APS

Palo Verde Nuclear
Generating Station

David Mauldin
Vice President
Nuclear Engineering
and Support

Tel: 623-393-5553
Fax: 623-393-6077

Mail Station 7605
PO Box 52034
Phoenix, Arizona 85072-2034

10 CFR 50.55a(a)(3)(i)

102-05298-CDM/TNW/GAM
June 21, 2005

U.S. Nuclear Regulatory Commission
Attn: Document Control Desk
Washington, DC 20555-0001

Dear Sirs:

Subject: Palo Verde Nuclear Generating Station (PVNGS)
Unit 3
Docket No. STN 50-530
List of References Associated with ASME Code Case N-499 to Support NRC Review of Inservice Inspection (ISI) Program Relief Request No. 33 for Pressurizer Base Material Heating

In letter 102-05296, dated June 19, 2005, Arizona Public Service Company (APS) requested NRC approval of proposed alternatives to 10 CFR 50.55a(c), "Reactor Coolant Pressure Boundary," for a portion of the PVNGS Unit 3 pressurizer base material surrounding the heater sleeves that was subjected to elevated temperatures (ISI Relief Request No. 33).

During telephone conferences on Monday, June 20 and Tuesday, June 21, 2005 regarding Relief Request No. 33, the following references were discussed:

1. Portions of ASTM DS 47, "Evaluations of the Elevated Temperature, Tensile and Creep - Rupture properties of C-Mo, Mn-Mo and Mn-Mo-Ni Steels," Prepared for MPC By G. V. Smith, 1971.
2. Portions of ASME Publication, "Symposium on Heat-Treated Steels for Elevated Temperature Service," September 1966; Article: "Characterization of Heat Treated Pressure Vessel Steels for Elevated Temperature Service," Edited by M. Semchysen, 1966.

A047

3. Portions of ASME-MPC Publication, "Analysis of Data from the Symposium on Heat-Treated Steels for Elevated Temperature Service," By E. B. Norris and R. D. Wylie, 1966.

4. DOE-HTGR-88383, "Tensile and Creep Properties of SA533 Grade B Class 1 Steel," December 1989.

5. DOE-HTGR-90286, "Documentation of ASME Code Case for Elevated-Temperature Service of MHTGR Reactor Vessel Materials," September 1991.

6. Combustion Engineering Report MML-89-142, "Creep and Tensile Properties of SA508 Class 3 Forging Material," December 1989.

7. Oak Ridge National Laboratory Letter 0409-49-90 regarding submission of data package for SA-533 Grade B, Class 1 plates, SA-508 Class 3 forgings and their weldments, dated April 20, 1990.

8. ASME Publication, "Criteria for Design of Elevated Temperature Class 1 Components in Section III, Division 1, of the ASME Boiler and Pressure Vessel Code," May 1976.

The applicable portions of the documents listed above are attached to this submittal. No commitments are being made to the NRC by this letter. If you have any questions, please contact Thomas N. Weber at (623) 393-5764.

Sincerely,

David Mauldin

CDM/TNW/GAM

Attachments: Applicable portions of the documents listed in this letter.

cc: All w/o attachments

B. S. Mallett	NRC Region IV Regional Administrator
M. B. Fields	NRC NRR Project Manager
G. G. Warnick	NRC Senior Resident Inspector for PVNGS

1. ASTM DS 47, "Evaluations of the Elevated Temperature, Tensile and Creep –Rupture properties of C-Mo, Mn-Mo and Mn-Mo-Ni Steels".

CH
4-7-88

EVALUATIONS OF THE ELEVATED TEMPERATURE TENSILE AND CREEP-RUPTURE PROPERTIES OF C-Mo, Mn-Mo and Mn-Mo-Ni STEELS

Prepared for the
METAL PROPERTIES COUNCIL
by G. V. Smith

DS 47

AMERICAN SOCIETY FOR TESTING AND MATERIALS

EVALUATIONS OF THE ELEVATED TEMPERATURE TENSILE AND CREEP-RUPTURE PROPERTIES OF C-Mo, Mn-Mo and Mn-Mo-Ni STEELS

Prepared by
G. V. Smith

ASTM DATA SERIES PUBLICATION DS 47

05-047000-02

List price $6.25

AMERICAN SOCIETY FOR TESTING AND MATERIALS
1916 Race Street, Philadelphia, Pa. 19103

REFERENCE: Smith, G. V., Evaluations of the Elevated Temperature Tensile and Creep-Rupture Properties of C-Mo, Mn-Mo and Mn-Mo-Ni Steels; ASTM Data Series DS 47. American Society for Testing and Materials, 1971.

ABSTRACT: This report evaluates the elevated temperature strength properties of carbon-moly steel, and various modified versions of that steel commonly identified as manganese-molybdenum or manganese-molybdenum-nickel steels. The data that have been evaluated encompass test results previously included in ASTM Data Series DS 6 (1953)[1] and DS6-S1 (1966)[2], and previously unpublished test results gathered by The Metal Properties Council.

Employing the method of least squares, trend curves depicting in ratio form the characteristic temperature variations of yield and tensile strengths have been developed. The rupture data have been evaluated by both direct isothermal interpolation or extrapolation, and by time-temperature parameters, to establish the temperature dependences of the average and minimum stresses to cause rupture in 1000, 10,000 and 100,000 hours. The secondary creep rate data have been evaluated by direct interpolation or extrapolation to determine the temperature dependences of average and minimum stresses to cause secondary creep rates of 0.1 and 0.01 percent per 1000 hours. These latter trend curves could be developed only for C-Mo steel, there being too few data for the remaining grades to warrant such evaluation. Elongation and reduction of area data are included for both the short time elevated temperature tensile tests and for the rupture tests.

Several summary figures immediately following this abstract, Figs. 1-6, show the temperature dependence of strength properties for the various grades evaluated in this report. In these figures, the yield and tensile strength curves have been computed from the respective ratio trend curves so that they correspond at room temperature to the specified minimum values of common ASTM specifications.

The body of the report provides in tables, text, and figures, details concerning the identification of the individual lots of material, the evaluation procedures, and the results.

KEY WORDS: elevated temperature, tensile strength, yield strength, creep strength, rupture strength, elongation, reduction of area, carbon moly and manganese moly steels, time-temperature parameter, data evaluation, mechanical properties.

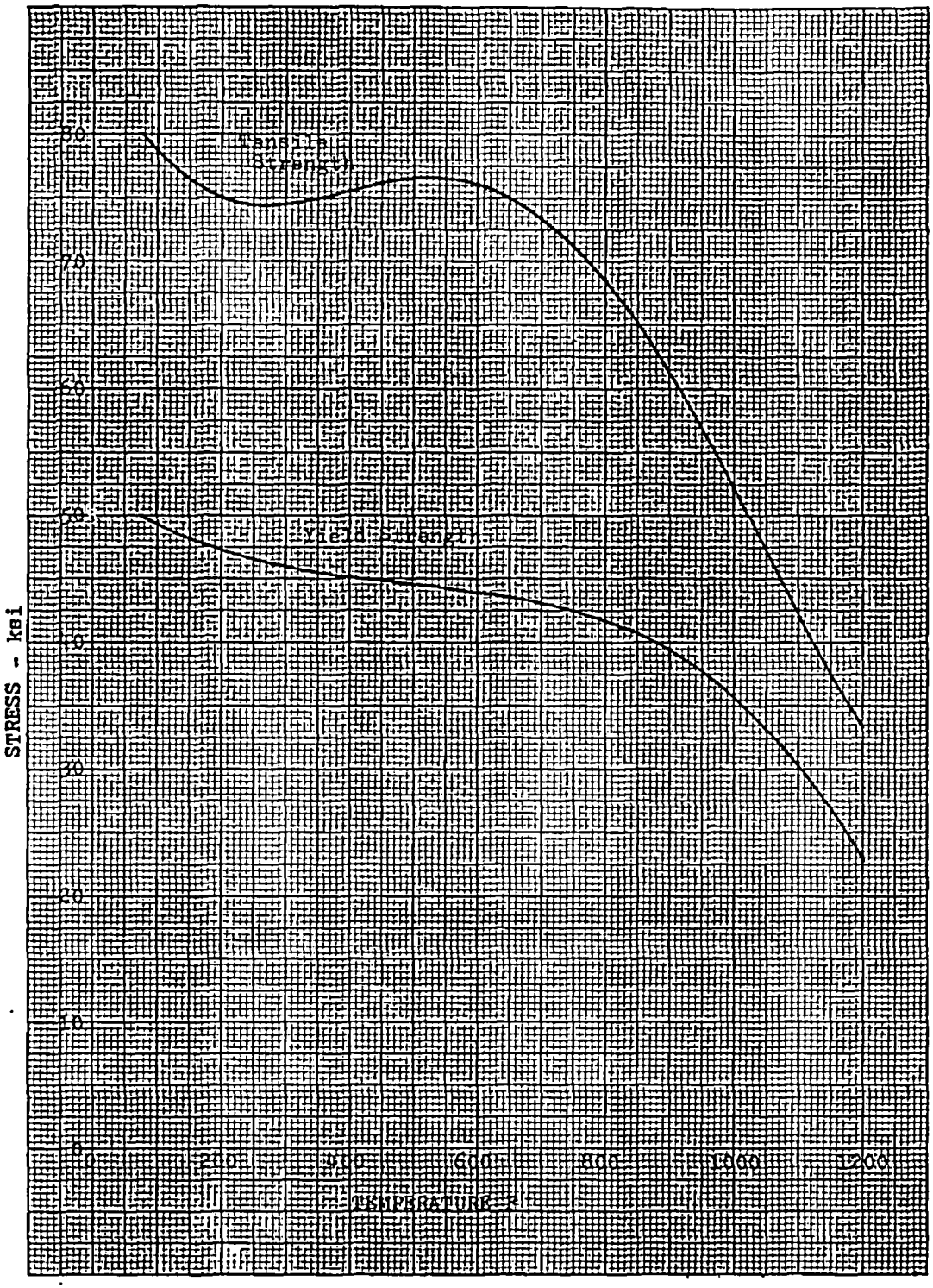

Fig. 2 Effect of temperature on yield strength and tensile strength of Mn-Mo-(Ni) steel, A 302 (or A 533, Class 1), adjusted to 50 and 80 ksi at 75 F.

INTRODUCTION

The materials evaluated in this report include C-Mo steel (0.5 percent molybdenum) which has been widely used in elevated temperature service over many years, and the newer Mn-Mo, and Mn-Mo-Ni modifications of this basic grade. Evaluations have been made for various heat-treated conditions, including quenching and tempering, and for various product forms. The report is another in a continuing series of evaluations sponsored by The Metal Properties Council (MPC)[16-18].

Included in the evaluations are data previously reported in ASTM's DS Data Series,[1,2,19] under sponsorship of the Joint ASTM-ASME Committee on the Effect of Temperature on the Properties of Metals, as well as data recently gathered by MPC from cooperating laboratories. Pertinent data reported many years ago in the 1938 Creep Data Compilation[6] have also been included. All of the data are identified in Table I as to ASTM specification, deoxidation practice, heat treatment, product form and size, grain size, and data source, to the extent that these were known, and in Table II with respect to chemical composition. Some of the data sets from DS 6 and DS 6S1[1,2] were excluded from the evaluation, owing to inadequate identification or non-conformance with specifications. The data gathered by MPC are tabulated in this report; data from DS 6 and DS 6S1 have not been copied into this report, but a coding key to the DS data that have been integrated into the evaluations is provided in Table I of the present report.

The tabular data for each of the several types of materials, or heat treatment variations of a given type of material, included in the evaluations, have been grouped separately, as follows:

Part 1: C-Mo steels (Specs. A204, A209, A335, A369, A182, A217)

Part 2: Mn-Mo and Mn-Mo-Ni Steel Plates (A302)

Part 3: Mn-Mo and Mn-Mo-Ni Steel Plates, Quenched and Tempered (A533)

Part 4: Mn-Mo Steel Forgings (A372, Class IV)

Part 5: Mn-Mo Steel Castings (A487, Classes 2N, 2Q)

Part 6: Mn-Mo Steel Plate, Quenched and Tempered (A514, Type C).

In considering the data of Part 1, a distinction has been preserved in the early stages of the evaluation as to product form (bar, plate, tube or pipe, casting), but in the final stage of trend curve evaluation, it has seemed appropriate to consider the data for different product forms as from one population. In the remaining Parts, the product form was unique to the individual Part.

The properties that have been evaluated in this report include yield and tensile strengths, and creep and rupture strengths. Unfortunately, the latter two properties could be evaluated only for Part 1, the number of data being either too few or nonexistent for the remaining Parts. For Part 1, rupture strength has been evaluated for three rupture intervals, namely; 1000, 10,000 and 100,000 hours, and creep strength for two secondary creep rates, namely 0.1 and 0.01 percent per 1000 hours. Elongation and reduction of area at fracture have been included in the report for both the tensile and rupture tests, when available.

Yield Strength, Tensile Strength, Elongation and Reduction of Area

The original tensile test results, excepting those previously reported in DS 6 and DS 6S1, are tabulated in Table III. Many of the reported values represent the average of replicate tests. As with the previous evaluations in this series, the tests are presumed to have been conducted generally at strain rates within the limits permitted by ASTM Recommended Practice E 21, and the yield strengths to represent either 0.2% offset, or the lower yield point. Unless otherwise indicated, elongation values represent a gage length of two inches, and in the case of plate material, test specimens were taken from the quarter thickness position.

Employing a data normalizing procedure that has proved useful in previous evaluations,[16-18] the elevated temperature yield and tensile strengths of individual lots have been ratioed to the room temperature yield and tensile strengths of the same lots. Then, each set of such ratios, representing individual data populations, e.g. C-Mo steel, has been evaluated by the procedure of least squares to establish a "ratio trend curve" of best fit through all the data. With the temperature dependence of strength expressed in terms of strength ratios, it becomes possible to compute strength trend curves for any specific room-temperature strength level of interest, within the limits encompassed by the original data.

The tensile test results for the different categories are plotted as dependent upon temperature in Figures 7-12, corresponding with the individual Parts into which the data have been grouped. In each figure, part (a) charts yield strength and yield strength ratio; part (b) charts tensile strength and tensile strength ratio; and part (c) charts elongation and reduction of area. No data for either weld metal or weldments are included in the figures inasmuch as no elevated temperature test results were received by MPC, nor were there data in an earlier report covering weld metal and weldments.[19]

Specific comments concerning the individual groups follow:

Part 1: C-Mo steels, Figs. 7a, b and c

Data for the different product forms, plate, pipe-tube, bar, and castings have been distinguished from one another. All of the plate materials fell within limits corresponding to Grade B of A204, with several lots also meeting the requirements of either Grade A or C. Considerable scatter is evident, especially for yield strength,* and normalizing the strength data by

*As suggested in an earlier publication[18], a significant portion of the scatter in yield strength probably reflects the difficulty of measuring small strains at elevated temperatures, the possible presence of residual stresses from straightening or specimen preparation procedures, and possible differences in strain rate, factors which have a lesser effect upon tensile strength than upon yield strength.

ratioing has not proved particularly effective in reducing scatter. Inspection of the ratio plots suggests somewhat greater yield strength ratios for plate than for bar, but this difference is not evident for tensile strength ratio. Unfortunately, the extent of overlap in temperature for these two product forms is limited, there being no plate data above 1000°F, and only isolated data for bar below 700°F. For the other two product forms, the number of data are quite limited. All in all, the character of the data is such that it has seemed appropriate to treat all of the yield and tensile strength ratios as belonging to the same individual populations for the purposes of the least squares analyses. The resulting regression lines of best fit, or trend curves, have been superimposed on the ratio plots, and are included in the tabulations of Table V.

The tensile strength ratios that resulted from the least squares analyses using a computer began increasing immediately above room temperature, and it is apparent that the two values at 200°F, having a ratio less than one, were "overwhelmed" by the weighting of all the other data. Since carbon and low alloy steels typically exhibit[17] a decreasing ratio immediately above room temperature, before dynamic strain aging can be manifested, the trend curve shown in Fig. 7b and included in Table V has been drawn visually for temperatures between room temperature and 700°F. It is of interest to note that the spread in tensile strength ratio at intermediate temperatures is probably in part associated with differences in strain-aging susceptibility of the different lots, the degree of susceptibility depending primarily upon nitrogen concentration, deoxidation practice and heat treatment. It is also of interest to note that the maximum susceptibility evident in Fig. 7b is on the order of that exhibited by carbon steel.[17]

Elongation and reduction of area of C-Mo steel also exhibit much scatter, Figure 7c, with some tendency for reduced ductility in the range of temperature in which dynamic strain aging is indicated in the tensile strength data. At higher temperature, ductility trends to higher levels. Plate and castings tend to exhibit somewhat less ductility than bar and pipe.

Part 2. Mn-Mo and Mn-Mo-Ni steel plates, Figs. 8a, b and c

The data that were available were reported to represent either grade B or Grade C of ASTM specification A302, and are so distinguished in Figs. 8a, b and c. However, it will be recognized that Grade B requirements overlap those of Grade A, and hence a number of the Grade B data may equally well represent Grade A material. Inspection of the ratio plots, Figs. 8a and b does not indicate any need to distinguish between grades B and C as to trend curves. Some data representing material having room temperature tensile strengths greater than permitted by spec. A302 have been included in the evaluation. Work previously reported,[20] as well as analysis of the present data, has indicated that for a specific grade of material the dependence of strength upon temperature, when expressed in ratio form, is insensitive to absolute strength level within wide limits. A common population has been assumed for the least squares regression analyses. The resulting trend curves have been superimposed upon the ratio plots, and included in Table V.

The trend curve for tensile strength indicates by the rise at intermediate temperatures a slight tendency for dynamic strain aging. However, the strength ratio remains below 1.0, in contrast to the C-Mo steels of Part 1, and the peak occurs at a slightly higher temperature, 550°F as compared to 400°F. Again, the scatter in strength ratio at the peak temperature is probably to be associated with differing susceptibilities to strain aging.

Perhaps reflecting the reduced strain-aging susceptibility indicated by the tensile strength results, there is little tendency for reduced ductility at intermediate temperatures, Fig. 8c. The scatter in ductility for the plate represented in Fig. 8c, is less than that evident in Fig. 7c, which represented various product forms.

Part 3. Mn-Mo and Mn-Mo-Ni steel plates, quenched and tempered, Figs. 9a, b and c

ASTM Spec. A533 includes 4 grades A, B, C and D corresponding with different levels of nickel within the range 0 to 1% and fixed amounts of the remaining elements, and 3 classes of tensile requirements, Classes 1, 2 and 3. Because the strength classes overlap one another and because experience has indicated an insensitivity of strength ratio to strength level, within a given material category, the plots of Figs. 9a, b and c distinguish only among the several grades. At least some data were available for each of the grades A, B and D, but none for grade C. Although it is possible that more adequate samples of data for the different grades might reveal differences amongst them, the character of the strength ratio data that are available are such that it has not seemed appropriate to distinguish at this time amongst the different grades. Hence the ratioed data have been considered as belonging to a common population. The trend lines resulting from the regression analyses are shown on the ratio plots and included in Table V.

The tendency for dynamic strain-aging has been lessened still further relative to the materials of Parts 1 and 2, with the tensile strength ratio trend curve essentially level at intermediate temperatures.

The ductility data, Fig. 9c, showed only limited scatter, with no evident differentiation amongst the three grades for which data are available.

Part 4. Mn-Mo steel forgings, Figs. 10, b and c

Data were available for only one lot of Mn-Mo steel forgings, and thus the conversion of the strength data into ratios serves only the purpose of making it possible to express the trend curves in ratio form. With data for only one lot, there is, of course, no way of knowing how representative the trend curves shown on the ratioed plots and in Table V are. The requirements of ASTM Specification A372, IV covering this material, overlap in many respects with those for the materials of Parts 2 and 3 of this report, and the strength ratios fall within the scatter bands of Figs. 8 and 9. However, the specified molybdenum content for A372, IV is only about one-half of that required of the other materials, and it has not seemed appropriate to include this material with the others. Clearly, further testing of this material is desirable.

Part 5. Mn-Mo steel castings, Figs. 11a, b and c

Data were available for 3 lots of this material, but each lot had been tested in both the normalized-and-tempered and quenched-and-tempered conditions, conforming to grades 2N and 2Q of ASTM Specification A487. The data are distinguished as to heat treatment in the plots. Ratioing of the strength data has been effective in reducing scatter, especially for tensile strength. Yield ratios for Grade 2N exhibit relatively high scatter, but except for this grade, the ratio trend curves shown in Figs. 11a and b and included in Table V seem reasonably well defined by the data from only three lots.

The ductility values, Fig. 11c, exhibit only modest scatter.

Part 6. Mn-Mo steel plate, quenched and tempered, Figs. 12a, b and c

Data were available for only two lots of material in this category, and although it is possible that the availability of further data at some future date may reveal that this material can be grouped with one or another of the other material groups evaluated in the present report, it has seemed desirable to treat it separately for the present. Interestingly, a relatively small difference between the strengths of the two lots has been even further reduced by ratioing, giving a measure of confidence in the trend curves that have been developed, Figs. 12a and b and Table V. Gaps in test temperature between room temperature and 300°F and between 300 and 600°F, do raise some uncertainty as to the true shapes in the range below about 600°F.

Comparisons of the Trend Curves

Tabular comparisons of the yield and tensile strength ratio trend curves are afforded for all of the material categories in Tables Va and Vb, respectively, and a graphical comparison is provided in Fig. 13 for the three categories for which there were significant volumes of data. It may be seen in Fig. 13 that the trend curves for material categories corresponding to Specifications A302 and A533 are reasonably similar to one another. For this reason, trend curves for the combined populations have also been developed, and are included in Tables Va and Vb. The common trend curves have been used for summary Figures 2 and 3.

Creep and Rupture Properties

The original creep and rupture data not previously reported in DS 6 and DS 6S1 (References 1 and 2) have been tabulated in Table IV, separated into Parts according to specification or nominal composition. Only a few data were available for Parts 2 and 3 (corresponding to specifications A302 and A533) and for Part 6 (A514C), and none at all were available for Parts 4 and 5 (A372IV and A487, 2N and 2Q). Only for Part 1 (C-Mo) were the data adequate to warrant evaluation to the extent of developing trend curves suitable for establishing allowable stresses.

As in earlier evaluations[17,18], both direct and indirect procedures have been employed in extrapolating the rupture data to 100,000 hours. The former procedure involves extending the isothermal relation between stress and rupture time, commonly plotted on log-log coordinates, to 100,000 hours, whereas the latter involves one or another time-temperature parameter. For reasons described in the earlier evaluations, the character of the available data is such that the indirect or parameter extrapolations have not been performed on an individual lot basis, but rather on a "universalized" basis, assuming universal values for the parameter constants.

Part 1. C-Mo steels

To show both the quantity of data and their scatter, all of the data are shown in isothermal scatter band plots of log stress versus log time for rupture (Figs. 14a, b and c); of log stress versus log secondary (or minimum) creep rate (Figs. 15a, b and c); and of percent elongation and reduction of area at rupture versus log time for rupture (Figs. 16 a-g). In each plot, data for different product forms are differentiated. A few data available for weld metal have been plotted, for purposes of visual comparison, but these have not otherwise been included in the evaluations. A few weld metal data for temperatures of 842, 932 and 1022°F have not been plotted, but inspection reveals that these are not inconsistent with the data for the several product forms, as true also of the plotted data. A few data for weldments (as contrasted with weld metal) have not been included in this report owing to the inhomogeneous nature of weldment test specimens, and the dependence of the results upon geometrical considerations.

Rupture Strength

The rupture data have been extrapolated isothermally to 100,000 hours both visually on an individual lot basis, giving weight to the longer time tests, and by extending the line of best fit resulting from least squares analysis of the scatter bands, assuming all of the data to have come from a common population. No clearly identifiable effect of product form is evident in the scatter bands, nor in the results of the individual lot extrapolations assembled into plots of strength versus temperature (see later). However, for some product forms, there are few or no data. In contrast to earlier evaluations in this series[16-18], these evaluations have indicated that the relation between log stress and log time to rupture may be bilinear or curvilinear. Thus, for a number of the isothermal scatter bands, the variance of the data was observed to decrease as the order of the assumed relation between the variables was increased beyond the first degree. In the individual-lot extrapolations some of the log-log plots (not included here) seemed to exhibit a break from one slope to another steeper one; such breaks might well be reflected as curvilinearity in the scatter bands. Unfortunately, departure from linearity introduces an element of uncertainty into the direct extrapolations, beyond the usual uncertainty associated with extending a linear line for one or more log cycles.

The results of the individual lot evaluations of the stress to cause rupture in 1000, 10,000 and 100,000 hours, by interpolation or extrapolation, as required, have been assembled in Table VI, and plotted in Figs. 17a and b. Most of the data of Figs. 17a and b represent bar stock. The

relatively few data for pipes or tube and for castings fall reasonably within the scatter of the bar data. Least squares evaluations were made for each rupture time, Figs. 17a, b, assuming the data to represent common populations; the resulting regression lines, of third order in each instance, have been superimposed upon the data, and included in tabular form in Table IX. It is of interest that the regression curves for the three intervals have similar shapes. Minimum position curves, derived from the mean curves by a procedure described previously[21], are also shown in Figs. 17a and 17b, and tabulated in Table IX.

In the least squares evaluations of the isothermal scatter bands, the longer time data were weighted by the expedient of excluding rupture times less than 50 hours, and time was taken as the independent variable, for reasons given earlier.[21] The results of the evaluations, in terms of the stresses to cause rupture in 1000; 10,000; and 100,000 hours, are assembled in Table VIII. For each of the temperatures evaluated, rupture strengths are shown corresponding to a first order relation between log stress and log time-for-rupture. In addition, for a number of temperatures, rupture strengths are given, corresponding to a second or third order equation, exhibiting a reduced variance. Even when the variance is reduced only marginally (expressed as a percentage), the 100,000 hour rupture strength, developed in all instances by extending the regression line, may be reduced significantly, and for larger reductions in variance, the reduction in strength is even greater. Note particularly, the 100,000 hour strength at 900°F corresponding to a third order equation. The differences in 10,000 hour and 1000 hour strengths corresponding to different orders of the regression equation are correspondingly less than those for 100,000 hours as might be expected, but may still be significant (as for example at 900°F). It must be concluded from a study of Table VIII that extension of the isothermal scatter regression line to 100,000 hours is an especially hazardous procedure, and increasingly so as the order of the assumed equation increases (see also reference 21). For this reason values for 100,000 hours rupture strength by this procedure have not been included in the comparisons of Table IX. However, 1000 hour and 10,000 hour rupture strengths have been included in Table IX (for the linear case only), as of possible comparative interest.

Two "universalized", time-temperature parameter evaluations were made, in which all of the rupture data, except those for rupture time less than 5 hours, were "parameterized", and the resulting scatter bands of stress versus parameter evaluated by the method of least squares. Universal values were assumed for the constants, and all data were assumed to come from a common statistical population. The parameters that were employed were firstly, the well-known Larson-Miller parameter, with an assumed value of 20 for the constant:

$$T(20 + \log t) = F_1(s);$$

and the more recent compromise parameter proposed by Manson:[22]

$$\log t + \frac{1}{40}\log^2 t - \frac{40,000}{T+460} = F_2(s) .$$

In either parameter, T is temperature in degrees Rankin, t is the rupture-time in hours, and $F_1(s)$ and $F_2(s)$ denote that the parameters are *different functions of the stress* s.

Scatter band plots showing the dependence of log stress upon the two parameters are provided in Figures 18a and b. Parameter values corresponding to 100,000 hours at specific temperatures have been superimposed upon the Figures. Also superimposed upon the plots are the results of least squares evaluations, taking parameter as the independent variable. Mean curves together with minimum curves (90% confidence) derived from the mean curves[21] are shown. Mean and minimum values for the stresses to cause rupture in 1000; 10,000 and 100,000 hours are included in Table IX, for comparison with the results derived by the other procedures employed.

Figure 19 shows a graphical comparison of the results for rupture in 10,000 and 100,000 hours, derived by regression of the temperature dependence of the individual lot extrapolations and by the two universalized parameter procedures. Both of the parameter evaluation procedures give a more conservative result than the procedure involving individual lot visual extrapolation, but the differences may be viewed as relatively modest. (In past evaluations of carbon steel[17] and 2 1/4 Cr-1 Mo[18], the individual lot procedure had given a more conservative result than the universalized Larson-Miller procedure.) Of the two parameter procedures, the Manson compromise parameter gave the more conservative result, as expected, with divergence increasing towards higher temperature. Since the parameter procedures provide an estimate of long time strength (e.g. 100,000 hours) from shorter time tests at higher temperatures, it follows that they are inherently unable to provide estimates of 100,000 hour rupture strengths over the entire range of temperatures for which there are test data (except as questionable extrapolations of the "master" parameter curve might be employed). Thus 100,000 hour rupture strengths can be derived in the present instance only to a maximum temperature of 1000°F, and even at this temperature, only a small portion of all the data actually define the corresponding value of parameter. To be sure, many engineers would not choose to use C-Mo steel above 1000°F because of the excessive scaling to be expected.

In choosing amongst the three sets of 100,000 hour rupture strengths in Table IX or Fig. 19, one obtained by direct and two by indirect extrapolation, the advantages by the direct individual lot extrapolation procedure of visual weighting of the longer time results seems to be outweighed by the uncertainties associated with possible bilinearity or curvilinearity. It follows then that greater weight should be given to the results of the indirect or parameter procedures, in spite of inherent reservations about such procedures, previously expressed.[21,20] Also, as previously noted, either parameter procedure leads to a more conservative estimate. The choice between the two parameter results is more difficult; several considerations seem appropriate. Firstly, the maximum difference between the two results is at 1000°F, at which the Manson compromise parameter result is 13% less than that by the Larson-Miller procedure; the difference diminishes progressively to zero at 800°F. Interestingly, the positions of the parameter master

curves are least well defined by data at 1000°F, and best defined at 800°F. Secondly, at 1000 hours, at which the direct result might be reasonably viewed as superior to the result of any indirect procedure, since it can be derived by interpolation, the Larson-Miller result more closely approximates the direct result. Similarly, at 10,000 hours, the need for extrapolation was minimal, with a few values derivable by interpolation, and again the Larson-Miller result more closely approximates the direct result. The foregoing train of reasoning suggests that the Larson-Miller procedure has given the most reasonable estimates of 100,000 hour rupture strength; and it is this result that has been integrated into the summary chart of Fig. 1. Also as a matter of possible interest, isothermal log stress vs. log time-for-rupture curves have been computed from the Larson-Miller master curve, and these have been superimposed upon the scatter bands, Figs. 14a, b and c.

Creep Strength

The secondary creep-rate data shown in the scatter bands of Figs. 15a, b and c were visually interpolated or extrapolated (by not more than about 1 log cycle) on an individual lot basis, to determine creep strengths corresponding to 0.1 and 0.01 percent per 1000 hours. Curvilinearity in the relation between log stress and log secondary creep rate in the region 0.1 to 0.01% per 1000 hours was evident for many of the individual lots. The results are assembled in Table VII and plotted in Figs. 20a and b. There is no effect of product form evident in the data, but the number of data for other than bar is severely limited. The scatter plots of strength vs. temperature have been evaluated by the method of least squares and the resulting lines of best fit (trend curves) superimposed upon the plots and tabulated in Table X. Minimum position trend curves, derived from the mean curves, are also given.

The trend curves for variation of creep strength with temperature, Fig. 20, exhibit a complex character, requiring a third or higher order equation, if the entire range of temperature is to be represented by a common curve. As a consequence, the result becomes sensitive to the distribution of data and at the mercy of the procedure; thus the indicated maximum in the 0.1% per 1000 hours creep strength at 850°F is of questionable validity. It is of interest to note that creep strength falls off rapidly above about 950°F, whereas at lower temperatures there seems to be a levelling tendency. (The variations of 1000 hour and 10,000 hour rupture strengths, Fig. 17a, exhibited a somewhat similar tendency.) This relative insensitivity of strength to temperature at the lower temperatures may be related to the tendency to secondary hardening conferred by molybdenum. The trend curves have been extended to the upper limit of temperature for which data were available, i.e. 1200°F, even though as indicated earlier, extensive scaling may be expected above about 1000°F.

Rupture Ductility

The elongation and reduction of area at rupture of C-Mo steel tend, on the whole, to be relatively low at longer rupture times, Figs. 16 a-g. Thus, at 850 and 950°F, where the trends are fairly well defined and which are in the range of practical interest, ductility at rupture at 10,000 hours is on the order of only 10 percent. This reduced ductility may reflect a trend to intergranular mode fracture at longer time, but no information concerning mode of fracture was made available by the contributors of data.

Parts 2 and 3. Mn-Mo and Mn-Mo-Ni steels (Specifications A302 and A533)

Since the yield strength ratio and tensile strength ratio curves for material corresponding to Specifications A302 and A533 were relatively similar, and since the number of creep and rupture test results available is limited, data from these latter tests have been plotted together, though differentiated by symbol. Figs. 21 a-b shows the interdependence between time-for-rupture and stress, Fig. 22, that for secondary creep rate and stress, and Fig. 23a, b that for rupture ductility and time-for-rupture (except that, in the interest of saving space, a few relatively short time rupture ductility results have not been plotted).

The rupture and creep data, extending to a maximum test duration of only about 1000 hours, are so limited in number that it has not seemed worthwhile to attempt the development of trend curves, particularly, when, based upon the behavior of normalized and tempered or quenched and tempered 2 1/4 Cr-1 Mo steel,[18] it is to be expected that the elevated temperature creep and rupture strengths will vary with the level of strength at room temperature, and hence depend upon the tempering temperature. However, individual lot interpolations or extrapolations were made, and these results are summarized in Tables VI and VII. Evidence of dependence upon room temperature strength is apparent when the level of the 900°F scatter band is observed to be higher than that for 850°F, Fig. 21a. The 900°F data represent lots having room temperature tensile strengths in the range 130-140 ksi (which, of course, exceeds the level permitted by specification), whereas the A533 data at 850°F represent a lot having a tensile strength at room temperature of only 87 ksi. Certainly, under the circumstances there is no possibility of differentiating between lots conforming to the two different specifications.

The limited ductility data extending only to 1000 hours test duration are essentially independent of rupture time and at a satisfactory level at 850°F, but trend downward at 950°F.

Part 6. Mn-Mo Steel Plate, Quenched and Tempered (A514, Type C)

The time-for-rupture, secondary creep rate, and rupture ductility for A514, Type C are plotted in Figs. 24, 25, and 26 a-b, respectively, but in view of the limited character of the data, and an expectation that the results depend sensitively upon level of strength at room temperature, no effort has been made to develop trend curves. However, interpolations and extrapolations of the data for the individual lots have been made, and the results are included in Tables VI and VII.

Acknowledgment

The evaluations of this report were developed for The Metal Properties Council under the guidance of a subcommittee of which Dr. M. Semchyshen is Chairman. Appreciation is expressed to the chairman and members of the subcommittee for helpful suggestions.

References

1. Report on the Elevated-Temperature Properties of Chromium-Molybdenum Steels; ASTM Data Series Pub. DS 6 (formerly STP No. 151); Oct. 1953.

2. Supplemental Report on the Elevated-Temperature Properties of Chromium-Molybdenum Steels, ASTM DS 6S1; June 1966.

3. Babcock and Wilcox Co.

4. U.S. Steel Corp.

5. General Electric Co.

6. Compilation of Available High-Temperature Creep Characteristics of Metals and Alloys; Joint ASME-ASTM Committee on Effect of Temperature on the Properties of Metals; March 1938; published by ASTM and ASME, Phil. and New York.

7. A. O. Schaefer: Review of Available Data on Steel in Heavy Sections for Pressure Vessel Applications; unpublished work, Pressure Vessel Research Committee, Welding Research Council, 1964; also 1968.

8. U.S. Steel Corp.

9. Lukens Steel Co.

10. Babcock and Wilcox Co.

11. Combustion Engineering, Inc.

12. Lehigh Univ., Department of Metallurgy and Materials Science: The Creep Rupture Properties of Pressure Vessel Steels - Data Summary, Sept. 1968.

13. S. S. Strunck, A. W. Pense, and R. D. Stout: The Properties of Spray-Quenched Thick-Section Steels; Welding Research Council Bulletin, No. 120, Feb. 1967.

14. Texas Electric Steel Casting Co.

15. Jones and Laughlin Steel Corp.

16. An Evaluation of the Yield, Tensile, Creep and Rupture Strengths of Wrought 304, 316, 321 and 347 Stainless Steels at Elevated Temperatures; ASTM Data Series DS 5S2 (1969).

17. An Evaluation of the Elevated Temperature Tensile and Creep-Rupture Properties of Wrought Carbon Steel; ASTM Data Series DS 11S1 (1970).

18. An Evaluation of the Elevated Temperature Tensile and Creep Rupture Properties of 2 1/4 Cr-1 Mo Steel; ASTM Data Series DS 6S2 (1971).

19. Elevated-Temperature Properties of Weld-Deposited Metal and Weldments, ASTM Special Technical Pub. No. 226 (1958).

20. G. V. Smith: Strength of 2 1/4 Cr-1 Mo Steel at Elevated Temperatures; Symposium on 2 1/4 Chrome-1 Molybdenum Steel in Pressure Vessels and Piping, Sept. 1970, Denver, Colorado. American Society Mechanical Engineers.

21. G. V. Smith: Evaluation of Elevated-Temperature Strength Data: Jnl. of Materials, 4, No. 4, Dec. 1969, pp. 878-908.

22. S. S. Manson: Time-Temperature Parameters -- A Re-Evaluation and Some New Approaches; published in "Time-Temperature Parameters for Creep-Rupture Analysis"; Amer. Society for Metals, Pub. No. D8-100 (1968).

Table I

Identification of Steels

Code No.	Spec. No.	Deoxid. Pract.	Heat[1] Treatment	Product Form-Size	Grain[2] Size	Ref.	Ref. Code No.
Part 1 - Carbon-Molybdenum Steels (Specs. A204, A209, A335, A369, A182, A217)							
1-1	-	Si+Al (1 lb.)	A1550	Bar, 1"	6-8$_M$	1	1
1-2	A182	-	HR	Plate 18×10×1.5"	-	1	2
1-3	A206	-	N1650, T1250	Rod, 1"	7$_M$	1	3
1-4	-	Si+Al (.4 lb.)	N1650	Forged	1-3$_M$	1	4
1-5	-	Si+Al (1.6 lb.)	N1650	"	6-8$_M$	1	5
1-6	-	Si	N1650	"	1-3$_M$	1	6
1-7	-	Al (.5 lb.)	N1700, T1300	Cast	3	1	7
1-8	-	CaMnSi (2 lbs.)	N1700, T1150	Cast	-	1	8
1-9	-	Si+Al	N1560, T1380	Wrought	-	1	9
1-10	-	-	N1650, T1300	"	8-9	1	10
1-11	-	-	N1650, T1300	"	8-9	1	11
1-12	-	Si+Al	N1650	"	8-9	1	12
1-13	-	Al (.5 lb.)	A1850	"	-	1	13
1-14	-	-	A1740, T1330, T1200	Cast	-	1	14
1-15	-	-	Annealed	Tube, 14 O.D.×1 1/4"w.	-	1	16
1-16	-	Al (2 lb.)	N1750, T1200	Cast	-	1	18
1-17	-	CaMnSi+Al (3 lbs.)	N1700, T1300	Cast	8	1	20
1-18	-	CaMnSi+Al (2 lbs.)	N1700, T1300	Cast	7	1	21
1-19	-	CaSi+Al (.5 lb.)	N1700, T1300	Cast	2-3	1	22
1-20	-	Al (2 lbs.)	N1700, T1300	Cast	6-7	1	23
1-21	-	Carbotram (4 lbs.)	N1700, T1200	Cast	7-8	1	24
1-22	-	Al (2 lbs.)	N1700, T1300	Cast	6-7	1	25
1-23	-	Al (.5 lb.)	N1700, T1300	Cast	3-4	1	26
1-24	-	None	N1700, T1300	Cast	3-6	1	27
1-25	-	Al (.5 lb.)	N1700, T1300	Cast	4	1	28
1-26	-	CaMnSi+Al (3 lb.)	N1700, T1300	Cast	7	1	29
1-27	-	CaSi+Al (2.5 lb.)	N1700, T1200	Cast	2-3	1	30
1-28	-	CaSi+Al (2.4 lb.)	N1700, T1200	Cast	7-8	1	31
1-29a	-	Al (1 lb.)	N1800	Bar	5	2	7-6a
1-29b	-	"	N1800, T1250	"	"	"	"
1-30a	-	"	N1950, T1250	"	5	2	7-6b
1-30b	-	"	N2000, T1250	"	-	"	"
1-31a	-	-	HR, T1300F	Bar 3/4"	-	2,3	7-18
1-31b	-	-	N1750, T1200	"	-	2,3	7-18
1-31c	-	-	N1650, T1200	"	-	2,3	7-18
1-32	-	-	T1400 (4 hrs)	Tube $2\frac{1}{2}$ O.D.×.3"	-	2,3	7-19
1-33	A209	Si+Al (1.6 lb.)	A1575 → 1200, AC	Bar 3/4"	6	2,3	7-20
1-34	A209	Si	" "	Bar 3/4"	-	2,3	7-21
1-35	A209	-	CD, T1300	Tube, 2 O.D.×.344"	-	3	-
1-36	-	-	A1600	Tube	-	3	-

(1) A-Annealed; N-Normalized; HR-Hot Rolled; Q-Quenched; T-Tempered or Stress Relieved; CD-Cold Drawn

(2) Actual grain size except when identified as M for McQuaid-Ehn

Table I - page 2

Code No.	Spec. No.	Deoxid. Pract.	Heat Treatment	Product Form-Size	Grain Size	Ref.	Ref. Code No.
1-37	-	-	1525 → 1200, AC	Wrought	-	3	-
1-38*	-	Si	N1650	Bar, 1"	1-3	4	-
1-39+	-	Si+Al (1.6 lb)	N1650	Bar, 1"	6-8	4	-
1-40	A204-B	-	N1650	Plate, 5 3/16"	-	4	-
1-41*	-	Si+Al (.4 lb)	N1650	Bar, 1"	1-3	4	-
1-42	-	-	T1270	Cast	-	5	-
1-43	-	-	N1650, T1250	Bar, 1"	$6\text{-}8_M$	6	1a
1-44a	-	-	N1650, Q1550, T1100	Bar, 1 1/8"	7_M	6	1b
1-44b	-	-	N1650, T1050	" "	3.5_M	6	1c
1-44c	-	-	N1650, Q1550, T1100	" "	4.5_M	6	1d
1-45	-	-	N1650, T1225	Bar, 1"	-	6	2
1-46**	-	Si-Al	A1550	Bar, 1"	8_M	6	3a
1-47	-	Si-Al	A1550	Bar, 1"	8_M	6	3b
1-48	-	Si-Al	A1550	Bar, 1"	$4\text{-}5_M$	6	3c
1-49	-	Si-Al	A1550	Bar, 1"	$6\text{-}8_M$	6	3d
1-50	-	-	N1650, T1200	Tube	-	6	4a
1-51	-	-	" "	"	-	6	4b
1-52	-	-	" "	"	-	6	4c
1-53	-	-	" "	"	-	6	4d
1-54	-	-	" "	"	-	6	4e
1-55	-	-	" "	"	-	6	4f
1-56	-	Killed	N1650, T1200 (1 wk.)	Bar, 1"	-	6	5a
1-57	-	Killed	N1650, T1200 (1 wk.)	Bar, 1"	-	6	5b
1-58	-	Killed	N1650, T1400 (1 wk.)	Bar, 1"	-	6	5c
1-59	-	Si-Al	N1650	Bar	-	6	6a
1-60	-	Si-Al	N1650, T1200 (5 hr)	Bar	-	6	6b
1-61	-	Si-Al	N1650, T1200 (168hr)	Bar	-	6	6c
1-62	-	Si-Al	N1650, T1300 (5 hr)	Bar	-	6	6d
1-63	-	Si-Al	N1650, T1300 (168hr)	Bar	-	6	6e
1-64	-	Si-Al	N1650, T1400 (5 hr)	Bar	-	6	6f
1-65	-	Si-Al	N1650, T1400 (168hr)	Bar	-	6	6g
1-66	-	-	N1650, T1110	Plate, 1 1/4"	-	6	7
1-67	-	-	Normalized	Bar, 1"	2_M	6	8a
1-68	-	Si	T1200	Plate, 1 1/2"	$2\text{-}4_M$	6	8b
1-69	-	Si	T1200	Plate, 1 1/2"	$2\text{-}4_M$	6	8c
1-70	-	-	T1200	Weld metal	-	6	9b
1-71	-	-	T1200	Weld metal	-	6	9c
1-72	-	-	As Received	Pipe	-	6	9a
1-73	A204-B	-	N1675	Plate, 5 1/4"	$4\text{-}5_M$	9	-
1-74	A204-B-C	-	N1700	Plate, 3"	-	9	-
1-75	A204-B-C	-	N1700, T1100	Plate, 3"	-	9	-
1-76	A204-B	-	N1700, T1100	Plate, 4 3/4"	-	9	-

* Identical with Code 1-6
\+ Identical with Code 1-5
* Identical with Code 1-4
** Identical with Code 1-1

Table I - page 3

Code No.	Spec. No.	Deoxid. Pract.	Heat Treatment	Product Form-Size	Grain Size	Ref.	Ref. Code No.
1-77	A204-B	-	N1700, T1100	Plate, 4 3/4"	-	9	-
1-78	A204-A-B	-	N1675	Plate, 6"	-	9	-
1-79	A204-B	-	N1650, T1150	Plate, 3 1/4"	-	9	-
1-80	"	-	N1650, T1200	" "	-	9	-
1-81	"	-	N1650, T1250	" "	-	9	-
1-82	-	-	T1200	Weld metal	-	19	1
1-83	-	-	T1200	" "	-	19	2
1-84	-	-	T1200	" "	-	19	3
1-85	-	-	T1275	" "	-	19	4
1-86*	-	-	T1112	" "	-	19	5
1-87*	-	-	T1202	" "	-	19	5
1-88	-	-	T1200	" "	-	5	-
1-89	-	-	T1275	" "	-	5	-
Part 2 - Manganese-molybdenum and manganese-molybdenum-nickel steels (Spec. A302)							
2-1	A302B	-	Norm. & Temp.	Plate, 6"	-	2	7-14a,b,c
2-2	"	-	" " "	Plate, 8 1/2"	-	2	7-15a,b
2-3	"	-	" " "	Plate, 3"	-	2	7-16a,b
2-4	A302B	FG;Al	N1775F(1), T1125	Plate, 8 1/8"	-	7	-
2-5	A302B	FG	Spray Quenched & Tempered	Plate, 15"	-	7	-
2-6	A302B	-	N1650, T1200	Plate, 4"	-	8	-
2-7	A302C	-	N1650, T1225, T1125	Plate, 2 7/8"	-	8	-
2-8	A302C	-	N1650, T1275	Plate, 5 9/16"	-	9	-
2-9	A302B		N1600, T1100	Plate, 6"	-	9	-
2-10	A302C	-	N1650	Plate, 2"	-	9	-
2-11	"	-	N1650, T1290	Plate, 2"	-	9	-
2-12	"	-	N1650, T1300	Plate, 2"	-	9	-
2-13	"	-	N1650, T1275	Plate	-	9	-
2-14	A302B	FG	Q1575, T1225, T1150	Plate, 10 1/2"	-	7	-
2-15	"	"	" " "	" "	-	7	-
2-16	"	"	" " "	" "	-	7	-
Part 3 - Manganese-molybdenum and manganese-molybdenum-nickel steels (Spec. A533)							
3-1	A533B,2,3	-	O1700, O1625, T1175	Plate, 6 3/8"	-	10	-
3-2	"	-	" " "	" "	-	10	-
3-3	"	-	" " "	" "	-	10	-
3-4	A533B,2	FG	Q1575, T12225, T1150	Plate, 7 7/8"	-	11	-
3-5	"	"	" " "	Plate	-	11	-
3-6	A533D,2,3	FG	Q1650, T1240	Plate, 1 3/4"	-	9	-
3-7	"	"	Quenched & Temp.	Plate, 1 3/4"	-	9	-
3-8	"	"	Q1675, T1225, T1075	Plate, 1 3/4"	-	9	-
3-9	A533D,2,3	-	O1675, T1225	Plate, 1 3/4"	-	9	-

(1) Spray quench to 600F
* Data identical with Codes 1-70 and 1-71

Table I - page 4

Code No.	Spec. No.	Deoxid. Pract.	Heat Treatment	Product Form-Size	Grain Size	Ref.	Ref. Code No.
3-10	A533A,1,2	-	Q1600, T1100, T1150	Plate, 6"	-	9	-
3-11	A533B,1	-	Q1650, T1240, T1150	Plate, 5 9/16"	-	9	-
3-12	A533B,1,2	-	Q1650, T1240, T1150	Plate	-	9	-
3-13	A533B,1	FG-Al	Q1600, T1225, T1150	Plate, 9 5/8"	-	7	-
3-14	"	"	" " "	" "	-	7	-
3-15	"	"	" " "	" "	-	7	-
3-16	A533B,3	-	Q1650, T1200	Plate, 2 3/8"	-	8	-
3-17[1]	A533A	-	Q1650, T1150	Plate, 3/4"-1"	-	12	-
3-18a[1]	A533B	-	" "	" "	-	12	-
3-18b	A533B,1	-	Q1650, T1200, T1100	Plate(2), 6"	-	13	-
3-18c	"	-	" " "	" (2), 12"	-	13	-
Part 4 - Carbon-Manganese-Molybdenum steel forgings (Spec. A372, Class IV)							
4-1	A372,IV	-	Q1650, T900	Pipe 24"O.D.×1.08"w	-	8	-
Part 5 - Carbon-Manganese-Molybdenum steel castings (Spec. A487, Class 2)							
5-1a	A487,2N	-	N1600, T1100	Casting	-	14	-
5-1b	A487,2Q	-	Q1600, T1225	"	-	14	-
5-2a	A487,2N	-	N1600, T1100	"	-	14	-
5-2b	A487,2Q	-	Q1600, T1225	"	-	14	-
5-3a	A487,2N	-	N1600, T1100	"	-	14	-
5-3b	A487,2Q	-	Q1600, T1225	"	-	14	-
Part 6 - Quenched and Tempered carbon-manganese-molybdenum steel plate (Spec. A514, Type C)							
6-1	A514C	-	Q1650, T1125	Plate, 1/2"	-	15	-
6-2	A514C	-	" "	" "	-	15	-

(1) Yield and tensile strengths at room temperature exceed limits of current specification.
(2) Heat treated to simulate thickness indicated.

Table II

Chemical Composition of Steels

Code No.	C	Mn	P	S	Si	Cr	Ni	Mo	Cu	Al	N	
Part 1 - Carbon-Molybdenum steels												
1-35	.18	.52	.009	.022	.28	.12	.08	.54	.08			
1-36	.19	.50	.008	.018	.26	.16	.12	.59	.10			
1-37	.14	.54	.015	.015	.22	.06	.08	.52	.08			
1-38	.16	.85	.020	.019	.24	.028	.015	.51	.03	.010	.005	
1-39	.13	.52	.012	.021	.16	.058	.042	.52		.044	.005	
1-40	.23	.85			.26			.54				
1-41	.22	.51	.012	.020	.17	.046	.048	.50	.09	.004	.005	V .001
1-42	.18	.58	.008	.008	.36	.12	.10	.53				
1-43	.18	.68	.030	.019	.20	.10	.12	.51	.26			
1-44	.16	.78	.032	.015	.25	.03	.04	.48				
1-45	.17	.51	-	-	.32	-	-	.46	-			
1-46	.13	.49	.011	.010	.25	-	-	.52	-			
1-47	.16	.49	.015	.018	.30	-	-	.49	-			
1-48	.16	.47	.016	.015	.23	-	-	.42	-			
1-49	.11	.19	.010	.012	1.35	-	-	.50	-			
1-50	.17	.52	-	-	.16	.05	-	.54	-			
1-51	.21	.48	-	-	.31	.05	.11	.53	-			
1-52	.15	.47	-	-	.13	.02	-	.55	-			
1-53	.15	.41	-	-	.19	.07	.14	.58	-			
1-54	.13	.50	-	-	.13	.06	-	.52	-			
1-55	.16	.45	-	-	.14	.06	-	.58	-			
1-56	.16	-	-	-	-	-	-	.50	-			
1-57	.10	-	-	-	-	-	-	.50	-			
1-58	.10	-	-	-	-	-	-	.50	-			
1-59	.11	.47	.010	.014	.17	-	-	.54	-			
1-60	.11	.47	.010	.014	.17	-	-	.54				
1-61	.11	.47	.010	.014	.17	-	-	.54				
1-62	.11	.47	.010	.014	.17	-	-	.54				
1-63	.11	.47	.010	.014	.17			.54				
1-64	.11	.47	.010	.014	.17			.54				
1-65	.11	.47	.010	.014	.17			.54				
1-66	.17	.50	-	-	.21	-	-	.54				
1-67	.16	.66	.016	.012	-	-	-	.54				
1-68	.17	.60	.01	.02	.22	-	-	.45				
1-69	.17	.60	.01	.02	.22			.45				
1-70	.06	.48	-	-	.03	-	-	.56				
1-71	.06	.48	-	-	.03	-	-	.56				
1-72	.12	-	-	-	-	-	-	.50				
1-73	.25	.75	.007	.024	.25	.05	.09	.45	.12	.010		
1-74	.25	.75	.007	.024	.25	.05	.09	.45	.12	.010		
1-75	.25	.75	.007	.024	.25	.05	.09	.45	.12	.010		
1-76	.25	.75	.007	.024	.25	.05	.09	.45	.12	.010		

Table II - page 2

Code No.	C	Mn	P	S	Si	Cr	Ni	Mo	Cu	Al	N
1-77	.25	.75	.007	.024	.25	.05	.09	.45	.12	.010	
1-78	.21	.62	.015	.024	.23	.08	.21	.47	.24	.012	
1-79	.20	.70	.008	.012	.17	.10	.16	.47	.21	.02	
1-80	.20	.70	.008	.012	.17	.10	.16	.47	.21	.02	
1-81	.20	.70	.008	.012	.17	.10	.16	.47	.21	.02	
1-82	.14	.44			.12			.59			
1-83	.13	.66			.18			.46			
1-84	.12	.52			.23			.48			
1-85	.08	2.32	.020	.021	.71			.48			
1-86	.06	.48			.03			.56			
1-87	.06	.48			.03			.56			
1-88	.08	.26			.10			.55			
1-89	.20	.65	.004	.003	.51			.52			
Part 2 - Manganese-molybdenum and manganese-molybdenum-nickel steels (Spec. A302)											
2-1	.25	1.36	.018	.036	.23			.49			
2-2	.25	1.36	.018	.036	.23			.49			
2-3	.25	1.36	.018	.036	.23			.49			
2-4	.20	1.27	.020	.028	.21			.48			
2-5	.22	1.45	.011	.015	.18	.29	.35	.50	.20	.037	
2-6	.18	1.26	.015	.012	.29	.09		.56			
2-7	.19	1.37	-	-	.20		.62	.55			
2-8	.21	1.27	.011	.016	.25	.10	.56	.60	.12	.014	
2-9	.20	1.28	.009	.018	.24	.07	.08	.47	.11	.031	
2-10	.22	1.30	.010	.017	.22	.07	.62	.52	.13	.029	
2-11	.23	1.30	.010	.015	.22	.06	.52	.42	.12	.039	
2-12	.23	1.30	.010	.015	.22	.06	.52	.42	.12	.039	
2-13	.24	1.32	.009	.016	.15	.11	.56	.55	.11	.019	
2-14	.20	1.46	.013	.010	.22			.48	.12		
2-15	.20	1.37	.010	.021	.19			.47	.12		
2-16	.20	1.42	.010	.014	.26			.47	.10		
Part 3 - Manganese-molybdenum and manganese-molybdenum-nickel steels (Spec. A533)											
3-1	.26	1.35	.012	.021	.26	.15	.61	.46	.28		
3-2	.25	1.37	.012	.024	.33	.13	.63	.46	.23		
3-3	.25	1.37	.013	.024	.32	.13	.65	.46	.23		
3-4	.22	1.56	.005	.013	.38	.07	.57	.51	.19	.03	
3-5	.22	1.31	.008	.025	.22	.15	.51	.49	.25	.048	
3-6	.19	1.48	.012	.022	.21	.29	.35	.50	.20	.037	
3-7	.20	1.37	.009	.017	.19	.08	.25	.48	.15	.041	
3-8	.18	1.18	.010	.016	.22		.31	.48			
3-9	.22	1.30	.011	.025	.24	.14	.25	.45	.23	.03	
3-10	.20	1.28	.009	.018	.24	.07	.08	.47	.11	.031	
3-11	.21	1.27	.011	.016	.25	.10	.56	.60	.12	.014	
3-12	.24	1.32	.009	.015	.15	.08	.56	.55	.11	.019	

Table II - page 3

Code No.	C	Mn	P	S	Si	Cr	Ni	Mo	Cu	Al	N
3-13	.22	1.29	.011	.018	.25	.16	.57	.46	.16	.062	
3-14	.22	1.30	.014	.020	.22	.10	.46	.50	.14		
3-15	.20	1.28	.010	.019	.25	.15	.58	.46	.25		
3-16	.25	1.34	.012	.023	.23	.10	.50	.53		.054	
3-17	.19	1.28	.013	.010	.22	-	-	.45			
3-18	.20	1.28	.019	.030	.21	.15	.53	.52	.27	.031	
Part 4 - Carbon-manganese-molybdenum steel (Spec. A372, Class IV)											
4-1	.44	1.56	.013	.021	.20			.21			
Part 5 - Carbon-manganese-molybdenum steel castings (Spec. A487, Class 2)											
5-1a,b	.30	1.10	.015	.015	.43	.26	.18	.18			
5-2a,b	.30	.87	.022	.018	.41	.21	.18	.19			
5-3a,b	.28	1.03	.016	.020	.38	.21	.16	.21			
Part 6 - Quenched and tempered carbon-manganese-molybdenum steel palte (A514C)											
									Ti		V	B
6-1	.18	1.17	.012	.023	.22	.03	.02	.24	.037	N.D.	.005	.002
6-2	.18	1.30	.012	.024	.25	.02	.02	.25	.04	N.D.	.005	.002

Table III - page 3

Code No.	Test Temp. °F	1000 psi Yield Stren.	1000 psi Tensile Stren.	Per Cent Elong.	Per Cent Red. Area
1-73	700	42.8	79.5	24.	48.
cont.	750	38.5	69.3	21.	52.
	800	40.3	69.5	20.	52.
	850	41.6	67.7	21.	49.
1-74	70	55.6	83.3	24.	51.
	500	57.8	97.8	21.	35.
	675	48.1	77.3	21.	54.
	850	51.5	76.7	20.	56.
	1000	46.0	62.7	20.	63.
1-75	70	51.7	78.8	28.	52.
	500	40.6	78.6	17.	41.
	675	43.5	79.6	23.	49.
	850	47.6	71.2	25.	51.
	1000	40.8	60.5	22.	54.
1-76	70	47.2	74.4	30.	51.
	500	42.8	79.7	24.	40.
	675	39.8	67.3	21.	49.
	850	41.9	70.4	20.	45.
	1000	36.3	58.2	23.	54.
1-77+	70	46.9	73.6	32.	52.
	500	44.5	78.5	21.	38.
	675	38.5	65.5	23.	49.
	850	36.8	66.7	23.	52.
	1000	42.2	57.0	24.	55.
1-78	70	46.6	73.2	31.	56.
	500	36.0	64.6	26.	52.
	675	33.5	65.3	25.	42.
	850	30.4	60.5	26.	61.
	1000	29.9	50.6	30.	68.
1-79	75	55.6	80.6	29.	61.
	750	31.4	75.8	28.	64.
1-80	75	55.1	78.6	31.	63.
	750	31.1	75.4	28.	63.
1-81	75	52.3	76.7	29.	66.
	750	31.4	69.0	31.	64.
Part 2 - Manganese-molybdenum and manganese-molybdenum-nickel steels (Spec. A302)					
2-4	75	77.0	98.5	23.	61.
	100	73.7	99.2	26.	65.
	150	70.2	96.4	21.	60.
	200	69.5	94.5	22.	66.
	300	68.1	91.0	22.	65.
	400	65.9	89.9	20.	56.

+ Test samples from 1/2 T position.

Table III - page 4

Code No.	Test Temp. °F	1000 psi Yield Stren.	1000 psi Tensile Stren.	Per Cent Elong.	Per Cent Red. Area
2-4	550	67.5	92.0	17.3	52.
cont.	700	65.9	92.0	24.	54.
2-5	75	85.6	104.9(1)	20.	50.
	1000	64.5	75.4	23.	66.
	1200	42.5	46.6	27.	55.
	1400	13.6	16.6	58.	51.
	1600	7.2	10.3	51.	44.
	1800	4.0	5.4	59.	57.
2-6	80	76.4	96.1	25.	69.
	200	70.1	90.0	23.	68.
	400	66.9	88.8	23.	67.
	600	66.5	94.0	27.	65.
	800	61.0	79.9	26.	73.
	1000	53.4	61.7	29.	83.
	1200	32.0	38.7	31.	91.
	1400	12.0	17.4	79.	92.
	1600	6.6	13.4	50.	92.
	1900	3.0	5.6	-	91.
2-7	80	71.6	88.1	27.	-
	500	55.0	82.4	21.	67.
	700	58.5	84.5	28.	74.
	900	49.6	68.6	21.	76.
2-8	80	54.2	100.8	26.	50.
	750	53.2	90.5	33.	64.
	850	50.1	74.9	34.	68.
	950	47.9	64.4	34.	72.
2-9	80	69.8	94.9	22.	56.
	750	58.9	84.8	23.	62.
	850	56.3	79.8	22.	64.
	950	53.4	71.7	25.	68.
2-10(2)	75	94.4	116.3(2)	22.	60.
	400	90.7	111.0	14.	46.
	600	84.4	111.9	26.	69.
	800	82.2	103.5	22.	71.
	1000	69.6	78.4	20.	69.
2-11	75	73.3	95.0	26.	69.
	400	67.2	93.4	24.	64.
	600	70.3	96.5	25.	61.
	800	67.3	81.0	28.	72.
	1000	54.4	63.3	26.	78.
2-12	75	64.2	90.5	28.	69.
	400	60.1	84.5	23.	68.
	600	61.1	95.8	32.	64.

(1) Slightly higher than permitted by spec. A302.
(2) Exceeds limit of spec. A302C.

Table III - page 5

Code No.	Test Temp. °F	1000 psi Yield Stren.	1000 psi Tensile Stren.	Per Cent Elong.	Per Cent Red. Area
2-12	800	56.2	76.7	22.	72.
cont.	1000	50.6	57.1	22.	80.
2-13	80	60.7	87.0	30.	65.
	750	47.3	79.1	30.	63.
	850	44.3	69.2	31.	69.
	950	43.7	61.2	31.	72.
2-14	75	61.7	81.4	27.	72.
	200	58.6	76.8	25.	67.
	400	53.2	74.2	22.	69.
	600	53.1	75.2	27.	65.
2-15	75	58.7	81.0	29.	70.
	200	56.5	76.4	25.	68.
	400	54.1	76.6	22.	69.
	600	51.0	74.1	27.	65.
2-16	75	62.8	83.5	29.	69.
	200	59.5	79.1	27.	67.
	400	54.6	75.7	26.	66.
	600	52.4	80.0	29.	62.

302=67

Part 3 - Manganese-molybdenum and manganese-molybdenum-nickel steels (Spec. A533)

533=87

3-1	75	87.2	108.1	24.	67.
	200	84.5	101.9	23.	66.
	400	78.5	97.5	22.	67.
	600	76.5	100.9	19.5	51.
	800	69.2	87.3	21.	63.
3-2	75	87.0	107.5	25.	66.
	200	82.0	101.0	24.	66.
	400	78.6	98.1	22.	63.
	600	78.0	101.3	21.	55.
	800	71.2	86.1	21.	69.
3-3	75	91.5	110.4	25.	67.
	200	86.1	102.9	24.	67.
	400	81.2	99.0	21.	63.
	600	81.8	103.5	21.	54.
	800	72.8	89.1	22.	66.
3-4	75	72.6	94.5	24.	65.
	300	65.4	85.5	23.	65.
	500	62.9	85.9	21.	64.
	700	60.9	84.6	25.	67.
	900	54.6	67.1	22.	74.
3-5	75	69.4	91.3	25.	66.
	550	61.8	88.0	23.	60.
	650	60.1	84.9	25.	61.
3-6	75	88.3	105.7	26.	-
	200	91.8	107.7	23.	71.
	400	88.4	105.3	22.	65.

Table III - page 6

Code No.	Test Temp. °F	1000 psi Yield Stren.	1000 psi Tensile Stren.	Per Cent Elong.	Per Cent Red. Area
3-6	600	84.8	111.1	20.	62.
cont.	800	78.1	97.7	22.	69.
	1000	66.7	74.4	24.	79.
3-7	75	82.8	100.5	25.	-
	200	81.0	98.3	23.	70.
	400	76.0	96.5	19.	70.
	600	74.7	106.5	24.	56.
	800	68.5	91.5	22.	64.
	1000	61.6	72.9	22.	79.
3-8	75	89.1	107.1	23.	64.
	700	76.4	100.6	18.7	60.
	800	71.9	92.2	19.0	63.
	900	68.5	83.2	18.5	67.
	1000	62.9	74.5	20.	72.
3-9	75	86.7	107.6	21.	64.
	300	77.3	97.0	22.	65.
	500	73.1	102.5	28.	63.
	700	71.7	100.0	27.	70.
	800	69.1	90.4	25.	66.
3-10	80	62.1	83.1	30. (1)	69.
	750	57.8	82.5	30. (1)	71.
	850	54.5	71.4	30. (1)	75.
	950	50.7	64.1	29. (1)	80.
3-11	80	64.5	87.0	29.	67.
5338-1	750	54.2	73.1	29.	66.
	850	50.9	67.0	33.	71.
	950	47.9	58.9	32.	79.
3-12	75	70.8	95.1	27.	63.
	750	59.5	79.7	31.	67.
	850	56.0	71.4	43.	72.
	950	53.0	62.7	31.	76.
3-13	75	65.3	87.3	26.	67.
	200	67.7	89.0	22.	66.
	400	56.7	78.3	22.	66.
	600	58.1	85.2	25.	66.
3-14 5338-1	75	64.6	87.1	27.	70.
	200	63.4	84.1	25.	69.
	400	52.2	75.5	23.	68.
	600	54.1	80.1	23.	66.
3-15	75	67.2	88.8	25.	67.
	200	64.8	84.6	24.	68.
	400	58.8	81.0	22.	66.
	600	57.3	83.2	22.	64.
3-16	80	100.0	117.0	21.	66.
	200	99.4	114.0	20.	65.
	400	91.4	111.0	20.	62.

(1) 1" gage length.

Table III - page 7

Code No.	Test Temp. °F	1000 psi Yield Stren.	1000 psi Tensile Stren.	Per Cent Elong.	Per Cent Red. Area
3-16	600	90.0	117.0	25.	66.
cont.	800	79.0	98.8	23.	72.
	1000	69.8	79.8	22.	82.
3-17	75	121.3	138.0	22.	70.
3-18a	75	121.5	130.5	20.	63.
3-18b	75	70.0	88.7	28.	69.
	200	64.8	82.5	25.	69.
	600	58.1	83.6	21.	60.
	900	51.7	64.6	22.	74.
	1100	44.2	45.5	26.	81.
3-18c	75	64.1	84.6	29.	69.
	200	56.7	77.5	28.	68.
	600	48.5	78.9	23.	58.
	900	41.4	58.4	28.	75.
	1100	36.1	39.8	38.	82.
Part 4 - Carbon-manganese-molybdenum steel forgings (Spec. A372, Class IV)					
4-1	75	95.9	125.9	19.	54.
	200	91.8	120.3	18.5	53.
	300	86.9	118.1	17.0	54.
	400	85.5	119.3	18.0	55.
	500	87.1	123.7	22.0	60.
	600	85.9	127.4	29.0	71.
	700	81.4	117.5	28.0	74.
	800	77.6	101.4	24.0	78.
	900	72.5	88.6	27.0	84.
	1000	63.3	74.4	25.5	85.
Part 5 - Carbon-manganese-molybdenum steel castings (Spec. A487, Class 2)					
5-1a	75	65.0	98.5	23.	41.
	300	62.5	90.0	28.	46.
	500	56.5	89.5	20.	39.
	700	55.0	91.2	22.	39.
5-1b	75	88.0	107.0	22.	48.
	300	85.0	101.5	18.0	48.
	500	78.0	101.0	18.0	44.
	700	78.0	103.7	24.0	46.
5-2a	75	59.0	88.5	24.0	43.
	300	50.0	80.0	26.0	51.
	500	41.0	80.0	23.0	41.
	700	40.0	81.0	24.0	42.
5-2b	75	77.0	98.0	24.0	57.
	300	71.0	92.0	22.0	56.
	500	65.0	89.0	21.0	53.
	700	65.0	97.0	27.0	59.

Table IV - page 6

Code No.	Temp. °F	Stress, ksi	Test Duration-Hours	Min. creep Rate-%/hr.	At Rupture % Elong.	At Rupture % Red. Area
1-72	932	20.0	1030. c	.0000194		-
	932	20.0	1030. c	.0000248		-
1-88	900	58.0	1.5	-	11.6	62.
		52.0	33.	-	5.7	18.
		46.0	136.	-	5.9	17.
		42.0	871.	-	3.0	10.
		38.0	343.	-	2.0	13.
		38.0	1035.	-	2.3	11.
1-89	1150	7.0	648.	-	15.6	44.
	1050	17.0	331.	-	14.5	33.
	1000	27.0	132.	-	25.4	48.
	900	27.0	10,046.	-	10.2	24.
	800	38.0	38,307.	-	13.3	58.
Part 2 - Manganese-molybdenum and manganese-molybdenum-nickel steels (spec. A302)						
2-8	830	57.5	219.	.01319	31.	70.
A302C	850	65.0	0.5	8.4	29.	64.
		62.5	1.9	6.2	29.	65
		57.5	48.6	.253	34.	66.
		55.0	445.	.0268	30.	64.
		52.5	2667. c	.00426	-	-
		50.0	1438. c	.00217	-	-
		45.0	5000. c	.0004	-	-
	900	32.5	171. c	.00125	-	-
	950	60.0	during loading	-	30.	70.
		47.5	10.3	1.76	42.	74.
		45.0	26.9	1.12	41.	73.
		40.0	101.	.077	37.	57.
		35.0	321.	.0218	17.8	35.
		30.0	1281.	.00651	19.5	25.
2-9 A302B	950	53.0	183.	-	11.4	13.8
		45.0	727.	-	7.5	10.0
		42.5	476.	-	8.6	11.6
Part 3 - Manganese-molybdenum and manganese-molybdenum-nickel steels (spec. A533)						
3-10	850	60.0	61.	.249	31.	68.
A533 B,2		57.5	95.	.154	34.	62.
	950	50.0	19.4	.870	39.	77.
		47.5	630.	.01165	22.	39.
		40.0	288.	.0337	35.	54.
		37.5	1198.	-	22.	25.
		35.0	1017.	.0033	16.5	25.
		32.5	1938. c	.00159		

Table IV - page 7

Code No.	Temp. °F	Stress, ksi	Test Duration-Hours	Min. creep Rate-%/hr.	At Rupture % Elong.	At Rupture % Red. Area
3-11	850	60.0	2.25	3.21	30.	71.
A533B1		55.0	18.6	.371	26.	69.
		52.5	21.	.423	29.	71.
		50.0	253.	.0326	31.	70.
		47.5	160.	.0358	30.	64.
		45.0	907.	.0034	31.	71.
		40.0	1000. c	.000679	-	-
	950	50.0	0.7	9.14	36.	74.
		45.0	7.0	.864	37.	78.
		40.0	54.	.1095	35.	76.
		35.0	188.	.0399	32.	61.
		30.0	657.	.0161	24.	38.
3-17	900	80.0	110.	-	33.	44.
A533A		70.0	265.	-	-	-
		60.0	905.	-	-	7.
	1000	57.0	15.	-	-	27.
		50.0	0.6	-	16.	66.
		45.0	10.7	-	21.	42.
		40.0	39.0	-	24.	42.
		33.5	53.	-	8.	-
		30.0	108.	-	-	10.
		25.0	271.	-	33.	21.
		20.0	740.	-	-	29.
	1100	20.0	23.3	-	-	41.
		15.0	103.	-	-	-
3-18a	900	80.0	14.	-	-	72.
A533B		70.0	186.	-	15.	21.
		60.0	283.	-	-	-
		50.0	535.	-	41.	11.
	1000	57.0	12.1	-	21.	35.
		50.0	19.2	-	19.	24.
		45.0	29.7	-	20.	22.
		40.0	27.5	-	38.	53.
		33.5	96.	-	23.	27.
		30.0	171.	-	14.	13.
		25.0	320.	-	27.	33.
		20.0	712.	-	-	29.
	1100	15.0	106.	-	70.	60.
Part 6 - Quenched and tempered carbon-manganese-molybdenum steel plate (A514 C)						
6-1	700	100.0	2.5	-	11.1	-
		95.0	650.	-	-	-
		92.0	717.	-	10.2	-
		90.0	526.	-	-	-
	800	90.0	5.3	-	-	-
		85.0	23.5	-	13.4	-

Table Va

Ratio of Elevated Temperature Yield Strength to
Room Temperature Yield Strength

Temp. °F	C-1/2 Mo	A302	A533	Combined A302-A533	A372,IV	A487,2N	A487,2Q	A514C
75	1.000	1.000	1.000	1.000	1.00	1.0	1.0	1.0
100	.988	.983	.990	.988	.990	.986	.990	.980
200	.940	.938	.951	.950	.947	.945	.959	.942
300	.902	.914	.923	.922	.917	.904	.925	.918
400	.870	.903	.903	.903	.902	.860	.890	.901
500	.845	.898	.887	.890	.896	.820	.860	.881
600	.818	.893	.870	.877	.886	.775	.859	.857
700	.788	.880	.848	.861	.862	.738	.858	.829
800	.749	.853	.817	.833	.815	-	-	.788
900	.698	.805	.770	.788	.746	-	-	.732
1000	.631	.729	.705	.718	.663	-	-	.654
1100	.545	.615	.617	.613		-		.549
1200	.435	.466	-	.463				
1300	.297							
1400	.140							

Table Vb

Ratio of Elevated Temperature Tensile Strength to
Room Temperature Tensile Strength

Temp. °F	C-1/2 Mo	A302	A533	Combined A302-A533	A372,IV	A487,2N	A487,2Q	A514C
75	1.000	1.000	1.000	1.000	1.00	1.0	1.00	1.00
100	.990	.981	.980	.983	.990	.980	.990	.990
200	.965	.928	.944	.937	.951	.930	.959	.970
300	1.035	.928	.935	.933	.939	.909	.935	.952
400	1.118	.948	.942	.946	.958	.902	.923	.942
500	1.125	.967	.947	.958	.986	.905	.928	.938
600	1.075	.966	.938	.952	.989	.909	.941	.922
700	1.010	.934	.908	.920	.939	.918	.968	.878
800	.935	.868	.850	.857	.828	-	-	.815
900	.840	.771	.764	.766	.686	-	-	.738
1000	.735	.653	.652	.653	.596	-	-	.650
1100	.590	.545	.518	.531				.545
1200	.440	.425		.417				-
1300	.295							
1400	.175							

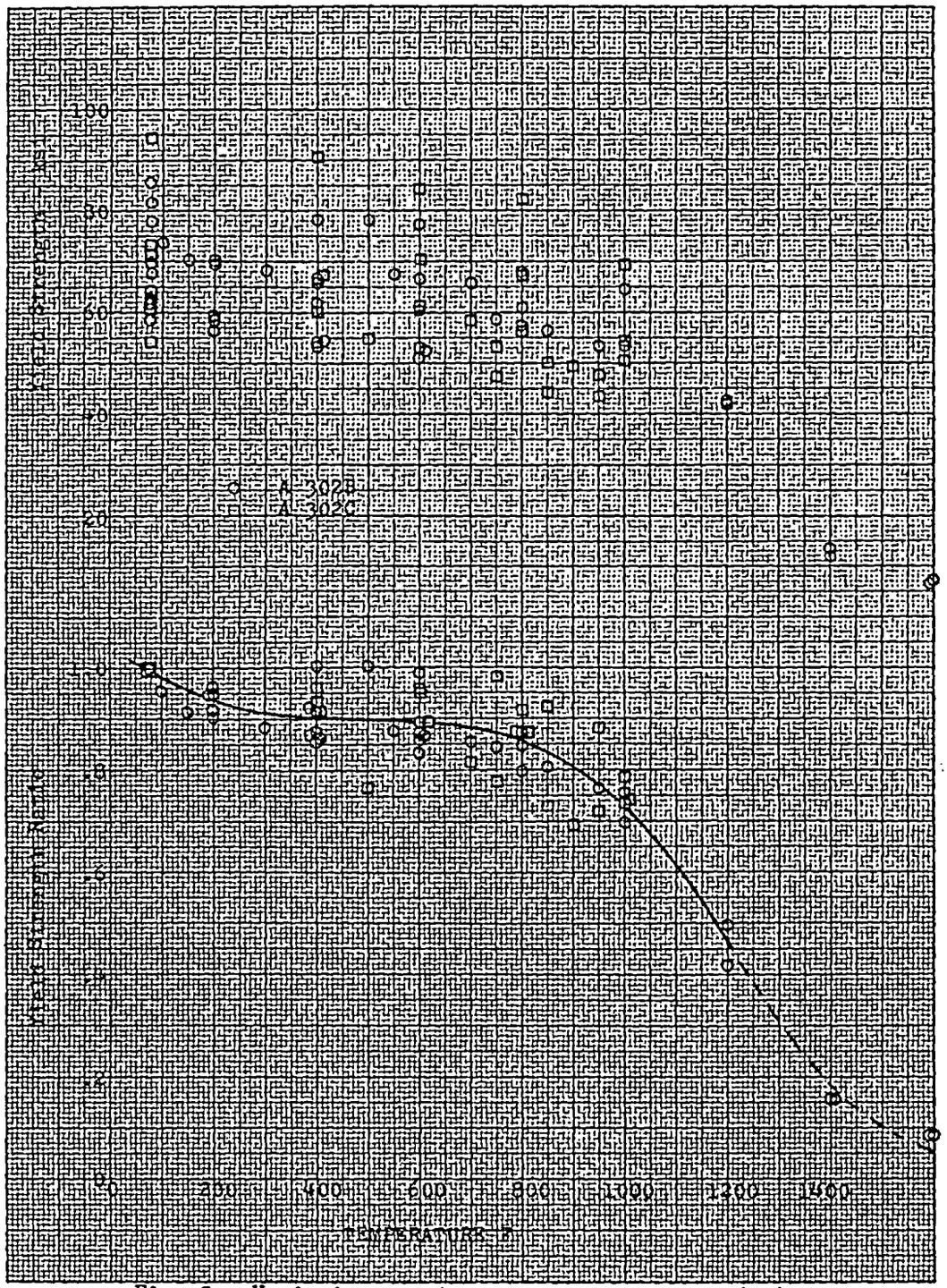

Fig. 8a Variation of yield strength of Mn-Mo-(Ni) steel, A 302, with temperature.

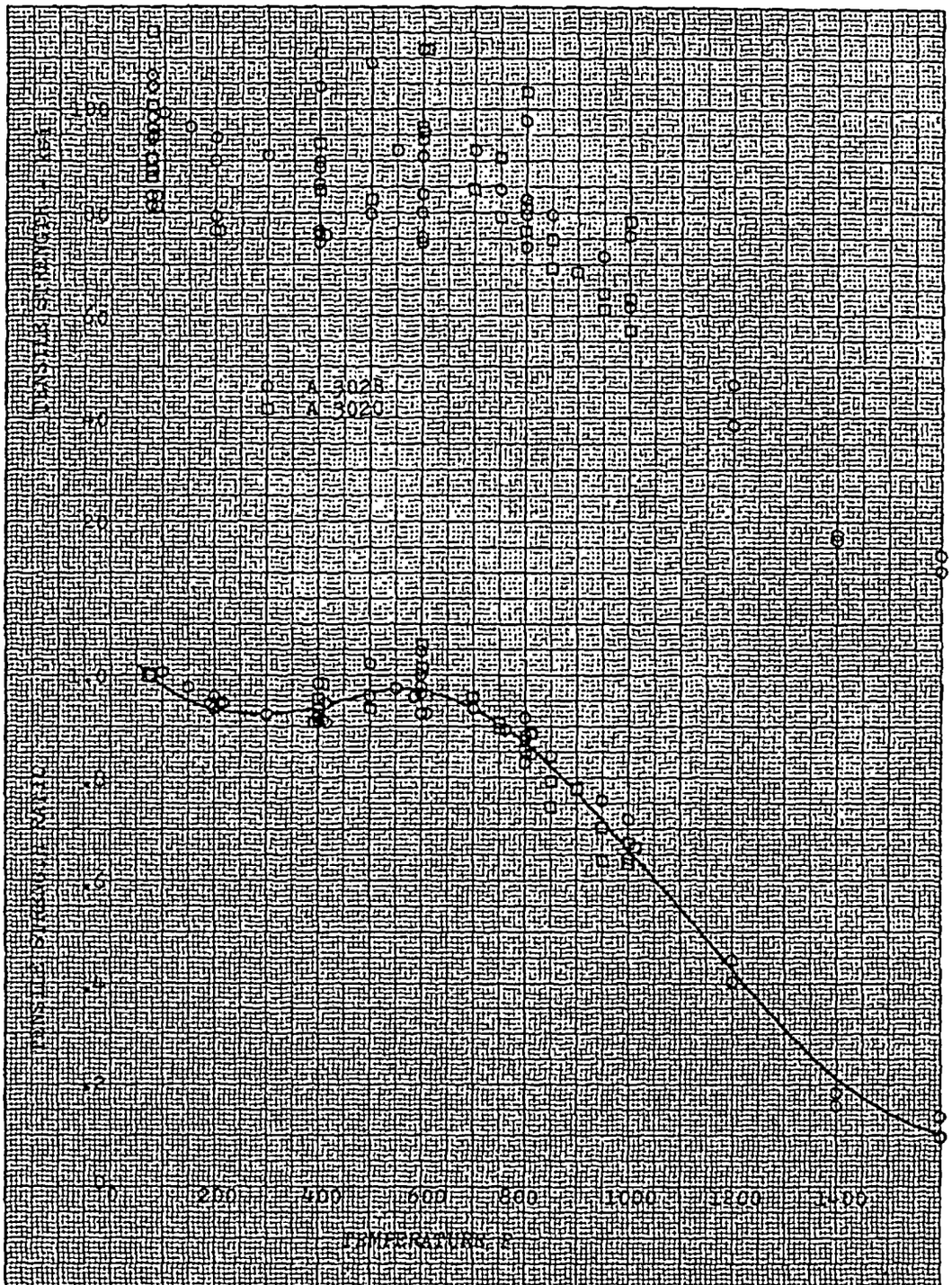

Fig. 8b Variation of tensile strength of Mn-Mo-(Ni) steel, A 302, with temperature.

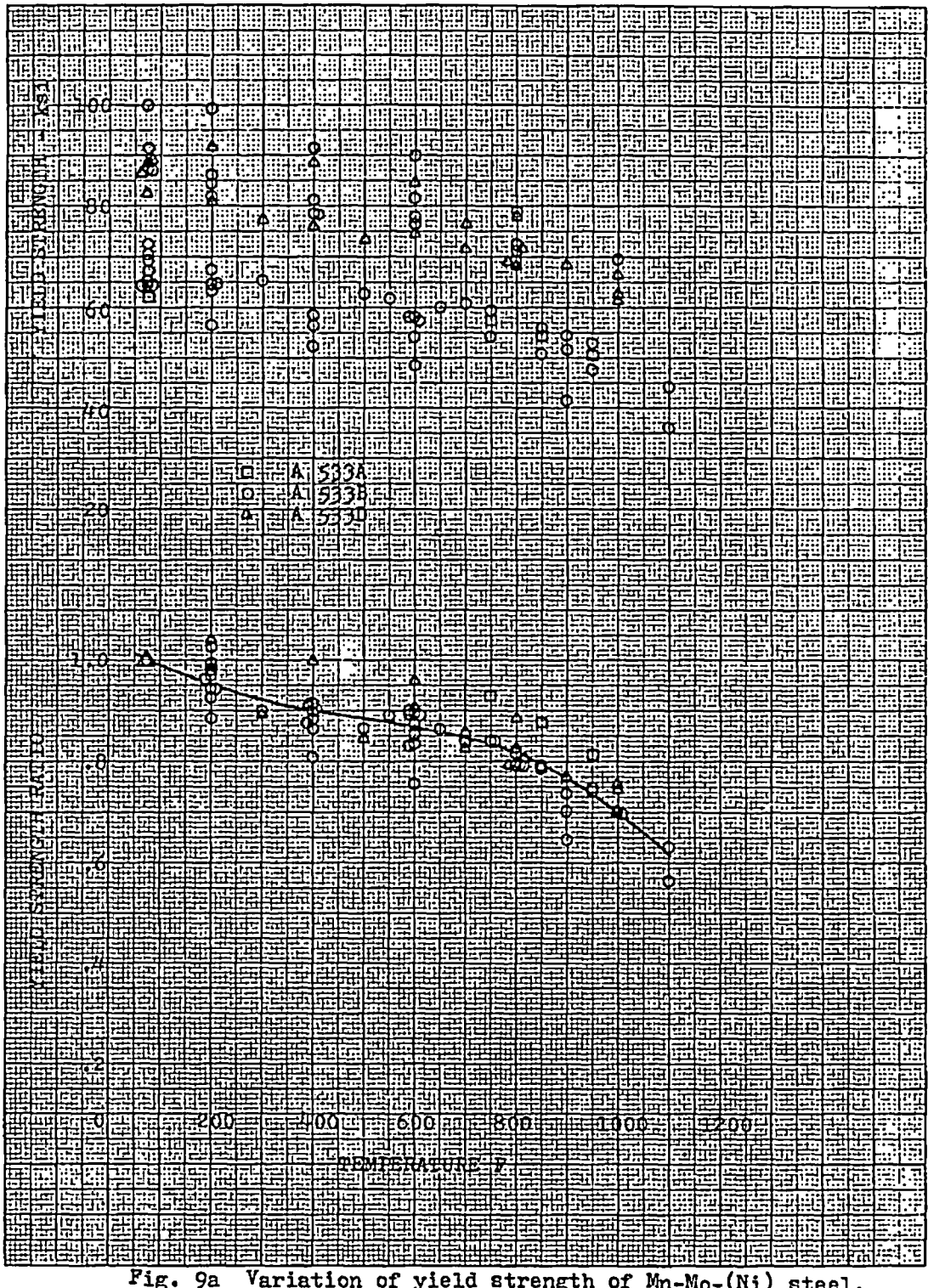

Fig. 9a Variation of yield strength of Mn-Mo-(Ni) steel, A 533, with temperature.

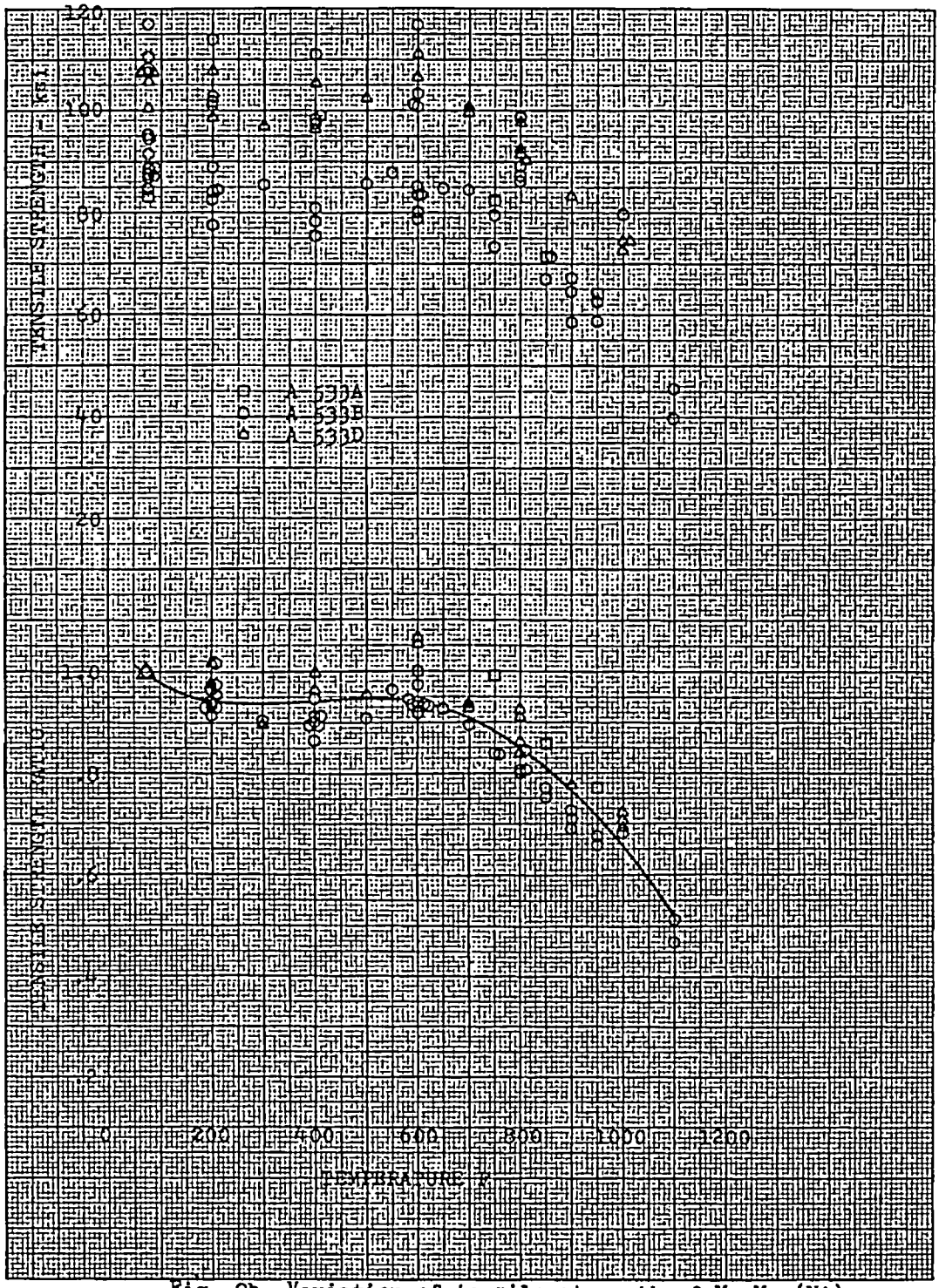

Fig. 9b Variation of tensile strength of Mn-Mo-(Ni) steel with temperature.

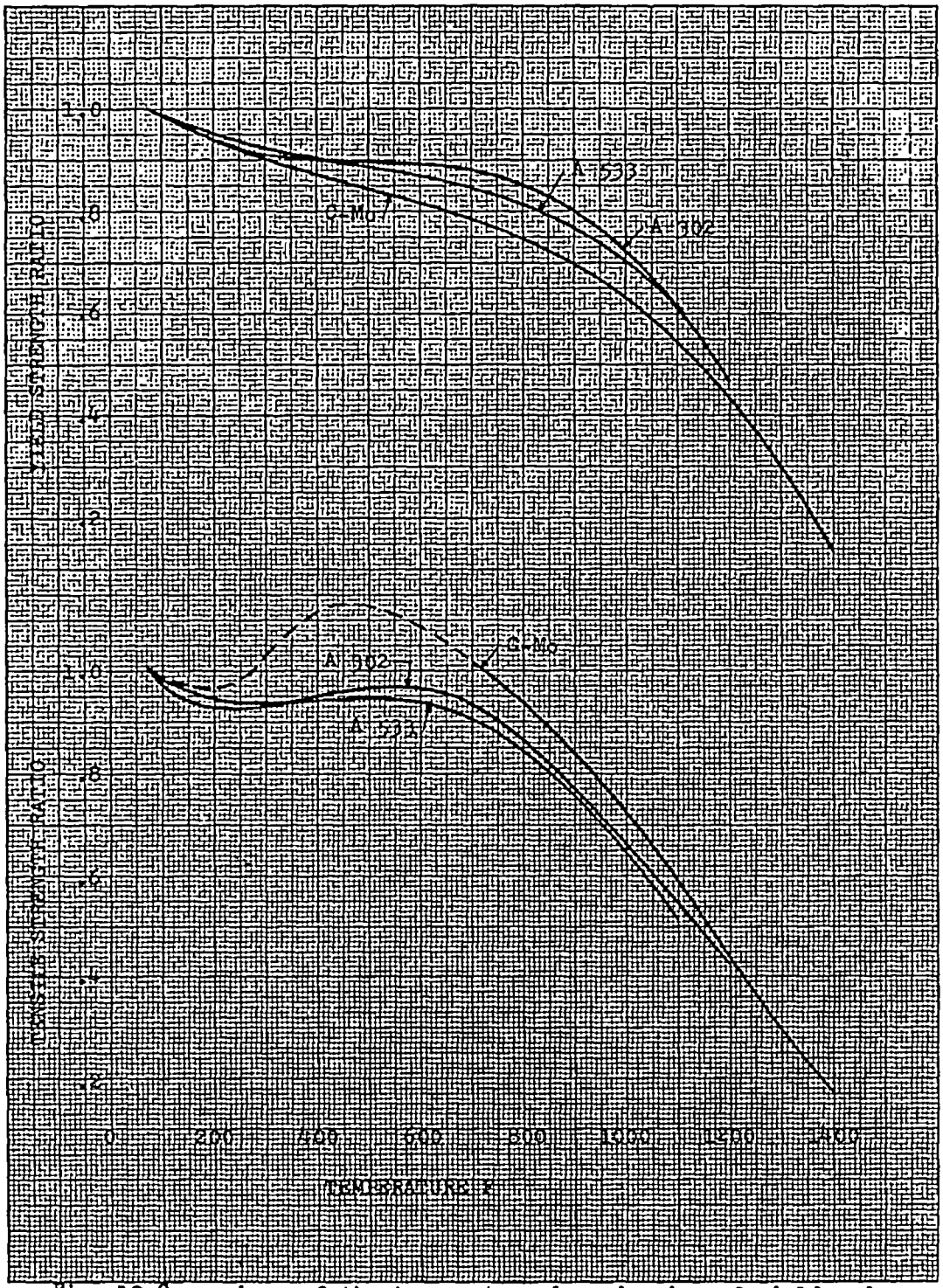

Fig. 13 Comparison of the temperature dependencies of yield and tensile strength ratios for C-Mo and Mn-Mo-(Ni), A 302 and A 533, steels.

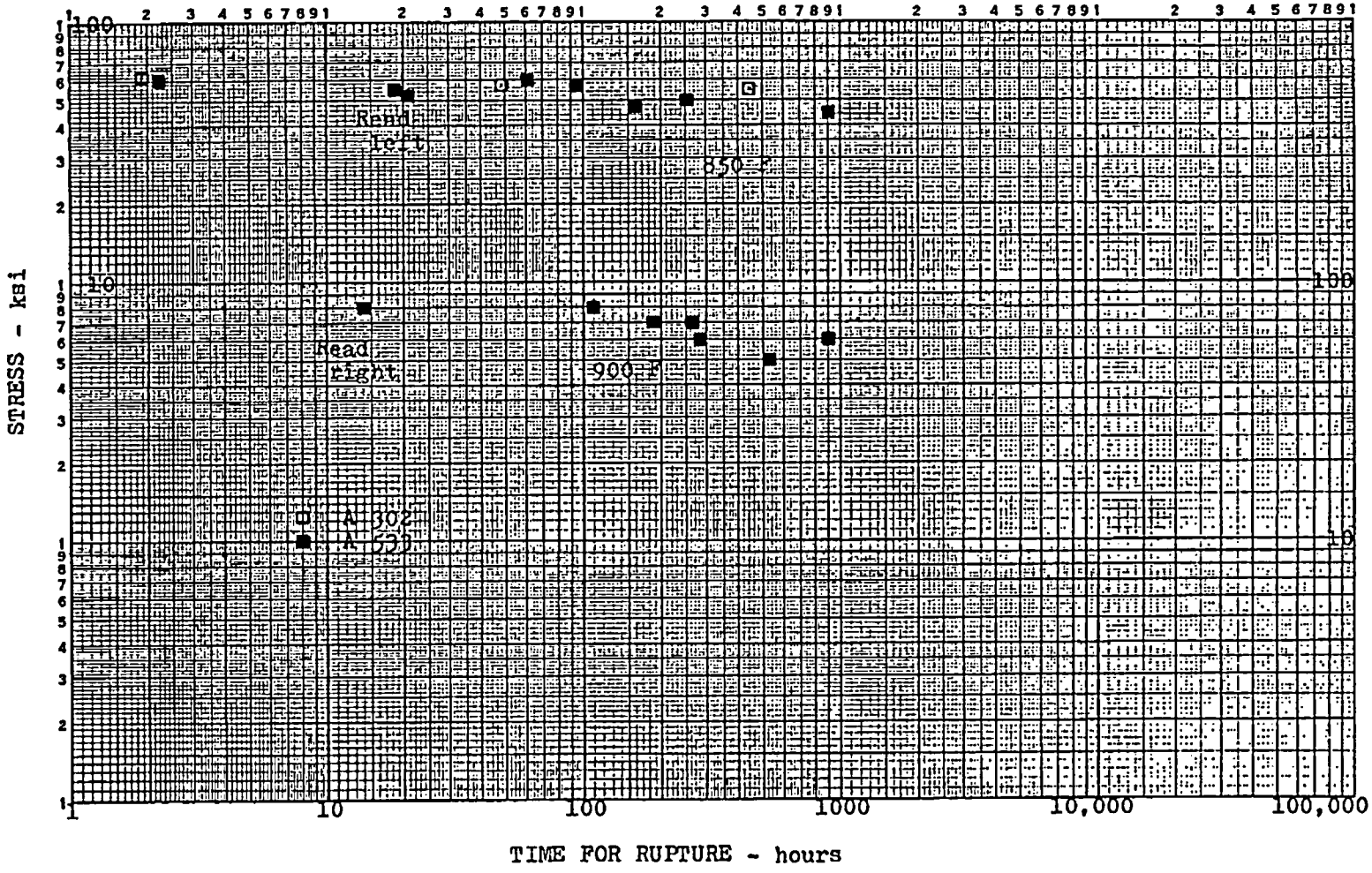

Fig. 21a Stress vs time for rupture of Mn-Mo steels.

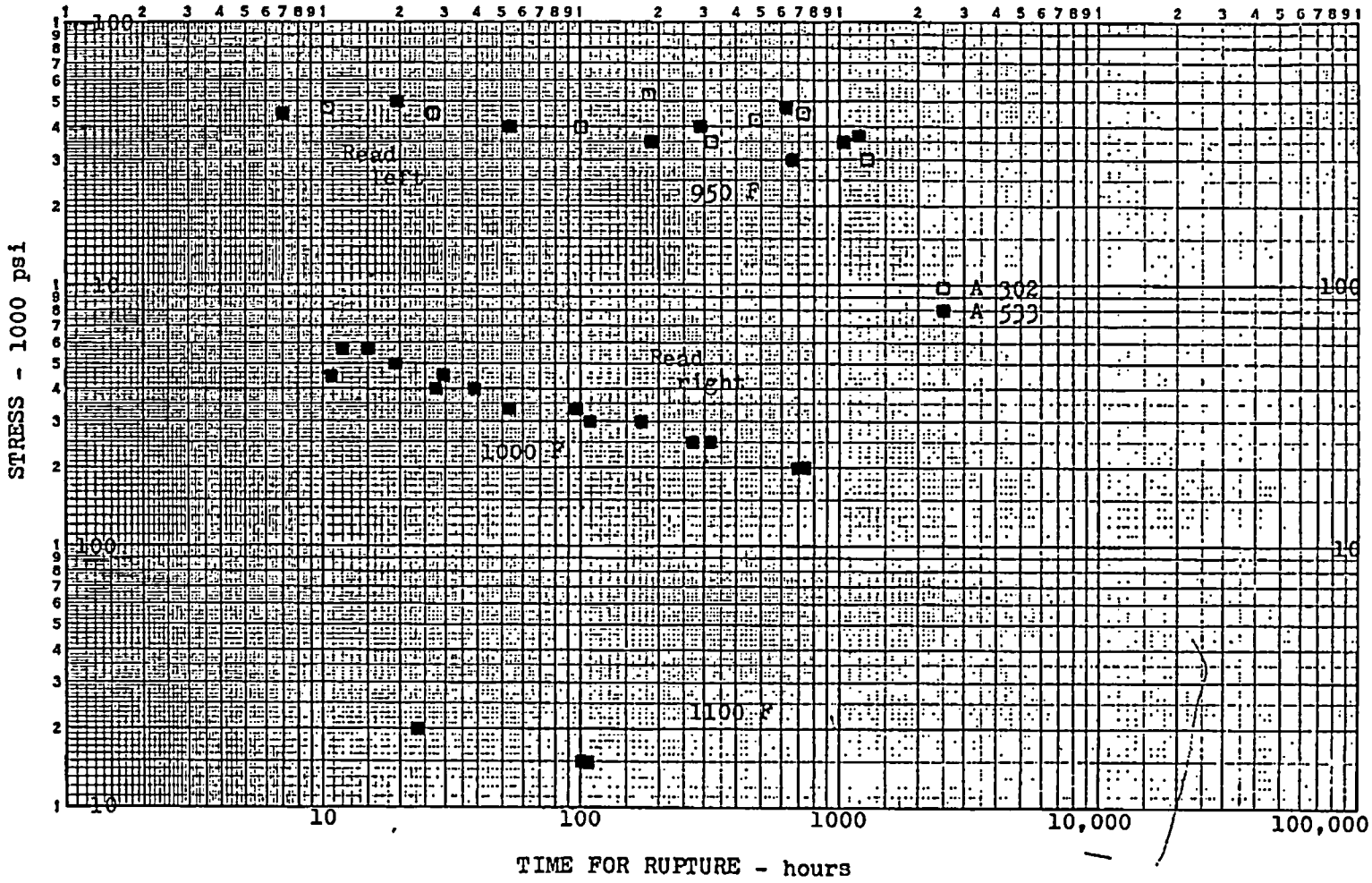

Fig. 21b Stress vs time for rupture of Mn-Mo steels.

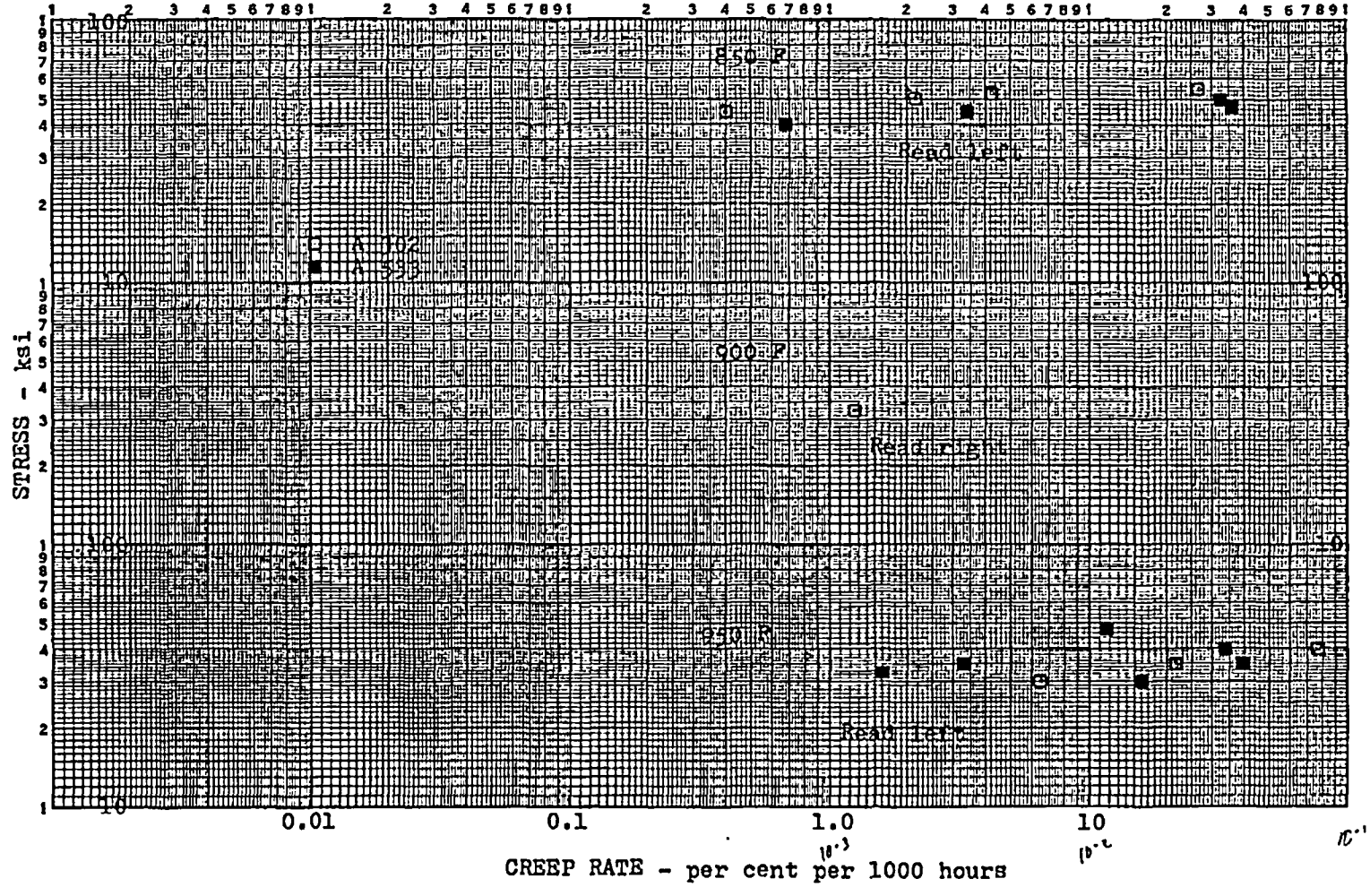

Fig. 22 Stress vs secondary creep rate of Mn-Mo steels.

2. ASTM Publication, "Symposium on Heat-Treated Steels for Elevated Temperature Service," September 1966; Article: "Characterization of Heat Treated Pressure Vessel Steels for Elevated Temperature Service."

SYMPOSIUM ON

HEAT-TREATED STEELS FOR ELEVATED TEMPERATURE SERVICE

TN
478
S85

SYMPOSIUM ON

HEAT-TREATED STEELS FOR ELEVATED TEMPERATURE SERVICE

SEPTEMBER 19-20, 1966
NEW ORLEANS, LOUISIANA

Held as Part of the
21ST ANNUAL PETROLEUM-MECHANICAL ENGINEERING CONFERENCE

Sponsored by
ASTM-ASME JOINT COMMITTEE ON EFFECT OF TEMPERATURE ON THE PROPERTIES OF METALS
and
METAL PROPERTIES COUNCIL OF THE ENGINEERING FOUNDATION

Edited by
M. SEMCHYSHEN
CLIMAX MOLYBDENUM COMPANY
ANN ARBOR, MICHIGAN

THE AMERICAN SOCIETY OF MECHANICAL ENGINEERS
United Engineering Center 345 East 47th Street New York, N. Y. 10017

Characterization of Heat Treated Pressure Vessel Steels for Elevated Temperature Service

A. W. PENSE and R. D. STOUT
Department of Metallurgy and Materials Science
Lehigh University
Bethlehem, Pennsylvania

Abstract

The extension of service conditions of pressure vessels to higher pressures and temperatures has stimulated consideration of steels capable of developing more useful combinations of such properties as strength, toughness, fatigue resistance, and creep-rupture strength. The Pressure Vessel Research Committee of the Welding Research Council has sponsored an extensive series of investigations at Lehigh University to assess the potential usefulness of quenched and tempered carbon and alloy steels in pressure vessels for elevated temperature service. The program included studies of stress-rupture properties, fatigue properties, tensile properties, and notch toughness. Eight pressure vessel steels, A212 Grade B, A387 Grade B, A517 Grades E and F, A533 Grades A and B, A 542 and A543 were included in the program and were studied in both the welded and unwelded condition.

The investigations showed that the steels could be placed into three groups on the basis of stress for rupture in 10,000 hours at 1000 F. As expected, the lowest strength was exhibited by the carbon steel, A212 Grade B. At an intermediate strength level were A533 Grades A and B, A517 Grade F and A543. In the highest strength group were A387 Grade B, A517 Grade E and A542. Using the same basis of comparison, i.e., 10,000 hour life at 1000 F, the steels could also be grouped on the basis of rupture ductility. The steel with the greatest ductility was the A212 Grade B steel. Materials with intermediate ductility were A542 and A517 Grade E. The A533 Grades A and B, A517 Grade F, A387 Grade B and A543 all had low rupture ductilities. This low ductility was associated with intergranular cracking during creep.

When welded, the rupture strengths of most of the steels were nearly comparable to their unwelded counterparts, although for three steels a slight loss in

rupture strength was observed and for one steel, A517 Grade F, a substantial loss was recorded. All of the alloy steels were susceptible to intergranular cracking in the coarse-grained heat-affected zone of the weld, while the carbon steel was free of this phenomenon.

Comparison of quenched and tempered and normalized and stress relieved steels revealed that below 800 F for the carbon steel and 950 F for the alloy steels, the quenched and tempered structure is superior to the normalized one for 10,000 hour life.

Studies of fatigue at elevated temperatures indicated that between 800 F and 1000 F, 100,000 cycle fatigue stresses were more limiting to service for the alloy steels than the stress for rupture in 100,000 hours. Above 1000 F, rupture stress became limiting for the alloy steels. For the carbon steel, rupture stresses were always limiting above 800 F. Below 800 F, one-quarter of the tensile strength was lower than either of these fatigue or stress rupture criteria for all the steels tested.

Exposure to elevated temperatures in the 500 F to 1200 F range without prior cold work did not significantly influence the notch toughness of the carbon steel, but the alloy steels had substantial losses in toughness after exposure to this temperature range. When strained prior to aging all of the steels tested had some toughness loss. The inherently good notch toughness of the alloy steels served to offset most of this loss.

Introduction

Service conditions for pressure vessels in the chemical and nuclear power industries have extended the application of the more familiar grades of steel to the practical limit of their capabilities. The high temperatures and operating pressures anticipated and even currently utilized for such vessels have resulted in increasingly heavy sections of the normalized grades of low-alloy steels. As a result, it becomes difficult to manufacture such heavy-walled vessels, and some of the concomitant properties normally considered essential to extended service, such as toughness, cannot easily be maintained.

Anticipating the increasing need for experimental data dealing with the elevated temperature properties of low-alloy high-strength steels, the Pressure Vessel Research Committee of the Welding Research Council in 1962 initiated a series of investigations at Lehigh University to explore the characteristics of low-alloy high-strength steels in the elevated temperature range. From the start of the investigation, it was determined that the greatest need was for a better understanding of the capabilities of quenched and tempered steels, particularly those with sufficient hardenability to respond favorably to heat treatment even in relatively heavy sections. Previous Pressure Vessel Research Committee investigations on quenched and tempered low-alloy steels had already established that favorable combinations of strength, toughness, high cycle fatigue resistance, and resistance to aging phenomena in the 500 F to 700 F range were possible in these steels, making them more attractive than their normalized counterparts in many cases.

The present PVRC studies, which are still continuing, have included investigations of the tensile properties, the fatigue properties and the stress-rupture properties at elevated temperatures of a variety of representative quenched and tempered

steels. The influence of section size and of fabrication operations such as welding were considered in the program, as well as properties such as ambient temperature strength and toughness that are complementary to properties at service temperatures. Special consideration has been given to alteration of low temperature properties due to elevated temperature exposure. As a part of this program, the tensile strength, fatigue strength and creep-rupture strength, particularly as they represent limiting stresses for design, have been investigated in the 700 F to 900°F range to determine over what temperature ranges each becomes limiting.

While a number of materials were included, the purpose of the PVRC program has not been to define the behavior of a given material but to develop the overall pattern of behavior that is typical of these materials. It is the characterization of the quenched and tempered steels that is the primary objective, with emphasis on the grouping of materials and generalizations about the kinds of mechanical properties at room and elevated temperature that are representative of this class of steels. In the presentation of the results of this work, therefore, emphasis will be placed on the general behavior of the quenched and tempered low-alloy high-strength steels and their suitability for elevated temperature service as a whole.

Review of Data

Materials and Heat Treatment

Most of the materials included in the original investigation are now covered by recent ASTM designations for quenched and tempered steels. The materials are listed by ASTM designation in Table I. Two of these steels, A212B, and A387B, which were studied in the quenched and tempered condition, are not yet covered in these compositions by ASTM quenched and tempered designations. The two steels in the A517 designation are more commonly known by their proprietary names "SSS-100" (Grade E) and "T-1" (Grade F). While the steels designated as A533, Grades A and B, fall within the chemistry limits for these grades, the room temperature mechanical properties of the specimens exceed the maximum tensile strength allowed by this specification. They are therefore A533 composition material only and this is so indicated when appropriate. The thicknesses of the plates tested and the heat treatment temperatures for the various steels are listed in Table I. The room temperature mechanical properties of the steels are listed in

Table I

Chemical Compositions, Heat Treatment Temperatures and Welding Electrodes

	C	Mn	P	S	Si	Ni	Cr	Mo	V	Ti	Cu	B	Aust. Temp.	Tempering Temp.	Welding Electr.
A212B	0.26	0.70	0.010	0.024	0.23	–	–	–	–	–	–	–	1650	1150	E7016
A533A	0.19	1.28	0.013	0.010	0.22	–	–	0.45	–	–	–	–	1650	1150	E10018
A533B	0.20	1.28	0.019	0.030	0.21	0.53	–	0.52	–	–	–	–	1650	1150	E10018
A387B	0.17	0.59	0.012	0.024	0.21	–	0.91	0.51	–	–	–	–	1675	1150	E11018
A542	0.11	0.37	0.010	0.010	0.26	–	2.20	0.96	–	–	–	–	1700	1150	E11018
A543	0.15	0.26	0.010	0.022	0.18	2.84	1.52	0.45	–	–	–	–	1700	1150	E11018
A517E	0.15	0.65	–	–	0.28	–	1.76	0.50	–	0.072	–	0.002	–	–	E11018
A517F	0.18	0.85	0.008	0.017	0.25	0.85	0.48	0.50	0.04	0.003	0.27	0.004	1700	1260	E11018

Welding done with a travel speed of 10 in. per minute, 200A, approx. 22V.

Table II. In most cas
thicknesses listed in
Figs. 16–20, are tak
in Fig. 16, some data

Steel	0.2 Yie
A212B	
A533B	
A387B	
A542	
A543	
A517E*	
A517F	

*Data courtesy of the Arm

Stress Rupture Data

Dead load stress r
in the program in both
these tests are shown
while the welded tests
this latter specimen t
deform together during
which are particularly
selected to produce fa
between 100 and 5000

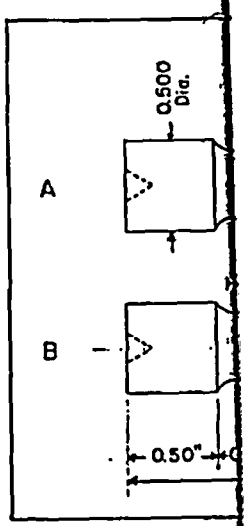

FIG

ns such as welding
mbient temperature
ervice tempera-
temperature proper-
gram, the tensile
/ as they repre-
700 F to 900 F
imiting.
: PVRC program
velop the over-
e characterization
e, with emphasis
of mechanical
ve of this class
re, emphasis will
low-alloy high-
vice as a whole.

e now covered by
e materials are
.2B, and A387B,
not yet covered
ions. The two
r proprietary
els designated as
grades, the room
naximum tensile
composition ma-
esses of the
steels are listed
eels are listed in

ding Electrodes

Aust. Temp.	Temper-ing Temp.	Weld-ing Electr.
1650	1150	E7016
1650	1150	E10018
1650	1150	E10018
1675	1150	E11018
1700	1150	E11018
1700	1150	E11018
2 —	—	E11018
1700	1260	E11018

Table II. In most cases, the data presented in this paper are for the steels and thicknesses listed in Table I. Some of the data, particularly those illustrated in Figs. 16–20, are taken from other heats of the same steel tested at Lehigh, and in Fig. 16, some data from the literature are included.

Table II

Room Temperature Mechanical Properties of the Quenched and Tempered Steels

Steel	0.2% Offset Yield Strength psi	Tensile Strength psi	Elongation in 1 in. %	Reduction of Area %
A212B	49,400	79,500	30.0	67.1
A533B	121,500	130,500	20.0	63.2
A387B	129,500	140,600	16.0	63.8
A542	119,000	137,000	25.0	70.4
A543	126,000	135,000	21.5	68.4
A517E*	107,500	117,800	19.5	68.9
A517F	119,000	131,000	19.5	63.2

*Data courtesy of the Armco Steel Company.

Stress Rupture Data

Dead load stress rupture tests were performed on the eight materials included in the program in both the unwelded and welded condition. The specimens used in these tests are shown in Fig. 1. The base plate test specimen is specimen A, while the welded tests were run on composite specimen B. It was the purpose of this latter specimen to force the base plate, weld metal and heat-affected zone to deform together during testing, thereby revealing those regions of the composite which are particularly sensitive to fracture initiation. Testing stresses were selected to produce failure in less than 10,000 hours with the majority of the data between 100 and 5000 hours [1], [2].

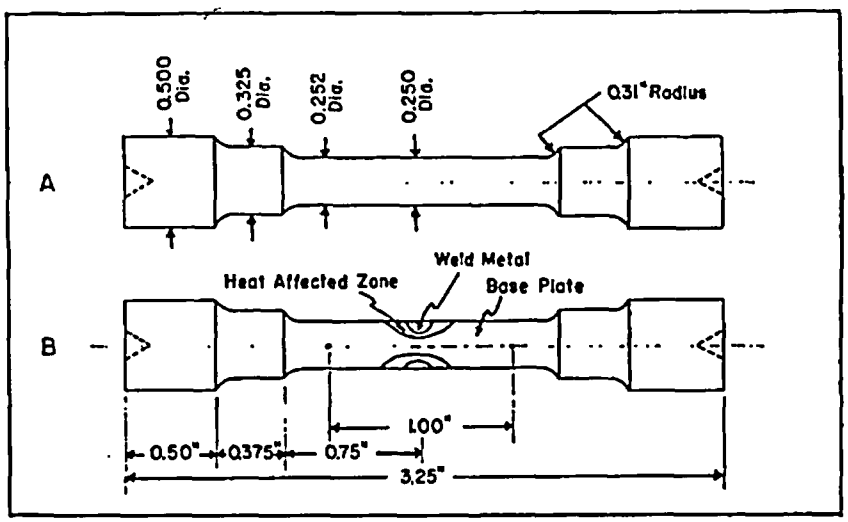

FIG. 1 – STRESS RUPTURE TEST SPECIMENS

A summary of these data for welded and unwelded specimens are found in Figs. 2–15. It should be noted that these figures include two kinds of information—the stress for rupture in 10, 100, 1000, 5000 and 10,000 hours, and the rupture ductility for these same time periods.

Base Plate Tests. The stress rupture data for the base plate specimens are presented in Figs. 2–8. For ease of comparison, selected rupture strength data taken from these curves are also listed in Table III. If we consider the rupture strength for 10,000 hour life at 1000 F, however, it is possible to classify the steels into three groups. In the lowest strength (5000 psi) category is the A212 Grade B steel. The next group, of intermediate strength (10,000–12,000 psi), contains four alloy steels including A533 Grades A and B, A517 Grade F and A543. The highest strength (20,000–23,000 psi) group includes three steels, A387 Grade B, A517 Grade E and A542. It may be observed that the intermediate strength group of steels consists of manganese-molybdenum (with or without nickel) and nickel-chromium molybdenum steels, while the highest strength group is primarily a chromium-molybdenum group. The material with the highest rupture strength of any tested in the program is the quenched and tempered 2¼ per cent chromium–1 per cent molybdenum steel (A542).

Although these groupings hold strictly only for 10,000 hour life at 1000 F, Table III indicates that much the same relationship between the steels continues to hold at lower temperatures and shorter times. The A542 and A517 Grade F are, however, proportionately somewhat higher in strength at lower temperatures and shorter times than indicated above.

Table III

Rupture Stresses for the Quenched and Tempered Steels

	Stress to Rupture (psi) in 1000 hr. at, °F				Stress to Rupture (psi) in 10,000 hr. at, °F			
	800	900	1000	1100	800	900	1000	1100
A212B	30,000	17,000	8,500	–	23,000	11,000	5,000	–
A533A	–	60,000	19,000	10,000	–	43,000	11,000	–
A533B	–	55,000	20,000	10,000	–	40,000	11,000	–
A387B	–	77,000	35,000	13,000	–	62,000	20,000	7,500
A542	–	88,000	41,000	15,000	–	75,000	23,000	8,000
A543	85,000	55,000	23,000	11,000	–	–	12,000	6,000
A517E*	82,000	60,000	35,000	16,000	79,000	48,000	20,000	10,000
A517F	89,000	74,000	32,000	8,500	85,000	52,000	13,000	4,000

*Data courtesy of the Armco Steel Company

Although the rupture strength of the steels appears to be of primary importance for service, rupture ductility may also be of interest. Reference to Figs. 2–7 reveals that the steels would be grouped in quite a different order on the basis of reduction of area at failure. The carbon steel A212 Grade B, has the best rupture ductility of any steel tested, always exhibiting reductions of area of 60 per cent or greater, a characteristic not observed with any of the alloy steels. The alloy steels can be divided into two groups on the basis of ductility. In the first group, ductility at failure decreases regularly as time for rupture increases, particularly in the 900 F to 1100 F range. However, up to 10,000 hours, the ductility remains

above 40 per cent re
Grade E and A542. I
drops below 40 per c
ing are A387 Grade E
be noted that the ste
those with the lowe
level have the lowe

Metallographic ex
has revealed that th
prior austenite grain
the lowest ductilitie
fracture, while exte
the test gage length
cluding microprobe
cracking.

Welded Composit
of the same steels
were welded withou
in Table I. The spe
in shallow grooves
mens transverse to

When comparing
noted that the same
the base plate tests
A533 Grades A and
or slightly greater i
Grade B and A543,
from welding and te
about the same mag
sensitive to weldin
the 800 F to 1000 F
rupture times longe

As Figs. 9–15
of A212 Grade B, h
times were increas
both in the weld me
rupture cracking di
was the coarse gra
a common characte
strongest in those
in the base plate t
steels the fracture
zone. The stress r
toe of the weld an
with final fracture
affected zone regi
appears that the te
intensified in the

above 40 per cent reduction of area. The two steels in this category are A517 Grade E and A542. In the second alloy steel group, the fracture reduction of area drops below 40 per cent, and in some cases well below 20 per cent. In this grouping are A387 Grade B, A517 Grade F, A533 Grades A and B and A543. It should be noted that the steels with the highest stress-rupture strength are not necessarily those with the lowest rupture ductility, but that the steels of intermediate strength level have the lowest ductilities.

Metallographic examination of specimens failing with low rupture ductilities has revealed that this phenomena is associated with intergranular cracking along prior austenite grains in the quenched and tempered structure. In specimens with the lowest ductilities, little if any plastic flow appears to be associated with the fracture, while extensive grain boundary sliding and cracking is evident throughout the test gage length. Extensive studies using light and electron microscopy, including microprobe analysis, did not reveal any specific cause for intergranular cracking.

Welded Composite Tests. The results of tests on welded composite specimens of the same steels shown in Figs. 2–8 are presented in Figs. 9–15. The steels were welded without preheat using the electrodes and welding parameters indicated in Table I. The specimen used, (Fig. 1B) was obtained by depositing weld metal in shallow grooves on opposite sides of the base plate and cutting out the specimens transverse to the weld beads.

When comparing the base plate and weld composite specimen results, it may be noted that the same general grouping of steels on the basis of rupture strength for the base plate tests is followed by the welded specimen tests. For four steels, A533 Grades A and B, A542 and A387 Grade B, the weld composite was equal to or slightly greater in rupture strength than the base plate. For two steels, A212 Grade B and A543, approximately 15 per cent reduction in rupture strength resulted from welding and testing at 900 F; while for A517 Grade E, a loss in strength of about the same magnitude occurred in the 1000 F to 1100 range. The material most sensitive to welding in terms of decreased rupture strength was A517 Grade F. In the 800 F to 1000 F range, rupture strengths were reduced by 30 – 40 per cent for rupture times longer than 100 hours in the welded condition.

As Figs. 9–15 indicate, failures in the welded specimens, with the exception of A212 Grade B, had an increasing tendency to occur in the weld zone as rupture times were increased. The term "weld zone" in these figures includes failures both in the weld metal and the heat-affected zone. In some of the steels, stress rupture cracking did occur in the weld metal, but the most common site of fracture was the coarse grained region of the heat-affected zone. While this appears to be a common characteristic of all the alloy steels tested, the tendency appears to be strongest in those steels that were the most susceptible to low ductility fracture in the base plate tests, (for example, A543 and A517 Grade F). In many of these steels the fracture was almost exclusively in the coarse grained heat-affected zone. The stress rupture cracks usually initiate at the specimen surface at the toe of the weld and progress along the heat-affected zone under the weld metal, with final fracture occurring through the base plate separating the two heat-affected zone regions. The fracture was along prior austenite grain boundaries. It appears that the tendency for intergranular cracking observed in the base plate is intensified in the microstructure in the coarse grained heat-affected zone.

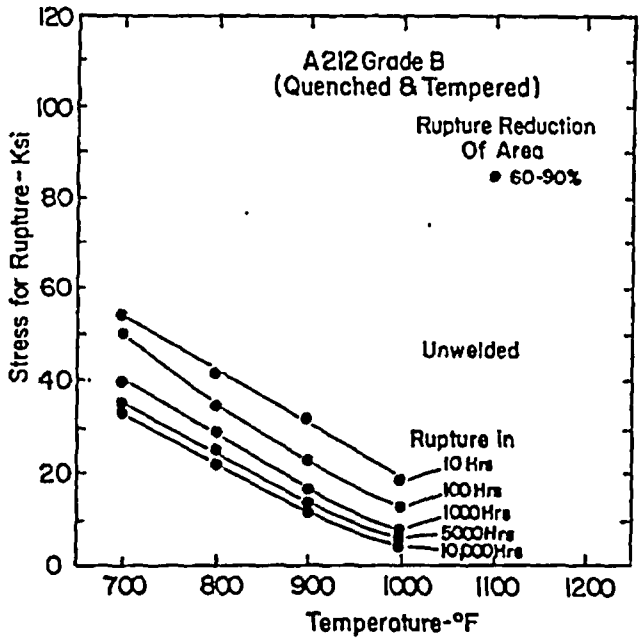

FIG. 2 – STRESS RUPTURE SUMMARY CURVE FOR A212 GRADE B, QUENCHED AND TEMPERED

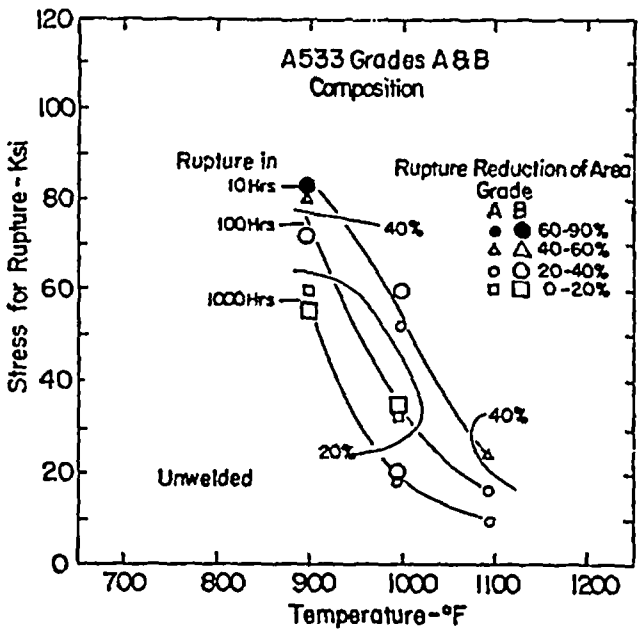

FIG. 3 – STRESS RUPTURE SUMMARY CURVE FOR A533 GRADES A AND B

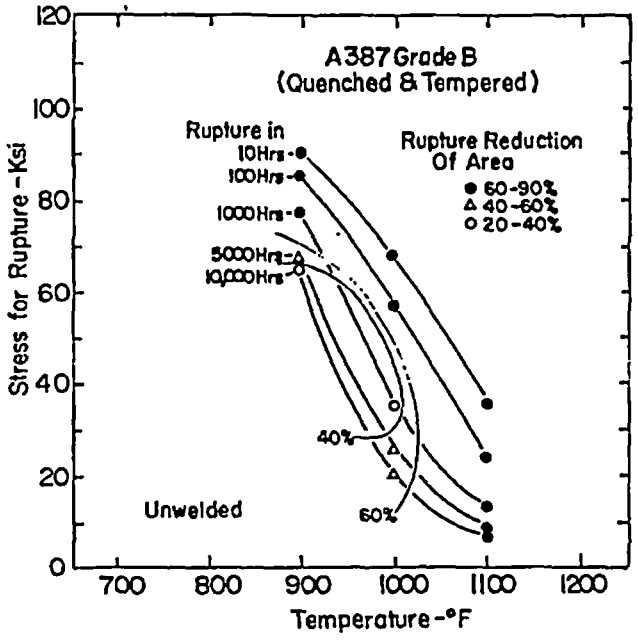

FIG. 4 – STRESS RUPTURE SUMMARY CURVE FOR A387 GRADE B, QUENCHED AND TEMPERED

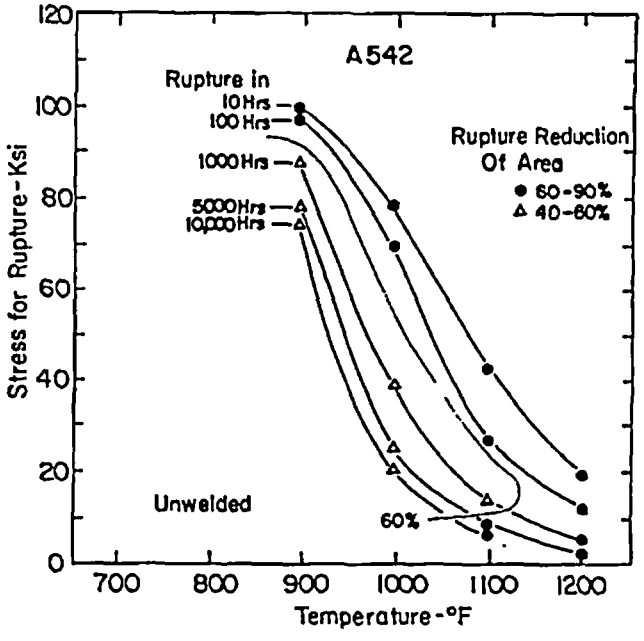

FIG. 5 – STRESS RUPTURE SUMMARY CURVE FOR A542

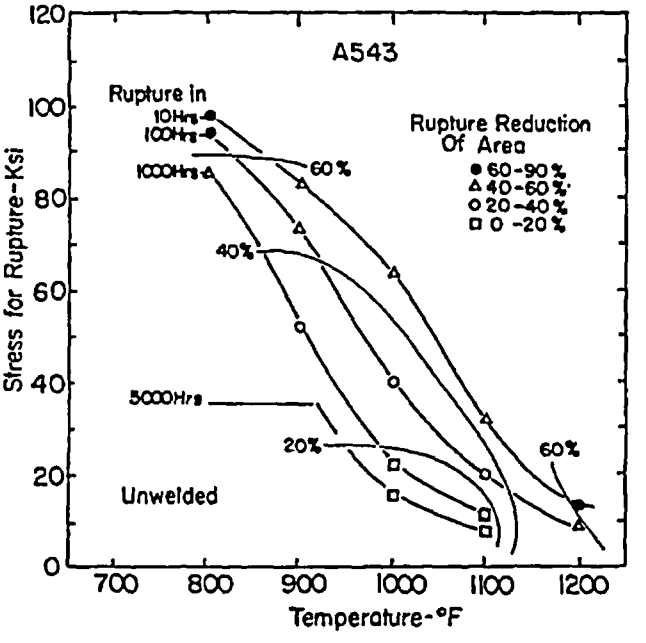

FIG. 6 – STRESS RUPTURE SUMMARY CURVE FOR A543

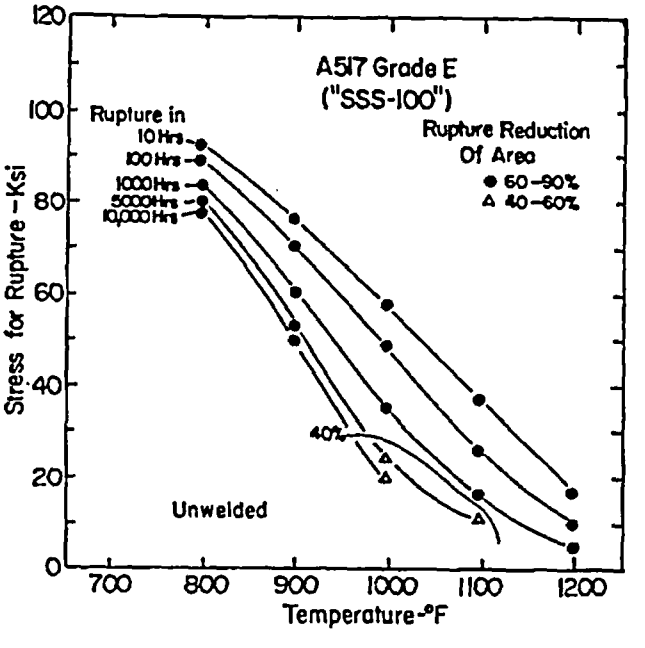

FIG. 7 – STRESS RUPTURE SUMMARY CURVE FOR A517 GRADE E

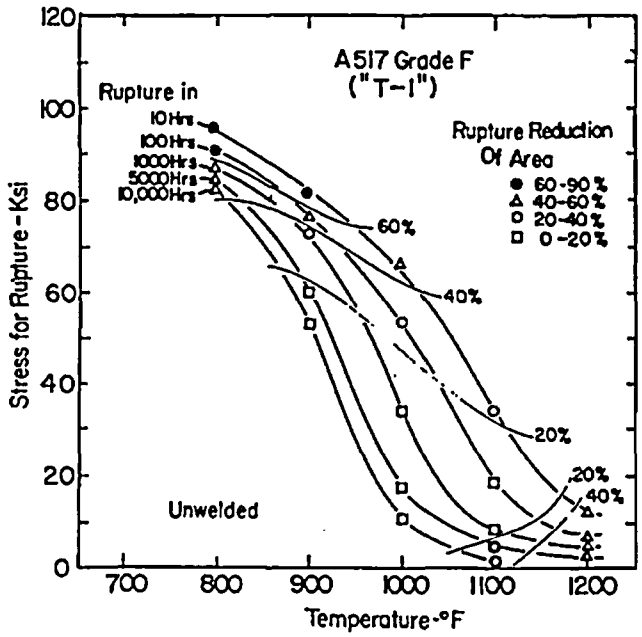

FIG. 8 – STRESS RUPTURE SUMMARY CURVE FOR A517 GRADE F

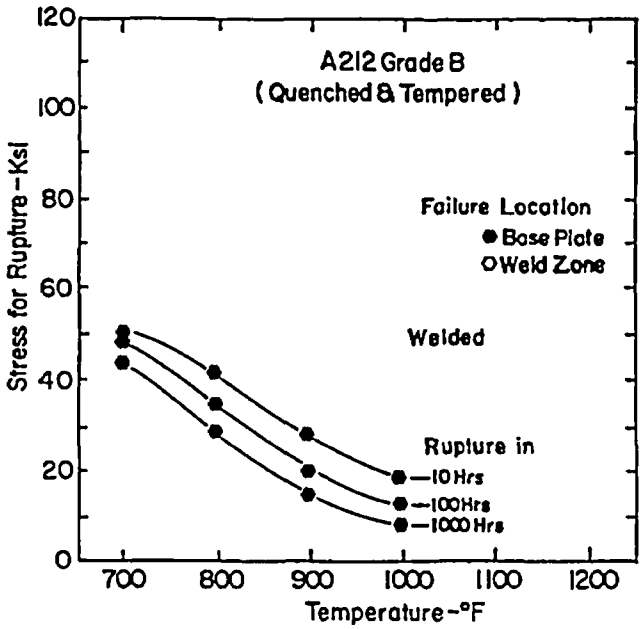

FIG. 9 – STRESS RUPTURE SUMMARY CURVE FOR WELDED A212 GRADE B QUENCHED AND TEMPERED

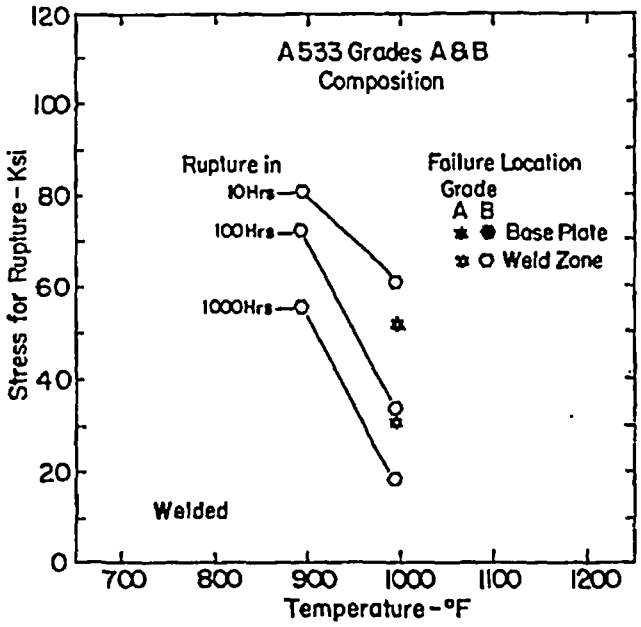

FIG. 10 – STRESS RUPTURE SUMMARY CURVE FOR WELDED A533 GRADES A AND B

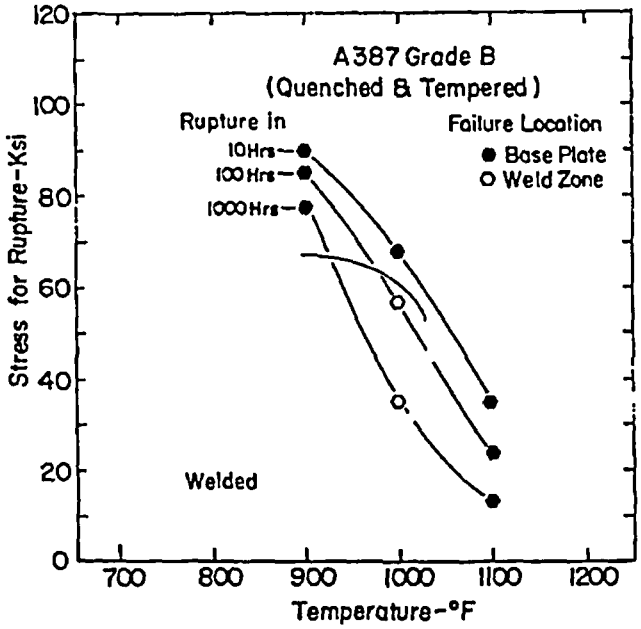

FIG. 11 – STRESS RUPTURE SUMMARY CURVE FOR WELDED A387 GRADE B QUENCHED AND TEMPERED

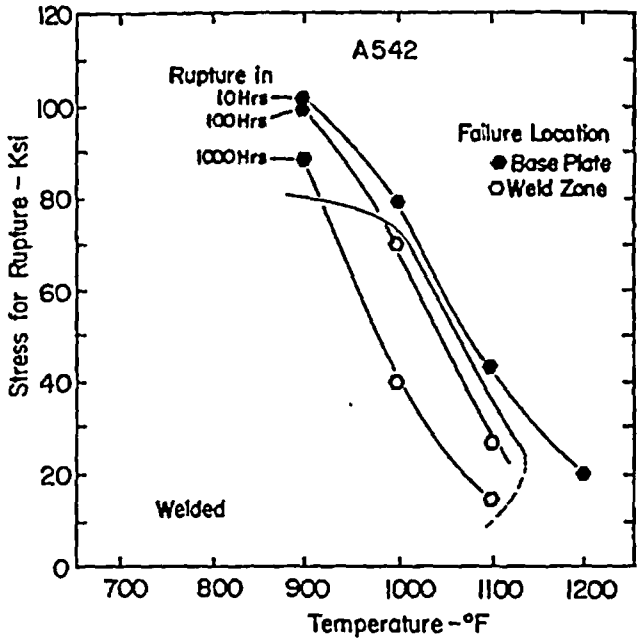

FIG. 12 – STRESS RUPTURE SUMMARY CURVE FOR WELDED A542

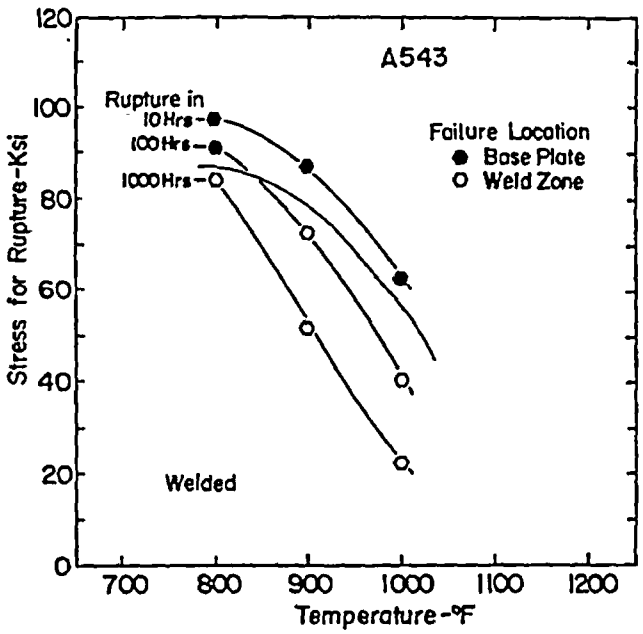

FIG. 13 – STRESS RUPTURE SUMMARY CURVE FOR WELDED A543

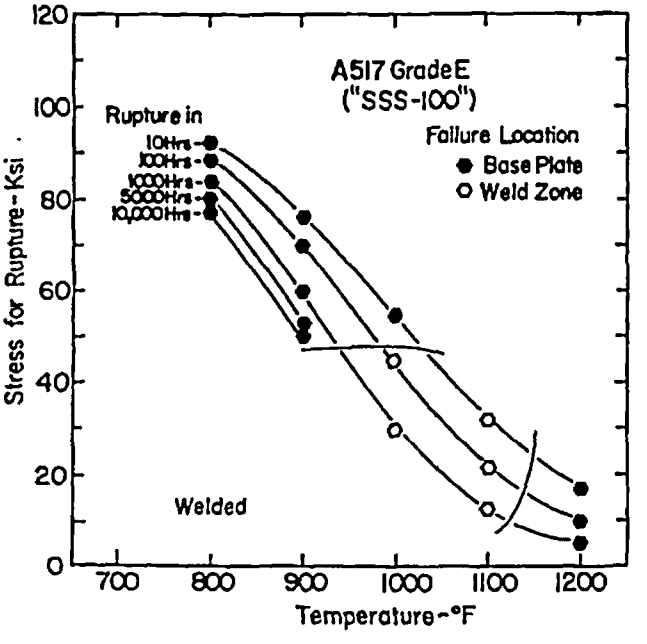

FIG. 14 – STRESS RUPTURE SUMMARY CURVE FOR WELDED A517 GRADE E

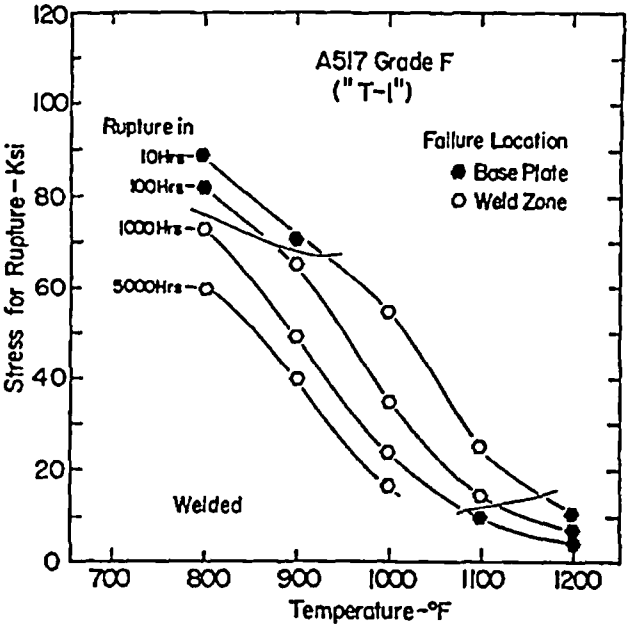

FIG. 15 – STRESS RUPTURE SUMMARY CURVE FOR WELDED A517 GRADE F

Although the r
have a bearing on
Lehigh University
weld zone crackin
thermal stress rel
current tests on r
relief that are ide
tests [2]. The ste
have the lowest r
tendency for heat-

Influence of Micro

Although quenc
normalized and st
strength and notch
tempered microstr
temperature range
normalized structu
elsewhere for carb
the temperature ra
depends on compo
Figs. 16 and 17. C
quenched and temp
and stress relieve

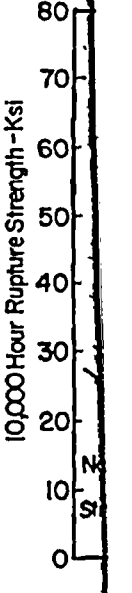

FIG.

Although the results of these tests are of significance to service, they also have a bearing on the heat treatment of these steels. Tests presently underway at Lehigh University appear to indicate that the steels which have a tendency for weld zone cracking may also be susceptible to heat-affected zone cracking during thermal stress relief. Such cracking has been reported in the literature [3], and current tests on restrained weldments have produced cracks during thermal stress relief that are identical in appearance to those produced in the stress-rupture tests [2]. The steels most susceptible to this phenomena appear to be those that have the lowest rupture ductilities in the base plate tests and have the greatest tendency for heat-affected zone failure in the welded composite tests.

Influence of Microstructure

Although quenched and tempered steels have a significant advantage over normalized and stress relieved steels from the standpoint of yield strength, tensile strength and notch toughness, it has been accepted that the quenched and tempered microstructure will be subject to spheroidization in the creep-rupture temperature range and therefore may be inferior in rupture strength to the coarser normalized structure. Comparison of stress-rupture data obtained at Lehigh and elsewhere for carbon and alloy steels has confirmed this general conclusion, but the temperature range over which the normalized microstructure is advantageous depends on composition. A comparison of this type for four steels is seen in Figs. 16 and 17. On the basis of 10,000 hour life, these figures show that the quenched and tempered microstructure does hold advantage over the normalized and stress relieved one up to 800 F for the A212 Grade B, up to 950 F for the

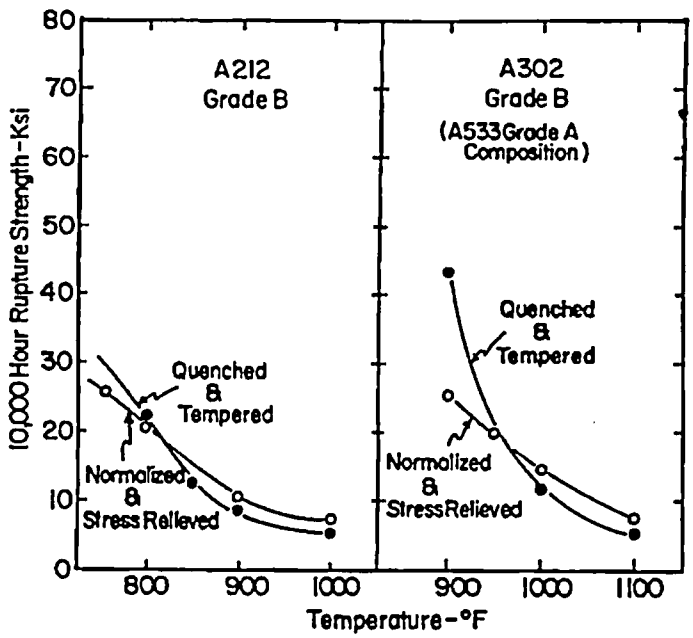

FIG. 16 – THE INFLUENCE OF MICROSTRUCTURE ON STRESS FOR RUPTURE IN 10,000 HOURS ON A212 GRADE B AND A302 GRADE B

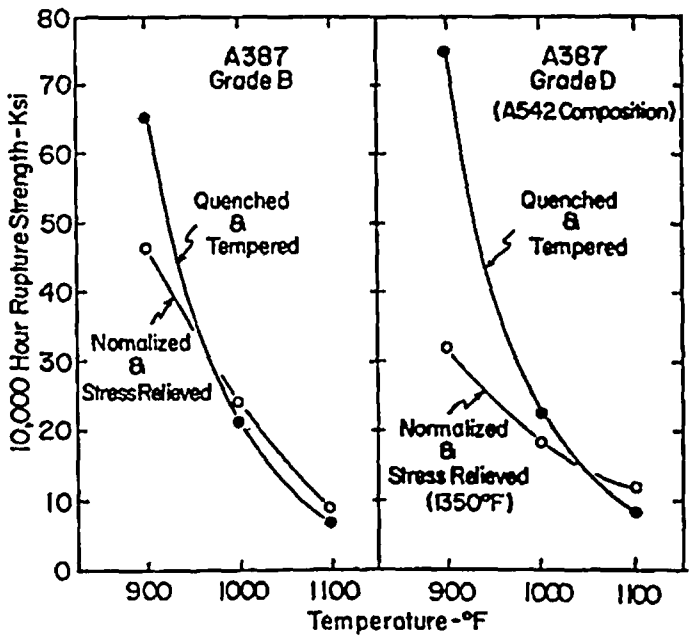

FIG. 17 – THE INFLUENCE OF MICROSTRUCTURE ON STRESS FOR RUPTURE IN 10,000 HOURS ON A387 GRADES B AND D

A302 Grade B (A533 Grade A composition) and for the A387 Grade B. The stress relief temperature (following normalizing treatment) in these cases is 1150 F. For the A387 Grade D (A542 composition) the stress relief temperature is one specifically selected to produce structural stability (1350 F), while the tempering temperature for the quenched steel is more typical of that used to produce high room temperature strength and satisfactory toughness (1150 F). Under these conditions of heat treatment the quenched and tempered structure is superior up to 1050 F.

Elevated Temperature Fatigue Data

While stress-rupture properties are of primary consideration in pressure vessel service above some threshold temperature, presumably greater than 650 F, it is of interest to know what role fatigue plays in this threshold range, and where the threshold temperature for creep-rupture may be expected to fall. Fig. 18 is a compilation of data that delineates some of these relationships in the threshold range, i.e., between 700 F and 1100 F. The one-quarter tensile strength curves and extrapolated stress-rupture curves (extrapolated one cycle on the conventional log stress-log rupture time curve) are derived from the current PVRC program. The fatigue curve is derived from a companion PVRC study using fully reversed cantilever bending specimens on the same quenched and tempered steels studied in the stress-rupture investigation [4]. These tests were conducted at 1100 cycles per hour and were strain controlled. The safety factor of four applied to this curve is a result of full scale pressure vessel tests sponsored by PVRC at Southwest Research Institute. The fatigue strength reduction factor for 100,000 cycle life based on vessel membrane strain in these full scale vessels as compared to

strain in Lehigh tests on the same material, was about four [5]. The curves shown in Fig. 18 suggest that fatigue failure should not be a serious problem in design with the carbon steel, but that for the two alloy steels this type of failure is a distinct possibility in preference to either tensile or stress-rupture failure if fatigue conditions are encountered in service. Some vessel applications involve cyclic operations applying fatigue cycles at slow rates in the elevated temperature range. Hence, in service lives that extend for a number of years, 100,000 cycle fatigue life and 100,000 hour rupture strength may both be of significance. In the temperature range between 800 F and 1000 F the stress for fatigue failure becomes more limiting from the design standpoint than the stress for rupture. Below 800 F, the quarter-tensile-strength at temperature criterion becomes limiting for design, while above 1000 F, stress rupture becomes the most important consideration. For the carbon steel, design below 850 F appears to be limited by one quarter of the tensile strength at temperature while above this temperature, stress rupture is limiting. Current studies on elevated temperature fatigue have been concerned with the influence of welding on this fatigue behavior. The results obtained thus far indicate that the fatigue resistance of the alloy steels is not impaired by the presence of weld metal or heat-affected zone structures in the specimen.

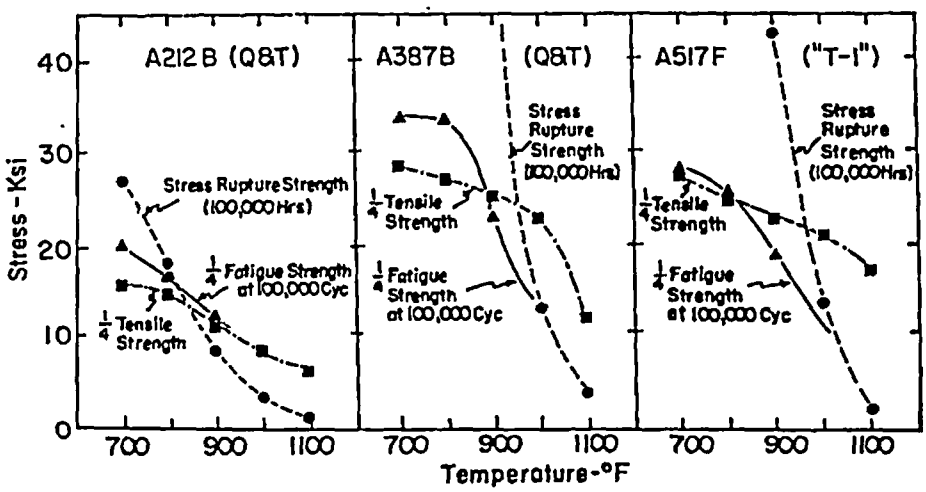

FIG. 18 – THE RELATIONSHIP BETWEEN TENSILE, STRESS-RUPTURE AND FATIGUE CRITERIA FOR QUENCHED AND TEMPERED A212 GRADE B, A387 GRADE B, AND A517 GRADE F

Elevated Temperature Exposure Data

All of the mechanical properties discussed thus far—tensile strength, stress-rupture strength and fatigue strength—are directly related to the behavior of the steels at the service temperature. One property not directly related to elevated temperature service but still of importance under certain conditions of fabrication and operation is notch toughness. Quenched and tempered steels are advantageous for pressure vessel service not only because of the improved yield and tensile strength, but also because of the decided improvement in notch toughness that

they provide. Even in relatively heavy section sizes, it has been shown [6] that adequate toughness can be maintained in quenched and tempered steels. Exposure to elevated temperatures, either with or without prior cold work, can lead to marked reductions in toughness. Figs. 19 and 20 illustrate the losses of toughness that have been found to occur. In Fig. 19, the toughness loss due to long-time exposure is illustrated for both light and heavy sections of four quenched and tempered steels, while in Fig. 20, the effect of short-time exposure to elevated temperatures after 5 per cent cold forming is illustrated. In these figures the term "light section" refers to a quenched and tempered plate approximately 1 in. in thickness, while "heavy section" refers to a plate approximately 12 in. in thickness. It should be observed that in the non-prestrained condition, the carbon steel A212 Grade B was not sensitive to toughness losses by exposure to the 500 F to 1150 F range. On the other hand, the initial transition temperature of this material was high compared to the alloy steels. When strain aged the embrittlement of the A212 Grade B is more substantial. In the unstrained condition, Fig. 19, the A533 Grade A material was also relatively insensitive to toughness losses up to 1150 F, where some loss is observed. The sensitivity of this material to aging phenomena after cold work is evident in Fig. 20. The most sensitivity to aging is found in the more complex alloy steels such as A543 and A517 Grade F. These materials show substantial toughness losses due to exposure either with or without prior cold work. The initial excellent toughness of these materials, however, serves to compensate to a large extent for these losses during exposure, rendering them superior to the carbon steel under most conditions of service.

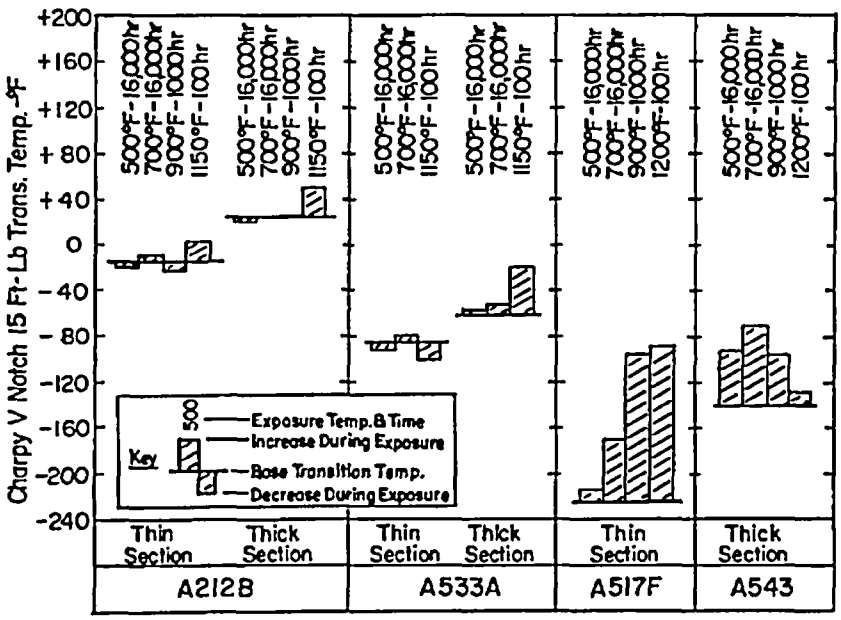

FIG. 19 – THE INFLUENCE OF ELEVATED TEMPERATURE EXPOSURE ON THE TOUGHNESS OF A212 GRADE B, A533 GRADE A, A517 GRADE F AND A543

ıas been shown [6] that
empered steels. Exposure
d work, can lead to
te the losses of tough-
ıness loss due to long-
:ions of four quenched
:-time exposure to ele-
rated. In these figures
:ed plate approximately
ıte approximately 12 in.
:ained condition, the
ss losses by exposure to
transition temperature of
n strain aged the em-
he unstrained condition,
nsensitive to toughness
sensitivity of this ma-
'ig. 20. The most sensi-
such as A543 and A517
sses due to exposure
ent toughness of these
:nt for these losses dur-
l under most conditions

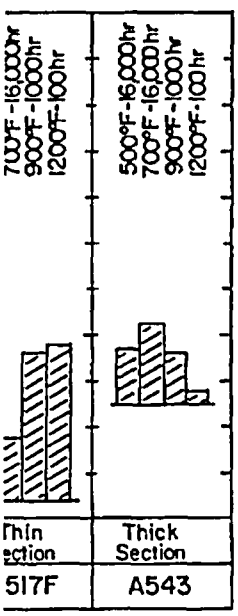

EMPERATURE
= A212 GRADE
ıND A543

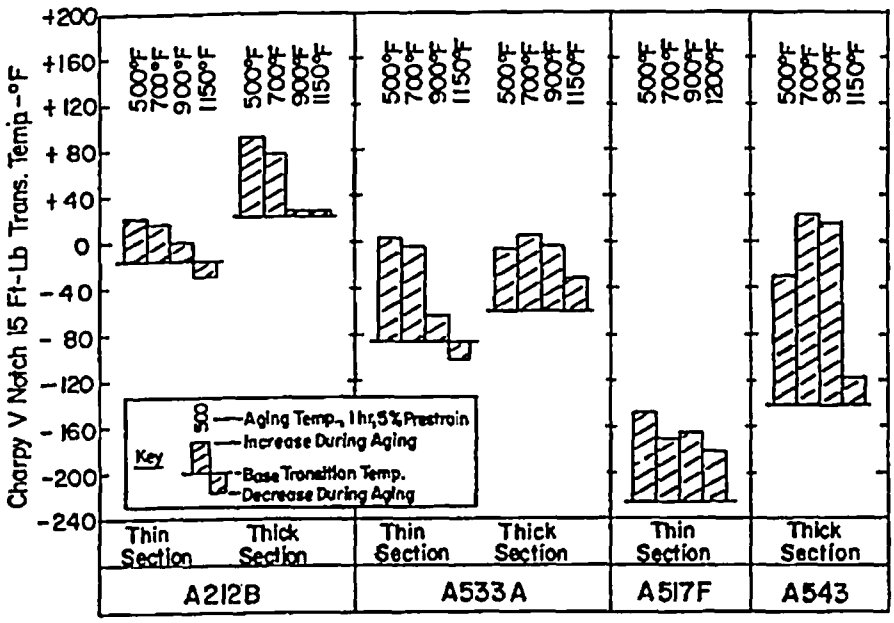

FIG. 20 – THE INFLUENCE OF 5 PER CENT STRAIN AND 1 HOUR EXPOSURE ON THE TOUGHNESS OF A212 GRADE B, A533 GRADE A, A517 GRADE F AND A543

Summary

This data review may be summarized as follows:

1. A comparison of the stress-rupture properties of eight quenched and tempered low-alloy high-strength steels in the 900 to 1100 F range has indicated that for 10,000 hour life at 1000 F, these steels may be grouped on the basis of rupture stress as follows:
   a) Rupture stress approximately 5000 psi – A212 Grade B steel.
   b) Rupture stress approximately 11,000 psi – A533 Grades A and B, A517 Grade F, and A543 steels.
   c) Rupture stress approximately 20,000 psi – A387 Grade B, A517 Grade E, and A542.
2. As time to rupture increases in the 900 to 1100 F temperature range, the reduction of area at failure decreases for the alloy steels. This decrease is associated with extensive intergranular cracking along prior austenite grains. For 10,000 hour rupture life at 1000 F, the steels may be grouped on the basis of rupture reduction of area as follows:
   a) Reduction of area greater than 60 per cent – A212 Grade B steel.
   b) Reduction of area between 40 and 60 per cent – A517 Grade E and A542.
   c) Reduction of area below 40 per cent – A387 Grade B, A517 Grade F, A543, and A533 Grades A and B.
3. The welded composite specimens were comparable or nearly comparable to the base plate in stress rupture strength for most of the steels. Four steels, A533 Grades A and B, A542 and A387 Grade B when welded displayed equal or greater

stress rupture strength than the base plate. Three steels, A212 Grade B, A543 and A517 Grade E suffered approximately 15 per cent loss in strength when welded compared to the base plate. One steel, A517 Grade F, lost 30 – 40 per cent of its rupture strength when welded.

4. The welded composite specimens of the alloy steels showed a tendency for low ductility intergranular fracture in the coarse-grained heat-affected zone of the welds. The materials most susceptible to this type of failure were those failing with low ductilities in the base plate tests. The carbon steel, A212 Grade B, was free of this type of fracture.

5. The quenched and tempered microstructure is superior in 10,000 hour stress rupture life to the normalized and stress relieved up to 800 F for the carbon steel A212 Grade B and up to 950 F for the three alloy steels, A387 Grade B, A533 Grade A and A542.

6. For applications where elevated temperature fatigue is a consideration, in the temperature range between 800 F and 1000 F the 100,000 cycle life stress is lower than the stress for rupture in 100,000 hours for A387 Grade B and A517 Grade F. For the carbon steel A212 Grade B, the rupture stress is less than the fatigue stress over this range. Below 800 F, one-quarter of the tensile strength is lower than either of the other two strength criteria for these three steels.

7. Exposure to elevated temperatures either with or without prior cold work can cause losses in notch toughness in the quenched and tempered low-alloy high-strength steels. The carbon steel A212 Grade B was not so seriously affected. Three alloy steels tested, A533 Grade A, A517 Grade F and A543 all had some substantial toughness losses due to exposure, but the inherently good notched toughness of these steels served to substantially offset the loss.

Acknowledgment

The authors gratefully acknowledge the financial assistance and technical cooperation of the Pressure Vessel Research Committee of the Welding Research Council, and of many of the companies represented by the council. Special acknowledgment is made to the United States Steel Corporation, the Armco Steel Company and The American Oil Company for their contribution of data to the program. The authors also are appreciative of the contribution of Mr. J. J. deBarbadillo of the Lehigh Staff to the program.

References

[1] V. S. Robinson, A. W. Pense and R. D. Stout, "The Creep Rupture Properties of Pressure Vessel Steels," *Welding Journal*, Vol. 43, *Research Suppl.*, pp. 534-s to 540-S, 1964.

[2] J. J. deBarbadillo, A. W. Pense and R. D. Stout, "The Creep Rupture Properties of Pressure Vessel Steels – Part II," *Welding Journal*, to be published, 1966.

[3] W. D. Doty, and G. E. Grotke, "Some Observations on the Weldability of Quenched and Tempered High-Yield-Strength Alloy Steels," *Conf. Proc.*, U. S. Navy Bureau of Ships, Washington, D. C., pp. 34 – 67, March 21–22, 1960.

[4] R. A. DePaul, A. W. Pense and R. D. Stout, "The Elevated Temperature Fatigue Properties of Pressure Vessel Steels," *Welding Journal*, Vol. 44, *Research Suppl.*, pp. 409-s to 416-s, 1965.

[5] J. H. Gross, "PRVC Interpretive Report of Pressure Vessel Research Section 2 – Materials Considerations," Welding Research Council Bull. No. 101.

[6] R. D. Stout, "Higher-Strength Steels for Weldments," *Welding Journal*, Vol. 39, *Research Suppl.*, pp. 273-s – 283-s.

3. ASTM Publication, "Analysis of Data from the Symposium on Heat-Treated Steels for Elevated Temperature Service."

ANALYSIS OF DATA FROM

SYMPOSIUM ON HEAT-TREATED STEELS FOR ELEVATED TEMPERATURE SERVICE

Prepared by:

E. B. NORRIS and R. D. WYLIE

Southwest Research Institute
Department of Materials Engineering

Prepared for:

THE METAL PROPERTIES COUNCIL
United Engineering Center
345 East 47th Street
New York, New York 10017

THE AMERICAN SOCIETY OF MECHANICAL ENGINEERS

United Engineering Center 345 East 47th Street New York, N. Y. 10017

Contents

	Page
Tables	ii
Illustrations	iv
Introduction	1
Evaluation of Data Presented at Symposium	1
Tensile and Creep Rupture Properties	1
Determination of Allowable Stresses	4
Notch Toughness Considerations	5
Notched Rupture Characteristics	5
Long Time Exposure Effects	5
Hydrogen Environmental Studies	5
Properties of Welds	5
Fatigue Studies	12
Recommendations for Future Work	12
General	12
Chemical Analysis Limits	12
Strength Determinations	13
Microstructural Stability	13
Fracture Toughness	13
Effect of Welding	14
Low Cycle Fatigue	14
Environmental Effects	14
Summary – Priority	14
References	15
Appendix A – Illustrations of Experimental Data	18
Appendix B – Tables of Experimental Data	40

Tables

Table		Page
I	Materials Evaluated in Symposium Papers	2
II	Three Classifications for 2-¼ Cr-1 Mo Data	2
III	Summary of 2-¼ Cr-1 Mo Stress Rupture Strength	3
IV	Stress Rupture Strength of Several Quenched and Tempered Steels	4
V	Comparison of Derived Allowable Stresses Based on 25 per cent of Minimum Tensile Strength for the Four Groups of Steels Evaluated	10
VI	Comparison of Derived Allowable Stresses Based on 33-⅓ per cent of Minimum Tensile Strength for the Four Groups of Steels Evaluated	11
B.I	Tensile Properties of A542 Steel Tempered at 1075 to 1125 F	41
B.II	Tensile Properties of A542 Steel Tempered at 1150 to 1200 F	42
B.III	Tensile Properties of A387 Grade D Steel Tempered at 1250 to 1350 F	43
B.IV	Tensile Properties of A212 Grade B Steel	44
B.V	Tensile Properties of A387 Grade B Steel	44
B.VI	Tensile Properties of A517 Grade F Steel Tempered at 1260 F	45
B.VII	Tensile Properties of A517 Grade E Steel	45
B.VIII	Tensile Properties of A387 Grade E Steel	46
B.IX	Tensile Properties of A508 Steel (Tempering Temperature 1050 F)	47
B.X	Room Temperature Tensile Properties of Several Quenched and Tempered Steels	47
B.XI	Stress Rupture Properties of A542 Steel Tempered at 1075 to 1125 F	48
B.XII	Stress Rupture Properties of A542 Steel Tempered at 1150 to 1200 F	49
B.XIII	Stress Rupture Properties of A387 Grade D Steel	50
B.XIV	Stress Rupture Properties of A212 Grade B Steel Tempered at 1150 F	51

B.XV Stress Rupture Properties of A387 Grade B Steel Tempered at 1250 to 1350 F 52

B.XVI Stress Rupture Properties of A387 Grade D Steel Tempered at 1150 F 53

B.XVII Stress Rupture Properties of A517 Grade F Steel Tempered at 1260 F 54

B.XVIII Stress Rupture Properties of A517 Grade B Steel Tempered at 1260 F 55

B.XIX Stress Rupture Properties of A517 Grade E Steel 56

B.XX Stress Rupture Properties of A517 Grade D Steel 57

B.XXI Stress Rupture Properties of A543 Steel 58

B.XXII Stress Rupture Properties of A533 Grade A Steel 58

B.XXIII Stress Rupture Properties of A533 Grade B Steel 59

B.XXIV Stress Rupture Properties of A387 Grade E Steel 59

B.XXV Stress Rupture Properties of 2-¼ Cr-1 Mo Weld Metal Quenched and Tempered 60

B.XXVI Stress Rupture Properties of 2-¼ Cr-1 Mo Weld Metal Stress Relieved 60

B.XXVII Selected Creep Rate Data on A542 Steel 61

B.XXVIII Summary of Code Strength Criteria for A542 Class 2 Steel 61

B.XXIX Summary of Code Strength Criteria for A542 Class 1 Steel 62

B.XXX Summary of Code Strength Criteria for A387 Grade D Steel Tempered to 75,000-psi Minimum UTS 63

B.XXXI Summary of Code Strength Criteria for the Remaining Low Alloy Steels Studied, Quenched and Tempered to 115,000 psi Minimum UTS 64

Illustrations

Figure		Page
1	Comparison of Allowable Stress Criteria for A542 Class 2 Steel	6
2	Comparison of Allowable Stress Criteria for A542 Class 1 Steel	7
3	Comparison of Allowable Stress Criteria for A387 Grade D Steel	8
4	Comparison of Allowable Stress Criteria Based on Tensile Strength Data for Various Quenched and Tempered Steels	9
A.1	Tensile Strength of A542 Class 2 Steel	19
A.2	Yield Strength of A542 Class 2 Steel	20
A.3	Tensile Strength of A542 Class 1 Steel	21
A.4	Yield Strength of A542 Class 1 Steel	22
A.5	Tensile Strength of A387 Grade D Steel	23
A.6	Yield Strength of A387 Grade D Steel	24
A.7	800 F Stress Rupture Properties of A542 and A387 Steels	25
A.8	850 F Stress Rupture Properties of A542 and A387 Steels	26
A.9	900 F Stress Rupture Properties of A542 and A387 Steels	27
A.10	1000 F Stress Rupture Properties of A542 and A387 Steels	28
A.11	Tensile Strength of Various Quenched and Tempered Steels	29
A.12	Yield Strength of Various Quenched and Tempered Steels	30
A.13	800 F Stress Rupture Properties of Various Quenched and Tempered Steels	31
A.14	900 F Stress Rupture Properties of Various Quenched and Tempered Steels	32
A.15	1000 F Stress Rupture Properties of Various Quenched and Tempered Steels	33
A.16	1100 F Stress Rupture Properties of Various Quenched and Tempered Steels	34
A.17	1200 F Stress Rupture Properties of Various Quenched and Tempered Steels	35
A.18	Stress Versus Larson-Miller Parameter for 2-¼ Cr-1 Mo Steels	36
A.19	Charpy V-Notch Impact Properties of 2-¼ Cr-1 Mo Steel	37
A.20	Charpy V- Notch Impact Properties of 2-¼ Cr-1 Mo Steel	38

Analysis of Data from Symposium on Heated-Treated Steels for Elevated Temperature Service

E. B. NORRIS and R. D. WYLIE

Southwest Research Institute
San Antonio, Texas

Introduction

The use of quenched and tempered low alloy steels for special purpose petrochemical vessels operating in the intermediate temperature range of 750 to 850 F has accelerated development of data on steels which are potentially useful for such vessels. As a result of this development, a conference was held September 19-20, 1966 at the annual meeting of the Petroleum Division of the ASME in New Orleans with the specific purpose of presenting the available data on these steels. The conference was jointly sponsored by the ASTM-ASME Joint Committee on the Effect of Temperature on the Properties of Metal and The Metals Properties Council. The newly organized Metals Properties Council contracted with Southwest Research Institute to review the data presented at the conference, to prepare a detailed analysis of the data for submission to the ASME Boiler Code Subcommittee on Properties of Metals, and to outline specific programs which may be required to provide needed data for this class of steels.

The following report presents the results of the study program.

Evaluation of Data Presented at Symposium

Tensile and Creep Rupture Properties

The mechanical property data presented at the Symposium on Heat Treated Steels for Elevated Temperature Service were obtained on materials representing ten chemistries covered by seven ASTM specifications, as summarized in Table I.

The tensile and stress rupture data were analyzed in a manner as consistent as possible with the methods employed by the Subgroup on Strength Properties for Steel and High Temperature Alloys of the ASME Boiler and Pressure Vessel Code. For the "elastic" range, this involves determining the tensile and yield trend curves, as a function of temperature, by lowering the average curves to the

Table I

Materials Evaluated in Symposium Papers

Alloy Class	ASTM Specifications
Carbon steel	A212-B*
½ Mn Mo	A533-A
½ Mn Mo-Ni modified	A533-B
1 Cr-½ Mo	A387-B*
2 ¼ Cr-1 Mo	A387-D*, A542
3 Cr-1 Mo	A387-E*
1 ¾ Cr-½ Mo	A517-E
¾ Ni-½ Cr-½ Mo	A517-F
Ni-Cr-Mo	A543
Ni-Cr-Mo-V	A508

*These specifications are for annealed or normalized and tempered material.

minimum specified values at room temperature. In the "creep" range, the average and minimum stresses to produce rupture in 100,000 hours and the average stress to produce a secondary creep rate of 0.01 per cent per 1000 hours are also required. However, the creep data presented at the Symposium were too limited to permit the latter calculation. The creep data will be discussed in more detail in a later section.

The bulk of the data reported were on the 2-¼ Cr-1 Mo steel composition. The chemistries and tensile properties reported showed that they met either the ASTM A542 or the ASTM A387 specification. For purposes of analysis, the data were divided into three groups or classifications as given in Table II. For each of these groups, the minimum ultimate strength and minimum yield strength trend curves were established, as shown in Figures A.1 through A.6, Appendix A. The first step was to construct an average curve for the ultimate or yield strength as a function of temperature. Secondly, a minimum trend curve was developed by reducing the average curve by the ratio of the minimum specified room temperature strength to the average room temperature strength. There was no adjustment made to this average curve for the purpose of establishing design stresses. The raw data used to construct these curves are given in Tables B.I through B.III, Appendix B.

The stress rupture data contained in Tables B.XI through B.XIII, Appendix B, were plotted on log-log coordinates in Figures A.7 through A.10, Appendix A. Individual rupture curves were constructed for each lot of material in Figures A.7

Table II

Three Classifications for 2-¼ Cr-1 Mo DATA

Group	Minimum UTS	Heat Treatment	Tempering Temperature
A542-2	115,000	Q & T	1075° to 1125°F
A542-1	105,000	Q & T	1150° to 1200°F
A387-D	75,000	N & T	1250° to 1300°F

through A.10. A lot was considered to consist of a material with a specific combination of heat of steel, heat treatment, material thickness, specimen location, etc. The log-log plots were extrapolated to 100,000 hours life if any individual test within a lot exceeded 1000 hours and if at least one lot in a group had a test result exceeding 3000 hours. The 100,000-hour rupture strengths so obtained are summarized in Table III.

Table III

Summary of 2-¼ Cr-1 Mo Stress Rupture Strengths

Group	Temp. (°F)	10^5-Hour Rupture Strength, ksi	
		Minimum	Average
A542-2	800	84.0	97.7
	850	60.0	64.0
	900	32.0	38.5
A542-1	800	73.0	76.0
	850	54.0	57.0
	900	36.0	42.5
A387-D	800	50.0	50.0
	850	—	—
	900	26.0	26.0

The tensile data on the remaining materials listed in Table I were grouped together for study because they were insufficient to permit evaluation of each alloy individually. The tensile data on these alloys are presented in Tables B.IV through B.X, Appendix B, and in Figures A.11 and A.12, Appendix A. Except for A212-B[2] and A508[7], the tensile data agreed well with the trend curves determined previously for A542-2. Also shown in Figure A.11 is a curve representing four times the allowable stresses given in Code Cases 1204 and 1298. The shape of this curve also agrees well with the 115,000-psi trend curve.

The individual stress rupture data utilized but not specifically tabulated in one paper [2] was obtained by consulting two additional references [12, 13]. These data, along with other data presented at the Symposium, are given in Tables B.XIV through B.XXVI, Appendix B, and in Figures A.13 through A.17, Appendix A. Although there is a large amount of test data, less than 13 per cent were over 1000-hours duration, and over half of all tests failed in less than 100 hours. For those materials (all single heat data) on which test results in excess of 3000 hours were reported, extrapolation to 100,000 hours were made and are given in Table IV.

The creep rate data reported at the conference were quite limited. Only those obtained on tests in excess of 5000 hours were considered, Table B.XXVII, Appendix B. The number of variables in this tabulation prohibits any detailed analysis, and the relatively high creep rates reported do not lend themselves to extrapolation to determine stresses for a creep rate of 0.01 per cent in 1000 hours.

Table IV

Stress Rupture Strength of Several Quenched and Tempered Steels

Group	Estimated 10^5-Hour Rupture Strength, ksi		
	800°F	900°F	1000°F
A387-B-QT	—	52.0	13.3
A517-E	71.0	40.0	13.0
A517-F	—	46.0	8.9

The stress rupture properties of the 2-¼ Cr-1 Mo class of materials were also studied with the aid of the Larson-Miller parameter technique, Figure A.18. A constant of 25 was employed instead of the normally used value of 20 because a better correlation between test temperatures was obtained. Two primary points can be noted in this figure. The first is the tendency for the two lower bands to merge. The second is the indication that the quenched and tempered groups not only merge but may cross, indicating that the material starting with the higher rupture strength may be the weaker after long periods of exposure to temperature and stress.

Determination of Allowable Stresses

In the "elastic" range, one of the factors for determining allowable stresses is the minimum tensile strength. Certain sections of the Code utilize one-quarter of this value, while others employ a factor of one-third. In the "creep" range, 80 per cent of the minimum and 60 per cent of the average 100,000-hour rupture strength are used along with the average stress to produce a minimum creep rate of 0.01 per cent per 1000 hours.

At the temperature of transition between the tensile-governing and the creep-governing curves, a "faired value" was taken as being equal to 75 per cent of the difference between the creep-governing value at a temperature 50 F higher and the tensile-governing value at a temperature 50 F lower. An example of this calculation is given below:

Temperature	Material	Governing Property and Allowable Stress
850 F	A542-2	25% UTS = 23,500 psi
900 F	A542-2	(To be determined)
950 F	A542-2	10^5-SR Strength = 11,000 psi

"Faired value" of Allowable stress at 900 F

$$= 11{,}000 \text{ psi} + \tfrac{3}{4}\,(23{,}500 \text{ psi} - 11{,}000 \text{ psi})$$
$$= 20{,}400 \text{ psi}$$

The 75-per cent factor was chosen because it provides a smooth transition between the two curves.

The allowable stresses based on each of the above criteria are tabulated in Tables B.XXVII through B.XXXI, Appendix B, and are presented graphically in

Figures 1 through 4. For A542 Classes 1 and 2, Figures 1, 2 and 3 show that based on the 25 per cent of minimum tensile strength criteria the "elastic" range extends to 850 F and that based on the 33 ⅓ per cent of minimum tensile strength criteria the "elastic" range is limited to 800 F. For the remaining quenched and tempered alloys (except A212-B carbon steel), the tensile data supported the use of the same 115,000-trend curve used for A542 Class 2. The stress rupture data were insufficient to reliably establish allowable stresses in the "creep" range. Based on this analysis, the suggested allowable stresses for the four groups of materials, using 25 per cent of the minimum tensile strength, are presented in Table V. A similar summary using 33 ⅓ per cent of the minimum tensile strength is contained in Table VI.

Notch Toughness Considerations

Except that in one paper [9], the Charpy V data presented were generally insufficient to construct transition curves. These data, presented in Figures A.19 and A.20, Appendix A, exhibit a large amount of scatter and a significant directional effect. A directional effect is also indicated by a second author [4].

Another important characteristic is the large range (30 to 80 ft-lb) reported in the drop weight NDT Charpy V correlation energy level [4, 9]. The Naval Reseach Laboratory has also reported large variations in correlation energy levels of over 100 ft-lb absorbed energy [16]. This observation raises a question concerning the adequacy of the Charpy V test in defining the fracture safe operating temperature range of a structure employing these higher strength materials.

Notched Rupture Characteristics

Combination smooth-notched bar rupture test results [3] indicate that strain aging may produce embrittlement at elevated temperatures, as evidenced by two failures in the notch at 1000 F.

Long Time Exposure Effects

The effect of long time exposures on the tensile and impact properties was studied by several investigators [4, 7, 9]. On the basis of tensile properties, the data indicated that below 1000 F there is no significant loss in tensile strength when exposed approximately a year, with or without stress. However, there appears to be an indication of embrittlement, as defined by the Charpy V test. In general, the as-quenched notch toughness of the quenched and tempered alloys are good. However, data were presented [7] which indicated that the Ni-Cr-Mo-V alloy was embrittled by aging, particularly at 800 F.

Hydrogen Environmental Studies

The effects of hydrogen on Cr-Mo steels was studied [6]. Although tests were limited to the lower strength grades (annealed, normalized and tempered), a reduction in stress-rupture strength was noted. This is of concern because the effect might be more pronounced on the high strength quenched and tempered grades.

Properties of Welds

The results reported on weld metal and heat affected zone properties were quite limited. One paper [2] employed a composite specimen containing a shallow

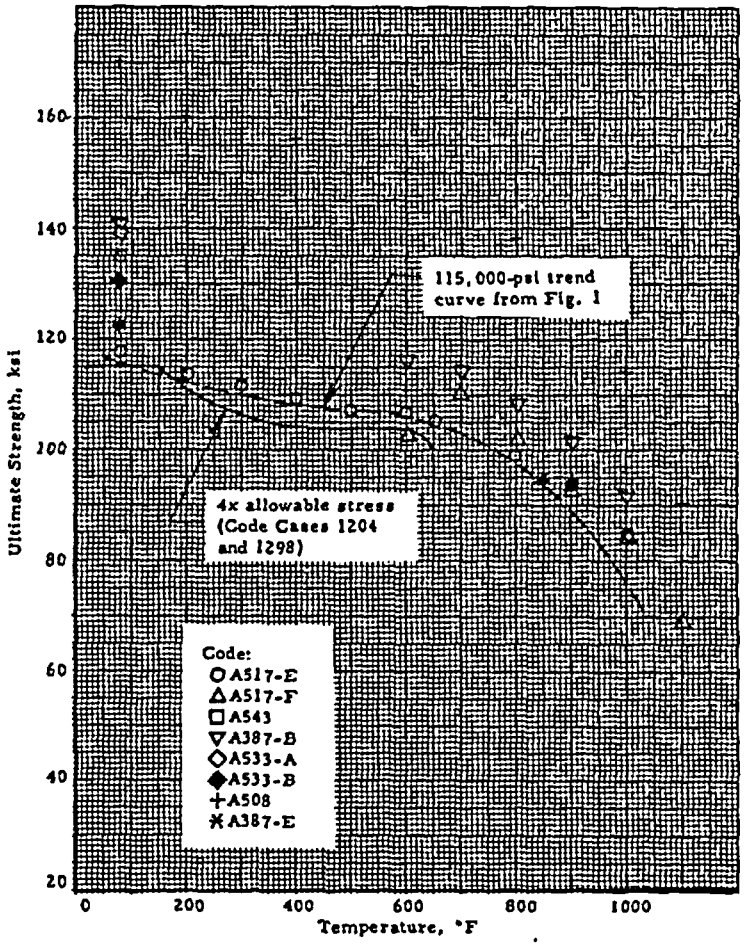

FIG. A.11 TENSILE STRENGTH OF VARIOUS QUENCHED AND TEMPERED STEELS

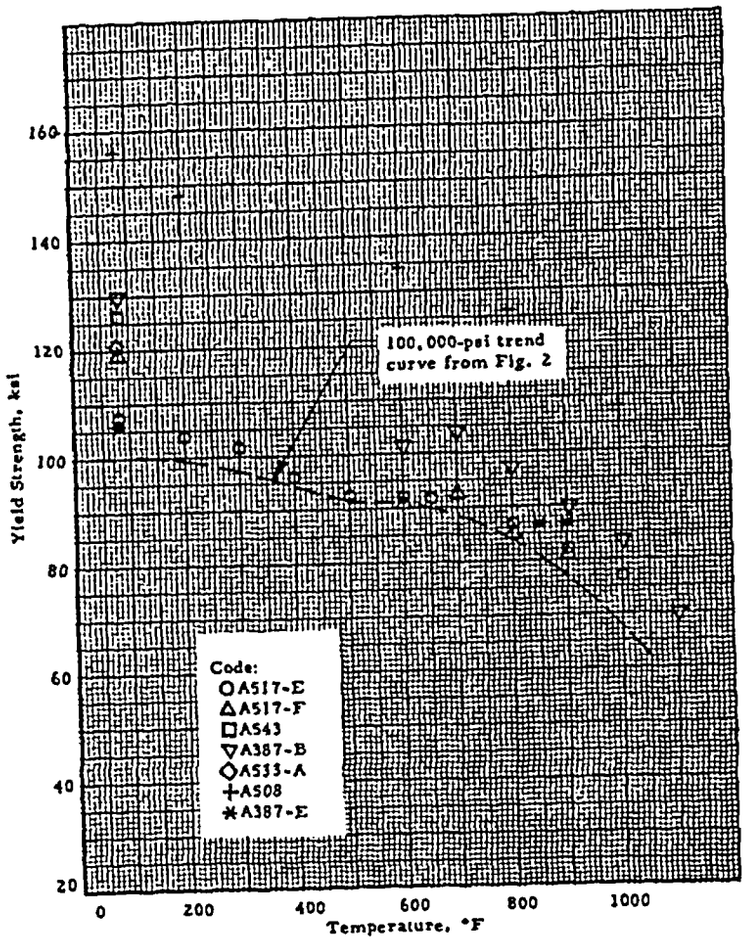

FIG. A.12 YIELD STRENGTH OF VARIOUS QUENCHED AND TEMPERED STEELS

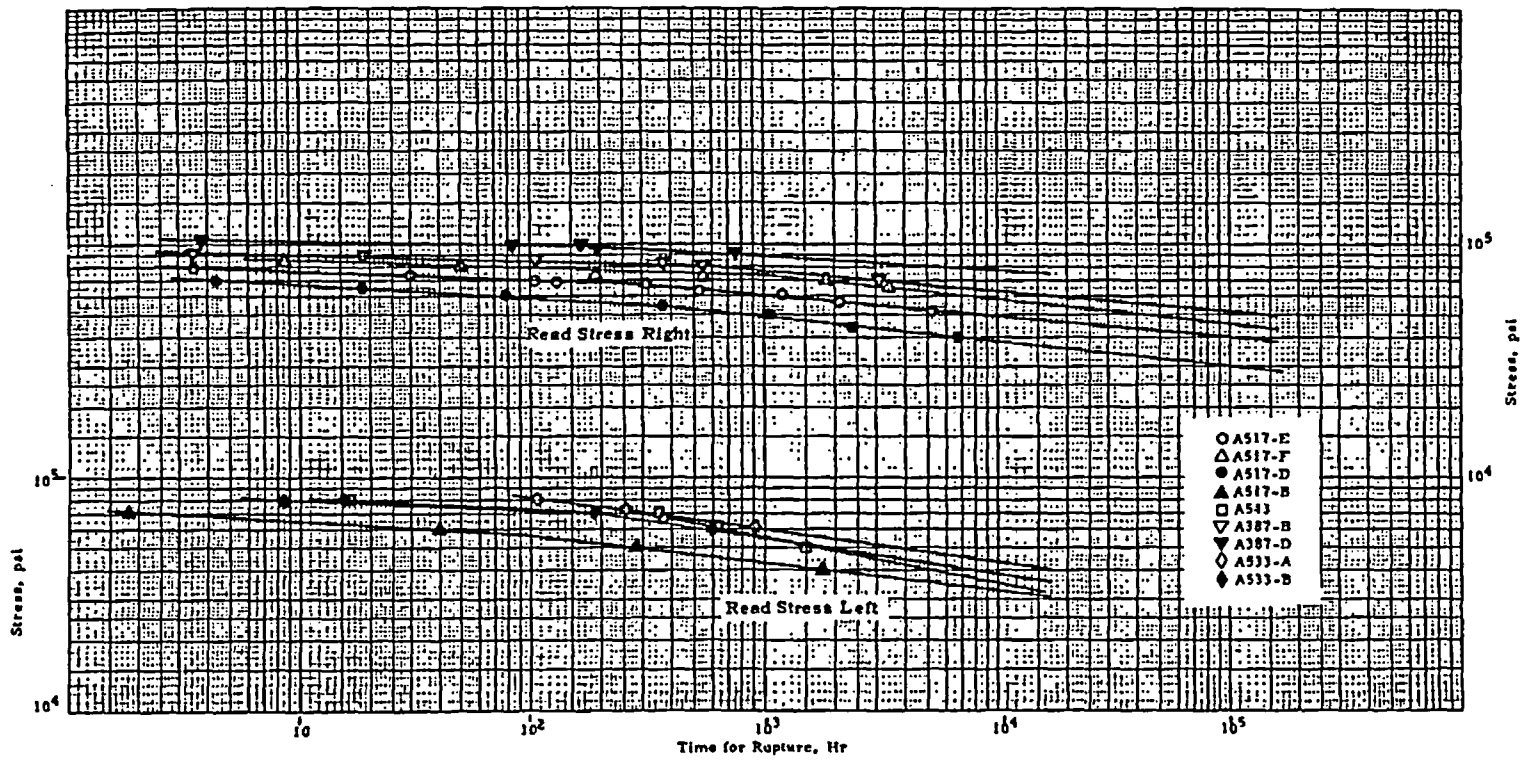

FIG. A.14 900 F STRESS RUPTURE PROPERTIES OF VARIOUS QUENCHED AND TEMPERED STEELS

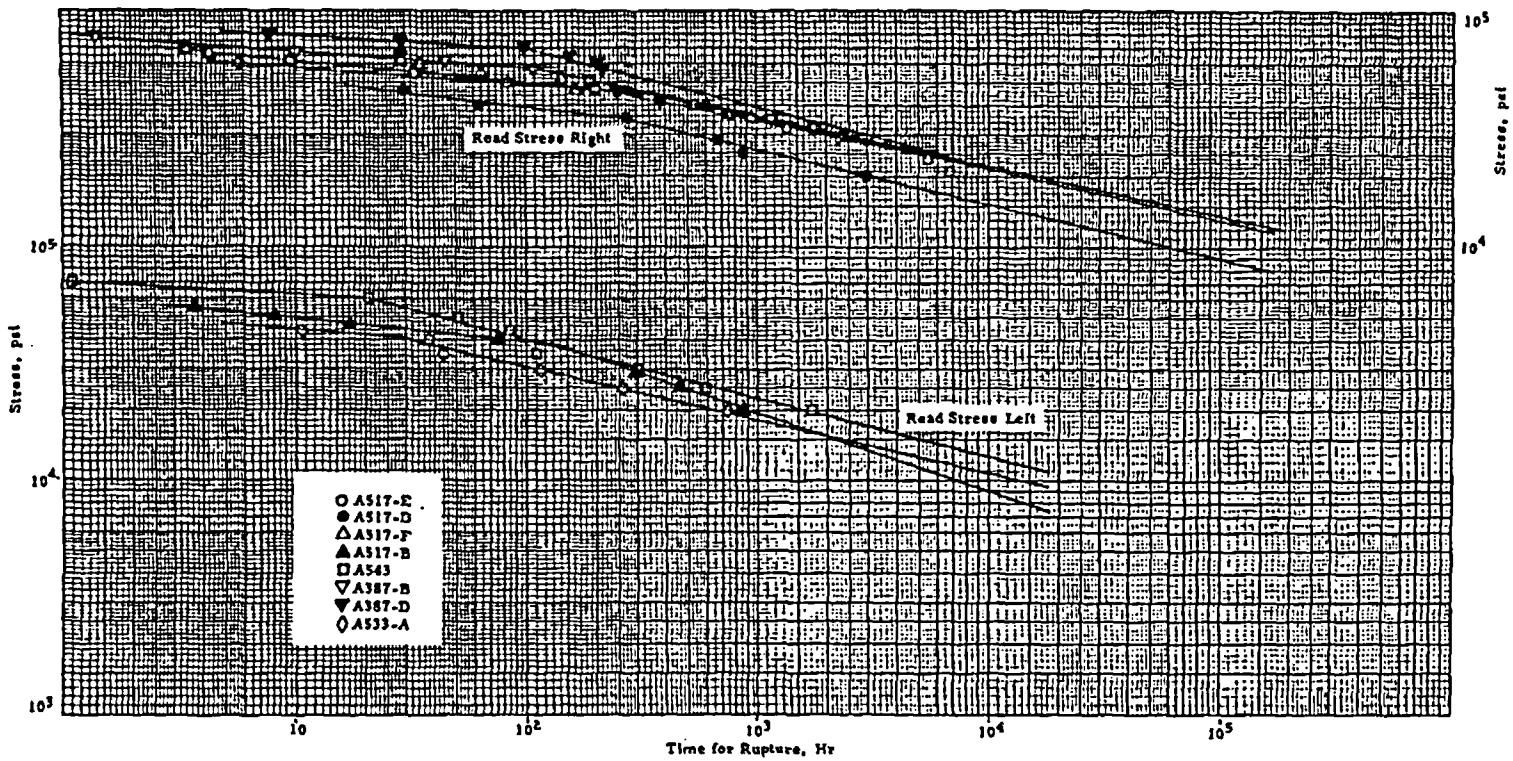

FIG. A.15 1000 F STRESS RUPTURE PROPERTIES OF VARIOUS QUENCHED AND TEMPERED STEELS

Table B.IX

Tensile Properties of A508 Steel (Tempering Temperature 1050°F)

Source*	Plate Gauge (in.)	Test Loc'n	Test Temp. (°F)	0.2% YS (ksi)	UTS (ksi)	Elong (%)	R.A. (%)
7	4-½	¼ T	RT	156.0	170.0	18.0	60.0
			200	148.0	160.0	15.0	55.0
			400	140.0	156.0	14.0	53.0
			600	134.0	150.0	16.0	59.0
			800	126.0	138.0	18.0	63.0
			1000	108.0	114.0	19.0	72.0
			1100	84.0	90.0	21.0	81.0
			1200	48.0	54.0	39.0	91.0

*See References for source.

Table B.X

Room Temperature Tensile Properties of Several Quenched and Tempered Steels

Source*	Alloy Ident.	Plate Gauge (in.)	Test Loc'n	0.2% YS (%)	UTS (ksi)	Elong (%)	R.A. (%)
2	A543			126.0	135.0	21.5	68.4
	A517F			113.0	121.0	26.0	59.7
	A517E			112.0	120.0	22.0	67.9
	A533A			121.3	138.9	22.5	70.5
	A533B			121.5	130.5	20.0	63.2

*See References for source.

Table B.XXI

Stress Rupture Properties of A543 Steel

Source*	Test Temp. (°F)	Stress (psi)	Rupture Life (hr)
13	800	94,000	51.0
		89,000	325.0
	900	80,000	16.5
		70,000	350.0
		64,000	360.0
		60,000	600.0
		50,000	1490.0
	1000	70,000	1.1
		60,000	21.0
		50,000	51.0
		45,000	85.0
		35,000	112.0
		30,000	307.0
		25,000	585.0
		20,000	1690.0
	1100	40,000	1.1
		30,000	14.5
		20,000	86.0
		15,000	307.0
	1200	15,000	6.1
		10,000	72.0

*See References for source.

Table B.XXII

Stress Rupture Properties of A533 Grade A Steel

Source*	Test Temp. (°F)	Stress (psi)	Rupture Life (hr)
13	900	80,000	108.0
		70,000	257.0
		60,000	920.0
	1000	57,000	14.5
		50,000	<1.0
		45,000	10.5
		40,000	38.5
		35,000	5.4
		30,000	114.0
		25,000	266.0
		20,000	725.0
	1100	20,000	24.0
		15,000	105.0

*See References for source.

Table B.XXIII

Stress Rupture Properties of A533 Grade B Steel

Source*	Test Temp. (°F)	Stress (psi)	Rupture Life (hr)
13	900	80,000	8.4
		80,000	15.8
		70,000	184.0
		60,000	585.0
	1000	58,000	11.4
		50,000	19.2
	1100	15,000	114.0

*See References for source.

Table B.XXIV

Stress Rupture Properties of A387 Grade E Steel

Source*	Plate Gauge (in.)	Test Loc'n	Test Temp. (°F)	Stress (psi)	Rupture Life (hr)
Quenched and Tempered (1125°F)					
4	7-11/16	¼ T	850	90.0	49.6
				85.0	114.0
				80.0	364.1
				76.0	1596.0
			900	85.0	20.6
				80.0	26.6
				75.0	230.0
				70.0	430.8
				68.0	453.8
				66.0	687.7
Normalized and Tempered (1225°F)					
4	7-11/16	¼ T	850	56.0	37.7
				55.0	28.1
				52.0	138.5
				50.0	305.5
			900	55.0	6.1
				50.0	42.6
				45.0	181.3
				45.0	187.9
				43.0	358.0

*See References for source.

4. DOE HTGR 88383, "Tensile and Creep Properties of SA533 Grade B Class 1 Steel," December 1989.

xtra

DOE-HTGR-88383
ORNL/TM-11338

HTGR

TENSILE AND CREEP PROPERTIES OF SA533 GRADE B CLASS 1 STEEL

APPLIED TECHNOLOGY

Any further distribution by any holder of this document or data therein to third parties representing foreign interests, foreign governments, foreign companies, and foreign subsidiaries or foreign divisions of U.S. companies shall be approved by the Associate Deputy Assistant Secretary for Reactor Systems, Development and Technology, U.S. Department of Energy. Further foreign party release may require DOE approval pursuant to Federal Regulation 10 CFR Part 810, and/or may be subject to Section 127 of the Atomic Energy Act.

AUTHORS/CONTRACTORS

Oak Ridge National Laboratory
H. E. McCoy

Oak Ridge National Laboratory
Oak Ridge, Tennessee 37831
operated by
MARTIN MARIETTA ENERGY SYSTEMS, INC.
for the
UNITED STATES DEPARTMENT OF ENERGY
December 1989

DOE-HTGR-88383
ORNL/TM-11338
Distribution
Category UC-522T

Metals and Ceramics Division

TENSILE AND CREEP PROPERTIES OF SA533 GRADE B CLASS 1 STEEL

H. E. McCoy

Date Published: December 1989

NOTICE: This document contains information of a preliminary nature. It is subject to revision or correction and therefore does not represent a final report.

Prepared for the
DOE Office of Advanced Reactor Programs
AF 20 10 15 2

Prepared by the
OAK RIDGE NATIONAL LABORATORY
Oak Ridge, Tennessee 37831-6285
operated by
MARTIN MARIETTA ENERGY SYSTEMS, INC.
for the
U.S. DEPARTMENT OF ENERGY
under Contract DE-AC05-84OR21400

CONTENTS

LIST OF TABLES v

LIST OF FIGURES vii

ABSTRACT 1

INTRODUCTION 1

EXPERIMENTAL DETAILS 2

MATERIAL 2

TEST METHODS 2

EXPERIMENTAL RESULTS 2

EFFECTS OF HEAT TREATMENT ON TENSILE PROPERTIES OF BASE METAL . 2

METALLOGRAPHIC EXAMINATION OF MATERIAL 3

MEASURED TENSILE PROPERTIES 3

MEASURED CREEP PROPERTIES 4

TEMPER EMBRITTLEMENT 6

DISCUSSION 7

SUMMARY 7

ACKNOWLEDGMENTS 7

REFERENCES 8

LIST OF TABLES

Table		Page
1	Summary of test materials	9
2	Summary of product chemical analyses	10
3	Specimen lot designations (modified heat number used in report)	11
4	Tensile properties specified by code and measured after various heat treatments	12
5	Tensile test of A533 base metal heat treated by ORNL HT 1 (Lot 1)	13
6	Tensile test of A533 base metal heat treated by ORNL HT 2 (Lot 2)	14
7	Tensile test of A533 base metal heat treated by CE (Lot 3)	15
8	Tensile test of A533 transverse weld (HT 9583A) heat treated by CE (Lot 4)	16
9	Tensile test of A533 weld metal (HT 9583A) heat treated by CE (Lot 5)	17
10	Tensile test of A533B base metal (HT 5795) heat treated by CE (Lot 6)	18
11	Tensile properties of A533B all weld metal (HT 5795) heat treated by CE (Lot 7)	19
12	Tensile properties of A533B transverse weld (HT 5795) heat treated by CE (Lot 8)	20
13	Tensile properties of A533B base metal (HT 9583B) heat treated by CE (Lot 9)	21
14	Tensile properties of A533B transverse weld (HT 9583B) heat treated by CE (Lot 10)	22
15	Tensile properties of A533B weld metal (HT 9583B) heat treated by CE (Lot 11)	23
16	Tensile properties of A533B base metal (HT 64535) heat treated by CE (Lot 12)	24
17	Creep data for A533B steel-heat 9583A	25

Table		Page
18	Creep data for A533B steel-heat 5795	26
19	Creep data for A533B steel-heat 9583B	27
20	Creep data for A533B steel-heat 64535	27
21	Effect of creep exposure on tensile properties	28

LIST OF FIGURES

Figure		Page
1	Yield strength of several lots of A533 base metal as a function of test temperature	29
2	Yield strength of three lots of weld metal as a function of temperature	29
3	Yield strength of three lots of transverse weld samples as a function of temperature	30
4	Yield strength for lots of base metal, transverse welds, and weld metal having the lowest strength	30
5	Yield strength of A533 base metal at a strain rate of $3.7 \times 10^{-5}s^{-1}$ as a function of temperature	31
6	Yield strength of A533 weld metal at a strain rate of $3.7 \times 10^{-5}s^{-1}$ as a function of temperature	31
7	Yield strength of transverse weld specimens of A533 at a strain rate of $3.7 \times 10^{-5}s^{-1}$ as a function of temperature	32
8	Yield strength at a strain rate of $3.7 \times 10^{-5}s^{-1}$ for lots of base metal, transverse weld samples, and weld metal as a function of temperature	32
9	Tensile strength of several lots of A533 base metal as a function of temperature	33
10	Tensile strength of several lots of A533 weld metal specimens as a function of temperature	33
11	Tensile strength of several lots of A533 transverse weld specimens as a function of temperature	34
12	Tensile strength for lots of base metal, transverse welds, and weld metal having the lowest strength	34
13	The ultimate tensile strength of several lots of base metal as a function of temperature	35
14	The ultimate tensile strength of several lots of weld metal as a function of temperature	35
15	The ultimate tensile strength of several lots of transverse weld specimens as a function of temperature	36

16 Ultimate tensile strength for lots of base metal, weld metal, and transverse weld metal having the lowest strength 36

17 Yield strength of Lot 6 measured at strain rates of $1.3 \times 10^{-4}s^{-1}$ and $3.7 \times 10^{-5}s^{-1}$ 37

18 Ultimate tensile strength of Lot 6 measured at strain rate of $1.3 \times 10^{-4}s^{-1}$ and $3.7 \times 10^{-5}s^{-1}$ 37

19 Larson-Miller correlation for Lots 1, 2, and 3 base metal crept to 1% strain 38

20 Larson-Miller correlation for Lots 3, 6, 9, and 12 base metal crept to 1% strain 38

21 Larson-Miller correlation for 1% strain showing average and minimum strengths for Lots 3, 6, 9, and 12 base metal . . 39

22 Larson-Miller correlation for tertiary creep for Lots 3, 6, 9, and 12 base metal 39

23 Larson-Miller correlation for rupture for Lots 3, 6, 9, and 12 base metal 40

24 Time to 1% strain as a function of time to rupture for Lots 3, 6, 9, and 12 base metal 40

25 Time to tertiary creep as a function of time to rupture for Lots 3, 6, 9, and 12 base metal 41

26 Fracture strain as a function of rupture time for Lots 3, 6, 9, and 12 base metal 41

27 Allowable stresses as a function of temperature for base metal based on various design criteria 42

28 Larson-Miller correlation for 1% strain in Lots 5, 7, and 11 weld metal 42

29 Larson-Miller correlation for 1% strain in Lots 5, 7, and 11 (combined) weld metal 43

30 Larson-Miller correlation for 1% strain in Lots 4, 8, and 10 transverse weld samples 43

31 Larson-Miller correlation for 1% strain in Lots 4, 8, and 10 (combined) transverse weld samples 44

32 Larson-Miller plot comparing the average properties of base metal, weld metal, and transverse weld samples 44

TENSILE AND CREEP PROPERTIES OF SA533 GRADE B CLASS 1 STEEL*

H. E. McCoy

ABSTRACT

Tensile and creep tests are being performed on several lots of base metal and weldments to determine the design stresses for 1% strain in 1000 h over the temperature range of 371 to 538°C. Short-term tensile tests indicate that the strength is least for base metal, intermediate for transverse weld specimens, and greatest for weld metal. Creep tests show much less variation, with about equivalent creep strength for base metal and transverse weld samples and slightly greater creep strength for weld metal. This is an interim report on a continuing program.

INTRODUCTION

The Modular High-Temperature Gas-Cooled Reactor (MHTGR) concept utilizes a pressure vessel constructed of SA533 Grade B Class 1 steel. The allowable stresses given for this material in Section III (Nuclear Construction) of the *ASME Boiler and Pressure Vessel Code* are for temperatures to 371°C (700°F).[1] It is anticipated that, in the operation of MHTGR's, Level C and D events may occur that last for a total of less than 1000 h in which the vessel temperature will be in the range of 371 to 538°C (700 to 1000°F). The purpose of the current testing is to determine the mechanical properties of this steel over the temperature range 371 to 593°C (700 to 1100°F) needed to support code approval for use of this steel under the Level C and D conditions.

The approach taken to this problem is that of measuring the tensile and creep properties of this steel over the temperature range of 317 to 593°C (700 to 1100°F). The construction will involve two basic welding processes, namely, tandem electrode submerged arc (machine) and shielded metal arc (manual). Hence, samples of welds made by these processes are included. The test materials currently being evaluated include three heats of base metal, two submerged arc welds, and one shielded metal arc weld. The current status of the testing is described in this report.

*Research sponsored by the Office of Advanced Reactor Programs, Division of HTGRs, U.S. Department of Energy, under contract DE-AC05-84OR21400 with Martin Marietta Energy Systems, Inc.

EXPERIMENTAL DETAILS

MATERIAL

The materials were procured from Combustion Engineering (CE), Chattanooga, Tenn., and information about the test materials is summarized in Table 1. All of the materials underwent the vendor chemical analysis and an analysis by CE; the results of these tests are shown in Table 2. The tests showed excellent agreement, and the material seemed to be of the composition specified by the *ASME Boiler and Pressure Vessel Code*.[2]

The type of specimen, the associated heat treatment, and vendor designation are given in Table 3. The lot numbers shown in the last column of Table 3 will be used throughout this report.

As will be discussed further, all three heat treatments resulted in mechanical properties that satisfied the code requirements: ultimate tensile strength in the range of 550-690 MPa (80-100 ksi), the minimum yield strength of 345 MPa (50 ksi), and the minimum elongation in 50.8 mm (2 in.) of 18.0%.

TEST METHODS

The tensile tests were run in accordance with ASTM E8, and the creep tests were run according to ASTM E139.[3] The specimen had a gage section 6.35 mm (0.25 in.) in diameter by 31.75 mm (1.25 in.) long. Extensometers were attached by set screws into small grooves outside the gage section so that the set screws would not induce rupture.

EXPERIMENTAL RESULTS

EFFECTS OF HEAT TREATMENT ON TENSILE PROPERTIES OF BASE METAL

The range of properties allowed by the code for this material is quite broad. The first piece of base material obtained from CE did not have the desired heat treatment. Individual test specimens were given the first heat treatment listed in Table 4, referred to as ORNL HT 1. The ultimate tensile strength of the material given this heat treatment is at the top of the code-specified range, with duplicate tests having values of 705 and 667 MPa (102.2 and 96.8 ksi). The heat treatment used by CE is the last one listed in Table 4. The ultimate tensile strength of the base metal is near the middle of the allowable range, and the other mechanical properties are acceptable.

The next heat treatments investigated were based on the premise that the most conservative results would be obtained by heat treating to the lower side of the allowable strength band. The material was solution annealed at 871°C, water quenched, and tempered at 663°C. After tempering for 30 h, the ultimate tensile strength was barely above the code minimum value. Tempering for 50 h at 663°C reduced the ultimate tensile strength considerably below the code minimum value. Thus, the heat treatment of

solution annealing at 871°C, water quenching, and tempering 30 h at 663°C was selected as ORNL HT 2. The mechanical properties of heat 9583 were evaluated following three heat treatments: ORNL HT 1 (Lot 1), ORNL HT 2 (Lot 2), and CE HT (Lot 3).

METALLOGRAPHIC EXAMINATION OF MATERIAL

Not all of the materials have been evaluated metallographically. The primary microconstituent is tempered bainite. The hardness of the base metal is 90 to 92 Rockwell B. The weld deposit is slightly harder with a hardness of 95 Rockwell B. There is a region in the base metal a short distance from the fusion line that is tempered during welding to a hardness of about 88 Rockwell B. Samples that transversed the fusion line (noted transverse weld samples) usually failed at this weaker location.

MEASURED TENSILE PROPERTIES

Tensile properties of the following were measured: A533 base metal, the deposited weld metal, and transverse across the fusion line. In the transverse specimens, the fusion line was midway along the gage length; weld metal is on one side, and base metal on the other. The test matrix consisted of test temperatures of 25, 317, 427, 482, 538, and 593°C. Specimens were tested at initial strain rates of 1.3×10^{-4} and $0.27 \times 10^{-4} s^{-1}$. In general, duplicate tests were run at each condition, but the availability of material was a limitation in a few cases.

The tensile test results for Lots 1 through 12 (see Table 3) are given in Tables 5 through 16. The data from these tables were used to construct Figs. 1 through 18. The yield strengths of the various lots of base material are shown in Fig. 1. The data for each lot were fit with a second-order polynomial, and the lines developed in this way are shown in Fig. 1. The Lot 1 material is the strongest, the Lot 2 material is second weakest, and Lot 6 is the weakest material. Lots 3, 6, 9, and 12 were given the standard CE heat treatment. The yield strengths of these four lots agree well at temperatures above 300°C, but there is considerable scatter at 25°C. The spread in the yield strengths of weld metal are shown in Fig. 2. Lots 5 and 7 were submerged arc welds, but their properties fall at the extremes. Lot 11 was a shielded metal arc weld, and its strength is close to that of submerged arc Lot 7. There is no obvious explanation for this variation in properties. The yield strengths of the three lots of transverse weld specimens are shown in Fig. 3. There is some variation in strength between the three lots, and the strength order is not the same as that shown in Fig. 1 for the base metal.

The minimum yield strength curves are shown in Fig. 4 for the 12 lots of material. These data have not been treated in any special way but are the lowest curves selected from Figs. 1, 2, and 3. The weakest weld metal was Lot 5, and the weakest transverse weld samples were from Lot 4. Comparison of the minimum curves in Fig. 4 shows that the order of yield strengths from least to greatest is base metal, transverse weld samples, and weld metal samples.

Curves are shown in Figs. 5, 6, and 7 for the yield strength determined at the slower strain rate ($0.27 \times 10^{-4}s^{-1}$). Curves are shown in Fig. 5 for the base metal, Fig. 6 for the weld metal, and Fig. 7 for the transverse weld specimens. The relative positions of the curves are similar to those noted in Figs. 1, 2, and 3 at the higher strain rate of $1.3 \times 10^{-4}s^{-1}$. The minimum curves from Figs. 5, 6, and 7 are shown in Fig. 8. The base metal (Lot 6) is the weakest, the transverse weld samples (Lot 8) are next highest, and the weld metal (Lot 5) is the strongest.

The ultimate tensile strengths of the various lots of base metal are shown in Fig. 9. Lot 1, which was heat treated to obtain the maximum allowable strength, is significantly stronger, but the other lots of material fall in a rather narrow band. The tensile strengths of the three lots of weld metal are shown in Fig. 10. The strengths of the two submerged arc welds fall at the extremes, and the shielded-metal arc weld has intermediate strength. The transverse weld sample properties are shown in Fig. 11. The spread in strengths between the three lots of material is very small.

The minimum ultimate tensile strength curves at the higher strain rate of $1.3 \times 10^{-4}s^{-1}$ are shown in Fig. 12. The spread in strength is rather small, but Lot 6 base metal has the lowest strength, Lot 5 weld metal has the highest strength, and Lot 8 transverse weld specimens have intermediate strength.

The ultimate strength curves at the lower strain rate of $0.27 \times 10^{-4}s^{-1}$ are shown in Fig. 13 for the base metal. Lot 1 has significantly higher properties, but the properties of the other base metals fall in a rather narrow band. The ultimate tensile strengths of the two submerged arc welds are shown in Fig. 14. There is a variation in strength of about 10% between the two lots of weld metal. The ultimate tensile strengths of the three lots of transverse weld specimens are shown in Fig. 15. The spread in strengths is quite small.

The minimum ultimate tensile strength curves at the lower strain rate of $0.27 \times 10^{-4}s^{-1}$ are shown in Fig. 16. The variation in strengths is small, but the order from weakest to strongest is base metal Lot 6, transverse weld samples Lot 4, and weld samples Lot 5.

The effect of strain rate on the yield and ultimate tensile strengths for Lot 6 base metal is shown in Figs. 17 and 18. The peak in strength predicted by the curves near 200°C is not real but is a result of the lack of data between 25 and 371°C. The yield and ultimate tensile strengths show an effect of strain rate at test temperatures of 538 and 593°C; there is no systematic influence of strain rate at lower temperatures.

The fracture elongation of all samples exceeded the 18% minimum required by the code. (See Tables 5 through 16 for exact values.) The reduction of area was about 75% for most samples.

MEASURED CREEP PROPERTIES

The creep results obtained thus far are summarized in Tables 17 through 20. A "D" after the discontinued time in the "T-R (time to rupture)" column indicates that the test was discontinued prior to rupture. Tests that do not have a reduction in area noted in the last column of each

table are still in progress. The creep results indicate, as did the tensile properties, that the order of strengths from least to greatest is the base metal, the transverse weld specimens, and the weld metal.

The time to 1% strain for Lots 1, 2, and 3 is correlated by use of the Larson-Miller parameter in Fig. 19. Lot 1 was heat treated by ORNL to the maximum allowable tensile strength, Lot 2 was heat treated by ORNL to the lowest allowable tensile strength, and Lot 3 was given the standard heat treatment by CE (Table 3). Lots 1, 2, and 3 were from the same heat of material. The line in Fig. 19 was fit to the Lot 3 data with a second-order polynomial. The Lot 1 data points, except one, fall above the line, indicating higher creep strength for Lot 1. The data for Lots 2 and 3 are interspersed, and there appears to be little, if any, difference in the creep strengths of the two lots.

The data for the base metal heat treated by CE (Lots 3, 6, 9, and 12) were analyzed as a group. There were 34 data points for the time to 1% strain. Similar analyses will be performed for the transverse weld and weld metal samples when more data become available; however, the design stresses probably will be determined by the properties of the base metal. The data for the four lots of base metal (all receiving the CE standard heat treatment) are shown in Fig. 20. The data were fit with a second-order polynomial on a Larson-Miller plot to give the average properties.

These same data were treated statistically to obtain the minimum properties using the premise that the minimum properties were less than the average properties by 1.65 times the standard deviation. The data in Fig. 20 were fit on the basis of the stress being the independent variable and the Larson-Miller Parameter (K/1000) (20 + log t) being the dependent variable, where K is the absolute temperature in degrees Kelvin and t is the time in hours. The standard deviation was determined to be 0.7453, and this value was used to establish the curve for minimum properties in Fig. 21. The crossover at the left side of the figure does not have any physical significance.

Because the test program has emphasized good definition of the stress-temperature-time relationships to low strains, most of the tests have not been taken to rupture. However, the rupture and tertiary creep data for Lots 3, 6, 9, and 12 were used to obtain estimates of the average properties. Eighteen data points were available for tertiary creep (intersection of line parallel and offset 0.2% from minimum creep rate with creep curve), and these are shown in Fig. 22. There were nine data points for rupture, and these are shown in Fig. 23.

The time to 1% strain is shown in Fig. 24 as a function of the time to rupture. The data are not distributed well enough to obtain a very accurate correlation, but they are approximated by the line shown in Fig. 24, represented by the equation

$$(T-1) = 0.688(T-R)^{0.874} \quad .$$

A similar correlation is shown in Fig. 25 for the time to tertiary creep as a function of the time to rupture. The line shown in Fig. 25 is represented by the equation

$$(T-t) = 1.48(T-R)^{0.83} \quad .$$

The symbols all have units of time; specifically, T-1 is the time to 1% strain, T-t is the time to the beginning of tertiary creep, and T-R is the time to rupture.

The fracture strain of the base metal samples is very dependent on test temperature, with higher temperatures favoring higher strains. The fracture strains from 10 base metal tests are shown as a function of rupture time in Fig. 26. The horizontal line is at 18% strain, and two tests fall at this minimum value; all other tests failed at higher strains. Even the 18% value is quite high compared with the 1% limit imposed by design.

Correlations were developed for base metal on the basis of 1% strain (average strength), 1% strain (minimum strength), and tertiary creep and rupture strengths based on average properties. These correlations were used to obtain allowable stresses at various temperatures based on a design life of 1000 h. These data are summarized in Fig. 27 for the four lots of base metal (Lots 3, 6, 9, and 12). The order of design stress at a given temperature from highest to lowest stress is based on rupture (average), tertiary creep (average), 1% strain (minimum), and 1% strain (average).

The three curves for the three lots of weld metal are shown in Fig. 28. The data points for the three lots fall rather close together, so they were fit as a single set of data (Fig. 29). The three individual curves for the three lots of transverse weld specimens are shown in Fig. 30. The spread between the three lots is quite small, so these data were combined as a single set to obtain the correlation shown in Fig. 31.

The comparative strengths of base, transverse weld, and weld metal specimens are shown in Fig. 32. The base metal and the transverse weld specimens have about the same creep strengths. The weld metal is slightly stronger.

TEMPER EMBRITTLEMENT

Most of the temper embrittlement studies of this alloy show that embrittlement is associated with the enrichment of grain boundaries with impurities such as phosphorus during welding. The worst embrittlement was noted in the heat-affected zone.[4-7] The heats of commercial material currently being evaluated are quite low in residual impurities such as phosphorus (Table 2), so it is not very likely that commercial heats of this material produced to the chemical specifications for nuclear use in Section II of the code will be susceptible to temper embrittlement. However, a small program is being carried out to demonstrate this point. In the meantime, it was felt that tensile tests at 25°C on creep samples discontinued after a few percent strain would reveal any significant embrittlement.

The results of tensile tests at 25°C on samples from discontinued creep tests are shown in Table 21. The creep tests involved exposures up to 7292 h to temperatures ranging from 371 to 593°C. The tensile results for samples that had only been heat treated before tensile testing are given in Table 21 for comparison. The ductilities (elongation and reduction of area) are higher for the samples creep tested before tensile testing than those tensile tested without the creep test history. Thus,

there is no indication of temper embrittlement in these materials based on these tests.

DISCUSSION

The data available are sufficient for only part of the analytical analyses necessary to determine allowable stresses at various temperatures. Numerous tests are in progress, and the data base will increase markedly over the next few months.

The tensile data indicate significant differences in strength, with base metal having the lowest, weld metal having the highest, and transverse weld metal samples falling in between. Under creep conditions, the spread in strengths is much smaller than in short-term tensile tests. Base metal and transverse weld samples have equivalent strengths, but weld metal is slightly stronger.

The Larson-Miller parameter with a second-order polynomial fit of the data has been used extensively in analyzing the data. This method has appeared satisfactory, but the data at parameter values of about 20 do not fit well. The data in this region will determine the design stress at 538°C, so it may be necessary to alter the analytical methods being used.

SUMMARY

Three lots of SA533 Grade B Class 1 plate were procured and are being evaluated. Two submerged arc welds and one shielded-metal arc weld were also procured for evaluation. Tensile tests were run on all materials at 25, 371, 427, 482, 538, and 593°C at two strain rates. These tests indicate that the short-term tensile strength varies appreciably, with base metal having the lowest strength and weld metal the highest strength. Transverse weld samples have intermediate strength. Numerous creep tests are complete on these materials, others are in progress, and still others remain to be started. The indication thus far is that the spread in strengths is smaller than noted in short-term tensile tests. Base metal and transverse weld samples have equivalent creep strength, and weld metal is slightly stronger.

Creep samples tested to fracture have fracture strains in excess of 18%. Several discontinued creep samples were subjected to short-term tension tests, and there was no evidence of embrittlement as a result of the creep exposure. A program to more systematically evaluate whether temper embrittlement occurs in this material is in progress.

ACKNOWLEDGMENTS

Research is sponsored by the Office of Advanced Reactor Programs, Division of HTGRs, U.S. Department of Energy, under contract DE-AC05-84OR21400 with Martin Marietta Energy Systems, Inc.

The author is grateful to P. L. Rittenhouse for programmatic direction and to C. R. Brinkman for technical assistance. Nancy Cole, CE, Chattanooga, Tenn., was very helpful in providing the test materials. D. F. Wilson and D. J. Alexander reviewed the manuscript and provided several helpful suggestions. Several technicians provided their expertise, including R. H. Baldwin, T. P. Kirkland, and H. D. Upton. The draft was typed by C. Erickson, and the final manuscript was prepared by B. Q. Bridges.

REFERENCES

1. *ASME Boiler and Pressure Vessel Code*, Section III, July 1, 1986, American Society of Mechanical Engineers.

2. *ASME Boiler and Pressure Vessel Code*, Section II, July 1, 1986, American Society of Mechanical Engineers.

3. "Metals – Mechanical Testing; Elevated and Low-Temperature Tests," in *1984 Annual Book of ASTM Standards, Vol. 03.01*, American Society for Testing Materials.

4. Masayoshi Haseguawa, Nobuya Nakajima, Nobuharw Kusunoki, and Kazuhiro Suzuki, "Effects of Copper and Phosphorus on Temper Embrittlement of Mn-Mo-Ni Low Alloy Steel (ASTM A533-B)," *Trans. Jpn. Inst. Met.* 16, 641–46 (1975).

5. S. G. Druce and B. C. Edwards, "On the Temper Embrittlement of Manganese-Molybdenum-Nickel Steels," *Nucl. Technol.* 55, 487–98 (November 1981).

6. W. A. Logsdon, "The Influence of Long-Time Stress Relief Treatments on the Dynamic Fracture Toughness Properties of ASME SA508 Cl 2a and ASME SA533 Gr B Cl 2 Pressure Vessel Steels," *J. Mater. Energy Sys.* 3(4), 39–50 (March 1982).

7. S. G. Druce, G. Gage, and G. Jordan, "Effect of Aging on Properties of Pressure Vessel Steels," *Acta Metall.* 34(4), 641–52 (1986).

Table 1. Summary of test materials

Heat number	Vendor	Plate thickness		Evaluated as[a]		
		cm	in.	BM	SA weld	SMA weld
D9583	Lukens	8.9	3.5	X	X	X
C5975	Lukens	24.9	9.625	X	X	
64535-1	Marrel Freres	24.5	9.625	X		

[a]BM = base metal, SA = submerged arc weldment, and SMA = shielded metal arc weldment.

Table 2. Summary of product chemical analyses

Element	Code specified[a]	Heat								
		D9583[b] (Lukens)	D9583[b] (CE)	D9583[c] (CE)	64535-1[b] (M. Freres)	64535-1[b] (CE)	C5795[b] (Lukens)	C5795[b] (CE)	C5795[c] (CE)	D9583[d] (CE)
C	0.25 (max)	0.19	0.18	0.11	0.22	0.21	0.20	0.22	0.13	0.10
Mn	1.07-1.62	1.31	1.27	1.41	1.45	1.43	1.45	1.44	1.53	1.27
P	0.015 (max)	0.012	0.010	0.008	0.009	0.006	0.01	0.008	0.009	0.008
S	0.018 (max)	0.003	0.002	0.006	0.006	0.004	0.015	0.021	0.015	0.014
Cu	0.12 (max)		0.08	0.04	0.04	0.04	0.07	0.06	0.04	
V	0.06		0.004	0.003	<0.005	0.001		0.003	0.004	0.008
Si	0.13-0.45	0.22	0.21	0.45	0.19	0.21	0.23	0.25	0.45	0.35
Mo	0.41-0.64	0.57	0.52	0.55	0.52	0.51	0.54	0.58	0.57	0.48
Ni	0.37-0.73	0.69	0.76	0.13	0.62	0.62	0.65	0.66	0.12	0.03
Cr		0.10	0.06			0.04		0.08	0.14	0.03
Cb, Ti, W		<0.01	<0.01			<0.01		<0.01	<0.01	<0.029
Co		0.01	0.013			0.014		0.016	0.011	0.005
Al		0.026	0.01		0.019			0.022	0.011	0.005
B		0.001	<0.001		<0.001			<0.001	0.001	<0.001
As, Sn		0.005	<0.01		<0.020			<0.007	<0.007	<0.005
Zr		<0.001	<0.001		<0.001			<0.001	<0.001	<0.001
N			0.006					0.01	0.006	

[a]ASME, Section II, Standard Chemical Requirements plus Special Reactor Beltline Requirements for Cu, P, S, and V.

[b]Base metal.

[c]Weld metal deposited by submerged arc process.

[d]Weld metal deposited by the shielded-metal arc process.

Table 3. Specimen lot designations
(modified heat number used in report)

Vendor heat number	Modified heat number	Form[a]	Heat treatment[b]	Lot number
D9583	9583A	BM	ORNL HT 1	1
D9583	9583A	BM	ORNL HT 2	2
D9583	9583A	BM	CE-STD	3
D9583	9583A	TW-SA	CE-STD	4
D9583	9583A	WM-SA	CE-STD	5
C5795	5795	BM	CE-STD	6
C5795	5795	WM-SA	CE-STD	7
C5795	5795	TW-SA	CE-STD	8
D9583	9583B	BM	CE-STD	9
D9583	9583B	TW-SMA	CE-STD	10
D9583	9583B	WM-SMA	CE-STD	11
64535-1	64535	BM	CE-STD	12

[a]BM - base metal specimen; TW - transverse weld specimen, fusion line in specimen center; WM - weld metal specimen; SA - weld made by the submerged arc process; and SMA - weld made by shielded metal arc process.

[b]ORNL HT 1 - 1 h/871°C/WQ/4 h/663°C; ORNL HT 2 - 1 h/871°C/WQ/30 h/663°C; and CE-STD - 2.5 h/871°C/WQ/ 2.5 h/663°C/20 h/607°C.

Table 4. Tensile properties specified by code and measured after various heat treatments

	Yield strength		Ultimate tensile strength		Elongation (%)
	MPa	ksi	MPa	ksi	
Code-specified	345 min	50 min	552–689	80–100	18 min
Heat-treated					
1 h/871°C/4 h/663°C[a] (1 h/1600°F/4 h/1225°F)	641 599	93.0 86.9	705 667	102.2 96.8	26.7 30.0
1 h/871°C/30 h/663°C[b] (1 h/1600°F/30 h/1225°F)	492	71.3	578	83.8	33.0
1 h/871°C/50 h/663°C (1 h/1600°F/50 h/1225°F)	426	61.8	518	75.2[c]	33.7
2.5 h/871°C/2.5 h/663°C/ 20 h/607°C[d] (2.5 h/1600°F/2.5 h/1225°F/ 20 h/1125°F)	492	71.3	621	90.1	35.0

[a]ORNL HT 1.

[b]ORNL HT 2.

[c]Below code minimum.

[d]CE HT.

Table 5. Tensile test of A533 base metal heat treated by ORNL HT 1 (Lot 1)

Specimen	Test temperature		Strain rate		Modulus		Yield strength		Tensile strength		Total elongation (%)	Uniform elongation (%)	Reduction of area (%)
	°C	°F	$10^{-4}s^{-1}$	$10^{-3}min^{-1}$	GPa	10^6 psi	MPa	ksi	MPa	ksi			
504	24	75	1.3	8.0	210	30.5	599	86.9	668	96.8	29.95	9.98	76.47
526	24	75	1.3	8.0	231	33.5	641	93.0	705	102.2	26.72	8.05	74.88
529	24	75	1.3	8.0	224	32.4	621	90.1	707	102.5	25.70	7.30	74.94
505	24	75	0.27	1.6	215	31.2	604	87.6	676	98.0	29.30	8.24	76.68
527	24	75	0.27	1.6	228	33.0	641	93.0	700	101.5	26.21	7.99	74.54
530	24	75	0.27	1.6	211	30.7	649	94.1	707	102.6	26.50	7.87	74.58
506	371	700	1.3	8.0	193	28.0	531	77.0	636	92.2	24.60	6.85	74.60
508	371	700	1.3	8.0	179	25.9	497	72.1	609	88.3	25.30	6.93	76.76
507	371	700	0.27	1.6	114	16.5	525	76.2	629	91.3	23.39	4.79	74.48
509	371	700	0.27	1.6	165	23.9	488	70.8	607	88.0	28.53	7.05	76.57
519	427	800	1.3	8.0	159	23.0	462	67.0	562	81.6	27.78	4.74	78.70
522	427	800	1.3	8.0	162	23.5	476	69.0	569	82.6	24.80	5.59	78.57
516	427	800	0.27	1.6	153	22.3	482	69.9	559	81.0	23.50	3.31	77.71
517	427	800	0.27	1.6	169	24.5	478	69.3	549	79.6	26.40	3.96	76.94
523	482	900	1.3	8.0	189	27.4	434	62.9	489	70.9	30.25	4.32	83.23
525	482	900	1.3	8.0	224	32.5	454	65.9	502	72.8	24.48	2.15	81.82
520	482	900	0.27	1.6	241	35.0	427	61.9	483	70.1	33.60	1.91	82.47
521	482	900	0.27	1.6	172	24.9	446	64.7	486	70.6	25.58	1.72	82.39
510	538	1000	1.3	8.0	151	21.9	376	54.6	411	59.6	33.51	1.40	85.58
512	538	1000	1.3	8.0	123	17.9	389	56.4	410	59.5	32.38	0.89	83.48
511	538	1000	0.27	1.6	107	15.6	331	48.1	368	53.4	46.51	1.16	84.20
513	538	1000	0.27	1.6	88	12.8	348	50.5	376	54.5	54.45	1.19	83.03
538	593	1100	1.3	8.0	100	14.6	286	41.5	307	44.5	57.15	1.62	82.30
539	593	1100	0.27	1.6	88	12.7	177	25.7	236	34.2	61.40	0.70	80.30

Table 6. Tensile test of A533 base metal heat treated by ORNL HT 2 (Lot 2)

Specimen	Test temperature		Strain rate		Modulus		Yield strength		Tensile strength		Total elongation (%)	Uniform elongation (%)	Reduction of area (%)
	°C	°F	$10^{-4}s^{-1}$	$10^{-3}min^{-1}$	GPa	10^6 psi	MPa	ksi	MPa	ksi			
905	24	75	6.7	40.0	185	26.9	491	71.3	578	83.8	33.00	11.54	78.56
910	24	75	6.7	40.0	210	30.5	478	69.3	597	86.6	32.10	12.38	77.09
911	24	75	6.7	40.0	218	31.6	470	68.2	593	86.0	32.25	11.47	77.67
920	24	75	0.27	1.6	214	31.0	485	70.3	582	84.4	31.10	11.16	77.84
912	371	700	6.7	40.0	189	27.3	393	57.0	551	80.0	35.72	11.30	78.61
921	371	700	0.27	1.6	216	31.3	370	53.7	539	78.1	30.11	9.60	74.96
913	427	800	6.7	40.0	189	27.4	371	53.8	495	71.8	32.55	8.84	79.02
922	427	800	0.27	1.6	144	20.9	357	51.8	479	69.5	32.50	7.66	80.14
914	482	900	6.7	40.0	193	27.9	346	50.2	419	60.8	32.28	6.31	82.13
923	482	900	0.27	1.6	167	24.2	329	47.7	392	56.8	36.25	4.15	84.21
915	538	1000	6.7	40.0	157	22.8	322	46.7	357	51.7	41.70	3.19	87.01
924	538	1000	0.27	1.6	125	18.1	283	41.0	314	45.5	47.70	1.39	77.55
916	593	1100	6.7	40.0	132	19.2	254	36.9	282	40.9	59.25	1.19	89.89
925	593	1100	0.27	1.6	84	12.2	174	25.2	220	31.9	62.00	1.23	88.15

Table 7. Tensile test of A533 base metal heat treated by CE (Lot 3)

Specimen	Test temperature		Strain rate		Modulus		Yield strength		Tensile strength		Total elongation (%)	Uniform elongation (%)	Reduction of area (%)
	°C	°F	$10^{-4}s^{-1}$	$10^{-3}min^{-1}$	GPa	10^6 psi	MPa	ksi	MPa	ksi			
600	24	75	1.3	8.0	238	34.5	492	71.3	624	90.5	31.65	9.20	73.93
601	24	75	1.3	8.0	199	28.8	491	71.2	619	89.7	29.32	9.73	75.14
602	24	75	0.27	1.6	255	37.0	478	69.3	604	87.6	29.66	9.20	74.58
603	24	75	0.27	1.6	208	30.2	562	81.5	663	96.1	29.30	8.47	75.61
604	371	700	1.3	8.0	191	27.7	407	59.1	547	79.3	29.59	8.30	77.34
605	371	700	1.3	8.0	221	32.1	413	59.9	553	80.2	28.35	8.82	76.51
606	371	700	0.27	1.6	201	29.2	461	66.9	574	83.2	26.18	5.67	75.55
607	371	700	0.27	1.6	199	28.9	410	59.4	562	81.6	29.00	9.45	77.26
609	427	800	1.3	8.0	192	27.8	392	56.8	494	71.6	29.75	6.72	80.47
610	427	800	1.3	8.0	213	30.8	427	61.9	513	74.4	27.10	5.25	81.37
611	427	800	0.27	1.6	136	19.7	346	50.2	508	73.7	28.60	6.82	81.22
612	427	800	0.27	1.6	183	26.6	438	63.5	510	74.0	18.00	3.60	80.43
613	482	900	1.3	8.0	125	18.1	334	48.5	453	65.6	30.25	4.69	84.33
614	482	900	1.3	8.0	165	24.0	378	54.8	435	63.1	30.28	3.48	83.50
615	482	900	0.27	1.6	127	18.4	362	52.5	415	60.2	33.40	6.14	82.55
616	482	900	0.27	1.6	183	26.5	368	53.4	414	60.2	36.15	3.06	85.39
617	538	1000	1.3	8.0	146	21.2	334	48.5	359	52.1	36.58	2.12	86.01
618	538	1000	1.3	8.0	161	23.4	334	48.3	363	52.6	35.45	1.72	84.95
619	538	1000	1.27	1.6	82	12.0	317	46.0	331	48.0	41.90	1.60	84.06
620	538	1000	0.27	1.6	119	17.3	321	46.5	341	49.4	42.40	1.15	84.80
630	593	1100	1.3	8.0	80	11.5	264	38.3	281	40.8	37.65	0.86	78.92
631	593	1100	1.3	8.0	110	16.0	257	37.3	282	40.9	66.42	0.78	87.91
632	593	1100	0.27	1.6	61	8.9	212	30.8	240	34.8	55.65	1.13	73.50
633	593	1100	0.27	1.6	47	6.9	209	30.3	240	34.8	45.08	1.09	71.34

Table 8. Tensile test of A533 transverse weld (HT 9583A) heat treated by CE (Lot 4)

Specimen	Test temperature		Strain rate		Modulus		Yield strength		Tensile strength		Total elongation (%)	Uniform elongation (%)	Reduction of area (%)
	°C	°F	$10^{-4}s^{-1}$	$10^{-3}min^{-1}$	GPa	10^6 psi	MPa	ksi	MPa	ksi			
700T	24	75	1.3	8.0	213	30.9	519	75.3	621	90.0	26.50	8.98	77.93
701T	24	75	1.3	8.0	227	32.9	511	74.1	622	90.2	24.75	6.69	75.04
702T	24	75	0.27	1.6	227	32.9	505	73.3	609	88.4	20.02	7.55	66.56
703T	24	75	0.27	1.6	231	33.5	509	73.9	616	89.3	26.78	8.83	67.76
704T	371	700	1.3	8.0	190	27.5	430	62.3	572	83.0	22.35	8.60	65.75
705T	371	700	1.3	8.0	245	35.5	424	61.5	565	82.0	27.18	8.21	77.23
706T	371	700	0.27	1.6	201	29.2	422	61.2	561	81.4	25.00	6.30	78.17
707T	371	700	0.27	1.6	195	28.3	429	62.2	564	81.8	21.49	6.02	75.87
709T	427	800	1.3	8.0	173	25.1	422	61.3	516	74.8	23.09	4.72	78.31
710T	427	800	1.3	8.0	188	27.3	406	58.9	505	73.2	24.10	4.60	79.94
711T	427	800	0.27	1.6	196	28.4	416	60.3	509	73.9	18.30	4.06	78.66
712T	427	800	0.27	1.6	233	33.7	405	58.7	498	72.2	24.18	3.95	80.49
714T	482	900	1.3	8.0	180	26.1	376	54.5	445	64.6	21.50	2.62	81.52
715T	482	900	1.3	8.0	160	23.3	353	51.1	447	64.8	26.00	3.09	83.84
716T	482	900	0.27	1.6	159	23.0	383	55.6	428	62.0	22.12	2.01	80.68
717T	482	900	0.27	1.6	136	19.8	368	53.4	426	61.7	20.50	2.19	82.29
718T	538	1000	1.3	8.0	176	25.6	334	48.5	376	54.5	24.55	1.46	83.52
719T	538	1000	1.3	8.0	141	20.4	341	49.4	377	54.6	21.32	1.38	82.60
720T	538	1000	0.27	1.6	179	25.9	335	48.6	351	50.9	25.05	0.87	81.23
721T	538	1000	0.27	1.6	149	21.5	328	47.6	349	50.6	25.90	1.15	84.16
724T	593	1100	1.3	8.0	134	19.5	258	37.5	293	42.5	26.90	0.28	84.61
725T	593	1100	1.3	8.0	103	14.9	268	38.9	285	41.4	29.33	0.75	86.79
726T	593	1100	0.27	1.6	83	12.3	205	29.7	235	34.0	25.10	1.01	81.51
727T	593	1100	0.27	1.6	71	10.3	229	33.2	253	36.7	28.18	0.95	80.59

Table 9. Tensile test of A533 weld metal (HT 9583A) heat treated by CE (Lot 5)

Specimen	Test temperature		Strain rate		Modulus		Yield strength		Tensile strength		Total elongation	Uniform elongation	Reduction of area
	°C	°F	$10^{-4}s^{-1}$	$10^{-3}min^{-1}$	GPa	10^6 psi	MPa	ksi	MPa	ksi	(%)	(%)	(%)
800	24	75	1.3	8.0	213	30.9	517	74.9	615	89.2	28.31	9.57	66.42
801	24	75	1.3	8.0	211	30.6	517	74.9	621	90.0	28.99	10.15	66.41
802	24	75	0.27	1.6	221	32.0	500	72.5	607	88.0	28.80	9.55	66.96
803	24	75	0.27	1.6	231	33.6	500	72.5	608	88.2	28.99	9.59	67.47
804	371	700	1.3	8.0	218	31.7	432	62.6	571	82.8	25.61	8.70	67.04
805	371	700	1.3	8.0	203	29.5	459	66.5	579	84.0	25.80	8.03	66.74
806	371	700	0.27	1.6	215	31.2	438	63.6	573	83.1	26.35	7.41	66.61
807	371	700	0.27	1.6	221	32.1	428	62.0	570	82.7	25.00	8.33	67.62
808	427	800	1.3	8.0	207	30.1	423	61.4	530	76.9	26.40	6.54	69.43
809	427	800	1.3	8.0	176	25.5	411	59.7	520	75.5	25.88	7.61	68.24
810	427	800	0.27	1.6	221	32.1	418	60.6	525	76.2	24.51	5.94	65.74
811	427	800	0.27	1.6	211	30.6	425	61.6	532	77.1	26.40	6.38	65.79
814	482	900	1.3	8.0	150	21.7	388	56.2	474	68.8	28.80	5.48	71.44
815	482	900	1.3	8.0	174	25.2	372	53.9	469	68.0	29.39	6.21	72.51
816	482	900	0.27	1.6	228	33.1	383	55.5	456	66.2	31.70	5.57	72.59
817	482	900	0.27	1.6	211	30.7	391	56.7	460	66.8	31.40	4.65	72.10
819	538	1000	1.3	8.0	215	31.2	372	53.9	408	59.2	34.49	2.53	77.79
820	538	1000	1.3	8.0	155	22.5	376	54.6	411	59.6	40.02	2.39	77.76
821	538	1000	0.27	1.6	164	23.8	339	49.1	374	54.2	30.35	2.15	73.82
822	538	1000	0.27	1.6	159	23.0	344	49.9	371	53.8	36.10	2.52	76.13
828	593	1100	1.3	8.0	102	14.8	308	44.7	319	46.2	56.12	0.99	81.21
829	593	1100	1.3	8.0	94	13.6	312	45.2	321	46.6	49.85	1.08	81.99
830	593	1100	0.27	1.6	151	21.9	254	36.8	281	40.8	56.35	1.07	63.61
831	593	1100	0.27	1.6	121	17.5	264	38.2	276	40.0	47.45	1.09	75.38

Table 10. Tensile test of A533B base metal (HT 5795) heat treated by CE (Lot 6)

Specimen	Test temperature		Strain rate		Modulus		Yield strength		Tensile strength		Total elongation	Uniform elongation	Reduction of area
	°C	°F	$10^{-4}s^{-1}$	$10^{-3}min^{-1}$	GPa	10^6 psi	MPa	ksi	MPa	ksi	(%)	(%)	(%)
B101	24	75	1.3	8.0	242	35.1	432	62.6	578	83.9	30.95	11.47	70.44
B102	24	75	1.3	8.0	202	29.3	451	65.4	596	86.4	30.95	11.33	68.09
B103	24	75	0.27	1.6	197	28.5	434	63.0	583	84.5	29.20	10.12	67.04
B104	24	75	0.27	1.6	226	32.8	429	62.2	569	82.5	30.10	10.86	67.83
B105	371	700	1.3	8.0	156	22.6	365	53.0	543	78.7	27.65	10.20	70.27
B106	371	700	1.3	8.0	118	17.1	366	53.1	539	78.1	30.15	9.86	72.56
B107	371	700	0.27	1.6	133	19.3	391	56.6	552	80.1	29.00	8.45	71.99
B108	371	700	0.27	1.6	156	22.7	409	59.4	560	81.3	28.35	8.25	71.85
B109	427	800	1.3	8.0	174	25.3	361	52.3	472	68.5	31.50	7.12	76.93
B110	427	800	1.3	8.0	108	15.6	398	57.7	494	71.7	29.22	7.98	73.88
B111	427	800	0.27	1.6	186	26.9	379	55.0	498	72.3	27.99	CHART	74.52
B112	427	800	0.27	1.6	123	17.9	340	49.4	479	69.4	32.60	7.70	75.14
B113	482	900	1.3	8.0	158	22.9	339	49.2	433	62.7	29.25	5.91	76.19
B114	482	900	1.3	8.0	150	21.7	311	45.1	419	60.8	34.51	6.72	78.08
B115	482	900	0.27	1.6	155	22.4	336	48.8	419	60.8	34.00	4.42	77.61
B116	482	900	0.27	1.6	107	15.6	315	45.7	404	58.6	39.60	5.95	80.38
B117	538	1000	1.3	8.0	109	15.8	312	45.2	361	52.4	43.60	3.77	82.67
B118	538	1000	1.3	8.0	105	15.3	320	46.4	368	53.4	45.75	2.38	81.25
B119	538	1000	0.27	1.6	116	16.9	299	43.3	332	48.2	51.75	2.68	72.46
B120	538	1000	0.27	1.6	104	15.1	283	41.0	325	47.1	48.60	3.44	77.62
B121	593	1100	1.3	8.0	95	13.7	245	35.5	273	39.6	55.88	1.58	77.36
B122	593	1100	1.3	8.0	97	14.1	258	37.5	277	40.1	63.40	1.27	76.81
B123	593	1100	0.27	1.6	102	14.8	201	29.2	235	34.1	56.53	0.76	58.44
B124	593	1100	0.27	1.6	103	15.0	224	32.5	250	36.3	59.72	1.08	56.37

Table 11. Tensile properties of A533B all weld metal (HT 5795) heat treated by CE (Lot 7)

Specimen	Test temperature		Strain rate		Modulus		Yield strength		Tensile strength		Total elongation (%)	Uniform elongation (%)	Reduction of area (%)
	°C	°F	$10^{-4}s^{-1}$	$10^{-3}min^{-1}$	GPa	10^6 psi	MPa	ksi	MPa	ksi			
B307	24	75	1.3	8.0	216	31.3	608	88.1	699	101.4	28.70	9.02	65.73
B308	24	75	1.3	8.0	222	32.3	582	84.3	673	98.1	26.35	8.23	66.88
B309	24	75	0.27	1.6	254	36.8	588	85.3	683	99.0	27.00	7.72	66.78
B310	24	75	0.27	1.6	207	30.0	615	89.1	687	99.6	25.30	7.61	67.37
B311	371	700	1.3	8.0	201	29.2	506	73.3	639	92.7	26.75	8.30	67.66
B312	371	700	1.3	8.0	200	29.1	506	73.4	638	92.6	23.90	7.07	68.61
B313	371	700	0.27	1.6	159	23.1	493	71.5	621	90.1	25.40	7.84	67.33
B314	371	700	0.27	1.6	192	27.8	500	72.6	634	92.0	22.90	7.31	65.67
B315	427	800	1.3	8.0	186	27.0	462	67.1	577	83.7	26.28	6.55	70.33
B316	427	800	1.3	8.0	168	24.4	456	66.1	563	81.7	23.20	6.46	56.68
B317	427	800	0.27	1.6	177	25.7	472	68.5	560	81.2	25.25	5.74	70.64
B318	427	800	0.27	1.6	153	22.2	463	67.2	566	82.0	25.02	6.20	68.14
B319	482	900	1.3	8.0	156	22.6	449	65.1	509	73.8	30.35	6.26	73.00
B320	482	900	1.3	8.0	149	21.6	457	66.3	523	75.8	27.08	5.08	70.58
B321	482	900	0.27	1.6	148	21.4	451	65.4	507	73.5	33.10	4.66	74.70
B322	482	900	0.27	1.6	142	20.6	441	64.0	492	71.3	33.35	4.51	71.03
B323	538	1000	1.3	8.0	141	20.4	396	57.4	430	62.3	41.40	1.68	77.47
B324	538	1000	1.3	8.0	143	20.7	419	60.7	453	65.7	37.80	1.84	77.30
B325	538	1000	0.27	1.6	173	25.2	382	55.4	412	59.8	51.25	1.78	74.68
B326	538	1000	0.27	1.6	130	18.9	396	57.4	420	60.9	40.50	1.01	74.23
B331	593	1100	1.3	8.0	107	15.4	304	44.2	330	47.9	45.60	0.67	42.81
B332	593	1100	1.3	8.0	112	16.3	311	45.2	330	47.8	50.55	0.97	47.88
B333	593	1100	0.27	1.6	162	23.5	272	39.4	290	42.1	58.65	0.50	53.07
B334	593	1100	0.27	1.6	162	23.5	281	40.7	292	42.3	52.50	0.95	54.07

Table 12. Tensile properties of A533B transverse weld (HT 5795) heat treated by CE (Lot 8)

Specimen	Test temperature		Strain rate		Modulus		Yield strength		Tensile strength		Total elongation (%)	Uniform elongation (%)	Reduction of area (%)
	°C	°F	$10^{-4}s^{-1}$	$10^{-3}min^{-1}$	GPa	10^{6} psi	MPa	ksi	MPa	ksi			
B200T	24	75	1.3	8.0	212	30.8	483	70.0	647	93.8	22.03	6.79	57.21
B201T	24	75	1.3	8.0	194	28.2	472	68.5	630	91.4	21.75	6.38	62.55
B202T	24	75	0.27	1.6	207	30.1	463	67.1	631	91.5	19.80	5.89	62.57
B203T	24	75	0.27	1.6	202	29.2	480	69.6	643	93.3	21.75	6.30	61.48
B204T	371	700	1.3	8.0	162	23.5	411	59.7	567	82.2	21.25	5.66	72.09
B205T	371	700	1.3	8.0	190	27.5	417	60.4	572	83.0	21.70	5.48	68.46
B206T	371	700	0.27	1.6	176	25.5	434	62.9	576	83.5	18.00	5.13	65.17
B207T	371	700	0.27	1.6	177	25.7	423	61.3	578	83.8	19.30	5.54	67.61
B208T	427	800	1.3	8.0	189	27.5	413	60.0	515	74.7	20.65	3.79	73.29
B209T	427	800	1.3	8.0	209	30.2	399	57.9	508	73.6	22.10	2.96	73.74
B210T	427	800	0.27	1.6	188	27.3	402	58.3	497	72.1	21.00	3.22	78.32
B211T	427	800	0.27	1.6	257	37.2	470	68.2	497	72.1	22.50	3.62	77.45
B212T	482	900	1.3	8.0	149	21.6	387	56.2	445	64.6	23.75	2.91	77.08
B213T	482	900	1.3	8.0	190	27.5	377	54.7	435	63.1	22.85	2.74	78.91
B214T	482	900	0.27	1.6	123	17.9	373	54.2	428	62.1	21.75	1.69	76.75
B215T	482	900	0.27	1.6	146	21.1	355	51.6	423	61.3	26.65	3.76	78.29
B216T	538	1000	1.3	8.0	119	17.3	351	51.0	377	54.7	25.12	1.76	80.35
B217T	538	1000	1.3	8.0	150	21.8	317	45.9	357	51.7	31.65		81.56
B218T	538	1000	0.27	1.6	177	25.7	322	46.7	354	51.3	26.43	1.48	77.69
B219T	538	1000	0.27	1.6	195	28.3	323	46.9	353	51.3	24.30	1.50	76.14
B220T	593	1100	1.3	8.0	78	11.3	277	40.2	304	44.0	25.12	1.04	72.92
B221T	593	1100	1.3	8.0	106	15.4	291	42.3	299	43.4	24.30	0.82	77.56
B222T	593	1100	0.27	1.6	77	11.1	214	31.0	239	34.7	30.20	1.34	65.56
B223T	593	1100	0.27	1.6	127	18.4	245	35.6	262	38.0	20.30	0.96	67.05

Table 13. Tensile properties of A533B base metal (HT 9583B) heat treated by CE (Lot 9)

Specimen	Test temperature		Strain rate		Modulus		Yield strength		Tensile strength		Total elongation (%)	Uniform elongation (%)	Reduction of area (%)
	°C	°F	$10^{-4}s^{-1}$	$10^{-3}min^{-1}$	GPa	10^6 psi	MPa	ksi	MPa	ksi			
C100	24	75	1.3	8.0	231	33.5	582	84.3	652	94.6	30.55	9.11	76.31
C101	371	700	1.3	8.0	196	28.4	406	58.9	543	78.8	30.25	8.49	79.12
C102	427	800	1.3	8.0	178	25.8	399	57.9	495	71.8	28.20	6.54	81.69
C103	482	900	1.3	8.0	214	31.1	384	55.7	438	63.5	27.99	3.78	84.75
C104	538	1000	1.3	8.0	140	20.3	327	47.4	352	51.1	40.90	1.86	86.60
C105	593	1100	1.3	8.0	100	14.5	240	34.8	258	37.4	20.00[a]	1.02	82.94

[a]Specimen broke in gage marks.

Table 14. Tensile properties of A533B transverse weld (HT 9583B) heat treated by CE (Lot 10)

Specimen	Test temperature		Strain rate		Modulus		Yield strength		Tensile strength		Total elongation (%)	Uniform elongation (%)	Reduction of area (%)
	°C	°F	$10^{-4}s^{-1}$	$10^{-3}min^{-1}$	GPa	10^6 psi	MPa	ksi	MPa	ksi			
C200T	24	75	1.3	8.0	210	30.4	569	82.6	643	93.2	23.70	7.47	69.02
C201T	24	75	1.3	8.0	192	27.9	568	82.4	647	93.9	23.35	7.19	70.25
C202T	24	75	0.27	1.6	211	30.6	554	80.4	633	91.8	25.58	8.52	72.29
C203T	24	75	0.27	1.6	194	28.1	487	70.6	646	93.7	21.50	7.09	70.96
C204T	371	700	1.3	8.0	148	21.4	474	68.8	586	85.0	21.00	6.44	68.57
C205T	371	700	1.3	8.0	184	26.7	471	68.3	582	84.3	23.20	6.67	70.82
C206T	371	700	0.27	1.6	173	25.1	474	68.8	583	84.5	20.80	6.72	69.69
C207T	371	700	0.27	1.6	183	26.5	472	68.4	579	84.0	23.22	6.33	72.30
C208T	427	800	1.3	8.0	184	26.7	451	65.4	538	78.0	20.05	5.68	72.31
C209T	427	800	1.3	8.0	160	23.2	459	66.6	538	78.0	22.01	4.88	73.87
C210T	427	800	0.27	1.6	176	25.5	451	65.4	528	76.6	24.40	5.21	74.74
C211T	427	800	0.27	1.6	177	25.7	443	64.2	504	73.1	22.80	1.17	78.39
C212T	482	900	1.3	8.0	148	21.4	422	61.2	486	70.4	23.25	4.29	76.69
C213T	482	900	1.3	8.0	172	25.0	427	61.9	475	68.9	22.25	4.13	76.19
C214T	482	900	0.27	1.6	158	22.9	420	60.9	464	67.3	26.41	4.09	78.64
C215T	482	900	0.27	1.6	138	20.0	431	62.5	475	68.9	24.10	3.45	71.58
C216T	538	1000	1.3	8.0	180	26.1	379	55.0	409	59.3	28.40	1.84	80.01
C217T[a]	538	1000	1.3	8.0	172	25.0	374	54.3	407	59.1	17.90	2.50	76.26
C218T	538	1000	0.27	1.6	148	21.4	355	51.4	383	55.5	34.10	1.69	80.07
C219T	538	1000	0.27	1.6	166	24.0	357	51.7	382	55.4	29.61	1.46	80.89
C220T	593	1100	1.3	8.0	124	18.0	294	42.6	316	45.9	35.93	1.09	80.21
C221T[a]	593	1100	1.3	8.0	149	21.7	294	42.6	316	45.8	12.68	0.93	67.21
C222T	593	1100	0.27	1.6	94	13.7	267	38.7	284	41.1	38.80	1.16	79.68
C223T	593	1100	0.27	1.6	121	17.6	263	38.2	282	41.0	38.90	0.82	82.98

[a]Specimen broke outside of gage marks.

Table 15. Tensile properties of A533B weld metal (HT 9583B) heat treated by CE (Lot 11)

Specimen	Test temperature		Strain rate		Modulus		Yield strength		Tensile strength		Total elongation (%)	Uniform elongation (%)	Reduction of area (%)
	°C	°F	$10^{-4}s^{-1}$	$10^{-3}min^{-1}$	GPa	10^6 psi	MPa	ksi	MPa	ksi			
C300	24	75	1.3	8.0	214	31.1	606	87.9	670	97.2	26.75	9.81	60.82
C301	371	700	1.3	8.0	171	24.8	486	70.5	596	86.4	30.50	8.63	68.65
C302	427	800	1.3	8.0	144	20.9	464	67.3	544	78.8	23.15	6.42	74.45
C303	482	900	1.3	8.0	134	19.4	438	63.5	484	70.3	25.42	4.78	76.58
C304	538	1000	1.3	8.0	133	19.4	395	57.2	417	60.5	37.75	2.70	82.22
C305	593	1100	1.3	8.0	139	20.1	319	46.3	332	48.1	39.55	0.98	77.89

Table 16. Tensile properties of A533B base metal (HT 64535) heat treated by CE (Lot 12)

Specimen	Test temperature		Strain rate		Modulus		Yield strength		Tensile strength		Total elongation (%)	Uniform elongation (%)	Reduction of area (%)
	°C	°F	$10^{-4}s^{-1}$	$10^{-3}min^{-1}$	GPa	10^6 psi	MPa	ksi	MPa	ksi			
D100	24	75	1.3	8.0	244	35.3	478	69.3	607	88.0	30.50	12.45	71.51
D101	24	75	1.3	8.0	219	31.8	481	69.8	622	90.2	30.52	10.89	70.29
D102	24	75	0.27	1.6	212	30.8	485	70.3	621	90.1	29.40	10.20	69.99
D103	24	75	0.27	1.6	247	35.8	481	69.8	616	89.3	29.35	10.52	70.37
D104	371	700	1.3	8.0	148	21.5	400	58.0	551	80.0	27.95	10.34	72.00
D105	371	700	1.3	8.0	204	29.6	395	57.3	556	80.7	30.65	9.45	72.48
D106	371	700	0.27	1.6	229	33.3	402	58.3	552	80.1	30.65	8.64	74.60
D107	371	700	0.27	1.6	133	19.2	404	58.6	549	79.6	30.00	8.58	74.44
D108	427	800	1.3	8.0	161	23.4	387	56.1	491	71.2	32.28	7.94	77.98
D109	427	800	1.3	8.0	148	21.5	394	57.2	495	71.8	29.00	7.16	77.53
D110	427	800	0.27	1.6	212	30.7	385	55.8	486	70.5	32.61	7.43	78.35
D111	427	800	0.27	1.6	173	25.2	377	54.7	472	68.5	29.10	6.66	78.58
D112	482	900	1.3	8.0	166	24.1	358	52.0	432	62.6	34.20	5.44	82.00
D113	482	900	1.3	8.0	173	25.0	359	52.1	437	63.4	33.99	4.69	79.65
D114	482	900	0.27	1.6	102	14.8	371	53.8	416	60.3	41.85	3.54	81.78
D115	482	900	0.27	1.6	143	20.8	347	50.4	415	60.2	35.25	4.28	80.59
D116	538	1000	1.3	8.0	197	28.6	342	49.6	350	50.8	45.42	2.29	84.46
D117	538	1000	1.3	8.0	194	28.2	333	48.3	355	51.5	41.85	2.20	86.30
D118	538	1000	0.27	1.6	141	20.4	308	44.6	340	49.3	41.00	1.70	86.06
D119	538	1000	0.27	1.6	116	16.8	310	45.0	332	48.1	48.50	1.92	76.39
D120	593	1100	1.3	8.0	94	13.6	249	36.2	271	39.3	68.35	1.04	88.00
D121	593	1100	1.3	8.0	88	12.8	278	40.4	280	40.6	35.30	1.06	85.46
D122	593	1100	0.27	1.6	114	16.6	194	28.1	237	34.4	44.62	1.59	82.22
D123	593	1100	0.27	1.6	65	9.4	215	31.1	244	35.3	63.10	1.39	86.26

Table 17. Creep data for A533B steel-heat 9583A

TEST NO	LOT NO	STRESS, KSI	TEMP, C	SR, %/H	T-0.1%	T-1%	T-2%	T-5%	T-1	T-R	LOADING S, %	CREEP S, %	RED IN AREA, %
25526	1 *	75	371	0.000078	0.3	7850				5494D	0.47	0.82	1.11
25513	1	67	371	0.000049	0.35					1491D	0.62	0.37	0
25517	1	61	427	0.00020	5	1460				1346D	0.34	0.95	0.64
25516	1	50	482	0.013	0.75	55	135	365	325	577	0.17	25.8	37.8
25515	1	25	482	0.00077	0.5	30				337	0.05	36.7	71
25512	1	45	538	X	0.1	1.3				13.8			
25514	1	40	538	0.27	0.1	2.8	6.4	18	12	30	0.35	25.5	72.3
25714	2	60	371	0.00019	0.1	1250	6650			5016D	1.71	1.8	6.65
25719	2	50	427	0.0022	0.1	87	500			1321D	0.55	3.85	6.73
25710	2	40	482	0.021	0.4	30	78	174	128	252	0.33	22.16	70.2
25718	2	35	482	0.0088	0.7	80	192	420	300	834	0.19	40.4	72.6
25961	2	30	482	0.0013	12.8	640	1260		1300	2015	0.2	3.87	2.37
25713	2	20	538	0.021	0.8	40	85	205	120	528	0.07	37.4	73.4
25721	2	12	538	0.0009	7	720	1840			3290	0.12	3.5	1.8
25966	2	9	593	0.029	1.3	30	85	162	160	707	0.06	50.6	37.5
25722	2	6	593	0.00043	15	227	440	1010	720	1388D		7.2	11.3
25968	2	4	593	0.0017	10.5	494	1078		1600	2352D	0.03	4.9	10.9
26208	2	3	593	0.00058	54	1270			1500	2323	0.01	1.8	
26214	2	2	593	0.00028	185	2270			1260	1857	0.01	0.9	
26213	2	1	593	0.00026	40	3182				2178	0.05	0.7	
25708	3	75	371	0.006	0.05	45	185	560	660	1004	2.67	21.69	73.5
25694	3	67	371	0.00012	0.1	2050	8500			7490D	1.44	1.74	2.7
25527	3	61	427	0.0062	0.1	48	175	630	670	1261	0.87	32.74	73.8
25707	3	55	427	0.00032	4	1200	4300			5115D	0.32	2.2	3.74
25520	3	40	482	0.0019	0.2	340	840	1840	1180	2612	0.09	16.78	35.1
25987	3	40	482	0.0022	4.4	340	790			1124D	0.21	2.8	2.21
25698	3	35	482	0.0011	12	800	1600	3220	1900	4172D	0.04	9.3	13.82
25518	3	20	538	0.021	1	35	85	230	270	620	0.1	52.6	45.8
25709	3	15	538	0.003	10	250	600	1350	900	2995	0.14	18.8	23.9
25724	3	12	538	0.0004	83	1820	3100		1950	4025D	0.02	2.8	7.3
26218	3	8	593	0.013	1.4	63.5	140	320	200	1320	0.06	79	88
25723	3	5	593	0.0018	25	478	920		870	1171D	0.02	2.6	7.1
25989	3	4	593	0.00048	38	1660				2592ID	0.07	1.4	7.3
26209	3	3	593	0.00058	9.5	1540				2324	0.18	1.5	
26215	3	2	593	0.00032	175	2625				1838	0.02	0.7	
26216	3	1	593	0.000064	1040					1837	0.03	0.15	
25696	4	67	371	0.000076	0.3	6100				664D	0.93	1.04	3.38
25528	4	61	427	0.0046	0.1	120	340	550	590	825	0.67	15.24	72.4
25519	4	40	482	0.0022	9	380	750	1295	80	1472	0.19	19.42	47.5
26188	4	40	482	0.0033	2.5	250	495		540	717D	0.24	3.2	11.9
25523	4	20	538	0.005	4	170	345	623	375	704	0.14	8.97	43.9
26211	4	8	593	0.0068	4.6	127	245	480	290	714	0.02	17.0	76.5
25983	4	4	593	0.0018	48	630	1200		1480	1652D	0.01	2.9	21.1
26210	4	3	593	0.0007	100	1400				2154	0.1	1.4	
26212	4	2	593	0.00029	200	3330				2152	0.03	0.7	
26217	4	1	593	0.00013	510					1767	0.01	0.3	
25697	5	67	371	0.000012	1					5543D	0.75	0.24	1.7
25529	5	61	427	0.000068	4	4300				6121D	0.71	1.12	1.37
25962	5	50	482	0.0015	3.9	490	1200		1740	2139	0.27	3.7	3.16
25525	5	40	482	0.00014	43	6350				7292D	0.25	1.2	1.34
26189	5	40	482	0.0002	73	5900				864D	0.15	0.29	0.4
25695	5	25	538	0.00077	17	940	1424	1980	1100	2414	0.54	23.6	45.6
25720	5	20	538	0.00041	135	1650	2400	3175	1550	3185D	0.13	5	5.85
25984	5	4	593	0.0003	180	2850	5350		4150	5028	0.03	1.9	
26207	5	2	593	0.000031	2750					2442	0.05	0.09	

Table 18. Creep data for A533B steel-heat 5795

TEST NO.	LOT NO.	STRESS, KSI	TEMP, C	SR, %/H	T-0.1%	T-1%	T-2%	T-5%	T-t	T-R	LOADING S, %	CREEP S, %	RED IN AREA, %
25972	6	70	371	0.00062	0.025	242	1700			2515D	3	2.5	5.14
25968	6	65	371	0.00016	0.1					956	1.97	0.7	
26194	6	65	371	0.00016	4.4	1960				4291	0.81	1.4	
25976	6	60	427	0.0031	0.05	45	240			679D	1.34	3.2	5.01
25973	6	50	427	0.000094	40					648D	0.31	0.23	
25971	6	45	427	0.000028	65					1201D	0.29	0.2	1.42
25975	6	35	482	0.00036	6.4	2000				3815D	0.28	1.8	
25969	6	27	482	0.000026	170					1319D	0.16	0.2	0
26190	6	20	538	0.0019	9.8	440	810	1395	720	1990	0.13	19.8	19.9
25970	6	15	538	0.001	23	900	1760		1960	2026D	0.07	2.5	3.94
25974	6	8	593	0.0041	10	230	478		825	960D	0.06	4.7	7.05
26488	6	4	593	0.0007	54.2	1195				1269	0.03	1.1	
25985	7	60	427	0.000076	22	8790				5035	0.32	0.7	
25981	7	35	482	0.0002	60	4450				3336D	0.14	0.8	
25982	7	15	538	0.00023	56	2788	4370		2800	4799	0.14	2.4	
25988	7	8	593	0.0026	0.1	350	630	1015	560	1171D	0.05	7.4	13.88
26484	7	4	593	0.00039	63	1850				1473	0.02	0.7	
25980	8	60	427	0.003	0.1	255	590			1172D	0.51	3.5	9.91
26203	8	40	482	0.019	7.5	460	985			1009D	0.21	2.1	9.51
25978	8	35	482	0.00063	55	1540	2600		2400	2622	0.16	2.1	2.31
25977	8	15	538	0.0009	31.5	970	1640		1340	1820D	0.08	2.5	14.3
25979	8	8	593	0.0077	2.5	107	202	370	170	362D	0.06	4.8	33.5
26220	8	4	593	0.00068	43	1300				1654	0.03	1.3	

Table 19. Creep data for A533B steel-heat 9583B

TEST NO.	LOT NO.	STRESS, KSI	TEMP, C	SR, %/H	T-0.1%	T-1%	T-2%	T-5%	T-t	T-R	LOADING S, %	CREEP S, %	RED IN AREA, %
26491	9	75	371	0.15	0.05	3	9.6	22.4	19.6	23.5	6.4	16.6	71.1
26193	9	61	427	0.016	0.1	32	96	256	212	2850	0.85	5.8	7.56
26191	9	30	482	0.00026	12.9	2970				4202	0.17	1.4	
26192	9	15	538	0.0016	3.6	450	960	2060	1160	22080	0.08	5.5	3.26
26488	9	8	593	0.005	4.5	165	340	765	450	1362	0.06	12	
26218	9	4	593	0.0006	36.9	1400				1774	0.01	1.21	
26492	10	75	371	0.00024	0.2	2504				852	1.76	0.6	
26206	10	61	427	0.00024	0.1	490	4383			2660	0.31	1.6	
26202	10	30	482	0.00014	86	6180				3026	0.14	0.6	
26487	10	15	538	0.0007	18.7	1180				1319	0.2	1.1	
26485	10	8	593	0.0048	4.7	170	380	750	460	1241	0.06	20	58.8
26200	10	4	593	0.00095	42	975				1344d	0.03	1.4	13.8
26490	11	61	427	0.00031	1.7	2645				980	0.55	0.6	
26204	11	50	482	0.0023	7.8	360	790	1650	1140	2906	0.31	26.4	37.7
26489	11	15	538	0.00013	3					1269	0.16	0.8	
26197	11	4	593	0.00019	273	3950				3982	0.02	1.1	

Table 20. Creep data for A533B steel-heat 64535

TEST NO.	LOT NO.	STRESS, KSI	TEMP, C	SR, %/H	T-0.1%	T-1%	T-2%	T-5%	T-t	T-R	LOADING S, %	CREEP S, %	RED IN AREA, %
26198	12	61	427	0.0051	0.1	45	170	740	1480	1964	1.09	25.1	71.6
26198	12	30	482	0.0003	27.2	2875				3476	0.15	1.3	
26199	12	15	538	0.00015	8.9	600	1270			1345D	0.1	2.3	1.4
26201	12	8	593	0.0092	0.35	90	210	480	420	1409	0.1	61.3	93.2
26195	12	4	593	0.001	100	1020	1800		1740	1945D	0.09	2.25	12.8

Table 21. Effect of creep exposure on tensile properties

							Results for exposed samples				Results for unexposed samples			
TEST NO	HEAT	LOCATION	HEAT TREAT	TEMP, C	STRESS,KSI	TIME, H	YS,KSI	UTS,KSI	ELONG,%	RA,%	YS,KSI	UTS,KSI	ELONG,%	RA,%
25971	5795	BASE	CE	427	45	1201	68.4	97.1	27	63.5	64	85.2	31	69.3
25973	5795	BASE	CE	482	50	648	71.0	99.7	26.8	63.6	64	85.2	31	69.3
25969	5795	BASE	CE	482	27	1319	64.5	85.6	30.2	65	64	85.2	31	69.3
25974	5795	BASE	CE	593	8	960	52.4	82.0	31.5	56.9	64	85.2	31	69.3
25526	9583A	BASE	ORML 1	371	75	5494	89.6	110	29	71.7	90	100.5	28.3	75.7
25513	9583A	BASE	ORML 1	371	67	1491	92.9	102.3	24.9	74	90	100.5	28.3	75.7
25714	9583A	BASE	ORML2	371	60	5016	75.3	85.2	29.3	75.8	70.3	85.2	32.5	77.0
25694	9583A	BASE	CE	371	67	7490	82.5	93.7	28.7	70.3	71.3	90.1	30.5	74.5
25719	9583A	BASE	ORML 2	427	50	1321	64.2	84.2	32.4	72.5	70.3	85.2	32.5	77.0
25517	9583A	BASE	ORML 1	427	61	1346	91.7	106	26.4	72.5	90	100.5	28.3	75.7
25707	9583A	BASE	CE	427	55	5115	74.5	94.2	32.1	70.7	71.3	90.1	30.5	74.5
25961	9583A	BASE	ORML 2	482	30	2015	60	83.4	33.4	74.9	70.3	85.2	32.5	77.0
25721	9583A	BASE	ORML 2	538	12	3290	55.8	77.8	35	76.2	70.3	85.2	32.5	77.0
25966	9583A	BASE	ORML 2	538	9	707	53.9	71.5	29.3	72.7	70.3	85.2	32.5	77.0
25722	9583A	BASE	ORML 2	593	5	1388	57.6	76.1	35.7	70.1	70.3	85.2	32.5	77.0
25696	9583A	TW	CE	371	67	6664	81.0	91.3	28.7	64.2	74.7	90.1	25.6	76.5
25697	9583A	WELD	CE	371	67	5543	83.2	92.9	23.3	66.4	74.9	89.6	28.6	66.4
25529	9583A	WELD	CE	427	61	6121	81.2	93.2	28.0	65	74.9	89.6	28.6	66.4
25525	9583A	WELD	CE	482	40	7292	72.3	91.6	27.9	60.2	74.9	89.6	28.6	66.4
25962	9583A	WELD	CE	482	50	2139	82.6	95.8	26.3	63	74.9	89.6	28.6	66.4
25720	9583A	WELD	CE	538	20	3105	50.1	78.4	24.7	62.1	74.9	89.6	28.6	66.4
25524	9583A	WELD	CE	538	20	2349	66.7	82.7	28.5	63.8	74.9	89.6	28.6	66.4

ORNL-DWG 89-18608

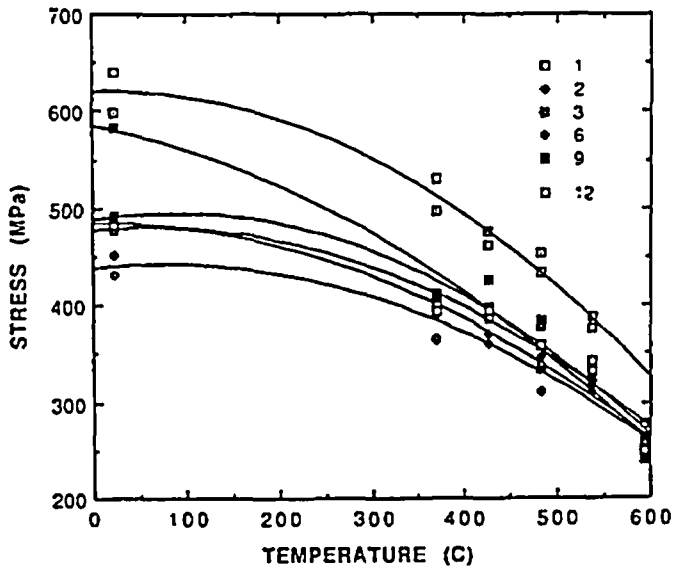

Fig. 1. Yield strength of several lots of A533 base metal as a function of test temperature.

ORNL-DWG 89-18609

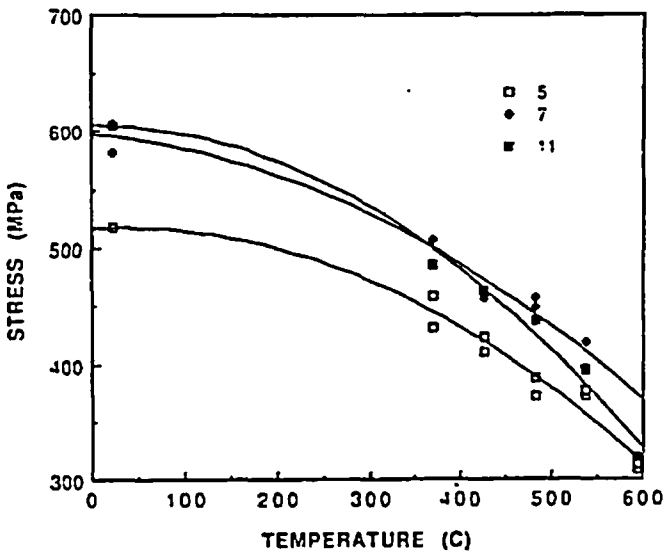

Fig. 2. Yield strength of three lots of weld metal as a function of temperature.

ORNL-DWG 89-18610

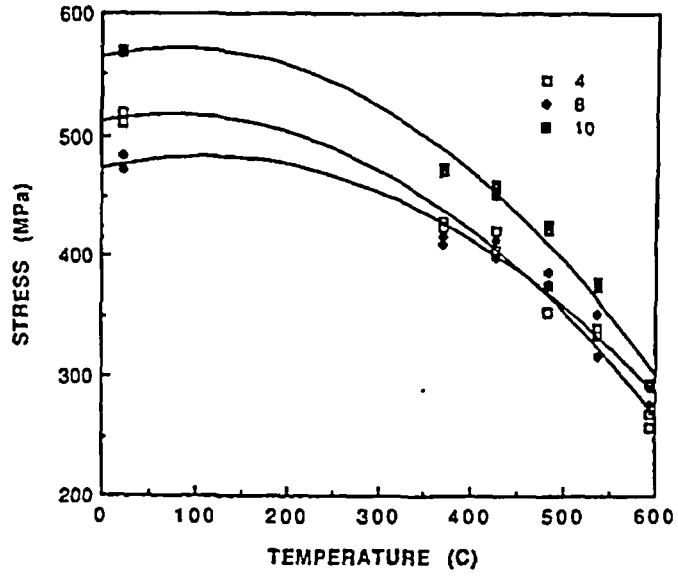

Fig. 3. Yield strength of three lots of transverse weld samples as a function of temperature.

ORNL-DWG 89-18611

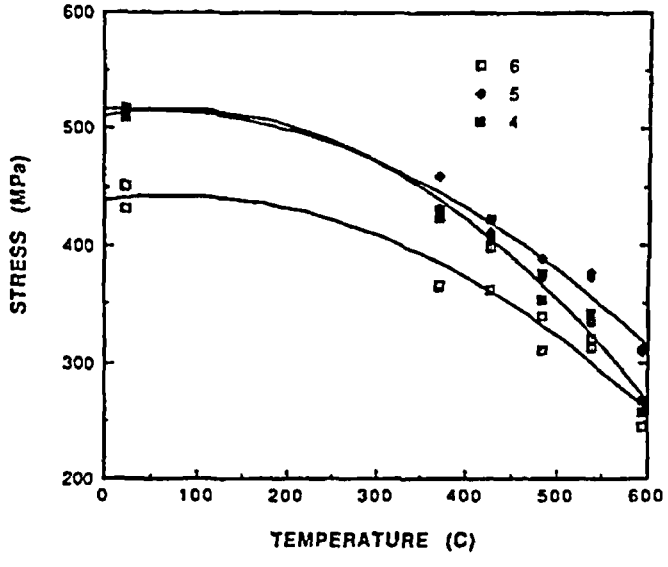

Fig. 4. Yield strength for lots of base metal, transverse welds, and weld metal having the lowest strength.

ORNL-DWG 89-18612

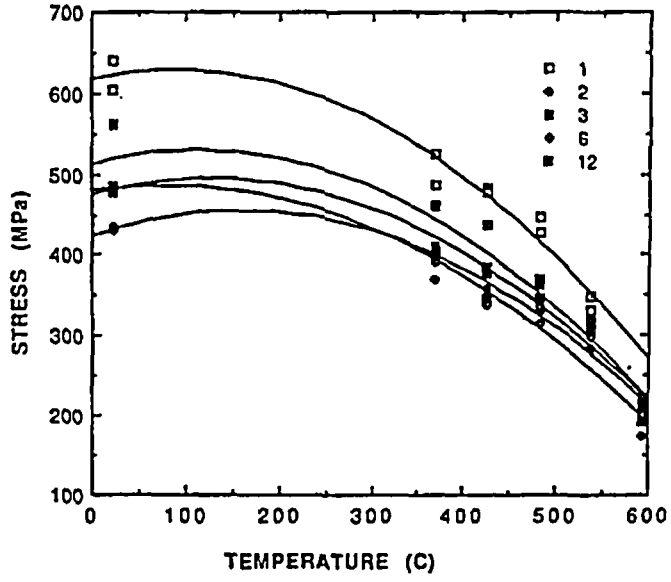

Fig. 5. Yield strength of A533 base metal at a strain rate of $3.7 \times 10^{-5} s^{-1}$ as a function of temperature.

ORNL-DWG 89-18613

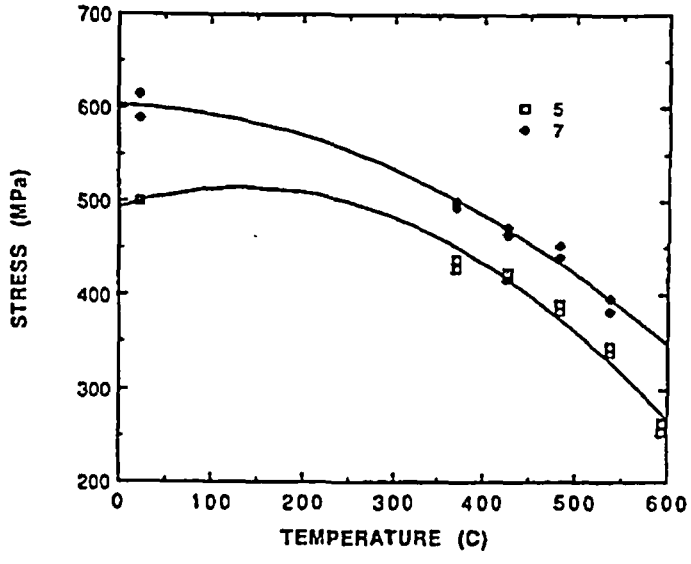

Fig. 6. Yield strength of A533 weld metal at a strain rate of $3.7 \times 10^{-5} s^{-1}$ as a function of temperature.

ORNL-DWG 89-18614

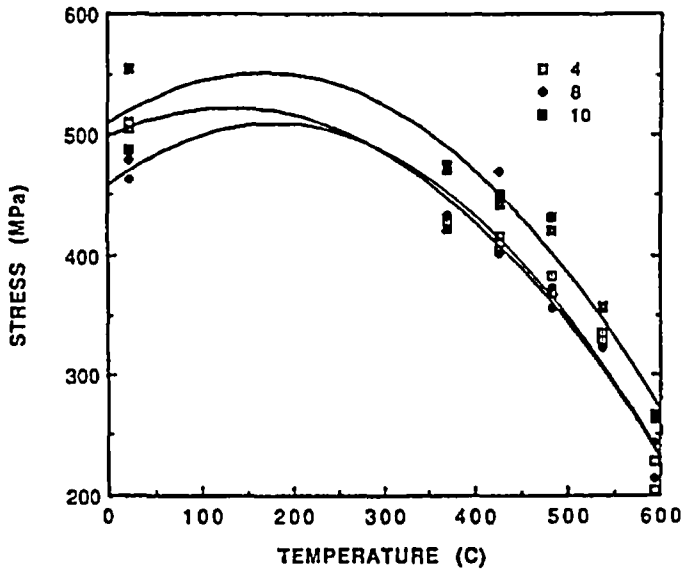

Fig. 7. Yield strength of transverse weld specimens of A533 at a strain rate of $3.7 \times 10^{-5} s^{-1}$ as a function of temperature.

ORNL-DWG 89-18615

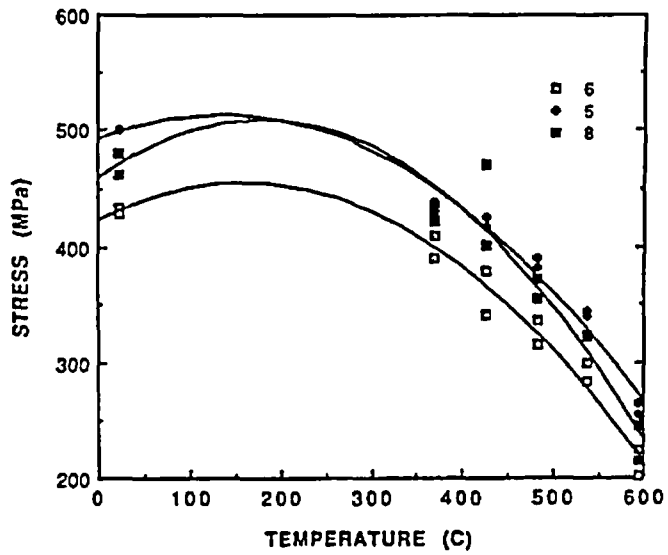

Fig. 8. Yield strength at a strain rate of $3.7 \times 10^{-5} s^{-1}$ for lots of base metal, transverse weld samples, and weld metal as a function of temperature.

ORNL-DWG 89-18616

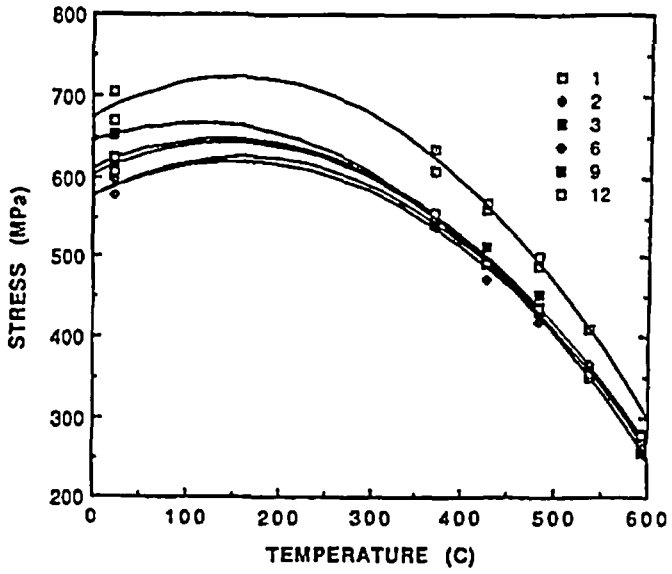

Fig. 9. Tensile strength of several lots of A533 base metal as a function of temperature.

ORNL-DWG 89-18617

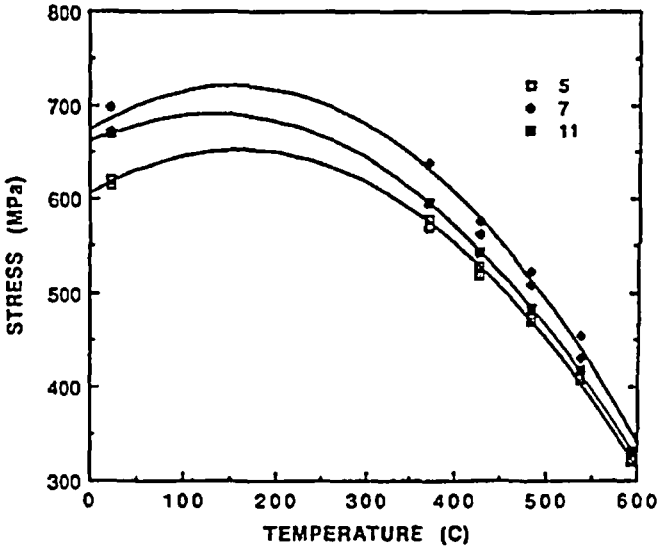

Fig. 10. Tensile strength of several lots of A533 weld metal specimens as a function of temperature.

ORNL-DWG 89-18618

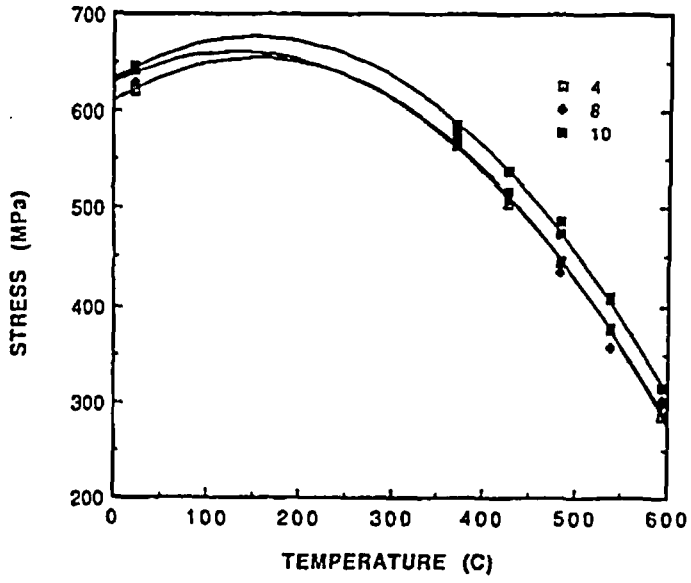

Fig. 11. Tensile strength of several lots of A533 transverse weld specimens as a function of temperature.

ORNL-DWG 89-18619

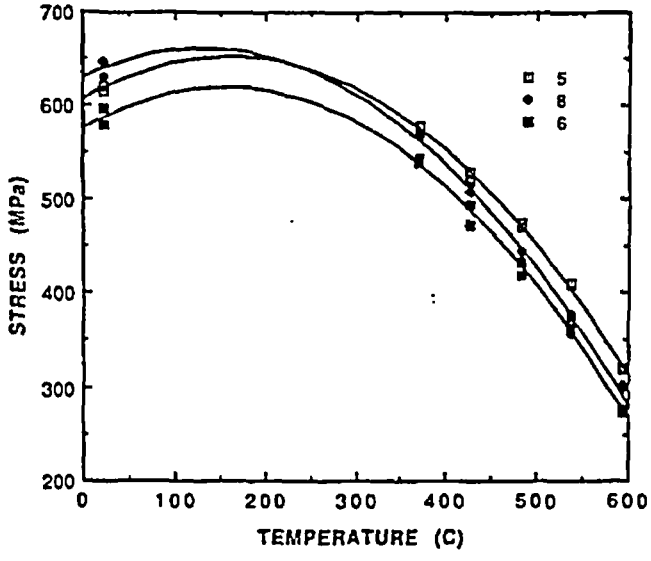

Fig. 12. Tensile strength for lots of base metal, transverse welds, and weld metal having the lowest strength.

ORNL-DWG 89-18620

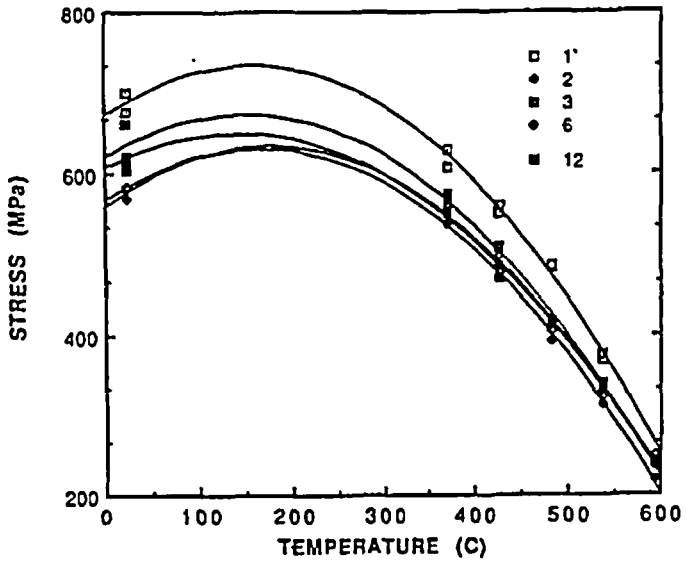

Fig. 13. The ultimate tensile strength of several lots of base metal as a function of temperature.

ORNL-DWG 89-18621

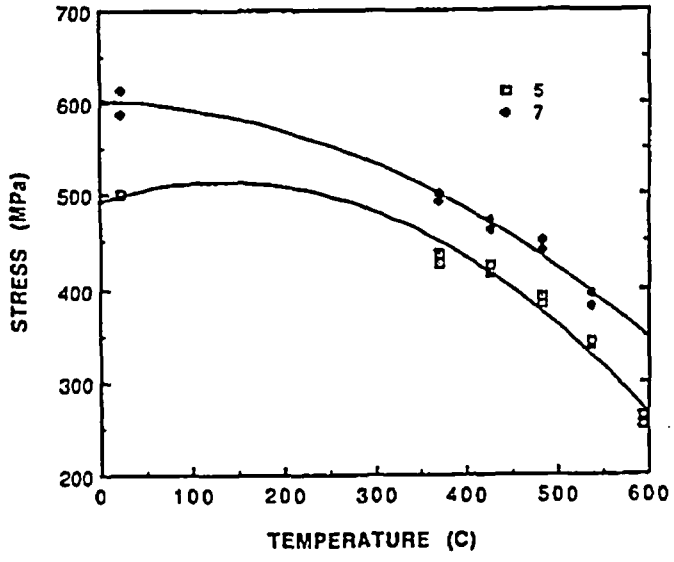

Fig. 14. The ultimate tensile strength of several lots of weld metal as a function of temperature.

ORNL-DWG 89-18622

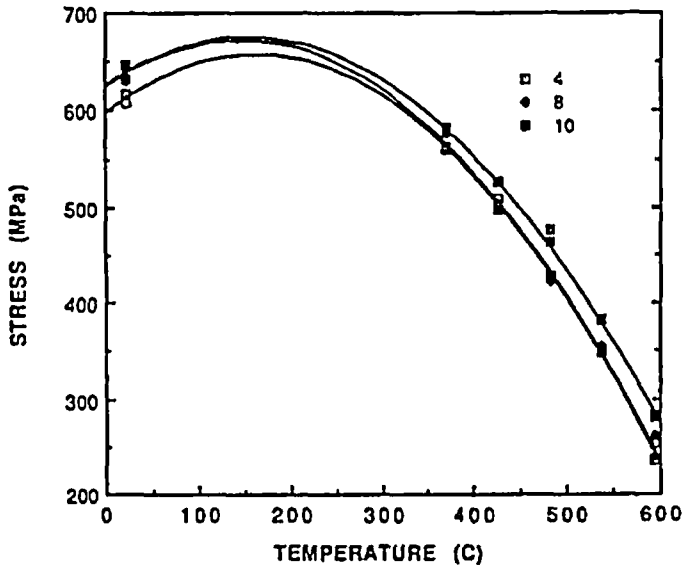

Fig. 15. The ultimate tensile strength of several lots of transverse weld specimens as a function of temperature.

ORNL-DWG 89-18623

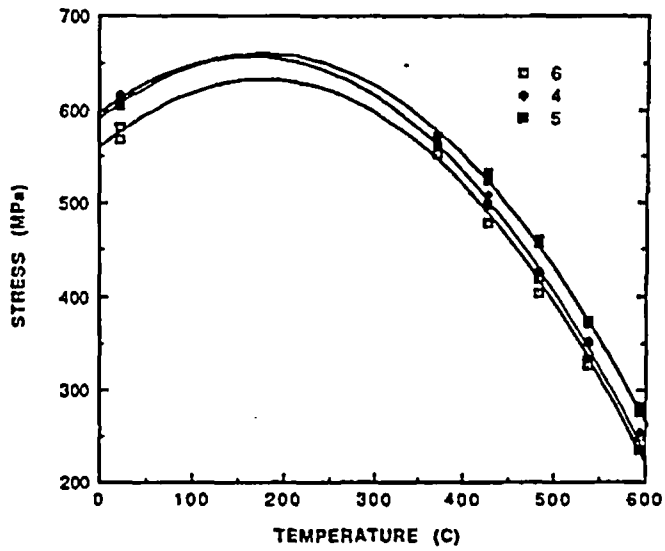

Fig. 16. Ultimate tensile strength for lots of base metal, weld metal, and transverse weld metal having the lowest strength.

ORNL-DWG 89-18624

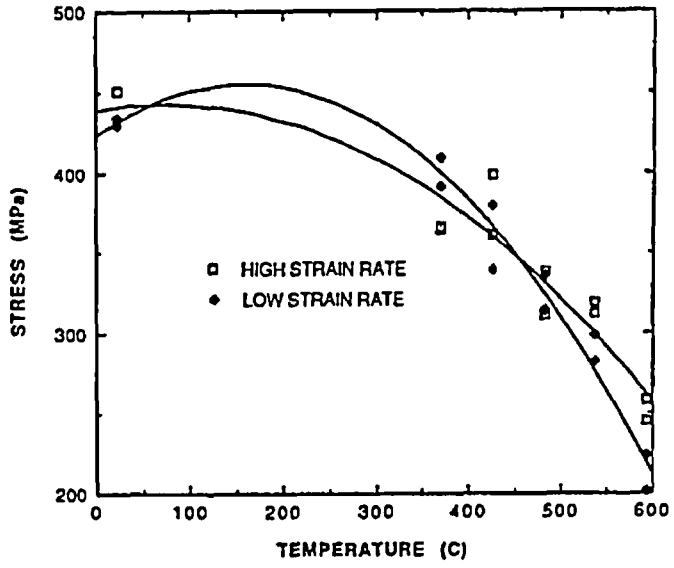

Fig. 17. Yield strength of Lot 6 measured at strain rates of $1.3 \times 10^{-4} s^{-1}$ and $3.7 \times 10^{-5} s^{-1}$.

ORNL-DWG 89-18625

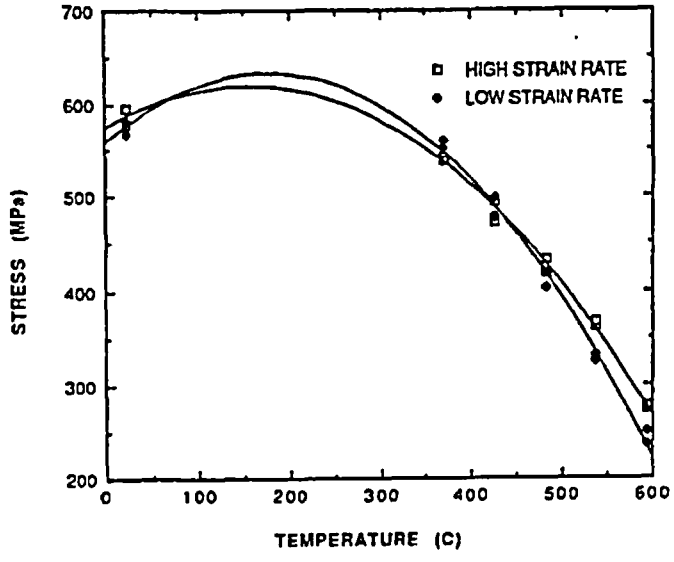

Fig. 18. Ultimate tensile strength of Lot 6 measured at strain rates of $1.3 \times 10^{-4} s^{-1}$ and $3.7 \times 10^{-5} s^{-1}$.

ORNL-DWG 89-18626

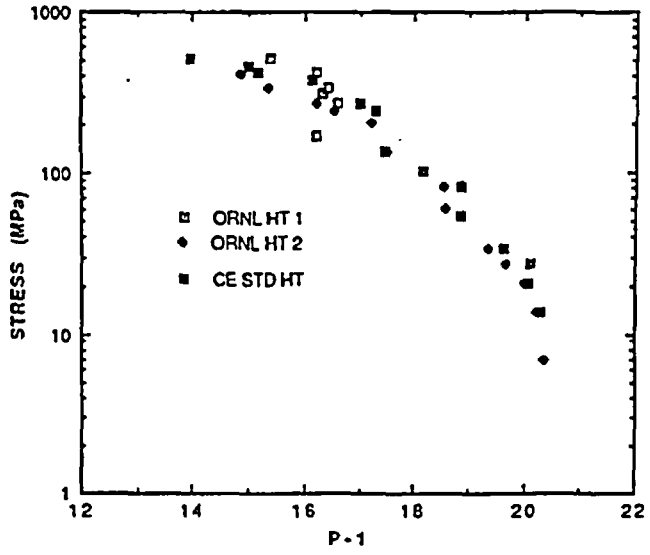

Fig. 19. Larson-Miller correlation for Lots 1, 2, and 3 base metal crept to 1% strain.

ORNL-DWG 89-18627

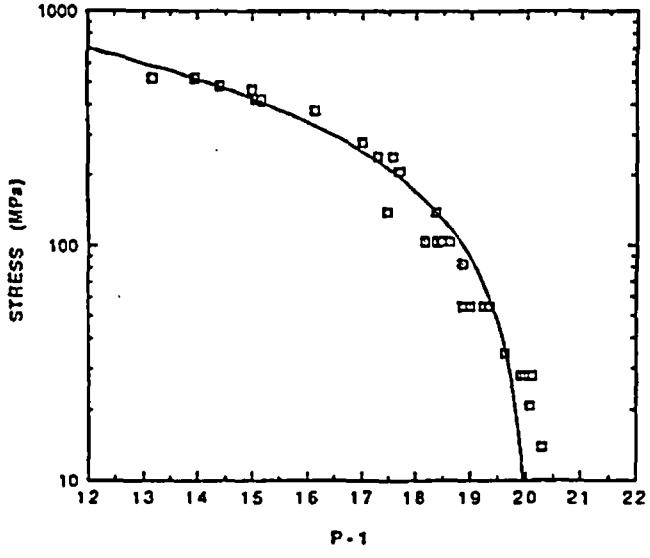

Fig. 20. Larson-Miller correlation for Lots 3, 6, 9, and 12 base metal crept to 1% strain.

ORNL-DWG 89-18628

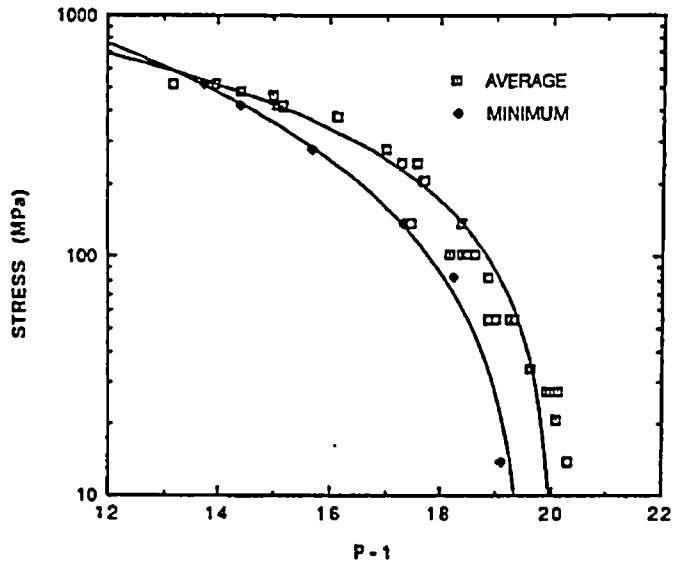

Fig. 21. Larson-Miller correlation for 1% strain showing average and minimum strengths for Lots 3, 6, 9, and 12 base metal.

ORNL-DWG 89-18629

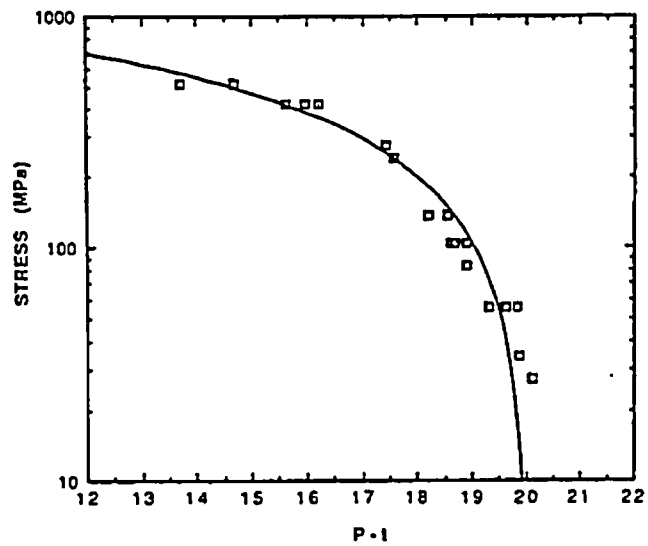

Fig. 22. Larson-Miller correlation for tertiary creep for Lots 3, 6, 9, and 12 base metal.

ORNL-DWG 89-18630

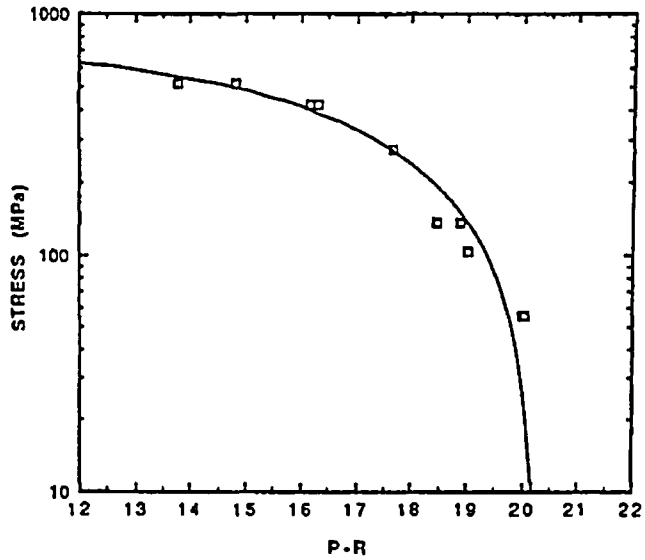

Fig. 23. Larson-Miller correlation for rupture for Lots 3, 6, 9, and 12 base metal.

ORNL-DWG 89-18631

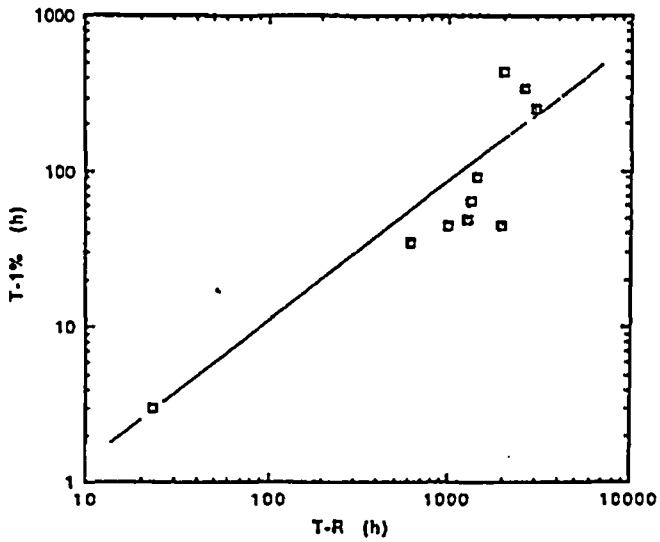

Fig. 24. Time to 1% strain as a function of time to rupture for Lots 3, 6, 9, and 12 base metal.

ORNL-DWG 89-18632

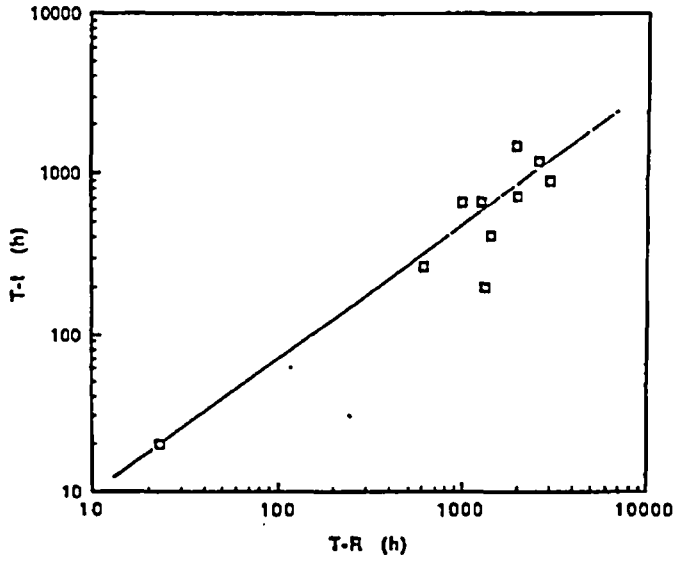

Fig. 25. Time to tertiary creep as a function of time to rupture for Lots 3, 6, 9, and 12 base metal.

ORNL-DWG 89-18633

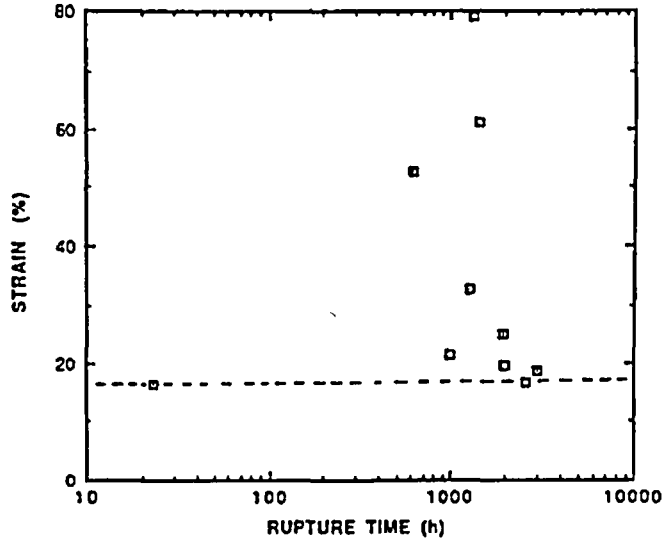

Fig. 26. Fracture strain as a function of rupture time for Lots 3, 6, 9, and 12 base metal.

ORNL-DWG 89-18634

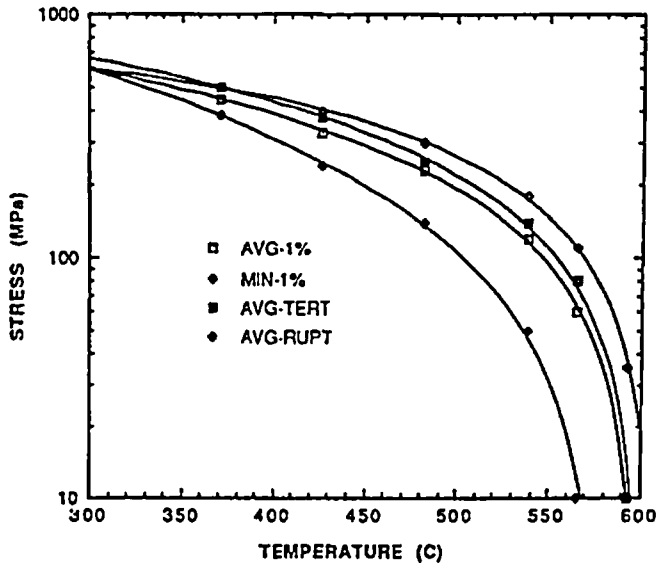

Fig. 27. Allowable stresses as a function of temperature for base metal based on various design criteria.

ORNL-DWG 89-18635

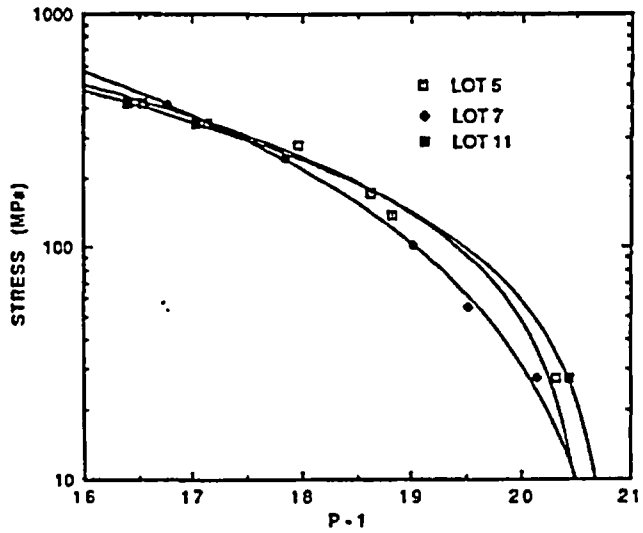

Fig. 28. Larson-Miller correlation for 1% strain in Lots 5, 7, and 11 weld metal.

ORNL-DWG 89-18636

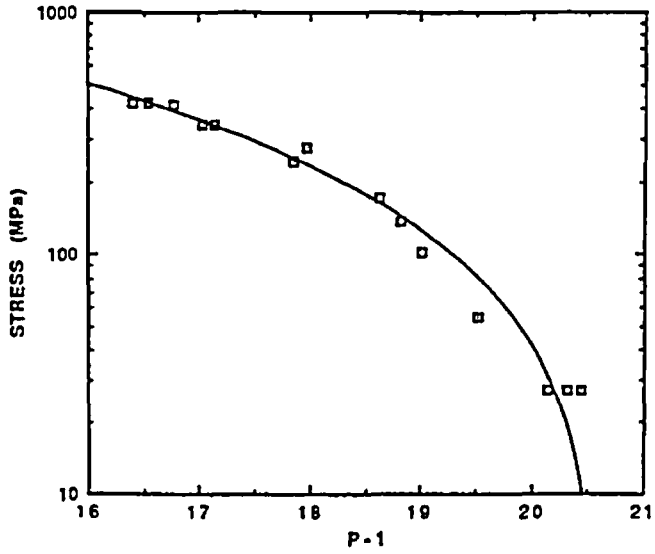

Fig. 29. Larson-Miller correlation for 1% strain in Lots 5, 7, and 11 (combined) weld metal.

ORNL-DWG 89-18637

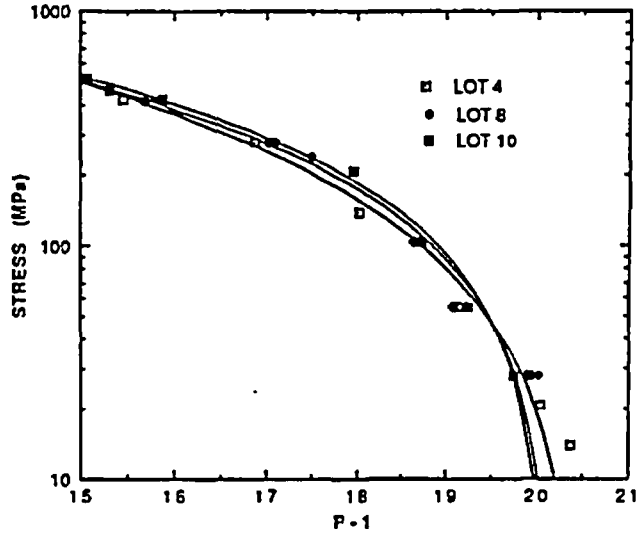

Fig. 30. Larson-Miller correlation for 1% strain in Lots 4, 8, and 10 transverse weld samples.

ORNL-DWG 89-18638

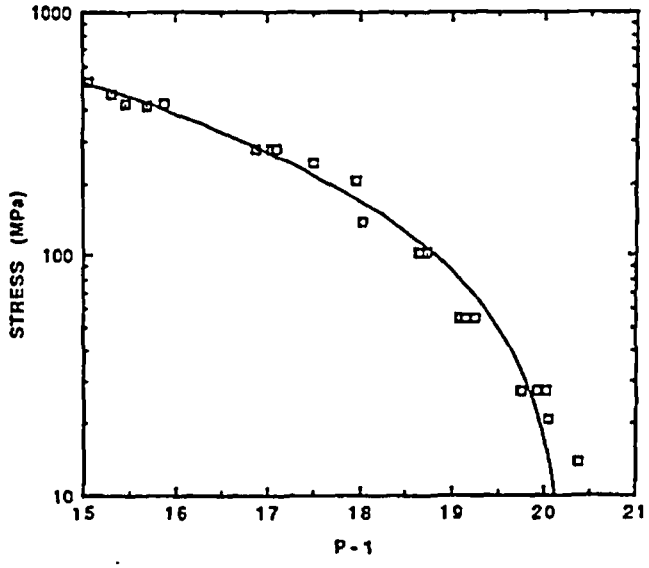

Fig. 31. Larson-Miller correlation for 1% strain in Lots 4, 8, and 10 (combined) transverse weld samples.

ORNL-DWG 89-18639

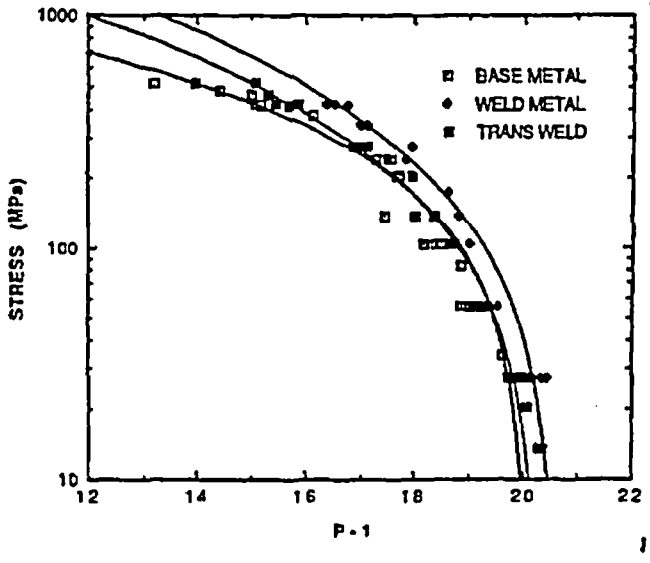

Fig. 32. Larson-Miller plot comparing the average properties of base metal, weld metal, and transverse weld samples.

DOE-HTGR 88383
ORNL/TM-11338
Distribution
Category UC-522T

INTERNAL DISTRIBUTION

1-2. Central Research Library
3. Document Reference Section
4-5. Laboratory Records Department
6. Laboratory Records, ORNL RC
7. ORNL Patent Section
8-10. M&C Records Office
11. C. A. Baldwin
12. W. P. Barthold (Consultant)
13. E. E. Bloom
14. J. A. Bucholz
15. T. D. Burchell
16-17. E. E. Clemmer
18. J. C. Cleveland
19. W. P. Eatherly (Consultant)
20. L. C. Emerson
21. E. C. Fox
22. U. Gat
23. R. K. Genung
24. H. A. Glovier
25. D. W. Heatherly
26. J. R. Hightower
27. F. J. Homan
28. D. T. Ingersoll
29. H. Jones
30. M. J. Kania
31. P. R. Kasten (Consultant)
32. T. S. Kress
33. J. C. Mailen
34-38. H. E. McCoy
39. F. R. Mynatt
40. N. H. Packan
41. P. L. Rittenhouse
42. J. P. Sanders
43. O. M. Stansfield
44. J. O. Stiegler
45-49. K. R. Thoms
50. D. B. Trauger
51. A. W. Trivelpiece

EXTERNAL DISTRIBUTION

52. COMBUSTION ENGINEERING, 1000 Prospect Hill Road, Windsor, CT 06095
    S. A. Caspersson

53. EG&G IDAHO, INC., P.O. Box 1625, WCB-E3, Idaho Falls, ID 83415
    E. Arbtin

54. GENERAL ATOMICS, P.O. Box 85608, San Diego, CA 92138-5608
    A. J. Neylan

55-57. JAPAN ATOMIC ENERGY RESEARCH INSTITUTE, Tokai-Mura, Ibaraki-Ken 319-11, Japan
    K. Fukuda
    T. Kondo
    K. Shiba

5. DOE-HTGR-90286, "Documentation of ASME Code Case for Elevated-Temperature Service of MHTGR Reactor Vessel Materials," September 1991.

CHRIS HOFFMANN

DOE-HTGR-90286
REV. 0

HTGR

DOCUMENTATION OF ASME CODE CASE FOR ELEVATED-TEMPERATURE SERVICE OF MHTGR REACTOR VESSEL MATERIALS

APPLIED TECHNOLOGY

Any Further Distribution by any Holder of this Document or Data Therein to Third Parties Representing Foreign Interests, Foreign Governments, Foreign Companies, and Foreign Subsidiaries or Foreign Divisions of U.S. Companies Shall be Approved by the Associate Deputy Assistant Secretary for Reactor Systems, Development and Technology, U.S. Department of Energy. Further Foreign Party Release May Require DOE Approval Pursuant to Federal Regulation 10 CFR Part 810, and/or May Be Subject to Section 127 of the Atomic Energy Act.

AUTHORS/CONTRACTORS

COMBUSTION ENGINEERING, INC.

ISSUED BY: COMBUSTION ENGINEERING, INC.
FOR THE DEPARTMENT OF ENERGY
CONTRACT DE-AC03-89SF17886

SEPTEMBER 1991

MHTGR TECHNOLOGY DEVELOPMENT PROGRAM

TASK 1603.3

REACTOR VESSEL MATERIALS

DOCUMENTATION OF ASME CODE CASE FOR ELEVATED-TEMPERATURE SERVICE OF MHTGR REACTOR VESSEL MATERIALS

Prepared by: Chris Hoffmann Date: 9-30-91
C. L. Hoffmann, Cognizant Engineer

Approved by: W.R. Gahwiller Date: 10/2/91
W. R. Gahwiller, Supervisor, Materials Technology

Approved by: S.M. Schloss Date: 10/2/91
S. M. Schloss, Manager, Materials/Chemical Technology

Approved by: SA Caspersson Date: 10/3/91
S. A. Caspersson, Project Manager

COMBUSTION ENGINEERING, INC.
ABB COMBUSTION ENGINEERING NUCLEAR POWER
MATERIALS/CHEMICAL TECHNOLOGY
WINDSOR, CONNECTICUT

DOE-HTGR-90286, Rev. 0

TABLE OF CONTENTS

Section	Title	Page
1.0	INTRODUCTION	1
2.0	SUMMARY	1
3.0	DISCUSSION	2
3.1	MHTGR VESSEL ELEVATED-TEMPERATURE SERVICE	2
3.2	INQUIRY TO ASME CODE	3
3.3	ASME COMMITTEE ORGANIZATION	3
3.4	APPROVAL PROCESS FOR THE MHTGR CODE INQUIRY	3
3.5	SUPPORTING MATERIALS TESTING PROGRAM	4
3.6	SUPPORTING DESIGN ANALYSIS	5
4.0	REFERENCES	5
APPENDIX I	INQUIRY AND REPLY FOR NEW CODE CASE APPROVED BY THE ASME CODE MAIN COMMITTEE	

LIST OF FIGURES

Figure No.	Title	Page
3-1	Committee Procedure for Adopting Proposed Changes to the Code	6
3-2	Flowchart for Code Committee Actions on Code Inquiry for MHTGR Elevated Temperature Service	7
3-3	Chronology of MHTGR Reactor Vessel ASME Code Case	8

MHTGR TECHNOLOGY DEVELOPMENT PROGRAM - TASK 1603.3

DOCUMENTATION OF ASME CODE CASE FOR ELEVATED-TEMPERATURE SERVICE

OF MHTGR REACTOR VESSEL MATERIALS

1.0 INTRODUCTION

The MHTGR vessel system includes an uninsulated, steel, reactor pressure vessel to allow decay heat removal by conduction and radiation during a total loss of coolant and/or coolant flow event. Certain low-probability conduction-cooldown events can raise metal temperatures of the reactor vessel above 370°C (700°F), the maximum temperature allowed by Section III of the ASME Boiler and Pressure Vessel Code for the selected pressure vessel materials. An Inquiry was submitted to the ASME Code Committee requesting a special Code Case which would provide allowable stresses and design rules for the limited elevated-temperature service of the MHTGR reactor vessel.

A materials test program was performed to provide the material properties required to obtain the Code Case approval. The time/temperature dependent behavior of the MHTGR pressure vessel materials was characterized for the range of times and temperatures occurring during conduction cooldown events. The test results were used as the basis for establishing time-independent and time-dependent stress allowables.

Analytical work was performed to determine the possible range of material response for the time-temperature conditions of the MHTGR duty cycle events. The results of the analysis were used to define the design rules for the Code Case.

The following discussion reviews the MHTGR elevated-temperature service conditions, design approach, and the technical issues associated with obtaining approval for the new Code Case. Previous progress on this task was reported in Reference 1.

2.0 SUMMARY

The design for limited elevated-temperature service of the MHTGR reactor vessel will be governed by the rules and allowable stresses of a new Code Case to the ASME Code. An Inquiry was submitted to the ASME Code Committee. The Inquiry and Proposed Reply received final approval of the ASME Code Main Committee on September 13, 1991. Following the Main Committee approval, the new Code Case is sent to the Board on Nuclear Codes and Standards (BNCS) for approval and is then published for public comment. The Code Case is available for use upon BNCS approval. C-E actively participated in the ASME Code committee meetings to obtain the approval of the new Code Case.

Materials data and analysis of elevated-temperature materials response were provided to demonstrate the capability of the MHTGR vessel materials. Elevated-temperature time-dependent materials properties were generated in test programs at ORNL and C-E. Both of these test programs were completed in FY 1990. The final data package was assembled following completion of all the testing and presented to the Code Committees at the May 1990 ASME meeting.

The data package included elevated-temperature tensile and creep data necessary for establishing allowable stresses. In addition, results from the temper embrittlement study, cyclic stress-strain curves, and elevated-temperature fatigue tests were presented. The elevated-temperature materials properties were used to establish allowable stresses for MHTGR design during Service Level C and D events at temperatures above 370°C (700°F) for limited times.

Analytical work to define the materials response to elevated-temperature service was performed by C-E and ORNL. The analyses demonstrated that a simplified set of design rules could not be developed to address all of the potential elevated-temperature design considerations. Based on the analytical results, the existing elevated-temperature design rules of ASME Section III Code Case N-47 were incorporated into the MHTGR Inquiry.

3.0 DISCUSSION

3.1 MHTGR VESSEL ELEVATED TEMPERATURE SERVICE

Reference 1 contained a detailed discussion of the MHTGR reactor vessel elevated-temperature service. The MHTGR reactor vessel is cooled by passive heat transfer, with no active decay heat removal systems. The design duty cycle of the MHTGR contains several low-probability events (Service Level C and D conditions) in which all forced circulation is lost. The elevated-temperature events are characterized by the following conditions:

1) Pressurized conduction cooldown, with a maximum metal temperature of approximately 410°C (770°F), with a time duration above 370°C (700°F) of approximately 150-200 hours, and

2) Depressurized conduction cooldown with a maximum metal temperature of approximately 470°C (880°F), with a time duration above 370°C (700°F) of approximately 400 hours.

Two events of each type are included in the MHTGR duty cycle. The number of events was restricted to reduce elevated-temperature creep-fatigue interaction concerns, while maintaining the flexibility within the duty cycle to return the MHTGR plant to service following one of these events. If two events of either type were to occur, the duty cycle for that event would be reduced to zero. Therefore, the maximum number of temperature cycles above 370°C (700°F) is effectively limited to a total of three. The maximum number of events permitting the return of the vessel system to operation is only two, since the vessel can only be returned to operation when the duty cycle provides for the possible reoccurrence of either event.

Allowable stresses for the SA 533 Grade B, Class 1 and SA 508 Class 3 pressure vessel steels were limited to 370°C (700°F) by Section III of the ASME Code. Section III designs are based only on the time-independent strength properties of materials. Time-dependent material behavior must be considered at elevated-temperatures. There was no provision in Section III for deriving and using allowable stresses in the elevated-temperature regime.

A request was made to the ASME Code Committee for a special Code Case to allow use of pressure vessel steels at temperatures above 370°C (700°F) for limited times. The ASME Code Section III design procedures, supporting data and allowable stresses are applicable to virtually the entire duty cycle with the exception of the low-probability Service Level C and D events. Obtaining approval of the new Code Case required establishing the necessary allowable stresses and supplementary design rules to be used in conjunction with existing ASME Code Section III data and rules for duty cycle events where temperatures are greater than 370°C (700°F).

3.2 INQUIRY TO ASME CODE

An Inquiry was prepared and submitted to the ASME Code Committees for consideration. The scope of the Inquiry enveloped the conditions for the anticipated Service Level C and D events in the MHTGR duty cycle. The general form of the Inquiry was as follows:

> May SA533 Grade B, Class 1 plates, SA508 Class 3 forgings and their weldments be used in Section III, Division 1, Class 1 construction at temperatures exceeding 700°F up to 1000°F during Service Level C or D events for limited times of exposure not to exceed 1000 hours?

The Inquiry remained essentially the same since it was originally submitted. However, the original Proposed Reply, which the Inquirer is required to provide to the ASME Code committee, underwent numerous revisions. The wording of the Inquiry and Reply approved by the ASME Code Main Committee is provided in Appendix I.

Approval by the ASME Code Committee resulted in the establishment of a new Code Case for the materials and design of the MHTGR vessel. The Code Case provides the Code Committee's response to the Inquiry in terms of design rules which will govern the limited elevated-temperature service of the MHTGR vessel and the time-temperature related allowable stresses which govern the vessel stresses at temperatures above 370°C (700°F).

3.3 ASME COMMITTEE ORGANIZATION

The overall organization of the ASME Code Committee was described in Reference 1. Appendix XX to Section III of the ASME Code describes the requirements for preparation of technical inquiries to the Code committee. Technical inquiries to the Code are forwarded to the appropriate Subcommittee(s) for review and action. Figure 3-1 shows a generalized flow chart of the committee procedure for considering and approving changes to the Code. Proposed changes to the Code must pass through the approval sequence shown in Figure 3-1 in order to be adopted into the Code or as a Code Case.

3.4 APPROVAL PROCESS FOR THE MHTGR CODE INQUIRY

The Inquiry was considered and approved by several Subgroups and/or Subcommittees of the ASME Code Committee and was evaluated in terms of both design and materials requirements. The MHTGR design is intended to adhere to the rules of Section III of the ASME Code for all other design and operating conditions. The design for the limited elevated-temperature service will be based on the supplemental rules and requirements of the Code Case.

Figure 3-2 shows the specific subgroups and subcommittees involved in addressing the C-E inquiry for MHTGR reactor vessel material elevated temperature service. Figure 3-3 shows a complete chronology of the ASME Code Case for the MHTGR reactor vessel, which was initiated in 1987.

Since the Inquiry was for a Section III Class 1 application, the overall responsibility for the Inquiry was with the Subcommittee on Nuclear Power (Section III). Due to the elevated-temperature requirements of the request, the Inquiry was assigned to the Subgroup on Elevated Temperature Construction. The Inquiry was addressed by Subgroups of the service subcommittees on properties and design in order to establish stress allowables based on the material properties and to provide the design rules that will be incorporated in the Code Case.

The Inquiry and Proposed Reply were initially approved by the Subgroup on Elevated-Temperature Design at the May 1990 ASME Code meeting. Additional approvals were obtained from the other Subgroups and Subcommittees indicated in Figure 3-2 at subsequent committee meetings, with the Main Committee approval obtained at the September 1991 meeting.

Progress on developing the committee response to the Code Inquiry required material property data for the SA533 and SA508 pressure vessel steels and weldments and the results of design analysis to demonstrate the material response to the time and temperature range requested in the Inquiry. The status of the materials test program and design analysis performed to support the Inquiry are discussed below.

3.5 SUPPORTING MATERIALS TEST PROGRAM

A test program was performed to provide the materials property information required to develop allowable stresses and design rules for the special Code Case. Testing was performed by Oak Ridge National Laboratories (ORNL) and Combustion Engineering's Metallurgical and Materials Laboratory. The test matrix included three heats of SA533 plate, one SA508 forging and three weldments (two submerged arc welds and one shielded metal arc weld). The testing performed on these materials was as follows:

1) Tensile testing from 700°F to 1100°F,

2) Creep testing at several different stress levels from 800°F to 1100°F for test times up to 2000 hours, and

3) Evaluation of the potential for thermal embrittlement of these materials by aging base and weld metal test specimens at 850°F and 950°F for 2000 hours and comparing Charpy impact test results for the aged and unaged materials.

The completed data package of the testing was provided to the ASME Code Committee in May 1990 (Ref. 1). The test data were used as the basis for establishing allowable stresses for the Code Case. The materials data submitted to the Code committee included room and elevated temperature tensile test data and trend curve analysis for establishing S_m values.

Information in the materials property data package provided all of the necessary material property information for Code Case N-47. The material properties have been incorporated as part of the Reply of the new Code Case (See Appendix I Figures and Tables). This data is required for performing the elevated-temperature design analysis according to Code Case N-47 rules. The elevated-temperature data included S_t values based on 1% creep strain in 1000 hours, onset of tertiary creep and stress rupture data. Creep and creep rupture equations were generated by analysis of the data. The package included information on creep strain to failure, isochronous stress-strain curves, cyclic stress-strain curves, elevated temperature fatigue curve and thermal aging.

3.6 SUPPORTING DESIGN ANALYSIS

In response to the suggestion of the ASME Subgroup on Elevated Temperature Design, evaluations of simplified geometries with an enveloping duty cycle were performed. A simple, plane-strain, symmetrical, cylindrical model was analyzed. The analyses were intended to bound the MHTGR transients that can occur for Service Level C events and provide an envelope for load-controlled and strain-controlled stresses subject to the criteria of Code Case N-47. The results of these analyses demonstrated where creep strains and creep-fatigue damage became significant.

Based on the results of the preliminary design analysis, the approach of using a bounding design envelope on primary and secondary stresses was discontinued. The analysis had shown that a bounding envelope would be overly restrictive, since it was attempting to generalize all possible stress conditions in the structure. The existing elevated-temperature design rules of Code Case N-47 were adopted for analyzing the MHTGR Level C and D events that exceeded 700°F.

4.0 REFERENCES

1) TR-MCC-149, Rev. 02, "Progress Report for FY 1990 on ASME Code Inquiry for Elevated-Temperature Service of Reactor Vessel Materials," Combustion Engineering, Inc., September 1990.

Figure 3-1

COMMITTEE PROCEDURE FOR ADOPTING PROPOSED CHANGES TO THE CODE

PROPOSED CHANGE - CORRESPONDENCE, TASK GROUP, WORKING GROUP

↓

SUBGROUP - (SECTION III HAS 6, SECTION XI HAS 7)

↓

SUBCOMMITTEE - VOICE VOTE

↓

MAIN COMMITTEE - (FIRST CONSIDERATION - 1 WRITTEN NEGATIVE BALLOT STOPS ACTION)

↓

MAIN COMMITTEE - (SECOND CONSIDERATION - 4 WRITTEN NEGATIVE BALLOTS DEFEAT ITEM, CANNOT BE BROUGHT BACK UNLESS IT IS CHANGED IN TECHNICAL CONTENT)

↓

BOARD ON NUCLEAR CODES AND STANDARDS

↓

PUBLIC REVIEW - (ANNOUNCED IN MECHANICAL ENGINEERING, ASME MONTHLY MAGAZINE, 4 MONTHS AFTER MAIN COMMITTEE MEETING)

↓

PUBLISHED - CODE CASE (4 TIMES A YEAR)
OR
ADDENDA (ONCE A YEAR)

FIGURE 3-2

ASME COMMITTEE WORK FLOW DIAGRAM

MHTGR CODE INQUIRY REQUEST FOR LIMITED ELEVATED TEMPERATURE SERVICE FOR REACTOR PRESSURE VESSEL MATERIALS

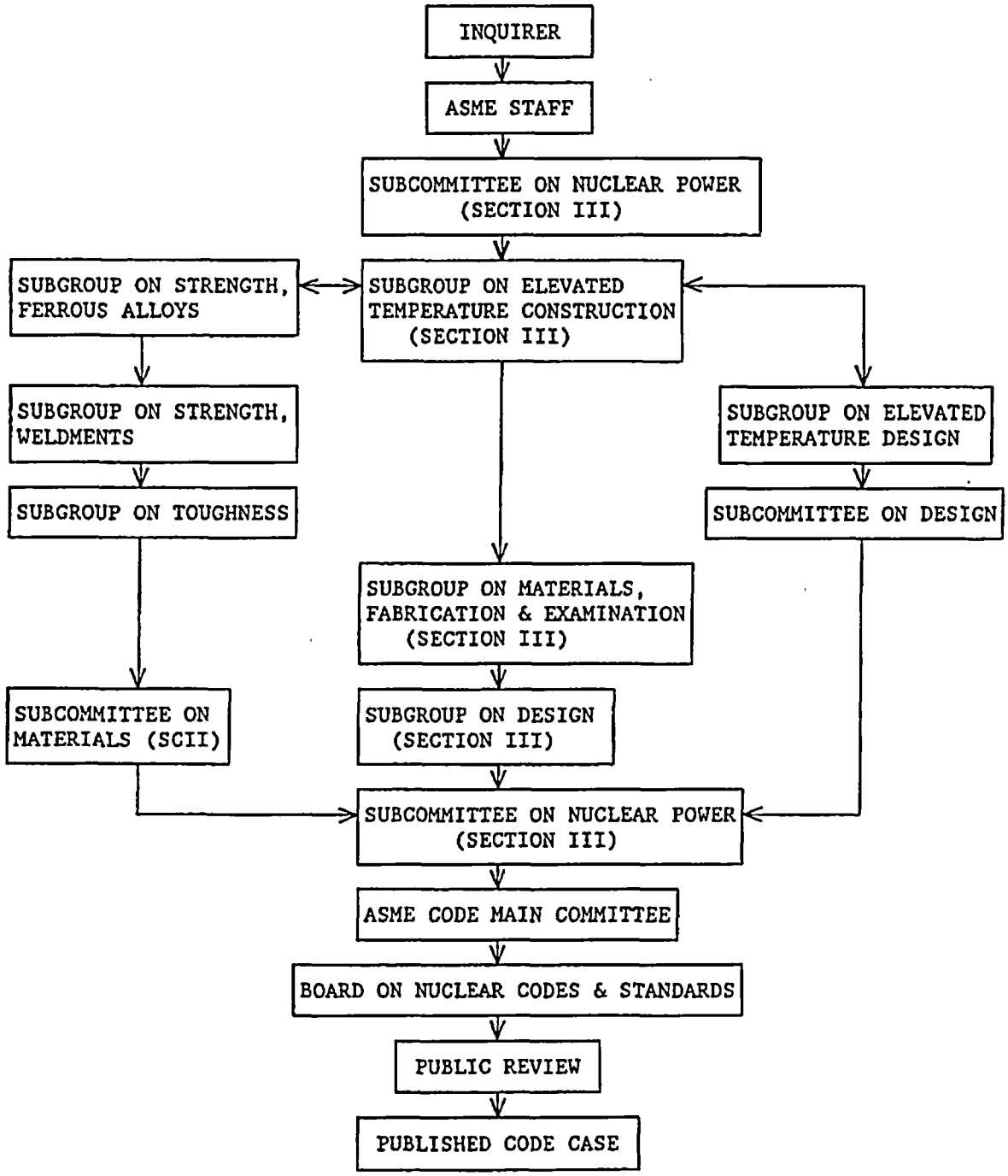

FIGURE 3-3

CHRONOLOGY OF MHTGR REACTOR VESSEL ASME CODE CASE

- CODE INQUIRY SUBMITTED TO ASME CODE COMMITTEE - 11/87
- INTERACTION WITH ASME CODE COMMITTEE AT QUARTERLY MEETINGS - 1987-1991
- MATERIALS TEST PROGRAMS COMPLETED BY ORNL AND C-E (MML) - 3/90
- REVISED INQUIRY/PROPOSED REPLY SUBMITTED TO CODE COMMITTEES - 5/90
- FINAL MATERIALS PROPERTIES DATA PACKAGE SUBMITTED - 5/90
- CODE CASE APPROVED BY ASME CODE MAIN COMMITTEE - 9/13/91

APPENDIX I

INQUIRY AND REPLY FOR NEW CODE CASE

APPROVED BY THE ASME CODE MAIN COMMITTEE

INQUIRY AND REPLY FOR NEW CODE CASE

APPROVED BY THE ASME CODE MAIN COMMITTEE

INQUIRY

May SA-533 Grade B, Class 1 plates, SA-508 Class 3 forgings and their weldments be used in Section III Division 1, Class 1 construction at temperatures exceeding 700°F up to 1000°F during Service Level C or D events for limited time of exposure not to exceed 1000 hours?

REPLY

It is the opinion of the committee that Class 1 nuclear components, fabricated from SA-533 Grade B, Class 1 plates, SA-508 Class 3 forgings and their weldments, may be used when metal temperatures exceed 700°F during Level C and D events in accordance with the following considerations:

(1) Metal temperatures shall not exceed 1000°F.

(2) The component design shall be based on a maximum cumulative time of 1000 hours when metal temperatures exceed 700°F.

(3) The number of anticipated events where metal temperatures exceed 800°F shall be limited to a total of 3.

(4) The rules for materials in Section III, Division 1, NB-2000 and Code Case N-47 for Class 1 Components in Elevated-Temperature Service shall apply to the materials of this case with the following additions:

   (a) The material specifications permitted by this Code Case are SA-533 Grade B Class 1, SA-508 Class 3 and their weldments.

   (b) The allowable stress intensities in Table 1 of this case shall be considered as extensions to the values of Tables I-1.0 in Appendix I for the materials and conditions addressed by this Case.

(5) The rules for design are:

   (a) The design rules of NB-3000 shall be satisfied for all Design and Operating Conditions for which metal temperatures do not exceed 700°F. The Design Conditions shall be as defined in NB-3000.

   (b) Metal temperatures exceeding 700°F are permitted only for Service Level C and D events. The applicable rules of Code Case N-47 for Class 1 Components in Elevated-Temperature Service shall be satisfied for these events.

The creep-fatigue interaction damage envelope shown in Figure 12 shall be used for the materials of this Case.
The mechanical and physical property values at elevated-temperatures are provided in Figures 1 thru 11 and Tables 1 thru 8 of this Case. The properties include:

(1) Isochronous Stress-Strain Curves,
(2) Yield Strengths,
(3) Stress-to-Rupture Values,
(4) Elevated-Temperature Fatigue Strength,
(5) Moduli of Elasticity, and
(6) Instantaneous and Mean Coefficients of Thermal Expansion.

The stress-rupture factors for welds shall have a value of 1.0 for the materials and conditions of this Case.

(c) In addition, the sum of the creep damage and fatigue damage, summed over the entire lifetime, shall not exceed the limit of Figure 12 anywhere in the structure. When performing the creep-fatigue interaction analysis, load history effects and residual stresses from prior low-temperature operation shall be considered in the evaluation. Since the fatigue curve at temperatures above 700°F is more restrictive than that for temperatures below 700°F, strain cycles which have one extremum at elevated-temperature and one extremum at low temperature shall be evaluated using the values in Figure 11 and Table 8.

(6) The following additional rules of the following Code Cases for elevated-temperature components shall apply:

(a) Code Case N-48, Fabrication and Installation of Elevated Temperature Components, Section III, Division I,

(b) Code Case N-49, Examination of Elevated-Temperature Nuclear Components, Section III, Class 1,

(c) Code Case N-50, Testing of Elevated-Temperature Components, Section III, Division 1, Class 1, and

(d) Code Case N-51, Protection Against Overpressure of Elevated-Temperature Components, Section III, Division 1, Class 1.

(7) The component stamping and Data Report shall indicate this case number and the revision applied.

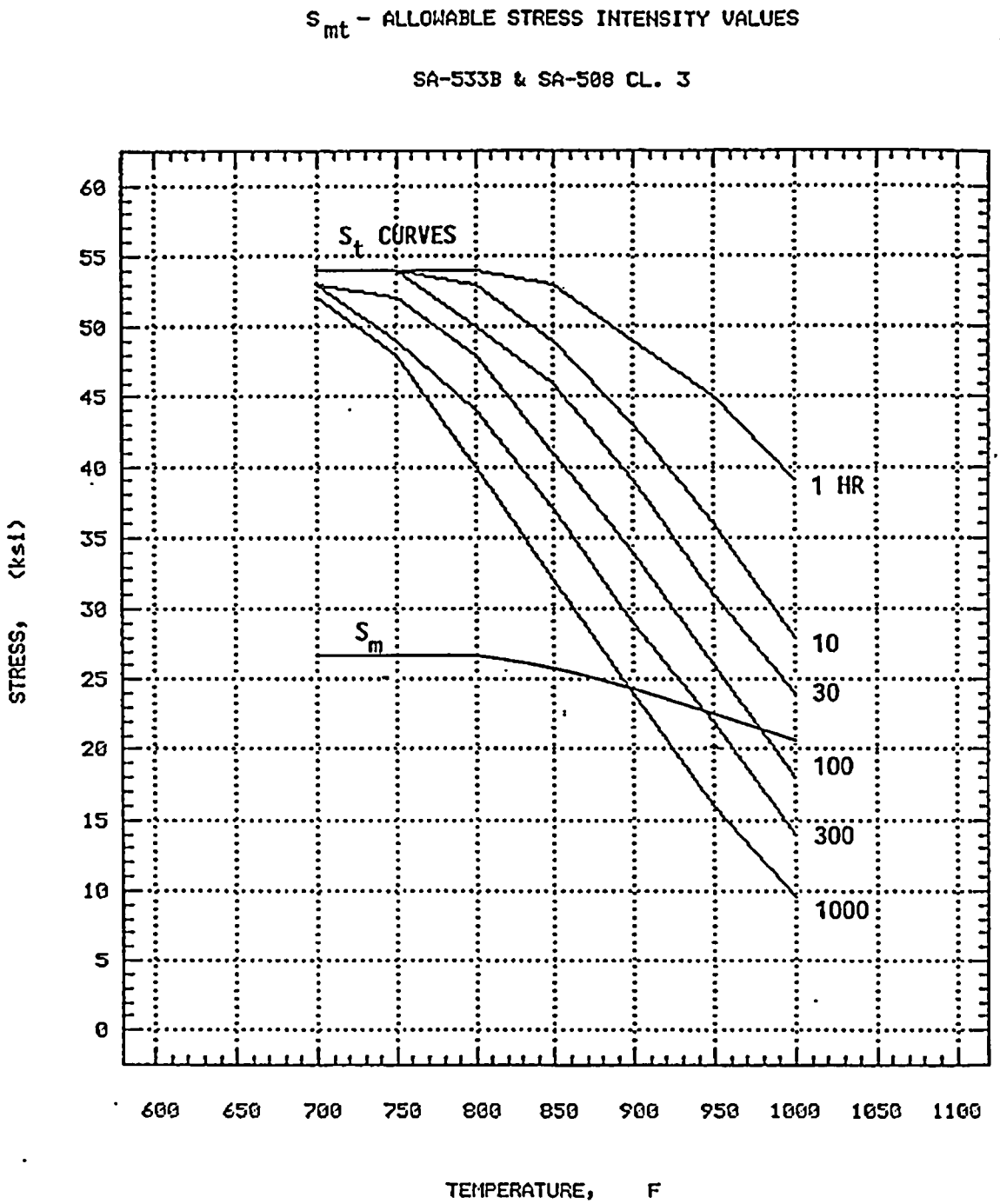

FIGURE 1 - S_{mt} VALUES FOR SA-533 GRADE B CLASS 1 AND SA-508 CLASS 3

Note: The S_{mt} values are the lower of the two stress intensity values, S_m (time-independent) and S_t (time-dependent).

TABLE 1

S_{mt} - ALLOWABLE STRESS INTENSITY VALUES FOR

SA-533 GRADE B CLASS 1 AND SA-508 CLASS 3

S_{mt} - ALLOWABLE STRESS INTENSITY VALUES, ksi

TIME AT TEMPERATURE, HOURS

TEMPERATURE (°F)	1	10	30	100	300	1000
700	26.7	26.7	26.7	26.7	26.7	26.7
750	24.9	24.9	24.9	24.9	24.9	24.9
800	24.2	24.2	24.2	24.2	24.2	24.2
850	22.7	22.7	22.7	22.7	22.7	22.7
900	21.3	21.3	21.3	21.3	21.3	21.3
950	20.2	20.2	20.2	20.2	20.2	16.0
1000	18.0	18.0	18.0	18.0	14.0	9.5

Note: The S_{mt} values are the lower of the two stress intensity values, S_m (time-independent) and S_t (time-dependent).

S_t - ALLOWABLE STRESS INTENSITY VALUES

SA-533B & SA508 CL. 3

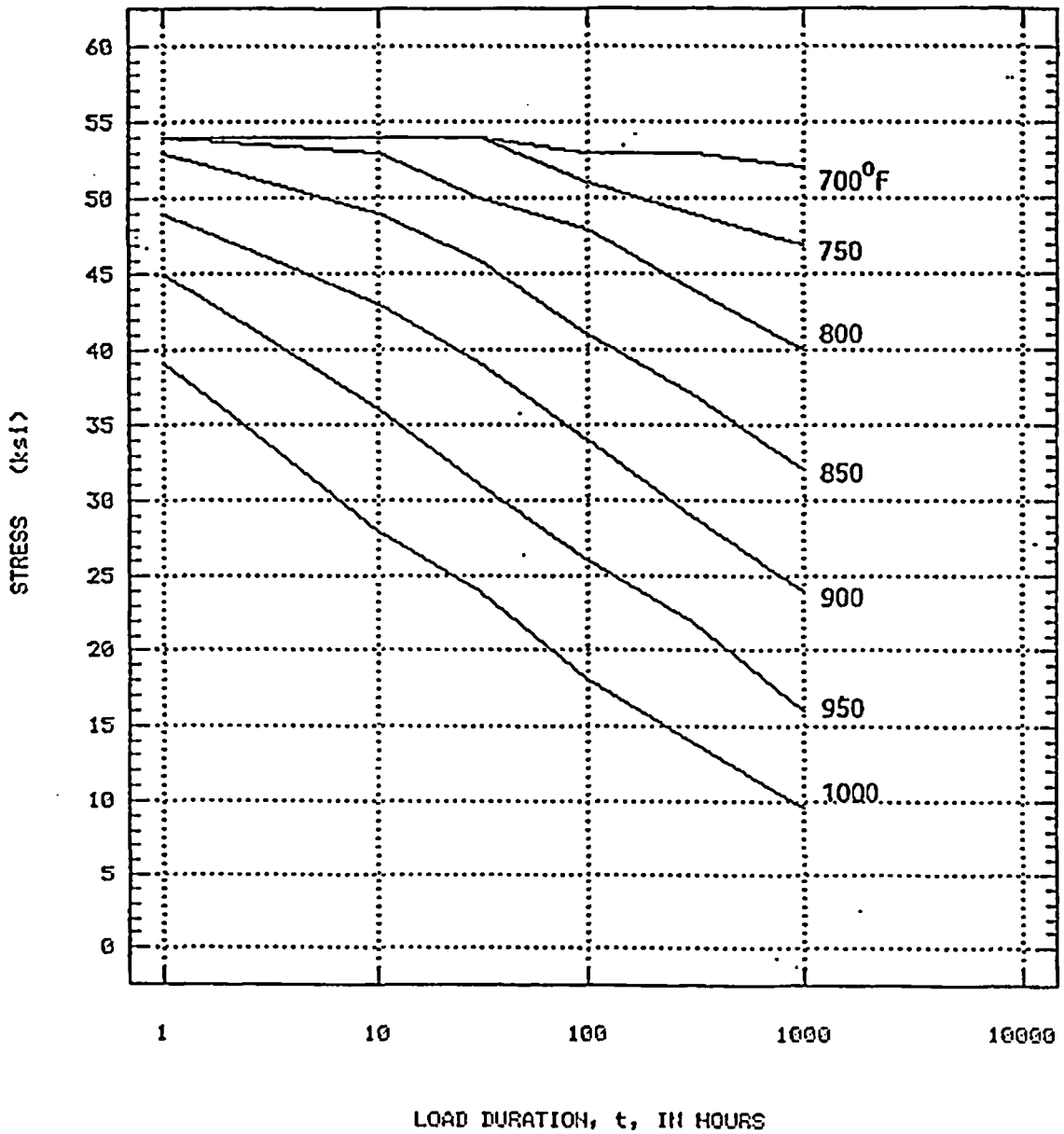

FIGURE 2 - S_t ALLOWABLE STRESS INTENSITY VALUES

TABLE 2

S_t - ALLOWABLE STRESS INTENSITY VALUES, 1000 psi

TEMPERATURE (°F)	TIME AT TEMPERATURE, HOURS 1	10	30	100	300	1000
700	54	54	54	53	53	52
750	54	54	54	52	49	47
800	54	53	50	48	44	40
850	53	49	46	41	37	32
900	49	43	39	34	29	24
950	45	36	31	26	22	16
1000	39	28	24	18	14	9.5

TABLE 3

S_m - ALLOWABLE STRESS VALUES, YIELD STRENGTH AND TENSILE STRENGTH VERSUS TEMPERATURE

TEMPERATURE (°F)	S_m (ksi)	YIELD STRENGTH (ksi)	TENSILE STRENGTH (ksi)
75	26.7	50.0	80.0
100	26.7	50.0	80.0
200	26.7	47.5	80.0
300	26.7	46.5	80.0
400	26.7	45.0	80.0
500	26.7	43.5	80.0
600	26.7	43.0	80.0
650	26.7	43.0	80.0
700	26.7	43.0	80.0
750	24.9	42.5	74.8
800	24.2	42.0	72.6
850	22.7	40.0	68.2
900	21.3	38.5	63.8
950	20.2	32.0	60.5
1000	18.0	34.5	53.9

EXPECTED MINIMUM STRESS-TO-RUPTURE

VALUES, 1000 psi SA-533B & SA-508 CL. 3

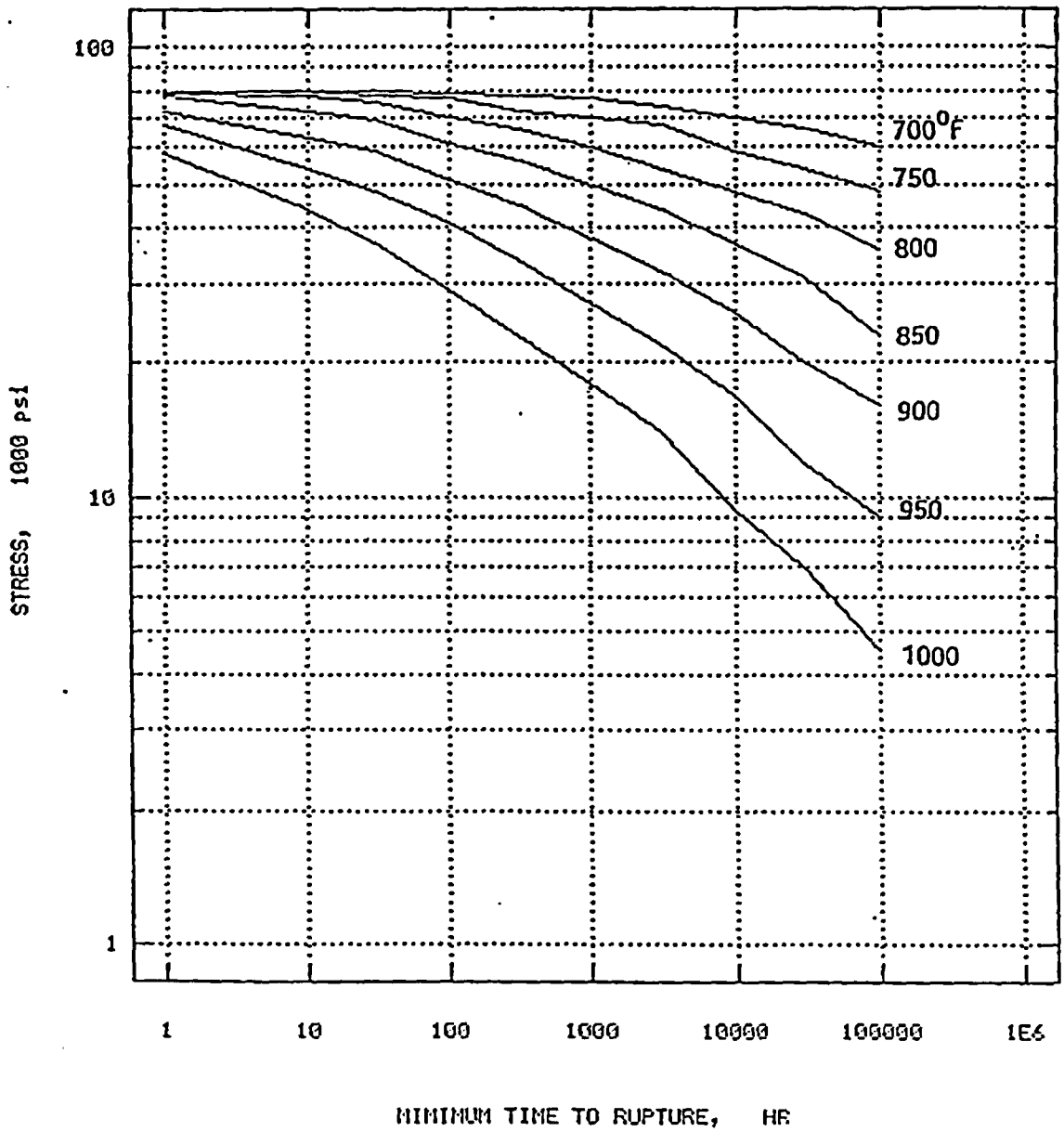

FIGURE 3 - STRESS-TO-RUPTURE (MINIMUM)

TABLE 4
EXPECTED MINIMUM STRESS-TO-RUPTURE VALUES (ksi).

TIME TO RUPTURE

TEMPERATURE (°F)	1	10	30	100	300	1000	3000	10000	30000	100000
700	80	80	80	79	78	77	74	70	66	60
750	80	80	78	77	72	70	67	59	54	48
800	79	78	75	70	66	60	54	48	43	36
850	78	72	69	61	56	50	44	37	31	23
900	72	63	59	51	45	38	32	26	20	16
950	67	54	48	41	34	27	22	17	12	9
1000	58	44	37	29	23	18	14	9.5	7	4.5

TABLE 5

MODULUS OF ELASTICITY VS. TEMPERATURE

TEMPERATURE (°F)	ELASTIC MODULUS (ksi) ($x10^3$)
-325	31.1
-200	30.5
-100	29.9
70	29.2
200	28.5
300	28.0
400	27.4
500	27.0
600	26.4
700	25.3
800	23.9
900	22.2
1000	20.1
1100	17.8

TABLE 6

INSTANTANEOUS COEFFICIENT OF THERMAL EXPANSION VS. TEMPERATURE

Instantaneous Coefficient of Thermal Expansion in/in - °F x 10^6		
Temp, °F	SA-533B Class 1 (Mn - 1/2Mo - 1/2Ni)	SA-508 Class 3 (3/4Ni - 1/2Mo - Cr - V)
70	7.02	6.41
100	7.13	6.53
150	7.29	6.73
200	7.45	6.93
250	7.60	7.12
300	7.74	7.30
350	7.88	7.49
400	8.01	7.66
450	8.13	7.84
500	8.25	8.03
550	8.36	8.21
600	8.46	8.35
650	8.55	8.51
700	8.63	8.64
750	8.71	8.78
800	8.78	8.90
850	8.84	9.04
900	8.90	9.13
950	8.95	9.22
1000	8.99	9.30

TABLE 7

MEAN COEFFICIENT OF THERMAL EXPANSION VS. TEMPERATURE

	Mean Coefficient of Thermal Expansion in/in - °F x 10^6	
Temp, °F	SA-533B Class 1 (Mn - 1/2Mo - 1/2Ni)	SA-508 Class 3 (3/4Ni - 1/2Mo - Cr - V)
70	----	----
100	7.06	6.50
150	7.16	6.57
200	7.25	6.67
250	7.34	6.77
300	7.43	6.87
350	7.50	6.98
400	7.58	7.07
450	7.63	7.15
500	7.70	7.25
550	7.77	7.34
600	7.83	7.42
650	7.90	7.52
700	7.94	7.59
750	8.00	7.68
800	8.05	7.76
850	8.10	7.85
900	8.14	7.89
950	8.19	7.98
1000	8.23	8.05

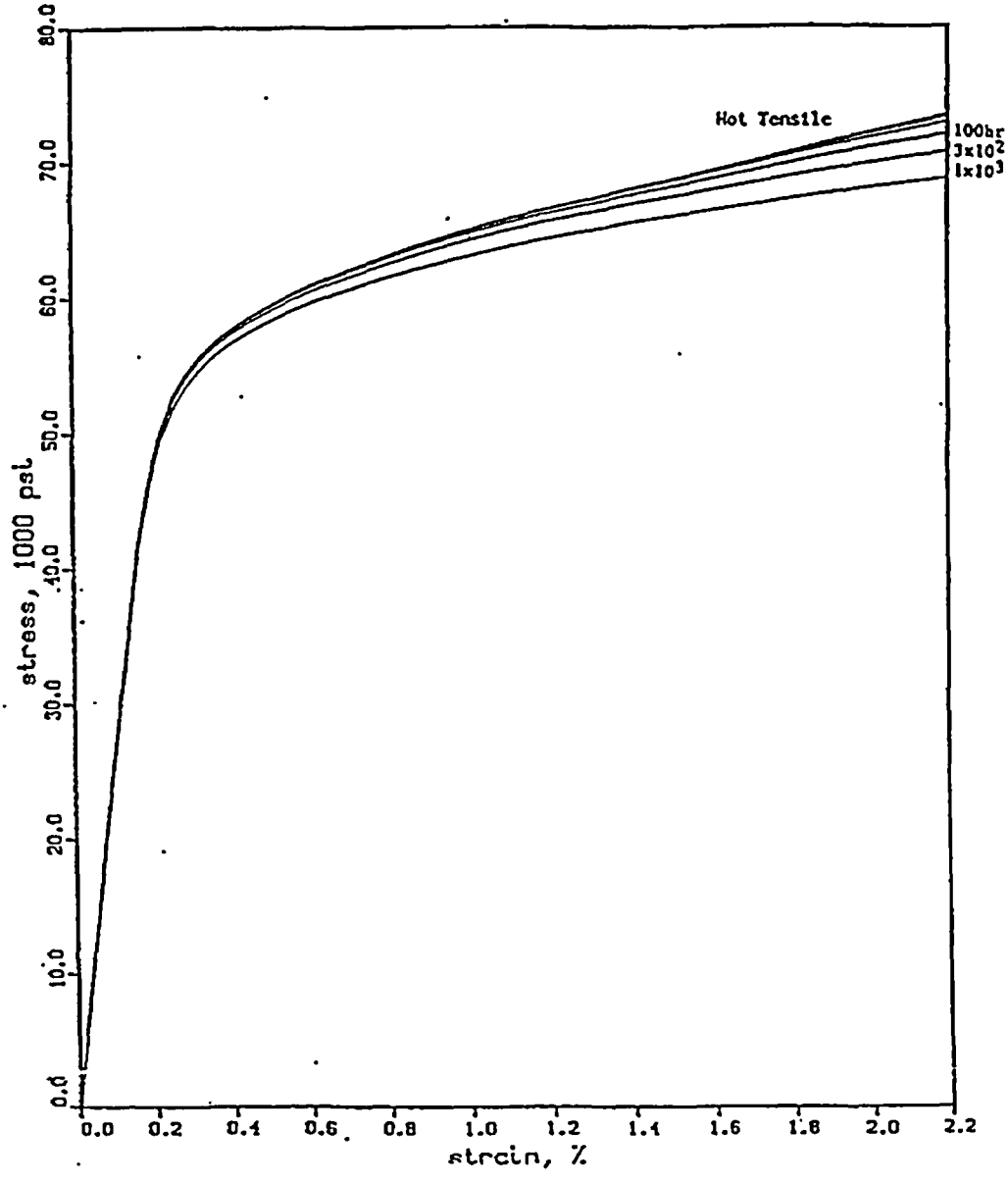

FIGURE 4 - ISOCHRONOUS STRESS-STRAIN CURVES FOR 700°F

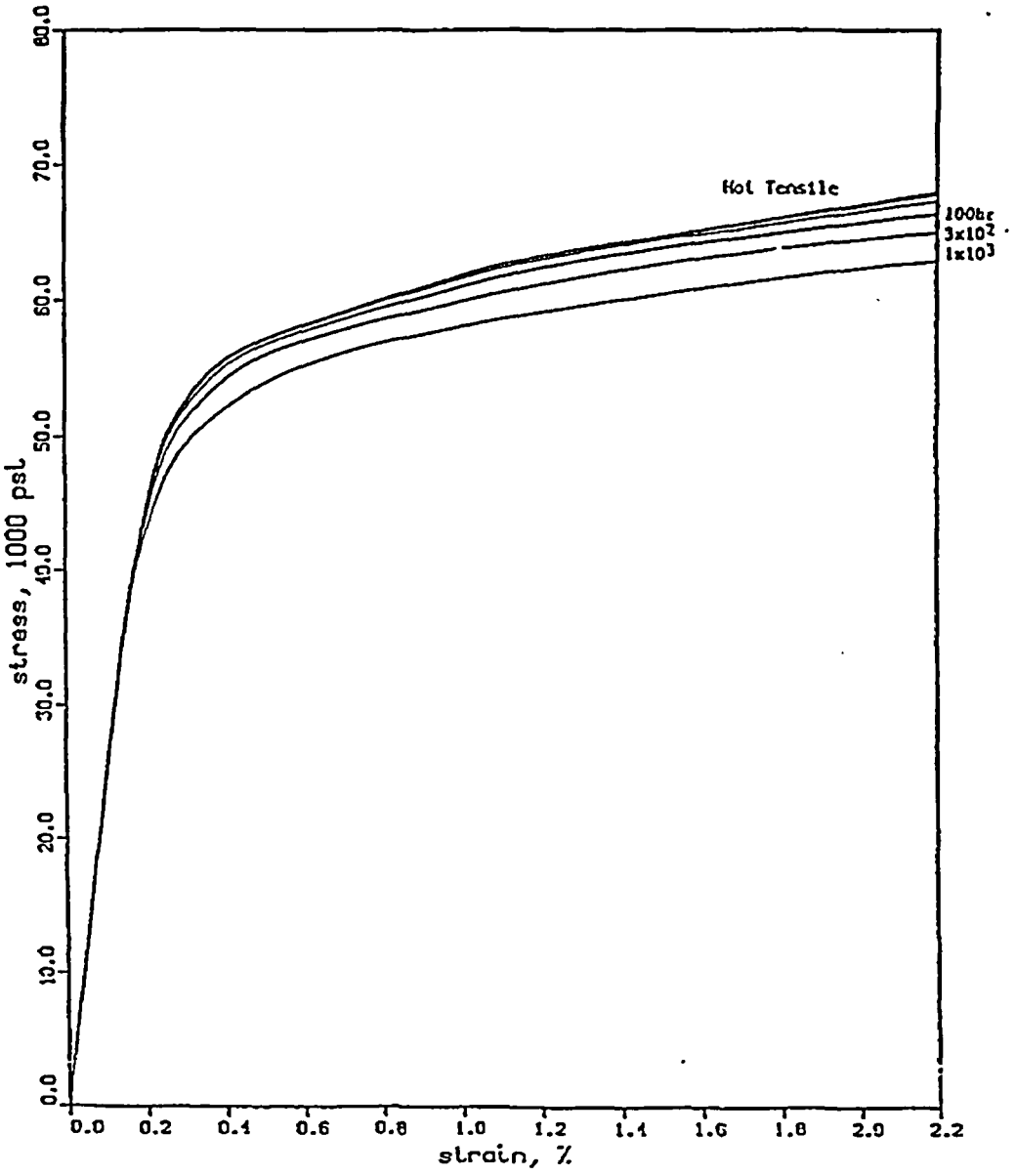

FIGURE 5 - ISOCHRONOUS STRESS-STRAIN CURVES FOR 750°F

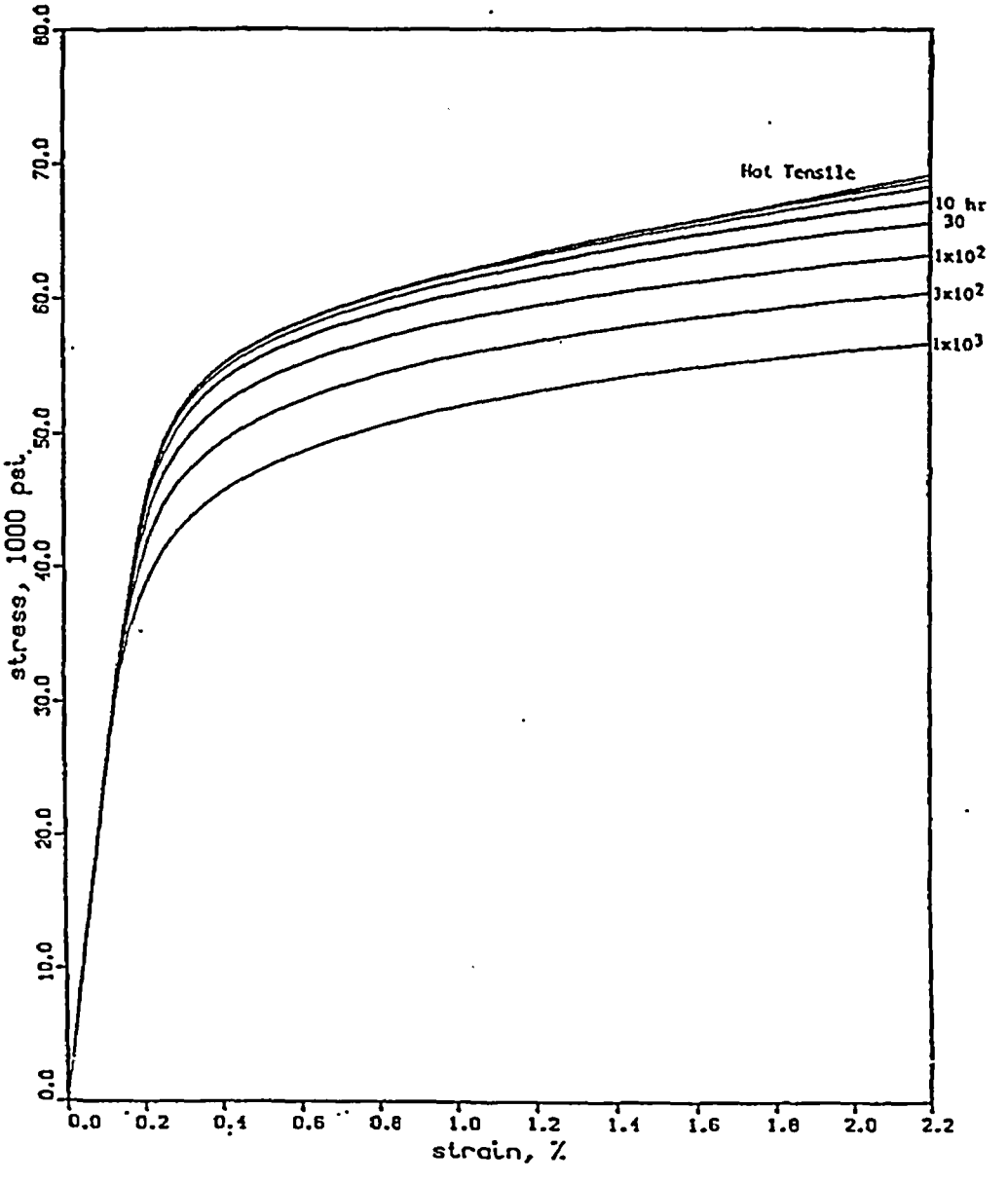

FIGURE 6 - ISOCHRONOUS STRESS-STRAIN CURVES FOR 800°F

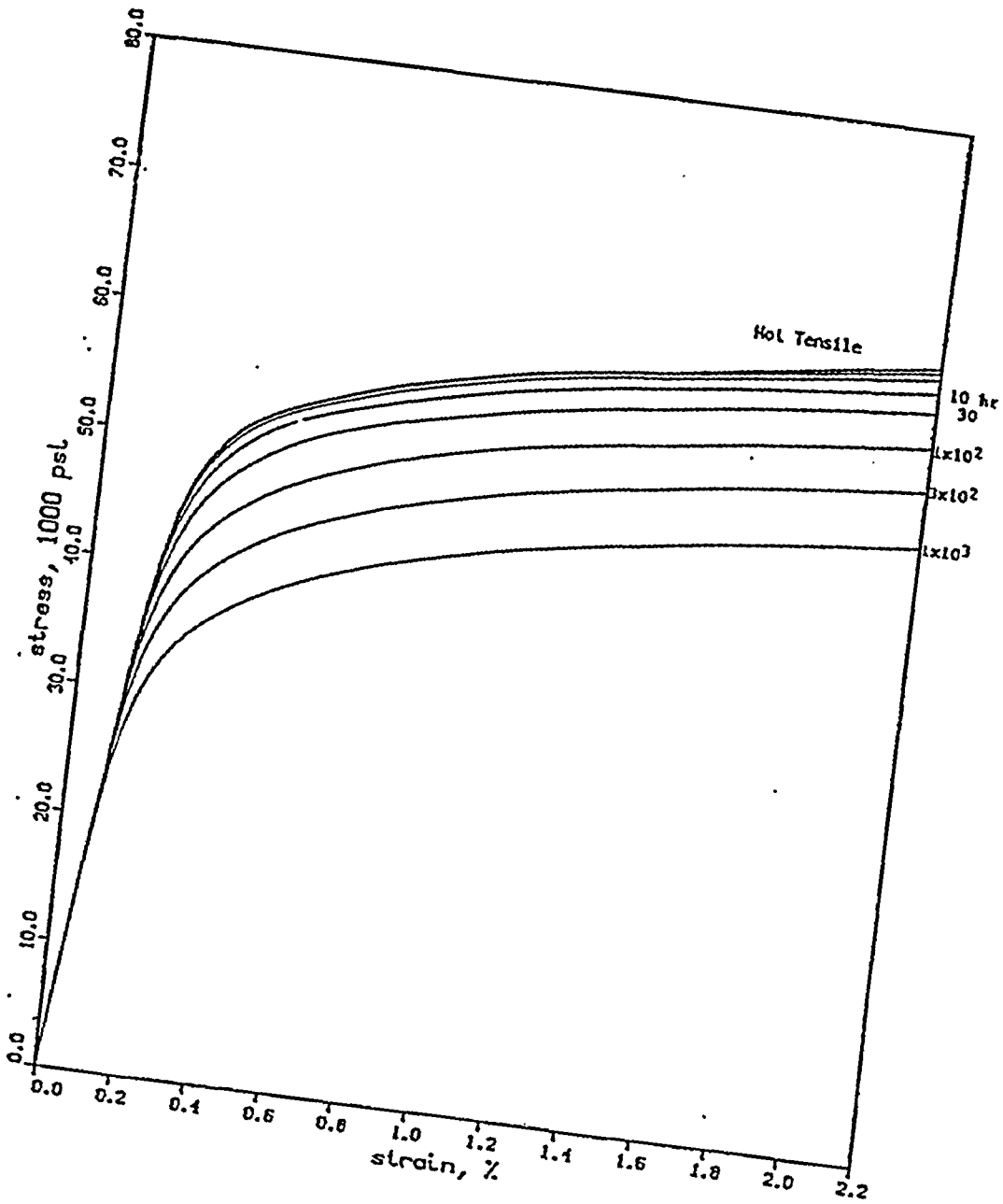

FIGURE 7 - ISOCHRONOUS STRESS-STRAIN CURVES FOR 850°F

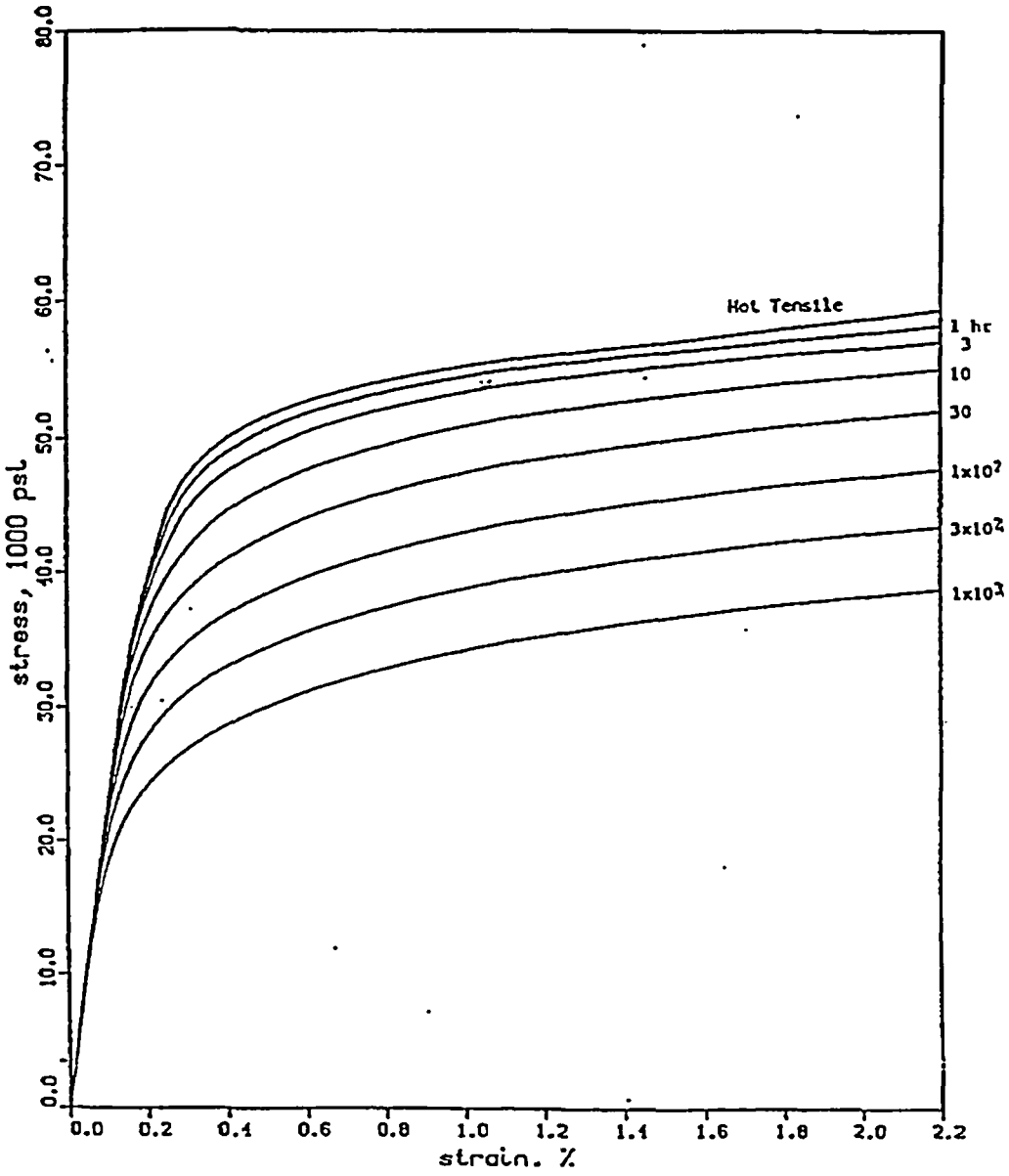

FIGURE 8 - ISOCHRONOUS STRESS-STRAIN CURVES FOR 900°F

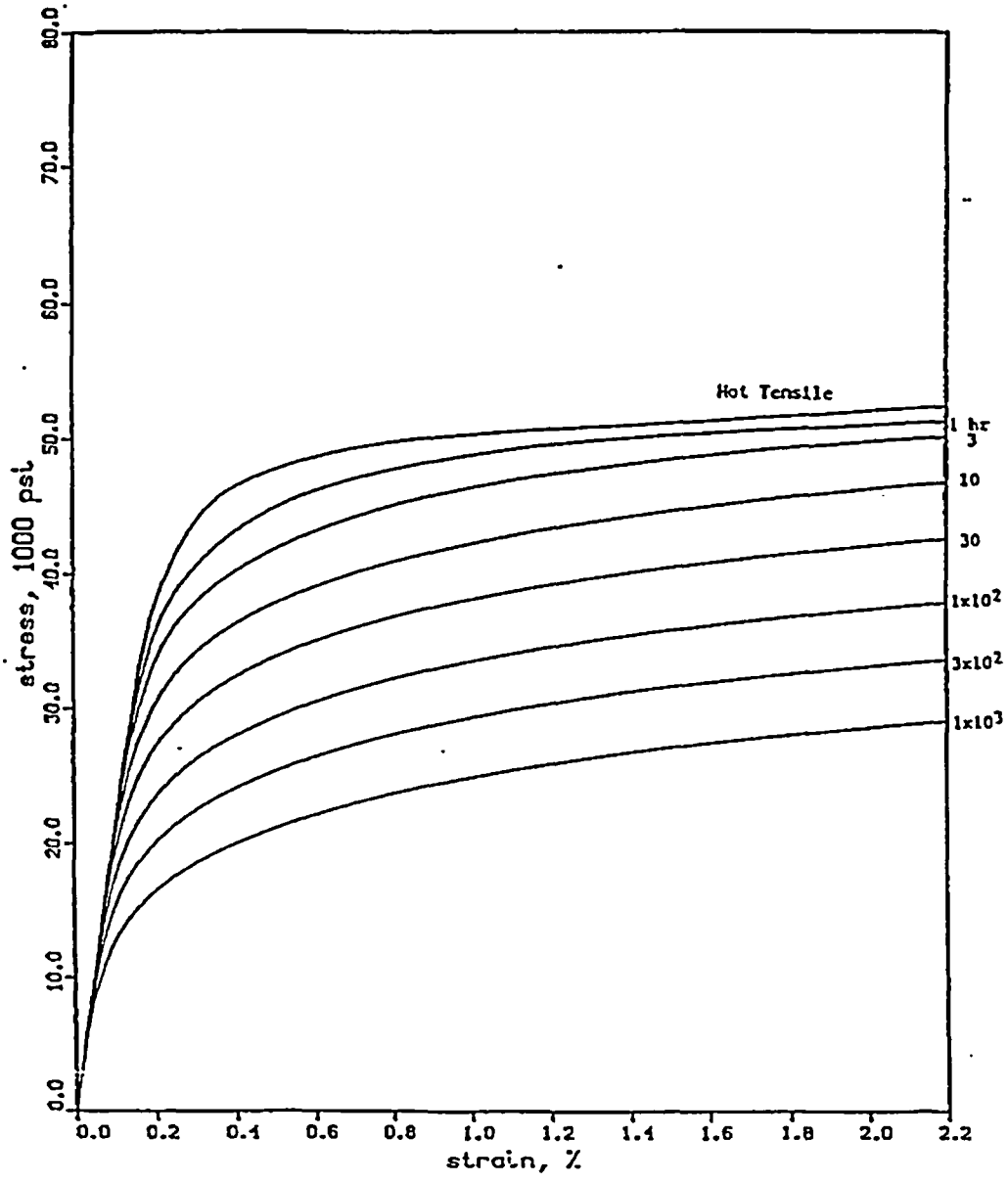

FIGURE 9 - ISOCHRONOUS STRESS-STRAIN CURVES FOR 950°F

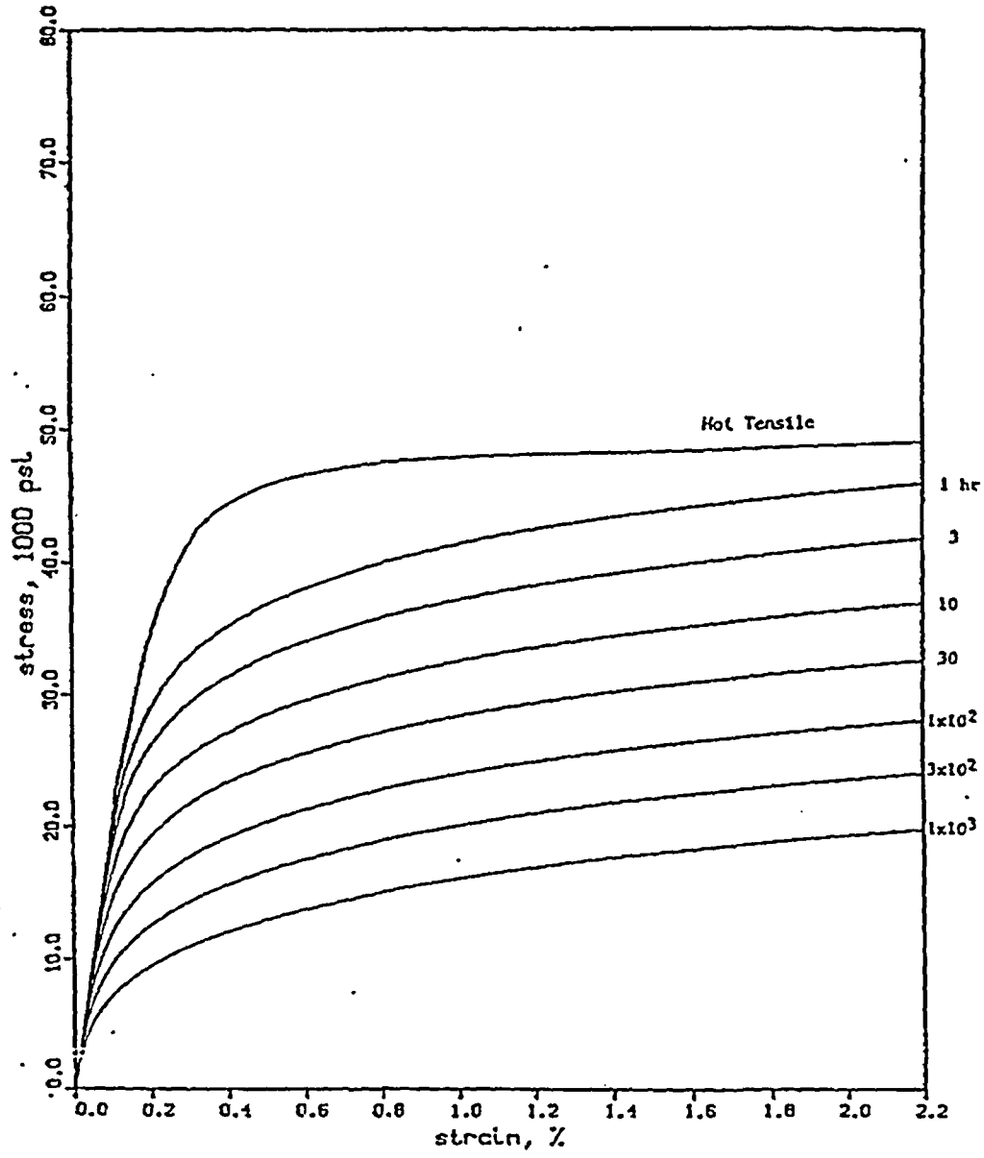

FIGURE 10 - ISOCHRONOUS STRESS-STRAIN CURVES FOR 1000°F

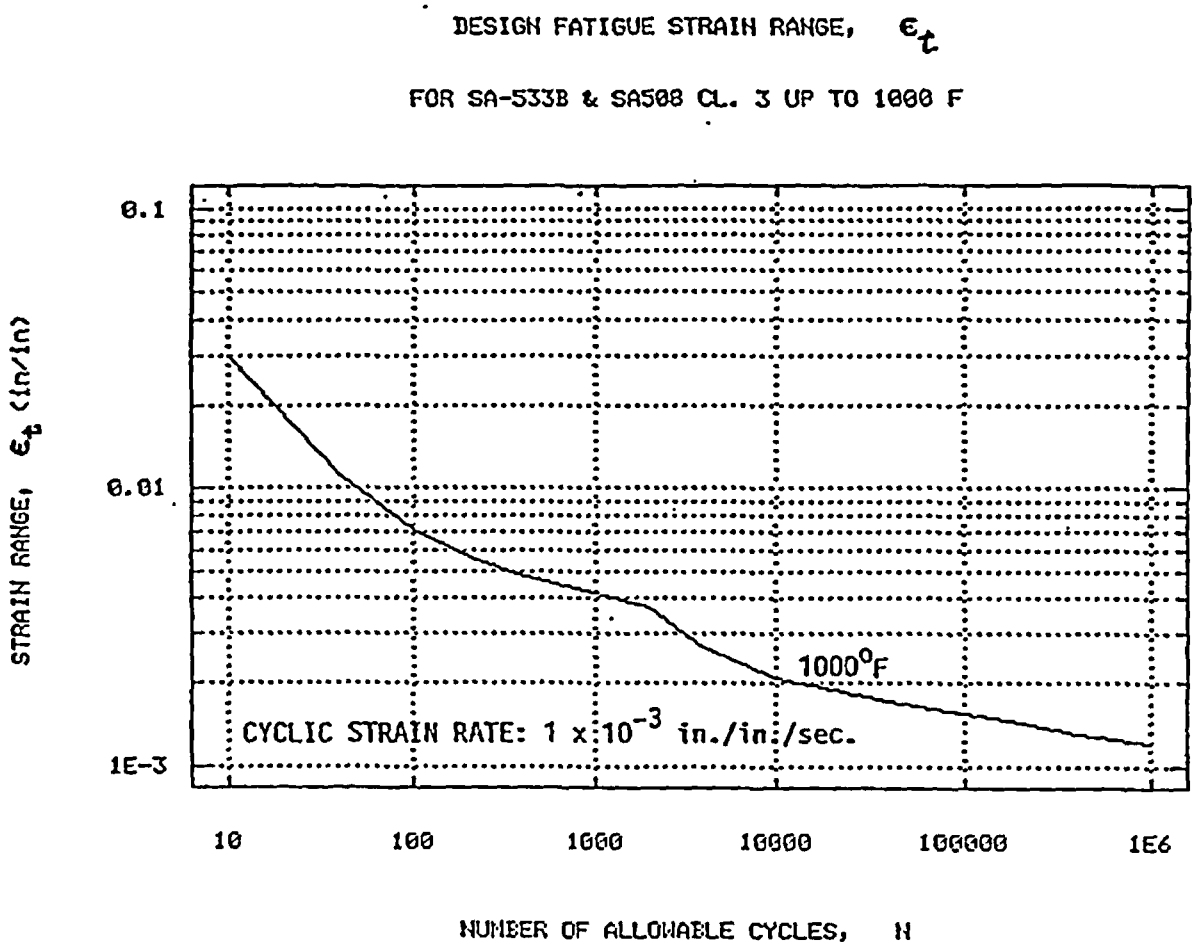

FIGURE 11 - DESIGN FATIGUE STRAIN RANGE FOR SA-533B CLASS 1 AND SA-508 CLASS 3

TABLE 8

DESIGN FATIGUE STRAIN RANGE FOR

SA-533 GRADE B CLASS 1 & SA-508 CLASS 3 UP TO 1000°F

N_D, NUMBER OF CYCLES [NOTE (1)]	C_t, STRAIN RANGE (in./in.) AT TEMPERATURE
10^1	0.030
4×10^1	0.011
10^2	0.0071
2×10^2	0.0056
4×10^2	0.0048
10^3	0.0042
2×10^3	0.0037
4×10^3	0.0027
10^4	0.0021
2×10^4	0.00190
4×10^4	0.00170
10^5	0.00155
2×10^5	0.00145
4×10^5	0.00130
10^6	0.00120

NOTE: (1) Cycle Strain Rate: 1×10^{-3} in./in./sec.

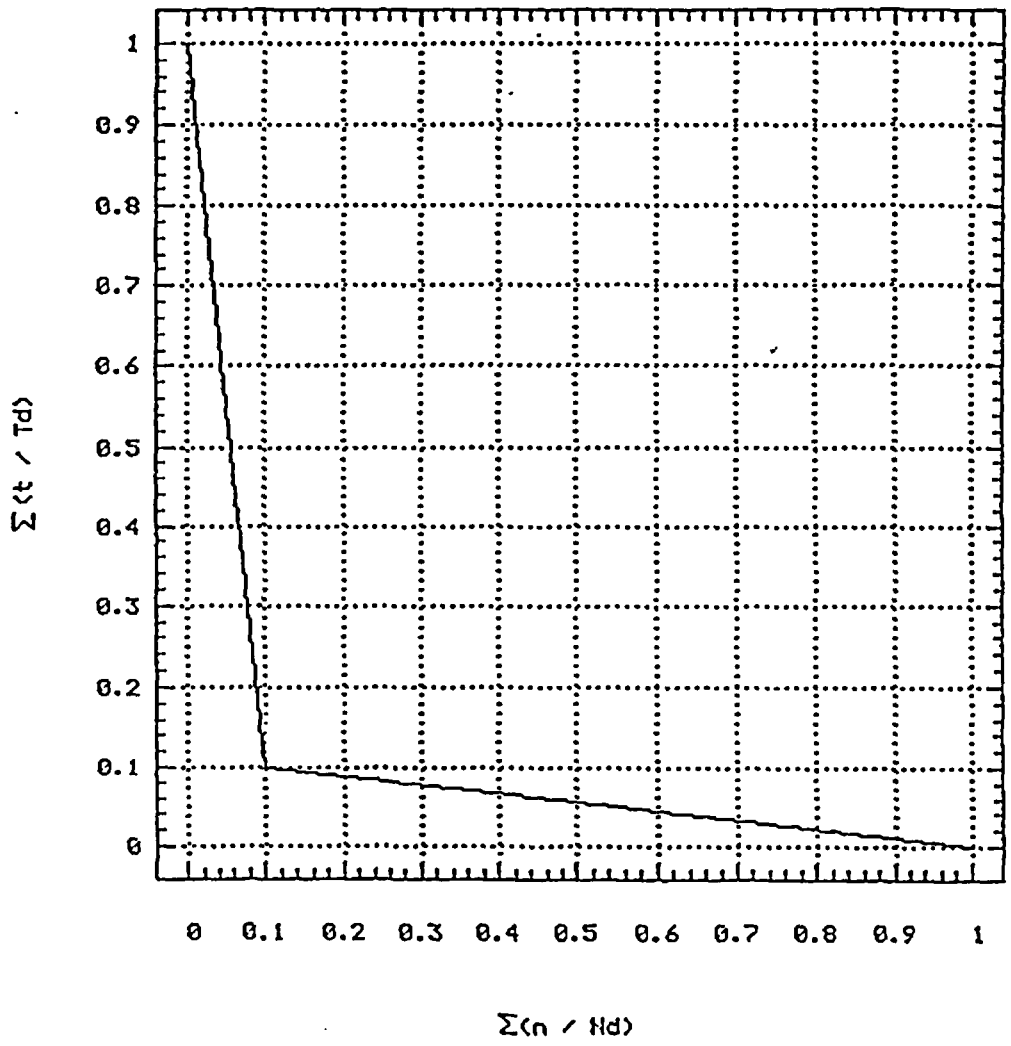

FIGURE 12 - CREEP-FATIGUE DAMAGE ENVELOPE

6. Combustion Engineering Report MML-89-142, "Creep and Tensile Properties of SA508 Class 3 Forging Material," December 1989.

Creep and Tensile Properties of SA508 Class 3 Forging Material

Project No. 900773
Job No. 98192177

MML-89-142

December 13, 1989

F. V. Ellis and J. E. Bynum

Metallurgical and Materials Laboratory
Combustion Engineering, Inc.
911 W. Main Street
Chattanooga, TN 37402

DISCLAIMER NOTICE

This report was prepared as an account of work sponsored by Oak Ridge National Laboratory. Neither Oak Ridge National Laboratory, nor Combustion Engineering, Inc., nor any person acting on their behalf:

a. makes any warranty or representation, express or implied, with respect to the accuracy, completeness, or usefulness of the information contained in this report, or that the use of any information, apparatus, method, or process disclosed in this report may not infringe privately owned rights; or

b. assumes any liabilities with respect to the use of, or for damages resulting from the use of any information, apparatus, method, or process disclosed in this report.

Creep and Tensile Properties of
SA508 Class 3 Forging Material

ABSTRACT

Creep and tensile properties were measured for a single heat of SA508 Class 3 forging material. The test material was given a heat treatment of 40 hours at 607C to simulate an extended post weld heat treatment. Duplicate tensile tests at strain rates of .008 $min.^{-1}$ and .0016 $min.^{-1}$ were conducted at room temperature, 371C, 427C, 482C, 538C and 593C. The yield and tensile strengths for the SA508 Class 3 material were lower than those for SA533 Grade B Class 1 steels which had been given a shorter term PWHT. The creep tests were conducted in air out to times of 3000 hours in the temperature range of 371C to 593C. The strain-time data were acquired and stored using a computer controlled data acquisition system. In addition to the rupture data, the minimum creep rate, time to end of secondary creep, and 0.2 percent offset tertiary time and strain data were obtained. All creep curves had the classical shape. For the primary plus secondary stage of creep, both power law and rational polynominal creep constitutive equations were good descriptors. For the tertiary creep stage, a creep equation was written based on a linear relationship between log creep strain rate and linear creep strain. Based on the tertiary creep equation, a rupture parameter was defined which correlates well with the observed rupture time. For the complete creep curve, a power law primary plus exponential tertiary model had better conformity to the observed creep curve than the Theta Projection. Metallographic examination of creep specimens indicated no significant hardness or microstructural changes for temperatures up to 482C and out to times of 2000 hours.

INTRODUCTION

Currently, the ASME Boiler and Pressure Vessel Code allowable stresses in Section III for the two common nuclear pressure vessel steels, SA508 Class 3 and SA533 Grade B Class 1, are given only to a maximum temperature of 371C. For a design application, both allowable stresses and design rules were required for limited duration elevated temperature service using these steels. A critical review of the available elevated temperature property data for Mn-Mo-Ni steels indicates the need for further testing in order to develop allowable stresses. One of the earlier studies sponsored by PVRC (DeBarbadillo, Pense, Stout, 1966) on A-302B (Ni) steel is inappropriate since the steel meets the chemical specification of A533B but exceeds the tensile strength requirement. One important aspect of this study was the testing of weldment as well as base material . The recent results reported by Reddy and Ayres (1982) on SA533B and SA508 give only short term data (approximately 48 hours maximum test duration) and emphasizes the creep strain-time properties with no rupture data provided. The American Society for Testing and Materials (ASTM) data series (Smith, 1971) gives rupture property data for six heats of Mn-Mo-Ni steels. Of these, only two heats would appear to meet the chemical and strength requirements for the SA533B Class 1 or SA508 Class 3 specifications. Although the data may be available from the original sources, other data needed for the allowable stress determination - time to 1% strain and time to tertiary creep - were not given in the ASTM data publication (Smith, 1971).

The objective of the current testing program was to measure the short term elevated temperature properties of SA508 Class 3 forging material required to support ASME Code approval for this steel under transient conditions in nuclear service. Only a limited testing program was conducted on the SA508 material, since similar properties to SA533 were anticipated for the two steels and a more comprehensive multiple heat testing program was being conducted by ORNL (McCoy, 1989) on SA533 Grade B Class 1 base materials, weldments, and compatible SA and SMA weld metals.

MATERIAL

The test material was a large diameter (approximately 5.3 m) reactor vessel closure head with a nominal wall thickness of 480 mm. An initial study (Borden, 1989) of the homogeneity of the flange material included chemical analyses, metallography, Charpy and tensile testing. Macroetched sections revealed inhomogeneities in the form of dark grey streaks scattered throughout the forging which were identified as resulting from alloy element segregation. Near the quenched surface the microstructure was 100 percent bainite. For the mid-thickness position, approximately 15 percent ferrite - 85 percent bainite was found. On a microscale, faint banding due to the varying proportions of ferrite and bainite in the microstructure was observed. The chemical composition for the SA508 Class 3 forging material is given in Table 1.

Prior to creep and tensile testing, the material was given a simulated post weld heat treatment of 607C ± 15C for 40 hours. The Vicker's hardness (20 kg load) was 188 (equivalent Rockwell B 91) following this heat treatment.

RESULTS AND DISCUSSION

The tensile and creep specimens had a 6.4 mm diameter cross section and a 31.8 mm gage length. Creep testing was performed on conventional lever-arm type constant load creep testing machines. These machines have automated beam leveling to accommodate specimen elongation. The tensile tests were conducted in a modified creep machine at two strain rates. All test data were acquired with a computerized data acquisition and process control system (Roberts and Cullen, 1973), (Bynum, 1989).

Tensile Properties

Results of the tensile tests at room temperature, 371C, 427C, 482C, 538C and 593C are listed in Table 2 and shown in Figures 1-4. The nominal strain rates for these tests were .0080 $min.^{-1}$ and .0016 $min.^{-1}$. Duplicate tests were performed at each temperature and strain rate for a total of 24 tests in the basic program. Because of the 64 MPa difference in ultimate tensile

strength between the replicate tests at 371C and 0.0080 min^{-1}, a third test was performed at this test condition. This third test agreed with the higher strength of 523 MPa. The yield and ultimate tensile strength data shown in Figures 1 and 2 were fit to cubic spline curves shown as solid lines in the figures. These fits are non-physical and should not be used to infer expected material behavior in the temperature range where test data does not exist.

The yield and tensile strengths for the SA508 Class 3 material are consistently lower than those found for the SA533B base material tested at equivalent strain rates (McCoy, 1989). This difference may be due to the longer simulated PWHT time of 40 hours for SA508 material compared to the 20 hours for the SA533B material. However, it should be noted that the room-temperature strength values are considerably less than those obtained on the same material tested at more "normal" strain rates in a different machine in the Metallurgical and Materials Laboratory after heat treating a section of the forging (Borden, 1989). These nine tests were conducted at strain rates on the order of .050 $min.^{-1}$ to verify that the heat treatment resulted in acceptable tensile properties. The yield strengths from the nine tests ranged from 416 MPa to 460 MPa and the ultimate tensile strengths ranged from 572 MPa to 611 MPa. An additional room-temperature test conducted at an intermediate strain rate of .024 $min.^{-1}$ (test AKNZ in Table 2) confirmed the higher strengths of the .050 $min.^{-1}$ strain rate tests. These higher strain rates are more representative of normal production type testing. Therefore, it appears that the tensile properties of the SA508 heat used in this investigation are highly strain-rate sensitive.

Tensile ductility of the SA508 material is shown in Figures 3 and 4 as a function of temperature at the two different strain rates. The total elongation (31.2 mm gage length) exceeds 20 percent over the entire temperature range. While both the reduction in area and the total elongation increase as the test temperature increases, the uniform elongation decreases with values approaching 2 percent at 593C.

Creep Properties

The criteria for establishing the ASME code time-dependent allowable stresses, S_t, for a specified time, t, is defined as the lower of the

following three time dependent values: (1) two-thirds of the minimum stress to produce rupture (2) 80 percent of minimum stress to cause tertiary creep and (3) the minimum stress to produce one percent total strain. For the intended application, the 10^3 hour allowable stresses were required for temperatures from 371C to 538C. The approach taken to gather the necessary data for the code analysis was to perform short term (approximately 3000 hours maximum duration) creep and stress rupture tests at five temperatures (371C, 427C, 454C, 482C, and 593C) with three stress levels at each temperature. The data analysis will be performed by ORNL and will use the creep and rupture properties obtained for both the SA533B and SA508 materials.

Strain versus time curves for each of the respective isothermal test temperatures of 371C, 427C, 482C, 538C and 593C are shown in Figures 5-9. Over the full range of stresses and temperatures, these curves exhibited the classical shape having primary, secondary and tertiary regimes. Time to a given creep strain data for the SA508 base material are given in Table 3. The creep strain is found by subtracting the loading strain (Table 3) from the measured total strain. Other measures of the creep curve -- minimum creep rate, Monkman-Grant constant (minimum creep rate times rupture time), time to end of secondary creep (t_2), and 0.2% offset tertiary time ($t_{0.2\%}$) and strain -- are given in Table 4.

Uniaxial stress rupture properties and Larson-Miller Parameter values are given in Table 5. The Larson-Miller Parameter, P, is defined as

$$P = T(C + \text{Log } t_r)$$

where T is absolute temperature, t_r is the rupture time, and C is the Larson Miller constant. The universal constant value of 20 was used in Table 5. The rupture test results are shown in Figure 10 plotted as log rupture stress versus log time. Various correlations have been proposed for relating rupture time to creep parameters other than stress. Figure 11 shows the minimum creep rate versus rupture time relation of Monkman-Grant. The time to end of secondary creep and time to 0.2% offset tertiary versus rupture time relations are shown in Figures 12 and 13. There is an apparent temperature dependence for both t_2 vs t_r and the $t_{0.2\%}$ vs t_r relations which could be easily modeled using heat-centered techniques.

The time to one percent creep strain data is shown in Figure 14 on a log stress versus log time basis and in Figures 15-18 on a log stress versus Larson-Miller Parameter basis using Larson-Miller constants (C) of 20.0, 20.8, 23.1 and 24.9, respectively. The solid line drawn in Figure 15 represents the mean of the 533B Class 1 material calculated by the relation given by McCoy (1989). The SA508 material is weaker in creep at the high stress region and tends to merge in the lower stress (approximately 55 MPa) region. This crossover in creep strength is similar to that reported by Pense and Stout (1966) for A302B steel. They showed that the 10,000 hour rupture strength for Q&T steel was vastly superior than that for N&T steel up to temperatures of 510C while the N&T steel had slightly better strengths at 538C and 593C. This change in rupture strengths was associated with the accelerated rate of spheroidization at the higher test temperatures for the Q&T microstructure compared to the coarser N&T microstructure. A similar microstructural based explanation may apply in the current study with the predominantly bainite microstructure of SA533B steel being less stable at the higher test temperatures compared to the ferrite-bainite (slower cooling rate) microstructure of the SA508 material. The solid line shown in Figures 16, 17 and 18 was drawn using a log stress plus stress master curve and a Larson Miller parameter fit to the data in Table 2 for different stress ranges. Comparison of the data in these figures indicates that the lower constant values correlate the low stress-high temperature data while higher constant values correlate the higher stress-low temperature data. It should be noted that the Dorn parameter correlations had lower standard deviations in log time to one percent creep strain than the Larson-Miller parameter.

Creep Constitutive Equations

The measured engineering strain, e, was converted to true strain, ϵ, using the following relation

$$\epsilon = \ln (1 + e)$$

Creep strain was found by subtracting the loading strain from the total strain. The resulting creep strain versus time curves were fit using several

relationships. Nonlinear-least squares fits were performed on the complete creep curves (through approximately 6% creep strain), the tertiary portion of the curves, and the portion from beginning through the end of secondary creep.

The primary plus secondary curve fit coefficients and models are given in Tables 6, 7 and 8. In general, the power law and the rational polynominal description were in good conformity to the creep curves while the exponential primary law tended to underpredict the initial creep and had higher standard deviations in creep strain than the other models.

The tertiary creep law is based on the observation that the plot of log creep strain rate versus creep strain is linear in the tertiary regime (Sandstrom and Kondyr, 1976). Using this relationship and integration, the following creep strain-time equation can be derived

$$\epsilon_c = -A \ln (C - Bt)$$

where ϵ_c is creep strain, t is time, and A, B and C are constants. A tertiary creep rupture parameter, P, can be defined by evaluating the tertiary equation at rupture and solving for the rupture time as follows

$$P = t_r = (C - e^{-\epsilon_r/A})/B$$

where ϵ_r is the true creep rupture strain.

For values of $\epsilon_r/A > 3$, the rupture parameter is given by the following approximate relation

$$P \simeq C/B$$

The values for the regression coefficients A, B, and C for the tertiary creep model are given in Table 9. The exact and approximate rupture parameters are also given in Table 9. Figure 19 shows a plot of log rupture time versus log tertiary creep rupture parameter (C/B) for the SA508 for Class 3 forging

material. It is intended that some of the creep tests in progress will be continued in order to extend this correlation out to longer times.

The complete creep curve models and regression coefficients are given in Tables 10 to 13. In general, it should be noted that the Theta Projection tended to underpredict the observed strain-time response in the primary regime while the power law primary plus exponential tertiary model had excellent conformity to the entire creep curve.

Metallography

Creep specimens exposed for the longest time at each temperature were metallographically prepared and examined to characterize the metallurgical structure. At 371C and 427C, no readily discernible microstructural changes or hardness decrease was observed as a result of the creep exposure for 3149 hours and 2566 hours, respectively. The specimen that ruptured in 2035.6 hours at 482C (LMP = 17600) also showed only very slight changes and is similar in both time and temperature to the maximum anticipated for the low probability transient condition. Both specimens exposed at the higher test temperatures had decreased hardness values and from slight to significant spheroidization of the microstructure. Figure 20 compares the microstructure of the creep specimens at 427C, 482C, 538C and 593C. The hardness values, converted to Rockwell B scale from measured Vicker's (20 kg load), and exposure duration are also given in Figure 20.

SUMMARY

Creep and tensile property data have been obtained for a single heat of SA508 Class 3 forging material in order to support a proposed Code Case to extend the allowable stress up to a maximum temperature of 538C and out to times of 10^3 hours.

REFERENCES

Borden, M. P., 1989, "Properties of SA508-Class 3 Reactor Vessel Closure Head Flange," Metallurgical and Materials Laboratory, Final Report MML-89-111, Combustion Engineering, Chattanooga, TN.

Bynum, J. E., 1989, "Automating a Creep Testing Laboratory for Real-Time Data Acquisition and Control Using an HP 1000 Computer System,", Proceedings of the 1989 INTEREX HP Users Conference, San Francisco, Paper 1004.

DeBarbadillo, J. J., Pense, A. W., and Stout, R. D., 1966, "The Creep-Rupture Properties of Pressure Vessel Steels - Part II," Welding Research Supplement, Welding Journal, pp. 357s-367s.

McCoy, H. E., 1989, "Tensile and Creep Properties of SA533 Grade B Class 1 Steel," Oak Ridge National Laboratory, Oak Ridge, TN.

Pense, A. W., and Stout, R. D., 1966, "Characterization of Heat Treated Pressure Vessel Steels for Elevated Temperature Service," Heat-Treated Steels for Elevated Temperature Service, ASME, NY, NY, pp. 8-26.

Reddy, G. B., and Ayres, D. J., 1982, "High Temperature Elastic-Plastic and Creep Properties for SA533 Grade B Class 1 and SA508 Materials," EPRI NP-2763, Electric Power Research Institute, Palo Alto, CA.

Roberts, B. W., and Cullen, T. M., 1973, "Computerized System Collects Creep Data," Metals Progress, pp. 49-64.

Sandstrom, R., and Kondyr, A., 1976, "Model for Tertiary-Creep in Mo-and Cr-Mo-Steels," Mechanical Behavior of Metals, Vol. 2, Pergamon Press, NY, NY, pp. 275-284.

Smith, G. V., 1971, Evaluations of the Elevated Temperature Tensile and Creep-Rupture Properties of C-Mo, Mn-Mo and Mn-Mo-Ni Steels, ASTM Data Series Publication DS-47, American Society for Testing and Materials, Philadelphia, PA.

Table 1

Chemical Composition of
SA508 Class 3 Forging Material

Element	Composition (Weight Percent)	SA508 Class 3 Requirements
C	0.19	0.25 max.
Mn	1.35	1.20 - 1.50
P	0.006	0.025 max.
S	0.003	0.025 max.
Si	0.31	0.15 - 0.40
Ni	0.78	0.40 - 1.00
Cr	0.14	0.25 max.
Mo	0.49	0.45 - 0.60
V	0.005	0.05 max.
Cb	0.001	
Ti	0.001	
Co	0.014	
Cu	0.06	
Al	0.012	
B	<0.001	
W	<0.001	
As	0.007	
Sn	0.006	
Zr	<0.001	

Table 2

Tensile Properties of SA508 Class 3 Base Material

Specimen Code	Test Temperature °C	Test Temperature °F	Strain Rate 10-3/min.	Yield Strength Mpa	Yield Strength ksi	Tensile Strength Mpa	Tensile Strength ksi	Total Elongation %	Uniform Elongation %	Reduction Of Area %
AJZZ	24	75	8.0	348	50.5	494	71.6	23.2	10.71	66.8
AKAZ	24	75	8.0	348	50.4	501	72.6	26.0	11.53	69.0
AKBZ	24	75	1.6	352	51.0	496	71.9	24.8	11.06	66.8
AKDZ	24	75	1.6	338	49.0	487	70.6	26.0	11.61	67.3
AKMZ	371	700	8.0	335	48.6	523	75.8	24.8	9.87	69.0
AKHZ	371	700	8.0	318	46.1	487	70.6	24.0	9.41	64.5
ALAZ	371	700	8.0	350	50.8	523	75.8	25.6	9.92	66.8
AKEZ	371	700	1.6	301	43.6	465	67.4	22.4	9.51	69.1
AKFZ	371	700	1.6	294	42.6	459	66.6	23.0	9.14	64.5
AKKZ	427	800	8.0	332	48.2	463	67.1	24.8	8.02	69.1
AKLZ	427	800	8.0	348	50.4	466	67.6	23.2	7.31	69.1
AKIZ	427	800	1.6	328	47.6	452	65.6	23.2	7.91	66.6
AKJZ	427	800	1.6	331	48.0	450	65.2	23.2	7.13	69.1
AKQZ	482	900	8.0	308	44.6	401	58.2	26.4	6.66	79.1
AKRZ	482	900	8.0	325	47.2	404	58.6	24.8	6.16	77.1
AKOZ	482	900	1.6	328	47.6	383	55.6	24.8	4.73	80.9
AKPZ	482	900	1.6	316	45.9	383	55.5	24.8	6.05	79.1
AKUZ	538	1000	8.0	292	42.3	330	47.8	33.2	3.14	82.6
AKVZ	538	1000	8.0	288	41.7	332	48.1	36.0	3.36	84.2
AKSZ	538	1000	1.6	270	39.2	303	43.9	41.6	2.73	85.0
AKTZ	538	1000	1.6	279	40.4	311	45.1	41.6	2.12	85.0
AKXZ	593	1100	8.0	223	32.4	254	36.8	44.8	2.72	88.6
AKZZ	593	1100	8.0	225	32.6	258	37.4	40.0	2.07	87.2
AKWZ	593	1100	1.6	194	28.1	220	31.9	41.6	2.18	85.7
AKYZ	593	1100	1.6	191	27.7	225	32.6	47.2	2.02	87.2
AKNZ	24	75	24.0	432	62.6	585	84.9	27.2	11.46	66.8

Table 3

Time to a Given Creep Strain Data for SA508 Class 3 Forging Material

Code	Stress (KSI)	Stress (MPa)	Loading Strain-%	Time to a Given Creep Strain - Hours 0.2%	0.5%	1%	2%	5%
			700F (371C)					
AMH	67	462.0	2.355	-	-	12	102	495
AMA	65	448.2	2.357	-	10.6	121	506	1952
ALU	60	413.7	1.597	.4	117	877		
			800F (427C)					
ALP	60	413.7	1.880	-	-	-	1.6	8
AMI	53	365.4	.979	.3	5.2	24	85	299
AMB	50	344.8	0.445	-	7.8	74	328	1177
ALS	45	310.3		0.237	16.5	198	1036	
			850F (454C)					
AMJ	45	310.3	0.339	1.2	11.0	45	134	387
AMK	40	275.8	0.186	26.6	191	616	1436	
			900F (482C)					
ALO	45	310.3	0.240	.2	1.8	5.8	15	35
AMD	40	275.8	0.238	1.6	8.6	26.9	67	166
ALY	35	241.3	0.160	12.3	71	207	475	1056
ALT	30	206.9	0.124	38.7	250	687	1519	
AMF	27	186.2	0.165	141.6	619	1500		
			1000F (538C)					
ALW	30	206.9	.119	0.9	3.5	8.1	17	39
AME	25	172.4	.043	3.6	13.7	35.0	-	-
AMO	25	172.4	.115	2.4	10.1	26.2	59	139
ALR*	20	137.9	.060	9.1	42	129	302	692
ALM	15	103.4	.098	36.7	194	531	1168	2500
AMC	12	82.7	.033	112.7	629	1492		
			1100F (593C)					
ALV	15	103.4	.038	1.0	5.1	14.5	34	82
AMG	12	82.7	.059	5.1	19.2	49	108	238
AMP	10	69.0	.033	8.7	38	94		
ALN	8	55.2	.033	19.4	96	223	431	876
ALX	4	27.6	.018	165.3	650	1432	2726	

*Specimen overtemperature by 10C for approximately 1 hour.

Table 4

Minimum Creep Rate, Monkman-Grant Constant, Time to End of Secondary Creep, 0.2% Offset Tertiary Time and Strain for SA508 Class 3 Forging Material

Code	Stress (KSI)	Stress (MPa)	Minimum Creep Rate - %/Hour	Monkman-Grant (%)	t_2 (Hrs.)	0.2% Offset Time-Hrs.	Tertiary Strain-%
			700F (371C)				
AMH	67	462.0	.0075	7.2	500	636	8.6
AMA	65	448.2	.002		1400	2311	8.2
			800F (427C)				
ALP	60	413.7	.38	5.1		9.5	7.4
AMI	53	365.4	.0138	9.5	220	354	6.9
AMB	50	344.8	.0034	8.7	800	1247	5.7
			850F (454C)				
AMJ	45	310.3	.010	8.5	165	308	4.3
			900F (482C)				
ALO	45	310.3	.107	6.9	12	24	3.4
AMD	40	275.8	.025	9.1	60	130	4.0
ALY	35	241.3	.0035	7.1	250	653	2.9
ALT	30	206.9	.0012		1000	2374	3.3
			1000F (538C)				
ALW	30	206.9	.106	8.0	14	28	3.4
AMO	25	172.4	.030	9.2	50	102	3.6
ALR	20	137.9	.0056	7.3	200	466	3.2
ALM	15	103.4	.0015		900	1628	3.0
			1100F (593C)				
ALV	15	103.4	.050	9.9	30	59	3.5
AMG	12	82.7	.016	9.5	70	143	2.7
AMP	10	69.0	.0089		90		
ALN	8	55.2	.0037	7.6	125	387	1.8
ALX	4	27.6	.00063		1800	2769	2.1

Table 5

Uniaxial Stress Rupture Properties of SA508 Class 3 Forging Material

Code	Stress (KSI)	Stress (MPa)	Rupture Time (Hours)	LMP*	Elong. (%)	Reduction In Area-%
			700F (371C)			
ALQ	75	517.1	.05	12040	23	64
AMH	67	462.0	959.8	14800	25	57
			800F (427C)			
ALP	60	413.7	13.5	14790	21	52
AMI	53	365.4	688.2	15980	24	69
AMB	50	344.8	2566.4	16390	32	73
			850F (454C)			
AMJ	45	310.3	853.7	16670	49	69
			900F (482C)			
ALO	45	310.3	64.1	16470	32	74
AMD	40	275.0	365.3	17040	49	75
ALY	35	241.3	2035.6	17600	30	37
			1000F (538C)			
ALW	30	206.9	75.9	17740	25	80
AMO	25	172.4	305.5	18240	40	65
ALR	20	137.9	1302.2	19130	36	75
			1100F (593C)			
ALV	15	103.4	197.7	19320	60	91
AMG	12	82.7	591.7	19730	80	87
ALN	8	55.2	2051.0	20190	60	92

*LMP is the Larson-Miller Parameter, P, defined as

$$P = T(K)\ (20 + \mathrm{Log}_{10}\ \mathrm{Time\ (Hours)})$$

Table 6

Power Law Primary Plus Secondary
Creep Curve Regression Coefficients

Code	Stress (KSI+)	K	n	$\dot{\epsilon}_m$ (%/Hr.)
		700F (371C)		
AMH	67	.587	.162	.00627
AMA	65	.300	.187	.00197
ALU	60	.221	.132	.000642
		850F (454C)		
AMJ	45	.18246	.333	.0078813
AMK	40			
		800F (427C)		
AMI	53	.2663	.320	.009981
AMB	50	.3106	.217	.002683
ALS	45	.0795	.325	.000276
ALS	45	.0768	.340	.000180
		900F (482C)		
ALO	45	.28826	.301	.08730
AMD	40	.15295	.358	.01879
ALY	35	.06503	.376	.00246
ALT	30	.065354	.224	.0010527
		1000F (538C)		
ALW	30	.1079	.287	.09879
AME	25	.072465	.565	.013029
AMO	25	.09816	.401	.02420
ALR	20	.07092	.400	.003976
ALM	15	.053426	.291	.0012715
AMC	12	.0304	.371	.000226
		1100F (593C)		
ALV	15	.16338	.293	.044475
AMG	12	.059809	.559	.009615
ALN	8	.05734	.315	.00269
ALX	4	.010775	.378	.00056419

$\epsilon_c = Kt^n + \dot{\epsilon}_m t$

+ 1 KSI = 6.895 MPa

Table 7

Exponential Primary Plus Secondary
Creep Curve Regression Coefficients

Code	Stress (KSI+)	θ_1 (%)	θ_2 (1/Hr.)	$\dot{\epsilon}_m$ (%/Hr.)
		700F (371C)		
AMH	67	.998	.694	.00776
AMA	65			
ALU	60	.352	1.058	.00093
		800F (427C)		
AMI	53	.720	.153	.01391
AMB	50	.669	.233	.00396
ALS	45	.310	.055	.00085
		850F (454C)		
AMJ	45	.482	.178	.011208
AMK	40			
		900F (482C)		
ALO	45	.343	1.482	.11072
AMD	40	.308	.365	.02511
ALY	35	.238	.093	.00373
ALT	30	.172	.071	.00127
		1000F (538C)		
ALW	30	.124	1.871	.10640
AMO	25	.203	.388	.02994
AME	25	.197	.246	.02276
ALR	20	.268	.0912	.00563
ALM	15	.182	.0577	.00158
AMC	12			
		1100F (593C)		
ALV	15	.257	.758	.05063
AMG	12	.202	.158	.01615
ALN	8	.132	.260	.00383
ALX	4	.075	.0426	.000629

$$\epsilon_c = \theta_1 (1 - e^{-\theta_2 t}) + \dot{\epsilon}_m t$$

+ 1 KSI = 6.895 MPa

Table 8

Rational Polynominal Creep Curve Regression Coefficients
For SA508 Class 3 Forging Material

Code	Stress (KSI+)	C (%)	p (1/Hr.)	$\dot{\epsilon}_m$ (%/Hr.)
		700F (371C)		
AMH	67	1.0646	.83497	.00756
AMA	65			
ALU	60			
		800F (427C)		
AMI	53	.82860	.20909	.013376
AMB	50	.80623	.20148	.0034609
ALS	45			
		850F (454C)		
AMJ	45	.56213	.23147	.010713
AMK	40			
		900F (482C)		
ALO	45	.40919	1.9423	.10601
AMD	40	.36681	.47142	.024190
ALY	35	.27355	.11611	.0035508
ALT	30	.21307	.076690	.0011496
AMF	27			
		1000F (538C)		
ALW	30	.14368	2.4885	.10514
AMO	25	.24667	.46827	.029147
AME	25	.26735	.23220	.021613
ALR	20	.31890	.11536	.0054166
ALM	15	.22626	.061773	.0014685
AMC	12			
		1100F (593C)		
ALV	15	.29389	1.0678	.049690
AMG	12	.27137	.15721	.015407
ALN	8	.15130	.35085	.0036738
ALX	4			

$\epsilon_c = Cpt/(1 + pt) + \dot{\epsilon}_m t$

+ 1 KSI = 6.895 MPa

Table 9

Tertiary Creep Curve Regression Coefficients
for SA508 Class 3 Forging Material

Code	Temp. (F)	Stress (KSI)	A (%)	B ($Hr.^{-1}$)	C	Monkman Grant-%	A B (%/Hr.)	Rupture Par. (Hours) C/B	Rupture Par. (Hours) P
AMH	700	67	3.5472	.00044010	.46709	7.2	.00156	1061	1057
AMA	700	65	7.0278	.0001498	.79966		.00105	5336	
AMI	800	53	8.1765	.001001	.85361	9.5	.00818	853	781
AMB	800	50	6.5431	.00028077	.80651	8.7	.00184	2872	2821
AMJ	850	45	7.9323	.0009288	.90134	8.5	.00737	970	963
ALO	900	45	5.6687	.013902	.91165	6.9	.07880	66	65
AMD	900	40	6.6791	.0026266	.91753	9.1	.01754	349	348
ALY	900	35	5.8241	.00047703	.93761	7.1	.00278	1966	1942
ALT	900	30	5.7847	.00014585	.93170		.000843	6388	
ALW	1000	30	6.1578	.012809	.94751	8.0	.07888	74	72
AMO	1000	25	7.4320	.0031179	.95118	9.2	.02317	305	302
ALR	1000	20	6.1206	.00070041	.93519	7.3	.00428	1335	1326
ALM	1000	15	5.8514	.0002100	.95997		.00123	4571	
ALV	1100	15	7.6095	.0050559	.94003	9.9	.03847	186	186
AMG	1100	12	7.4976	.0019004	.97388	9.5	.01425	512	512
ALN	1100	8	7.5924	.0005473	1.0062	7.6	.004155	1838	1835
ALX	1100	4	2.648	.00018357	.97672		.000486	5320	

$$\epsilon_c = -A \ln (C - Bt)$$

$$P = (C - e^{-\epsilon_r/A})/B;$$

Define rupture parameter, P, as

for $\epsilon_r/A > 3$ $P = C/B$

Table 10

Modified Theta Projection Regression Coefficients
For SA508 Class 3 Forging Material

Code	Stress (KSI+)	A (%)	α (hr^{-1})	B (%)
		700F (371C)		
AMH	67	4.5574	.0045705	.084342
		800F (427C)		
AMI	53	4.3012	.00634	.20527
		850F (454C)		
AMJ	45	3.2824	.0060798	.18871
		900F (482C)		
ALO	45	2.5378	.065284	.28846
AMD	40	2.7300	.013710	.27620
ALY	35	2.3486	.0019268	.42162
		1000F (538C)		
ALW	30	2.3082	.043787	.67508
ALR	20	2.4695	.0029282	.41212
ALM	15	2.1530	.000800	.4685
		1100F (593C)		
ALV	15	2.8000	.022679	.46211
AMG	12	2.3530	.0071674	.65130
ALN	8	1.6373	.001446	1.4454

$$\epsilon_c = A\,(1-e^{-\alpha t}) + B\,(e^{\alpha t}-1)$$

Rupture Parameter, P, defined as

$$P = 1/\alpha \ln((\epsilon_r - A)/B)$$

where

ϵ_r = true rupture creep strain

+ 1 KSI = 6.895 MPa

Table 11

Theta Projection Regression Coefficients
For SA508 Class 3 Forging Material

Code	Stress (KSI+)	θ_1 (%)	θ_2 (hr^{-1})	θ_3 (%)	θ_4 (hr^{-1})
		700F (371C)			
AMH	67	1.1845	.23784	7.8177	.00076069
		800F (427C)			
AMI	53	.98908	.07042	8.1661	.0012956
		850F (454C)			
AMJ	45	.64508	.08376	8.7066	.0010257
		900F (482C)			
ALO	45	.52630	.60865	3.5850	.022633
AMD	40	.43781	.16860	6.3077	.0032132
ALY	35	.36425	.031352	3.7160	.00075258
		1000F (538C)			
ALW	30	.42294	.22343	3.3333	.022001
ALR	20	.40627	.036399	3.9854	.0010893
ALM	15	.33558	.011152	3.1011	.00036104
		1100F (593C)			
ALV	15	.35939	.36571	6.7031	.0063152
AMG	12	.30535	.090205	4.2198	.0030879
ALN	8	.14050	.23369	3.6661	.0009461

$$\epsilon_c = \theta_1(1 - e^{-\theta_2 t}) + \theta_3(e^{\theta_4 t} - 1)$$

+ 1 KSI = 6.895 MPa

Table 12

Power Law Primary Plus Exponential Tertiary
Creep Curve Regression Coefficients
For SA508 Class 3 Forging Material

Code	Stress (KSI+)	K	n	θ_3 (%)	θ_4 (1/Hr.)
		700F (371C)			
AMH	67	.43571	.292	1.2320	.0019527
		800F (427C)			
AMI	53	.22642	.426	1.6185	.0029152
		850F (454C)			
AMJ	45	.16702	.406	2.0696	.0023087
		900F (482C)			
ALO	45	.31873	.424	1.4753	.034231
AMD	40	.14802	.446	2.1305	.0057862
ALY	35	.061437	.409	1.8866	.0010469
		1100F (538C)			
ALW	30	.15403	.683	1.0910	.034275
ALR	20	.067694	.445	1.8022	.0015968
ALM	15	.040160	.398	1.8292	.00046175
		1100F (593C)			
ALV	15	.16942	.426	3.1328	.0096733
AMG	12	.07616	.455	2.4914	.0039988
ALN	8	.09017	.104	3.5066	.00096906

$$\epsilon_c = Kt^n + \theta_3 \left(e^{\theta_4 t} - 1\right)$$

+ 1 KSI = 6.895 MPa

Table 13

Power Law Primary Plus Tertiary Creep
Curve Regression Coefficients
For SA508 Class 3 Forging Material

Code	Stress (KSI+)	K	n	A (%)	B ($Hr.^{-1}$)	C
			900F (482C)			
AMD	40	.22765	.298	5.4308	.0031433	1.0153
ALY	35	.36886	.122	5.2892	.00056307	1.0640
			1000F (538C			
ALW	30	.13257	.488	4.9427	.014575	1.0003
ALR	20	.22238	.201	5.2717	.0008210	1.0320
			1000F (538C)			
ALV	15	.38538	.185	7.0709	.0056853	1.0319

$\epsilon_c = Kt^n - A \ln (C - Bt)$

+ 1 KSI = 6.895 MPa

FIGURE CAPTIONS

Figure 1. Tensile strength properties for SA508 Class 3 forging material as a function of temperature at a nominal strain rate of .0080 $min.^{-1}$.

Figure 2. Tensile strength properties for SA508 Class 3 forging material as a function of temperature at a nominal strain rate of .0016 min^{-1}.

Figure 3. Ductility of SA508 Class 3 forging material as a function of temperature at a nominal strain rate of .0080 $min.^{-1}$.

Figure 4. Ductility of SA508 Class 3 forging material as a function of temperature at a nominal strain rate of .0016 $min.^{-1}$.

Figure 5. Strain time curves for SA508 material at 371C.

Figure 6. Strain time curves for SA508 material at 427C.

Figure 7. Strain time curves for SA508 material at 482C.

Figure 8. Strain time curves for SA508 material at 538C.

Figure 9. Strain time curves for SA508 material at 593C.

Figure 10. Stress rupture properties for SA508 base material.

Figure 11. Log minimum creep rate versus log rupture time data for SA508 base material.

Figure 12. Log time to end of secondary creep versus log rupture time for SA508 base material.

Figure 13. Log time to 0.2% offset tertiary creep versus log rupture time for SA508 base material.

Figure 14. Log stress versus log time to one percent creep strain data.

Figure 15. Log stress versus Larson-Miller parameter (C = 20) data for time to one percent creep strain.

Figure 16. Log stress versus Larson-Miller parameter (C = 21) data for time to one percent creep strain.

Figure 17. Log stress versus Larson-Miller parameter (C = 23) data for time to one percent creep strain.

Figure 18. Log stress versus Larson-Miller parameter (C = 25) data for time to one percent creep strain.

Figure 19. Log rupture time versus log tertiary creep rupture parameter.

Figure 20. Comparison of microstructure and hardness values for creep specimens tested at 427C, 482C, 538C and 593C.

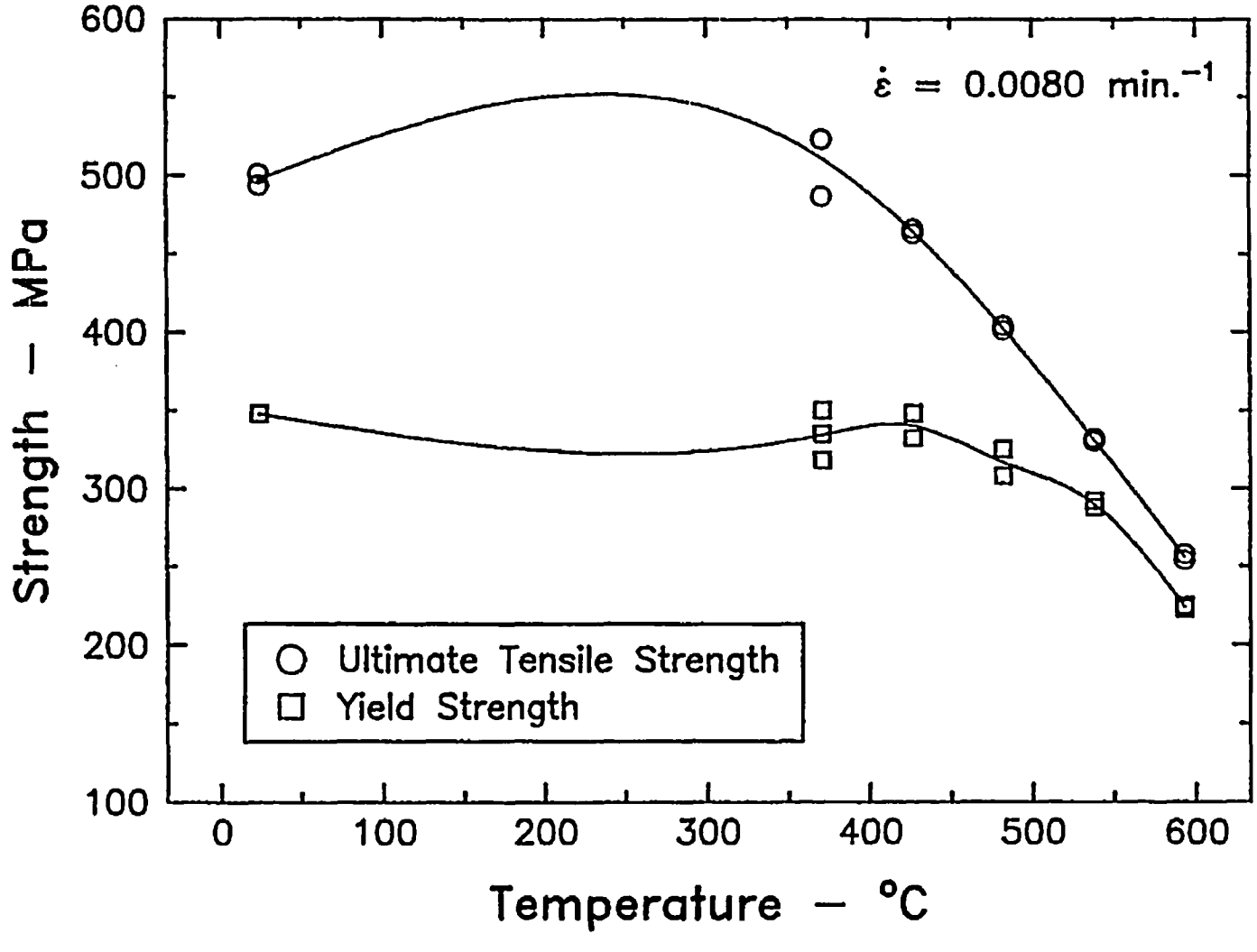
600
500
400
300
200
100
0
100
200
300
400
500
600
Strength – MPa
Temperature – °C
$\dot{\varepsilon}$ = 0.0080 min.$^{-1}$
Ultimate Tensile Strength
Yield Strength

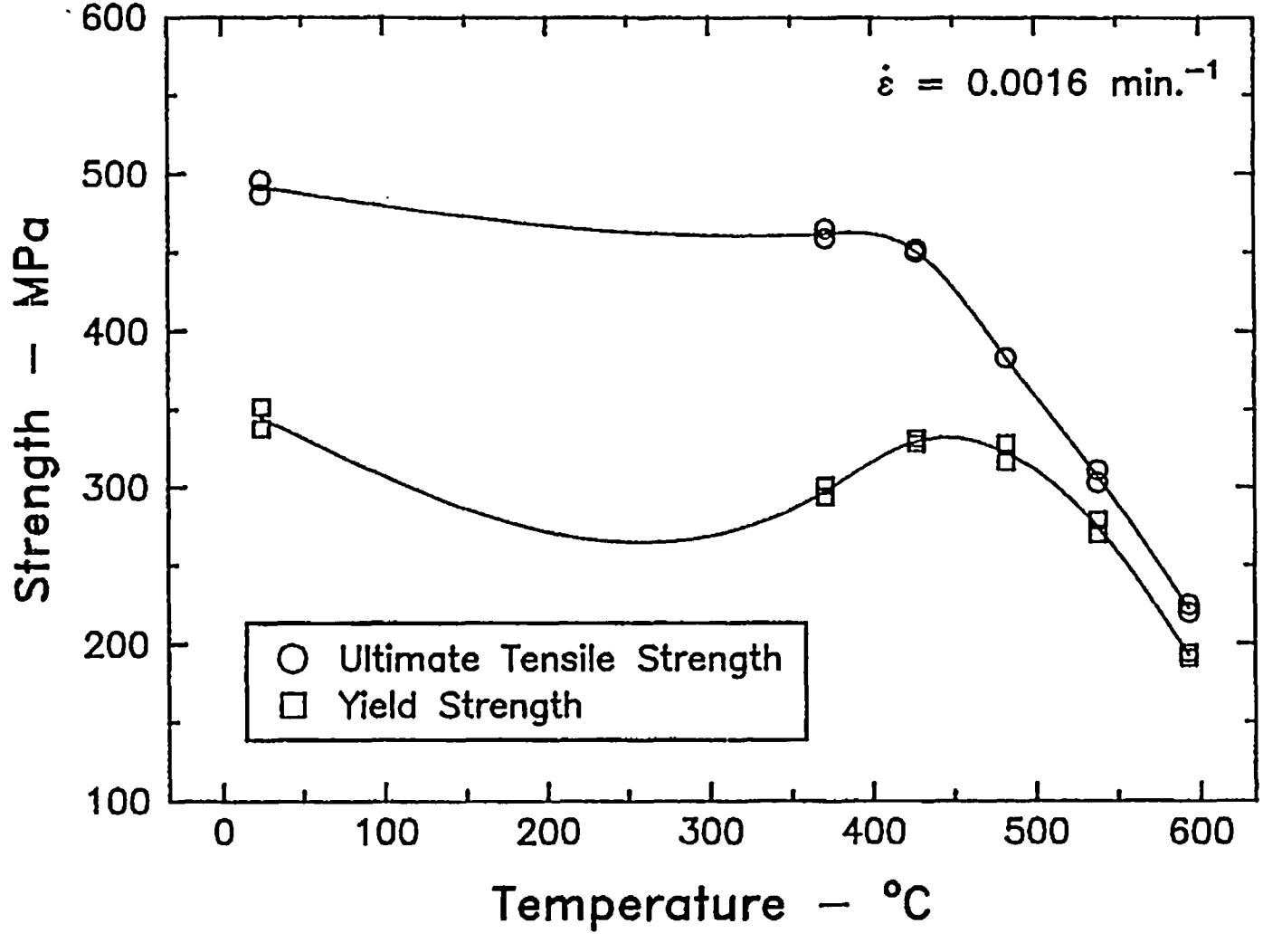
$\dot{\varepsilon}$ = 0.0016 min.$^{-1}$
Ultimate Tensile Strength
Yield Strength
Strength – MPa
Temperature – °C
600
500
400
300
200
100
0
100
200
300
400
500
600

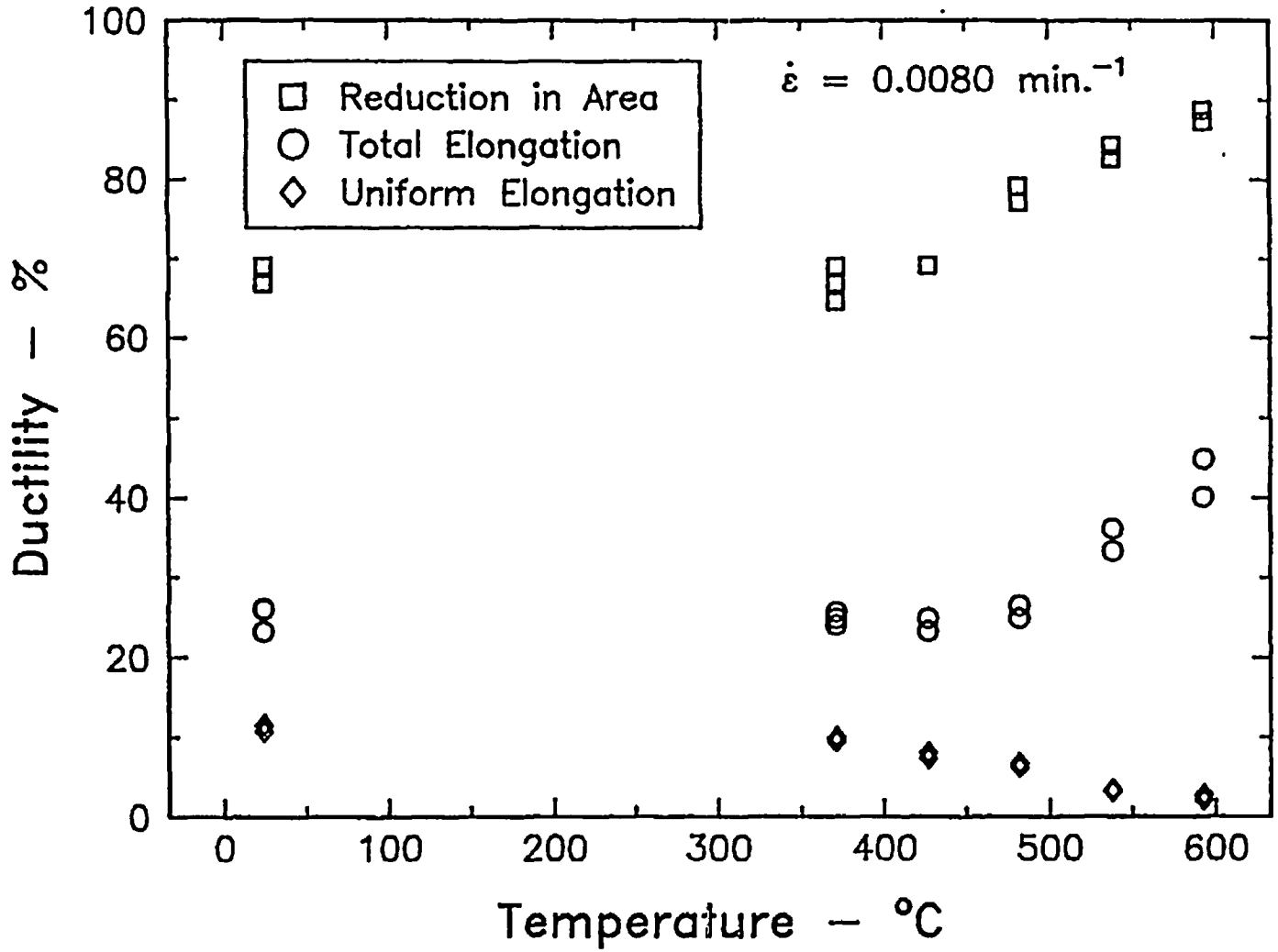
Reduction in Area
Total Elongation
Uniform Elongation
$\dot{\varepsilon}$ = 0.0080 min.$^{-1}$
Ductility – %
Temperature – °C
0
20
40
60
80
100
0
100
200
300
400
500
600

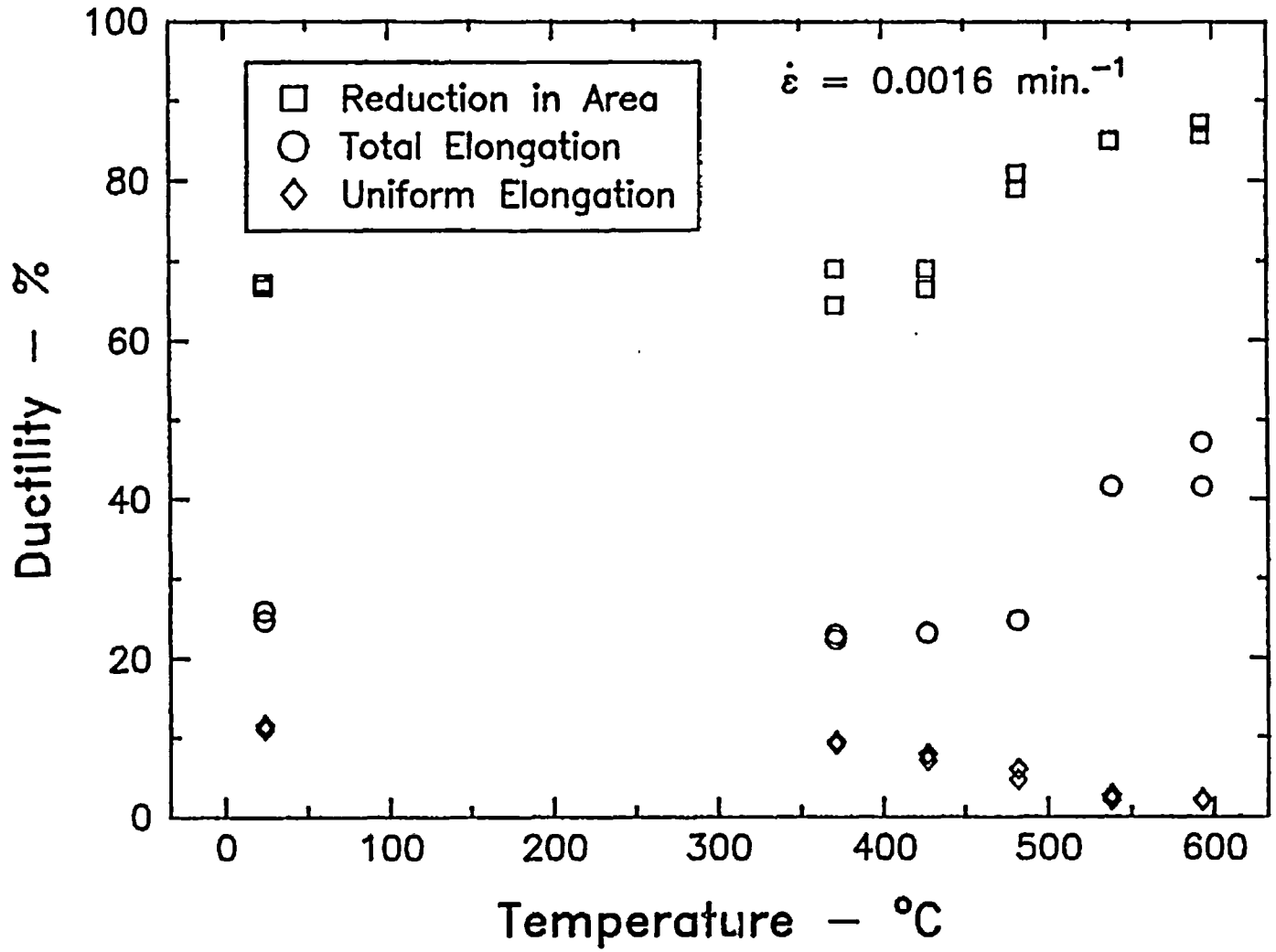
Reduction in Area
Total Elongation
Uniform Elongation
$\dot{\varepsilon}$ = 0.0016 min.$^{-1}$
Ductility – %
Temperature – °C
0
20
40
60
80
100
0
100
200
300
400
500
600

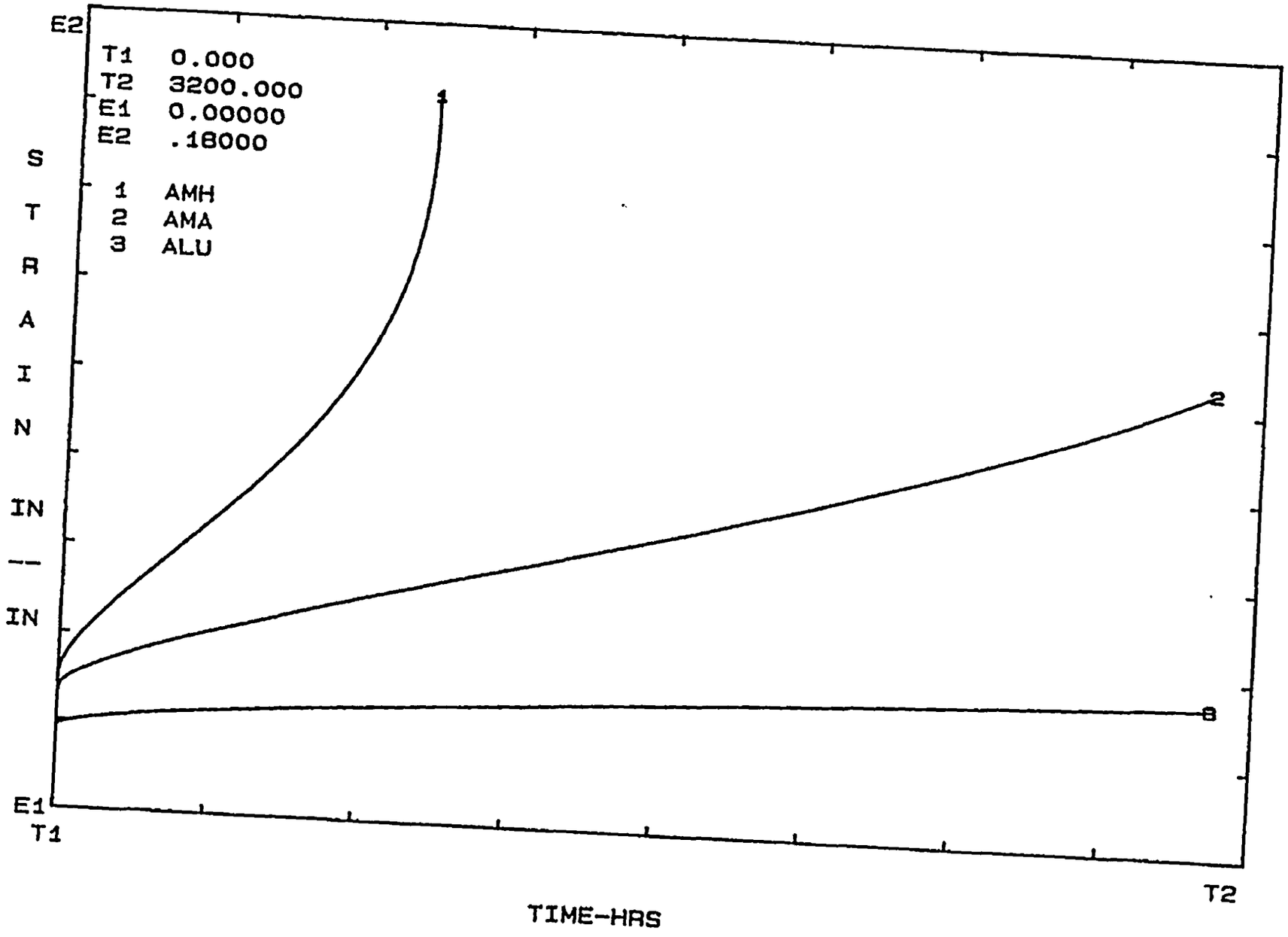
T1 0.000
T2 3200.000
E1 0.00000
E2 .18000
1 AMH
2 AMA
3 ALU
E2
E1
T1
T2
STRAIN
IN
--
IN
TIME-HRS
1
2
3

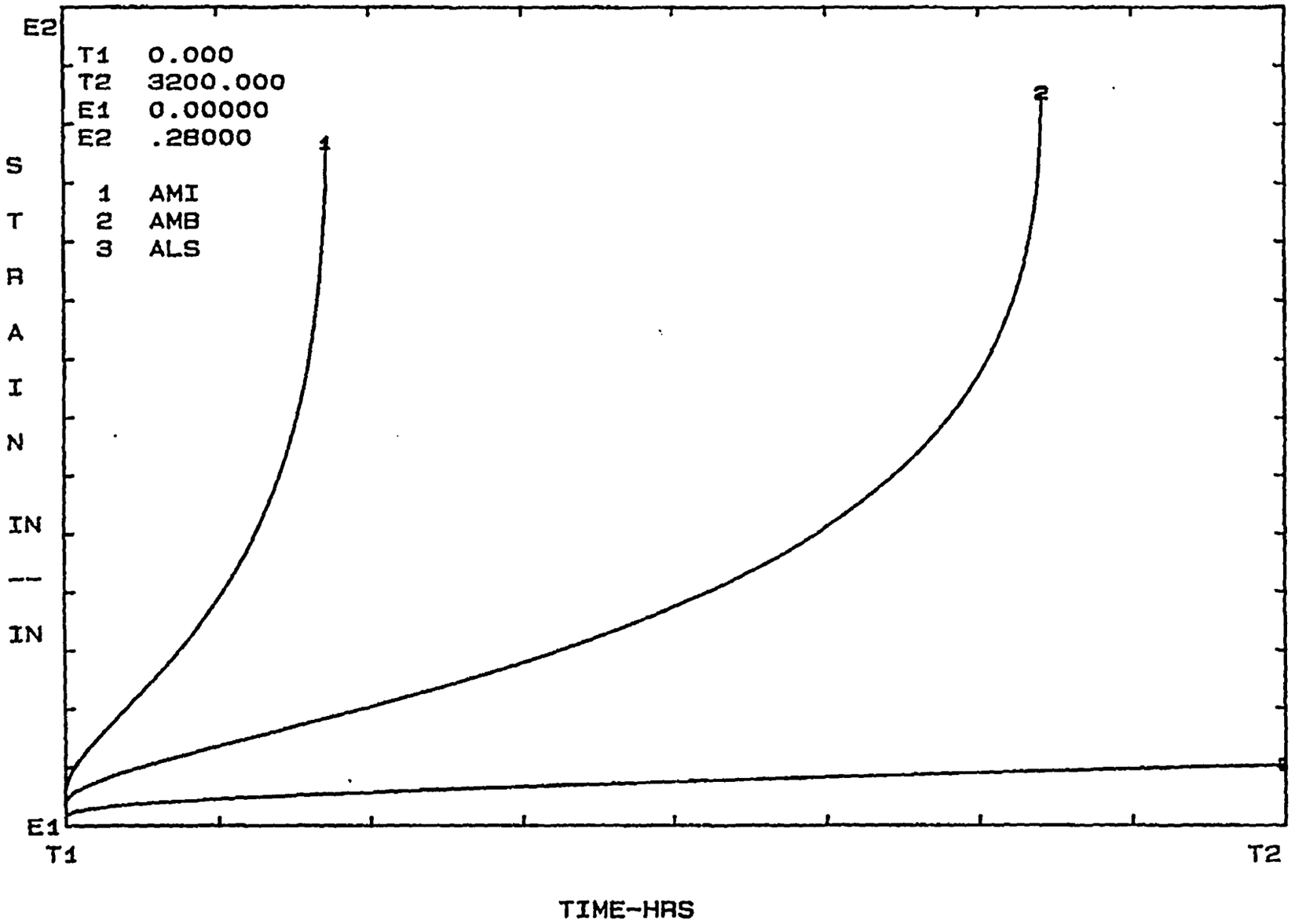
E2
T1 0.000
T2 3200.000
E1 0.00000
E2 .28000
1 AMI
2 AMB
3 ALS
STRAIN
IN
--
IN
E1
T1
T2
TIME-HRS
1
2

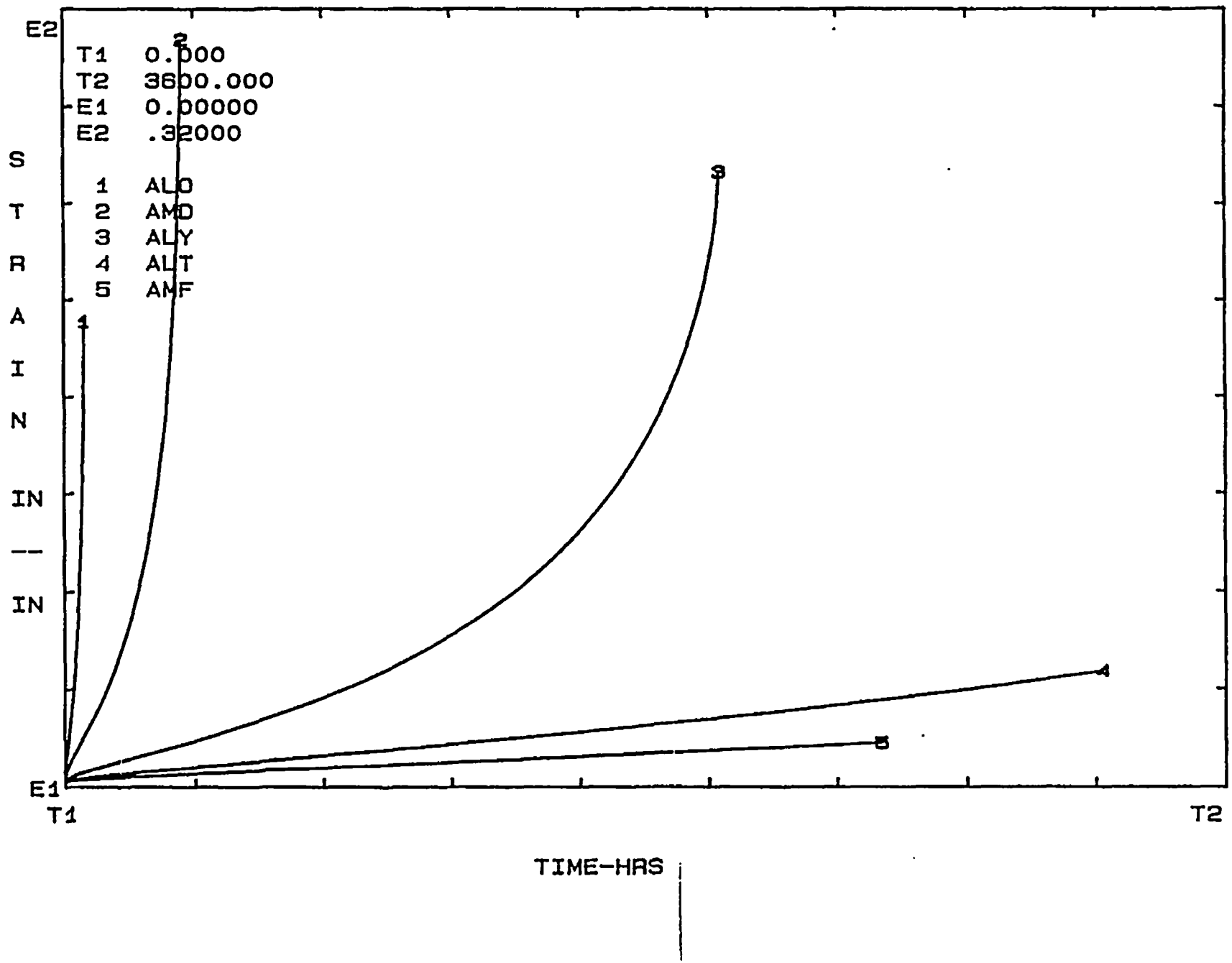
E2
T1 0.000
T2 3600.000
E1 0.00000
E2 .32000
1 ALO
2 AMO
3 ALY
4 ALT
5 AMF
STRAIN
IN
--
IN
E1
T1
T2
TIME-HRS

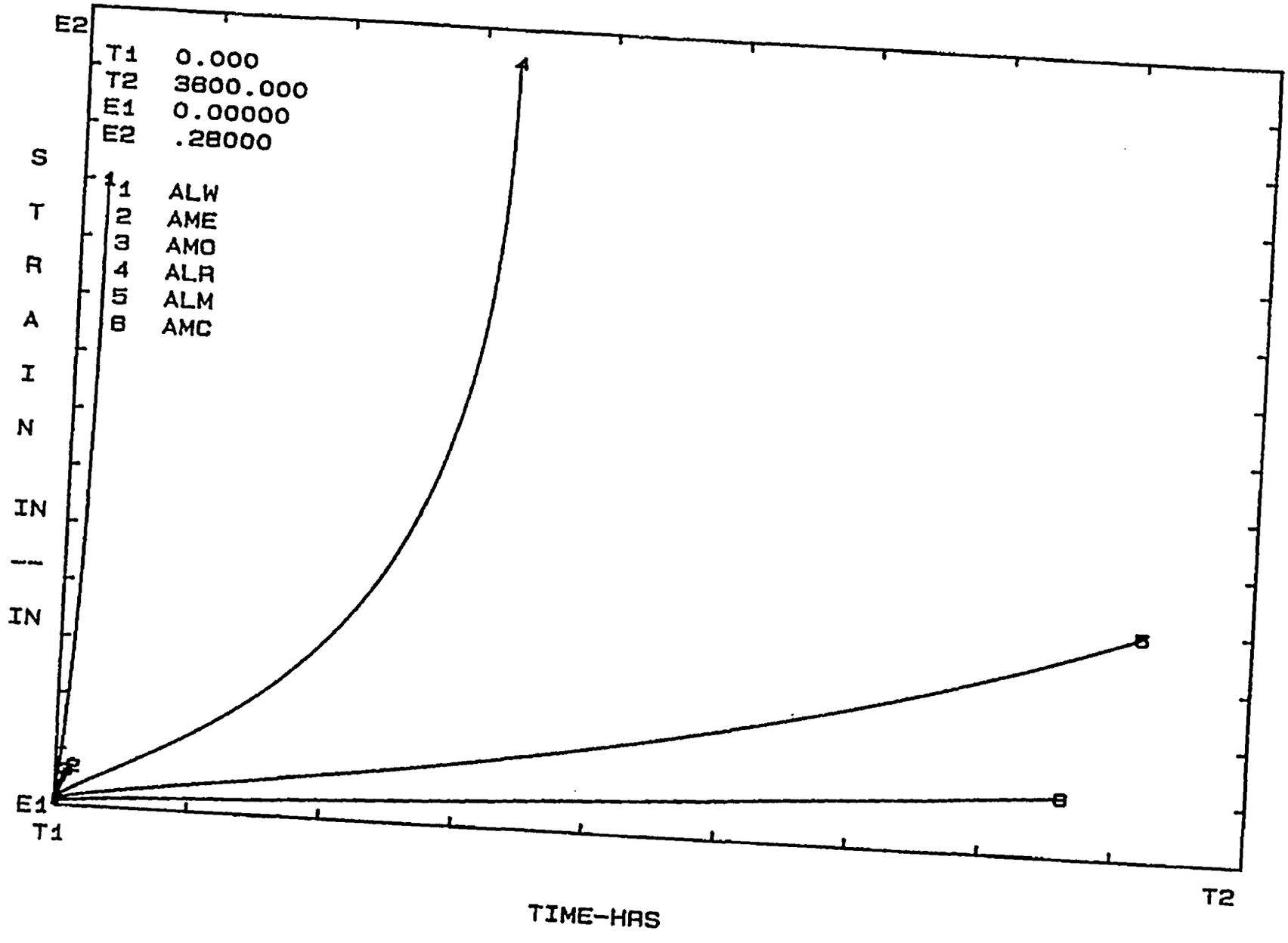
E2
T1 0.000
T2 3600.000
E1 0.00000
E2 .28000
1 ALW
2 AME
3 AMO
4 ALR
5 ALM
6 AMC
STRAIN
IN

IN
E1
T1
T2
TIME-HRS

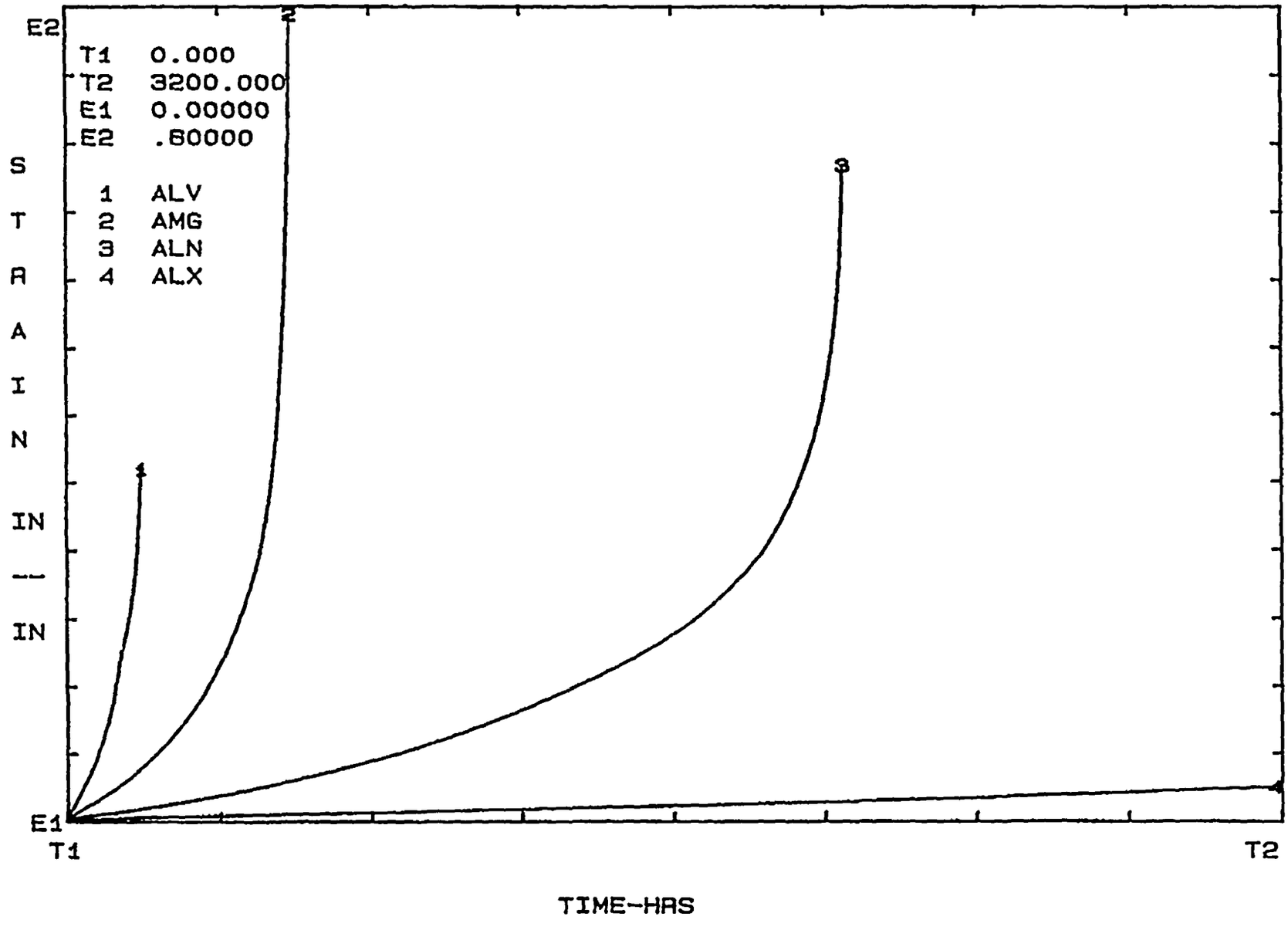
E2
T1 0.000
T2 3200.000
E1 0.00000
E2 .60000
1 ALV
2 AMG
3 ALN
4 ALX
STRAIN
IN
--
IN
E1
T1
T2
TIME-HRS

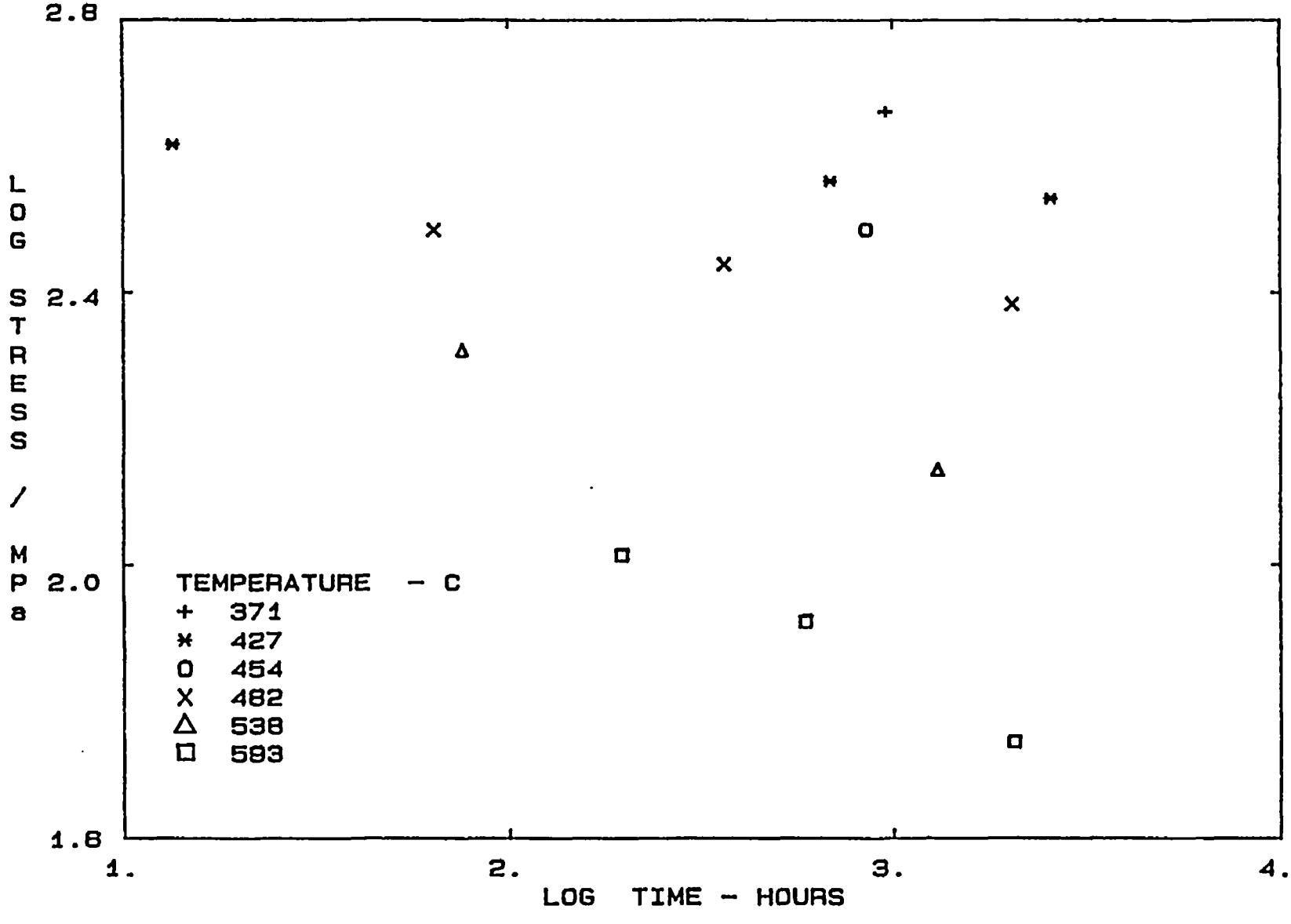
2.8
2.4
2.0
1.6
LOG STRESS / MPa
1.
2.
3.
4.
LOG TIME - HOURS
TEMPERATURE - C
+ 371
* 427
O 454
X 482
Δ 538
□ 593

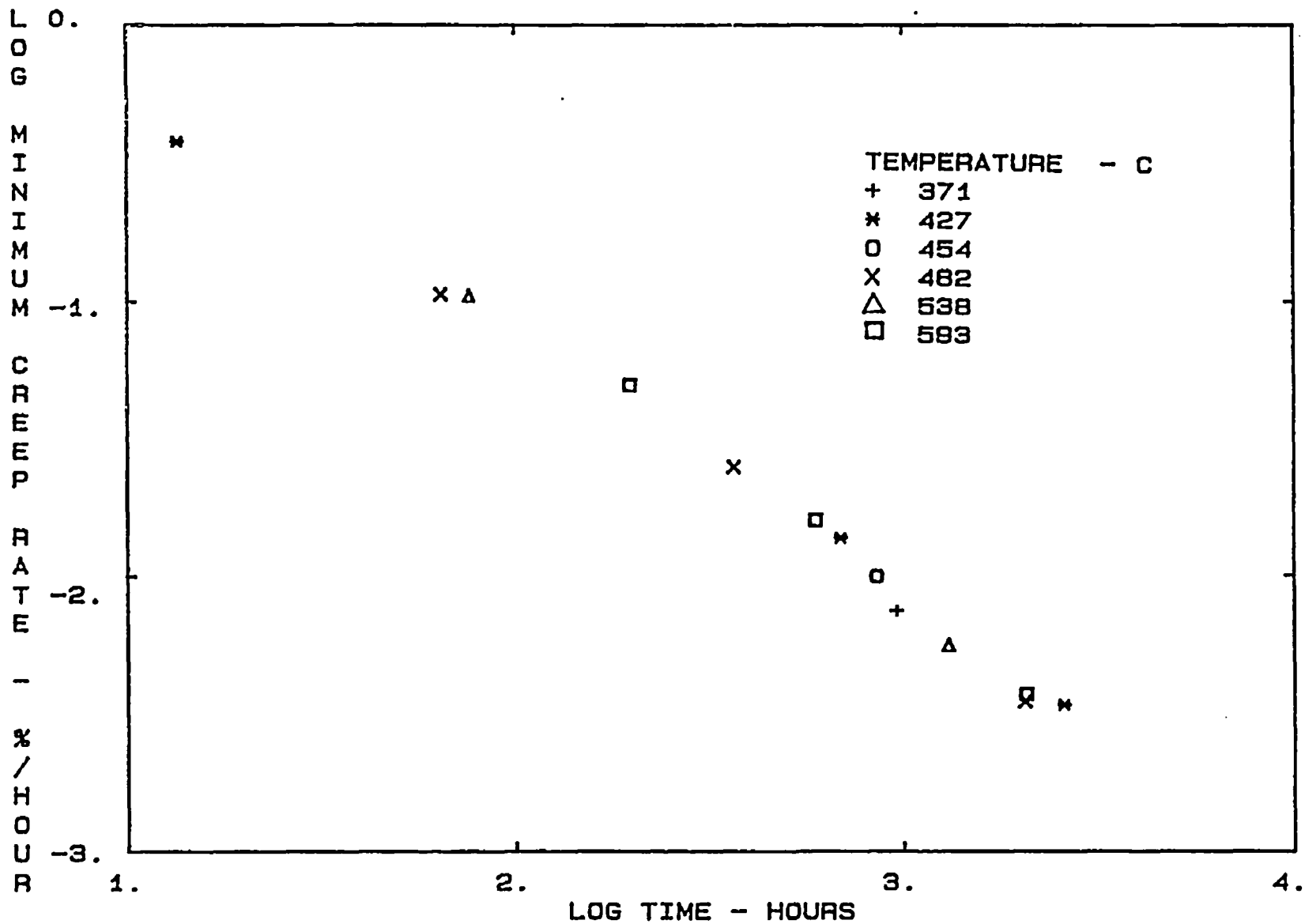
LOG MINIMUM CREEP RATE - %/HOUR
0.
-1.
-2.
-3.
1.
2.
3.
4.
LOG TIME - HOURS
TEMPERATURE - C
+ 371
* 427
O 454
X 482
Δ 538
□ 593

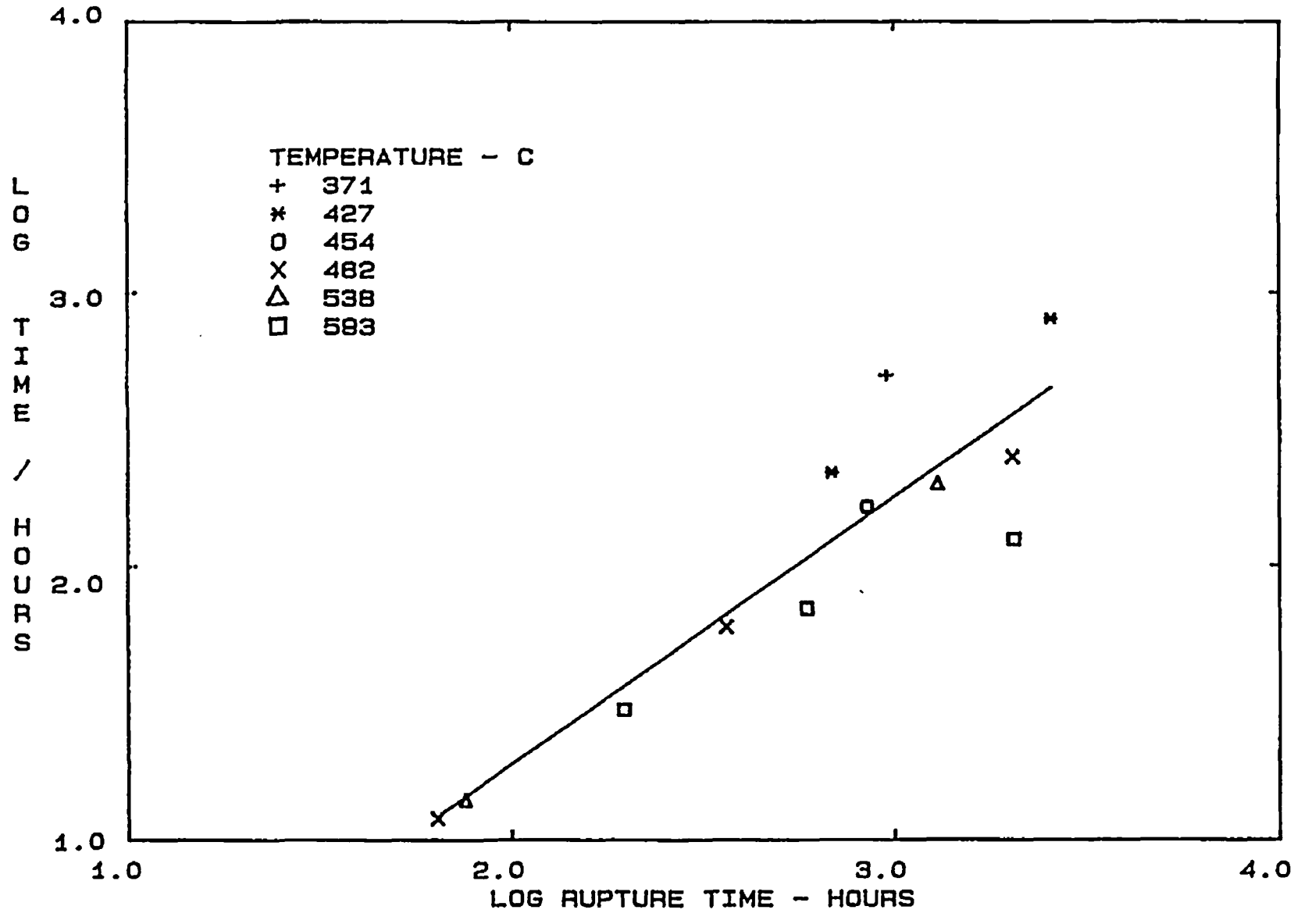
TEMPERATURE - C
+ 371
* 427
O 454
X 482
Δ 538
□ 583
LOG TIME / HOURS
4.0
3.0
2.0
1.0
1.0
2.0
3.0
4.0
LOG RUPTURE TIME - HOURS

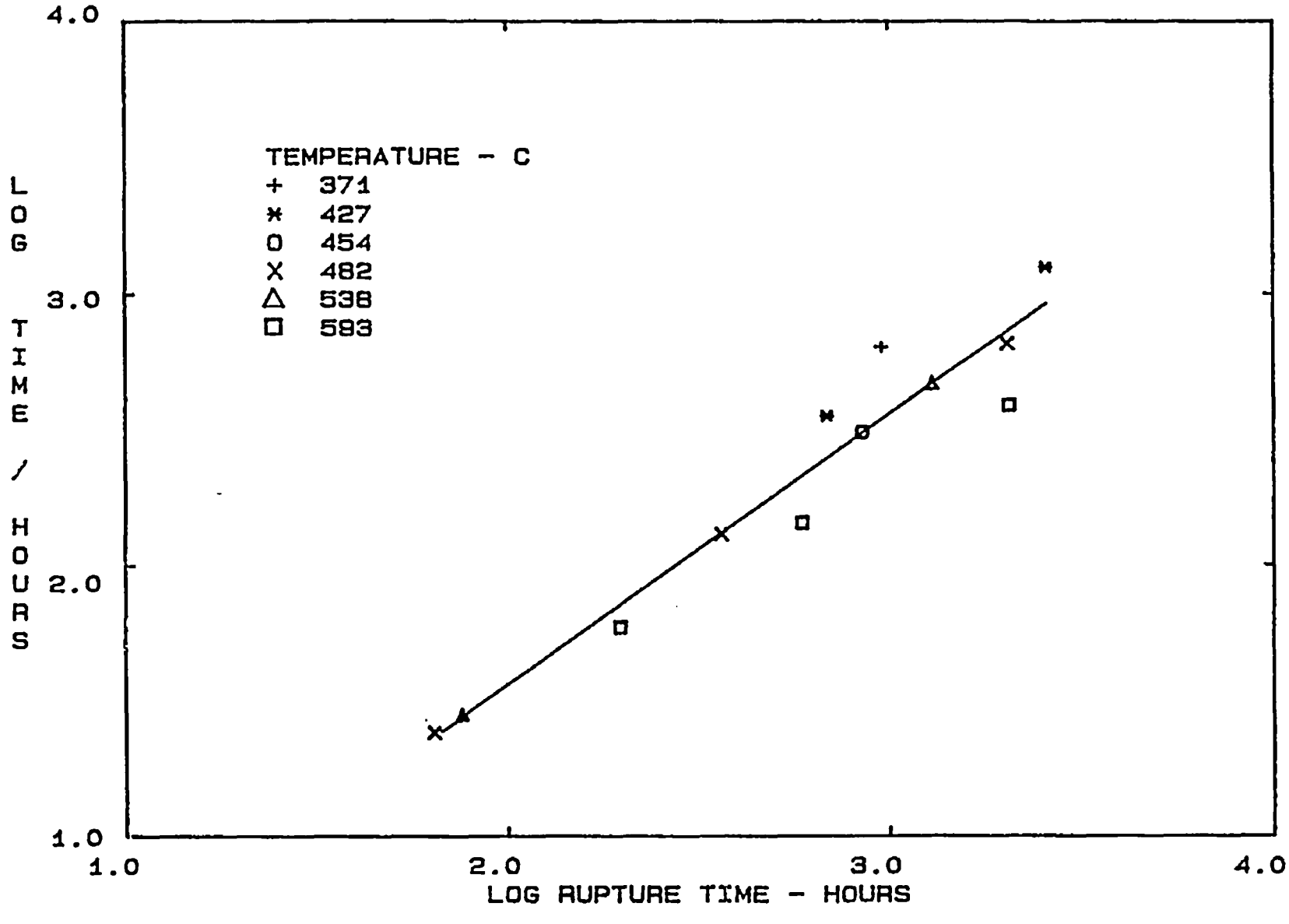
TEMPERATURE - C
+ 371
* 427
O 454
X 482
△ 538
□ 593
LOG TIME / HOURS
4.0
3.0
2.0
1.0
1.0
2.0
3.0
4.0
LOG RUPTURE TIME - HOURS

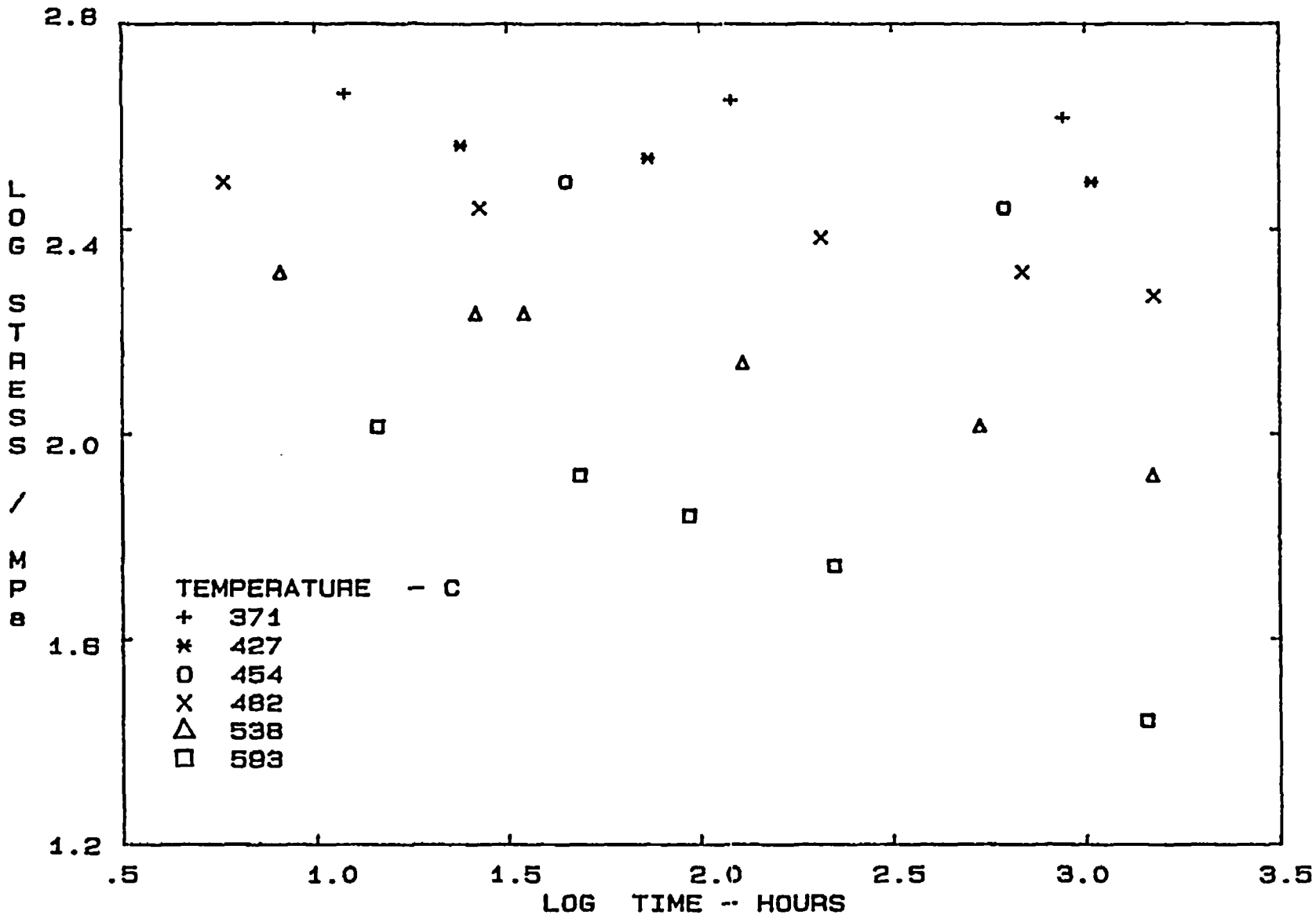
2.8
2.4
2.0
1.6
1.2
LOG STRESS / MPa
.5
1.0
1.5
2.0
2.5
3.0
3.5
LOG TIME -- HOURS
TEMPERATURE - C
+ 371
* 427
O 454
X 482
Δ 538
□ 593

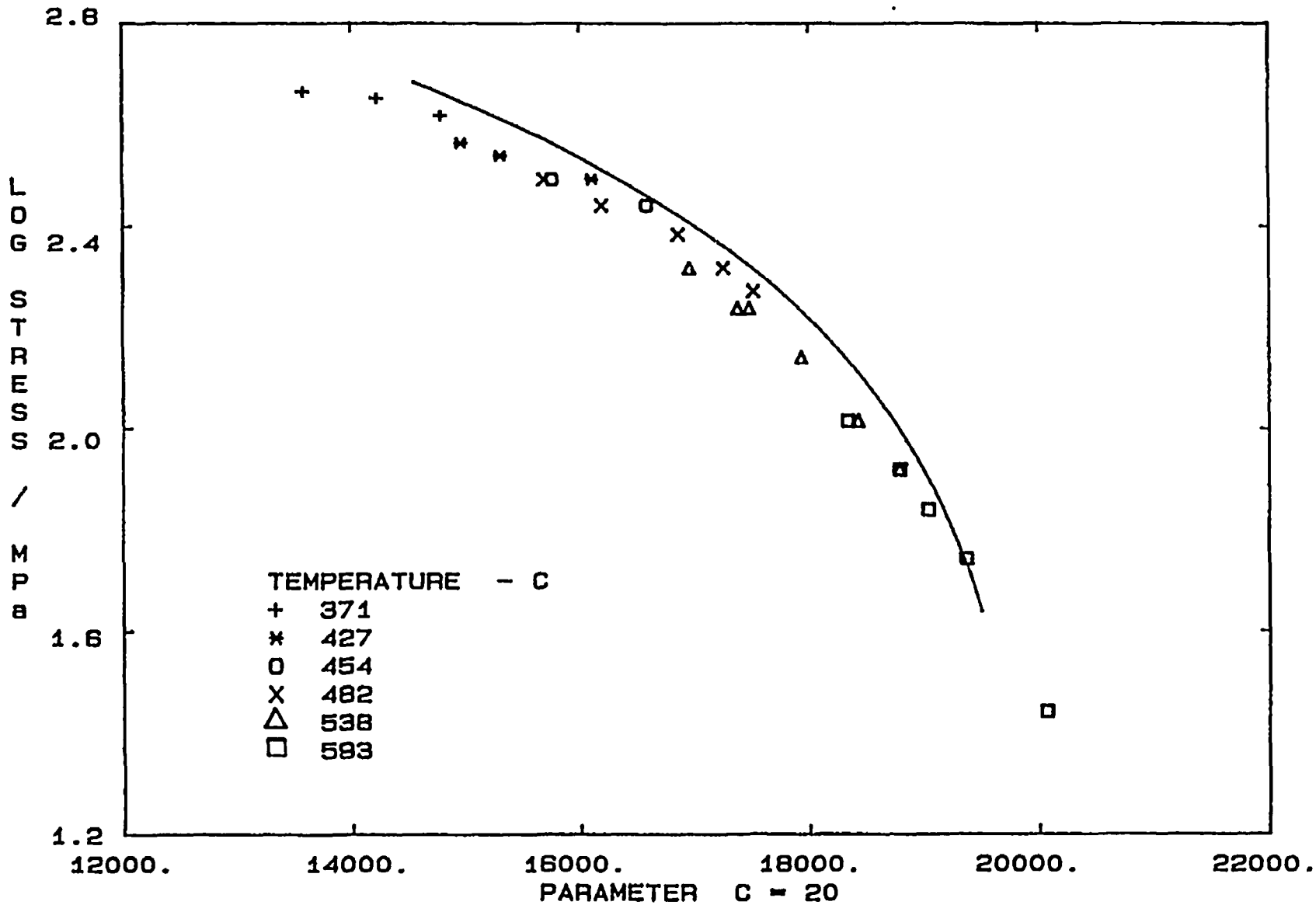
2.8
2.4
2.0
1.6
1.2
LOG STRESS / MPa
12000.
14000.
16000.
18000.
20000.
22000.
PARAMETER C = 20
TEMPERATURE - C
+ 371
* 427
O 454
X 482
Δ 538
□ 593

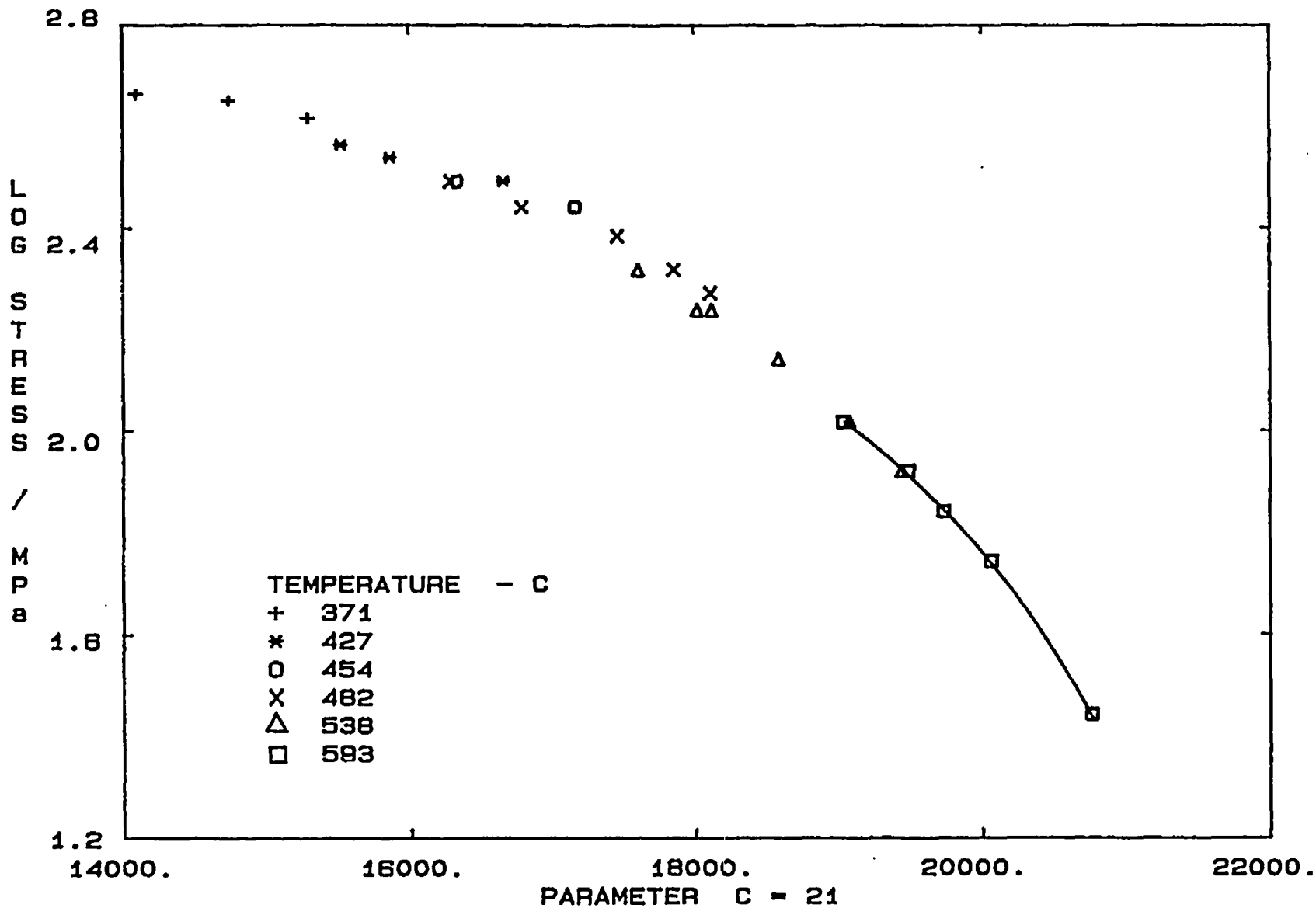
2.8
2.4
2.0
1.6
1.2
LOG STRESS / MPa
14000.
16000.
18000.
20000.
22000.
PARAMETER C = 21
TEMPERATURE - C
+ 371
* 427
O 454
X 482
Δ 538
□ 593

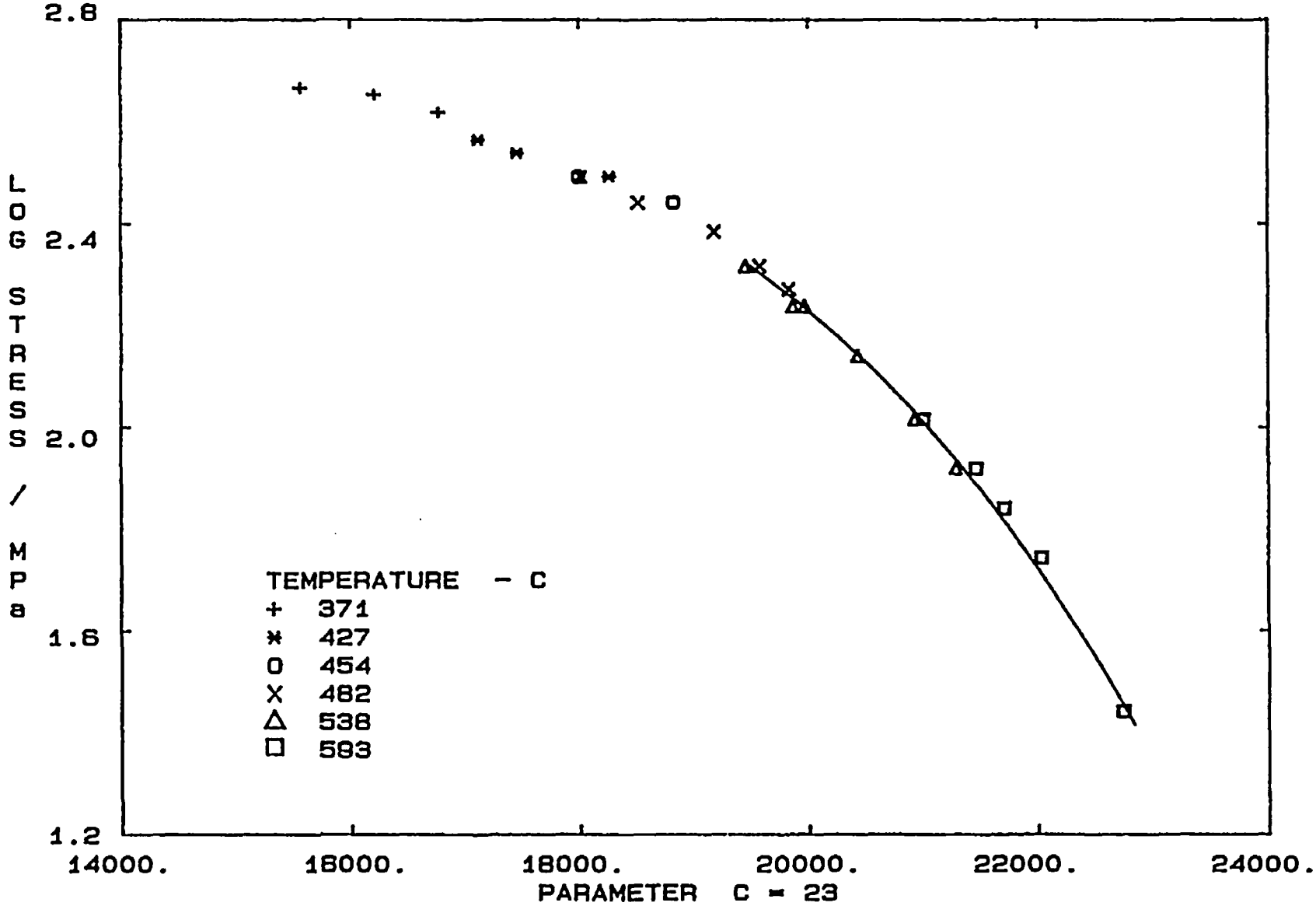
2.8
2.4
2.0
1.6
1.2
LOG STRESS / MPa
14000.
16000.
18000.
20000.
22000.
24000.
PARAMETER C = 23
TEMPERATURE - C
+ 371
* 427
O 454
X 482
Δ 538
□ 593

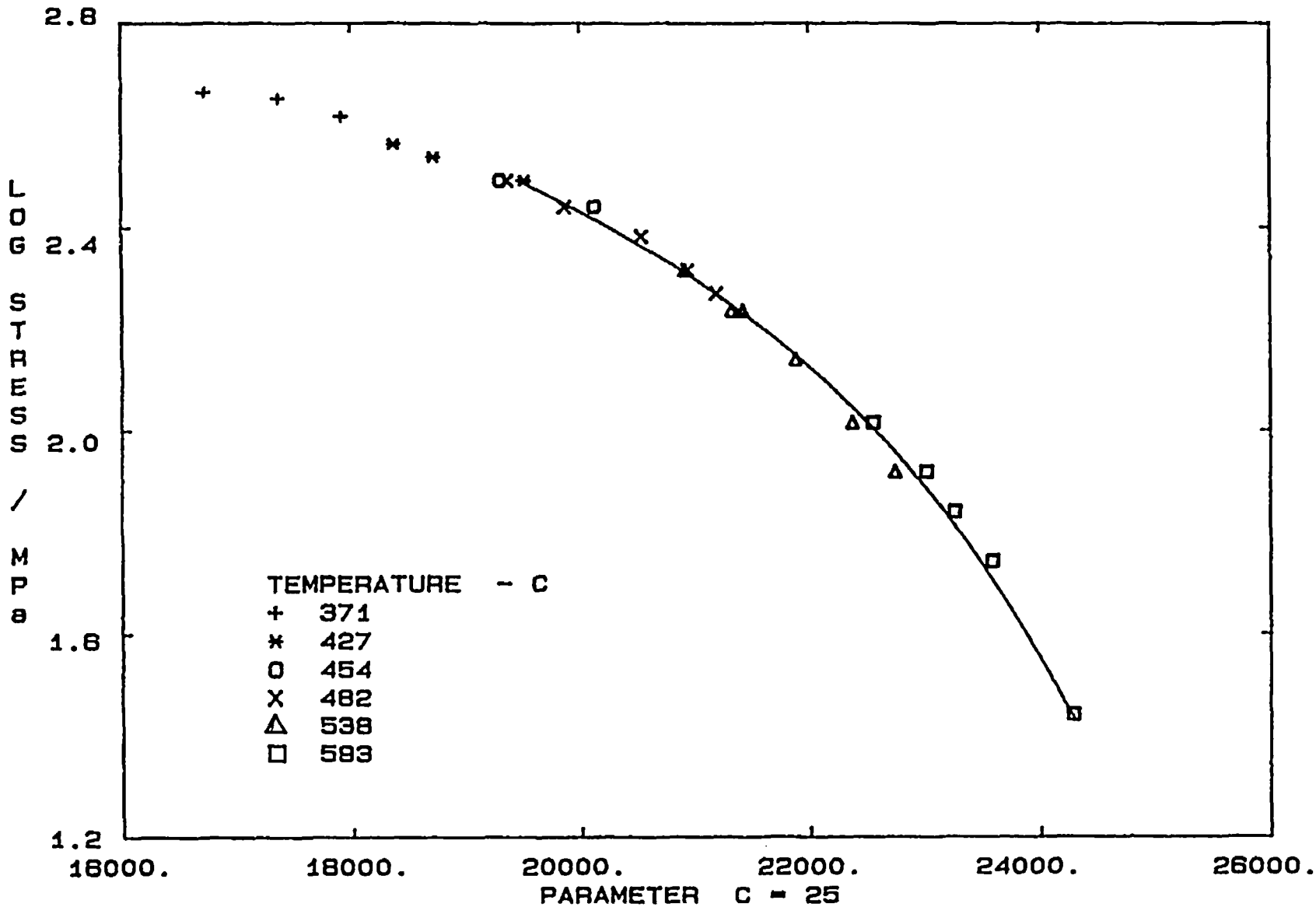
2.8
2.4
2.0
1.6
1.2
LOG STRESS / MPa
16000.
18000.
20000.
22000.
24000.
26000.
PARAMETER C = 25
TEMPERATURE - C
+ 371
* 427
O 454
X 482
Δ 538
□ 593

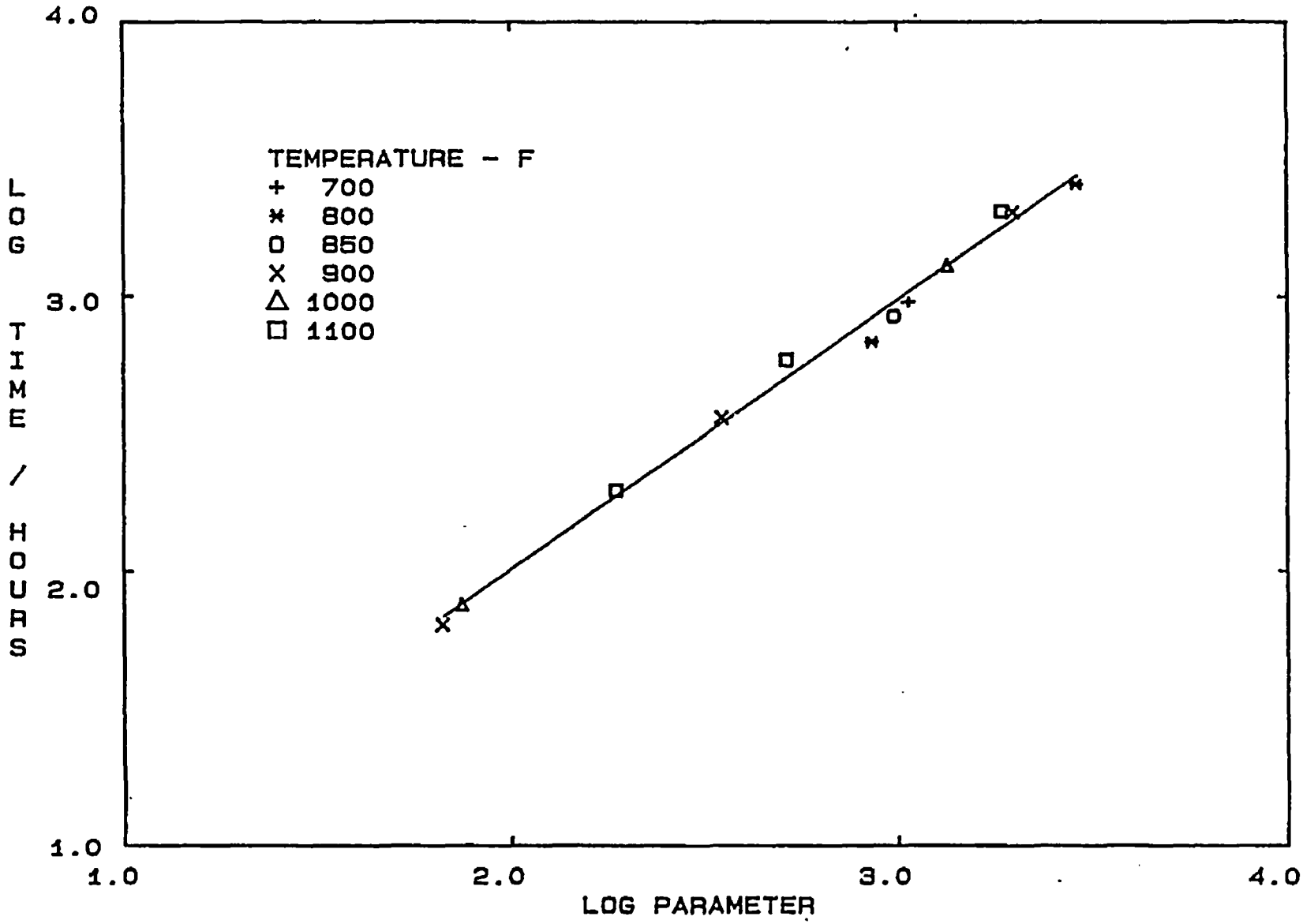
TEMPERATURE - F
+ 700
* 800
O 850
X 900
△ 1000
□ 1100
LOG TIME / HOURS
4.0
3.0
2.0
1.0
1.0
2.0
3.0
4.0
LOG PARAMETER

427C 2566.4 Hours
92 R_B

482C 2035.6 Hours
91 R_B

538C 1302.2 Hours
88 R_B

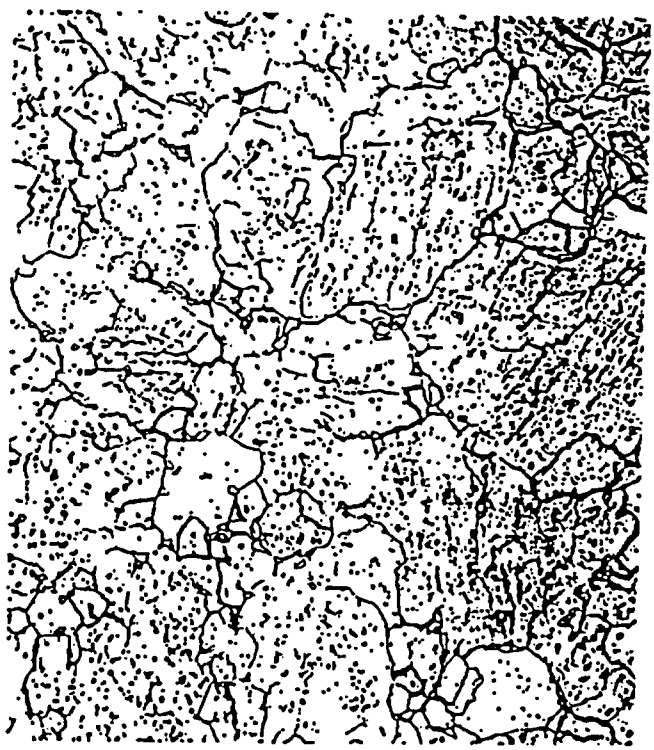

593C 2051.0 Hours
81 R_B

Figure 20. Comparison of microstructure and hardness values for creep specimens tested at 427C, 482C, 538C and 593C (1000X).

APPENDIX A

QA Documentation

The following copies of the QA documents for creep testing machine 5 are typical of the records on file for all such machines in the Metallurgical and Materials Laboratory of Combustion Engineering, Inc. located in Chattanooga, Tennessee. Copies of documents for other machines are available on request.

CREEP MACHINE CALIBRATION

Creep Machine

Machine No. : 5
C-E Asset No. : 8023
Machine Capacity : 12000. pounds
Lever Arm Ratio : 20:1

Morehouse Proving Ring

Serial No. : 4563
Capacity : 6000 pounds
NBS Reference No. : 737.229759
Calibration Date : 08/07/89

Proving Ring Temperature = 24.2 C

Pan Weight Lbs.	Applied Load Lbs.	Prov. Ring Reading Div.	Prov. Ring Defl. Div.	Prov. Ring Defl. at 23C Div.	Prov. Ring Load Lbs.	Error of Mach Lbs.	% Error
0.	0.	45.4					
40.	800.	107.3	61.9	61.88	798.97	1.03	.13
100	2000	199.8	154.4	154.35	2003.88	-3.88	-.19
160	3200	291.1	245.7	245.62	3204.81	-4.81	-.15
220	4400	381.6	336.2	336.09	4406.96	-6.96	-.16
280	5600	471.1	425.7	425.57	5607.69	-7.69	-.14

Date : 30 OCT., 1989

Calibrated by J. E. Bynum

CREEP MACHINE LOAD CELL CALIBRATION

Creep Machine No. : 5
Load Cell Manufacturer : Revere
Model No. : USP1-5-A
Serial No. : 245043
Capacity : 5000. pounds.
Excitation Voltage : 16.850 volts

Pan Weight Lbs.	Applied Load Lbs.	Load Cell Reading mv	Load Cell Reading Lbs.	Load Cell Error Lbs.	% Error
40.	800.	8.057	805.67	-5.67	-.709
100	2000.	20.058	2005.82	-5.82	-.291
160	3200.	32.069	3206.87	-6.87	-.215
220	4400.	44.053	4405.27	-5.27	-.120
280	5600.	56.032	5603.24	-3.24	-.058

Date : 17 NOV., 1989 Calibrated by J. E. Bryson

ASL CAPACITANCE TRANSDUCER CALIBRATION

ASL Transducer

Model No. : 1083B
Serial No. : 1109
Creep Machine : 5
Transducer : A

Calibration Source

Federal Products Corp. Micrometer
Model No. : 6888
C-E Asset No. : 8220
Resolution : 0.00001 inch

Micrometer Reading inch	Micrometer Change inch	Transducer Reading inch	Transducer Change inch	Error of Transducer inch	% Error
0.00000		.903886			
.10000	.10000	.803898	.099988	.000012	.012
.20000	.20000	.704067	.199819	.000181	.091
.30000	.30000	.604097	.299789	.000211	.070
.40000	.40000	.504071	.399815	.000185	.046
.50000	.50000	.404023	.499863	.000137	.027
.60000	.60000	.303936	.599950	.000050	.008
.70000	.70000	.203897	.699989	.000011	.002
.80000	.80000	.103831	.800055	-.000055	-.007
.85000	.85000	.053773	.850113	-.000113	-.013

Date : 17 NOV., 1989

Calibrated by E. Bryson

ASL CAPACITANCE TRANSDUCER CALIBRATION

ASL Transducer

Model No. : 1083B
Serial No. : 1068
Creep Machine : 5
Transducer : B

Calibration Source

Federal Products Corp. Micrometer
Model No. : 6888
C-E Asset No. : 8220
Resolution : 0.00001 inch

Micrometer Reading inch	Micrometer Change inch	Transducer Reading inch	Transducer Change inch	Error of Transducer inch	% Error
0.00000		.905220			
.10000	.10000	.805213	.100007	-.000007	-.007
.20000	.20000	.705225	.199995	.000005	.002
.30000	.30000	.605236	.299984	.000016	.005
.40000	.40000	.505263	.399957	.000043	.011
.50000	.50000	.405296	.499924	.000076	.015
.60000	.60000	.305325	.599895	.000105	.017
.70000	.70000	.205364	.699856	.000144	.021
.80000	.80000	.105389	.799831	.000169	.021
.85000	.85000	.055410	.849810	.000190	.022

Date : 17 NOV., 1989

Calibrated by J. E. Bagnum

THERMOCOUPLE ANALOG INPUT CALIBRATION

Creep Machine 5 Center Thermocouple Input

Leeds & Northrup Millivolt Potentiometer
Model Number 8686
Serial Number 18181921
Calibration Date 9-29-89

Kaye Instruments Ice Point Reference
Model Number K140-8
Serial Number 1295

Input Channel	Input Temp.-F	Min. mv	Max. mv	Avg. mv	Avg. Temp.-F	Temp. Diff.-F	% Error
224	600	12.850	12.857	12.853	599.81	.188	.031
224	700	15.140	15.173	15.167	699.50	.496	.071
224	800	17.510	17.516	17.513	799.58	.417	.052
224	900	19.865	19.870	19.867	899.35	.653	.073
224	1000	22.237	22.242	22.239	999.58	.416	.042
224	1100	24.603	24.607	24.604	1099.56	.437	.040
224	1200	26.953	26.956	26.954	1199.25	.753	.063
224	1300	29.292	29.294	29.293	1299.14	.857	.066
224	1400	31.594	31.597	31.595	1398.42	1.575	.113
224	1500	33.875	33.881	33.879	1498.25	1.752	.117

Date: 17 NOV., 1989

Calibrated by J. E. Bagnum

THERMOCOUPLE ANALOG INPUT CALIBRATION

Creep Machine 5 Top Thermocouple Input

Leeds & Northrup Millivolt Potentiometer
Model Number 8686
Serial Number 18181921
Calibration Date 9-29-89

Kaye Instruments Ice Point Reference
Model Number K140-8
Serial Number 1295

Input Channel	Input Temp.-F	Min. mv	Max. mv	Avg. mv	Avg. Temp.-F	Temp. Diff.-F	% Error
108	600	12.771	12.829	12.822	598.46	1.544	.257
108	700	15.119	15.155	15.149	698.72	1.284	.183
108	800	17.469	17.499	17.495	798.79	1.211	.151
108	900	19.848	19.858	19.856	898.89	1.114	.124
108	1000	22.224	22.230	22.227	999.08	.919	.092
108	1100	24.592	24.595	24.594	1099.10	.899	.082
108	1200	26.950	26.953	26.951	1199.11	.889	.074
108	1300	29.289	29.293	29.292	1299.08	.922	.071
108	1400	31.574	31.578	31.576	1397.63	2.370	.169
108	1500	33.863	33.866	33.865	1497.63	2.368	.158

Date: 17 NOV., 1989

Calibrated by J. E. Bazaar

7. Oak Ridge National Laboratory Letter 0409-49-90 regarding submission of data package for SA-533 Grade B, Class 1 plates, SA-508 Class 3 forgings and their weldments, dated April 20, 1990.

Letter 0409-49-90

OAK RIDGE NATIONAL LABORATORY
OPERATED BY MARTIN MARIETTA ENERGY SYSTEMS, INC.

POST OFFICE BOX 2008
OAK RIDGE, TENNESSEE 37831

April 20, 1990

Mr. A. W. Dalcher
Chairman, SG-ETC
General Electric Company
6835 Via Del Oro
P. O. Box 530954
San Jose, CA 95153-5354

Mr. Michael Gold
Chairman, SG-SFA (SC II)
Babcock & Wilcox
20 S. Van Buren Ave.
Barberton, OH 44203

Mr. R. I. Jetter
Chairman, SG-ETD
Rockwell International
Energy Technology Engineering Center
P. O. Box 1449
Canoga Park, CA 91304

Gentlemen:

Submission of Data Package for SA-533 Grade B, Class 1 Plates, SA-508 Class 3 Forgings and Their Weldments

Attached find the data package and analysis for the above named materials. We are requesting that discussion of this data package be placed on your agenda, for the May Code Meetings in Nashville.

Sincerely,

Chuck

C. R. Brinkman
Group Leader
Mechanical Properties

CRB:las.

Attachment

cc: J. M. Corum
G. L. Hoffman
H. E. McCoy
M. Prager
B. Roberts

CE REQUEST FOR CODE CASE FOR

SA533B CL1 AND SA508 CL 3

INQUIRY NUMBER N87-37

REVISION 1

APRIL 17, 1990

SUPPORTING DATA PACKAGE(ORNL)

TABLE OF CONTENTS

1.0 MATERIALS

1.1 a BASE METALS - SA533 PLATES & SA 508 FORGING
b IDENTIFICATION OF MATERIALS, HEAT NO.'S
c HEAT TREATMENTS OF MATERIALS
d CHEMICAL ANALYSES COMPARED TO SPECIFICATIONS
e MECHANICAL PROPERTIES COMPARED TO SPECIFICATIONS

1.2 a WELDMENTS
b IDENTIFICATION OF WELDMENT & WELDING PROCESS
c WELDMENT HEAT TREATMENT (PWHT)
d WELD METAL CHEMISTRY
e WELD METAL MECHANICAL PROPERTIES

2.0 Sm DATA - TENSILE PROPERTIES

2.1 TENSILE PROPERTIES FOR EACH MATERIAL
RT, 700, 800, 900, 1000, 1100
COMPARISON TO CODE VALUES IN SECTION III APPENDICES
TABLES I-2.1 YIELD STRENGTH VALUES (RT TO 1000F)
I-3.1 TENSILE STRENGTH VALUES (RT TO 1000F)

~~2.2~~ see 2.4 RATIO TREND CURVE ANALYSIS FOR Sm VALUES
COMPARISON TO CODE VALUES IN TABLES I-2.1 & I-3.1

2.3 PLOTS OF TENSILE & YIELD STRENGTH TREND CURVES
RATIO VALUES VERSUS TEMPERATURE (RT TO 1100F)
COMPARISON TO CODE VALUES IN TABLES I-2.1 & I-3.1

2.4 TABLE OF Sm ALLOWABLE STRESS VALUES (N-47 I-14.5)
TIME INDEPENDENT VALUES AS A FUNCTION OF TEMPERATURE
INCLUDE YIELD AND TENSILE STRENGTHS IN TABLE

2.5 PHYSICAL PROPERTIES TO 1000F (N-47 I-14.7 TO I-14.9)
MODULUS OF ELASTICITY & COEFFICIENT OF THERMAL EXPANSION

3.0 St DATA - CREEP PROPERTIES

3.1 TABLE OF CREEP DATA FOR EACH MATERIAL

3.2 LARSON-MILLER CORRELATIONS FOR 1%, TERTIARY & RUPTURE
ALL MATERIALS SHOWING AVERAGE AND MINIMUM CURVES

3.3 STRESS VERSUS TEMPERATURE PLOTS FOR 1%, TERTIARY & RUPTURE

3.4 STRESS VERSUS TEMPERATURE PLOT
MINIMUM STRESS TO 1%, 80% TERTIARY, & 67% RUPTURE STRESS

3.5 STRESS VERSUS TIME PLOTS (N-47 I-14.4)
St ALLOWABLE STRESS VALUES
ISOTHERMAL CURVES FOR 700, 750, 800, 850, 900, 950 AND 1000F

3.6 TABULATED St ALLOWABLE STRESS VALUES (N-47 I-14.4)
COLUMNS FOR 1, 10, 30, 100, 300 AND 1000 HOURS
ROWS FOR 700, 750, 800, 850, 900, 950 AND 1000 DEGREES F

3.7 PLOT OF MINIMUM STRESS TO RUPTURE VALUES (N-47 I-14.6)
STRESS VERSUS MINIMUM TIME TO RUPTURE
ISOTHERMAL CURVES FOR 700, 750, 800, 850, 900, 950 AND 1000F

3.8 TABULATED MINIMUM STRESS TO RUPTURE VALUES (N-47 I-14.6)
COLUMNS FOR 1, 10, 30, 100, 300 AND 1000 HOURS
ROWS FOR 700, 750, 800, 850, 900, 950 AND 1000 DEGREES F

3.9 ISOCHRONOUS STRESS-STRAIN CURVES (N-47 T-1800)
ISOCHRONOUS CURVES FOR 1, 10, 30, 100, 300 AND 1000 HOURS
CURVES PLOTTED FOR 700, 750, 800, 850, 900, 950 AND 1000 F

4.0 Smt ALLOWABLE STRESS VALUES

4.1 TABLE OF ALLOWABLE STRESS, Smt, VALUES (N-47 I-14.3)
COLUMNS FOR 1; 10, 30, 100, 300 AND 1000 HOURS
ROWS FOR 700, 750, 800, 850, 900, 950 AND 1000 DEGREES F

4.2 PLOT OF ALLOWABLE STRESS, Smt, VALUES (N-47 I-14.3)
ALLOWABLE STRESSES VERSUS TEMPERATURE Sm AND St CURVES
ISOCHRONAL CURVES FOR 1, 10, 30, 100, 300, AND 1000 HOURS

5.0 FATIGUE AND CYCLIC STRESS-STRAIN DATA

5.1 FATIGUE CURVE AT 1000 F (N-47 T-1420-1)
STRAIN RANGE VERSUS CYCLES

6.0 TEMPER EMBRITTLEMENT

6.1 SUMMARY OF LITERATURE FINDINGS

6.2 RESULTS OF TENSILE TESTS ON CREEP TESTED SPECIMENS
COMPARISON OF INITIAL VERSUS POST-CREEP PROPERTIES

6.3 TENSILE TEST RESULTS ON THERMALLY AGED SPECIMENS
COMPARISON OF INITIAL VERSUS AGED PROPERTIES
(900F AND 1000F FOR 1000 HOURS)

6.4 CHARPY IMPACT TEST RESULTS ON THERMALLY AGED SPECIMENS
COMPARISON OF INITIAL VERSUS AGED PROPERTIES
(AGED AT 900F AND 1000F FOR 1000 HOURS)

7.0 SUBJECTS NOT COVERED ELSEWHERE

7.1 Comparison of SA533 base metal and weldment properties.
7.2 Comparison of Properties of SA533 and SA508.
7.3 Guide used in preparing this document.
7.4 Direction of questions.

1.1.a,b IDENTIFICATION OF HEAT NUMBERS AND HEAT TREATMENTS FOR SA533B

MATERIAL	HEAT NUMBER	VENDOR	FORM	HEAT TREATMENT(a)
SA 533 PLATE	D 9583	LUKENS	3.5 INCH PLATE	A
SA533 PLATE	C 5975	LUKENS	9.625 INCH PLATE	A
SA533 PLATE	64535-1	MARREL FRERES	9.625 INCH PLATE	A

(a) A=2.5 h at 871C, WQ, 2.5 h at 663C, air cool, 20 h at 607C, air cool.

1.1.c CHEMICAL ANALYSIS OF SA533B COMPARED WITH SPECIFICATION.

Element	Code specified[a]	Heat number / Source of analysis: D9583 Lukens	D9583 CE	64535-1 M. Freres	64535-1 CE	C5795 Lukens	C5795 CE
C	0.25 max	0.19	0.18	0.22	0.21	0.20	0.22
Mn	1.07-1.62	1.31	1.27	1.45	1.43	1.45	1.44
P	0.015 max	0.012	0.010	0.009	0.006	0.010	0.008
S	0.018 max	0.003	0.002	0.006	0.004	0.015	0.021
Cu	0.12 max		0.08	0.04	0.04	0.07	0.06
V	0.06		0.004	<0.005	0.001		0.003
Si	0.13-0.45	0.22	0.21	0.19	0.21	0:23	0.25
Mo	0.41-0.64	0.57	0.52	0.52	0.51	0.54	0.58
Ni	0.37-0.73	0.69	0.76	0.62	0.62	0.65	0.66
Cr		0.10	0.06		0.04		0.08
Cb, Ti, W		<0.01	<0.01		<0.01		<0.01
Co		0.01	0.013		0.014		0.016
Al		0.026	0.010	0.019			0.022
B		0.001	<0.001	<0.001			<0.001
As, Sn		0.005	<0.010	<0.020			<0.007
Zr		<0.001	<0.001	<0.001			<0.001
N			0.006				0.010

[a]ASME, Section II, Standard Chemical Requirements plus Special Reactor Beltline Requirements for Cu, P, S, and V.

1.1.d COMPARISON OF SPECIFIED AND MEASURED TENSILE PROPERTIES AT ROOM TEMPERATURE

MATERIAL	CONDITION(a)	YIELD STRENGTH		ULTIMATE TENSILE STRENGTH		ELONG	RED IN AREA
		MPa	ksi	MPa	ksi	%	%
SA533B, CL 1	SPEC	345 min	50 min	552-689	80-100	18 min	
SA533B, CL 1	A	492	69.4	621	88.4	29.5	71

a) A= 2.5h/871C/2.5h/663C/20h/607C

1.2.a IDENTIFICATION OF WELDMENTS AND WELDMENT PROCESSES FOR SA533.

Heat number	Vendor	Plate thickness		Evaluated as[a]	
		cm	in.	SA weld	SMA weld
D9583	Lukens	8.9	3.5	X	X
C5975	Lukens	24.9	9.625	X	

[a]BM - base metal, SA - submerged arc weldment, and SMA - shielded metal arc weldment.

1.2.b WELDMENT HEAT TREATMENTS(PWHT)

THE POST WELD HEAT TREATMENT USED FOR SA533 WAS 20 HOURS AT 607C.

1.2.c CHEMICAL COMPOSITIONS OF DEPOSITED WELD METAL IN SA 533. BASE METAL COMPOSITIONS GIVEN FOR COMPARISON.

Element	Code specified[a]	Heat								
		D9583[b] (Lukens)	D9583[b] (CE)	D9583[c] (CE)	64535-1[b] (H. Freres)	64535-1[b] (CE)	C5795[b] (Lukens)	C5795[b] (CE)	C5795[c] (CE)	D9583[d] (CE)
C	0.25 (max)	0.19	0.18	0.11	0.22	0.21	0.20	0.22	0.13	0.10
Mn	1.07-1.62	1.31	1.27	1.41	1.45	1.43	1.45	1.44	1.53	1.27
P	0.015 (max)	0.012	0.010	0.008	0.009	0.006	0.01	0.008	0.009	0.008
S	0.018 (max)	0.003	0.002	0.006	0.006	0.004	0.015	0.021	0.015	0.014
Cu	0.12 (max)		0.08	0.04	0.04	0.04	0.07	0.06	0.04	
V	0.06		0.004	0.003	<0.005	0.001		0.003	0.004	0.008
Si	0.13-0.45	0.22	0.21	0.45	0.19	0.21	0.23	0.25	0.45	0.35
Mo	0.41-0.64	0.57	0.52	0.55	0.52	0.51	0.54	0.58	0.57	0.48
Ni	0.37-0.73	0.69	0.76	0.13	0.62	0.62	0.65	0.66	0.12	0.03
Cr		0.10	0.06			0.04		0.08	0.14	0.03
Cb, Ti, W		<0.01	<0.01			<0.01		<0.01	<0.01	<0.029
Co		0.01	0.013			0.014		0.016	0.011	0.005
Al		0.026	0.01		0.019			0.022	0.011	0.005
B		0.001	<0.001		<0.001			<0.001	0.001	<0.001
As, Sn		0.005	<0.01		<0.020			<0.007	<0.007	<0.005
Zr		<0.001	<0.001		<0.001			<0.001	<0.001	<0.001
N			0.006					0.01	0.006	-

[a]ASME, Section II, Standard Chemical Requirements plus Special Reactor Beltline Requirements for Cu, P, S, and V.

[b]Base metal.

[c]Weld metal deposited by submerged arc process. AWS CLASSIFICATION NO. EH14, TYPE F-80 FLUX(LINDE 124). EH14 SPECIFIED TO HAVE LOW Cu, LOW P.

[d]Weld metal deposited by the shielded-metal arc process. AWS CLASSIFICATION NO. E8018GSR.

1.3 MATERIAL NUMERICAL IDENTIFICATION CODES USED IN DATA PROCESSING.

Vendor heat number	Modified heat number	Form[a]	Heat treatment[b]	Lot number
D9583	9583A	BM	CE-STD	3
D9583	9583A	TW-SA	CE-STD	4
D9583	9583A	WM-SA	CE-STD	5
C5795	5795	BM	CE-STD	6
C5795	5795	WM-SA	CE-STD	7
C5795	5795	TW-SA	CE-STD	8
D9583	9583B	BM	CE-STD	9
D9583	9583B	TW-SMA	CE-STD	10
D9583	9583B	WM-SMA	CE-STD	11
64535-1	64535	BM	CE-STD	12

[a]BM - base metal specimen; TW - transverse weld specimen, fusion line in specimen center; WM - weld metal specimen; SA - weld made by the submerged arc process; and SMA - weld made by shielded metal arc process.

2.1 TENSILE PROPERTIES OF SA533B CL1-SR-0.0016/min

HEAT NUMBER	TEMPERATURE	YIELD	AVG YIELD	CODE YIELD(a)	UTS	AVG UTS	CODE UTS(b)	TOTAL ELONGATION	UNIFORM ELONGATION	REDUCTION OF AREA
	F	ksi	ksi	ksi	ksi	ksi	ksi	%	%	%
9583A	75.00	69.30	69.35	50.00	87.60	88.35	80.00	29.68	9.20	74.58
9583A	75.00	81.50			96.10			29.30	8.47	75.61
5795	75.00	63.00			84.60			29.20	10.12	67.04
5795	75.00	62.20			82.50			30.10	10.86	67.83
64535	75.00	70.30			90.10			29.40	10.20	69.99
64535	75.00	69.80			89.30			29.35	10.52	70.37
5795	200.00	58.40	58.40	47.50	78.10	78.10	80.00	26.80	10.23	67.04
5795	300.00	63.70	63.70	46.10	85.40	85.40	80.00	23.38	7.60	64.00
5795	400.00	54.00	54.00	45.10	79.50	79.50	80.00	28.20	10.65	66.50
5795	500.00	60.10	60.10	44.50	86.10	86.10	80.00	22.95	9.38	67.14
5795	600.00	52.70	52.70	43.80	80.70	80.70	80.00	30.65	10.51	68.07
9583A	700.00	66.90	59.87	43.10	83.20	80.98	80.00	26.18	5.67	75.55
9583A	700.00	59.40			81.60			29.00	9.45	77.26
5795	700.00	56.60			80.10			29.00	8.45	71.99
5795	700.00	59.40			81.30			28.35	8.25	71.85
64535	700.00	58.30			80.10			30.85	8.64	74.60
64535	700.00	58.80			79.60			30.00	8.58	74.44
64535	750.00	56.00	56.00	42.30	73.60	73.60	80.00	30.90	7.71	76.12
9583A	800.00	50.20	54.77	41.60	73.70	71.43	80.00	28.60	6.82	81.22
9583A	800.00	63.50			74.00			28.00	3.60	80.43
5795	800.00	55.00			72.30			27.99		74.52
5795	800.00	49.40			69.40			32.60	7.70	75.14
64535	800.00	55.80			70.70			32.61	7.43	78.35
64535	800.00	54.70			68.50			29.10	6.66	78.58
64535	850.00	52.10	52.10	40.60	63.80	63.80	76.60	34.95	4.75	80.08
9583A	900.00	52.50	50.77	39.40	60.20	60.05	72.70	33.40	6.14	82.55
9583A	900.00	53.40			60.20			36.15	3.06	85.39
5795	900.00	48.80			60.80			34.00	4.42	77.61
5795	900.00	45.70			58.60			39.60	5.95	80.38
64535	900.00	53.80			60.30			41.85	3.54	81.78
64535	900.00	50.40			60.20			35.25	4.28	80.59
64535	950.00	48.70	46.70	37.80	51.30	51.30	67.30	50.75	2.12	86.75
9583A	1000.00	46.00	44.44	35.90	48.00	48.35	62.20	41.90	1.60	84.06
9583A	1000.00	46.50			49.40			42.40	1.15	84.80
5795	1000.00	43.30			46.20			51.75	2.68	72.46
5795	1000.00	41.00			47.10			48.60	3.44	77.62
64535	1000.00	44.60			49.30			41.00	1.70	86.06
64535	1000.00	45.00			48.10			48.50	1.92	78.39
64535	1050.00	35.20	35.20		39.00	39.00		56.60	1.13	86.25
9583A	1100.00	30.80	30.33		34.80	34.95		55.65	1.13	73.50
9583A	1100.00	30.30			34.80			45.08	1.09	71.34
5795	1100.00	29.20			34.10			56.53	0.78	58.44
5795	1100.00	32.50			36.30			59.72	1.08	56.37
64535	1100.00	28.10			34.40			44.62	1.59	82.22
64535	1100.00	31.10			35.30			63.10	1.39	86.26

a) Table I-2.1, Appendices, Section III, Division 1

See note on next page.

Tensile tests were performed at crosshead speeds of 0.01 and 0.002 inches/min. The specimen gage length was 1.25 inches, so the strain rate was either 0.008 or 0.0016 in/in/min. The values used in the data analysis were from the tests at the lower strain rate. However, the yield stress and the UTS were not significantly different at the two rates at temperatures from room temperature through 1000F, and either set of data could have been used with the same results.

2.3 RATIO ANALYSIS FOR SA533B TENSILE PROPERTIES

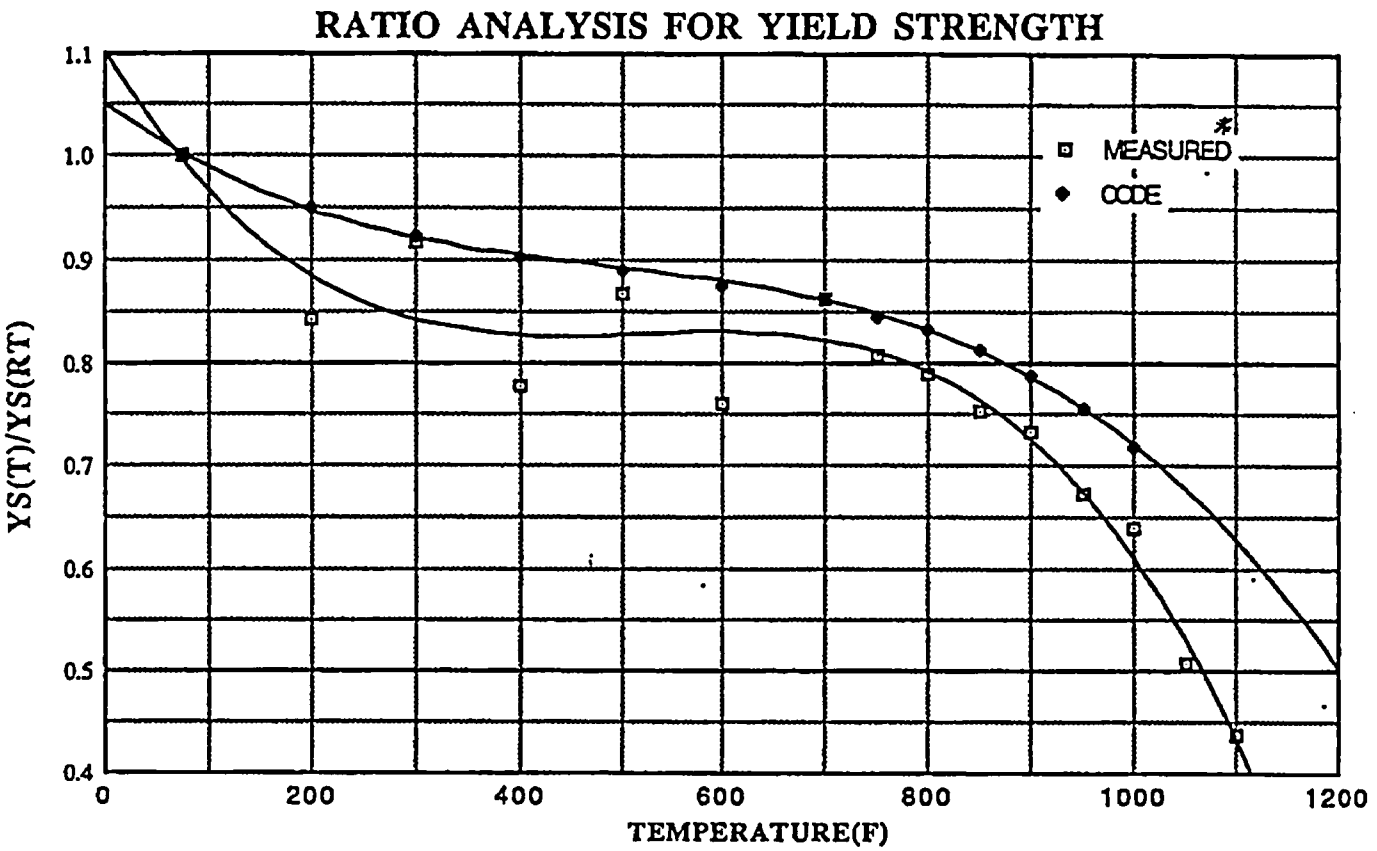

* Average results from duplicate tests on three heats of material (see Table 2.1).

2.3 RATIO ANALYSIS FOR SA533B TENSILE PROPERTIES

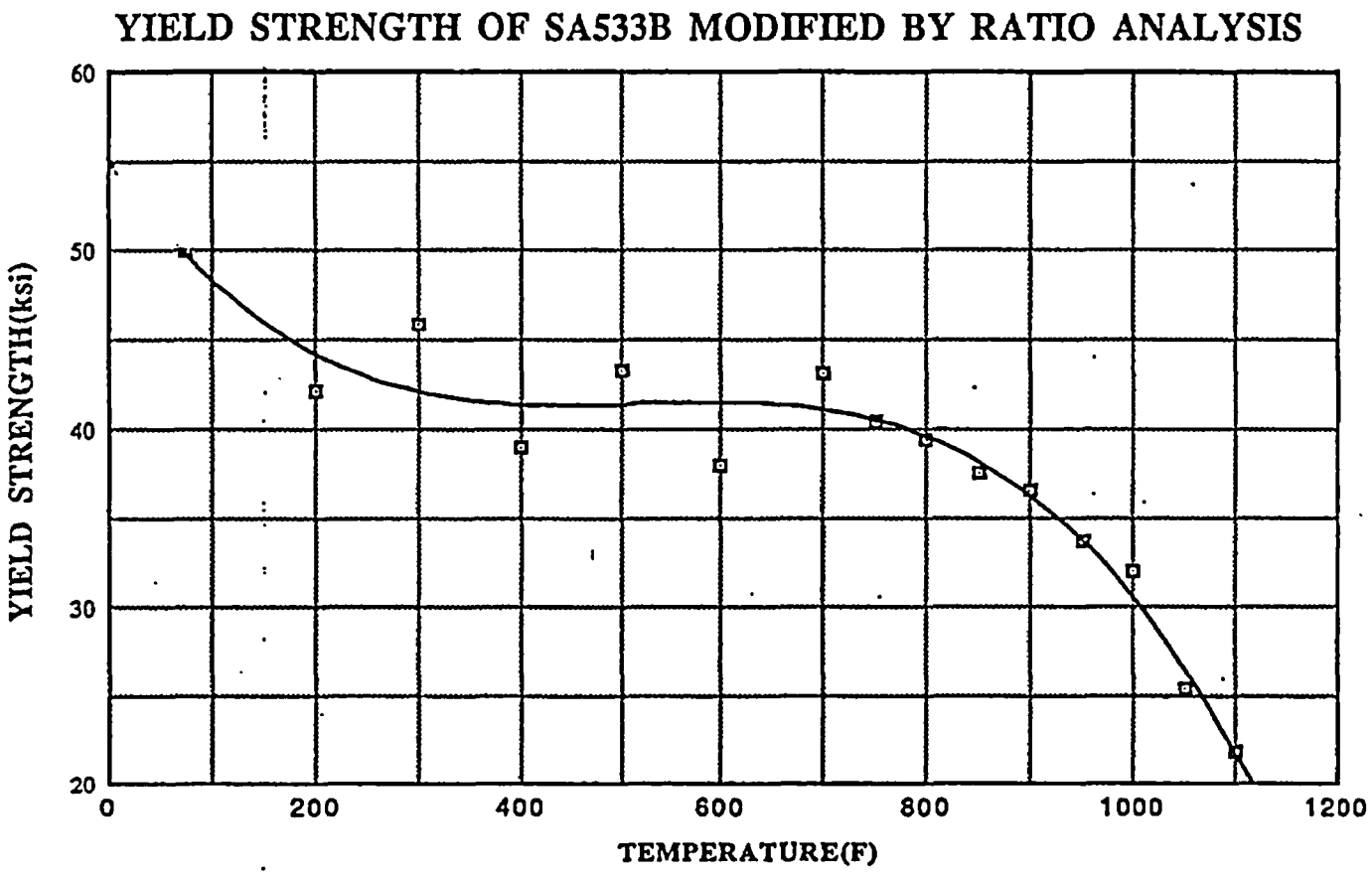

2.3 RATIO ANALYSIS FOR SA533B TENSILE PROPERTIES

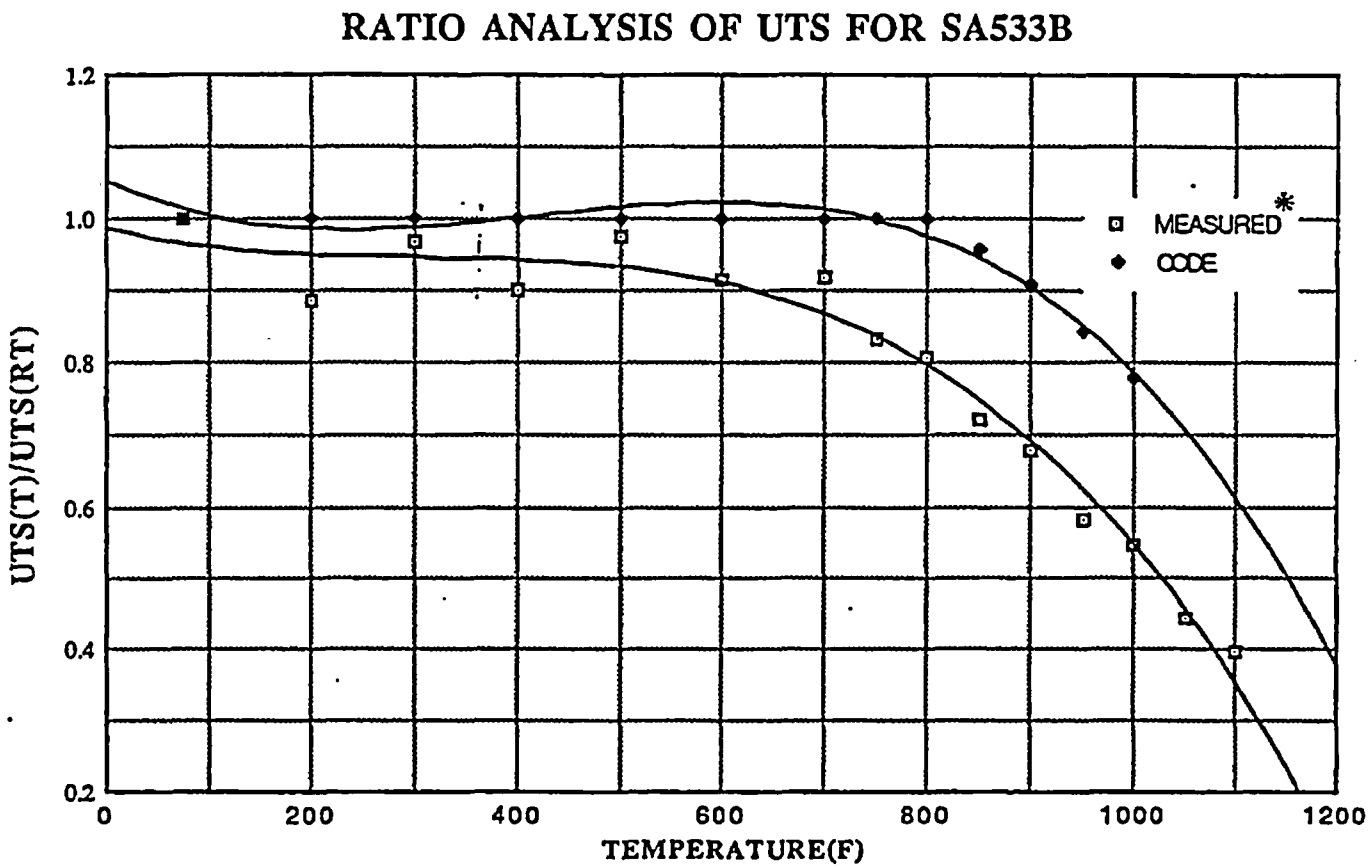

* Average results from duplicate tests on three heats of material (see Table 2.1).

2.3 RATIO ANALYSIS FOR SA533B TENSILE PROPERTIES

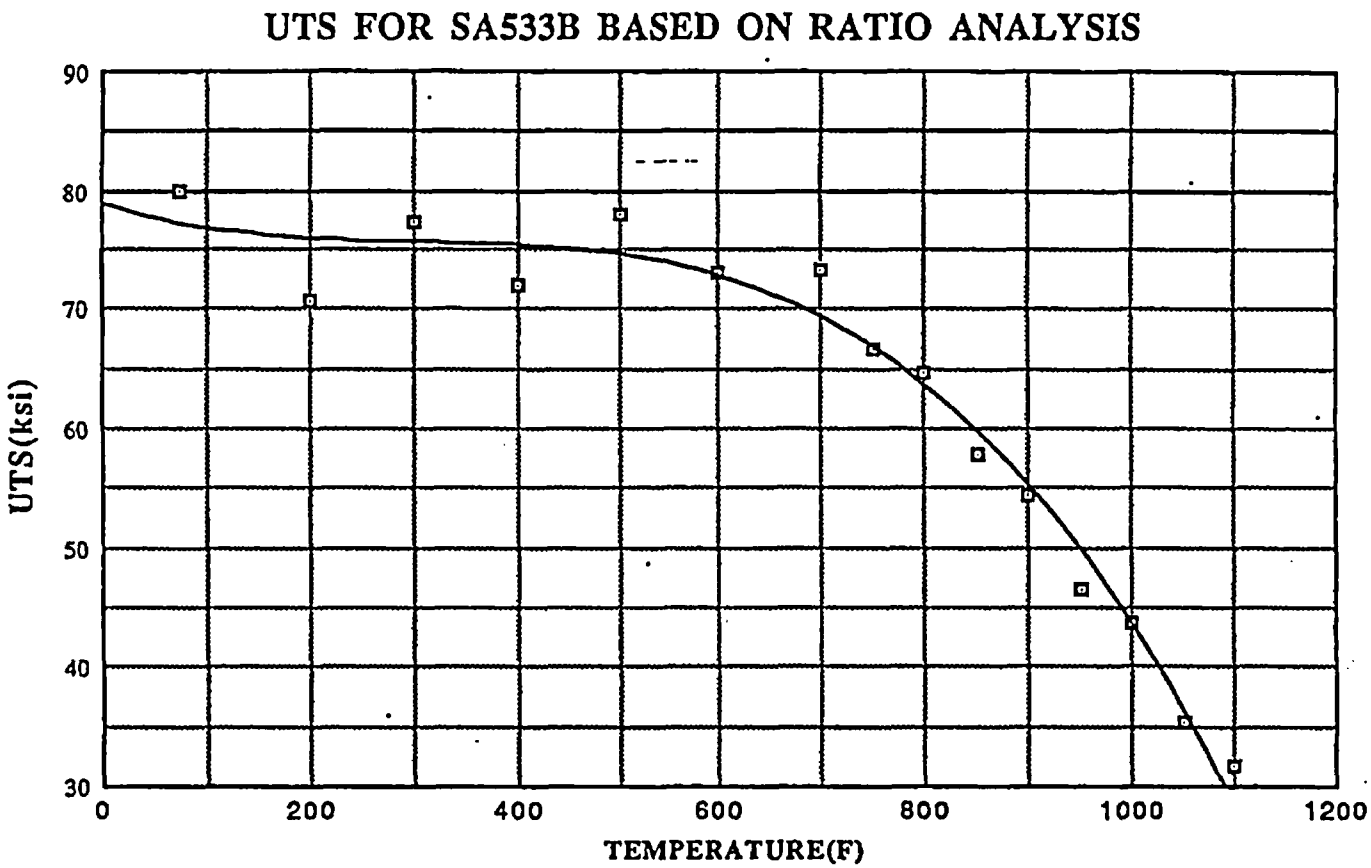

2.4 ALLOWABLE STRESSES(Sm) VS TEMPERATURE FOR SA533B

TEMPERATURE °F	(b) DERIVED S_m ksi	(c) YIELD STRESS ksi	(d) UTS ksi	CODE S_m(a) ksi	RECOMMENDED S ksi
75	26.4	50.0	80.0	26.7	26.7
100	26.4	48.0	80.0	26.7	26.7
200	26.4	44.0	80.0	26.7	26.7
300	26.4	42.0	80.0	26.7	26.7
400	26.4	41.5	80.0	26.7	26.7
500	26.4	41.5	80.0	26.7	26.7
600	26.4	41.5	80.0	26.7	26.7
650	26.1	41.5	79.2	26.7	26.7
700	25.0	41.0	75.9	26.7	26.7
750	24.3	40.5	73.7		~~24.3~~ 24.6
800	23.1	39.5	69.9		~~23.1~~ 23.3
850	21.8	38.0	66.0		~~21.8~~ 22.0
900	20.0	37.0	60.5		~~20.0~~ 20.1
950	18.2	33.5	55.0		~~18.2~~ 18.3
1000	16.0	31.0	48.4		~~16.0~~ 16.1

(a) Table 1-1.1, Appendix I, Section III, ASME Boiler and Pressure Vessel Code, Class I Components.

(b) Derived S_m equals 1/3 x (UTS column).

(c) Yield Stress is taken directly from the yield trend curve based on the ratio analysis and a room temperature value of 50 ksi.

(d) UTS is the lesser of 1) 80 ksi(minimum specified room temperature UTS or (2) 1.1 times the elevated temperature UTS from the trend curve.

2.5 MODULUS OF ELASTICITY vs TEMPERATURE FOR SA533B

TEMPERATURE	ELAST MOD	SOURCE
F	1000000 psi	
-325	31.1	SECT. III, APP I, TABLE I-60
-200	30.5	
-100	29.9	
70	29.2	
200	28.5	
300	28.0	
400	27.4	
500	27.0	
600	26.4	
700	25.3	
800	23.9	
900	22.2	SECT VIII, DIV 1, TAB UF-27
1000	20.1	
1100	17.8	

2.5 THERMAL EXPANSION OF SA533B

TEMPERATURE F	SA533B INST.COEF.	SA 533B MEAN COEF.
70.00	7.02	-
100.00	7.13	7.06
150.00	7.29	7.06
200.00	7.45	7.25
250.00	7.60	7.34
300.00	7.74	7.43
350.00	7.88	7.50
400.00	8.01	7.58
450.00	8.13	7.63
500.00	8.25	7.70
550.00	8.36	7.77
600.00	8.46	7.83
650.00	8.55	7.90
700.00	8.63	7.94
750.00	8.71	8.00
800.00	8.78	8.05
850.00	8.84	8.10
900.00	8.90	8.14
950.00	8.95	8.19
1000.00	8.99	8.23

Units on both parameters are in/in x°F x 10^{-6}

Source of data is: "R. A. Moen, "Thermophysical Properties of Ferrous Structural Alloys," HEDL-TME 78-47, UC-79b,h, April 1978.

3.1 CREEP DATA FOR SA533B STEEL

TEST NO.	LOT NO.	STRESS, KSI	TEMP, C.	SR, %/H (a)	T-0.1% (b)	T-1% (b)	T-2% (b)	T-5% (b)	T-t (b)	T-R (b)	LOADING S, %	CREEP S, %	RED IN AREA, %
25708	9583A	75	371	0.006	0.05	45	195	660	660	1004	2.62	21.69	73.5
25694		67	371	0.00012	0.1	2050	9500			7490D	1.44	1.74	2.7
25527		61	427	0.0062	0.1	48	175	630	670	1261	0.87	32.74	73.5
25707		55	427	0.00032	4	1200	4300			5115D	0.32	2.2	3.24
25520		40	482	0.0019	0.2	340	840	1840	1180	2612	0.09	16.76	35.1
25987		40	482	0.0022	4.4	340	790			1124D	0.21	2.8	2.21
25698		35	482	0.0011	12	800	1600	3220	1900	4172D	0.04	9.3	13.82
25518		20	538	0.021	1	35	85	230	270	620	0.1	52.6	45.8
25709		15	538	0.003	10	250	600	1350	900	2995	0.14	18.8	23.9
25724		12	538	0.0004	83	1820	3100		1950	4025D	0.02	2.8	7.3
26502		15	566	0.013	1	66	135	295	195	615	0.09	46.6	52.7
26497		10	566	0.0038	2.9	220	460	1040	620	3378	0.04	56.2	64.8
26817		3	566	0.00016	145	5375				1487D	0.02	0.4	0
26219		8	593	0.013	1.4	63.5	140	320	200	1330	0.06	79	88
25723		5	593	0.0019	25	478	920		870	1171D	0.02	2.6	7.1
25989		4	593	0.00046	36	1660				25921D	0.07	1.4	7.3
26208		3	593	0.00058	5.5	1540	3050	6350	3500	9399D	0.18	8	27.4
26215		2	593	0.00015	175	4150				5295D	0.02	1.2	12.4
26216		1	593	0.000053	1040					3810D	0.03	0.9	11.1
25972	5795	70	371	0.00062	0.025	242	1700			2515D	3	2.5	5.14
25968		65	371	0.00016	0.1					956	1.97	0.7	
26194		65	371	0.00063	4.4	1960				7895D	0.81	1.8	4.9
25976		60	427	0.0031	0.05	45	240			679D	1.34	3.2	5.01
25973		50	427	0.000094	40					648D	0.31	0.23	
25971		45	427	0.000028	65					1201D	0.29	0.2	1.42
25975		35	482	0.00036	8.4	2000				3815D	0.28	1.8	
25969		27	482	0.000026	170					1319D	0.16	0.2	0
26190		20	538	0.0019	9.8	440	810	1395	720	1990	0.13	19.8	19.9
25970		15	538	0.001	23	900	1780		1960	2026D	0.07	2.5	3.94
26501		15	566	0.0061	4.1	160	310	600	420	1163	0.09	42.7	47.5
26503		10	566	0.00014	12	625	1150	2350	950	3628D	0.09	10	5.54
25974		8	593	0.0041	10	230	478		825	960D	0.06	4.7	7.05
26488		4	593	0.0007	54.2	1195	2250	4575	1900	8400D	0.03	15.8	26.5
26499		2	593	0.00019	454	5000				4973D	0.06	1	14.75
26491	9583B	75	371	0.15	0.05	3	9.6	22.4	19.8	23.5	6.4	16.6	71.1
26509		70	371	0.00057	0.19	675	2375			2976D	1.7	2.3	3.3
26193		61	427	0.016	0.1	32	96	256	212	285D	0.85	5.8	7.58
26821		35	482	0.00072	17.2	1200				669D	0.11	0.8	0
26191		30	482	0.00026	12.9	2970	6100	11200	6500	11572D	0.17	5.5	3.6
26192		15	538	0.0018	3.6	450	960	2060	1160	2208D	0.08	5.5	3.26
26505		10	566	0.0026	5.9	325	700	1850	1250	3648D	0.09	16	9.8
26486		8	593	0.005	4.5	165	340	765	450	2241	0.08	62.8	67.1
26218		4	593	0.0006	36.9	1400	3100	5550	3350	9046D	0.01	10.4	25
26196	64535	61	427	0.0051	0.1	45	170	740	1480	1964	1.09	25.1	71.8
26198		30	482	0.0003	27.2	2675	5400		5700	6671D	0.15	2.8	0.4
26820		20	538	0.0074	2.3	100	225	520	290	834D	0.21	11	16.1
26199		15	538	0.00015	8.9	600	1270			1345D	0.1	2.3	1.4
26510		10	566	0.0031	0.08	260	580	1260	800	2782D	0.13	15.9	107
26201		8	593	0.0092	0.35	90	210	480	420	1409	0.1	61.3	93.2
26195		4	593	0.001	100	1020	1800		1740	1945D	0.09	2.25	12.8

(a) minimum creep rate

(b) Times given in hours to various creep strain percentages, t=tertiary, and r=rupture.

3.2 LARSON-MILLER CORRELATION FOR 1% STRAIN, AVERAGE AND MINIMUM PROPERTIES

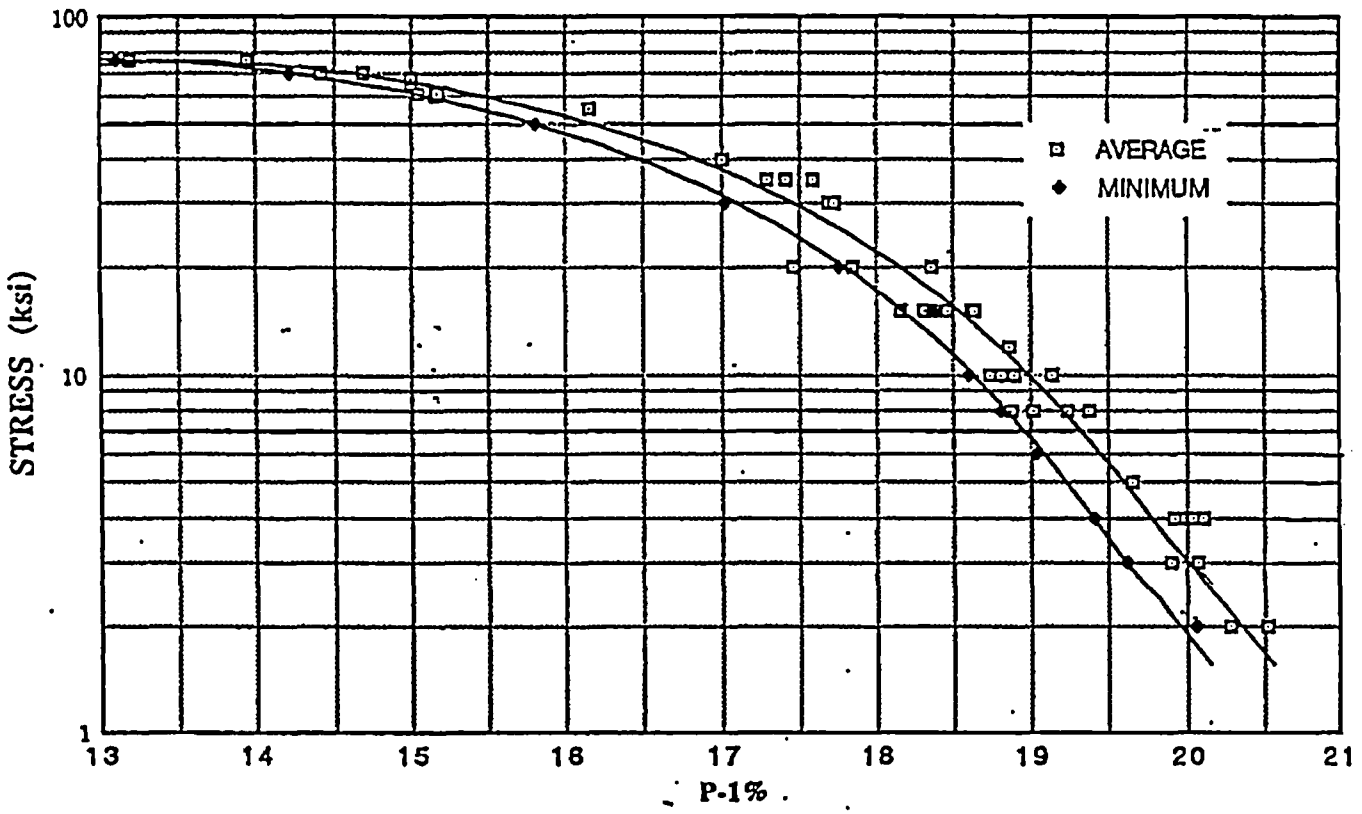

P-1% is a modified Larson-Miller parameter defined as equal to

$$K/1000(20+\log t)$$

where: K=temperature in degrees Kelvin,
t= time to 1% strain in hours.

NOTES:

(a) Minimum properties defined as the average value minum 1.65 multiples of the standard deviation.

(b) Larson-Miller constant variation between 15 and 25 had no effect on R^2.

3.2 LARSON-MILLER CORRELATION FOR TERTIARY CREEP, AVERAGE AND MINIMUM

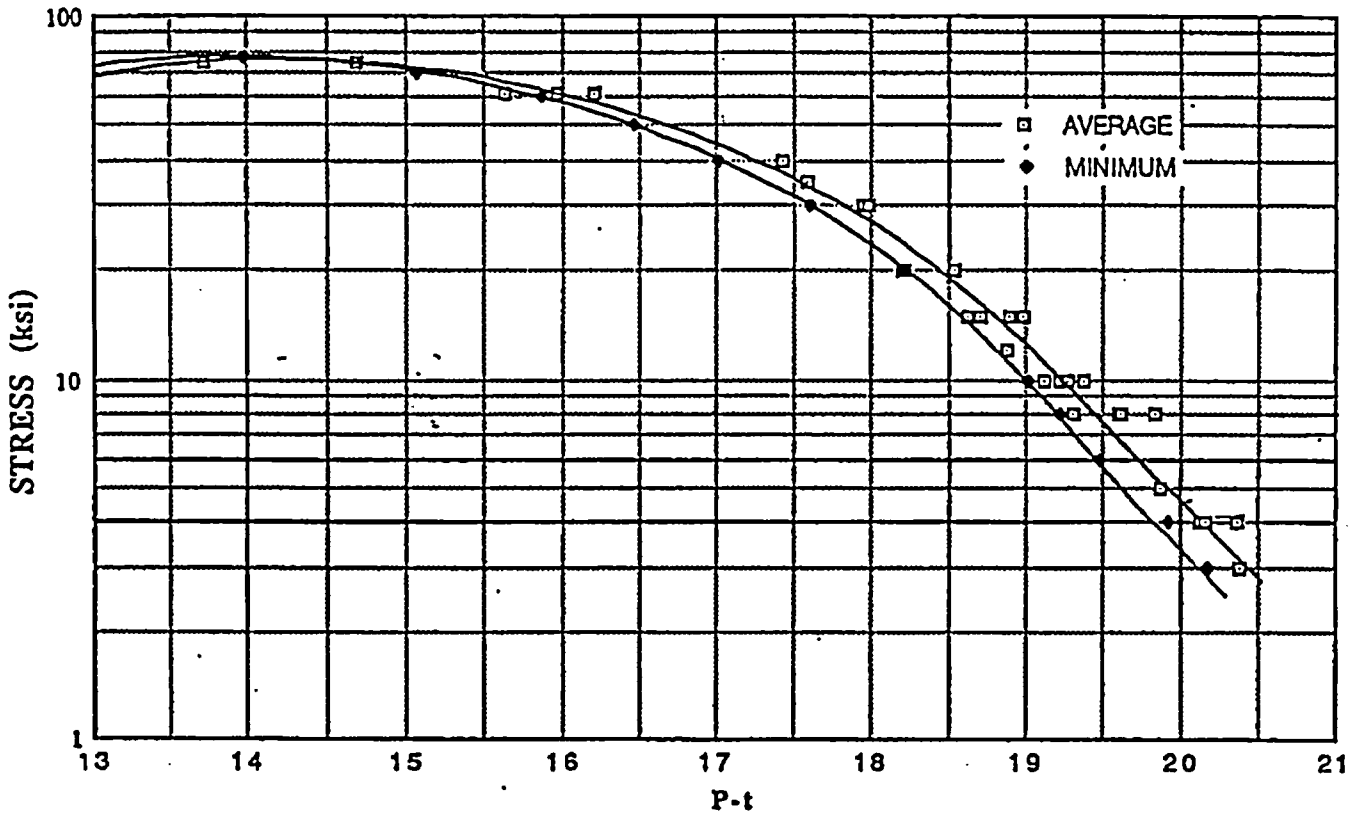

P-t is a modified Larson-Miller parameter defined as equal to

$$K/1000(20+\log t)$$

where: K=temperature in degrees Kelvin,
t= time to tertiary creep (based on 0.2% strain offset) in hours.

3.2 LARSON-MILLER CORRELATION FOR RUPTURE-AVERAGE AND MINIMUM

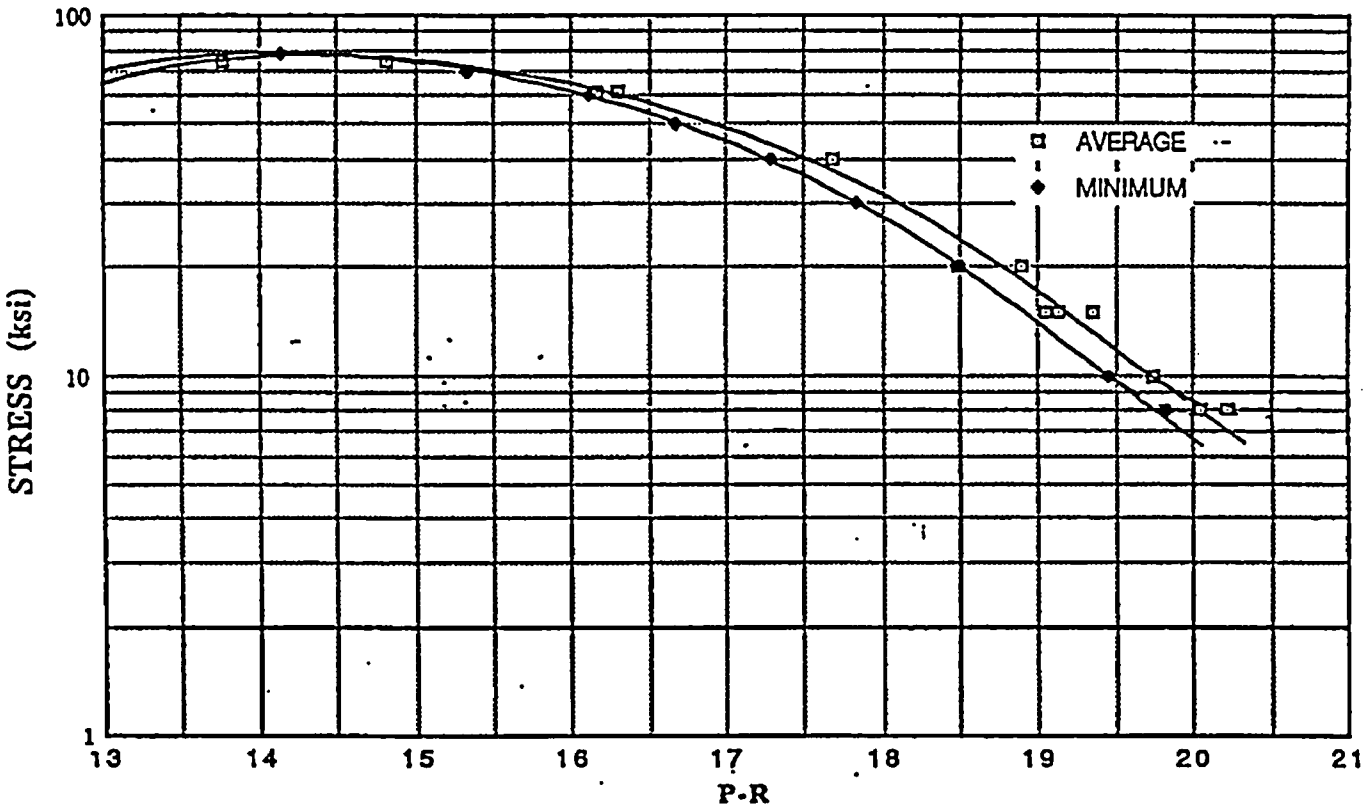

P-R is a modified Larson-Miller parameter defined as equal to

$$K/1000(20+\log t)$$

where: K=temperature in degrees Kelvin,
t= time to rupture in hours.

3.3 MINIMUM STRESS FOR NOTED EVENT IN 1000 HOURS AT TEMPERATURE

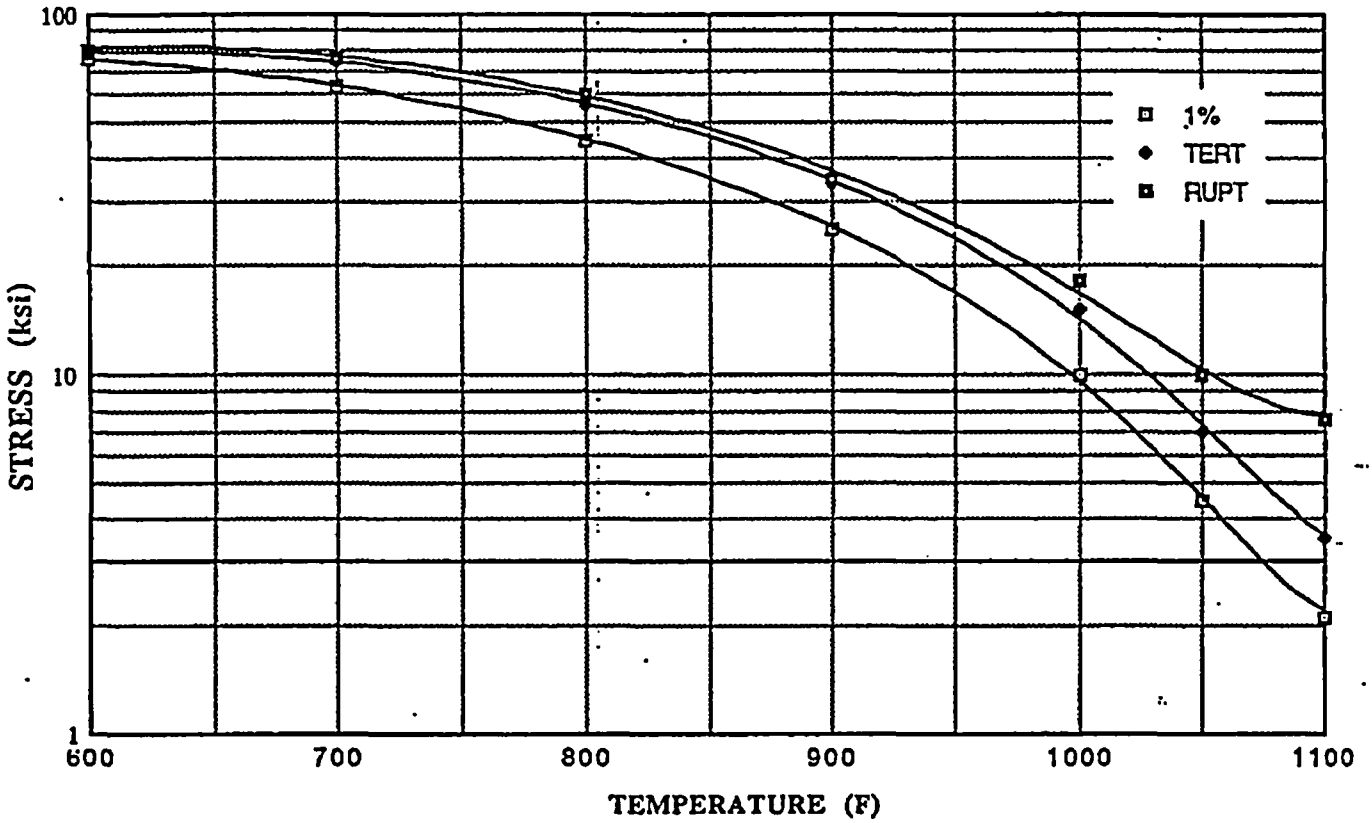

3.4 MINIMUM STRESS vs TEMPERATURE FOR 1% CREEP, 80% TERTIARY, AND 67% RUPTURE

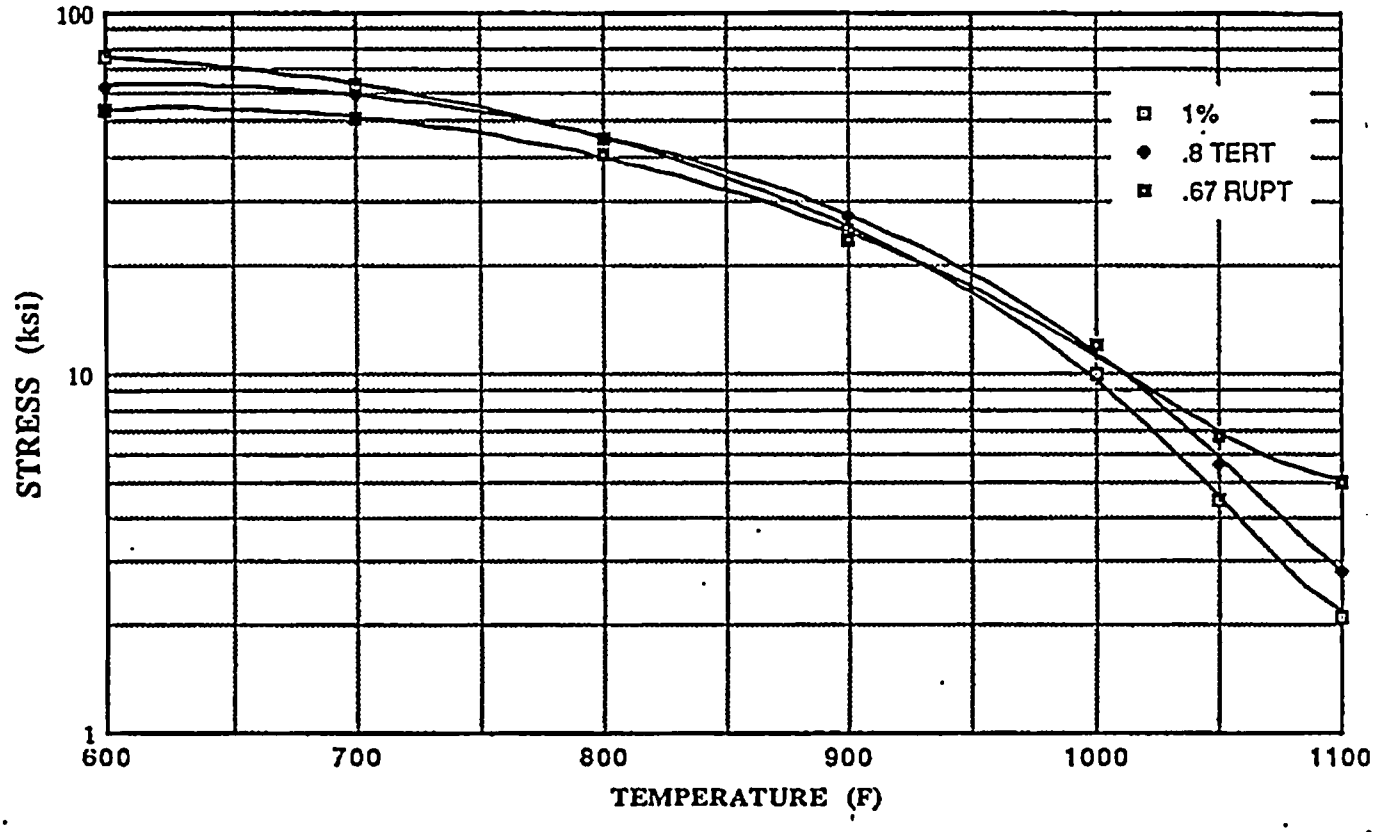

3.5 S_t vs TIME-ISOTHERMAL CURVES

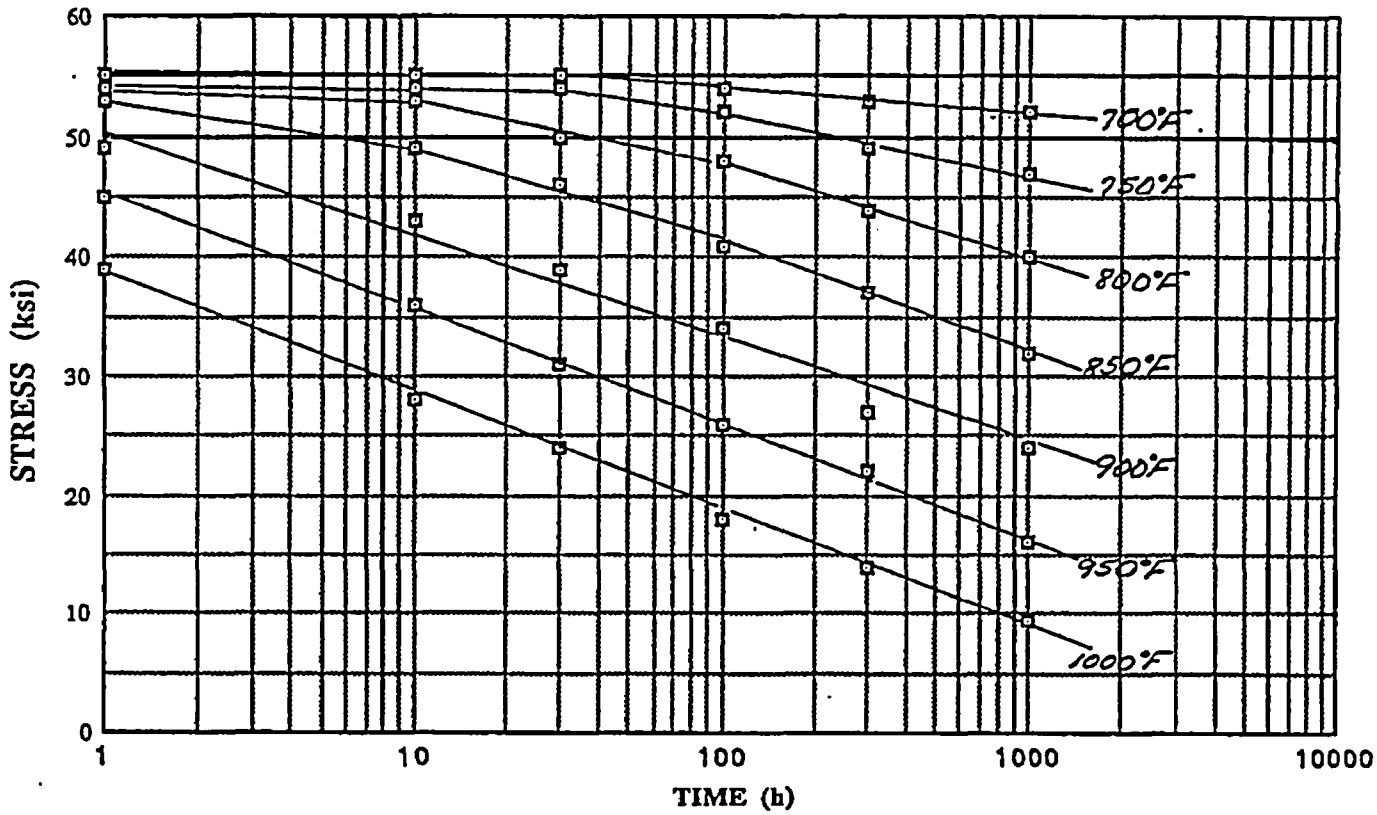

3.5 S_t vs TIME-ISOTHERMAL CURVES

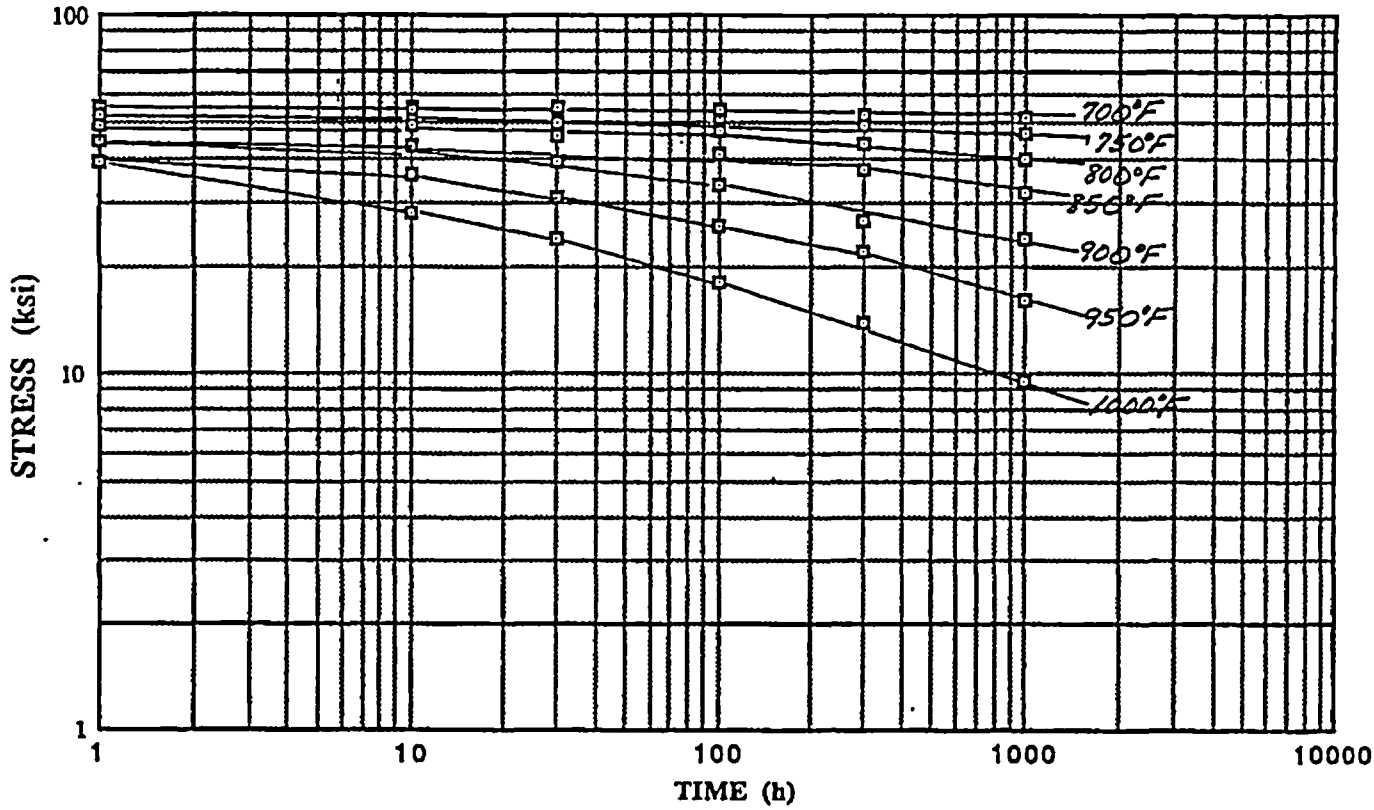

3.6 S_t-Allowable Stress Intensity Values, 1000 psi

Temp. F	1h	10h	30h	100h	300h	1000h
700	54	54	54	53	53	52
750	54	54	54	52	49	47
800	54	53	50	48	44	40
850	53	49	46	41	37	32
900	49	43	39	34	27 -29	24
950	45	36	31	26	22	16
1000	39	28	24	18	14	9.5

3.7 MINIMUM STRESS TO RUPTURE AS A FUNCTION OF TIME AND TEMPERATURE

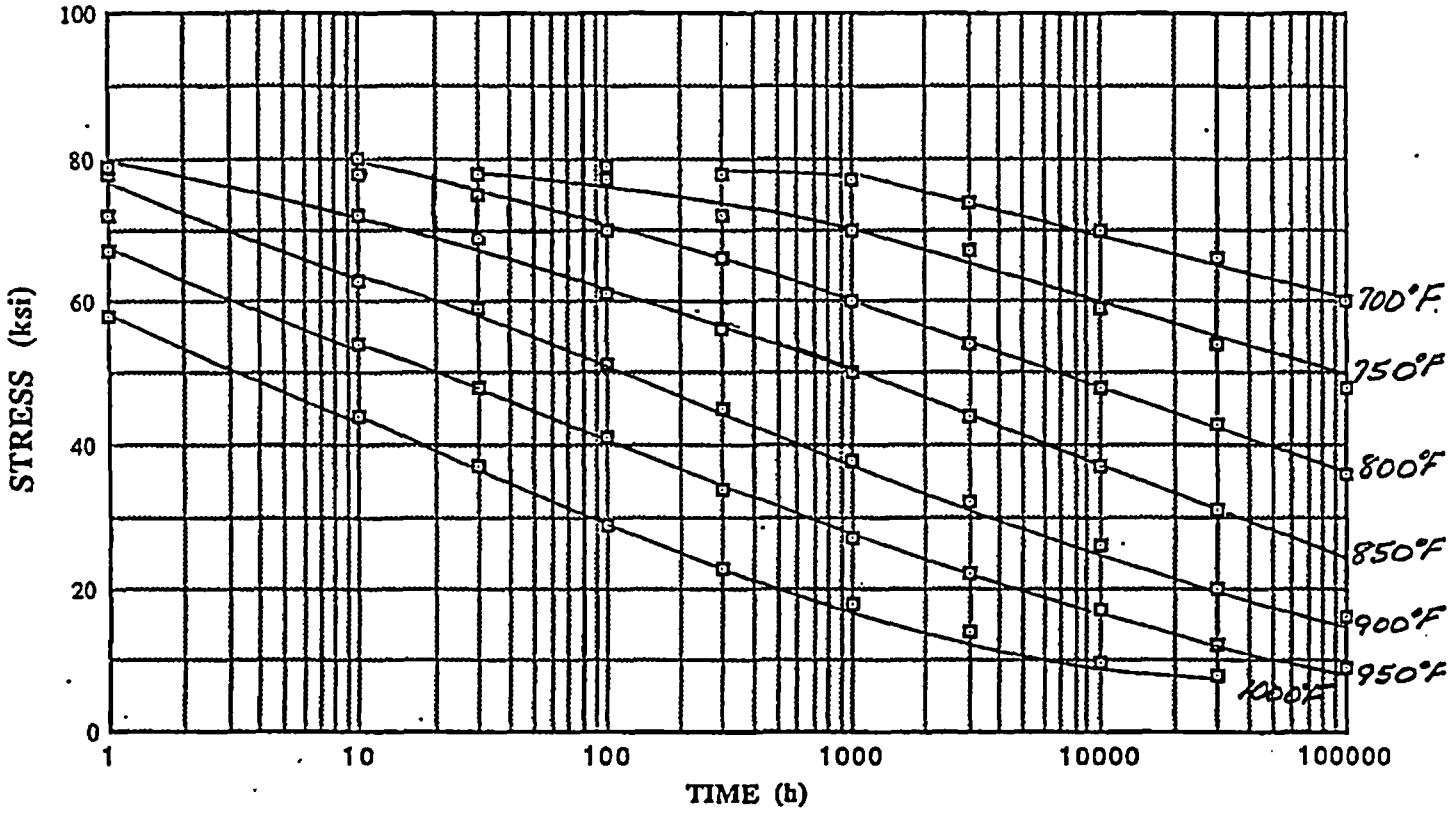

3.7 MINIMUM STRESS TO RUPTURE AS A FUNCTION OF TIME AND TEMPERATURE

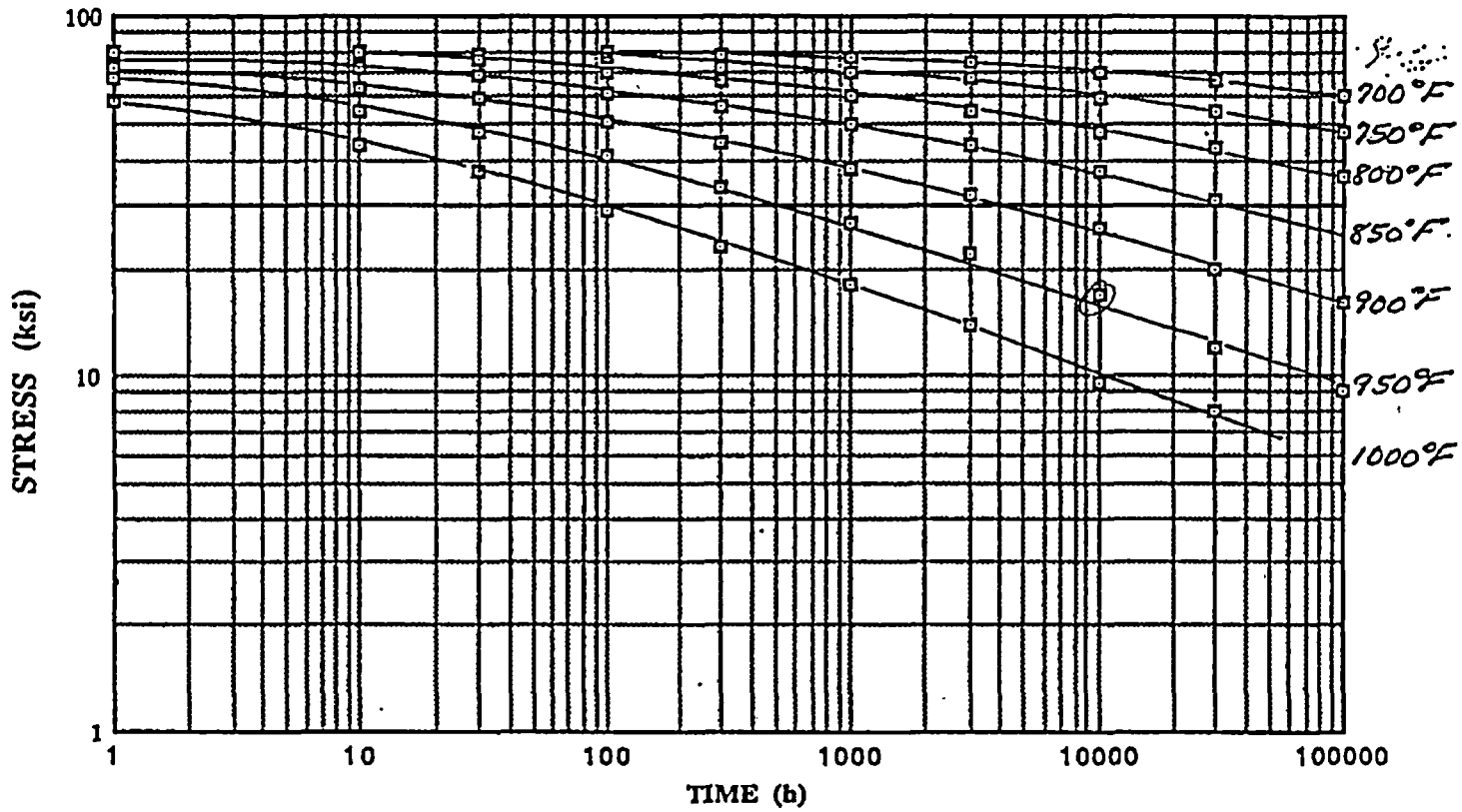

3.8 MINIMUM STRESS-TO-RUPTURE VALUES, ksi

TEMPERATURE F	1h ksi	10h ksi	30h ksi	100h ksi	300h ksi	1000h ksi	3000h ksi	10000h ksi	30000h ksi	100000h ksi
700	80	80	80	79	78	77	74	70	66	60
750	80	80	78	77	72	70	67	59	54	48
800	79	78	75	70	66	60	54	48	43	36
850	78	72	69	61	56	50	44	37	31	23
900	72	63	59	51	45	38	32	26	20	16
950	67	54	48	41	34	27	22	17	12	9
1000	58	44	37	29	23	18	14	9.5	8	4.5

7

3.9 These isochronus stress-strain curves were prepared by W. K. Sartory of ORNL. The modulus of elasticity values in 2.5 and an ORNL-derived creep equation were used in formulating these curves.

3.9 Isochronous stress-strain curve for SA533B at 700 F.

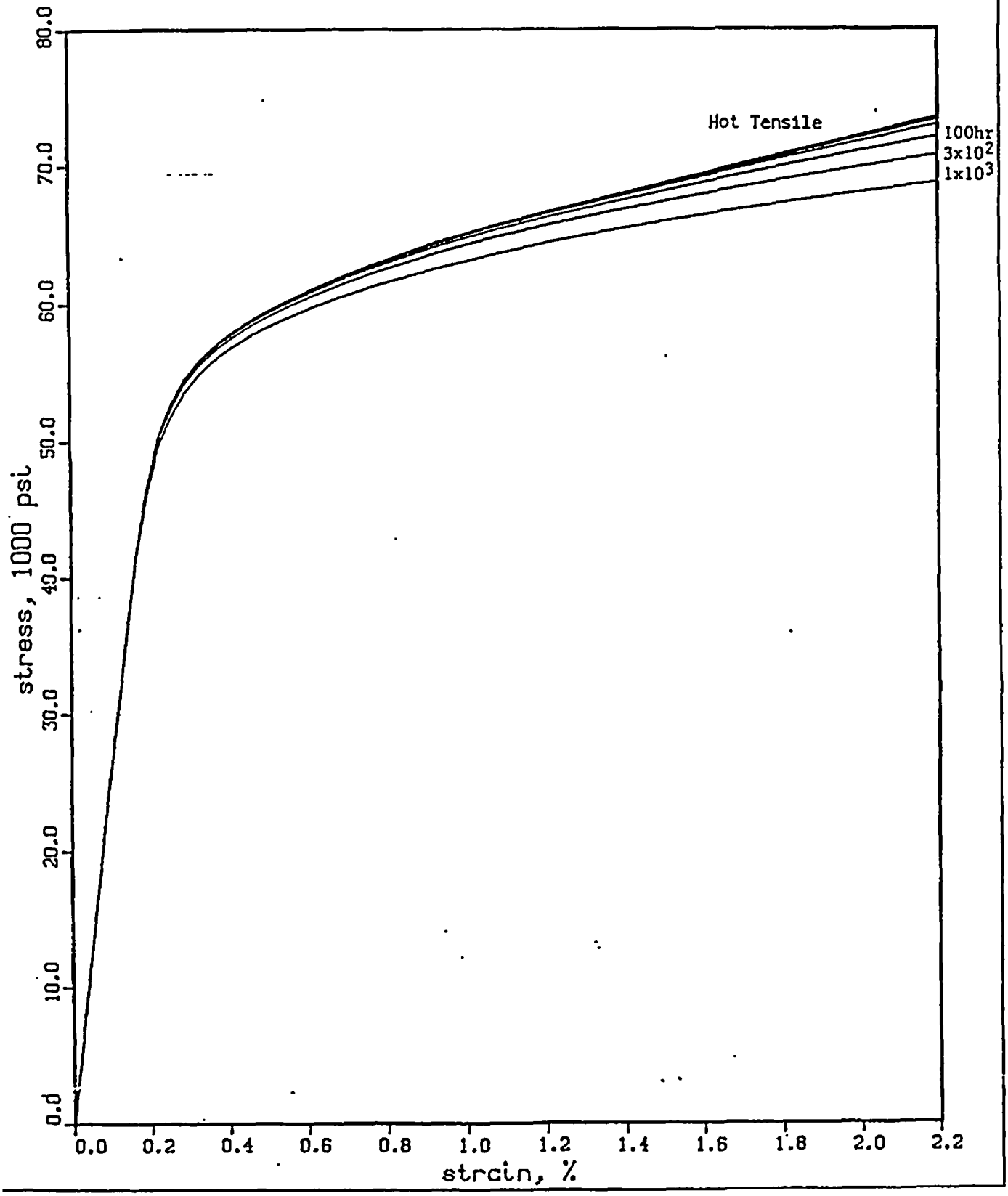

3.9 Isochronous stress-strain curve for SA533B at 750 F.

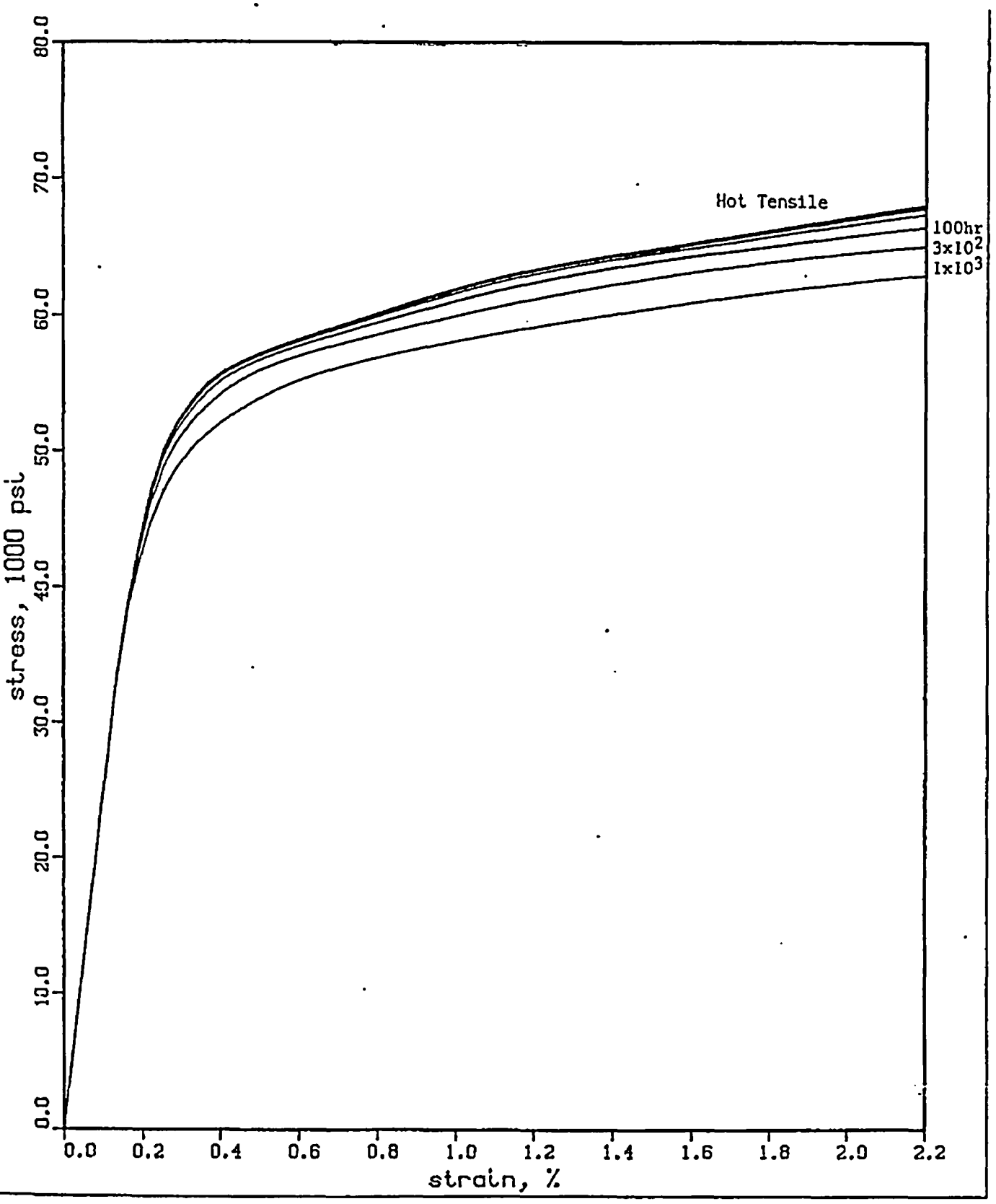

3.9 Isochronous stress-strain curve for SA533B at 800 F.

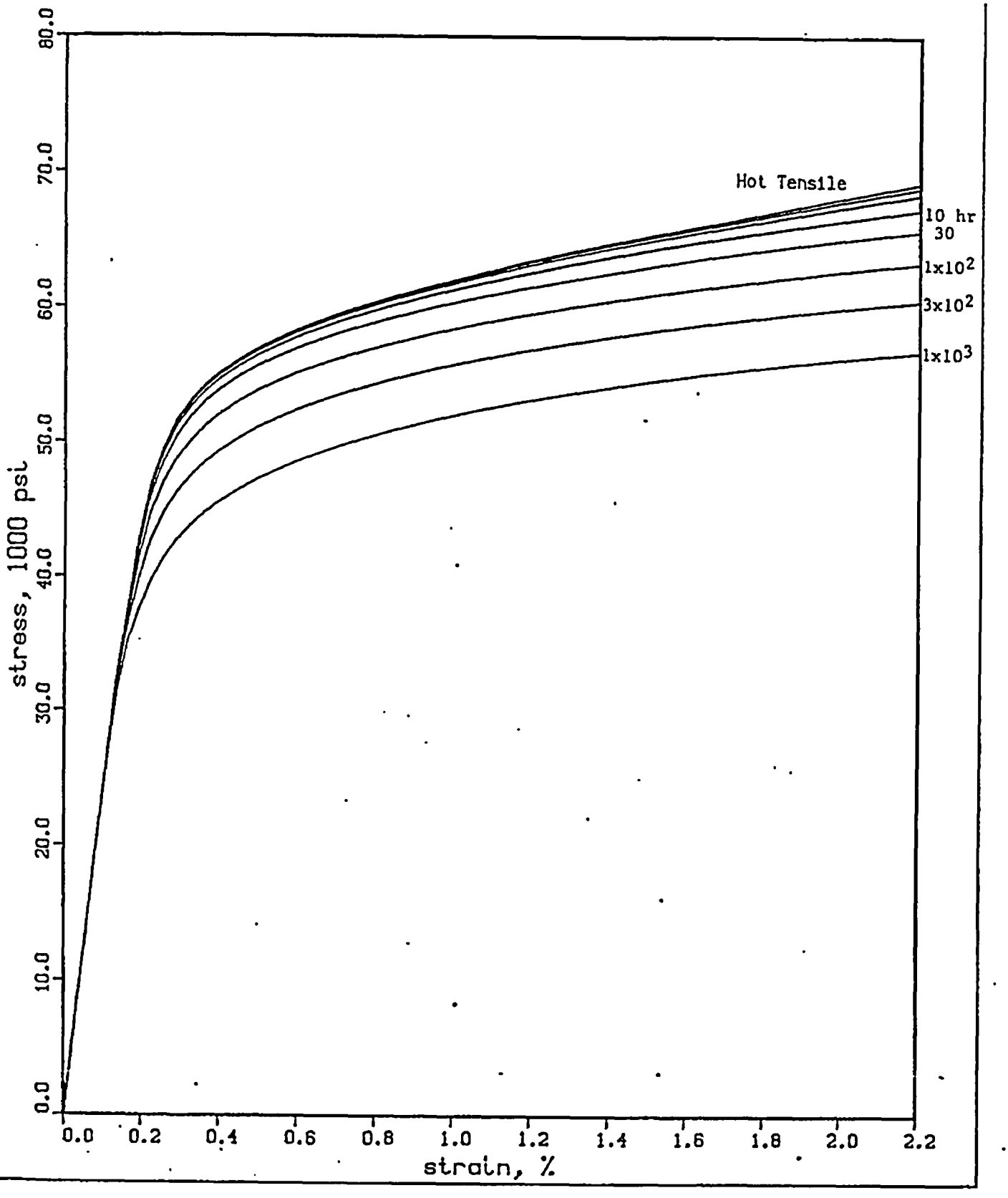

3.9 Isochronous stress-strain curve for SA533B at 850 F.

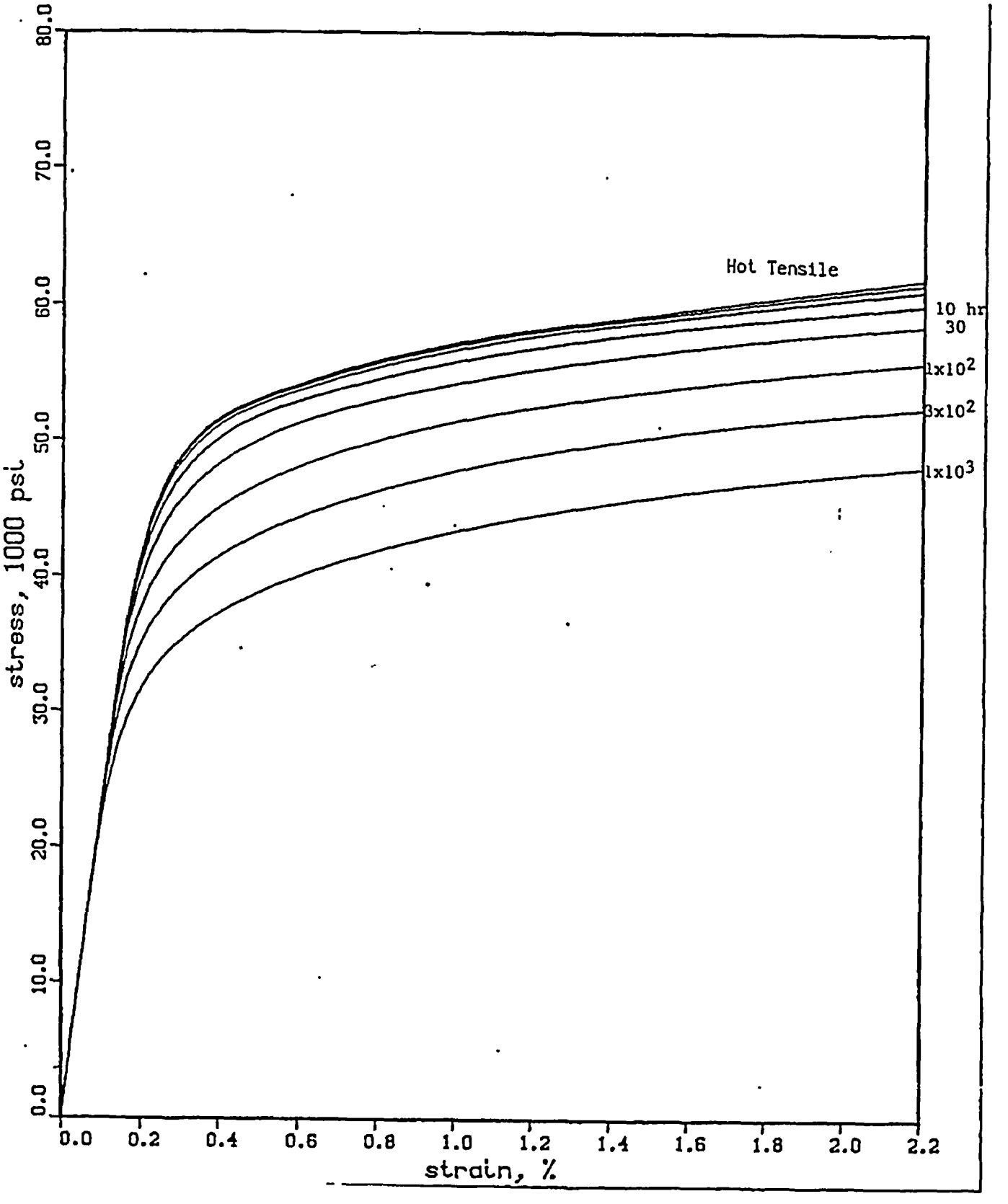

3.9 Isochronous stress-strain curve for SA533B at 900 F.

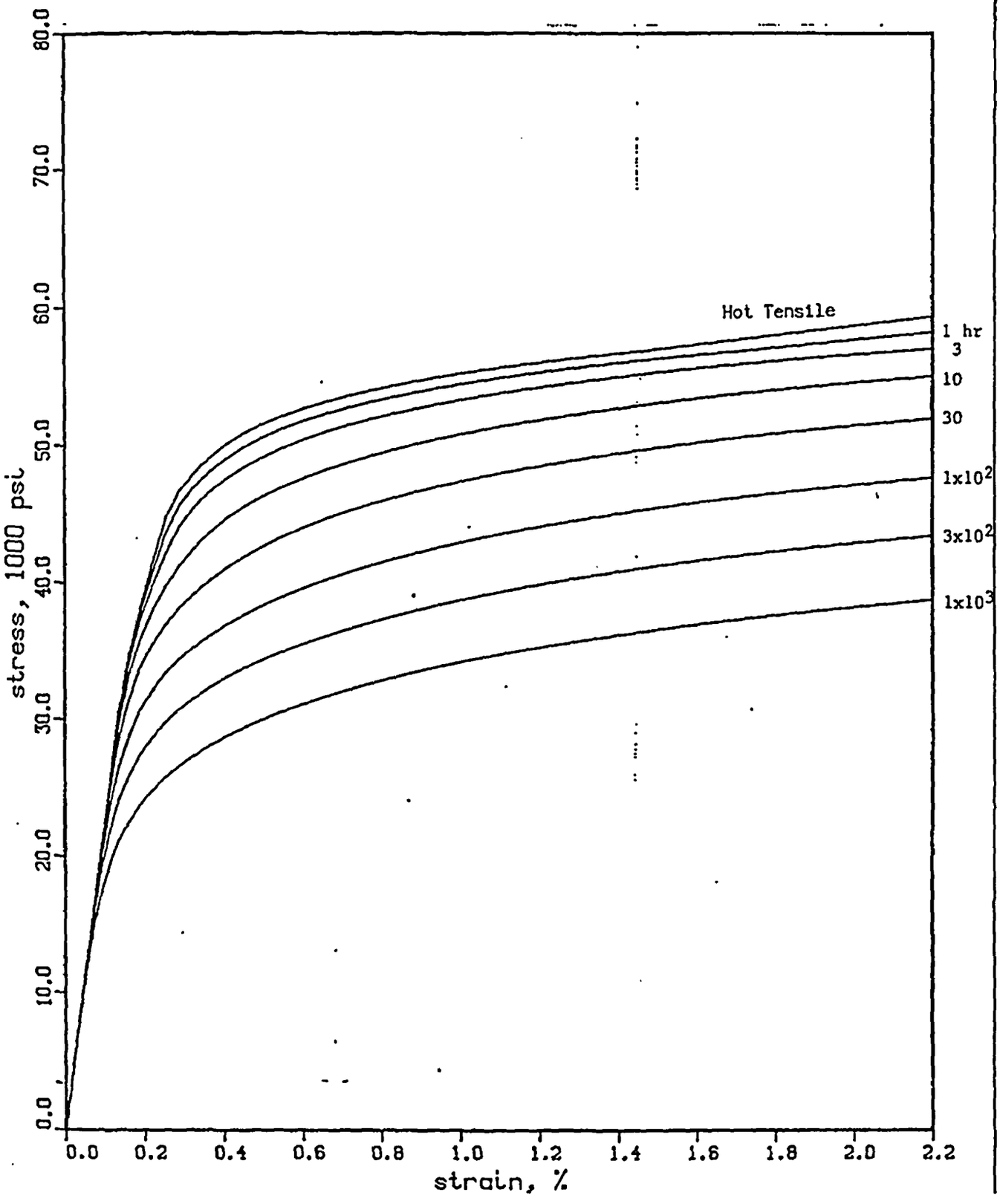

3.9 Isochronous stress-strain curve for SA533B at 950 F.

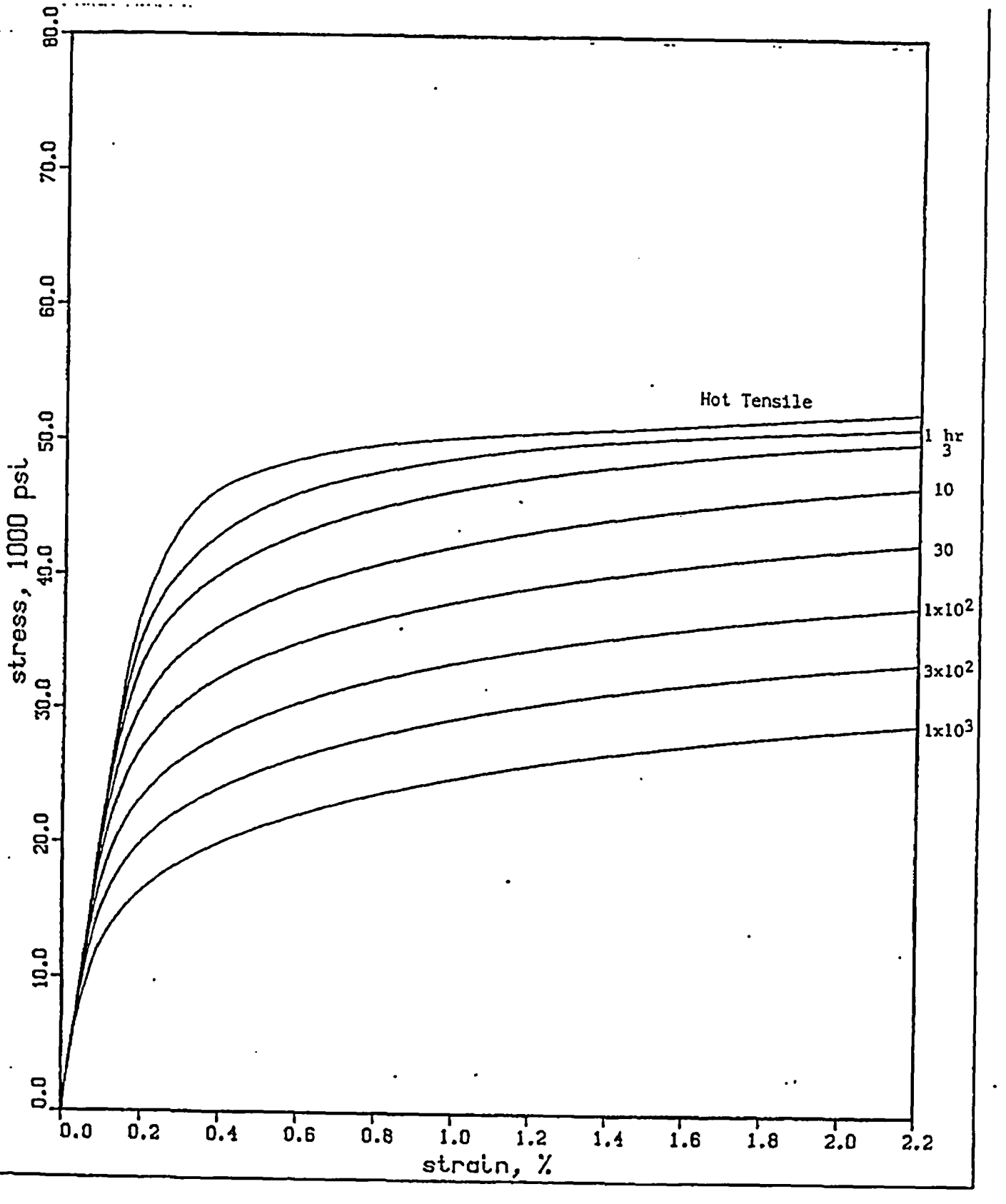

3.9 Isochronous stress-strain curve for SA533B at 1000 F.

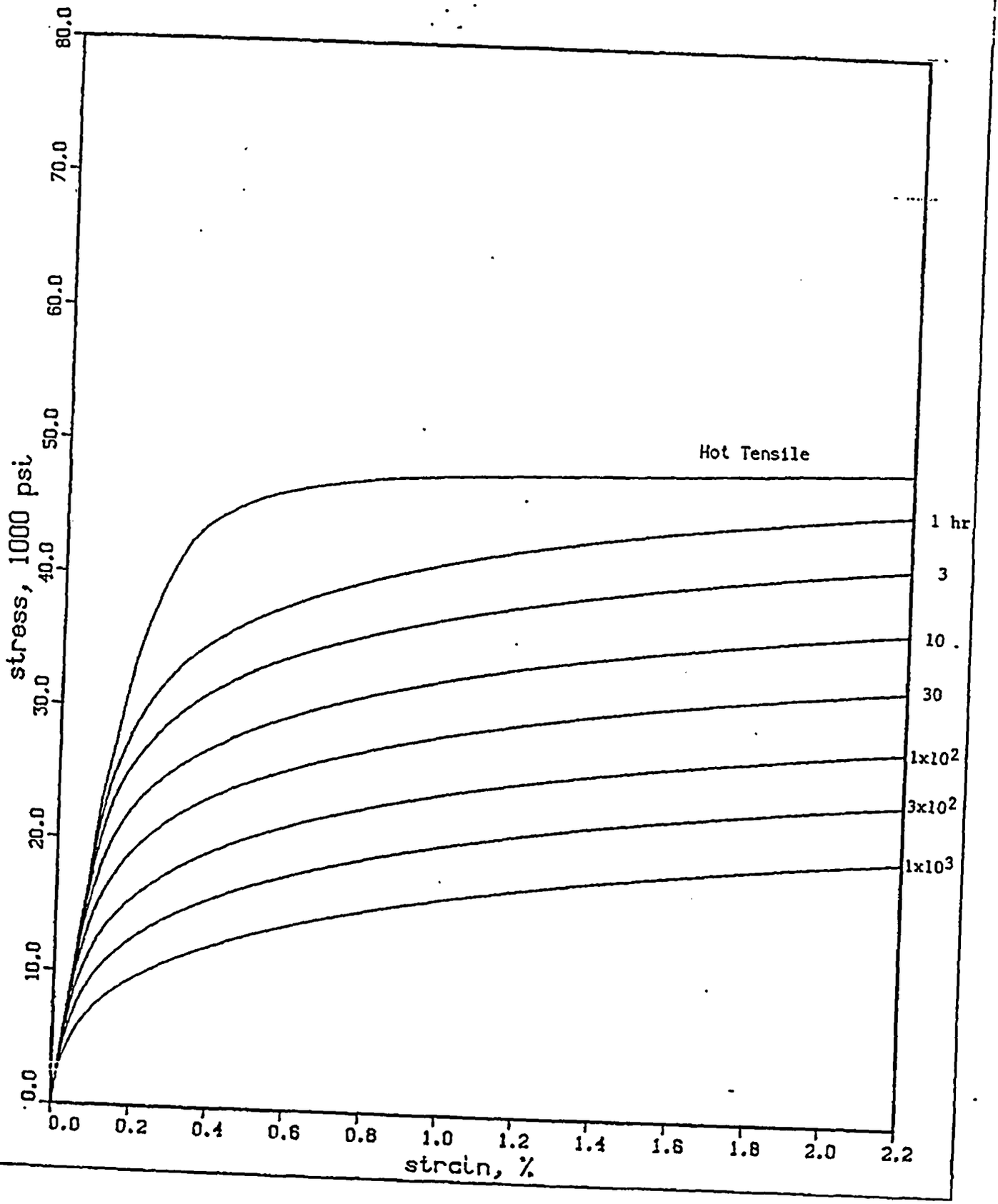

4.1 ALLOWABLE STRESS INTENSITY VALUES, Smt(ksi)

TEMPERATURE	1h	10h	30h	100h	300h	1000h
F	ksi	ksi	ksi	ksi	ksi	ksi
700.0	26.7	26.7	26.7	26.7	26.7	26.7
750.0	24.3	24.3	24.3	24.3	24.3	24.3
800.0	23.1	23.1	23.1	23.1	23.1	23.1
850.0	21.8	21.8	21.8	21.8	21.8	21.8
900.0	20.0	20.0	20.0	20.0	20.0	20.0
950.0	18.2	18.2	18.2	18.2	18.2	16.0
1000.0	16.0	16.0	16.0	16.0	14.0	9.5

4.2 PLOT OF ALLOWABLE STRESS VALUES (S_m) vs TEMPERATURE

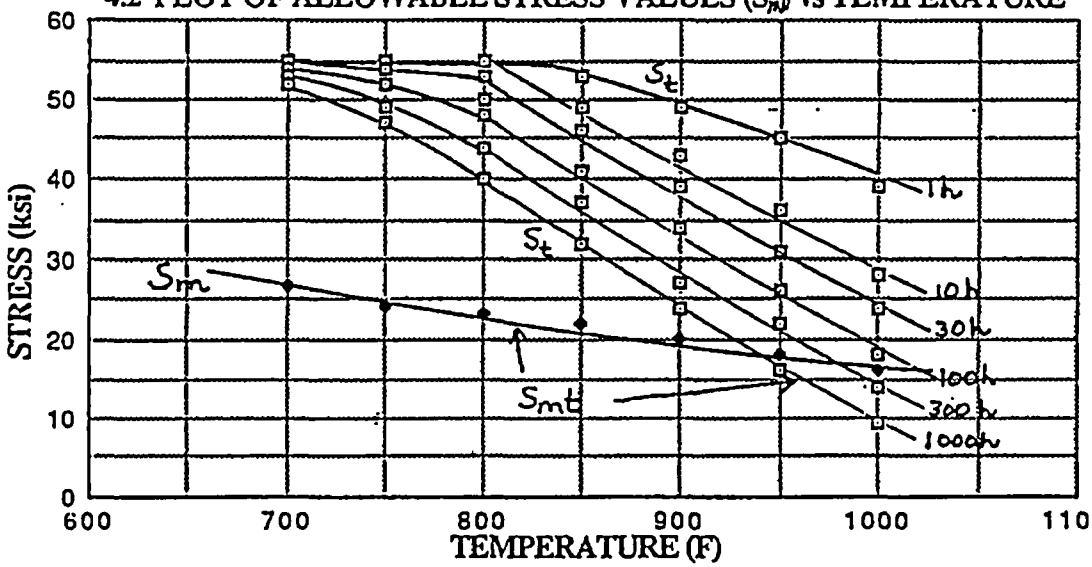

5.1 FATIGUE DATA AT 1000F FOR SA533B

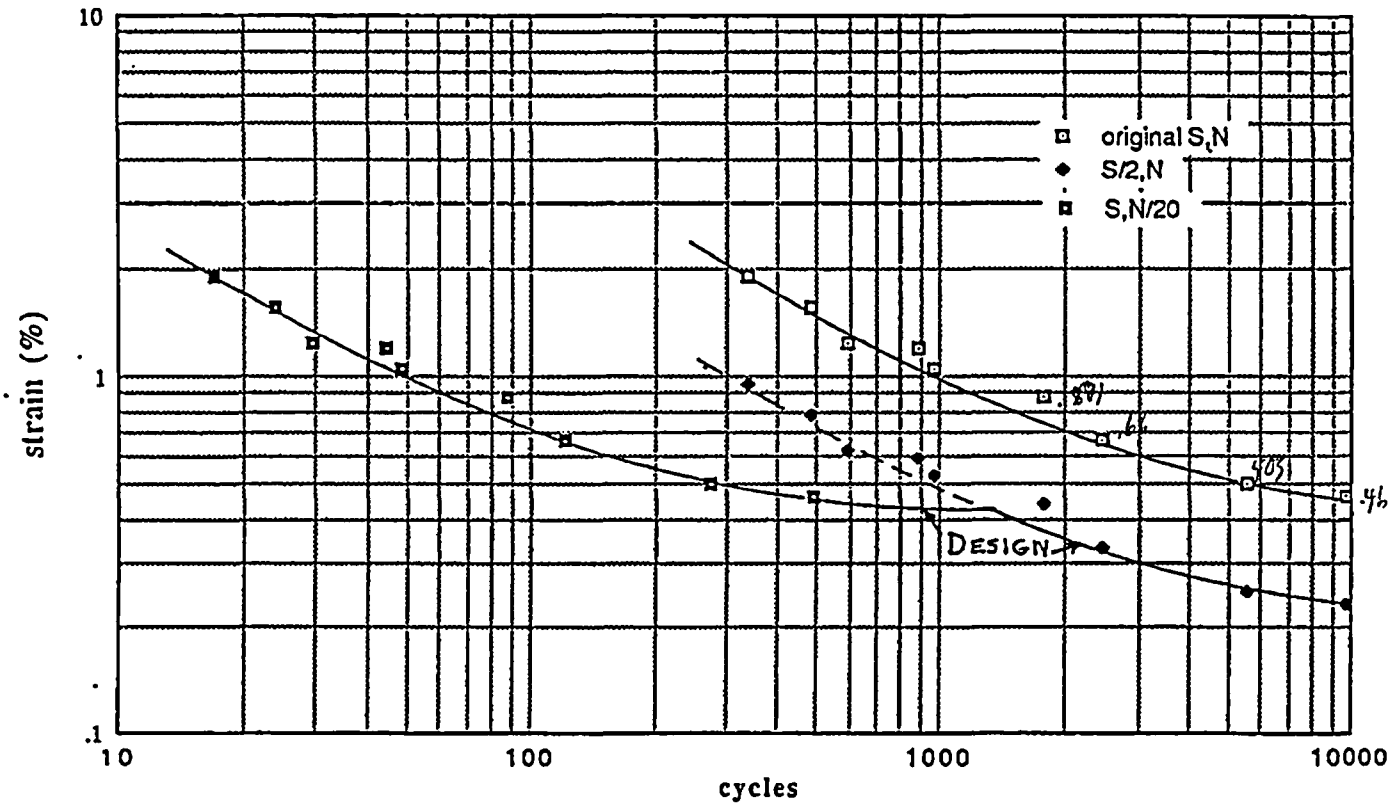

6.1

6.

TEMPER EMBRITTLEMENT

Most of the temper embrittlement studies of this alloy show that embrittlement is associated with the enrichment of grain boundaries with impurities such as phosphorus during welding. The worst embrittlement was noted in the heat-affected zone.[4,7] The heats of commercial material currently being evaluated are quite low in residual impurities such as phosphorus (Table 2), so it is not very likely that commercial heats of this material produced to the chemical specifications for nuclear use in Section II of the code will be susceptible to temper embrittlement. However, a small program is being carried out to demonstrate this point. In the meantime, it was felt that tensile tests at 25°C on creep samples discontinued after a few percent strain would reveal any significant embrittlement.

REFERENCES

4. Masayoshi Haseguawa, Nobuya Nakajima, Nobuharw Kusunoki, and Kazuhiro Suzuki, "Effects of Copper and Phosphorus on Temper Embrittlement of Mn-Mo-Ni Low Alloy Steel (ASTM A533-B)," *Trans. Jpn. Inst. Met.* 16, 641-46 (1975).

5. S. G. Druce and B. C. Edwards, "On the Temper Embrittlement of Manganese-Molybdenum-Nickel Steels," *Nucl. Technol.* 55, 487-98 (November 1981).

6. W. A. Logsdon, "The Influence of Long-Time Stress Relief Treatments on the Dynamic Fracture Toughness Properties of ASME SA508 Cl 2a and ASME SA533 Gr B Cl 2 Pressure Vessel Steels," *J. Mater. Energy Sys.* 3(4), 39-50 (March 1982).

7. S. G. Druce, G. Gage, and G. Jordan, "Effect of Aging on Properties of Pressure Vessel Steels," *Acta Metall.* 34(4), 641-52 (1986).

6.2 Effect of creep exposure on tensile properties at 75F.

							creep exposure before tensile				tensile without exposure			
TEST ID.	HEAT	LOCATION	HEAT TREAT	TEMP, C	STRESS,KSI	TIME, H	YS,KSI	UTS,KSI	ELONG,%	RA,%	YS,KSI	UTS,KSI	ELONG,%	RA,%
25971	5795	BASE	CE	427	45	1201	68.4	87.1	27	63.5	64	85.2	31	69.3
25973	5795	BASE	CE	482	59	648	71.8	89.7	26.8	65.6	64	85.2	31	69.3
25969	5795	BASE	CE	482	27	1319	64.5	85.6	30.2	65	64	85.2	31	69.3
25974	5795	BASE	CE	593	8	960	52.4	62.8	31.5	56.9	64	85.2	31	69.3
25526	9583A	BASE	ORIEL 1	371	75	5494	89.6	110	29	71.7	90	100.5	28.3	75.7
25513	9583A	BASE	ORIEL 1	371	67	1491	92.9	102.3	24.9	74	90	100.5	28.3	75.7
25714	9583A	BASE	ORIEL 2	371	60	5016	75.3	85.2	29.3	75.8	70.3	85.2	32.5	77.8
25694	9583A	BASE	CE	371	67	7490	82.5	83.7	28.7	70.3	71.3	90.1	30.5	74.5
25719	9583A	BASE	ORIEL 2	427	50	1321	64.2	84.2	32.4	72.5	70.3	8502	32.5	77.8
25517	9583A	BASE	ORIEL 1	427	61	1346	91.7	106	28.4	72.5	90	100.5	28.3	75.7
25707	9583A	BASE	CE	427	55	5115	74.5	94.2	32.1	70.2	71.3	90.1	30.5	74.5
25961	9583A	BASE	ORIEL 2	482	30	2015	60	83.4	33.4	74.9	70.3	85.2	32.5	77.8
25721	9583A	BASE	ORIEL 2	538	12	3290	55.8	77.8	35	76.2	70.3	85.2	32.5	77.8
25966	9583A	BASE	ORIEL 2	538	9	707	53.9	71.5	29.3	72.7	70.3	85.2	32.5	77.8
25722	9583A	BASE	ORIEL 2	593	5	1308	57.6	76.1	35.7	78.1	70.3	85.2	32.5	77.8
25696	9583A	TW	CE	371	67	6664	81.6	91.3	28.7	64.2	74.7	90.1	25.6	76.5
25697	9583A	WELD	CE	371	67	5543	83.2	92.9	23.3	66.4	74.9	89.6	28.6	66.4
25529	9583A	WELD	CE	427	61	6121	81.2	93.2	28.8	65	74.9	89.6	28.6	66.4
25525	9583A	WELD	CE	482	40	7292	72.3	91.6	27.9	60.2	74.9	89.6	28.6	66.4
25962	9583A	WELD	CE	482	50	2139	82.6	95.8	26.3	63	74.9	89.6	28.6	66.4
25720	9583A	WELD	CE	538	20	3165	50.1	78.4	24.7	62.1	74.9	89.6	28.6	66.4
25524	9583A	WELD	CE	538	20	2349	66.7	82.7	28.5	63.8	74.9	89.6	28.6	66.4

The results of tensile tests at 25C on samples from discontinued creep tests are shown above. The creep tests involved exposures up to 7292h to temperatures ranging from 371 to 593C. The tensile results for samples that had only been heat treated before tensile testing are given for comparison. The ductilities (elongation and reduction of area) are higher for the samples creep tested before tensile testing than those tensile tested without the creep test history. Thus, there is no indication of temper embrittlement in these materials based on these data.

6.3 Tensile specimens were prepared of SA533B and these were aged for 1000h at 900 and 1000F. The specimens were tested and the results are given in the following table. Specimens were tested at room temperature and at the aging temperature. Test data for unaged specimens are also give for comparison. Aging did not have a detectable effect on the ductility parameters (elongation and reduction of area). Thus these results indicate that temper embrittlement is not a problem under these conditions.

TENSILE PROPERTIES OF A533B TRANSVERSE WELD (HT#5795) AGED MATERIAL

HEAT TREATMENT	TEST TEMPERATURE °C	°F	STRAIN RATE 10-4/sec	10-3/min	MODULUS GPa	10+6psi	YIELD STRENGTH MPa	ksi	TENSILE STRENGTH MPa	ksi	TOTAL ELONGATION %	UNIFORM ELONGATION %	REDUCTION OF AREA %
AS RECEIVED	24	75	1.3	8.0	210	30.4	451	65.5	602	87.3	22.40	6.48	66.81
AS RECEIVED	24	75	1.3	8.0	220	31.9	470	68.2	632	91.7	20.51	6.50	62.03
AGED/1K/482°C	24	75	1.3	8.0	202	29.2	480	69.6	641	93.0	20.50	6.48	64.41
AGED/1K/482°C	24	75	1.3	8.0	189	27.4	463	67.2	631	91.5	23.59	5.84	63.07
AGED/1K/538°C	24	75	1.3	8.0	206	29.8	428	62.1	567	82.2	23.95	6.44	66.95
AGED/1K/538°C	24	75	1.3	8.0	219	31.7	438	63.5	595	86.2	22.40	5.99	63.33
AS RECEIVED	482	900	1.3	8.0	176	25.5	360	52.1	430	62.4	25.35	3.03	77.92
AS RECEIVED	482	900	1.3	8.0	171	24.7	362	52.6	435	63.1	23.60	2.71	78.56
AGED/1K/482°C	482	900	1.3	8.0	.158	23.0	380	55.2	455	66.0	21.70	3.04	77.31
AGED/1K/482°C	482	900	1.3	8.0	128	18.6	354	51.3	435	63.1	25.20	3.33	79.59
AS RECEIVED	538	1000	1.3	8.0	135	19.6	338	49.0	358	51.9	26.20	1.61	81.03
AS RECEIVED	538	1000	1.3	8.0	120	17.4	330	47.8	365	53.0	25.00	1.61	80.30
AGED/1K/538°C	538	1000	1.3	8.0	134	19.5	305	44.2	334	48.5	27.00	1.56	83.58
AGED/1K/538°C	538	1000	1.3	8.0	148	21.4	304	44.2	330	47.9	25.60	1.66	83.10

6.4 Impact specimens were prepared of SA533B and these were aged for 1000h at 900 and 1000F. These specimens were tested and the results are presented below. The results do not indicate that temper embrittlement occurs under these conditions.

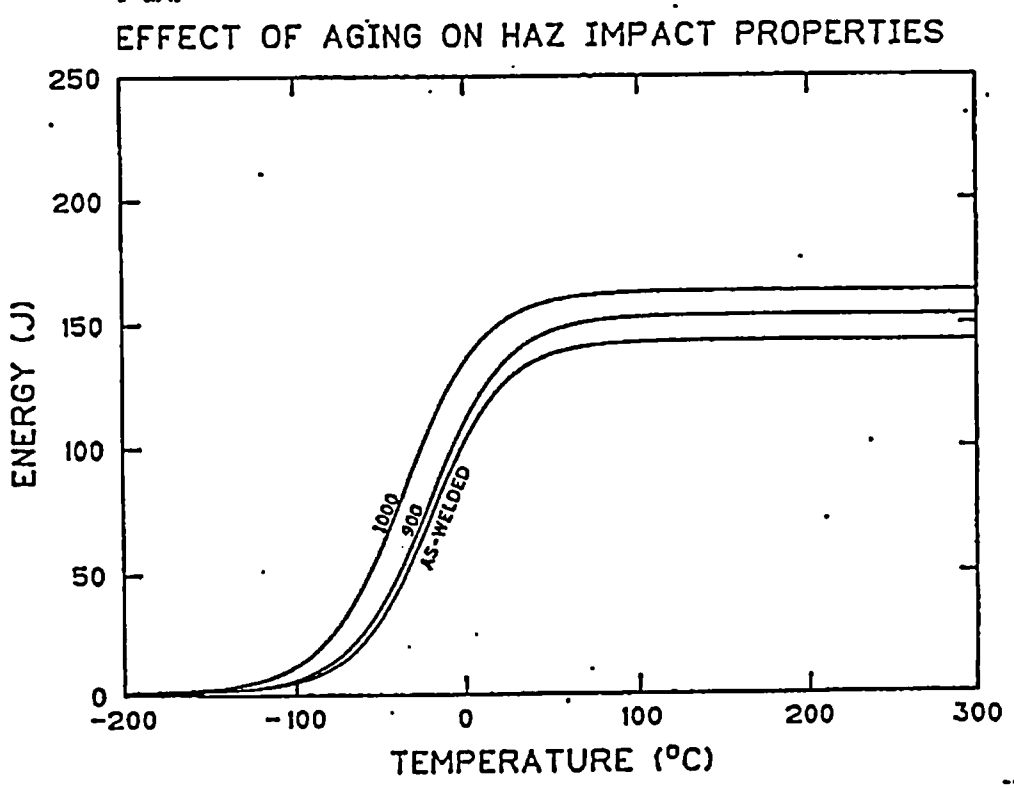

Table 1. Charpy impact data

Condition	Transition temperature (°C)			Upper-shelf energy (J)
	T_0	$T_{40.7}$	$T_{67.8}$	
As-welded	-21	-42	-24	143
900°F for 1000 h	-22	-46	-28	154
1000°F for 1000 h	-37	-64	-46	163

7.1 COMPARATIVE PROPERTIES OF BASE METAL AND WELDMENTS FOR SA533B.

Numerous tests were performed on base metal, weld metal, and transverse weld samples. The data presented in this submission are almost entirely for the base metal. The next two figures compare the yield and ultimate tensile strengths of the three types of material. Base metal has the lowest strength, so design values based on base metal properties should be conservative.

The third plot shows a comparison of the strengths of these same materials in creep. The differences in strength are smaller in creep than in short-term tensile tests, but the base metal is still weaker. Thus the use of base metal properties should be conservative.

7.1 7.1

The numbers on these plots refer to the lot designations defined in table 1.3.

ORNL-DWG 89-18611

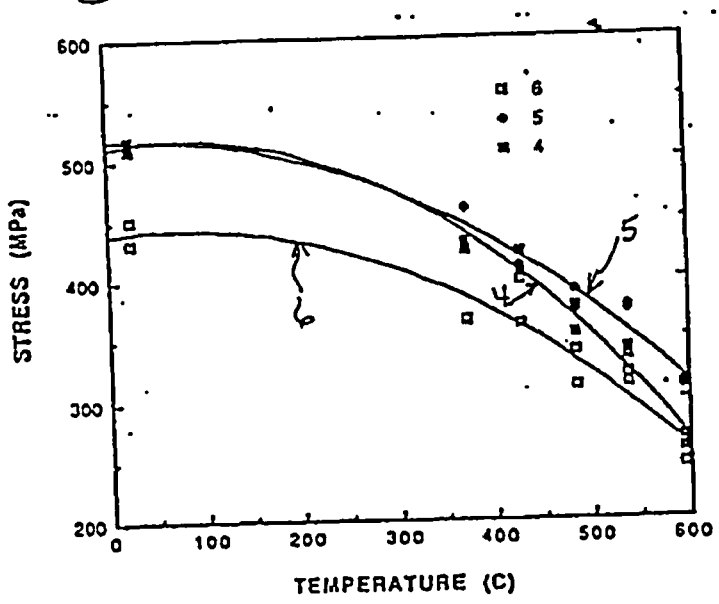

Fig. 4. Yield strength for lots of base metal, transverse welds, and weld metal having the lowest strength.

ORNL-DWG 89-186

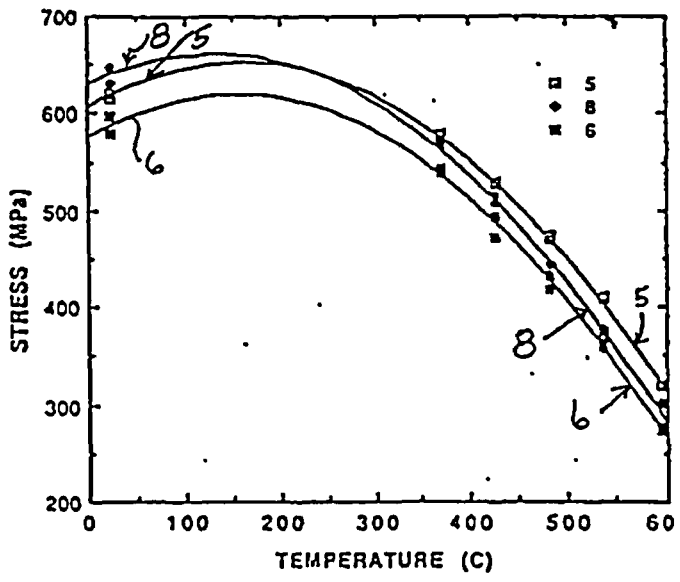

Fig. 12. Tensile strength for lots c base metal, transverse welds, and weld metal having the lowest strength.

ORNL-DWG 89-18639

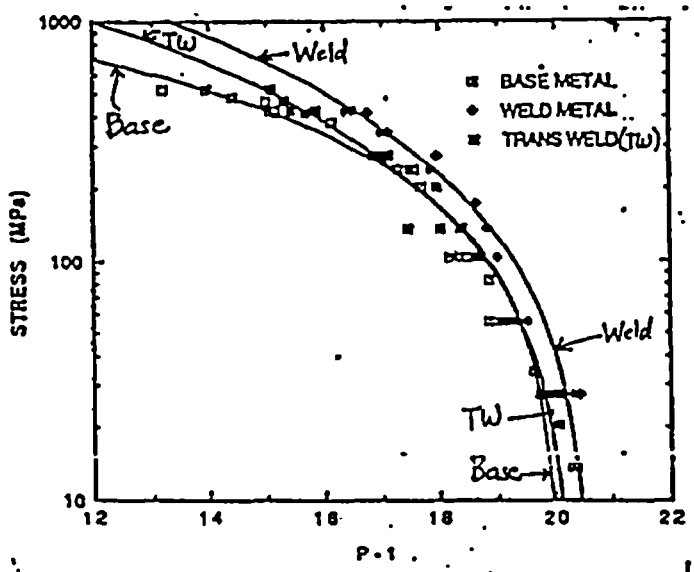

7.2 Comparison of Properties of SA533 and SA508.

SA533B AND SA508, CL3 HAVE SIMILAR CHEMICAL REQUIREMENTS(a)

ELEMENT	CONTENT (%)	
	SA533B	SA508, CL3
carbon	0.25 max	0.25 max
manganese	1.07-1.62	1.20-1.50
phosphorus	0.015 max	0.015 max
sulfur	0.018 max	0.018 max
silicon	0.13-0.45	0.15-0.40
molybdenum	0.41-0.64	0.45-0.60
nickel	0.37-0.73	0.40-1.00
copper	0.12 max	0.10 max
vanadium	0.06 max	0.05 max

(a) ASME, Section II, standard chemical requirements plus special reactor beltline requirements for Cu, P, S, and V.

7.2 Comparison of Properties of SA533 and SA508.

SA533B AND SA508, CL3 HAVE SIMILAR MECHANICAL PROPERTY REQUIREMENTS

MATERIAL	YIELD STRENGTH ksi	UTS ksi	ELONGATION %	REDUCTION OF AREA %
533	50 min	80-100	18 min	
508	50 min	80-105	18 min	38 min

7.2 Comparison of Properties of SA533 and SA508.

COMPARISON OF SA533 AND SA508 TENSILE PROPERTIES AT A STRAIN RATE OF 0.0016/min

	SA533-AVG 3 HEATS				SA508-ONE HEAT			
TEMPERATURE	YIELD STRENGTH	UTS	ELONGATION	RED OF AREA	YIELD STRENGTH	UTS	ELONGATION	RED OF AREA
F	ksi	ksi	%	%	ksi	ksi	%	%
75	69.4	88.4	29.0	69.0	66.9	91.4	31.3	64.7
400	54.0	79.5	28.2	66.5	69.3	94.7	20.6	53.0
700	59.9	81.0	28.3	74.0	59.6	90.1	24.4	67.7
800	54.8	71.4	30.1	77.2	56.3	81.2	31.0	71.6
900	50.8	60.1	38.4	80.3	56.0	70.9	34.0	78.8
1000	44.4	48.4	45.0	80.8	49.4	55.3	53.3	76.8
1100	30.3	35.0	55.0	75.2	34.9	38.2	54.0	58.5

The ultimate tensile strength controls S_{mt} from room temperature through 900F. Since the UTS of SA508 equals or exceeds that of SA533, S_{mt} for SA533 and SA508 should be the same at temperatures from 75 through 900F.

7.2 Comparison of Properties of SA533 and SA508.

COMPARISON OF CREEP PROPERTIES OF SA533 AND SA508

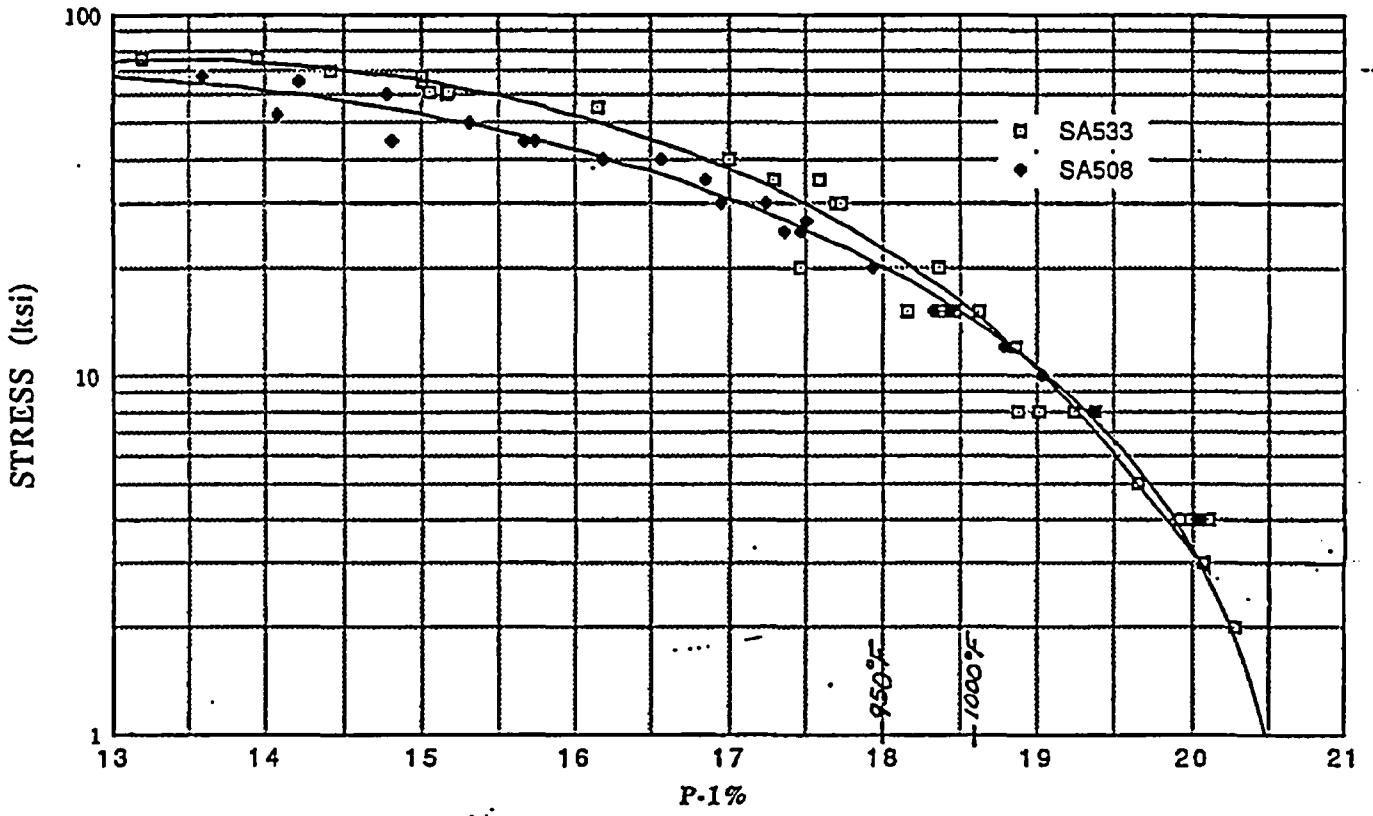

P-1% is a modified Larson-Miller parameter defined as equal to

K/1000(20+ log t)

where: K=temperature in degrees Kelvin,
t= time to 1% strain in hours.

The creep strength of SA508 is slightly lower than that of SA533 at the left side of the above graph. However, at the right side(longer times and higher temperatures) the properties of the two materials converge. S_{mt} is controlled by creep only at 950 and 1000F, and 1000h at these two temperatures are marked on the above plot. In this range the properties are about the same for the two materials, so the values of S_{mt} based on creep would not be significantly different.

7.3 Guide used in preparing this document.

Unless stated otherwise, the correlation methods described in the following document were used in preparing this data package.

7.3

From Back-up Document To Code Case 1592 (N-47) - 1976 -

APPENDIX A
PROCEDURES EMPLOYED TO ESTABLISH THE BASIC TIME AND TEMPERATURE STRESS INTENSITIES AND ISOCHRONOUS STRESS-STRAIN CURVES[1]

A.1 MAXIMUM ALLOWABLE VALUE OF GENERAL PRIMARY-MEMBRANE STRESS INTENSITY FOR DESIGN CONDITIONS

The symbol S_o is used for this value. The S_o values are identical to the values for S given in Section VIII, Division 1 of the Code.

A.2 TIME-INDEPENDENT DESIGN STRESS INTENSITY

The symbol S_m is used for this value. These values are based on tensile and yield strengths of the material. The criteria employed are defined as follows:

(a) The allowable stress intensity value, S_m, for ferritic steels and nonferrous metals and alloys, except those covered in paragraph (b) below, is the least of the following four values:

(1) one-third of the specified minimum tensile strength at room temperature

(2) one-third of the short-term tensile strength at temperature (as defined in A.2.1 in this Appendix).

The ratio of UTS_T/UTS_{RT}, for austenitic stainless steel, is found in ASTM DS5-S2.

(3) two-thirds of the specified minimum yield strength at room temperature

(4) two-thirds of the short-term 0.2% offset yield strength at temperature (defined as the ratio of yield strength at temperature divided by the yield strength at room temperature, multiplied by the minimum specified room temperature yield strength).

The ratio of YS_T/YS_{RT}, for austenitic stainless steel, is found in ASTM DS-S2. The strength is determined at a strain rate of 0.0005 min.[1]

(b) The allowable stress intensity value, S_m, for austenitic steels, nickel-chromium-iron and nickel-iron-chromium alloys is the lowest of the following four values:

(1) one-third of the specified minimum tensile strength at room temperature

(2) one-third of the tensile strength at the operating temperature

(3) two-thirds of the specified minimum yield strength at room temperature

(4) 90% of the yield strength at the operating temperature

A.2.1 YIELD AND TENSILE STRENGTH

The procedures for establishing yield and ultimate strengths are discussed below:

The yield and tensile strength data available for a particular material grade are normalized by ratioing the elevated temperature strength of individual lots to the room temperature strength of the same lots, and then all sets of such ratios representing a

[1] Not applicable to bolting materials.

particular grade are evaluated by the method of least squares to establish the curve of best fit for the data. The resulting *strength-ratio trend curve* is considered to represent the typical or characteristic variation of yield or tensile strength with temperature. Using such a ratio trend curve, it becomes possible to compute strength trend curves for any particular room temperature strength level of interest within the limits encompassed by the original data.

Since the design stress intensity criteria include fractions of the specified yield and tensile strengths, it is necessary to factor the ratio trend curves against the specified minimum yield and tensile strengths to define what may be termed minimum position yield and tensile strength curves. At temperatures above room temperature, the property *yield strength at temperature* is taken, for purposes of the criteria, to be this minimum position value. However, the property *tensile strength at temperature* is taken as the smaller of:

(a) specified minimum tensile strength at room temperature; or
(b) a value 10% greater than the minimum position value cited above.

A.3 TIME-DEPENDENT DESIGN STRESS INTENSITY[2]

The symbol S_t is used for the basic time and temperature dependent allowable stress intensity for load-controlled stresses. S_t values are the least of each of the three quantities:

(a) two-thirds of the minimum stress to cause rupture in time t;
(b) 80% of the minimum stress to cause the onset of tertiary creep in time t; and
(c) the minimum stress to produce one percent total strain in time t.

A.3.1 MINIMUM STRESS-TO-CAUSE-RUPTURE IN TIME t

The basic data and a description of the rupture strength evaluation procedures employed for several of the materials included in Case 1592 (i.e., Types 304 and 316 Stainless Steel) may be found in Metal Property Council data evaluations [Smith (17) and Simmons and Van Echo (18)].

Two principal procedures are employed in evaluating the dependence of the stress-to-rupture upon time and temperature. A choice between the results, based on engineering judgment, is then made.

In the first procedure, the isothermal relation between stress and time for rupture of individual lots is interpolated or extrapolated, as required, to identify the stress-to-cause-rupture in 100, 1000, 10,000, etc., hr. Plotting on log-log coordinates tends to linearize the variation, and thereby facilitate extrapolation, particularly at lower temperatures. At higher temperatures, the variation tends to curvilinearity at longer times, and extrapolation involves greater risk. The results of such interpolations or extrapolations for individual lots, as they vary with temperature, are then evaluated by the method of least squares to define an average rupture strength-temperature trend curve. A trend curve for minimum rupture strength is derived from the mean trend curve by subtracting 1.65 multiples of the standard deviation of the sample. If certain implicit assumptions hold (e.g., that the data are normally distributed, or that the average is without error), this minimum trend curve defines a lower boundary for 95% of the data. Inspection of the data plots has always shown that this is approximately true.

[2] Based on data determined from tests performed on air.

7.3 7.3

The second evaluation procedure that has been employed is an indirect one, involving one or another time-temperature parameter. One of the simplest of these, widely used, is Larson and Miller's

$$P = T(C + \log t) = F(S)$$

where T is the temperature in degrees Rankin, t is the time for rupture in hours; C is a material constant, and $F(S)$ denotes that the parameter depends upon stress. Ordinarily, the available data are not adequate to permit evaluation of individual lots by the parameter procedure, as would be desirable; instead, the total data population must be treated as a common population on a universalized basis, assuming the constant C to remain invariant from lot to lot within the data population. Accordingly, the scatter band for the stress-parameter variation is evaluated by the method of least squares to determine an average curve of best fit, from which average values of rupture strength as dependent upon temperature can be derived. A minimum curve is developed, as in the previously described procedure, by subtracting 1.65 multiples of the standard deviation of the sample from the average curve.

A.3.2 MINIMUM STRESS-TO-INITIATE-TERTIARY-CREEP IN TIME t

For the ferrous alloys included in Case 1592, Leyda and Rowe (19) had reported that the time to initiate tertiary creep is a fixed fraction of the time for rupture for a given material at a specific temperature. Thus, for 2¼ Cr-1 Mo and Types 304 and 316, the minimum stress-to-initiate-tertiary-creep was computed from the minimum-stress-to-rupture data. For the high-nickel alloys, tertiary creep information was developed by examination of available creep curves. In all instances, the initiation of tertiary creep was assessed visually. Extrapolations to lower temperatures were made by time-temperature parameter methods exactly analogous to those described for rupture strength, except that the time for tertiary creep to begin became the measured quantity.

A.3.3 MINIMUM STRESS TO CAUSE 1% TOTAL STRAIN IN TIME t

In common with the criterion for stress to initiate tertiary creep, the criterion on minimum stress for 1% total strain is new to the ASME Code. For purposes of Section I and Section VIII, Division 1, creep strength has for many years been evaluated in terms of the stress causing a secondary creep rate of 0.01% per 1000 hr. In the new criterion, stress to cause 1% total strain can be evaluated in an exactly analogous manner as the stress to cause rupture or to initiate tertiary creep—the dependence upon stress tends to parallel that of rupture time—or it can be derived directly from the isochronous stress-strain curves. Both approaches have been employed in developing the material for Case 1592.

A.4 ISOCHRONOUS STRESS-STRAIN CURVES

For relatively short times, isochronous stress-strain curves may be derived by taking constant time sections through a family of creep curves, such as those of Fig. 2. However, this approach to their derivation is not generally practicable (unless forming only a part of a multi-approach procedure) since the time scale of interest extends beyond the feasible limit of experimental testing. Extrapolative procedures are required for the longer test times and for strains below 1%. For generating the isochronous stress-strain curves in Case 1592, two procedures have been employed. In one of these, the curves are developed by performing evaluations exactly analogous to those described for developing information on the stress to reduce 1% strain, except that other specific strains encompassing the range of interest are also evaluated and the various parts assembled in plots of stress versus strain for different fixed times.

7.3

7.-

In a second procedure, the strain has been expressed as an analytical function of time according to the general form:

$$\epsilon = \epsilon_{loading} + \epsilon_{transient} + \epsilon_{steady\ state}$$

where each of the parts is a function of stress and temperature. The individual parameters of the equation are then evaluated from the experimental results generated in conventional creep tests.

More complete descriptions of these procedures may be found in *The Generation of Isochronous Stress-Strain Curves*, ASME, 1972(4).

7.4 Direction of questions.

QUESTIONS

QUESTIONS ON THE DATA PACKAGE SHOULD BE DIRECTED TO:
H. E. MCCOY, 615-574-5115.
OR
CHRIS HOFFMAN, 203-285-4929
OR
C.R BRINKMAN, 615-574-5106

8. ASME Publication, "Criteria for Design of Elevated Temperature Class 1 Components in Section III, Division 1, of the ASME Boiler and Pressure Vessel Code," May 1976.

Criteria for Design of Elevated Temperature Class 1 Components in Section III, Division 1, of the ASME Boiler and Pressure Vessel Code

May 1976

The American Society of Mechanical Engineers
345 East 47 Street
New York, N.Y. 10017

Copyright © 1976
The American Society of Mechanical Engineers
All Rights Reserved

No part of this document may be reproduced in any form, in an electronic retrieval system, or otherwise, without prior written permission from the publisher.

Library of Congress Catalog Card Number: 75-28980

Printed in the United States of America

FOREWORD

Experience in performing stress analysis of nuclear power plant components in accordance with the ASME Code Cases for elevated temperature service has indicated a need for a document to provide the background criteria for the rules of these Code Cases. Accordingly, this document was prepared.

To assure technical accuracy of this document, numerous reviews of the document material were performed during the period of preparation. The design criteria described herein were developed over a period of several years. It is not to be expected that this document will answer all the questions which will be asked, but it is hoped that it will provide a starting point.

Contents

1.0 Introduction 7
2.0 Elevated Temperature Material Behavior 8
3.0 Structural Failure Modes Considered 10
4.0 Stress and Strain Categories, and Controlled Quantities 13
5.0 Design Rules for Load-Controlled Stresses in Structures other than Bolts 15
- 5.1 Criteria for Design Conditions
- 5.2 Criteria for Operating Conditions—Introduction
- 5.3 General Primary Membrane Stress Intensity Limits for Operating Conditions
- 5.4 Allowable Stress Intensities for Loading Involving Bending
- 5.5 Use-Fraction Summations

6.0 Design Rules and Limits on Strain for Structural Integrity 22
- 6.1 Reasons for and Objectives of Strain Limits
- 6.2 Limits on Cumulative Inelastic Strain for Structural Integrity
- 6.3 Phenomena of Plastic and Creep Ratcheting
- 6.4 Methods of Satisfying Strain Limits Using Elastic Analyses

7.0 Creep-Fatigue 35
- 7.1 Correlation and Evaluation Methods
- 7.2 Derivation of the Creep-Fatigue Interaction Rules
- 7.3 Creep and Fatigue Design Curves
- 7.4 Mean Stress and Multiaxial Effects
- 7.5 Rotating Principal Strains
- 7.6 Rules and Limits for Use with Inelastic Analysis
- 7.7 Rules and Limits for Use with Elastic Analysis

8.0 Design Rules and Limits for Buckling and Instability 58
- 8.1 Elevated Temperature Design Factors
- 8.2 Dependence on Post-Buckling Behavior
- 8.3 Time Design Factor
- 8.4 Effect of Initial Imperfections
- 8.5 Strain-Controlled Buckling

9.0 Special Limits and Consideration 62
- 9.1 Requirements for Welds
- 9.2 Rules and Limits for Bolts
- 9.3 Elastic Follow-up
- 9.4 Load Environment Histograms

10.0 References 73
Appendix A 79
List of Figures 83

1.0 INTRODUCTION

The purpose of this publication is to set forth the criteria, reasoning, and supporting data for existing ASME Boiler and Pressure Vessel Code Section III, Division 1, rules for design of Class 1 pressure boundaries of components intended for elevated temperature service. The term *elevated temperature* refers to temperatures that exceed those for which allowable stress values are given in Section III.

The key consideration that sets these high temperature rules apart from the Section III, Subsection NB rules is creep effects. Unlike Subsection NB design rules which primarily guard against time-independent failure modes, the elevated temperature rules are applicable for service conditions where creep effects are significant.

These elevated temperature design rules for Section III have been under development for a number of years, but the last half-decade has been the period of most growth. The latest rules have been provided through Case 1331 (1)[1] and its successor, Case 1592 (2). It is intended that this publication explain the basis of the rules in Case 1592 and aid in the application of the rules.

In nonnuclear applications, the design of pressure boundary components for elevated temperature service dates back forty years. Over those years, vessels designed by the rules of Section I (Power Boilers) and Section VIII, Division 1 (Pressure Vessels) of the ASME Code have established a record of successful elevated temperature operation. This success is due to a combination of factors: (1) the ease of inservice inspection for such vessels has made it possible to detect incipient failure conditions before gross failures could occur, (2) the variety of operating and environmental conditions have been successfully addressed outside the Code rules by individual engineering effort, and (3) the Code design rules have required extra wall thickness for service where creep phenomena are significant.

In Section I and Section VIII, Division 1, the design rules employ allowable stress criteria which utilize creep rate and stress-rupture properties in addition to short-term tensile strength properties. However, these Sections do not have mandatory requirements for a detailed stress analysis but set the wall thickness necessary to keep the basic hoop stress below the tabulated allowable stress, and they rely on the design rules for details and the design factor to hold secondary bending and high localized stresses at a safe level consistent with experience. Even though these Sections employ criteria based on the average stress to provide a creep rate of 0.01% per 1000 hr and the average and minimum stress to produce rupture in 10^5 hr, it is not to be inferred that 10^5 hr (or any definite interval) is the intended design life for such construction. The foreword to the ASME Code states that the objective of its rules "is to afford reasonably certain protection of life and property and to provide a margin for deterioration in service so as to give a reasonably long safe period of usefulness." Neither Section I or Section VIII, Division 1, have mandatory requirements for a cyclic fatigue analysis. The Power Piping Code (ANSI B31.1), which extends into elevated temperature application, gives allowable values for the thermal stresses which are produced by expansion of piping systems and varies the allowable stresses with the number of expected cycles. However, a complete evaluation of localized and combined peak stresses and and associated fatigue life assessment is not required.

* ANSI B31.1

As discussed in the ASME Publication, *Criteria of the ASME Boiler and Pressure Vessel Code for Design by Analysis* (3), the Code Committee recognized that additional design considerations and rules were desired for nuclear components. These components would be exposed to severe service conditions (e.g., highly cyclic loadings, recurring severe thermal shocks) where superior reliability was required to offset potentially serious consequences of failure. These needs led to the preparation of the design rules in Section III, Division 1. The specialized service of nuclear components also made it feasible to expand the Code rules to cover all service conditions, whereas the diversity of service for Section VIII vessels made such a choice unwise.

[1] All references appearing in the bibliography are indicated by numbers in parentheses.

Section III rules are intended to prevent three different types of failure which are as follows:

(1) Bursting, gross distortion, and elastic instability (buckling) from a single application of pressure are prevented by the limits placed on primary stresses.
(2) Progressive distortion is prevented by the limits placed on primary-plus-secondary stresses. These limits generally assure shakedown to elastic action after a few repetitions of the loading.
(3) Fatigue failure is prevented by the limits placed on the peak stresses.

Rules to account for creep, stress-rupture, or other time-independent failure modes were not included in Section III.

After rules in Section III were initially developed for low-temperature design, there was an effort to extend the rules to elevated temperature design. By 1963, the first version of Case 1331 was approved. Subsequent versions of Case 1331 appeared, but it was not until 1971 and Case 1331-5 that extensive rules and limits were given to address the additional failure modes associated with elevated temperature operation. Additions and improvements led to the -6, -7, and -8 versions of Case 1331. With the further preparation of rules for use in elevated temperature construction, the Code Case for elevated temperature design was changed to the present Case 1592.

This publication first provides a brief discussion of metal behavior when operated at elevated temperatures (i.e., in the creep range) under sustained and cyclic loadings. Then the relevant structural failure modes are described, and an explanation of the associated design rules and limits is provided. Special limits and considerations relative to the design procedure are also presented. Throughout this publication, comparisons of elevated temperature and low temperature design rules are made.

2.0 ELEVATED TEMPERATURE MATERIAL BEHAVIOR

When discussing elevated temperature material behavior, it is common to distinguish between elevated temperature and low temperature behavior by whether or not significant creep effects are present. As an introduction to the time-dependent effects associated with creep, results from experiments using uniaxial test specimens will be employed.

Consider a uniaxial tensile specimen subjected to a load-induced stress level at a given test temperature. As shown in Fig. 1 (a), if the temperature is low enough so that no significant creep occurs, the stress and strain both achieve their maximum value at a time t_0 and remain constant at the maximum values for as long as the load is maintained. There are no time-dependent stress or strain changes after time t_0, and the stress and strain magnitudes are related to each other independent of time. However, if the test temperature is high enough for creep effects to be significant, the strain will increase with time after load application as depicted in Fig. 1(b), and may ultimately lead to rupture of the specimen. If, on the other hand, the elevated temperature uniaxial test is one where the specimen is initially strained a fixed amount and then held, the stress-strain history would be similar to that shown in Fig. 1(c). The reduction of stress under the constant imposed total strain of Fig. 1(c) is usually referred to as *relaxation due to creep* effects. In both of the above elevated temperature tests, either stress or strain is time and temperature dependent. Also, the amount of creep strain or relaxation is stress and strain level dependent. Figure 2, sketches (a) and (b) depict the effects of initial stress level on typical elevated temperature creep and relaxation behavior. Elevated temperature material behavior is a function of time, temperature, and stress level, and each material has its own creep characteristics and stress-temperature-time domain where creep is significant.

Standard material specimen creep tests commonly used for characterizing basic creep properties are constant-temperature, constant-load tests of uniaxial tensile specimens. The terms commonly used to describe the stages of these creep tests are shown in Fig. 3.

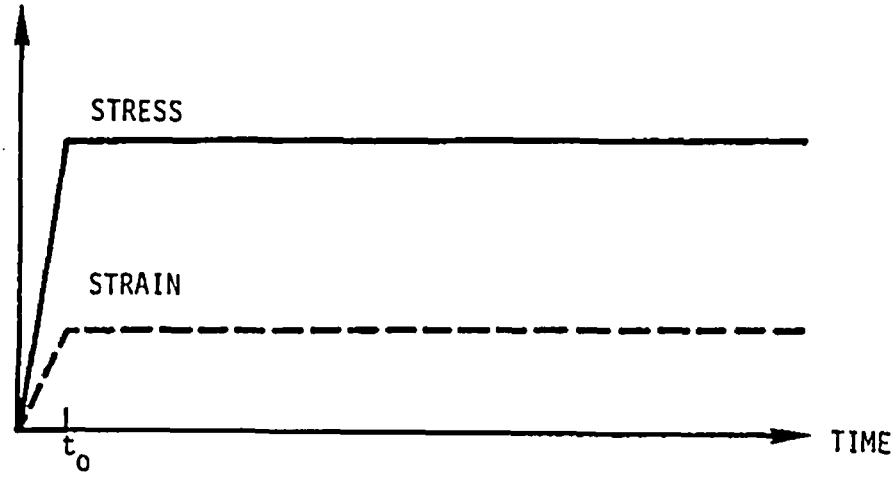

Fig. 1(a) HISTORIES FROM A LOADING AT LOW TEMPERATURE

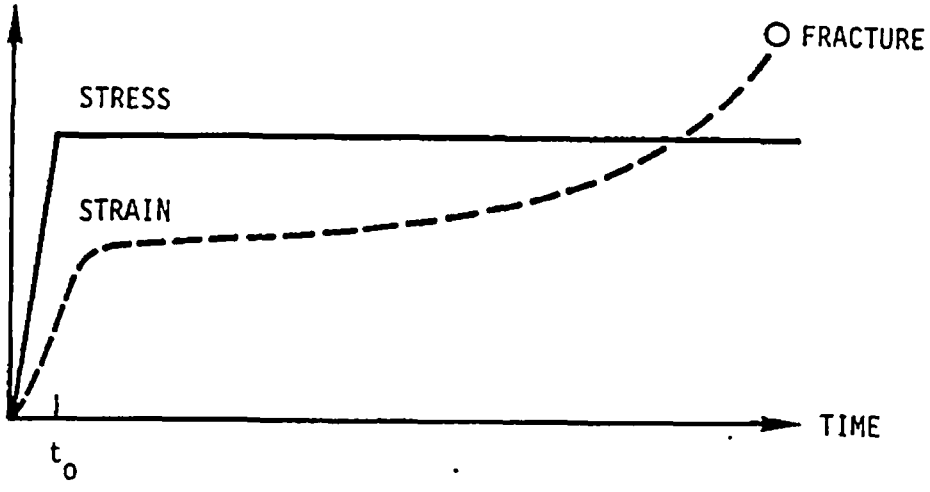

Fig. 1(b) HISTORIES FROM A LOAD-CONTROLLED LOADING AT ELEVATED TEMPERATURE

Figure 4 shows the typical manner of presenting stress-rupture data. If one were to cross plot the value of total strain (elastic-plus-plastic-plus-creep) as a function of stress at a given constant end-of-test time, a curve commonly referred to as an *Isochronous stress-strain curve* would result. Typical isochronous stress-strain curves are given in Fig. 5. Isochronous stress-strain curves are very convenient for presenting basic material creep data. The isochronous stress-strain curves for all pressure boundary materials allowed in Case 1592 are found in its Appendix T. General descriptions of the generation of the isochronous stress-strain curves are given in Appendix A of this document. More complete descriptions of these procedures may be found in the ASME publication, *The Generation of Isochronous Stress-Strain Curves* (4).

So far, the material behavior in the creep regime has been discussed in terms of time-dependent deformation and fracture characteristics for sustained load conditions. When cyclic load conditions exist, fracture and incremental cumulative deformation (ratcheting) can be significantly

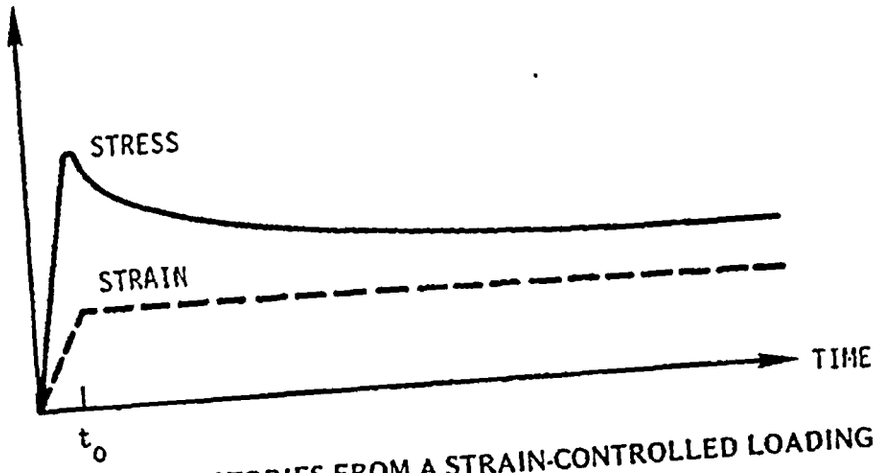

Fig. 1(c) HISTORIES FROM A STRAIN-CONTROLLED LOADING AT ELEVATED TEMPERATURE

accelerated by elevated temperature effects. For example, Fig. 6 [from Weeks (5)] shows typical reductions in strain-controlled fatigue life as a function of hold times. Moreover, many variables associated with the elevated temperature operation affect the material cyclic life. These variables include: (a) the temperature; (b) the loading level (load wave-form, frequency, strain rate, hold time, and total exposure time); (c) thermally activated metallurgical transformations; (d) the environmentally induced factors such as irradiation, oxidation, erosion, and corrosion; and (e) the material form and its fabrication process with the degree of cold work.

3.0 STRUCTURAL FAILURE MODES CONSIDERED

The structural failure modes considered are the following:

(1) ductile rupture from short-term loadings
(2) creep rupture from long-term loadings
(3) creep-fatigue failure
(4) gross distortion due to incremental collapse and ratcheting
(5) loss of function due to excessive deformation
(6) buckling due to short-term loadings
(7) creep buckling due to long-term loadings

In determining what rules were appropriate to elevated temperature design, the first step was to define the failure modes that the rules should preclude. The failure modes above were developed by adding to the Section III failure modes the (2), (3), and (7) modes.

Up to this point, discussion of failure modes has centered on the failure as related to the applied loading. As in Section III, the elevated temperature Code Case provides guidance for all possible load applications and loading sequences. However, the Owner and the Designer must recognize that environmental effects are a key area not specifically addressed by the Code Case rules. All the stress-rupture and creep-fatigue data used in developing the Code Case limits were taken from tests performed in an air environment.

Also, subtle changes in mechanical properties brought about by elevated temperature, aging, or by synergistic effects resulting from the combined influence of aging, recovery, and environment-related mechanisms are not necessarily accounted for by the Code. The reader is referred to references (6) through (16).

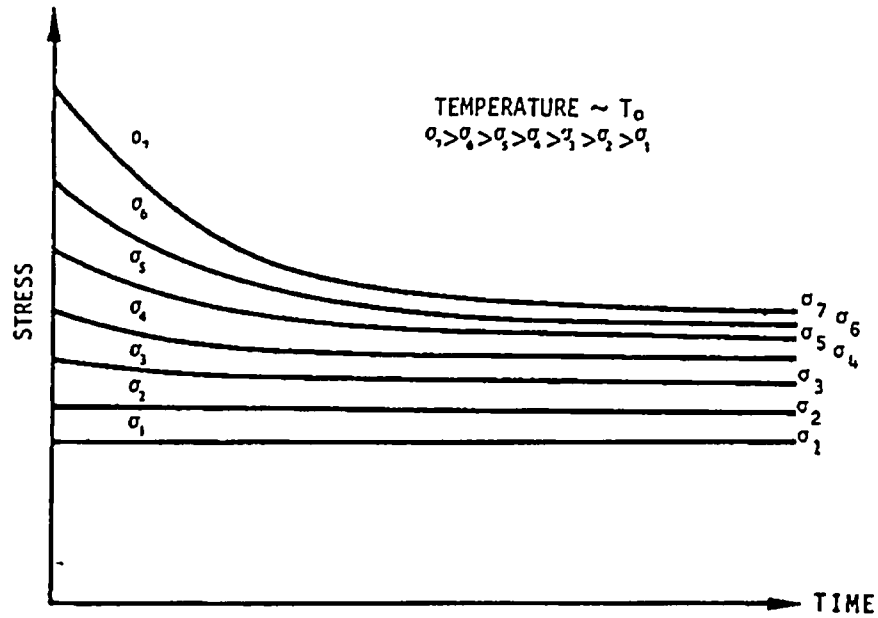

(a) STRESS RELAXATION CURVES AT FIXED TEMPERATURE

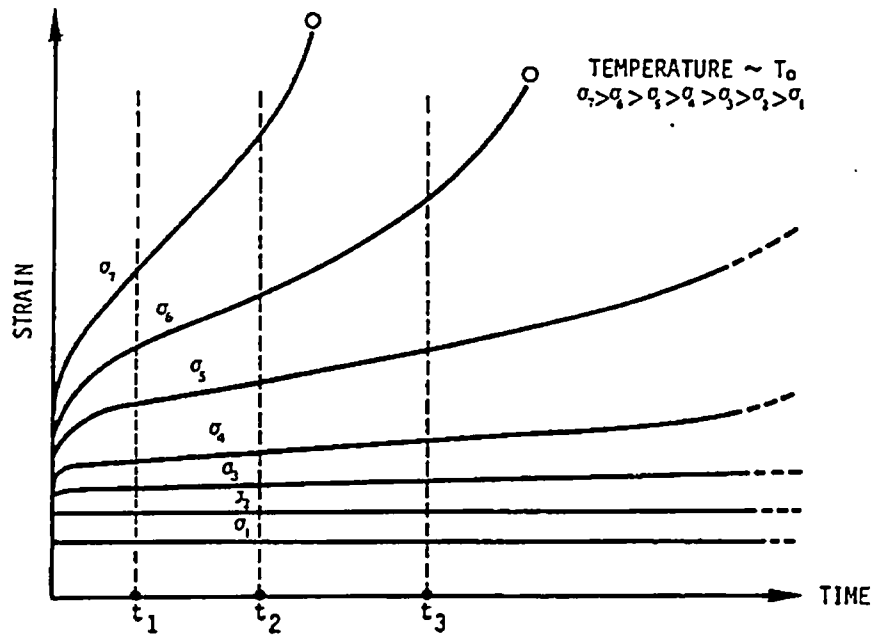

(b) CREEP CURVES AT FIXED TEMPERATURE

Fig. 2 EFFECT OF STRESS LEVEL ON ELEVATED TEMPERATURE BEHAVIOR

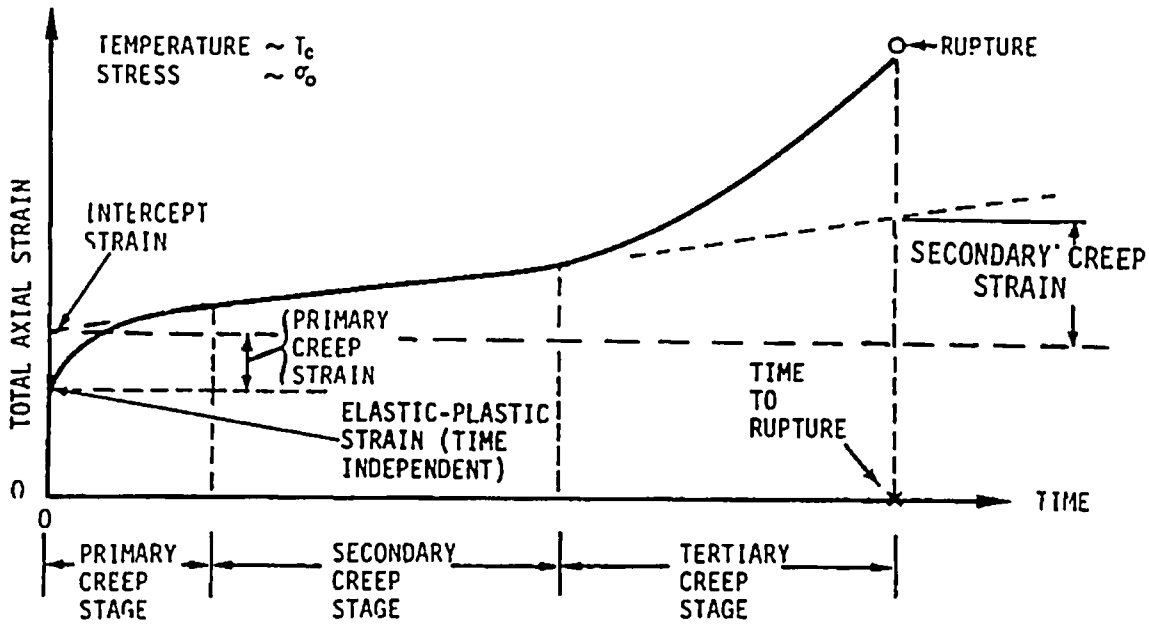

STRAIN HISTORY AND NOMENCLATURE

Fig. 3 DATA FROM THE STANDARD CREEP TEST

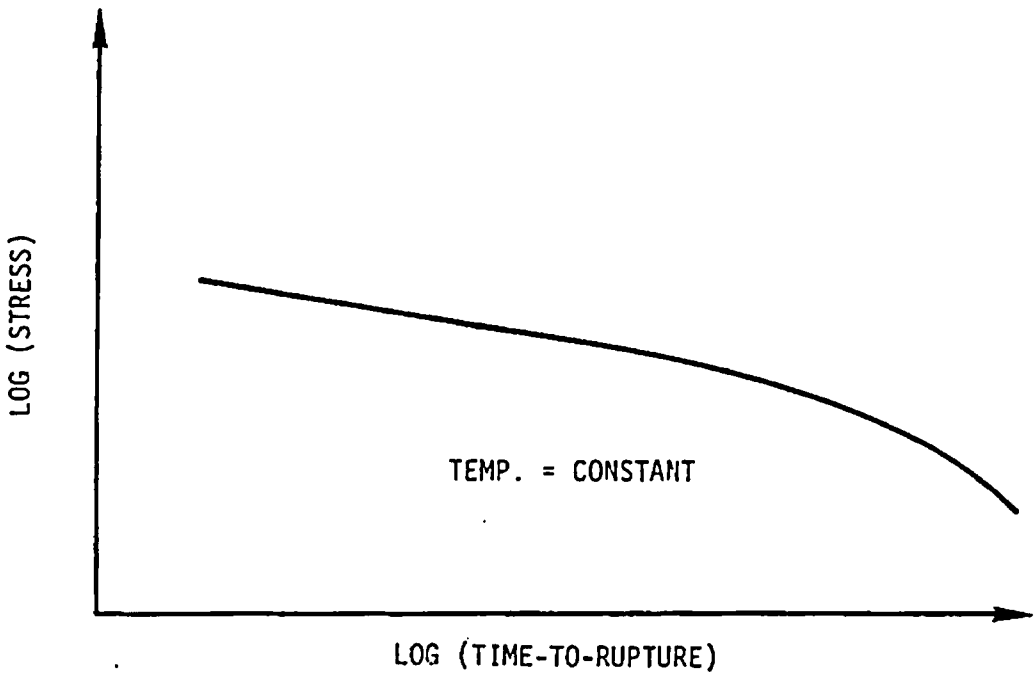

Fig. 4 STRESS-RUPTURE DATA FROM CONSTANT TEMPERATURE CREEP TESTS

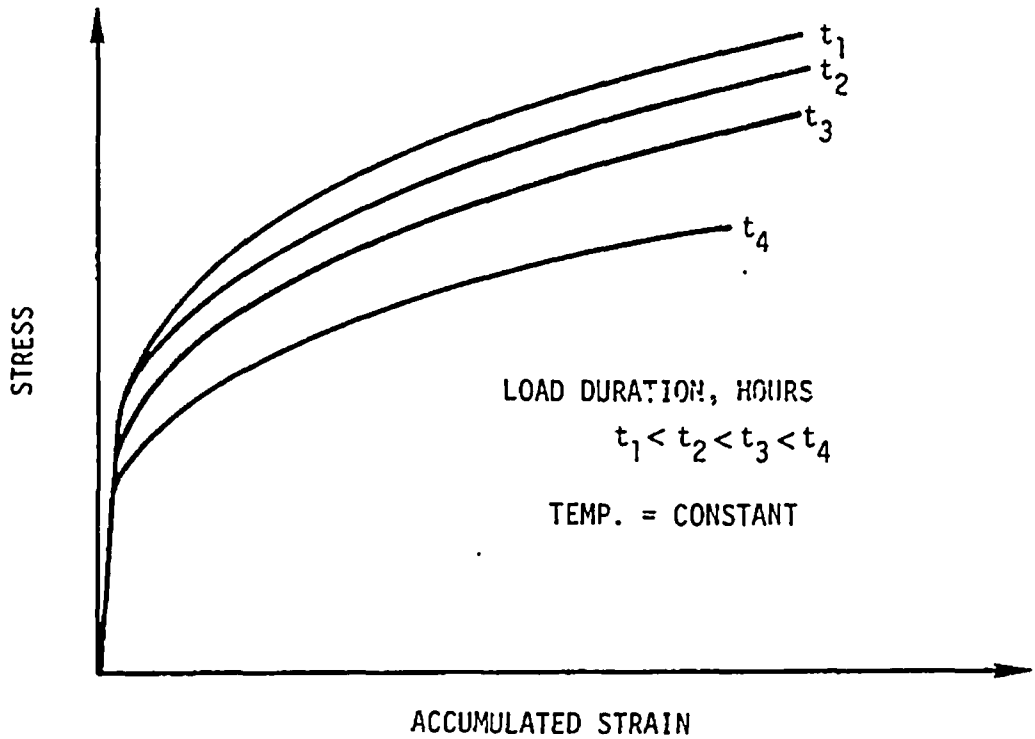

Fig. 5 ISOCHRONOUS STRESS-STRAIN CURVES FROM CREEP TESTS AT CONSTANT TEMPERATURE

Another design consideration area not controlled by Case 1592 is the area relating to functional performance. This area is left to the Designer to assure adequate performance as required by the Owner.

4.0 STRESS AND STRAIN CATEGORIES, AND CONTROLLED QUANTITIES

The elevated temperature rules follow the approach of Section III, NB-3000 in categorizing different types of stress and strain and applying different limits to each category. The categories and symbols used are generally the same as in Section III with limits related to primary, secondary, and peak stresses and strains.

As the structural behavior at elevated temperatures can be significantly different than at low temperatures, it was recognized that different grouping of the stress and strain categories for purpose of applying limits was needed. Thus, placing limits on quantities related to the type of expected structural behavior under loading was adopted. The two basic types of controlled quantities are:

(a) load-controlled quantities;
(b) deformation-controlled quantities.

The load-controlled quantities are stress intensities which result from equilibrium with applied loads during plant operation. As in Section III, the stress intensity is defined as twice the maximum shear stress and equal to the largest algebraic difference between any two of the three principal stresses. The load-controlled quantities are determined using linearly elastic material models. The familiar primary stress intensities are load-controlled quantities.

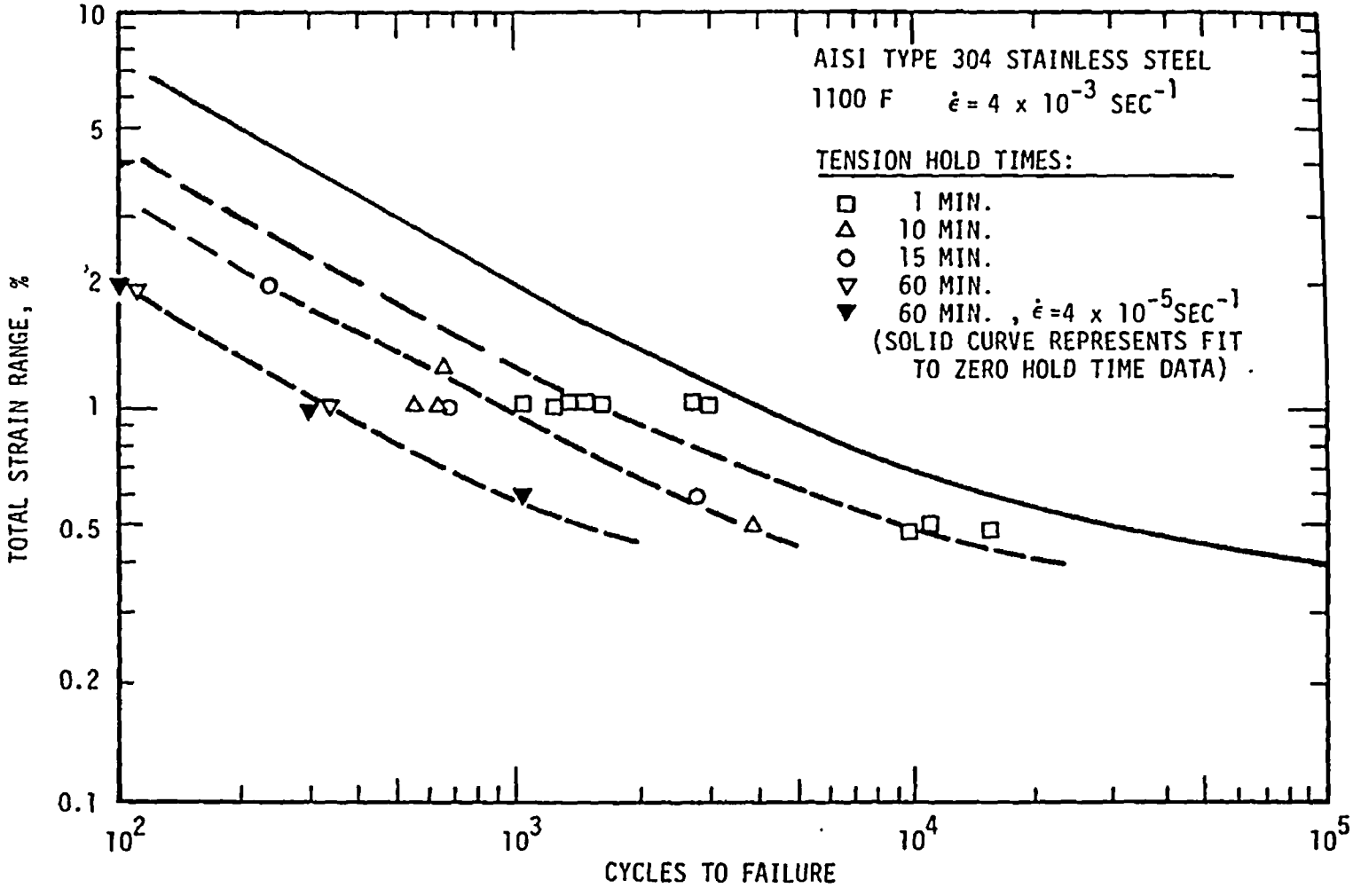

Fig. 6 EFFECT OF TENSION HOLD TIME ON THE FATIGUE LIFE OF AISI TYPE 304 STAINLESS STEEL AT 1000 F IN AIR

Deformation-controlled quantities are stresses, strains, and deformations which result from load deflection and strain compatibility. These quantities may vary with both time and the applied loads, and creep effects may be a major time-dependent influence. Thus, accurate analytical evaluation of deformation-controlled quantities usually requires inelastic stress analysis when creep effects are significant. The stress intensities usually categorized as secondary and peak in NB-3000 are usually considered to be deformation-controlled quantities. An exception, however, is made in regard to the expansion stress, P_e, defined in NB-3222.3. Such stress must be treated as either primary or secondary. Thermal expansion net axial and net shear force on the structural cross section are categorized as primary, P_m or P_L, load-controlled quantities. Thermal expansion leading to net bending stresses in piping are treated as secondary, Q, stresses unless elastic follow-up effects preclude the reduction of the thermal expansion bending stress through small deformations. If elastic follow-up effects (which are discussed later in more detail) are significant, instead of performing a detailed inelastic stress analysis it is conservative to consider the thermal expansion bending stress as a primary bending, P_b, stress and then use the elastic stress analysis rules for assessing compliance with the design rules and limits.

The grouping of stress and strain categories according to the controlled quantities and the operating conditions is illustrated in the flow diagram of Fig. 7. Notice that the "Load-Controlled Stress Limits" column depicts a design evaluation procedure similar to NB-3000, but the various operating conditions are handled with different parameters. For example, whereas the Design Condition limits are also used for primary stress control for Operating Conditions in NB-3000, the elevated temperature procedure controls primary stress intensities by placing limits on both Design Conditions and Operating Conditions.

The Design Conditions still retain single-value stress limits, S_o, based on extrapolated 10^5 hr properties—similar to Sections I and VIII, Division 1. Unlike Section III, the Operating Conditions have their own load-controlled stress limits in the Code Case. Time-of-loading becomes an additional variable so that elevated temperature stress limits, S_t, S_m, and S_{mt}, are a family of curves such as those shown in Fig. 8. This separation of load-controlled stress limits allows short-time loads (e.g., earthquake and severe shock loads) to have stress limits based on short-term tensile properties. Short-time loads need not be considered in the analysis for the Design Conditions since these same loads will be considered under the limits for Operating Conditions.

As shown in Fig. 7, the "Strain and Deformation Limits" for elevated temperature design cover Normal, Upset, and Emergency Operating Conditions, but no limits are placed on Design Conditions or Faulted Operating Conditions. The inclusion of coverage for Emergency events with strain and deformation limits is a new feature of the elevated temperature design methods.

It was recognized that the low temperature Section III limits on primary-plus-secondary stress intensity range will not, due to creep effects, necessarily assure that an elevated temperature structure will *shake down* to elastic action in gross areas when fixed strain ranges are repetitively applied. Thus, the primary-plus-secondary stress intensity limits of Section III were replaced by strain limits, where inelastic analyses are performed, and by more conservative rules where elastic analyses are employed.

5.0 DESIGN RULES FOR LOAD-CONTROLLED STRESSES IN STRUCTURES OTHER THAN BOLTS

The basic feature of a load-controlled stress is that it is necessary to satisfy equilibrium of the structure under externally applied loads. As a result, deformations will not generally relieve load-controlled stresses. In developing the rules for components at elevated temperature, the Committee was faced with the precedent established by Sections I and VIII and by the previous elevated temperature Case 1331-4 which used elevated temperature allowables based on 10^5 hr creep rupture properties and a creep rate of 0.01% per 1000 hr.

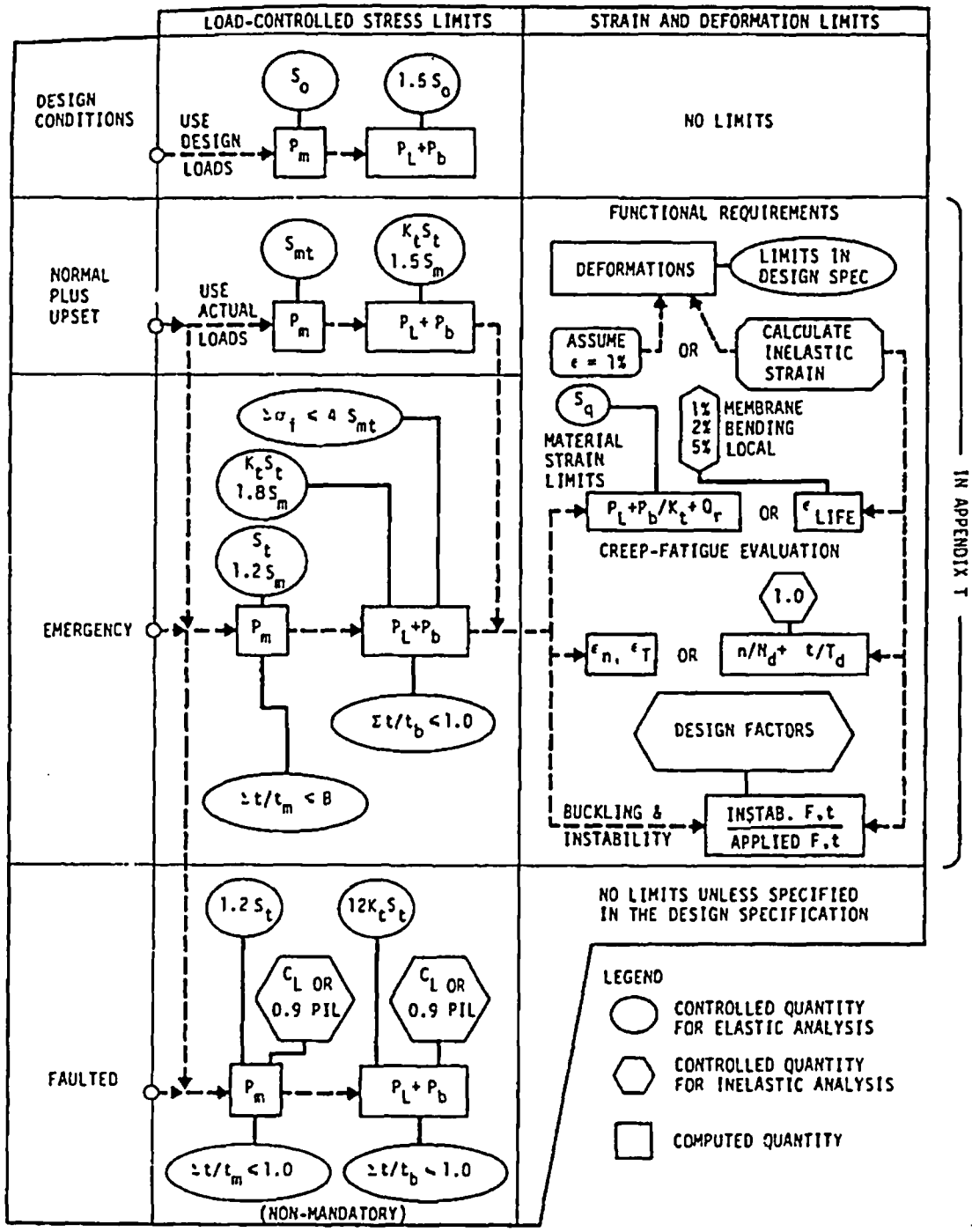

Fig. 7 FLOW DIAGRAM FOR ELEVATED TEMPERATURE ANALYSES

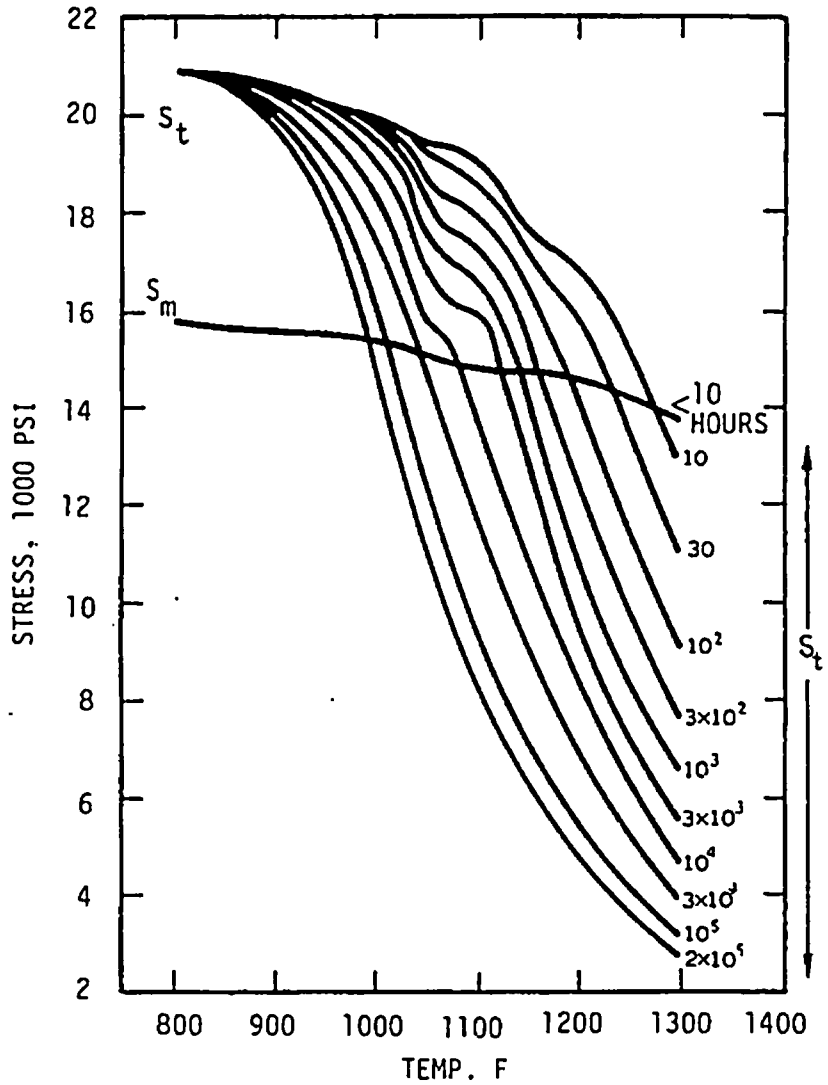

Fig. 8 S_{mt} ALLOWABLE STRESS, TYPE 316 STAINLESS STEEL

The ASME Code wanted to explicitly recognize the actual service life for Section III, Class 1 components and still utilize the proven methods of Section I and VIII. The result is two sets of primary stress allowables, one for Design Conditions and the other for Operating Conditions.

5.1 CRITERIA FOR DESIGN CONDITIONS

The Design Condition allowable stress values, S_o, are the same as Section I and Section VIII, Division 1. For Design Conditions for Case 1592, the allowable primary membrane stress is S_o and the allowable primary membrane-plus-bending stress is 1.5 S_o.

5.2 CRITERIA FOR OPERATING CONDITIONS – INTRODUCTION

For Operating Conditions, the allowable stress criteria are more complex. The first problem is to identify the numerical criteria to be used in setting the actual allowables. Then there is the problem of accounting for different loads for differing times and temperatures. It was decided to retain the basic Section III criteria for determining the time-independent allowable stress, S_m.

To that is added a time-dependent criteria, S_t. Another term, S_{mt}, was identified as the lower of S_m or S_t for a particular time or temperature. The S_t values are the least of three quantities:

(1) two-thirds of the minimum stress to cause creep rupture in time, t;
(2) 80% of the minimum stress to cause the onset of tertiary creep in time, t; and
(3) the minimum stress to produce 1% total strain in time, t.

The evaluation procedures employed in developing the S_t values for Case 1592 are described in Appendix A of this document.

5.3 GENERAL PRIMARY MEMBRANE STRESS INTENSITY LIMITS FOR OPERATING CONDITIONS

The Normal, Upset, Emergency, and Faulted Conditions have general primary membrane stress intensity limits as shown in the following table.

Loading Condition	P_m Limit is Lesser of
Normal and Upset	S_m or S_t
Emergency	1.2 S_m or S_t
Faulted	Section III limits or 1.2 S_t

The time, t, which corresponds to the total duration of the loading at temperature, T, during the entire design life of the component, is used for determining the S_t value. Note that there is no significant increase in the time-dependent (S_t related) limits for Emergency or Faulted loading conditions. Also, the time-independent (S_m related) limits are the same as those of Section III.

5.4 ALLOWABLE STRESS INTENSITIES FOR LOADING INVOLVING BENDING

The limits for local membrane plus bending stress intensities in Case 1592 are tabulated below.

Loading Condition	$P_L + P_b$ Limit is Lesser of
Normal and Upset	1.5 S_m or $K_t S_t$
Emergency	1.8 S_m or $K_t S_t$
Faulted	Section III limits or 1.2 $K_t S_t$

In Section III the 1.5 factor applied to S_m for Normal and Upset loading is the limit load *shape factor* for a solid rectangular section bar loaded in bending, assuming a perfectly plastic material. Thus, *collapse* of the bar due to attainment of limit loads is precluded in design by limiting the elastically calculated $P_L + P_b$. In elevated temperature design, where creep effects can exist, the K_t factor is intended to recognize the additional load-carrying capacity in bending due to the effects of creep on the distribution of stress and strain throughout the section which results in a reduction in the actual maximum bending stress below the elastically calculated value.

In Case 1331, versions -5 through -8, a factor K was used in the allowable stress intensities for primary membrane-plus-bending and in the strain limits for elastic analysis. The notation for this factor was changed in Case 1592 from K to K_t,[2] and it was made dependent on the actual cross section being considered.

The definition of the factor K_t and of the more traditional section factor K is illustrated in Fig. 9, which depicts the stress-distribution in a beam under pure bending. The elastically calculated distribution is linear and has a maximum value denoted by P_b. If P_b does not exceed the material yield stress, then the linear distribution is also the actual distribution at zero time. As creep occurs, the stress-distribution becomes nonlinear, as shown in Fig. 9, and it continues to change with time. However, as the transient creep becomes depleted in the outer fiber portions of the cross section, the stress-distribution change diminishes and approaches a stable distribution

[2] In the Winter 1972 Addenda to the 1971 Edition of Section III, K denotes the more traditional *shape factor* or *section factor* based on an elastic-ideally plastic material response. Thus, there was a conflict in notation.

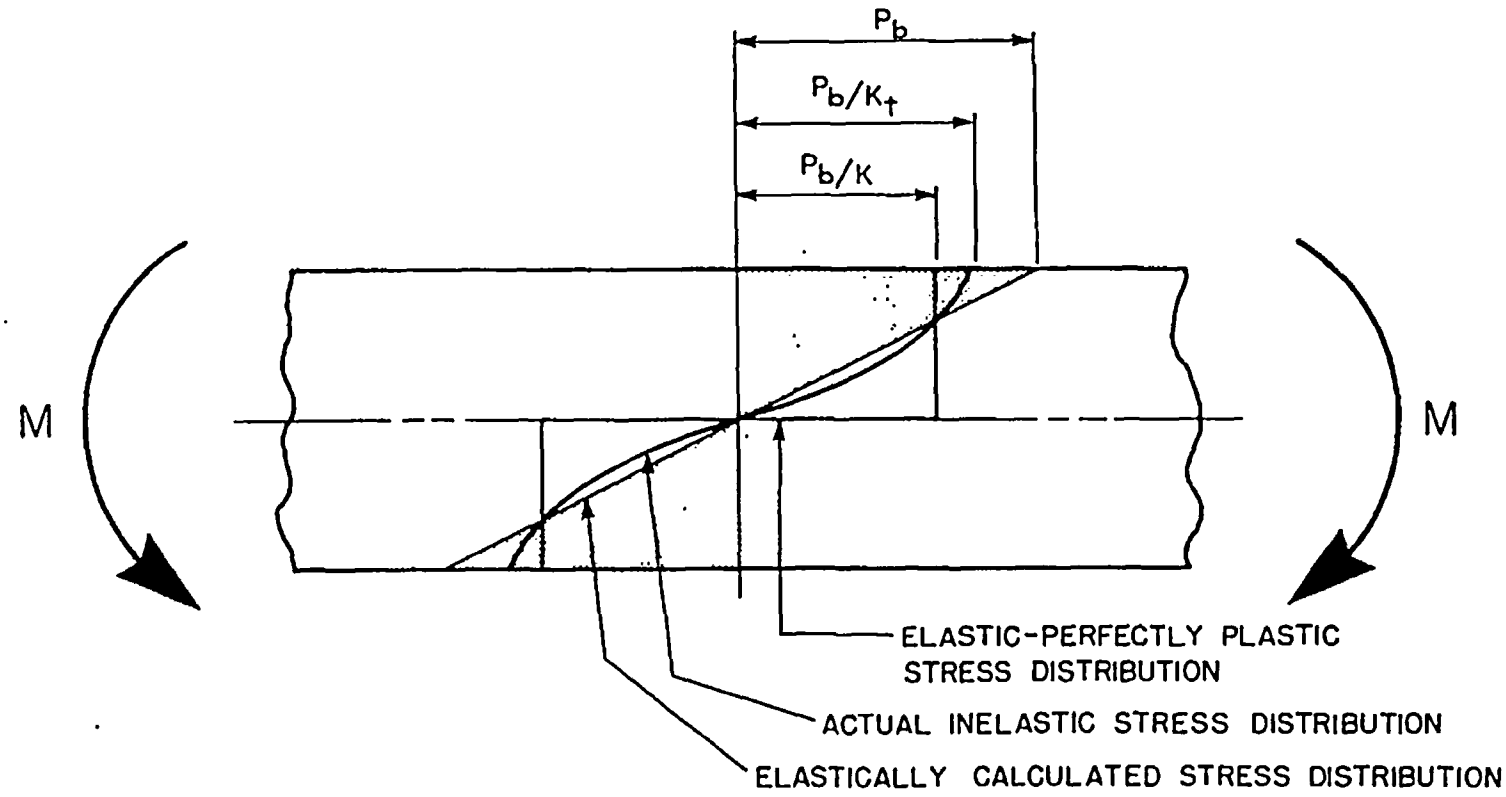

Fig. 9 ELASTICALLY CALCULATED PRIMARY BENDING STRESS DISTRIBUTION COMPARED TO ACTUAL TIME-DEPENDENT INELASTIC STRESS DISTRIBUTION

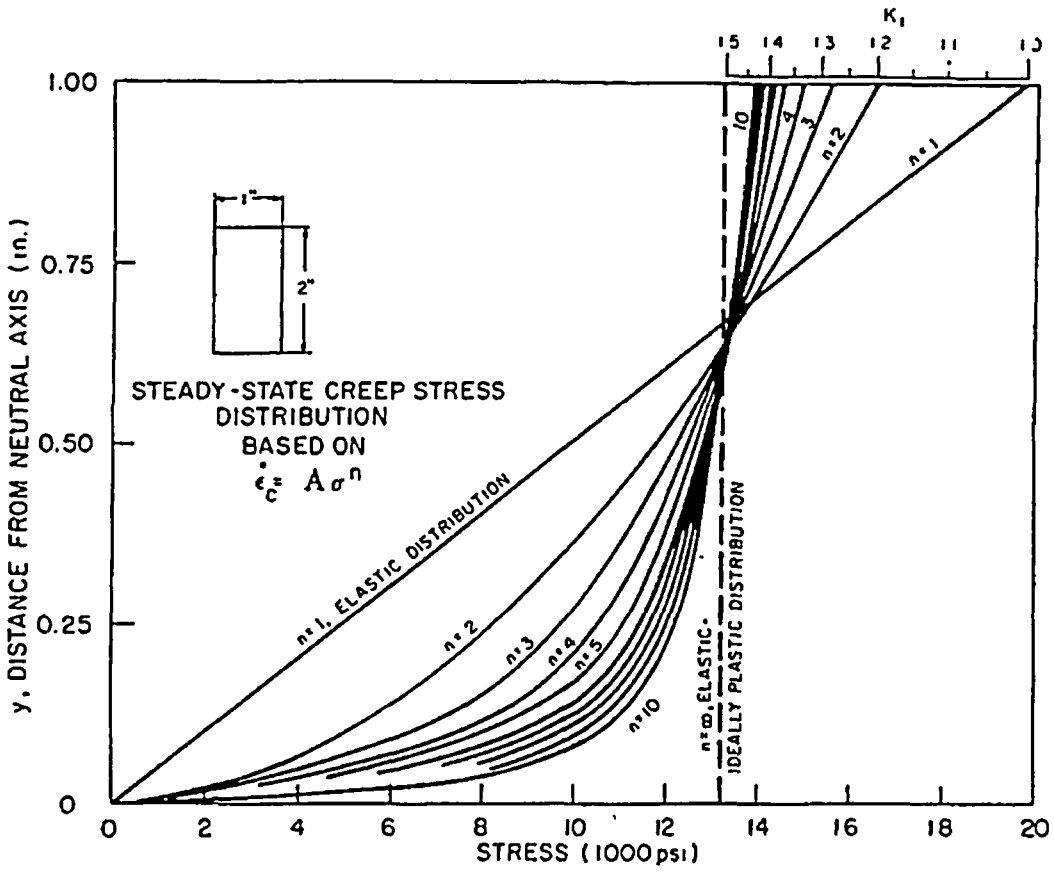

Fig. 10 STEADY-STATE CREEP STRESS DISTRIBUTION ACROSS A RECTANGULAR BEAM IN PURE BENDING AND HAVING A STEADY-STATE CREEP LAW OF THE FORM, $\dot{\epsilon}_c = A\sigma^n$

throughout the section. Creep analysis of the pure bending of a rectangular section beam, neglecting primary creep and assuming the secondary creep rate is proportional to the n power of stress, reveals that the distribution of stress is independent of time for any given n value. The stress-distribution ranges from linear through the section when n is unity, to perfectly plastic when n is infinite (see Fig. 10). However, at any given time during the creep period, the actual maximum stress is less than P_b and is denoted by P_b/K_t, and the factor K_t is a time-, temperature-, and material-dependent quantity, as well as being dependent on the cross-sectional shape of the beam.

To investigate the role of the K_t factor and the values which should be used in the Code Case, a number of elastic-creep and elastic-plastic-creep beam bending analyses using material properties for Types 304 and 316 Stainless Steel were performed. The resulting inelastic stress distributions and maximum stresses were examined relative to the K_t factor. The objective of these comparisons was to identify K_t values for Code Case use that would, for simplicity, be independent of time and would conservatively represent the long-term, steady-state creep stress. This work is reported by J. M. Corum (54).

Results of typical beam bending analyses are shown in Figs. 10 and 11. These figures show the steady-state creep stress distributions in a solid rectangular beam and in a tubular beam or pipe

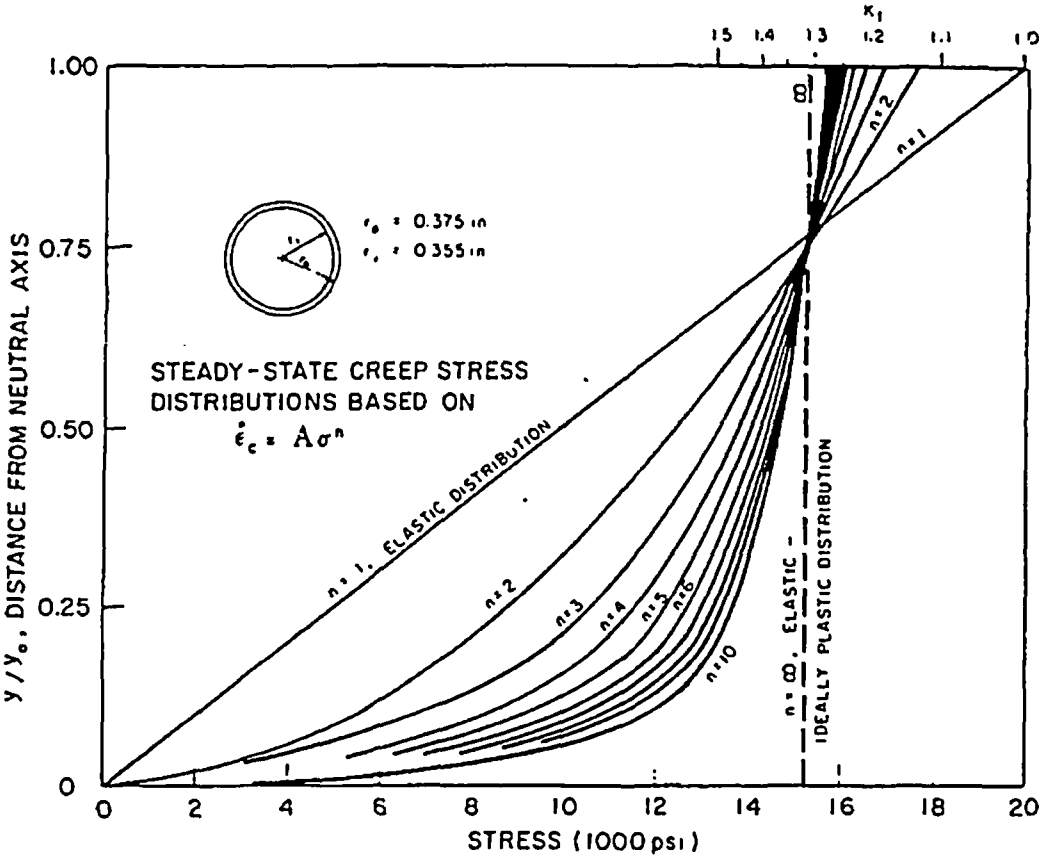

Fig. 11 STEADY-STATE CREEP STRESS DISTRIBUTIONS ACROSS A THIN, CIRCULAR TUBE IN PURE BENDING AND HAVING A STEADY-STATE CREEP LAW OF THE FORM, $\dot{\epsilon}_c = A\sigma^n$
[Note that for the particular thickness used, the value of K_t for $n = \infty$ or for elastic-ideally-plastic response is approximately 1.31. The limiting value as the thickness goes to zero is 1.27]

or circular cross section for various values of n in the assumed steady-state creep equation $\dot{\epsilon}_c = A\sigma^n$. For the rectangular section, K_t varies from about 1.28 to 1.38 for n between 3 and 6, the usual range for the materials of interest at low stresses.

Additional calculations based on the steady-state creep portion of the two-exponential creep law recommended in L. D. Blackburn (20) were used to examine Types 304 and 316 Stainless Steel beams in the 900 to 1200 F temperature range. For elastically calculated stresses ranging from 5,000 to 15,000 psi, it was found that the ratios of the maximum steady-state stress to the elastic stress varied from 0.70 to 0.74, giving a K_t value ranging from 1.35 to 1.43.

These results show that a value of 1.25 for pure bending conditions is reasonable and conservative for steady-state stress distributions in rectangular cross sections. On the same basis, however, Fig. 11 indicates that 1.25 is high for a thin circular tube. A comparable value to the 1.25 would be about 1.15 for the circular section. This illustrates the dependence that K_t must have on the cross-sectional shape.

For pure bending, the formula for K_t chosen for Case 1592 is

$$K_t = 1 + k_s$$

where

$$k_s = \alpha(K - 1)$$

The factor K is the section factor for the cross section being considered. Values of K for various sections are tabulated in Table A-9221(a)-1 of Appendix A of Section III. Presently, α is specified as 0.5. With this value, K_t for a rectangular beam ($K = 1.5$) in pure bending is 1.25; for a thin tube ($K = 1.27$), 1.14; and for an I-beam with a very thin web ($K = 1$), 1.0.

5.5 USE-FRACTION SUMMATIONS

The purpose of the use-fraction summations is to allow the Designer to take credit for the fact that a component may not be operating at a single temperature or stress level throughout its entire operating history. Thus, one is permitted to use higher allowables associated with shorter periods of operation, provided that the creep damage associated with the entire operating history at elevated temperatures is taken into account.

To account for varying loads at variable times and temperatures, a modified linear damage use-fraction approach was employed. This damage rule takes the form

$$\sum_i \left(\frac{t_i}{t_{ia}}\right) \leq B$$

where:

t_i = the total duration of time at a particular stress level and temperature during the service life of the component

t_{ia} = the allowable time of operation at the same stress level and temperature

Σt_i = the total operating time at temperatures in the creep regime

B = factor which is equal to unity or, alternatively, it can be specified to be less than unity in the Design Specifications to account for nonlinearities in the use-fraction rule

The time used in the denominator of the use-fraction is the time to reach the time-dependent stress limit, S_t, for a primary stress P_m at temperature T.

For primary membrane-plus-bending loads, the stress limits are increased by a factor K_t which accounts for the stress redistribution in bending for various cross sections due to plastic flow. Emergency Conditions, in addition to Normal and Upset Conditions, are included in the use-fraction summation.

6.0 DESIGN RULES AND LIMITS ON STRAIN FOR STRUCTURAL INTEGRITY

The incremental growth of a component subjected to pressure loading with superimposed cyclic thermal stresses may lead to distortion or fracture unless the accumulated strain is kept within allowable limits. For low temperature service when the creep influence is negligible, the stress regimes for which freedom from ratcheting may be demonstrated are described by NB-3222.5 of Section III. However, for operation where creep and relaxation cannot be neglected, the stress regime, E, as shown in the Bree (22, 23) diagram of Fig. 12, is the only regime where the response of the structure is ratchet-free. In many nuclear power plant components it is not feasible to keep all elastically calculated stresses less than the yield strength. In such components, plastic/creep cycling and ratcheting can be allowed, provided that both effects can be limited, calculated, and kept within safe allowable values.

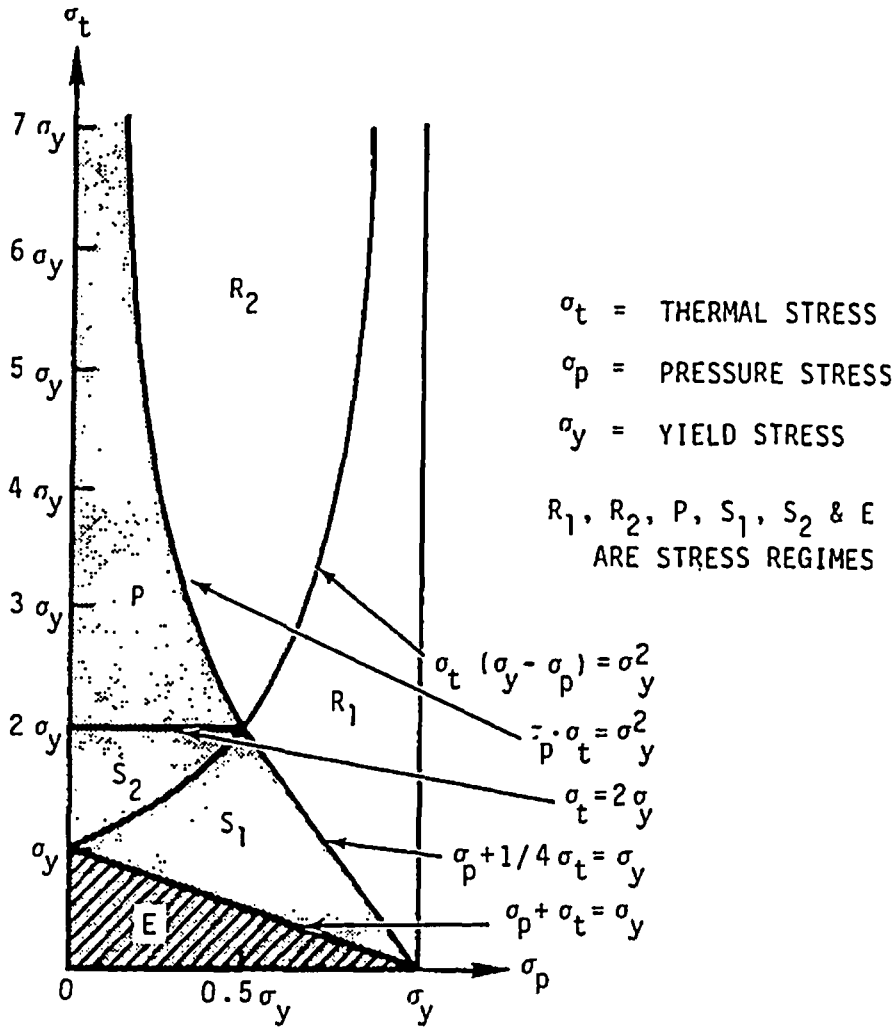

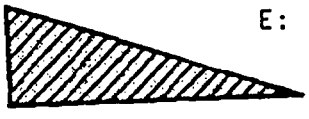

E: REGIME OF NO CREEP RATCHETING OR PLASTIC RATCHETING
[Note however that creep due to σ_p can exist.]

S_1, S_2, P & E: REGIMES OF BOUNDED CREEP/PLASTIC RATCHETING ANALYZED IN REFERENCE 28

R_1 & R_2: REGIMES OF PROGRESSIVE RATCHETING

Fig. 12 STRESS REGIMES
[Taken from Bree (22)]

6.1 REASONS FOR AND OBJECTIVES OF STRAIN LIMITS

Conceptually, the elevated temperature rules for primary stresses, creep-fatigue and buckling should provide an adequate basis for design. However, there are sufficient limitations to the current state of knowledge of elevated temperature materials behavior that additional rules for strain and deformation were deemed necessary to ensure structural integrity. These strain and deformation limits are not necessarily related quantitatively to specific failure modes. However, they have been formulated to help ensure the applicability of the other rules of the Code Case,[3] provide additional comparative design data, and provide additional quantified assessment relative to the failure modes of:

(1) creep rupture from long-term loadings;
(2) creep-fatigue failure;
(3) gross distortion due to incremental collapse and ratcheting.

Materials test data related to the first of the above failure modes is presented in Jakub and Moen (24). The data depicted in Fig. 13(a) and (b), demonstrate that prior creep deformation strains tend to reduce residual short-term tensile elongation and creep ductility (as measured by total elongation) as time-to-rupture increases.

For the creep-fatigue failure mode, much of the current data, even at elevated temperatures, has been obtained from tests which involve zero mean strain. Strain cycles between two fixed values as shown in Fig. 14(a) are typical in actual components.

For low temperatures the NB-3000 rules for primary-plus-secondary stress intensity limits rely on the simplified shakedown concept and $3S_m$ (or $2S_y$) limits along with the simplified thermal ratchet rules to allow gross section yielding and ratcheting (increasing mean strain) to occur only during the first few load cycles.

At elevated temperatures, creep strains make it necessary to handle the more general strain history as shown in Fig. 14(b). Due to creep effects, the simple $3S_m$ limit does not assure shakedown to gross area elastic action [Townley and Poynor (25) and Penney and Marrietts (26)]. Thus, strain concentrations higher than the stress concentrations may occur and the use of strain-controlled, zero-mean-strain fatigue data may not be sufficiently conservative.

It was recognized that a repetitive application of severe load cycles which induce large cumulative inelastic strains and ratcheting could cause exhaustion of the material ductility and lead to fracture in fewer cycles than would be indicated by normal creep-fatigue design rules. An approximate method for evaluating the effect of cumulative permanent strain of fatigue is given by B. F. Langer (27). It was felt that limiting the cumulative strains to a sufficiently low level in both gross and local areas would help ensure the applicability of the existing fatigue data. Thus, due to the lack of thorough experimental verification for creep-fatigue phenomena, the strain limits were also considered warranted for backing up the applicability of the creep-fatigue rules.

Finally, in the gross distortion failure mode, the limits on inelastic cumulative strain provide a direct control on incremental collapse and ratcheting.

In addition to the direct applications to failure modes, strain limits provide a vehicle to add quantitative rules for the design and location of welds. The present elevated temperature design rules require the use of material models that neglect the changes of mechanical properties at the welds—the entire structural model uses base material properties. However, the rules also restrict the limits for the calculated strains in the weld regions. (See discussion on welds in the Special Limits and Considerations section.) The decision to reduce all of the allowable strain limits at welds by a significant factor was a positive step to keep weld locations outside of areas expecting large creep strains.

[3] This function is similar to the role of the $3S_m$ limit of Section III.

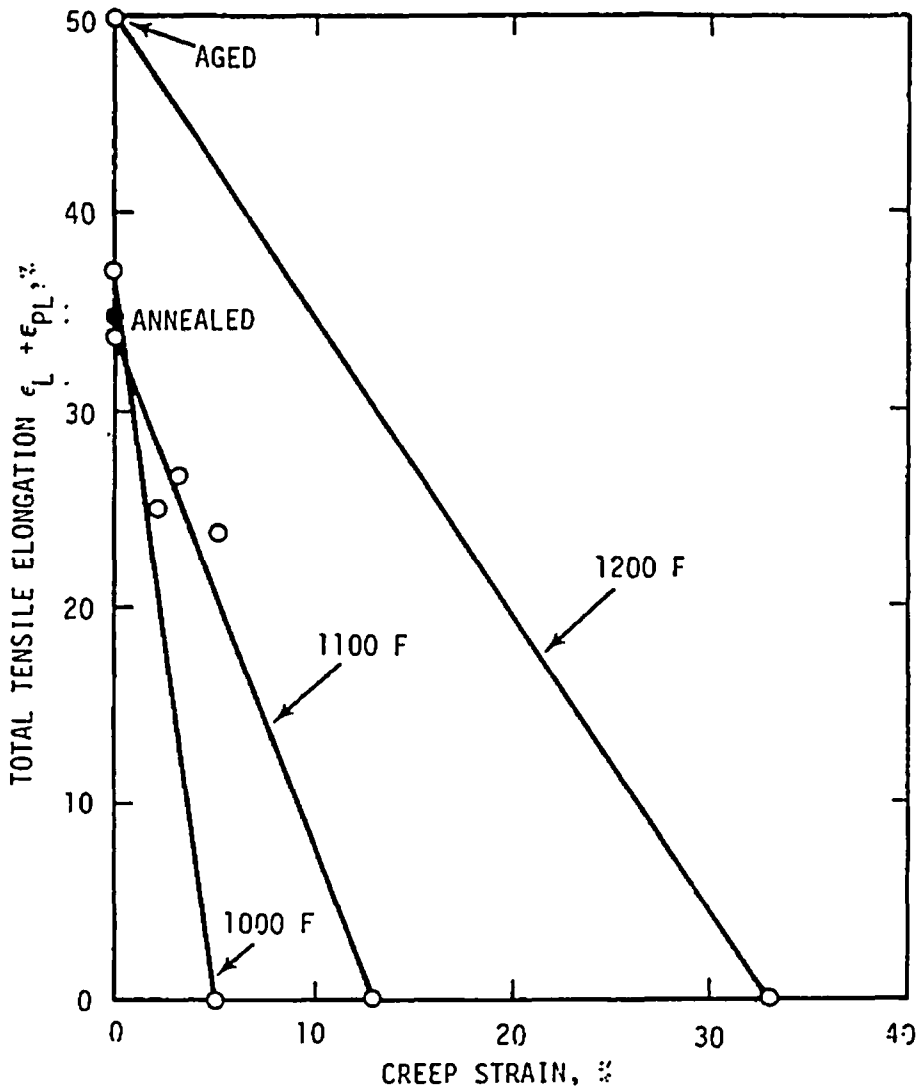

Fig. 13(a) EFFECT OF PRIOR CREEP DEFORMATION ON TENSILE ELONGATION OF TYPE 304 STAINLESS STEEL

The strain limits are also related to the small deformation theory which has been the cornerstone for analyses of structures at low temperatures. The same small deformation or small strain assumptions are retained by the majority of current computer structural models being used for elevated temperature analysis. However, the possibility of unlimited creep or relaxation strains have required that some way be found to ensure that the theory still applies. If one overall rule cannot ensure compliance, then there must be some measure which tells when large deformation theory must be applied. At present the strain limits in Case 1592 are set low enough that they effectively ensure that small deformation theory is applicable for most structural analyses of elevated temperature components. Obvious exceptions include some buckling instability analyses and thin-walled large deflection shell analyses.

For structural design of metal components, stress and strain are two obvious material state parameters which can be calculated and thus be considered as candidates for Code-allowable limits.

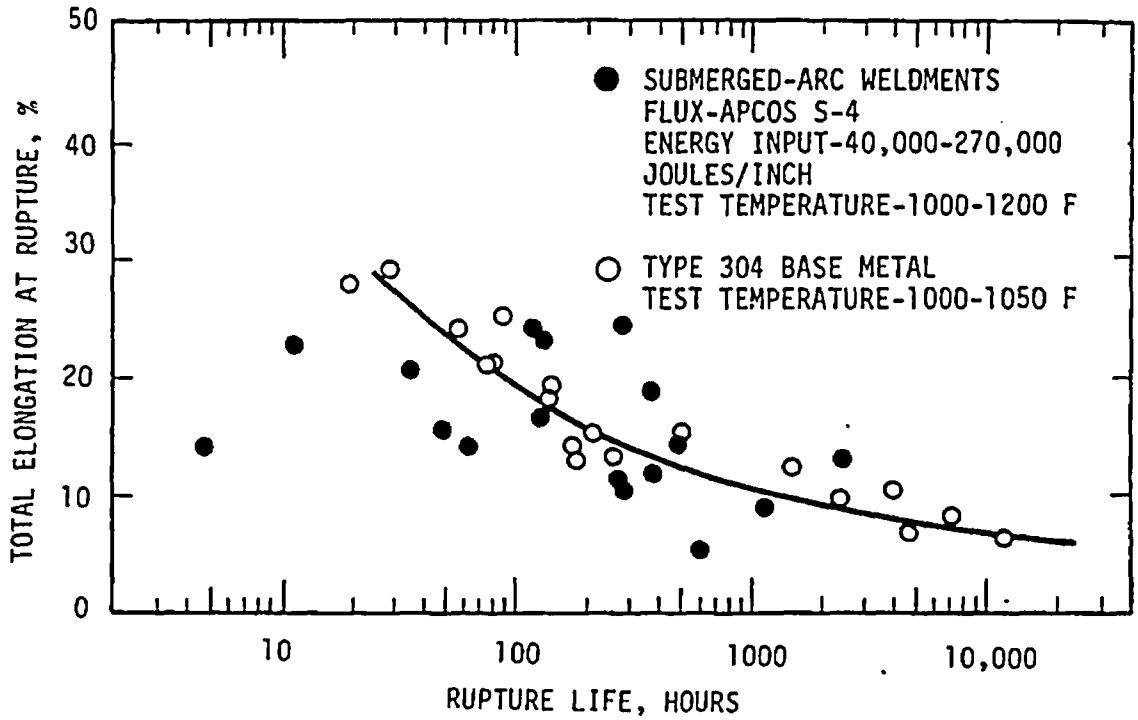

Fig. 13(b) VARIATION OF CREEP DUCTILITY WITH RUPTURE LIFE FOR SELECTED AUSTENITIC STAINLESS STEEL SUBMERGED-ARC WELDMENTS

The two quantities are not independent of each other since a complete history of one should, theoretically, provide a good description of the history of the other parameter. The strain parameter, which is still the most common physical measurement in experiments on elevated temperature structures, is more closely related to structural deformations. Thus, the Committee concluded that strain was the more useful parameter for setting Code-allowable limits at elevated temperatures. Appendix T of Case 1592 reflects this decision..

6.2 LIMITS ON CUMULATIVE INELASTIC STRAIN FOR STRUCTURAL INTEGRITY

In choosing what the controlled strain parameters and their limits should be, the state-of-the-art analysis methods were considered. For analysis economy it was and still is desirable to relate the limits to elastically calculated parameters. However, recognizing that the significant elevated temperature structural response is often inelastic, it was judged that inelastic stress analyses, rules, and limits were also necessary. Accordingly, for the less informative elastic analysis evaluations, conservative but often restrictive design rules and limits were developed. The rules and limits for inelastic analysis, being less restrictive and considered to provide more informative and accurate control, are a means to demonstrate component design adequacy even if the elastic analysis screening rules cannot be satisfied.

The elevated temperature Code Case places the following limits on the maximum accumulated inelastic strain for parent material (see T-1310 of Case 1592):

(1) strains averaged through the thickness, 1%
(2) strains at the surface, due to an equivalent linear distribution of strain through the thickness, 2%
(3) maximum local strains, 5%

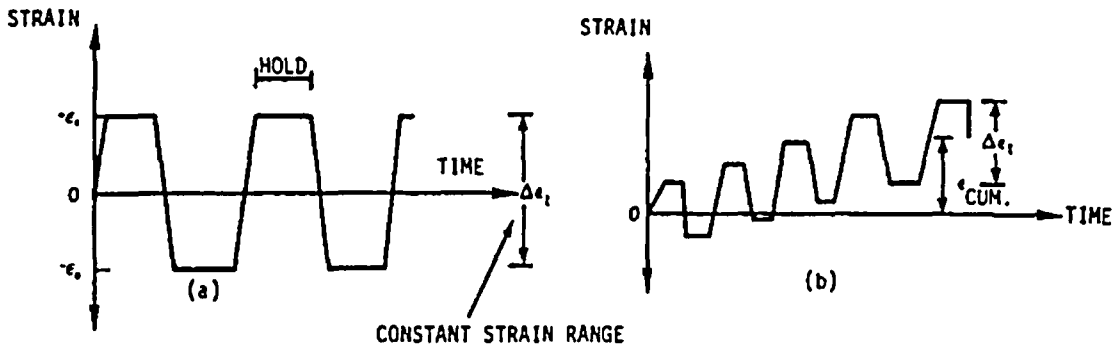

Fig. 14 TYPICAL STRAIN-TIME RESPONSES

The above limits apply to computed strains accumulated over the expected operating lifetime of the element under consideration and computed for some steady-state period at the end of this time during which significant transients are not occurring. These limits apply to the maximum positive value of the three principal strains. A positive strain is defined as one for which the length of the element in the direction of the strain is increased. The principal strains are computed from the strain components ($\epsilon_x, \epsilon_y, \epsilon_z, \gamma_{xy}, \gamma_{xz}, \gamma_{yz}$). When the strain is computed at several locations through the thickness, the strains are first averaged and linearized on a component level and then combined to determine the principal strains for comparison to the limits on average and surface strains. The limits for discontinuity strains are based on the computed strains at the point of interest.

Inelastic strains accumulated in weld regions are computed using parent material properties and these calculated strains are limited to one-half the strain values permitted for the parent material. (See Section 9.1 of this document.)

6.2.1 Membrane Strain Limits

The membrane strain limit magnitude of 1% was selected to accomplish the goals outlined in Section 6.1 of this document.

6.2.2 Bending and Local Strain Limits

High linearized bending strains may result in a large deflection which could compromise the integrity and reliability of the structure, particularly in the case of the thin-walled structures commonly found in elevated temperature systems. Classical small deformation theory, used for most high temperature design analyses, may also be compromised if linearized bending strains are not carefully limited. Thus, a 2% limit due to a linearized bending strain distribution was deemed appropriate.

The local creep fracture ductility in the creep regime was not considered sufficiently high so that local strain accumulations could be ignored. Monotonic creep tests have shown that the creep strain at fracture can be very low—well under 10%. It was desired to limit creep strains to a value under 5%. However, because of the practical difficulties that occur in trying to partition strains between plastic and creep strains, the limit of 5% was used for the total accumulated local strain.

6.2.3 Application of Strain Limits

The strain limits are applied to the maximum accumulated inelastic strain. This is illustrated by Fig. 15. The steps in the strain cycle are as follows:

o–a initial elastic strain
a–b subsequent creep strain due to sustained load

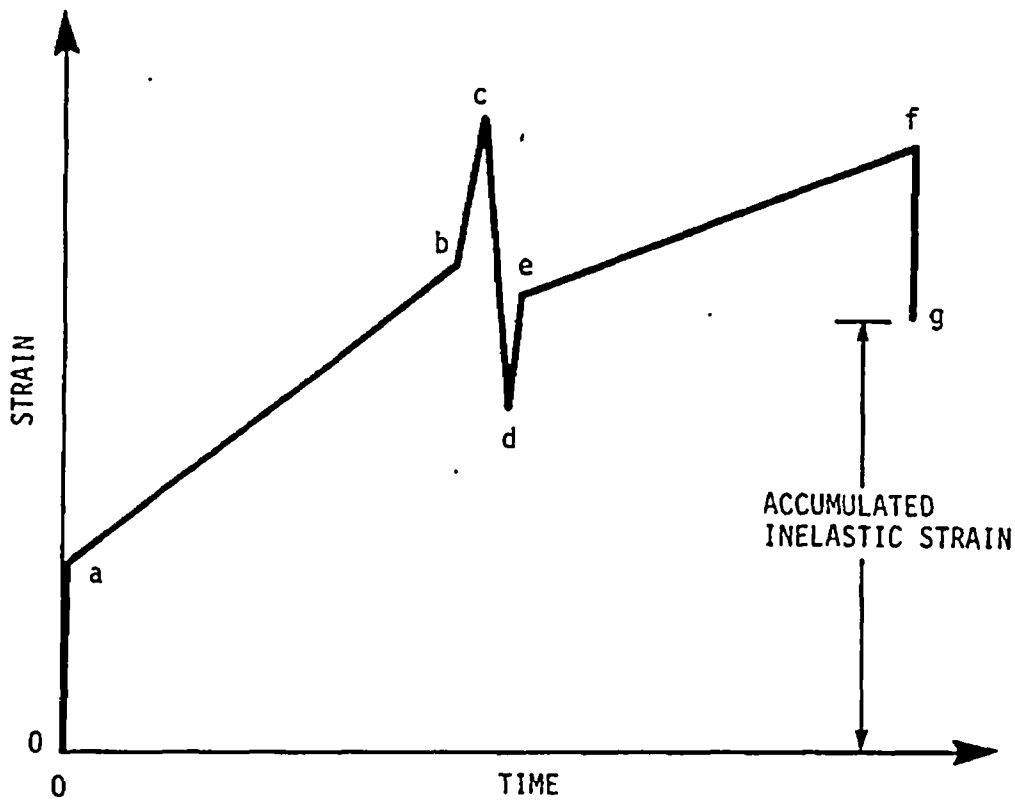

Fig. 15 STRAIN-TIME HISTORY SCHEMATIC

b–e	strain cycle resulting from superimposed thermal transient [Note that there is a net decrease in the strain]
e–f	additional creep strain due to sustained load or residual stresses
f–g	recovery of elastic strain due to removal of primary membrane stress

The strain limits apply to the accumulated inelastic strain, o – g.

The strain quantity limited by these criteria is the maximum principal tensile strain. The tensile strain was chosen since it was felt that this is the most appropriate index for the onset of tensile failure.

6.3 PHENOMENA OF PLASTIC AND CREEP RATCHETING

Ratcheting is defined in Case 1592 as progressive cyclic inelastic deformation that can occur in a component that is subjected to cyclic variations of mechanical secondary stress, thermal secondary stress, or both, in the presence of a sustained primary stress. The ratcheting phenomenon is of particular concern in elevated temperature reactor systems because of the cyclic stress conditions induced by frequent, and often rapid, temperature changes.

Several different mechanisms can contribute simultaneously, or singly, to the ratcheting phenomenon. The specific structural problem determines whether or not all of the various mechanisms come into play and the relative importance of each mechanism. However, an insight into the ratcheting phenomenon can be obtained by considering a simplified example in which the basic mechanisms are assumed to be present.

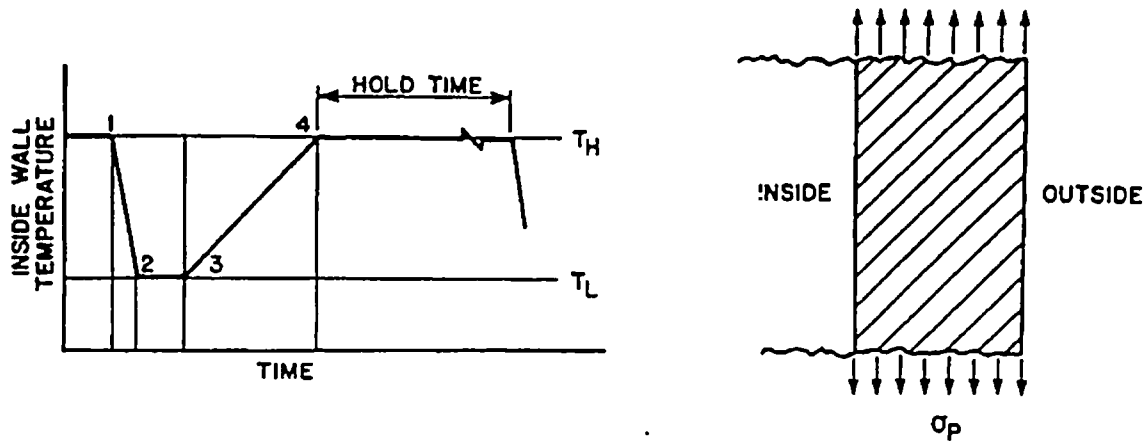

(a) COMPONENT WALL

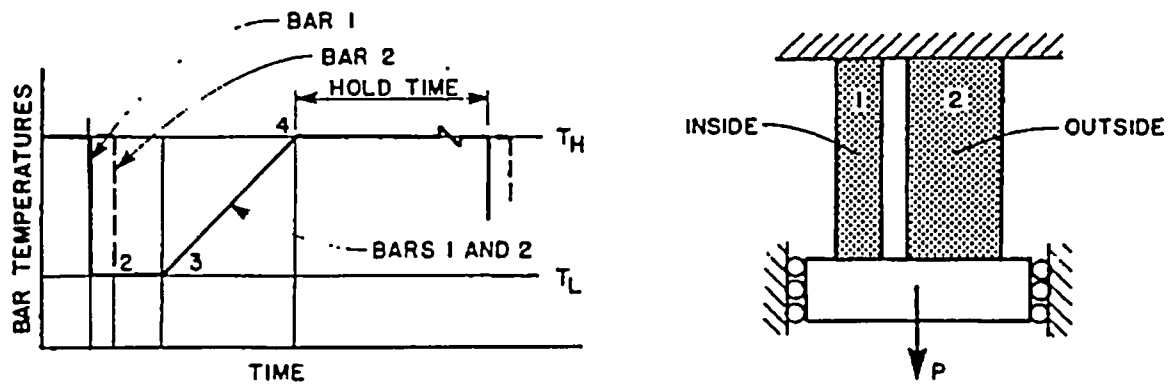

(b) SIMPLE TWO-BAR REPRESENTATION

Fig. 16 SIMPLE EXAMPLE OF CONDITIONS LEADING TO ELEVATED TEMPERATURE RATCHETING

Such an example is depicted in Fig. 16(a). Here, a component which carries a sustained primary membrane stress, σ_P, is also subjected to a periodic thermal down-shock on the inner surface, as represented by the histogram on the left in Fig. 16(a). Assume that the material creeps at the temperature T_H and that the temperature drop from T_H to T_L is sufficiently rapid for a relatively small inner portion of the component wall to drop almost to T_L, while the outer portion remains near the original temperature, T_H. Eventually the entire wall reaches T_L. The temperature is then slowly increased uniformly back to T_H. This is followed by a period of steady operation before another thermal down-shock occurs.

Now consider the possible effects of the down-shock. During the temperature drop, high secondary stresses are induced, and if these stresses are sufficiently large, plastic yielding will occur on both the inner and outer surfaces of the wall. Yielding has two effects in this example: it results in an increment of plastic growth, and it leaves a residual stress pattern in the wall at the beginning of the subsequent hold period. The residual stress pattern adds to the existing primary membrane stress, σ_P, and, because the creep response of the material generally has a nonlinear dependence on stress, more net creep strain is accumulated during the hold period than would have occurred due to the membrane stress σ_P alone. This effect is referred to as *enhanced creep*, and it adds to the progressive growth caused by the thermal down-shock. Finally, since the residual stresses are self-equilibriating, they tend to relax during the hold period. Relaxation alters the stress pattern during the subsequent thermal down-shock in such a manner that the time-independent plastic increment of growth may be larger than it would have been had the down-shocks not been separated by a hold period in the creep regime.

To better understand each of the assumed mechanisms in this simplified example, consider the simple two-bar representation of the component wall that is shown in Fig. 16(b). Bar 1, which has a smaller cross-sectional area than bar 2, represents the inner portion of the component wall in which the temperature drops rapidly during the down-shock. Bar 2 represents the larger outer portion of the wall which experiences a less rapid temperature drop. The bars are constrained to the same length, and they jointly carry the primary load, P, which initially produces a uniform tensile stress σ_P in both bars. The temperature history for the bars is shown on the left in Fig. 16(b). The temperature of bar 1 drops from T_H to T_L and subsequently the temperature of bar 2 drops. The slow heat-up and the hold period are the same as in the actual component wall.

With this simple representation, we can follow the ratcheting process step by step:

(1) As bar 1 is cooled, its stress increases from σ_P until it yields in tension. When bar 1 reaches T_L, bar 2, which is still at T_H, carries a reduced load that may even be compressive.

(2) As the temperature of bar 2 subsequently drops from T_H to T_L, its stress increases again until it also yields in tension. At the same time the stress in bar 1 decreases and becomes compressive.

(3) If we assume, for simplicity, that neither the elastic modulus nor the yield stress vary with temperature, then no stress change occurs during the reheat phase of the cycle as both bars are heated together from T_L back to T_H.

(4) At the beginning of the hold period, both bars have yielded in tension. The assembly is longer than it was in its initial elastic state, and it can continue to grow longer with each succeeding cycle. This growth is *time-independent plastic ratcheting.*

(5) Also at the beginning of the hold period, the stress in bar 2 is tensile, while a compressive stress exists in bar 1. The averaged stress in the two bars is, of course, still σ_P. If the first down-shock were followed immediately by another down-shock with no intervening creep period, the residual stresses in the bars resulting from the first down-shock would alter the stresses during the subsequent down-shock, and in this particular case reduce the subsequent increment of plastic ratcheting.

(6) Consider now the hold period. Bar 2 is subjected to tensile stress greater than σ_P, and creeps more than it would if the stress were σ_P. This increased time-dependent growth rate or enhanced creep, which is a direct consequence of the thermal down-shock, (referred to as *enhanced creep*) contributes to the ratcheting increment during each cycle.

(7) As creep occurs during the hold period, the compressive stress in bar 1 unloads and becomes tensile as the tensile stress in bar 2 is transferred to bar 1. Further, the beneficial effect of the residual stresses in reducing the increment of plastic ratcheting in the subsequent down-shock (step 5) is lost.

Although actual specified loading cycles are likely to be much more involved, this simple example serves to illustrate that ratcheting at elevated temperatures is a complex phenomenon consisting, generally, of both time-independent plastic ratcheting and time-dependent creep ratcheting. Depending on the particular thermal and mechanical loading histories, the temperatures, and the material behavior, plastic ratcheting and creep ratcheting may occur alone or together, and one type may or may not interact with the other.[4] Likewise, in actual service, events of varying types and severities are intermixed. The residual effects of one event may remain to combine with, and possibly reinforce, the effects of a subsequent event.

Thus, because of the complexity of the ratcheting phenomenon, a reasonable prediction of the *actual* incremental growth from cycle to cycle in a component subjected to a realistic operating history can generally come only from a detailed inelastic analysis. The elevated temperature Code Case provides screening rules that are based on elastic analysis results and which identify whether ratcheting is or is not a problem to be further evaluated. Also, the Code Case provides a procedure for obtaining an upper bound estimate of ratcheting strains using only the results of an elastic analysis. Since these rules and procedures ignore many of the complexities of the ratcheting phenomenon and the possible interactions involved, they are necessarily very conservative. Nonetheless, they often allow the Designer to evaluate complex inelastic structural behavior without resorting to a costly and time consuming inelastic structural analysis.

6.4 METHODS OF SATISFYING STRAIN LIMITS USING ELASTIC ANALYSES

6.4.1 Rules to Preclude Plastic or Creep Ratcheting

If the primary stress intensity and the range of cyclic secondary stress intensity are small enough that they define a point in the elastic *E* regime of Fig. 12, then no progressive ratcheting in a component will occur. Thus, the elevated temperature Code Case has some screening equations intended for use with elastic analysis stress results that are based on the equations defining the *E* regime of Fig. 12. This equation is

$$[P_L + (P_b/K_t)]_{MAX} + (Q_R)_{max} \leq S_y \qquad (1)$$

where

S_y = the average of the yield strength values at the maximum and minimum wall-averaged temperature during the operating conditions being evaluated

$[P_L + (P_b/K_t)]_{MAX}$ = the maximum value of the primary stress intensity, adjusted for bending via K_t, during the operating conditions being evaluated

$(Q_R)_{MAX}$ = the maximum range of the secondary stress intensity during the operating condition being considered

Note that the above Equation 1 is evaluated by adding primary and secondary stress *intensities*. This is different from the normal NB-3000 approach where stress levels of different categories are combined at the stress component level prior to determining the stress intensity level.

Equation 1 assures that there will be no plastic ratcheting. Further, it assures that there will be no creep ratcheting provided that the average wall temperature at one of the stress extremes defining each secondary stress range, Q_R, is below the creep regime. The latter temperature is defined in the Code such that creep effects do not control the primary stress limits for 10^5 hr of operation.

In cases where the average wall temperature at one of the stress extremes defining the secondary stress cycle is not below the creep regime, creep ratcheting can be avoided by reducing S_y in Equation 1 to a stress value which is low enough to avoid significant creep relaxation. This value was selected as $1.25S_t$ taken at the highest average wall temperature during the cycle at 10^4 hours.

[4] Creep ratcheting can occur in the absence of any plastic flow, for example, if a component is subjected to a sustained primary membrane stress and a cyclic radial temperature gradient.

The above screening limits are intended to preclude plastic and creep ratcheting. However, it is very difficult to design elevated temperature equipment within these limits because the thermal stress ranges are usually too high. Moreover, it is completely safe to allow plastic and creep ratcheting provided that the resulting accumulated strains are kept within safe limits. Further elastic screening limits are, therefore, given in the Code Case which bound the total accumulated inelastic strains to the specified limiting values.

6.4.2 Rules to Limit Accumulated Strains with Creep Ratcheting

A relatively new method, the O'Donnell-Porowski method (28), developed under the sponsorship of the Pressure Vessel Research Committee, gives a way of evaluating the total inelastic strains that could be accumulated under creep ratcheting conditions. Only the results of *elastic* stress analyses are needed in this method to obtain quantitative upper bounds using the creep properties of the material. The creep acceleration due to the secondary thermal stresses is included by deriving an equivalent creep stress σ_c for the particular combination of primary and secondary stresses which exists. The creep properties can be obtained through use of the isochronous stress-strain curves which are included in the Code Case.

A cylindrical vessel subjected to internal pressure and a cyclic temperature drop through the wall is solved in detail in O'Donnell-Porowski (28). The resulting upper bound strains are rigorously derived, based on an elastic-perfectly-plastic material model. The equivalent creep stress, accounting for the accelerated creep due to thermal cycling, is shown in Fig. 17.

The effective creep stress, σ_c, may then be obtained using Fig. 17,[5] or the closed form solution given in O'Donnell-Porowski (28). These stresses are then used in isochronous stress-strain curves to obtain upper bounds for the total inelastic strain accumulation, including the strains due to creep ratcheting.

Since these results were derived for a cylindrical vessel, their use is restricted to axisymmetric structures subjected to axisymmetric loading away from local structural discontinuities. However, nonaxisymmetric loads such as the bending of a pipe or vessel may often be conservatively included as axisymmetric loads, and the present rules may be applied.

Further, the average wall temperature at one of the stress extremes defining each secondary stress range Q_R must be below the creep regime, since no relaxation at the cold extreme of the cycle was considered in O'Donnell-Porowski (28). Minimum isochronous curves, assumed to be 25% lower than the "average" curves given in the Code Case, should be used. The total service life may be subdivided into temperature-time blocks, and the strain increment for each block may be evaluated separately. However, the times used in selecting the isochronous curves should sum to the total operating life. The strain increments for each time-temperature block are added to obtain the total strain. The resulting value is limited to 1% for base metal and ½% for weld regions.

6.4.3 Operating Cycle Definition for Ratcheting Evaluation

In applying the ratcheting rule as just described, it is important to note the significance of cycle definition. The intent of the term $[P_L + (P_b/K_t)]_{MAX}$ is to consider the maximum value of load-controlled stress throughout the operating life, and the intent of the expression *Q range* is to consider the maximum secondary stress range throughout life. This is shown schematically on Fig. 18. The reason for this can be illustrated by a hypothetical example, as shown by Fig. 19. Assume that one initially has a pure applied radial thermal gradient, and the resultant thermal stress is less than S_q, as defined in Case 1331 and Case 1592, and is maintained for a sufficiently long time that the true stress in the wall in the presence of the thermal gradient relaxes down to a very low value (O-A-B). Assume now that the radial thermal gradient is removed. One will then have a superimposed residual stress which very nearly equals the original thermal stress in

[5] Note that the $(Q_R)_{MAX} = 3$ limit on the abscissa in Fig. 17 was used for convenience in scaling the drawing and has no other significance.

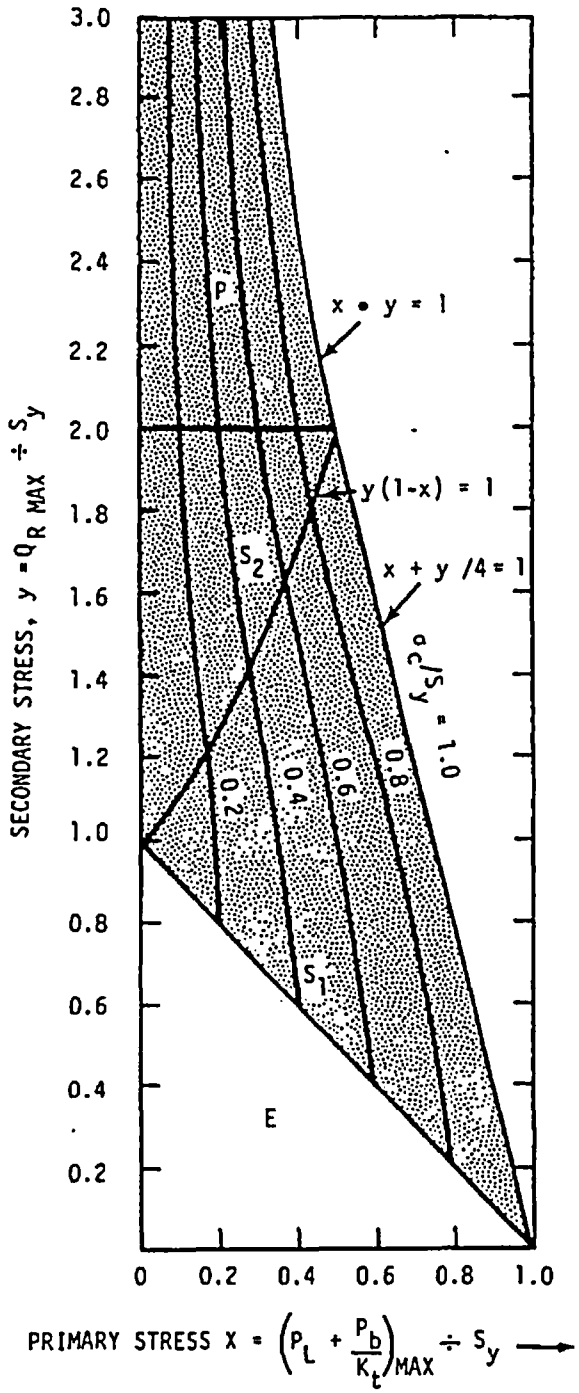

Fig. 17 EFFECTIVE CREEP STRESS, σ_c, FOR UPPER BOUNDS ON TOTAL ACCUMULATED INELASTIC STRAIN WITH CREEP RATCHETING

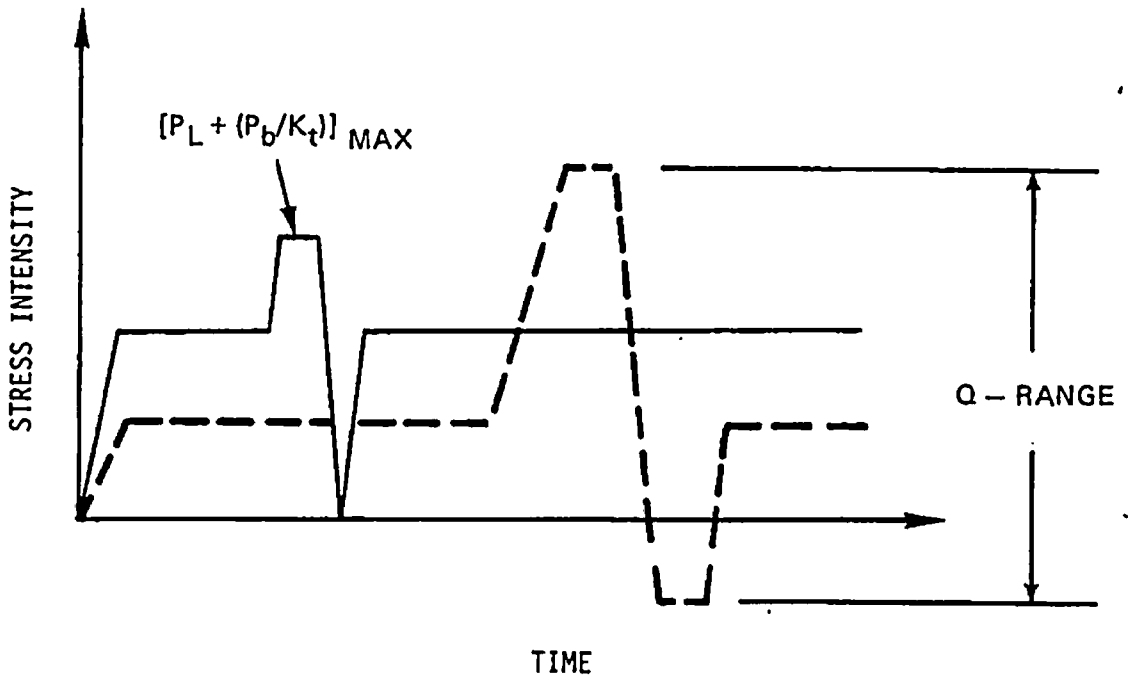

Fig. 18 LOAD HISTORY FOR AN EXAMPLE WITH RATCHETING

the presence of a radial gradient (Point C). If one now applies a pressure cycle which approaches the maximum allowable primary stress, then an incremental deformation can result (D-E). If one now holds the pressure stress until the residual thermal stress relaxes out (E-F), then removes the pressure stress (G), the cycle can be repeated. Applying this to the special case where two separate cycles are defined, one a thermal cycle and the other a pressure cycle, then each of these cycles can be shown to independently satisfy the elastic analysis ratcheting rules and yet, taken together, they will result in incremental deformation.

The interpretation of the rules given in the above example is clearly conservative. If the applied radial thermal gradient is only present for a very short time and no stress relaxation occurs, then the removal of the radial gradient will leave no residual stress to interact with the applied primary stress in the pressure cycle. In extending the elastic analysis rules, the possibility of using different bounding techniques on different cycles was explicitly recognized in the Code Case [T-1324(e)]. Thus it is possible to use inelastic analysis methods to calculate the strains for a selected number of maximum strain cycles provided that one adequately accounts for the interaction effects with the remaining cycles being elastically evaluated.

6.4.4 Experimental and Rigorous Inelastic Analysis Verification of Elastic Ratcheting Rules

An experimental and analytical study of ratcheting in a simple structural component is described in Corum and Sartory (30). A straight pipe from a well-characterized heat of Type 304 Stainless Steel was subjected to a series of thermal down-shocks followed by sustained periods of elevated temperature operation under internal pressure. The test was performed in a special sodium test facility built for the purpose. The inelastic analysis predictions were obtained using a one-dimensional finite-element procedure. Good agreement between the measured and predicted ratcheting behavior was found.

To further validate the upper bound method, an analysis [Pickel et al. (31)] was accomplished which applied the upper bound method to over fifty thin-walled cylinders subjected to sustained

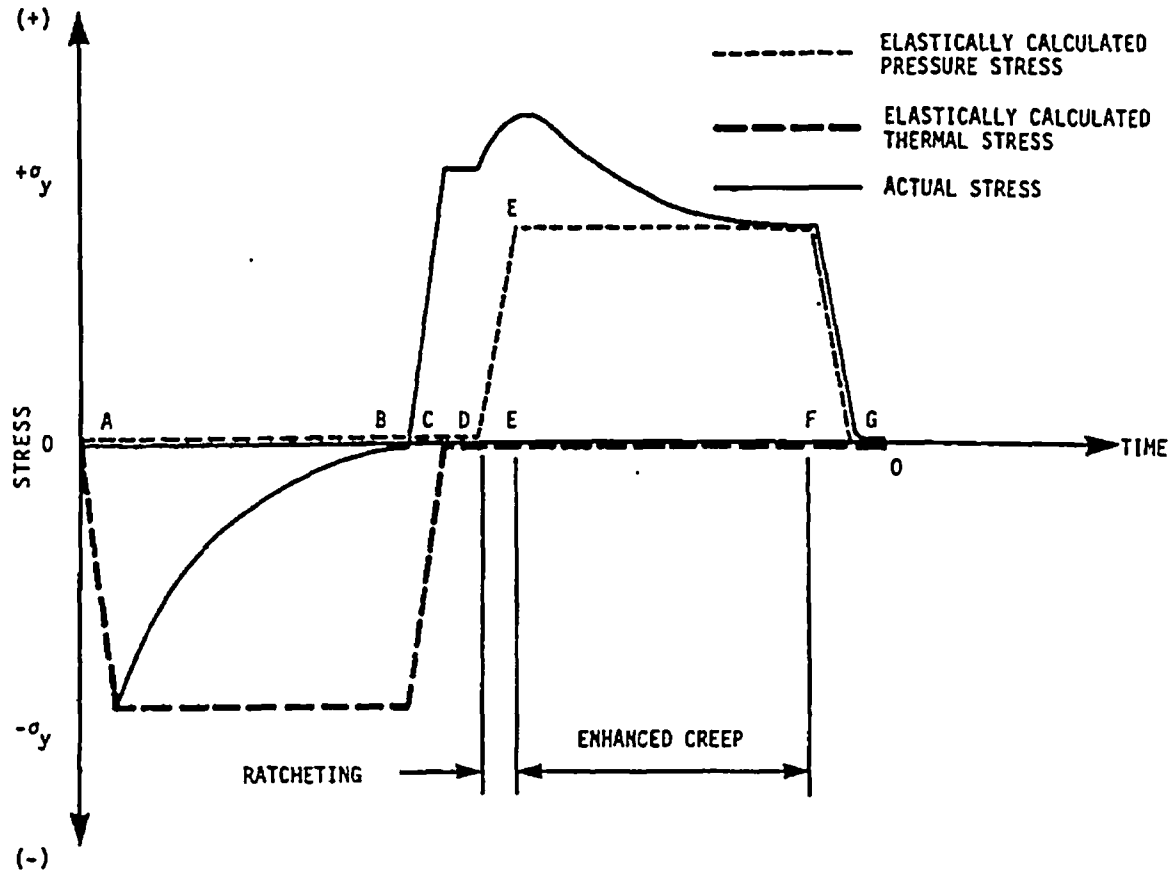

Fig. 19 STRESS HISTORY FOR AN EXAMPLE WITH RATCHETING

primary and cyclic secondary stresses that had been analyzed using a rigorous inelastic finite element computer code. Comparison of results showed the upper bound results to always be conservative relative to the rigorous inelastic analysis results.

7.0 CREEP-FATIGUE

Following a discussion of the correlations and evaluation methods that were considered by the Code Committee, the basis for the interaction rules is presented. Then, the text describes the creep and fatigue design curves, mean stress and multiaxial effects, and the rotating principal strains. Finally, the background and intent of the rules and limits for use with elastic and inelastic analysis are treated.

7.1 CORRELATION AND EVALUATION METHODS

Many theoretical correlations and evaluation methods for creep-fatigue have been proposed during the last twenty years without conclusive evidence that a universal method exists (32)–(46).

Kitagawa and Weeks (47) compare five analytical methods (including the methods of Campbell (39) and Coffin (60)) for correlating the results of hold-time fatigue testing. Linear damage rules using time ratios for creep damage appear to be at least as good as, and perhaps better than, linear damage rules using strain ratios or the frequency-modified fatigue life equation of Coffin (60).

The Committee chose the creep-fatigue interaction approach wherein damage due to creep is accounted for on a time-fraction basis and damage due to fatigue is accounted for by using Miner's cumulative damage criteria. The allowable total damage is based upon observed material behavior and is a function of the calculated damage for both creep and fatigue.

7.2 DERIVATION OF THE CREEP-FATIGUE INTERACTION RULES

Subarticle T-1400 describes the general rules for the damage summation which is used to assess the adequacy of the component to withstand the specified cyclic thermal and mechanical loadings. These rules were originally based on the behavior of AISI Type 304 Stainless Steel when subjected to hold times at peak tensile strain.

Material specimen creep-fatigue tests data covering the effect of hold time on the life of Type 304 Stainless Steel were described in references (48) through (51). Hold times were introduced individually both in the tension and compressive portions of the fatigue cycle and under several different strain rates. The strain rates varied from 6.4×10^{-2} in/in/sec to 4×10^{-6} in/in/sec. Hold times introduced into the fatigue cycles ranged from 0.1 to 600 minutes. Strain ranges varied from 0.25% to 4%; however, most of the strain rate and hold time data were generated on ½% and 2% total strain ranges.

Using data in references (32), (34), (48–51), the effect of hold times introduced into a fixed strain cycle are shown in Fig. 21. Note that a marked reduction in fatigue life is observed when only tensile hold periods are introduced into the fatigue cycle at fixed strain. Fig. 22, taken from references (32), (33), (43), (52) and (53), compares hold time effects for various strain ranges for 2¼ Cr - 1 Mo, 1 Cr - 1 Mo, and 1 Cr - 1 Mo - 0.25 V steels.

It is observed from Figs. 21 and 22 that hold time has significant influence on cyclic life, but mainly in the low strain ranges which are the ranges of most interest to pressure vessel Designers. Most of the available test data are for strain ranges greater than the range of interest to the Designer. It was thus necessary for the Committee to choose a method of correlation and, with this method and the available data, extrapolate to strain ranges and time of interest to the Designer.

The life-fraction rule (T-1411 of Case 1592) was adopted based largely upon a life-fraction evaluation of available data by Campbell (39).

An interaction value was also determined from this evaluation. The life-fraction concept was not based solely on stainless steel behavior. It was also applied by Wundt (40) to very limited test data on 1 Cr - 1 Mo - 0.25 V steel of Krempl and Walker (53), and the general behavior appeared the same as for austenitic steels. Other investigators [references (38), (41), (47)] have applied the life-fraction rule to different alloys as well as austenitic stainless steel and observed similar behavior. Subsequent to providing creep fatigue rules and fatigue curves for austenitic stainless steel in Case 1331-5, an evaluation of Ni-Fe-Cr, Alloy 800H hold time data was made and fatigue curves and a *D* value for this alloy were included in Case 1331-7. The hold time rules for stainless steel were based on 1200 F behavior. Thus, at temperatures lower than 1200 F, the rules were anticipated to be conservative. Subsequent test data at 1000, 1050, and 1100 F [references (55), (56), and (57)] have shown the data to fall within normal scatter, further supporting the Code rules.

7.3 CREEP AND FATIGUE DESIGN CURVES

Equation 5 of T-1411 of Case 1592 or Equation 14 of Cases 1331-5, -6, -7, and -8 is the linear life-fraction relationship discussed previously. The terms are explained in the Case; however, the following additional description is offered.

The Fig. 15 fatigue curves of Case 1331-5, -6, -7, -8, and Fig. T-1420-1 of Case 1592 are design curves. The design curve is constructed by reducing the best-fit curve of continuous cycling

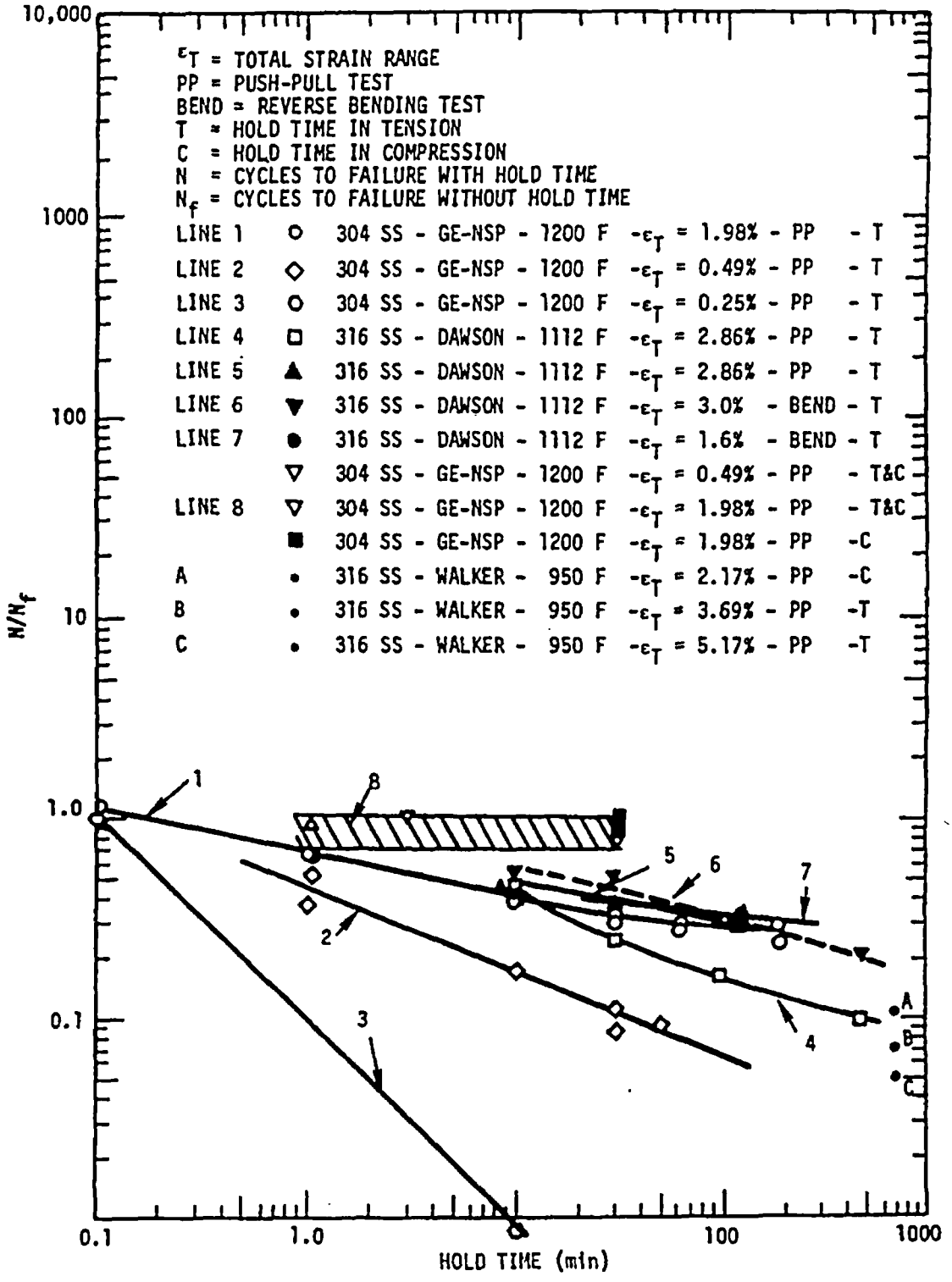

Fig. 21 EFFECT OF HOLD-TIME ON FATIGUE LIFE OF AUSTENITIC STAINLESS STEEL

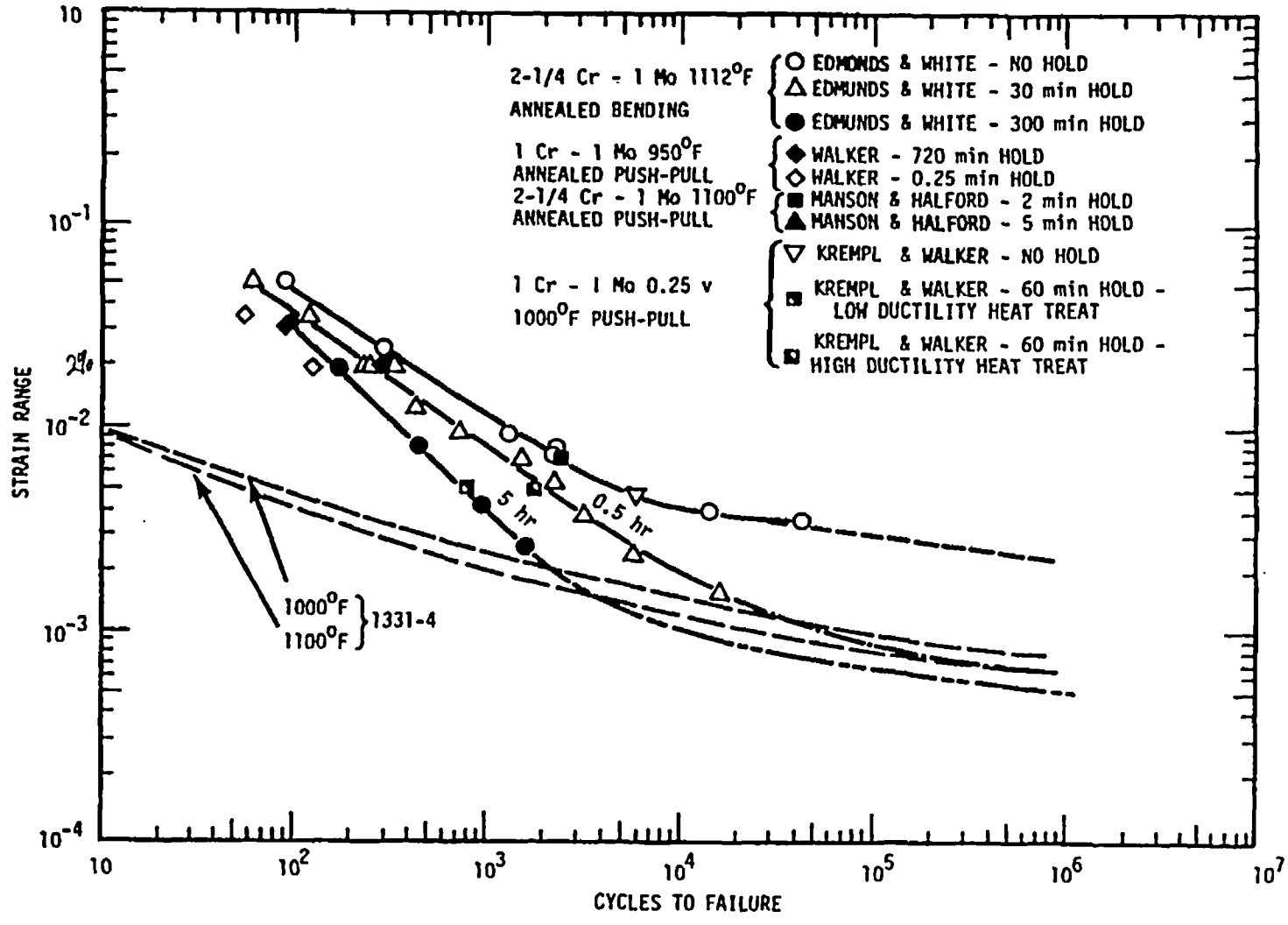

Fig. 22 EFFECT OF HOLD-TIME ON FATIGUE LIFE OF VARIOUS STEELS

fatigue data by a factor of 2 on total strain range or a factor of 20 on life, whichever results in a minimum value. The present curves are higher on the low cycle end than the Case 1331-4 curves. Extra design margin was built into the original 1331-4 curves to account for hold times, slow strain rates and inaccuracy in calculating inelastic strain by elastic methods. The current curves do not contain design margins for the above conditions and these conditions must be evaluated by other steps of the fatigue analysis. Figure 15 and T-1420-1 curves are generally used only for inelastic analysis where strain-time relations are rigorously calculated using appropriate plasticity and creep solution methods. The rigorous inelastic analysis eliminates the need for extra design margin since the strain range can be computed more accurately than by elastic methods. Also, the effects of hold times and slow strain rates are calculated by the second half of Equation 14 and Case 1331-5, -6, -7, and -8 and Equation 5 of Case 1592 using the integral form for creep damage shown in 5.3(b) and T-1420.

Figure 15 and T-1420-1 curves may be used for elastic analysis only for cases of continuous cycling at strain rates equal to or greater than those shown on the fatigue curves. If there are hold times at elevated temperatures or if the cycling is slow, then creep damage is being introduced which is not accounted for in the elastic analysis rules of 5.3(c)(2) and T-1433.

Figure 15 of Case 1331-5, -6, -7, and -8, and T-1420-1 fatigue curves for austenitic stainless steel do not show a difference between 1000 F and 1200 F. Test data from references (48)–(51), and (65) were plotted for temperatures of 800 F, 1200 F, and 1300 F. Data for 1000 F, Jaske et al. (59), appear very similar to the 1200 F data of references (48)–(51). In fact, some of the 1000 F data points fell below the average 1200 F curve. The 1200 F curve was then used as a representative curve from 1000 F to 1200 F. Curves between 800 F and 1000 F were interpolated by linear scaling on the log-log scale since there were no data in-between. The 1300 F data, Brinkman, et al. (65), fell distinctively below the 1200 F data and a separate curve was constructed for 1300 F.

Subsequent to originating the Fig. 15 and T-1420-1 fatigue curves, test data ranging from 800 F to 1200 F, references (55) and (63), indicate a definite difference between 1000 F and 1200 F. Figure 10 of Weeks et al. (55) compares the temperature effect. Fatigue data for Ni-Fe-Cr, Alloy 800H were available from references (57) and (64) for 800 F, 1000 F, 1200 F and 1400 F. Figure 15 and T-1420-1 curves for these temperatures were constructed in the same manner as for austenitic stainless steel. Intermediate temperature curves were interpolated linearly on a log-log scale. Figure 11 curves were constructed using the Fig. 15 and T-1420-1 curves as a base line and modifying them to account for the life reduction associated with slow strain rates and hold times. Figure 11 and T-1430-1 curves are reduced below those in Fig. 15 and T-1420-1 to account for creep damage due to hold times and slow strain rates. The hold-time effect is more severe than the strain rate effect, and thus, the curve is constructed based upon the fatigue life reduction determined for hold times at fixed strains.

The hold-time tests at fixed strain result in pure relaxation, hence the curves in Figs. 11 and T-1430-1 are reduced to account for creep damage due to pure relaxation of peak residual stresses. The relaxation damage is based upon uniaxial test specimen relaxation curves. Creep damage due to primary stresses and the relaxation of secondary stresses is not contained in Fig. 11. This creep damage effect is calculated separately in 5.3(c)(2) and T-1433.

The stress-to-rupture curves, Figs. 16 and I-14.6 (from which the values of T_d are obtained), are minimum stress-to-rupture curves. The factor K' is used to adjust the minimum curve to some other percentage of stress to cause rupture. The K' factor of 0.9 adjusts the curve to about a 89% of the minimum stress-to-rupture curve. In comparison, the primary membrane allowable curve, S_t, is based principally on two-thirds of minimum stress-to-rupture. The primary bending life-fraction summation is based upon a maximum of 1.25 (2/3) or 83 ⅓% of minimum stress-to-rupture by using the factor K_t from Equation 7, 3223(c) as a divisor for the calculated $P_L + P_b$ stress.

7.4 MEAN STRESS AND MULTIAXIAL EFFECTS

Very little data exists for mean stress effects at elevated temperature. Chow et al. (58) contains three data points for the effect of mean stress on high-cycle fatigue and indicates that the effect is small.

For strain-controlled, inelastic cycling, mean stresses tend to cyclically relax to zero. This tendency is more prominent at higher temperatures as shown by comparing Type 304 Stainless Steel data at 1000 F and 1200 F in Jaske et al. (59). In this work it was shown that significant mean stresses can be introduced by variable-amplitude straining. It is also generally known that mean stress effects become more important when the inelastic strains are small and the cyclic life is large.

Adjustment of the fatigue curves for stainless steels to account for mean stress effects was considered using the method described in the ASME Criteria Document for Section III, Class 1 Components (3). Using this *modified Goodman diagram* approach, it was found that no adjustment was indicated. At the end of the fatigue curve (10^6 cycles) plastic straining is still occurring (neglecting cyclic hardening) and the adjusted mean stress is zero.

Weeks et al. (55) indicates that there is very little effect on creep-fatigue life of austenitic stainless steels when a mean strain of up to 1.5% is imposed during the tests. This indicates that the effects of creep ratcheting do not significantly alter the creep-fatigue life when creep ratcheting strains are small. Thus, the Committee has not taken action to modify the fatigue curves for mean stress or strain as there are insufficient data to identify a definite need.

Compressive stresses are considered to be equally as damaging as tensile stresses in computing creep damage. The uniaxial test results of references (48), (49), and (55) would indicate that compressive stresses should be considered less damaging than tensile stresses since strain-controlled low cycle fatigue tests with hold times at fixed strain in compression indicated very little reduction in fatigue life, while tensile hold-time tests indicated a large reduction in fatigue life (Fig. 21). However, the uniaxial loading case does not generally appear in pressure-containing components. The state of stress is most always multiaxial. Until there is additional multiaxial load fatigue data (61), and a method to separate out the compressive strain effects in a general multiaxial stress/strain condition, the Committee chose to use the conservative and simpler approach of treating compressive and tensile strain as equally damaging.

7.5 ROTATING PRINCIPAL STRAINS

The rules for rotating principal strains are based on the applicability of the effective strain range for predicting fatigue behavior in multiaxial stress states. In Manson (62) this is presented in terms of the principal strains as

$$\Delta\epsilon_{equiv} = \frac{\sqrt{2}}{3}\left\{[\Delta(\epsilon_1 - \epsilon_2)]^2 + [\Delta(\epsilon_2 - \epsilon_3)]^2 + [\Delta(\epsilon_3 - \epsilon_1)]^2\right\}^{1/2}$$

which can be rewritten as

$$\Delta\epsilon_{equiv} = \frac{\sqrt{2}}{3}[(\Delta\epsilon_1 - \Delta\epsilon_2)^2 + (\Delta\epsilon_2 - \Delta\epsilon_3)^2 + (\Delta\epsilon_3 - \Delta\epsilon_1)^2]^{1/2}$$

where the algebraic strain (positive for tension) must be used in calculating the change in strain $\Delta\epsilon_i$. However, when the principal directions change during the cycle, the analysis must consider the six strain components. That is, the equivalent change in strain is calculated from the change in strain component from some reference time, t_{ref}.

$$\Delta\epsilon_x(t) = \epsilon_x(t) - \epsilon_x(t_{ref})$$

$$\Delta\epsilon_y(t) = \epsilon_y(t) - \epsilon_y(t_{ref})$$

etc.

The equivalent change in strain at any time during the fatigue cycle is

$$\Delta\epsilon_{equiv}(t) = \frac{\sqrt{2}}{3}[(\Delta\epsilon_x - \Delta\epsilon_y)^2 + (\Delta\epsilon_y - \Delta\epsilon_z)^2 + (\Delta\epsilon_z - \Delta\epsilon_x)^2 + \frac{3}{2}(\Delta\gamma_{xy}{}^2 + \Delta\gamma_{yz}{}^2 + \Delta\gamma_{zx}{}^2)]^{1/2}$$

The fatigue damage is estimated based on the maximum equivalent change in strain. This may require the calculations at several times during the cycle when the external conditions are not obvious.

At the present time there are no test data for fatigue under changing principal directions to confirm the validity of the above approach. However, the above approach reduces to

$$\Delta\epsilon_{equiv} = \Delta\epsilon_1$$

for uniaxial tests with large plastic strains ($\epsilon_2 = \epsilon_3 = 0.5\epsilon$). It also provides improved agreement with the change in stress intensity approach at low temperature. This was considered desirable to reduce any discontinuity of the design criteria at the limits of applicability of Subsection NB of Section III.

7.6 RULES AND LIMITS FOR USE WITH INELASTIC ANALYSIS

From the inelastic analysis, the stress-strain-time relationships are determined. The linear life-fraction summation of creep damage may then be represented by an integral form

$$\int_0^t \frac{dt}{T_d}$$

The original inelastic rules contained in Case 1331-5 were based on the behavior of austenitic stainless steel described in Conway (48) and the analysis of these data which was documented in Campbell (39). Only 1200 F tests data were available so it was assumed that the creep-fatigue interaction for other temperatures would be the same as that at 1200 F. Test data from references (55) and (63) at 1100 F support this original assumption. Figure 23 reproduced from Campbell (39) plots the original 1200 F failure data. Figure 24 shows a bilinear trend curve generated by a statistical evaluation of the Conway (48) data and documented in Campbell (39). From this data the *D* value for austenitic stainless steel was derived for Case 1331-5.

Figure 25 [reproduced from Brinkman et al. (63)] compares actual failure data at 1100 F with design allowable points of Case 1592. It can be seen that there is considerable scatter and the design factor on life varies from a minimum of approximately four to greater than 40. Figure 26 [reproduced from Weeks et al. (55)] shows the distribution of design factor in bar form for Type 304 Stainless Steel at 1100 F. The design factor ranges from about 7 to 40 for tests where hold times in tension only were introduced. With hold times in compression, the design factor on life increases significantly. This difference in life for tension versus compressive hold-time stresses was discussed previously.

When Ni-Fe-Cr, Alloy 800H was introduced into Case 1331-7, data at 1000, 1200 and 1400 F contained in Jaske et al. (64) were analyzed in Corum (54) in the same manner as was done in Campbell (39) for austenitic stainless steel. Figure 27 taken from Corum (54) shows considerably more scatter than for austenitic stainless steel. The creep-fatigue interaction curve, Fig. 27, shows that a *D* value of unity was reasonable.

Examination of Fig. 27 reveals that, when damage is primarily due to creep, the *D* value of unity is more conservative.

7.7 RULES AND LIMITS FOR USE WITH ELASTIC ANALYSIS

Elastic analysis rules and limits for creep-fatigue evaluation were intended to be more conservative than inelastic rules. To effect this, a number of assumptions, techniques, and rules were

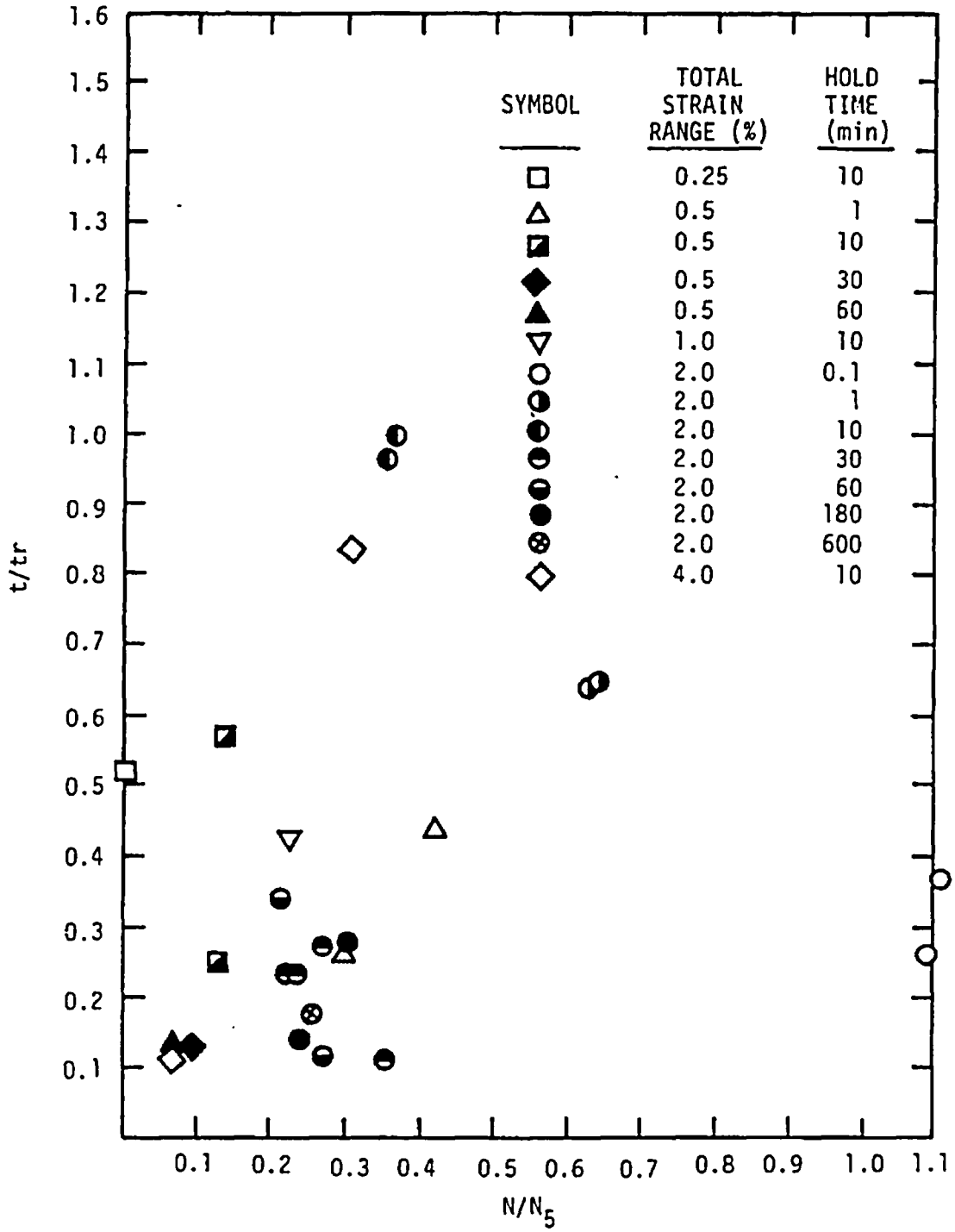

Fig. 23 CREEP vs. FATIGUE DAMAGE AT 5% LOAD DROP-OFF, TYPE 304 STAINLESS STEEL AT 1200 F [Campbell (39)]

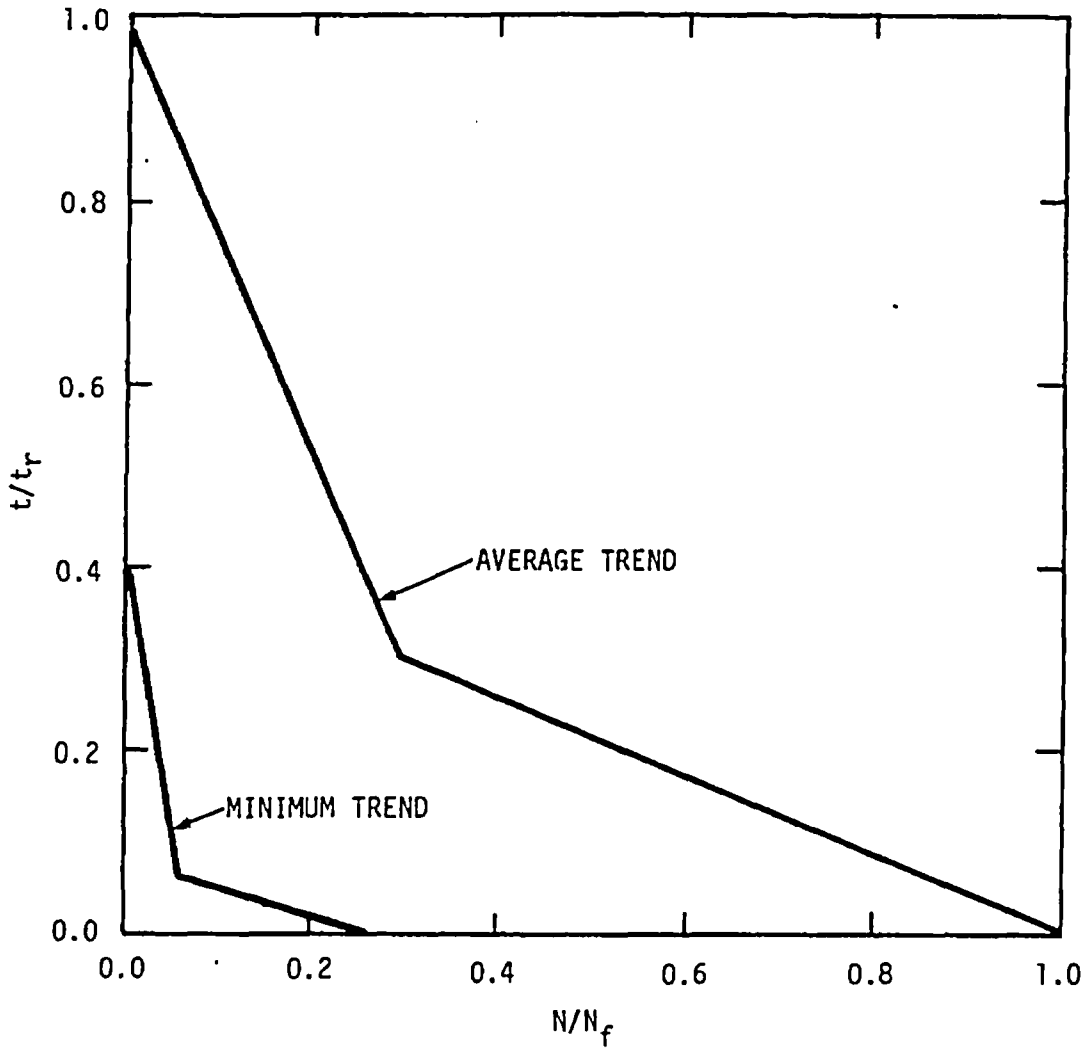

Fig. 24 AVERAGE AND MINIMUM TREND CURVES FOR CREEP-FATIGUE INTERACTION FOR TYPES 304 AND 316 STAINLESS STEELS

employed. These are listed below.

(1) Adjusted fatigue curves were developed to account for creep damage due to peak stress relaxation during hold times and slow strain rates.
(2) A technique was developed for determining the maximum strain range in the presence of inelastic deformation for use with the fatigue curve.
(3) Rules were established for evaluating the creep damage due to secondary and primary stresses.
(4) The rule for determining combined creep-fatigue damage was established.

Most of the above assumptions, techniques, and rules are quite conservative.

To obtain adjusted fatigue curves that incorporate creep damage due to relaxation of peak stresses, the continuous-cycling fatigue curves for use with inelastic analysis were used for the

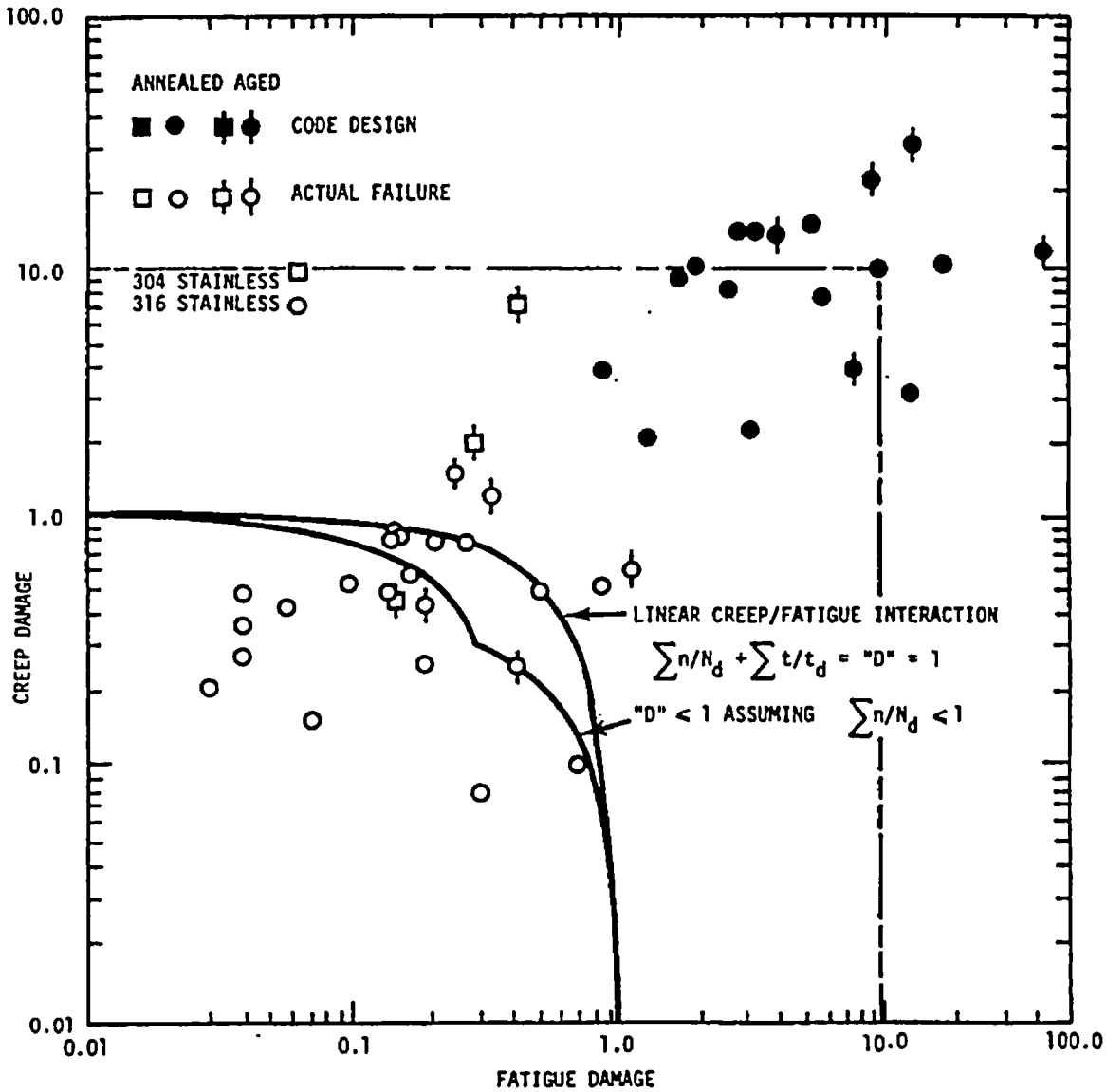

Fig. 25 COMPARISON OF CODE CREEP-FATIGUE ALLOWABLES TO EXPERIMENTAL DATA

unadjusted baseline data. This data is given in Fig. 15 of Case 1331-5, -6, -7, -8 and Fig. T-1420-1 of Case 1592. The fatigue curves were constructed in the same manner as was done for the lower temperature Section III curves incorporating a design factor of 2 on strain range or 20 on cycles, whichever is less.

7.7.1 Adjustment of Fatigue Curves

In order to determine the effects of slow strain rates and hold times, the fatigue-life-reduction factors were plotted from available data [references (48) through (51) for austenitic stainless steels, and references (57) and (64) for solution annealed Ni-Fe-Cr, Alloy 800H]. Such plots for

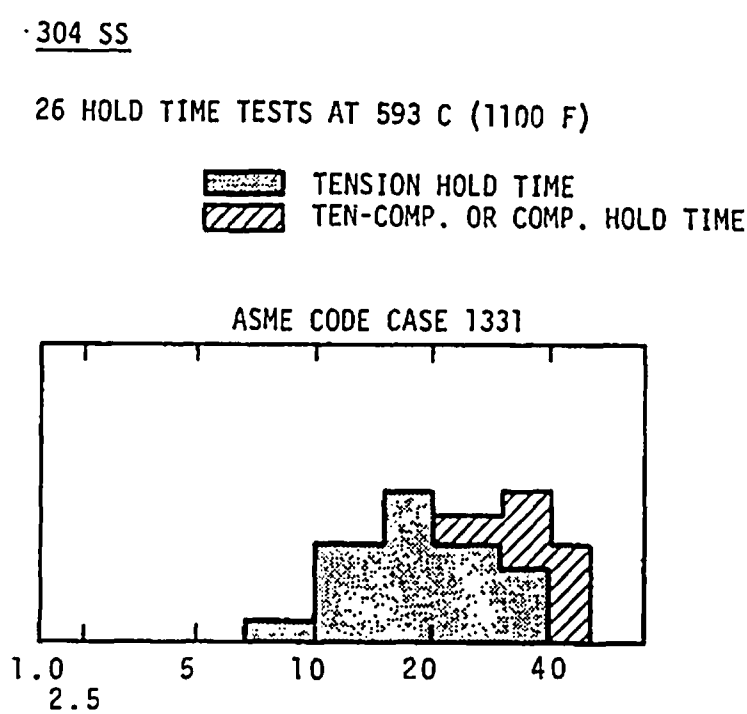

Fig. 26 DISTRIBUTION OF ACTUAL-TO-CALCULATED LIFE RATIOS FOR STRAIN-CONTROLLED CREEP-FATIGUE TEST SPECIMENS

austenitic stainless steel are shown in Figs. 28 and 29. The fatigue design curves are based on a strain rate of 10^{-3} in/in/sec or 3.6 in/in per hr. It was assumed that at 10^{-3} in/in/sec strain rate, the damage mechanism was pure fatigue or that any creep damage included in the data would be already built into the fatigue curves. Therefore, the fatigue-life-reduction factor was defined to be equal to 1.0 at a strain rate of 10^{-3} in/in/sec. All the data points in Fig. 28, with the exception of one for $\dot{\epsilon} = 4 \times 10^{-6}$ in/in/sec, span two orders of magnitude in strain rate.

The fatigue-life-reduction versus hold-time curves in Fig. 29 are derived from actual data in Conway (48) and Berlinz and Conway (49) for Type 304 Stainless Steel at 1200 F. Extension of the curves beyond data points was accomplished by analytically extending the relaxation curves of Conway (48) and computing creep damage by

$$\int_0^t \frac{dt}{t_r}.$$

The equation used in Campbell (39) and Conway (48) to fit the relaxation curve was used to extend the curves for longer hold times.

Figure 29 shows data points used to plot the fatigue-life-reduction curves. Open points are for actual test data and solid points are for computed values. Since strain ranges greater than 0.01 will rarely be encountered in actual service, the curve for $\epsilon_T = 0.01$ was used for $\epsilon_T \geqslant 0.01$.

The fatigue-life-reduction curve for $\epsilon_T = 0.001$ was constructed using part of the relaxation curve for $\epsilon_T = 0.0025$. It was desirable to use relaxation curves for the actual strain range in question; however, there were no available data on $\epsilon_T = 0.001$. Use of the lower portion of a

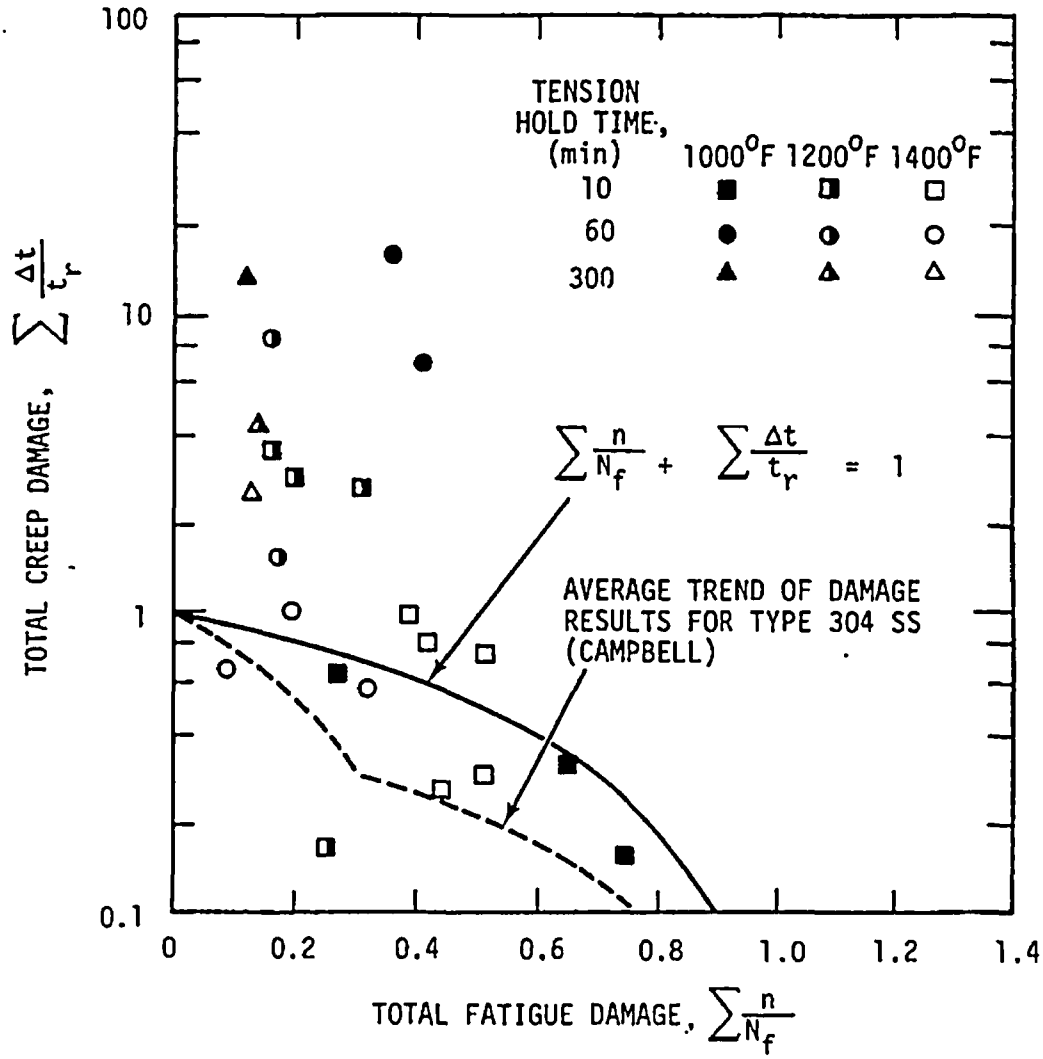

Fig. 27 CREEP-FATIGUE DAMAGE INTERACTION FOR TENSION HOLD-TIME TESTS OF SOLUTION ANNEALED Ni-Fe-Cr, ALLOY 800H

0.25% relaxation curve for the $\epsilon_T = 0.001$ relaxation curve should be, if anything, conservative since examination of relaxation curves for higher strain ranges shows that strain hardening slows down the relaxation process, thus increasing calculated creep damage for this case.

The maximum fatigue-life-reduction factors for hold-time effects given in Fig. 29 determined the actual curve used to modify Fig. T-1420-1 to obtain Fig. T-1430-1 in the Code Case. All test data indicate that the hold-time effects are more significant than slow strain rate effects. Hence, the fatigue-life-reduction curves generated for hold-time effects were used to construct Fig. T-1430-1 of the Code Case.

The low cycle end of Fig. T-1430-1 was constructed by reducing the number of cycles to failure for a given strain range in Fig. T-1420-1 by the maximum life-reduction factors for hold-time effects. The high cycle end of Fig. T-1430-1 was constructed in a different manner. The fatigue curves of Fig. T-1420-1 of the Code Case were extended at a slope of −0.12 on a log-log scale.

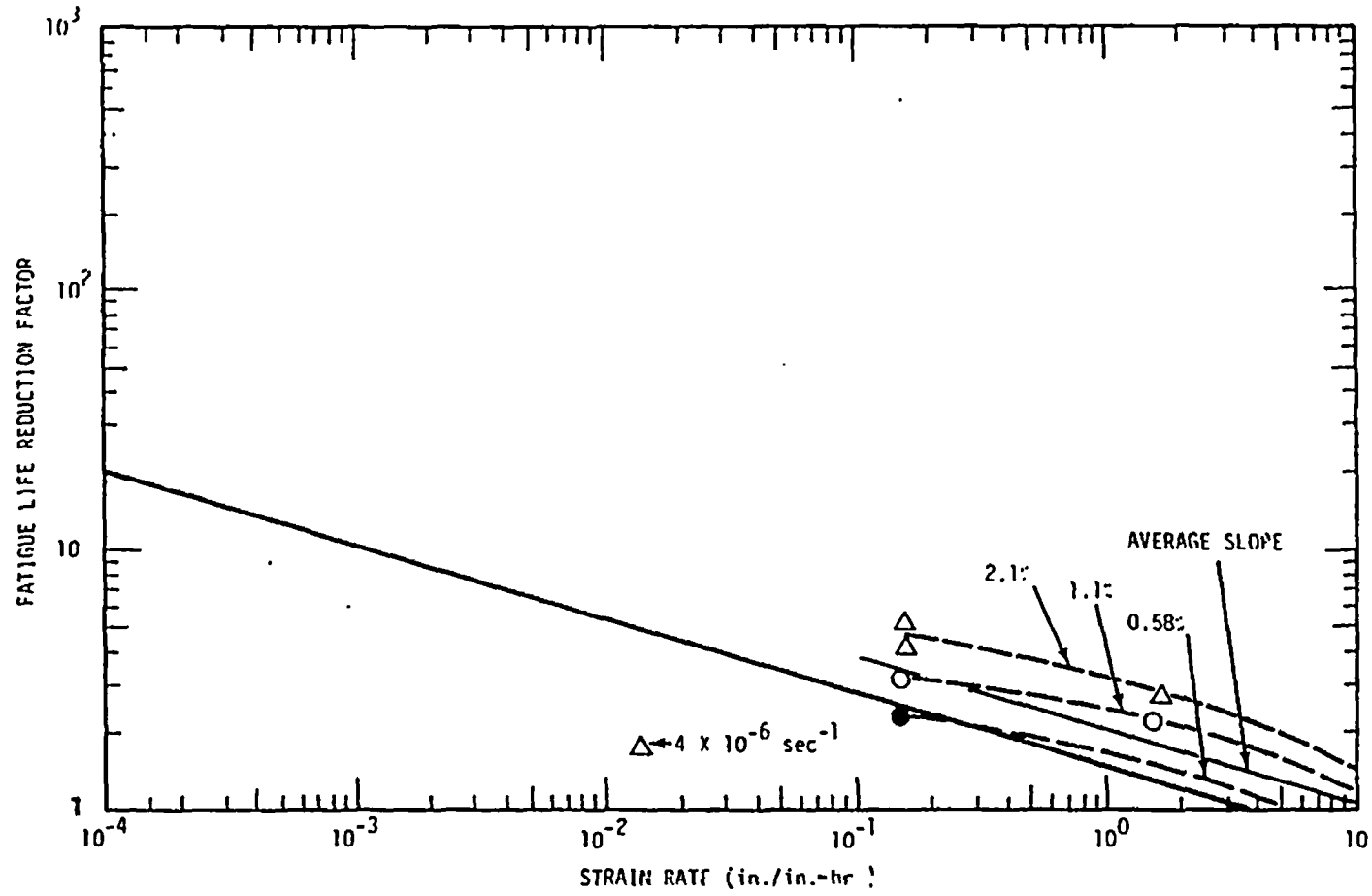

Fig. 28 STRAIN RATE EFFECTS ON FATIGUE LIFE REDUCTION

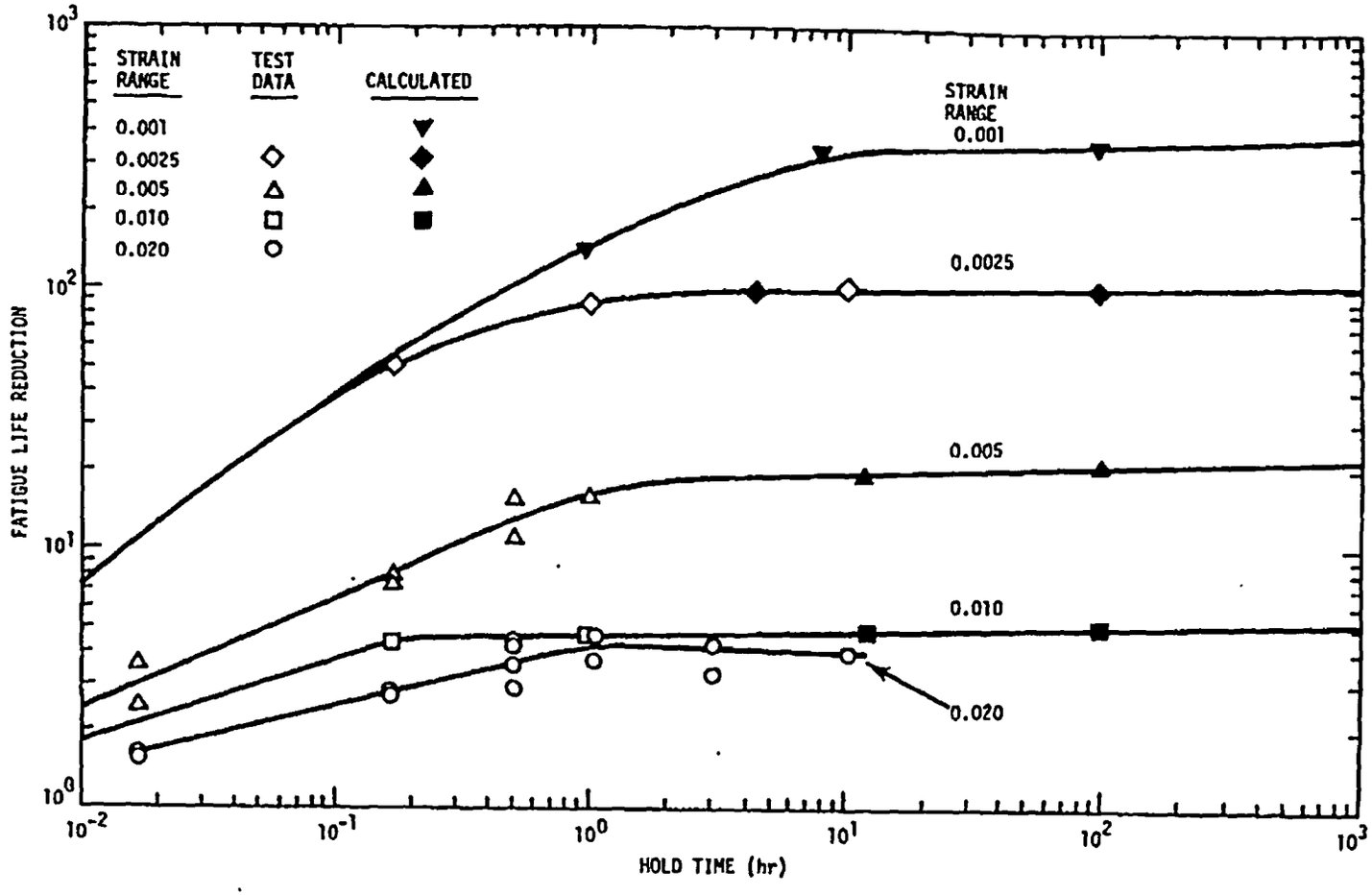

Fig. 29 HOLD-TIME EFFECTS ON FATIGUE LIFE REDUCTION FOR TYPES 304 AND 316 STAINLESS STEEL

Then, the fatigue-life-reduction factors from Fig. 29 were used to establish the high cycle end of the Fig. 11 and T-1430-1 fatigue curves of the Cases 1331 and 1592, respectively. Fatigue curves for Ni-Fe-Cr, Alloy 800H were generated in a similar manner.

7.7.2 Maximum Strain Range Prediction Equation for Use With Elastic Analysis

Strain concentrations significantly larger than the elastically calculated stress concentrations can occur when gross yielding or creep strains are occurring in the material surrounding local concentrations. In a low temperature Section III (NB-3000) design, this is prevented by the use of basic stress limits which assure shakedown to elastic action, or else a strain-concentration factor has to be applied to the elastically calculated stress-intensity range prior to entering the fatigue curve. This strain-concentration factor is based on the shape of the stress-strain curve. An extension of this method into the creep range using isochronous stress-strain curves was attempted. Unfortunately, this Section III simplified elastic-plastic approach appeared to be unconservative in some cases. The Committee then undertook the evaluation and correlation of the Krempl (66) test data using the Stowell (67) and Neuber (68) methods of predicting strain concentrations.

Test data, elastic-plastic finite element analysis, and the methods of Neuber and Stowell were compared. It was concluded that use of either the Neuber or the Stowell relationship for predicting strain in a notch (when the gross section is inelastic) is conservative. Mowbray and McConnelee (69) and Topper and Gowda (70) give further justification for the applicability of the Neuber method. The use of Neuber or Stowell equations with isochronous stress-strain curves was thus deemed to be conservative and represent methods by which elastic analysis may be used to compute peak strains in the creep range.

Application of either the Neuber or Stowell methods requires an iterative solution technique, a feature not desired for ASME Code rules. Therefore, an equation not requiring iteration was developed to simplify the calculation and yet maintain conservatism when the net section is undergoing inelastic strain due to creep or plasticity. The equation developed and given as Equation 16 of Case 1331-5, -6, -7, -8, and Equation 7 of T-1432 of Case 1592 is as follows:

$$\epsilon_T = K_\epsilon \epsilon_e + K_\epsilon^2 \epsilon_p + K_T \epsilon_F$$

where

ϵ_T = the derived maximum strain for the loading condition
ϵ_e = the elastic strain in the region under consideration, exclusive of strain concentrations
K_ϵ = the theoretical elastic strain-concentration factor
ϵ_p = the inelastic strain in the region under consideration, exclusive of strain concentrations and peak thermal strains
ϵ_F = peak thermal strain associated with the peak thermal stress intensity as defined in Section III
K_T = strain-concentration factor applied to peak thermal strain component, ϵ_F

The value, ϵ_p, is determined by subtracting the elastic strain component; ϵ_e from the calculated total nominal strain. The total nominal strain, ϵ_n, is the sum of the load-controlled strain and deformation-controlled strain, exclusive of strain concentration and peak thermal strain. The load-controlled strain is determined by entering the appropriate isochronous stress-strain curve at a stress intensity equivalent to the load-controlled stress intensity in the region under consideration. The deformation-controlled strain is determined from the elastically calculated stress intensity due to the applied deformation.

$$\epsilon_n = \epsilon_{\text{load-controlled}} + (S_{\text{strain-controlled}}/E)$$

This maximum strain range equation becomes very conservative if there is significant inelastic behavior in the net section. However, it was judged that proper design would not produce

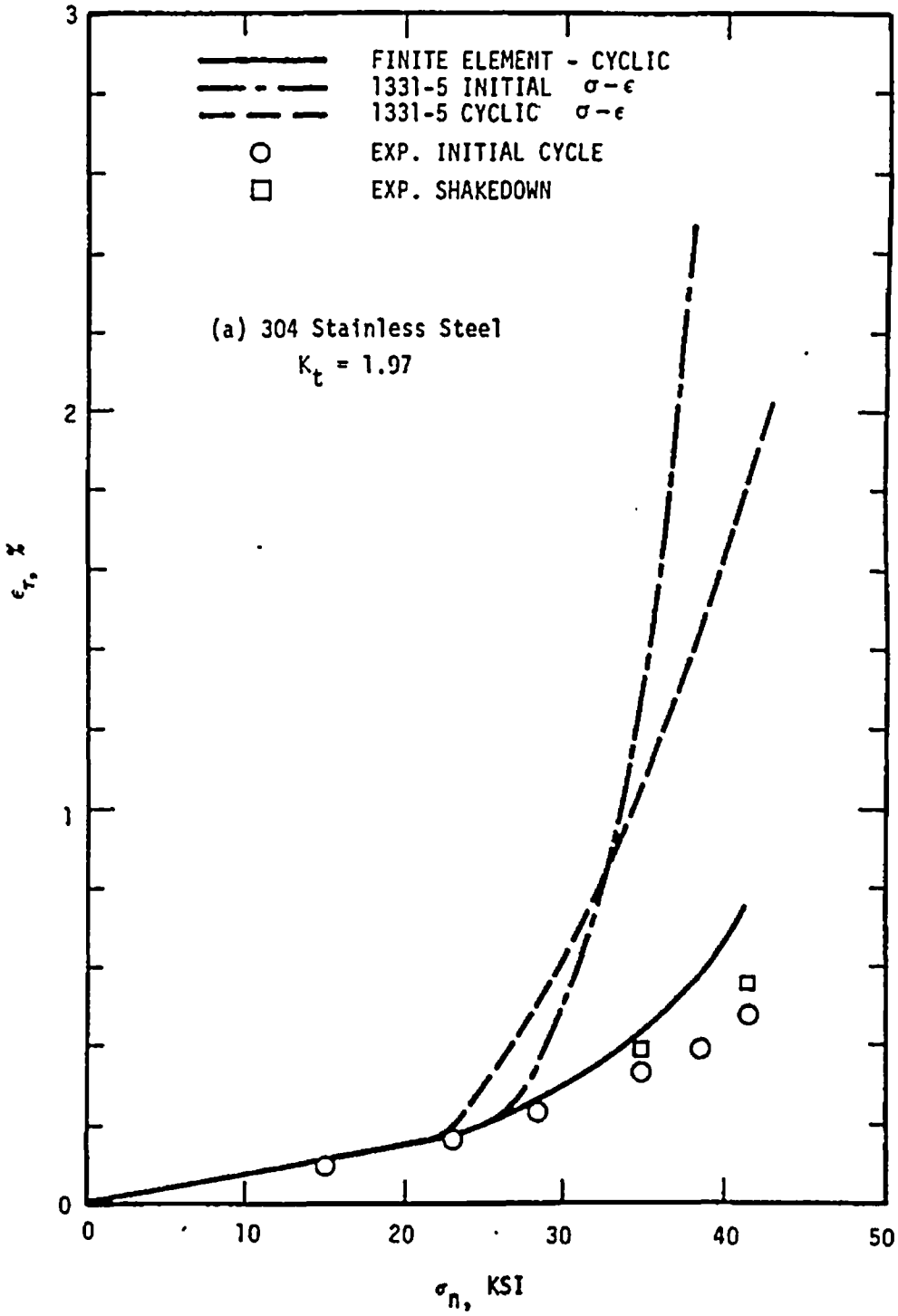

Fig. 30(a) COMPARISONS OF ANALYTICAL AND EXPERIMENTAL STRAIN RANGES FOR A NOTCHED BAR

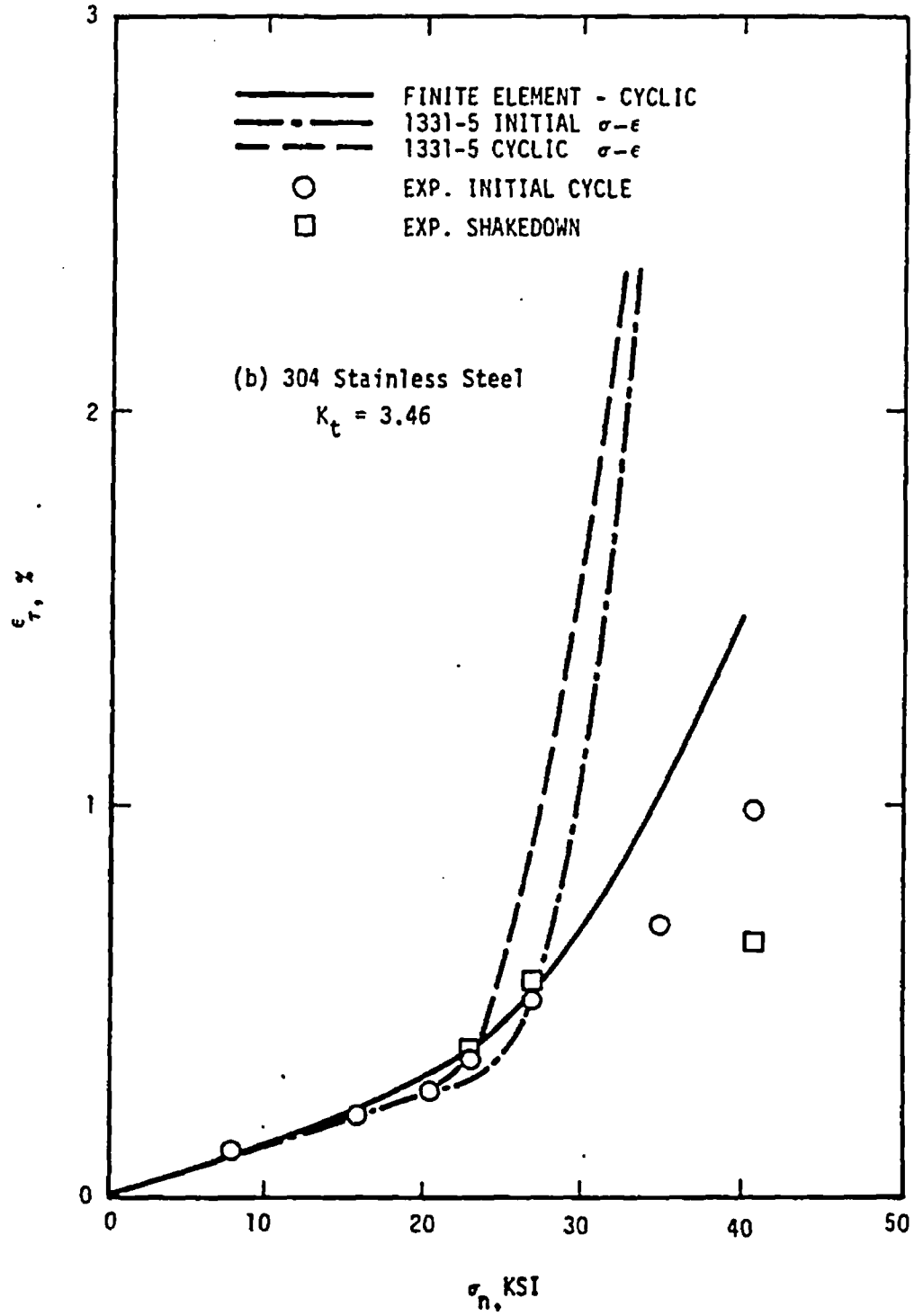

Fig. 30(b) COMPARISONS OF ANALYTICAL AND EXPERIMENTAL STRAIN RANGES FOR A NOTCHED BAR

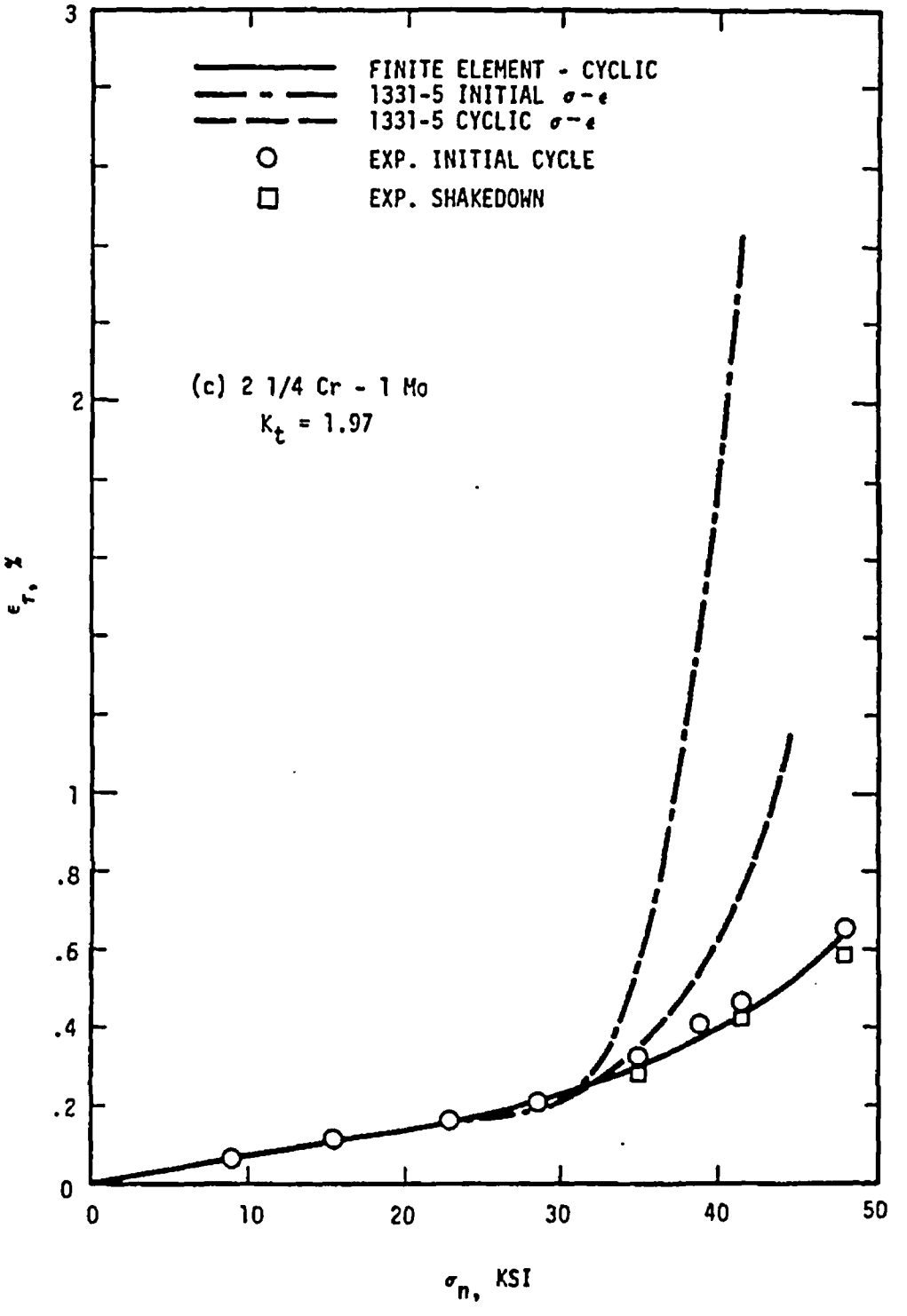

Fig. 30(c) COMPARISONS OF ANALYTICAL AND EXPERIMENTAL STRAIN RANGES FOR A NOTCHED BAR

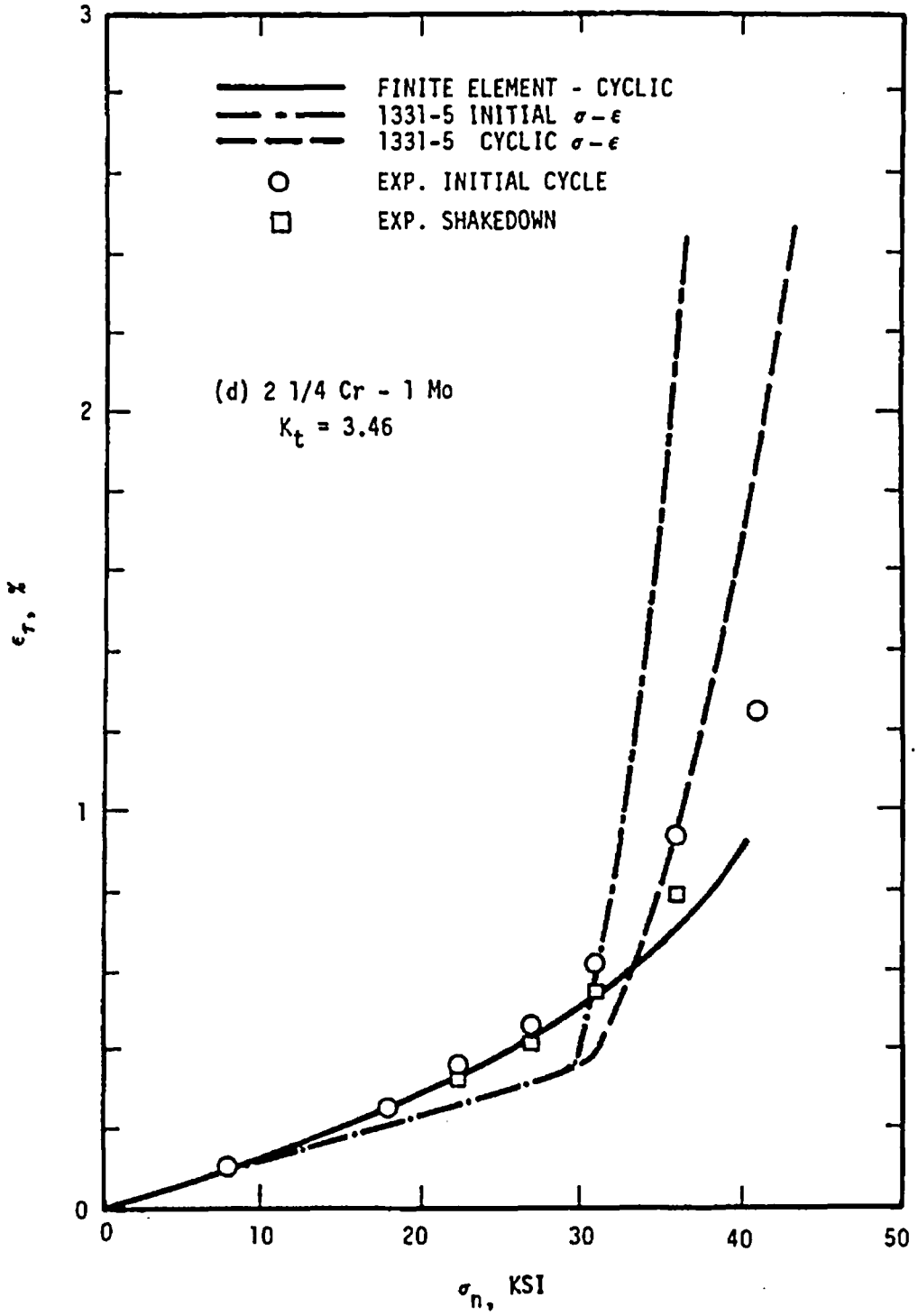

Fig. 30(d) COMPARISONS OF ANALYTICAL AND EXPERIMENTAL STRAIN RANGES FOR A NOTCHED BAR

significant gross inelastic behavior except for a very few infrequent and severe events, hence the apparent extra conservatism should not be detrimental to the design of components. Figures 30(a) through (d) gives a typical comparison of the Code Case equation, the Neuber equation, experimental data, and finite element analysis results.

When Case 1331-5 was published, the maximum strain range prediction equation contained only two terms:

$$\epsilon_T = K_e \epsilon_e + K_e^2 \epsilon_p$$

This resulted in extra large and unwarranted design factors when a skin-type peak thermal strain occurs from a thermal transient and the skin effect is small in comparison to the size of the geometric discontinuity. With the release of Case 1331-7, the equation was expanded to separate out the peak thermal strain from the remainder of the inelastic strain (ϵ_p). There is no guidance in the Code Case for determining what value K_T should have; K_T would normally be 1.0 for smooth surfaces, but in the case where there are surface irregularities that are small in comparison to the skin effect depth of the peak thermal strain, there should be a value of $K_T > 1.0$ applied. In the case of a weld which is not ground flush, an appropriate K_T should be applied.

Case 1331-5 required that all welds meet stringent contour requirements analogous to the flush weld requirements for Section III. Upon the release of Case 1331-7, the weld contour control was relaxed but a stress analysis of the finished joint was required using stress-concentration and strain-concentration factors appropriate for the worst surface geometry. The ASME Code does not tabulate stress-concentration and strain-concentration factors for welds or other discontinuities except for those included in piping stress indices. The Designer must determine his own K_T and K_e factors and justify them in the Stress Report.

7.7.3 Elastic Analysis Rules for Evaluating Creep Damage Due to Primary-plus-Secondary Stresses

As discussed previously, the fatigue curves for use with elastic analysis are adjusted to account for creep damage during pure relaxation of peak residual stresses. Creep damage from primary and secondary stresses are evaluated separately. The rules established in the Code Case use the time-fraction approach of

$$\sum_i \left(\frac{t}{T_d}\right)_i$$

for determining creep damage.

Consider the following simplified loading histogram.

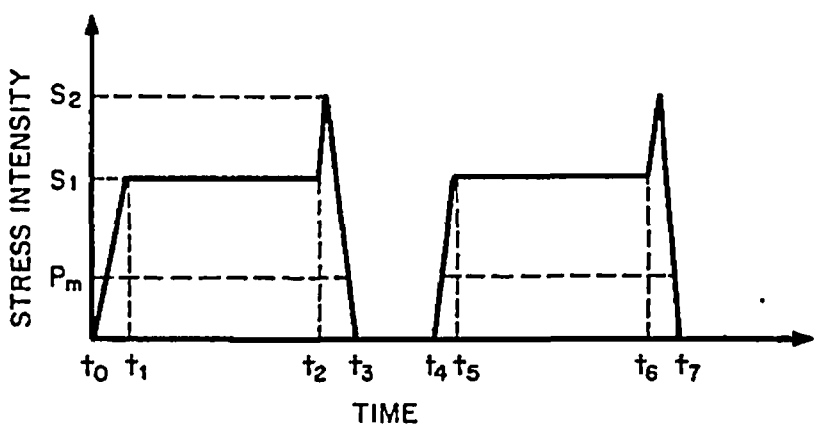

P_m = primary stress intensity
S_1 = sustained primary-plus-secondary stress intensity for sustained operating conditions between cycles
S_2 = transient primary-plus-secondary stress intensity

Case 1331-8 and Case 1592 specified that creep damage from primary-plus-secondary stresses resulting from sustained operating conditions between cycles be evaluated by considering that the stress intensity used for obtaining T_d be the lesser of the minimum specified yield strength of the material under evaluation, or $P_m + 0.5\ S_r$, where $S_r = S_1$ because only the sustained operating conditions between cycles are evaluated.

In Case 1331-5 the stress used for creep damage evaluation was different than that described above. Paragraph 5.3(c)(3) of Case 1331-5 required that creep damage from primary and secondary stresses shall be evaluated with no differentiation between sustained and transient conditions. For Case 1331-5 the stress intensity to be used for obtaining T_d would be the minimum specified yield strength, or $P_m + 0.5\ S_r = S_2$ on the previous figure since all operating conditions during the cycle are considered.

The philosophy and assumptions that were used to arrive at the above rules are further discussed below.

Relaxation of residual stresses due to mechanical and thermal loading are a function of the temperature, primary stress, prior strain history, and elastic follow-up. Since the above effects cannot be assessed by elastic analysis, it was assumed in Case 1331-5 that the secondary stresses would not relax during the cycle and that the creep damage must be assessed as though the stresses were primary. The maximum calculated elastic primary-plus-secondary stress intensity is not, however, a realistic stress intensity to use for creep damage since the material will yield and the stresses will redistribute. Hence, the stress to be used was assumed to be the lesser of σ_y or $P_m + 0.5\ S_r$. The assumption implies that if $(P_L + P_b + Q)$ range is greater than $2\sigma_y$, the maximum practical stress that can be sustained during a hold period is σ_y. If $(P_L + P_b + Q)$ range is less than $2\sigma_y$, then after a few repeated cycles the stress will redistribute to a value of approximately $P_m + 0.5\ S_r$, where S_r is the maximum range of $(P_L + P_b + Q)$.

With the issuance of Case 1331-7 and -8, the wording was changed so as to consider only the $P_L + P_B + Q$ for sustained operating conditions in order to remove some of the conservatism inherent in Case 1331-5. The logic behind the change was that residual secondary stresses caused by short-term thermal and mechanical transients would relax just the same as peak stresses relax, and creep damage due to the relaxation process would already be accounted for by use of the Fig. 9 (or Fig. T-1430-1 in Case 1592) fatigue curve. The only additional creep damage of concern would involve primary-plus-secondary stresses due to sustained mechanical or thermal loading. In this situation the secondary stresses are conservatively assumed to not relax.

7.7.4 Rules for Determining Allowable Creep-Fatigue Damage for Use With Elastic Analysis

The combined creep-fatigue damage allowable was set at $D = 1.0$ in the cumulative damage equation of

$$\sum_{i=1}^{p}\left(\frac{n}{N_J}\right)_i + \sum_{k=1}^{q}\left(\frac{t}{T_d}\right)_k \leq D$$

The value of D was chosen to be unity for use with the elastic analysis creep-fatigue rules. It was felt that the conservatisms already inherent in the adjusted fatigue curves and the creep damage rules were sufficient to obviate the need for a reduced value of D as in the inelastic creep-fatigue rules.

The procedures used to evaluate the creep-fatigue damage are straightfoward for simple shapes and loading such as a notched bar subjected to alternating tension and compression, but be-

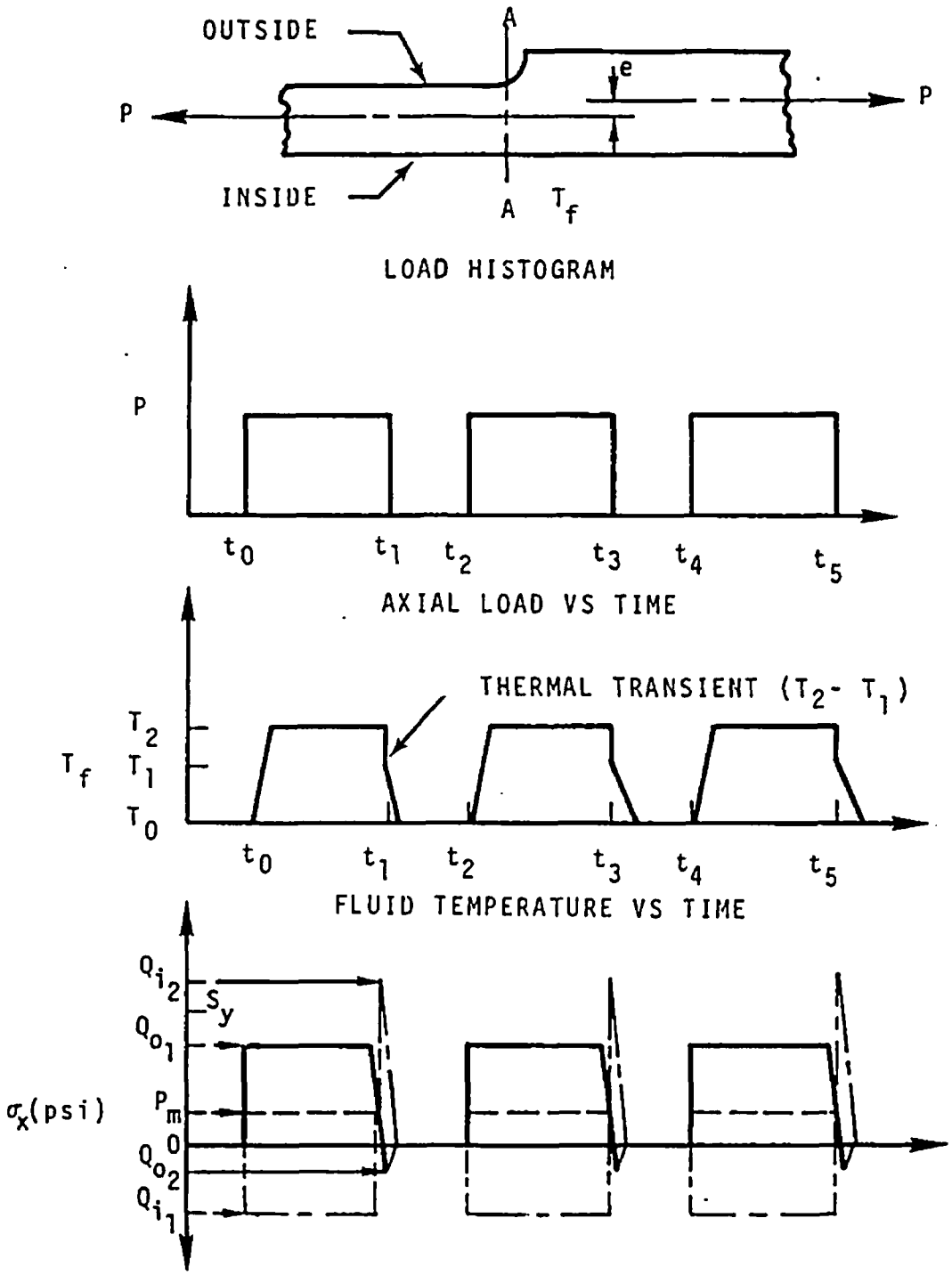

Fig. 31 SAMPLE PROBLEM IN PLANE STRESS

P = LOAD

T_f = FLUID TEMPERATURE

e = ECCENTRICITY OF LOAD PATH

$M_p = Pe$

M_T = THERMAL MOMENT = $\frac{S}{t^2}\int_0^t \cdot_{\alpha} y\, dy$

$\cdot$ = STRESS INTENSITY = $\cdot_{\alpha}$

S_y = YIELD STRESS

S_{LC} = LOAD-CONTROLLED STRESS INTENSITY = P/A

S_{DC} = DISPLACEMENT CONTROLLED STRESS INTENSITY = $\frac{M_p C}{I} + \frac{M_T C}{I}$

K_t = THEORETICAL ELASTIC STRESS CONCENTRATION FACTOR K_t FOR THE FILLET

ϵ_{LC} = LOAD-CONTROLLED STRAIN FROM ISOCHRONOUS STRESS STRAIN CURVE

ϵ_{DC} = DISPLACEMENT CONTROLLED STRAIN, S_{DC}/E.

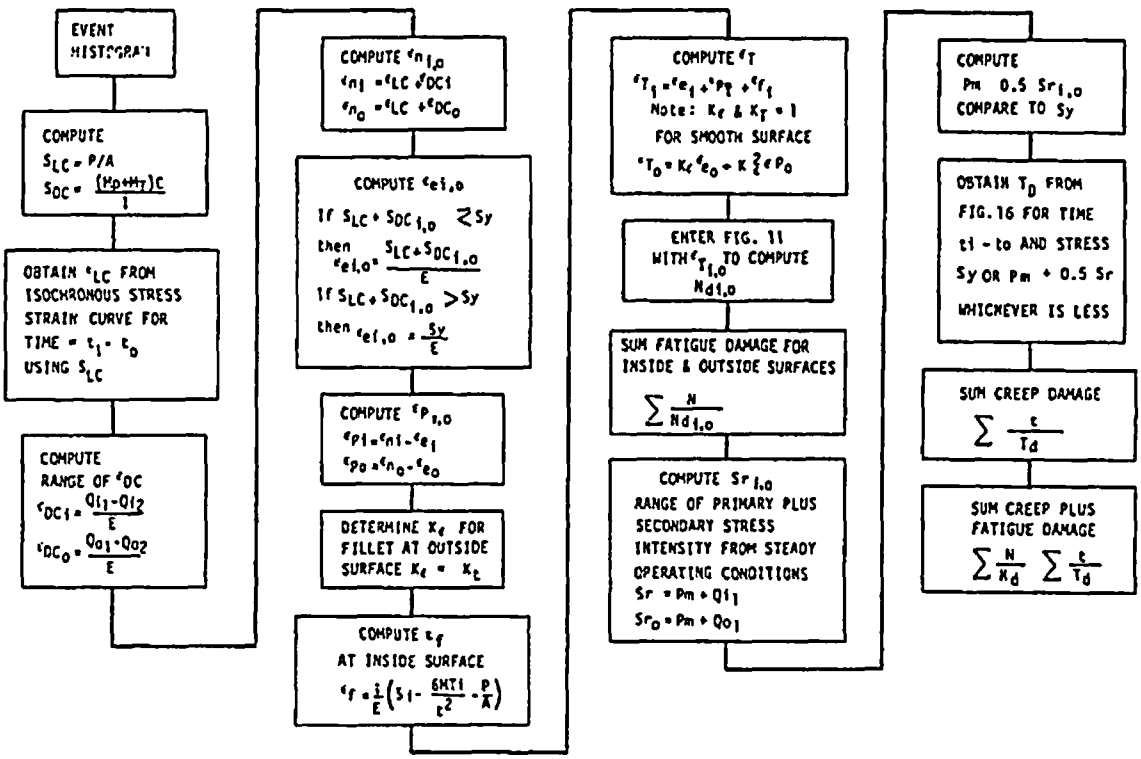

Fig. 32 ANALYSIS FLOW DIAGRAM

comes much more difficult when the component geometry and loading history are complex. Thus, a flow chart for an example problem, which exercises all the features of the elastic analysis procedures but does not contain the complexity of multiaxial geometry and loading, is presented in Figs. 31 and 32.

8.0 DESIGN RULES AND LIMITS FOR BUCKLING AND INSTABILITY

The buckling and instability design limits given in Case 1592 differ fundamentally from those provided in Section III in two ways:

(1) Section III provides charts for determining allowable stresses in spherical shells and cylindrical shells with or without stiffening rings loaded by external pressure, and for determining allowable stresses in cylindrical shells under axial compression. Design limits are not provided for other configurations or other loading conditions. Case 1592 provides minimum design factors for calculated buckling loads or times for any case where instability due to compressive loads or strains may be a possible failure mode. However, it does not provide methods or charts for calculating buckling loads for specific cases.

(2) The design charts of Section III include the effects of initial imperfections, where appropriate, and the effects of temperature upon the short-time stress-strain curve but do not account for the effects of creep. The design limits of Case 1592 are applicable for long-term loadings at elevated temperature where creep effects may become significant and require that the effects of geometric imperfections and tolerances be considered explicitly in all calculations.

8.1 ELEVATED TEMPERATURE DESIGN FACTORS

The design factors of Table T-1520-1 are specified to provide a margin of safety against two types of buckling failure: elastic or elastic-plastic buckling that may occur instantaneously at any time in life, and creep buckling which may cause geometrical instability as a result of creep enhancement of initial imperfections with time. The essential difference between elastic and elastic-plastic buckling and creep buckling is that elastic and elastic-plastic buckling occur with increasing load (or strain) independent of time, whereas creep buckling is time-dependent and may occur even when the loads are constant. Elastic and elastic-plastic buckling depend only on the geometrical configuration and short-time material response at the time of application. Creep buckling occurs at leads or strains below the elastic or elastic-plastic buckling loads or strains as a result of accumulated creep strains over a period of time. Creep buckling is highly dependent upon the geometrical configuration as well as the time-dependent material response.

In most cases creep buckling occurs in two stages: an increase in initial geometrical imperfections with time due to creep, and instantaneous buckling when the critical deformation is reached for the particular loading condition. Therefore, separate design factors are specified (1) for load and strain to provide a margin of safety against instantaneous collapse at any time during life, and (2) for time to account for the uncertainty in the magnitude of initial imperfections.

8.2 DEPENDENCE ON POST-BUCKLING BEHAVIOR

The margin of safety provided by the design factors of Table T-1520-1 is dependent upon the post-buckling behavior of the component. Three distinct types of post-buckling behavior may be identified as illustrated by curves 1, 2, and 3 of Fig. 33. The solid lines represent the behavior of theoretically perfect components; the dashed lines represent the behavior of real components with initial imperfections; and P_{cr} is the buckling load that would be calculated using small deformation theory for perfect components.

Components that behave according to curve 1 show considerable post-buckling strength; i.e., it takes an increase in load beyond the theoretical buckling load, P_{cr}, to get significant deforma-

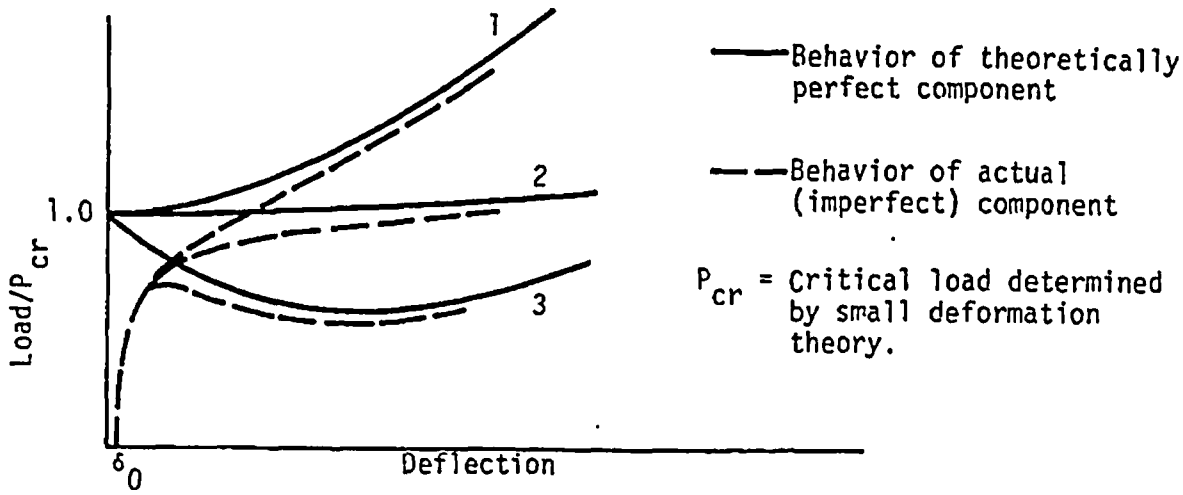

Fig. 33 TYPICAL BUCKLING BEHAVIOR

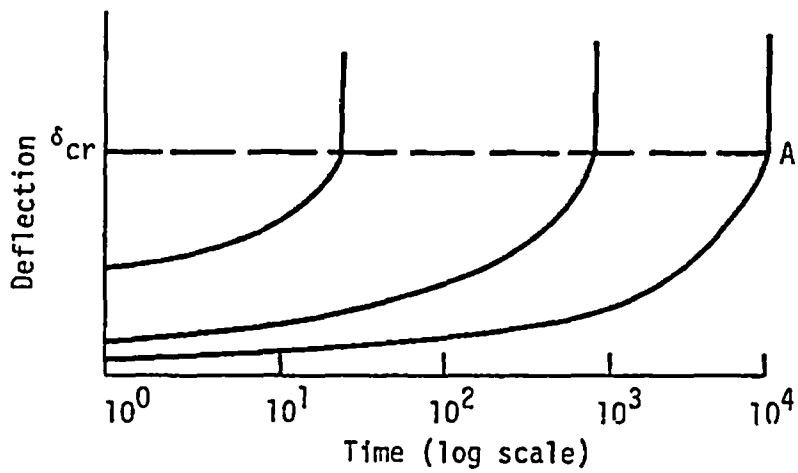

Fig. 34 CREEP BUCKLING DEFLECTION-TIME CHARACTERISTICS

tion. Rectangular plates compressed in the long direction with edges supported parallel to the load typify this type of behavior. Components that behave according to curve 2 show little or no post-buckling strength; i.e., as the load approaches the theoretical buckling load, the deformation increases very rapidly toward catastrophic collapse. Columns loaded axially and cylinders under external pressure typify this type of behavior. Components that behave according to curve 3 show post-buckling instability; i.e., equilibrium states exist at loads well below the theoretical buckling load, P_{cr}, and real components tend to jump to these equilibrium states by processes often described as *snap-through* or *oil-canning*. It is well known that thin-walled cylinders loaded axially buckle into a diamond pattern at loads on the order of one-half of the theoretical buckling load, P_{cr}. Spheres under external pressure and cylinders loaded in torsion also exhibit post-buckling instability.

It is apparent that buckling loads calculated for theoretically perfect components using small deformation theory provide conservative estimates for components with post-buckling strength. Magnification of initial deformation is small even at the theoretical buckling load. For components with little post-buckling strength, initial deformation is magnified as the load approaches P_{cr}. However, if initial deformation is sufficiently small, the load that causes significant magnification can approach P_{cr} very closely, so that P_{cr} provides an upper bound but close approximation to the buckling load. Magnification of larger initial deformations may become unacceptably large at loads well below P_{cr}. In this case it is necessary to calculate the actual load deflection curve, taking account of initial deformation and perhaps using large deformation theory. For components that show post-buckling instability, P_{cr} grossly overestimates the buckling load.

It is intended that the load factor of 3.0 for elastic buckling be applied to the actual buckling load, taking into account the effects of geometric imperfections and tolerances whether initially present or induced by service.

Consideration of geometrical imperfections is required to provide an adequate design margin for components which are imperfection-sensitive (post-buckling unstable), typified by the behavior shown in curve 3 of Fig. 33. For components that are imperfection-insensitive (post-buckling stable), typified by the behavior shown in curves 1 and 2 of Fig. 33, the load-controlled design factor of 3.0 may be shown to provide a sufficient margin of safety without inclusion of the effects of geometrical imperfections so long as their magnitudes are modest. For these components, the effects of geometrical imperfections are relevant only to creep buckling calculations.

A reduced design factor of 2.5 is used for elastic-plastic buckling where the effect of plasticity is significant, in recognition of the fact that strain-hardening tends to make the post-buckling behavior more stable and thereby reduces sensitivity to geometric imperfections. It is well known, for example, that when an axially loaded cylinder buckles in the bellows mode, typical of inelastic buckling, predicted buckling loads coincide closely with those actually measured.

8.3 TIME DESIGN FACTOR

The magnitude of the time design factor for creep buckling was selected, based on observed scatter in typical creep buckling test data, to account for uncertainty in initial imperfection and sensitivity to creep rate. The sensitivity of creep buckling time to initial imperfections is illustrated by the deformation-time relations in Fig. 34. Although typical of the behavior of axially compressed columns and cylinders under external pressure, these curves generally represent the behavior of any component with at least some post-buckling strength, such as those represented by curves 1 and 2 of Fig. 33. In general, a structural component will deviate initially from the perfect geometrical shape (straight, round, cylindrical, etc.) by some small amount. Under a system of loads, below those that would cause elastic or inelastic instability, the initial deflection is magnified with time as a result of creep. The deflection increases until the geometrical configuration becomes unstable, as shown at point A in Fig. 34, and buckling

occurs. The final buckling load in this situation would be dependent upon the instantaneous elastic or inelastic properties of the material at the time of buckling.

As can be seen in Fig. 34, a small difference in initial deflection is associated with a large difference in the time-to-buckling. Geometrical deviations within the range of manufacturing tolerances can easily result in variations of a decade or more in buckling time. It might be argued that the manufacturing tolerance would provide a safe upper limit on initial imperfection. But that only applies to the material as supplied. Fabrication and heat treatment can alter the geometry so that the actual magnitudes of initial imperfections in the as-fabricated condition are not well known. Considering the extreme sensitivity of buckling time to initial imperfection and the sensitivity of creep rate to various material parameters, a time design factor of 10 is not overly conservative.

A time design factor was considered to be necessary to provide an adequate margin of safety based on the current state of knowledge. However, it was recognized that considerable difficulty will occur in predicting component behavior at times up to 10 times design life.

In addition to properties, the question arises as to what load history to assume beyond the end of life. It would be prohibitively expensive to reproduce a detailed inelastic analysis of a complex load history for 10 times the design life. The intent of the Code Case is to identify the dominant features of the load history and construct, for repeated application, a simplified load history which has the same net response. The simplified load history could be as simple as a steady state load condition.

It is apparent that, although the time design factor is philosophically desirable, there is considerable computational difficulty with its application. Further Code development is presently underway to establish alternate limits which account for sensitivity to initial imperfections and variation in material creep rates without requiring calculations for times greater than the design life.

8.4 EFFECT OF INITIAL IMPERFECTIONS

Section T-1520(b) implies rather strongly the need for a complete and detailed inelastic analysis to account for the effect of geometry changes due to creep. In reality there are many situations in which a simplified analysis, which may assume an idealized component geometry, is perfectly adequate to assure structural stability. In this regard it should be noted that the design factor of 10 on time essentially assures that creep enhancement of initial geometric imperfections will be negligible for the design life. The geometrical configuration will not deviate significantly from the initial configuration and the instantaneous buckling load (load design factor) will remain essentially constant during life. Therefore, if the design factor of 10 on time is met and there is reasonable margin above the required load design factor at the beginning of life, calculation of the load design factor at every point in time is not needed.

8.5 STRAIN-CONTROLLED BUCKLING

In the determination of design factors, distinction is made between load-controlled buckling and strain-controlled buckling [see T-1510(b)]. Load-controlled buckling is characterized by situations where the application of load continues after buckling; i.e., the load is not relieved by buckling. Strain-controlled buckling is characterized by loads which are strain limited, thus, in a sense, relieved by buckling. Examples of load-controlled buckling include spheres and cylinders under external pressure, columns and cylinders loaded axially by a dead weight, and piping elements loaded by a moment or torque due to dead weight or seismic motion of connecting components. Examples of strain-controlled buckling included heated plates and shells restrained from in-plane thermal expansion, buckling of a cylinder near the intersection with a hemispherical head due to internal pressure, and buckling of plates and shells due to severe local variations in temperature which cause large compressive stresses. Thus, load-controlled buckling is

characterized by catastrophic collapse whereas strain-controlled buckling is a self-limiting process. Once the structure deforms, the strain is accommodated and the load is relieved. As a matter of fact, in the deformed state, the structure is able to accommodate increasing amounts of strain mismatch with smaller changes in the deformed shape. Initial deformation, rather than increasing additional deformation, tends to decrease additional deformation. Although strain-controlled buckling must be avoided or conservatively bounded to guard against failure by fatigue, excessive strain, and interaction with load-controlled instability, the minimum strain design factor can be lower than the minimum load design factor because of the self-limiting nature of deformation in the post-buckled state and the relative insensitivity to initial imperfections. Thus a design factor of 1.67 is used for strain-controlled buckling. A design factor on time is not required because strain-induced loads are reduced concurrently with resistance of the structure to buckling when creep is significant.

Note that for thermally induced, strain-controlled buckling, the material properties should be taken as those at the actual operating temperature in calculating strain design factors. Although, strictly speaking, this is nonconservative, the nonconservatism vanishes as the actual strain approaches the calculated buckling strain. Furthermore, the strain design factors are not employed to guard against uncertainty in operating temperatures.

9.0 SPECIAL LIMITS AND CONSIDERATIONS

9.1 REQUIREMENTS FOR WELDS

A significant portion of the rules for low temperature design in Subsection NB are concerned with weld materials, design at welds, fabrication of welds, and inspection of welds. However, the analysis requirements for weld regions are minimal, and the weld region is modeled as an extension of the base material with identical properties. The attitude of the Code rules toward weldments did not stem from a belief that weld regions are the same as base material. Instead the attitude reflects a belief that welds can be made as strong as base metal by means of proper control of weld fabrication, materials, and processes, and further, that bend tests will assure that the actual welds will have the necessary ductility in the weld region. With these controls on fabrication and materials, weld regions may be considered at least as strong as the base metal, and they can be conservatively modeled as extensions of base material.

For elevated temperature design, two new concerns caused the prior weld region assumptions to be re-examined. The first concern was that the long-term exposure to elevated temperatures could lead to changed mechanical properties by way of diffusion processes within the material. These are difficult to detect by tests on the deposited weld metal since the heat-affected zone between weld and base materials consists of a continuously changing chemistry of alloys over a region often a fraction of an inch thick. The second concern was that a weldment with strength greater than base metal may produce a poor structural joint since differences in material plasticity and creep properties can lead to discontinuity stress and strain patterns similar to those characteristic of a bimetallic junction with different coefficients of thermal expansion. This could lead to extra strain in the neighborhood of weld metal that in turn could lead to failure during elevated temperature service.

The Code personnel judged that weld regions needed good ductility more than an abundance of strength beyond that of the base metal. Unfortunately, the major source of data on weld region materials was generated only for austenitic stainless steel material and seldom covered anything but properties of the weld metal itself. Even this limited data showed that weld ductility, as expressed in elongation at fracture, was often far below values for base metal, especially in uniaxial creep-rupture testing [see Fig. 13(b)]. The Committee believed that more than words of general guidance were required for weld regions. Thus, the rules of Appendix T (see T-1710) not only warn of limited ductility but also restrict total *calculated* inelastic strain values. Due

to the lack of data for weld region materials, the restriction is only an interim measure for influencing component designs, and the degree of conservatism is not known for the method.

The method requires that weld regions be *assumed* to have properties identical to the surrounding base metal, but the calculated total inelastic strains shall not exceed one-half the values allowed in base metal. This is *not* the same as saying that all parts of the weld regions have one-half the ductility of base metal. Even with these restrictions, some parts of the weld region may undergo greater elongation than in the nearby base metal.

9.2 RULES AND LIMITS FOR BOLTS

9.2.1 Design Conditions

The intent of *Design Condition* rules is to keep the primary stresses below the lesser of one-third the expected minimum yield strength and the criteria for allowable stresses established in Section VIII, Division 1 of the ASME Code. The primary stresses are those required to resist the internal design pressure and to provide an adequate seal in terms of Section III requirements. Section VIII criteria govern the allowable stresses at elevated temperatures where time-dependent properties predominate; however, for most of the temperature range, time-independent properties govern. The combination of the lesser of one-third yield strength and Section VIII allowable stresses provide a smooth transition of design allowables between Section III bolting rules at low temperatures and the extension of Section III to elevated temperature.

9.2.2 Maximum Average Stress Through the Bolt Due to Pressure Loading

The intent of this paragraph in Case 1592 is to limit the normal pressure stress sustained by the bolt to the lesser of one-third the yield strength at temperature or $\frac{1}{2} S_t$ of a structural material. The S_{mt} values for bolting are one-half of those values given for structural materials in Case 1592. A design factor of approximately 2 is utilized in Section III for S_m values of bolts as compared to structural materials, and this philosophy was also used for the elevated temperature rules.

9.2.3 Maximum Membrane Stress in a Bolt Cross Section

The intent herein is to specify a maximum membrane stress for bolt preload which allows the Designer to neglect creep-rupture damage in his structural evaluation. If the bolt preload membrane stress is kept to the lesser of two-thirds yield strength and S_t value for a structural material, then creep-rupture damage in the shank does not have to be evaluated as a function of the number of bolt-tightening applications.

If the Designer wishes to preload a bolt in excess of the stress limits established above for various reasons such as minimizing potential leakage, he may do so, but at the expense of evaluating the creep rupture damage for each bolt-tightening application.

9.2.4 Maximum Membrane-Plus-Bending Stress in the Bolt Periphery

These rules and limits are intended to limit the bolt cross-sectional stress induced by a combination of bending-plus-membrane loadings that may result from flange rotation. The maximum periphery stress value is limited to the lesser of the yield strength or $2K_t S_t$ [the S_t values are those taken for bolting given in curves of I-14.13 of Case 1592]. The stresses are allowed to exceed this value provided the possibility of creep-rupture due to bending is guarded against by computing the creep-rupture life fraction expended for each bolt torque application. This calculation assumes that the bolt is orientated in the same position for each torque application so that the maximum bending stress is always applied to the same bolt region. The allowable use fraction of 0.67 was obtained by multiplying the use fraction of 0.5 for membrane loading by K_t for a solid circular cross section.

9.2.5 Creep-Fatigue

Because of the critical application of bolts at high temperature, fatigue exemptions are not permitted as in design for low temperature. For notches as exemplified by screw threads, fatigue-strength-reduction factors of 4.0 have been shown to be adequate. Unless it can be shown by tests that a lower value is justified, the use of lower stress-concentration factors is not permitted. A strength-reduction factor of 1.8 is used for creep-rupture as well.

9.2.6 Emergency and Faulted Conditons

The philosophy for Section III is extended to elevated temperature in that Emergency and Faulted events must be considered if they exist; however, the S_m and S_{mt} values for structural materials (Table I-14.3) may be utilized for the evaluation.

9.2.7 Strain Limits

The strain limits for structural materials are also applied to bolting. The previously discussed limits should preclude membrane and bending strains from exceeding 1 and 2% strains, respectively. Bending strains of 2% could exceed the functional requirements of most bolt applications; therefore, the membrane limits should be carefully studied in terms of the specific applications to ascertain whether or not they should be reduced.

9.3 ELASTIC FOLLOW-UP

There are two areas of the Code Case which require consideration of *elastic follow-up*. One area is the classification of secondary stresses with a "large amount of elastic follow-up" as a load-controlled quantity in paragraph 3213(a).

The only definition of elastic follow-up currently in the Code Case is contained in paragraph 3138 which is a modified version of the discussion in the Power Piping Code, B31.1, on local overstrain. The definition and examples of paragraph 3138 relate to the classification of load-controlled quantities. In practice, piping is the most common application of the paragraph 3138 definition and the term "large amount of elastic follow-up" would usually apply to an analysis of a complete pipe line. It is difficult to quantitatively describe what is "significant elastic follow-up."

Robinson (71) in 1955 published a paper which explored the possibility of localized creep strain concentrations in elevated temperature piping systems. Robinson started with the example of a bolt in a rigid flange, which is a case of pure relaxation, and continued through to the case of four large bending loops in series with four smaller loops of half-size pipe in parallel. Figure 35 is a summary of the behavior of a bolt in an unyielding flange. The stress and creep strain as a fraction of initial elastic extension are shown as a function of time. In this example, the creep extension in 10,000 hr is 0.75 times the initial elastic extension. Figure 36 is a similar plot for a simple bending loop. In this case, the creep extension is 0.97 times the initial elastic extension. The final stress is also somewhat higher. Finally, Fig. 37 plots the results for smaller diameter pipe loops in series with large diameter pipe. In this case, the 10,000 hr creep strain is 3.47 times the initial elastic extension and the final stress is significantly higher than the pure relaxation case.

In the context of the stated rules in 3213(a), which are largely based on the results of Robinson and others [references (71), (72), and (73)], the intent is to consider restrained thermal expansion stress in systems with localized weak areas, such as Fig. 37, as primary. However, restrained thermal expansion in a well-balanced system, as represented by Fig. 36, should not be considered primary.

The other part of the Code Case which considers elastic follow-up is in Appendix T, and it relates to the application of elastic analysis to the satisfaction of strain limits. Further illustration of elastic follow-up concepts is necessary in order to explain the intent of the rules in Appendix T.

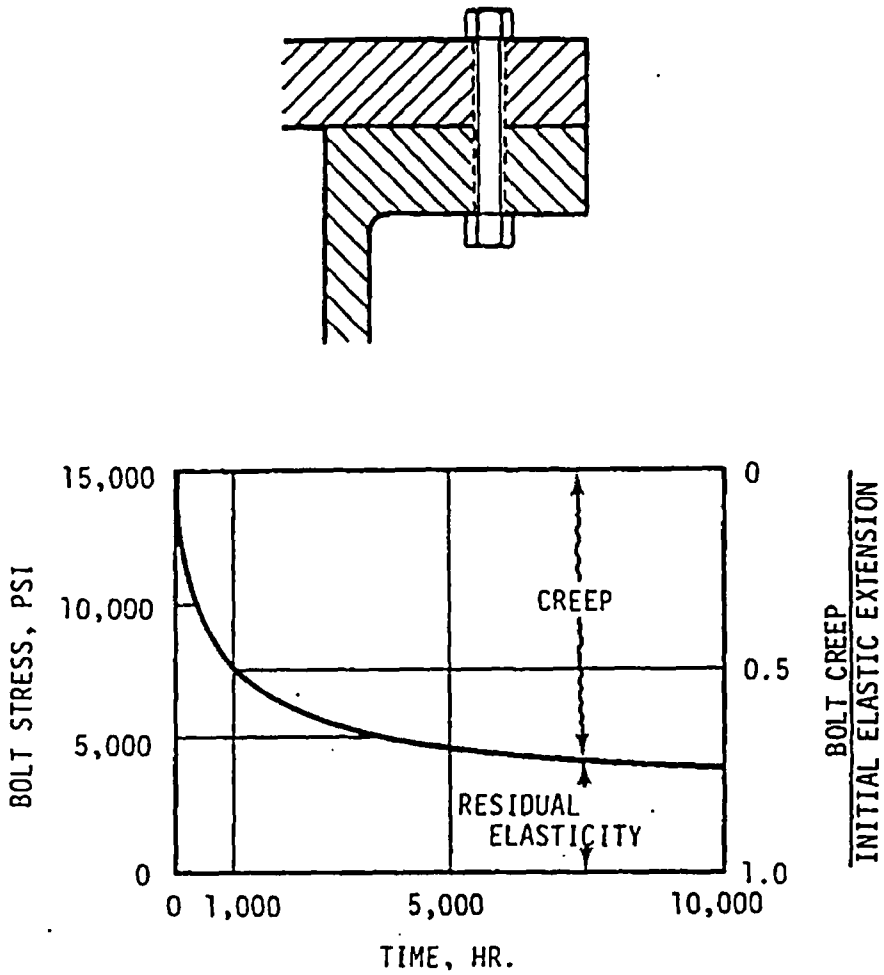

Fig. 35 BEHAVIOR OF BOLT IN AN UNYIELDING FLANGE

Consider two bars in series as shown in Figs. 38 through 40 subjected to a displacement, δ. The stress and strains associated with the displacement, δ, would nominally be considered deformation-controlled quantities. However, depending upon the relative stiffness of the two bars, the stresses in each will require separate interpretation of the Code Case rules. Consider the following cases:

In Fig. 38, the area of bar A is very much larger than B. In this case all the deformation will take place in B. This is analogous to a local thermal stress such as a small hot spot in a vessel wall. In essence, there is no elastic follow-up because the displacement-induced load in B causes a negligible change in the displacement of A. Therefore, the resultant load history in B can be considered solely on the basis of creep-fatigue.

In Fig. 39, A and B are of equal area and length and operate at the same temperature. When subjected to a displacement δ, the bars deflect an equal amount and this displacement does not change even if yielding or creep takes place. This case is analogous to the stresses produced in a vessel wall due to a radial thermal gradient. Radial thermal gradients remote from discontinuities produce stresses which are a function of the radius only, and the net strain is a function of

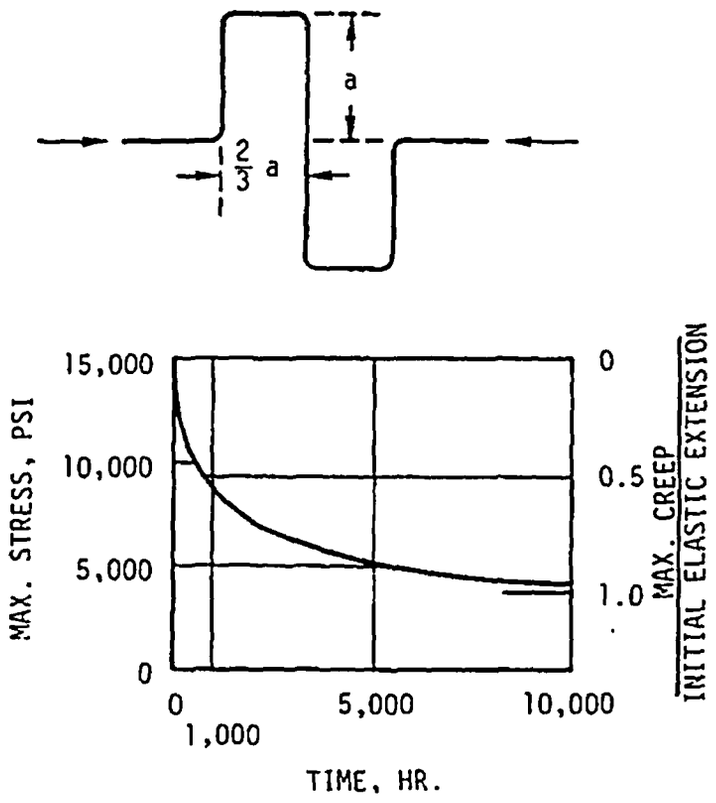

Fig. 36 BALANCED LOOP BEHAVIOR

the superimposed primary stress. The case of a cylinder under primary stress with a superimposed cyclic thermal stress is the basis of the rules for the application of elastically calculated stresses to the prediction of strain. Thus, stresses due to radial, through-the-wall, temperature variations are specifically exempted from the restriction that secondary stresses must be considered primary in applying the O'Donnell-Porowski (28) technique incorporated in T-1323 of Case 1592. The intent, as will be subsequently described, is to consider displacement-induced stresses with elastic follow-up as primary in applying the O'Donnell-Porowski technique.

In Fig. 40, where there is elastic follow-up, the area of B is smaller than A but still strong enough to cause an initial deflection in A. First, consider the mutual deflections of A and B if the elastically calculated stress in A is less than its yield strength. The elastically calculated deflections of A and B will be as shown. However, since the actual stress in B will not exceed its yield strength, the actual load and resultant deflection in A will be less than the elastically calculated load and deflection. Since the deflection in A and B must add up to the total applied deflection, the deflection of B will be greater than elastically calculated. This is an example of elastic follow-up. Next, consider the relative deflections of A and B assuming that creep is taking place; the area of B is smaller than A and A's initial deflection is significant with respect to B. Since the stress in B is greater than the stress in A, the stress in B will relax at a faster rate. As the stress in B relaxes, the stress and deformation of A will decrease (i.e., tend toward its unloaded position) and the deformation of B will increase; again this is elastic follow-up. Furthermore, if A is a relatively long bar, which stores a large amount of elastic energy, then it will tend to exert an almost constant load on B since the deformation of the relatively short bar, B, will

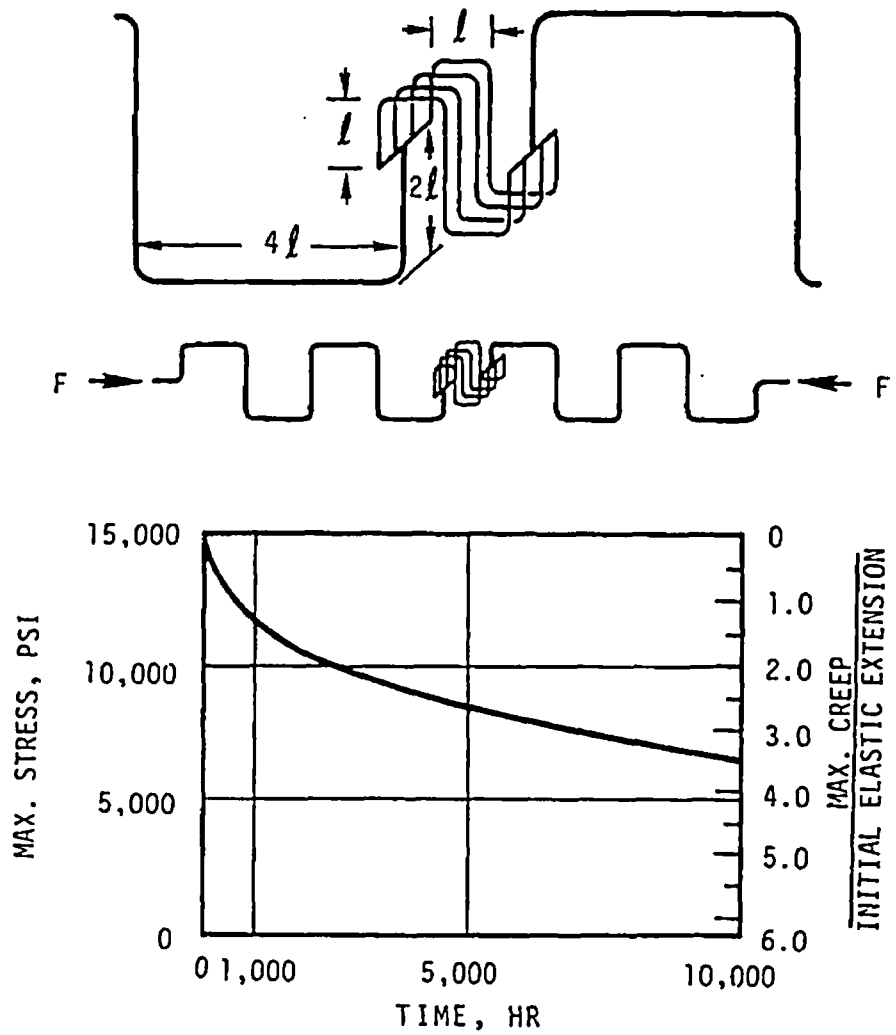

Fig. 37 FOUR LARGE BENDING LOOPS IN SERIES WITH FOUR SMALLER LOOPS OF HALF-SIZE PIPE IN PARALLEL

not relieve the load in the long bar, A. Thus, if there is a large amount of elastic follow-up, the load on B will be practically constant and can be considered primary even though the initial source of the load was a displacement. The presence of elastic follow-up results in a more constant load, slower stress relaxation, and more strain accumulation as compared to cases where there is no elastic follow-up. In effect, a purely elastic analysis will tend to underestimate the creep-fatigue damage (because of slower stress relaxation) and strain in the presence of elastic follow-up. This has important implications to the implementation of elastic methods for calculating the strain accumulation in some common structural configurations.

Consider the case of the stresses produced by the temperature difference between a nozzle and the shell to which it is attached. This can be idealized as a *built-in cylinder* as shown in Fig. 41. The initial elastically calculated deflection curve is shown as O-A. If there were no moment resistance at the built-in joint, then it would behave structurally as a pinned joint as shown by curve O-D. If the initial stress at the built-in end exceeds yield, then a partial plastic hinge will

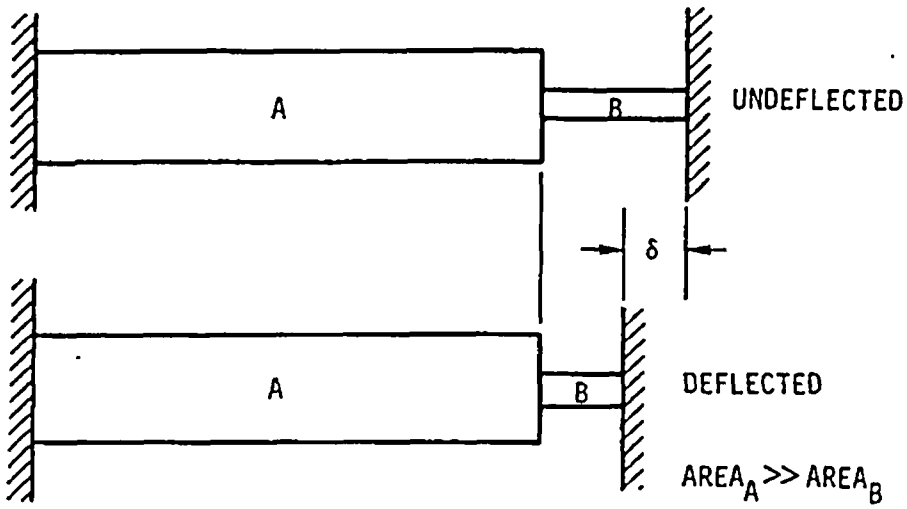

Fig. 38 TWO-BAR MODEL WITH STRAIN CONCENTRATION BUT NO ELASTIC FOLLOW-UP

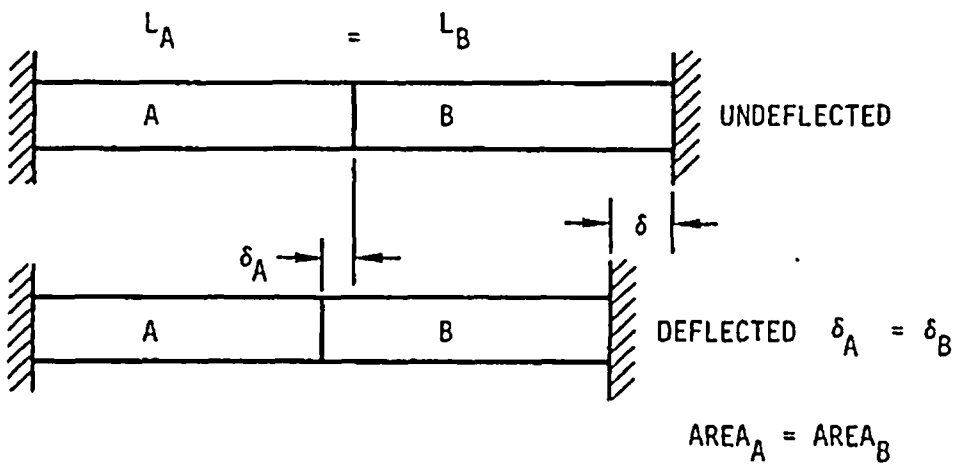

Fig. 39 TWO-BAR MODEL WITH NO STRAIN CONCENTRATION OR ELASTIC FOLLOW-UP

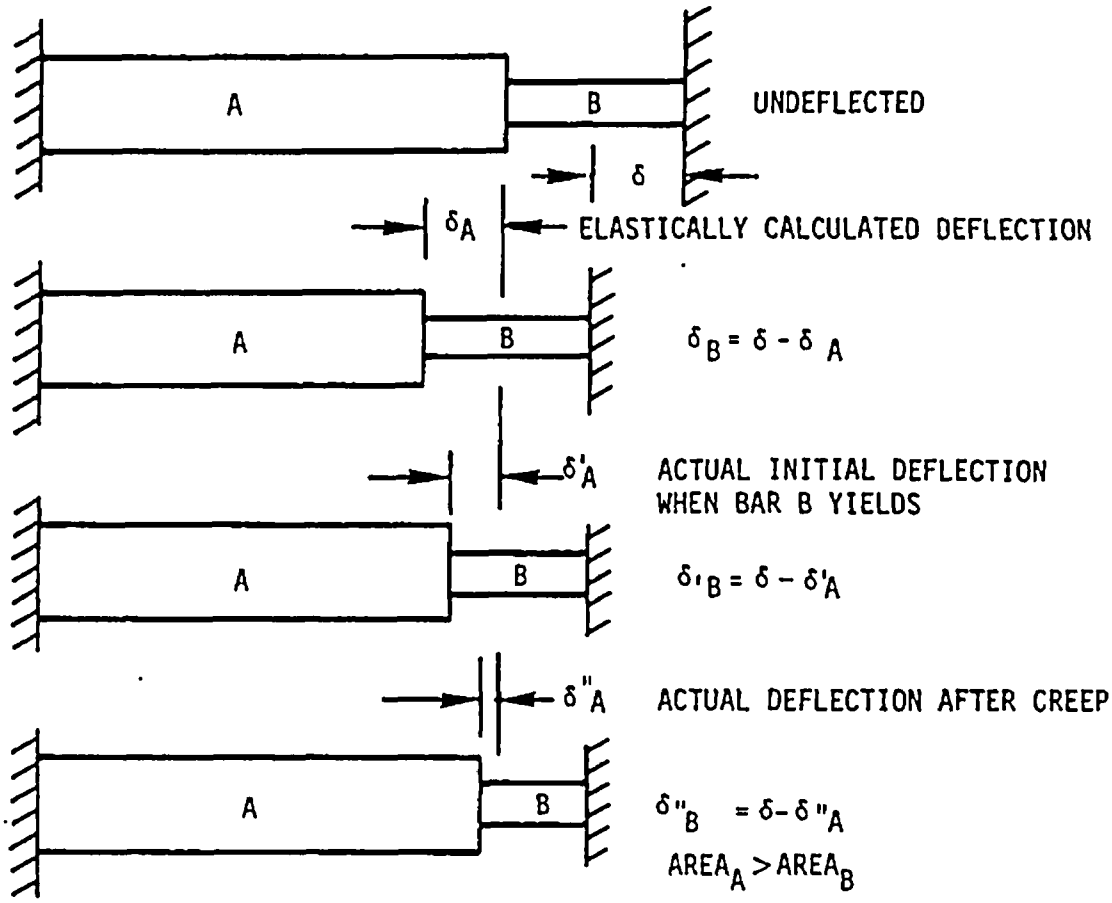

Fig. 40 TWO-BAR MODEL WITH ELASTIC FOLLOW-UP AND STRAIN CONCENTRATION

result with an increase in strain at the joint as shown by O-B. If the joint creeps, there will be further strain redistribution as shown by curve O-C. In effect, the angular rotation of the relatively localized high stress area at the joint is being driven by the lower stressed, beam-on-elastic-foundation behavior of the cylinder. Thus, the built-in cylinder is an example of elastic follow-up. If one were to apply the results of the elastic analysis directly, as in the case of stresses generated by a through-the-wall gradient, then the surface strain at the built-in end would be underestimated. This is the reason for the restriction in T-1324(d) which states that any secondary stress with elastic follow-up must be considered primary for purposes of that evaluation. This is conservative in that it assumes the *built-in cylinder* effect will have a large amount of stored elastic energy. Unfortunately, there have not been sufficient inelastic analysès of actual joints as of the drafting of these rules to permit anything other than this conservative assumption. However, it is recognized that specific geometries, materials, operating conditions, and analytical assumptions may be demonstrated to be sufficiently conservative that the noted restrictions on secondary stresses need not be invoked. If this is the case, the justification for not considering secondary stresses with elastic follow-up as primary stresses must be included in the stress report.

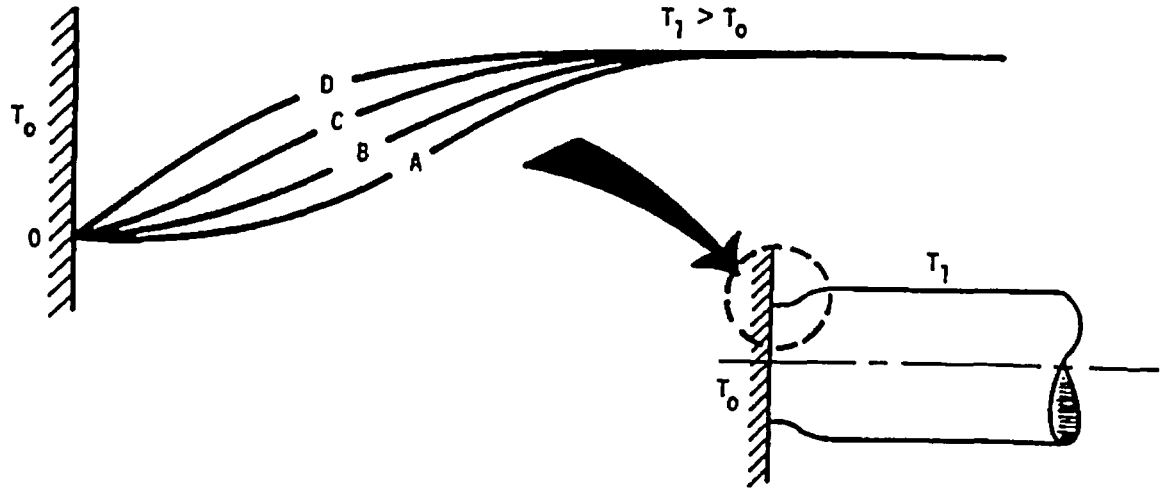

Fig. 41 BUILT-IN CYLINDER WITH ELASTIC FOLLOW-UP

Note that the restrictions of T-1324(d) do not apply to T-1322 and T-1323. This is because the stress limits for these cases are sufficiently conservative that the additional restrictions on elastic follow-up of secondary stresses are not warranted.

9.4 LOAD ENVIRONMENT HISTOGRAMS

A histogram, which is required by the Design Specification for each component, is a graphical representation of how the design parameters (such as pressure, temperature, force or flow) change with time during a particular event, and a histogram can depict the sequential order of events during the lifetime of a plant. These are the events that must be considered in the design of the component. In this larger sense, the histogram can depict more than a single loading event; it may contain a set of operational cycles, giving the various loadings, the number of occurrences of each, the order in which they are anticipated, and the expected time interval between events. The term *load histogram* and *expected loading history* are often used synonomously with histograms.

9.4.1 Event Order and Time Duration Effects

When material behavior is nonlinear (such as creep at elevated temperature), the order and time duration of the loads applied to a structure influence the total deformation and length of life of the structure. Different order and time duration of loads will yield different strain ranges for loading, creep deformation, and stress distributions for stress-rupture evaluation. The rate at which an elevated temperature structure recovers and readjusts its stress distribution following a transient load depends on the structure configuration, level and distribution of the primary stresses, and the creep properties of the material. Low creep strength materials usually relax the high residual stresses in a short time period so that the influence of the high residual stresses does not have a major effect on the component stress-rupture life, although the relaxation of the residual stress may be at the expense of some additional creep deformation. If the transient load leaves a residual stress distribution, these stresses will be added algebraically to the stress field of the next applied load and may thus increase or decrease the total stress. The total stresses, in turn, influence the creep strain rates and damage from stress-rupture for this applied load, especially during the early period of this time interval. The order of the transients will have its greatest influence when the time between the events is not sufficient to establish a stable stress distribu-

tion in the part. Further, the order of transients will also influence the magnitude of the calculated stresses and strains in a structure which is made of a material of high creep strength and subjected to small primary stresses and high secondary (including thermal) stresses. Such structures have an ability to retain residual stresses.

9.4.2 Design Specification Considerations

The Design Specifications require a histogram of the Normal and Upset operating conditions for the design life of the plant. Experience in the design of elevated temperature equipment has shown that an even spacing of the various transient events throughout the plant life is not a realistic histogram. As an illustration, consider the normal startup and shutdown events. At the beginning of operations there will be a number of these events at rather close spacing because of problems during the shakedown period. At a base loaded plant, there will be long intervals between these events. As the plant becomes older, it will be used only during the normal work week and placed on standby operation for the weekend. In the future this may be three days or more. Also as the plant becomes older, the unplanned shutdown becomes more frequent because of aging equipment. Finally the plant will be used only for peaking service because of its high cost of operation when compared with newer equipment in the system.

Electrical load patterns differ from one utility to another, and this part of the histogram is controlled by local conditions. The reaction of the various parameters such as temperature, pressure, and time to various transients depends on plant design and modes of operation. Thus, both the Owner of the plant, or his agent, and the system Designer have input to the histogram, much of which must be forecast with some degree of uncertainty.

The influence of the loading histogram may be factored into the design of the structural components in several ways. One procedure which would entail excessive cost would be to analyze each period of operation as it occurs on the histogram. Another procedure would be to find a recurring sequence of events and do the analysis on this section of the histogram and then consider the total damage as a multiple of the recurring events. However, there are several different stages in the plant life which depend on plant age and the ever changing social and economical pattern of the region in which the plant is located. At each stage in plant life, certain events will occur in approximate cyclic behavior in order that damage could be determined for each stage and then summed for total damage.

Another less detailed procedure would analyze each cyclic transient from steady-state operating conditions where each cyclic event would cover a time span that included the transient and the time required to bring the plant back to Normal operating conditions with a stable stress distribution. As an example, if a transient resulted in a plant shutdown, the total cyclic event would include the Upset transient, the shutdown, the startup, and sufficient time at Normal operating conditions to establish a stable stress distribution in the part being analyzed. Some modes of plant operation, for instance working in two shifts, do not allow sufficient time for a stable stress distribution to be established before the cyclic events are repeated. In this case two or more events should be analyzed back-to-back to establish a stable cyclic behavior. This procedure would handle Emergency events which are unpredictable in a similar manner. This method considers the influence of the residual stress system from the transient but neglects the order of the transients. However, the fatigue damage could be based on the maximum strain ranges over all transients regardless of order of events. Moreover, it is possible to order the events in a manner which will influence the magnitude of the calculated stresses and strains to some extent, especially if events occur at a frequency which does not allow a stable stress distribution to be formed.

For all cases a certain minimum factor of safety is required because of the inability to forecast the actual operating history of the plant, the variations in material properties, the limits of mathematically modeling the structural behavior of the component, and the lack of a theoretical basis for evaluating the combined damage from creep and fatigue. Different procedures for

evaluating creep and fatigue damage may require different factors of safety because of the amount of details involved in the analysis. In many cases a high degree of precision in one facet of the analysis is not justified when other phases of problems are not amenable to a similar determination.

In conclusion, the Design Specifications require a histogram which must be factored into the stress analysis of the particular component. Varied procedures are available to estimate the creep and fatigue damage from the periodic operating history of the plant. There is no typical histogram for all the components, or all components of the system. Also, histograms will vary for different types of systems and are dependent on the regional social and economical climate of the plant location because of the wide variation in electrical load demand. A realistic histogram requires input by the Owner to describe load demand throughout plant life and by the system Designer to describe Upset transients and maintenance replacement periods.

10.0 REFERENCES

1. Code Case 1331-4, -5, -6, -7, -8, ASME Boiler and Pressure Vessel Code, Case Interpretations, 1971 Edition, The American Society of Mechanical Engineers, New York.

2. Code Case 1592, ASME Boiler and Pressure Vessel Code, Code Cases, 1974 Edition, The American Society of Mechanical Engineers, New York.

3. *Criteria of the ASME Boiler and Pressure Vessel Code for Design by Analysis,* The American Society of Mechanical Engineers, New York, 1969.

4. *The Generation of Isochronous Stress-Strain Curves,* The American Society of Mechanical Engineers, New York, 1972.

5. R. W. Weeks, *Mechanical Properties Test Data for Structural Materials Quarterly Progress Reports,* October 1973, ORNL-4936, Oak Ridge National Laboratory.

6. G. V. Smith, W. B. Seens, H. S. Link, and R. R. Molenock, "Microstructural Instability of Steels for Elevated Temperature Service," *Proceedings of The American Society for Testing and Materials,* 51: 895-917 (1951).

7. A. J. Lovell, L. D. Blackburn, and J. J. Holmes, *Quarterly Progress Report, Irradiation Effects Progress Report,* Hanford Engineering Development Laboratory, WHAN-FR-40-1, (January 1970).

8. D. Fahr, *Fuels and Materials Development Program Quarterly Progress Report,* ORNL-TM-3703, Oak Ridge National Laboratory, (December 1971).

9. M. C. Murphy and G. D. Branch, "Metallurgical Changes in 2.25 Cr-Mo Steels During Creep-Rupture Test" *Journal of Iron Steel Institute,* 209 (Pt. 7): 546 (July 1971).

10. K. Natesan, T. F. Kassner, and Che-Yu Li, "Effect of Sodium on Mechanical Properties and Friction-Wear Behavior of LMFBR Materials," *Reactor Technol.* 15(4): 242 (Winter 1972-1973).

11. C. R. Brinkman, G. E. Korth, and R. R. Hobbins, "Estimates of Creep-Fatigue Interaction in Irradiated and Unirradiated Austenitic Stainless Steels," *Nuclear Technology* 16(1): 297 (October 1972).

12. C. R. Brinkman, *Mechanical Properties Test Data for Structural Materials Quarterly Progress Report April 30, 1974,* ORNL-4963, Oak Ridge National Laboratory.

13. C. R. Brinkman and G. E. Korth, "Heat-to-Heat Variations in the Fatigue and Creep-Fatigue Behavior of AISI Type 304 Stainless Steel at 593°C," *Journal of Nuclear Material* 48: 293-306 (1973).

14. H. E. McCoy and R. D. Waddell, "Mechanical Properties of Several Products from a Single Heat of Type 304 Stainless Steel," Presented at the Winter Annual Meeting of the ASME, Detroit, 1973, published

15. W. E. White and I. Le May, "Some Effects of Microstructure on the Creep Behavior of AISI Type 316 Stainless Steel," p. 1, *Symposium on Elevated Temperature Properties of Austenitic Stainless Steels,* The American Society of Mechanical Engineers, New York, 1974.

16. H. E. McCoy, "Tensile and Creep Properties of Several Heats of Type 304 Stainless Steel," ORNL-TM-4709, Oak Ridge National Laboratory, November 1974.

17. G. V. Smith, "An Evaluation of the Yield, Tensile, Creep, and Rupture Strengths of Wrought 304, 316, 321, and 347 Stainless Steels at Elevated Temperatures," ASTM Data Series DS5S2 American Society for Testing and Materials, Philadelphia, February 1969.

18. W. F. Simmons and J. A. Van Echo, "The Elevated Temperature Properties of Stainless Steels," ASTM Data Series Publication DS5S1, American Society for Testing and Materials, Philadelphia, December 1965.

19. W. E. Leyda and J. P. Rowe, "A Study of the Time for Departure from Secondary Creep for Eighteen Steels," ASM Technical Report No. P9-101, American Society for Metals, Metals Park, Ohio, 1969.

20. L. D. Blackburn, "Isochronous Stress-Strain Curves for Austenitic Stainless Steels," in *The Generation of Isochronous Stress-Strain Curves*, p. 15-48, The American Society of Mechanical Engineers, New York, 1972.

21. *Liquid Metal Fast Breeder Reactor Materials Handbook*, Hanford Engineering Development Laboratory, HEDL-TME 71-32.

22. J. Bree, "Elastic-Plastic Behavior of Thin Tubes Subjected to Internal Pressure and Intermittent High-Heat Fluxes with Application to Fast Nuclear-Reactor Fuel Elements," *Journal of Strain Analysis*, Vol. 2, No. 3, 1967.

23. J. Bree, "Incremental Growth Due to Creep and Plastic Yielding of Thin Tubes Subjected to Internal Pressure and Cyclic Thermal Stresses," *Journal of Strain Analysis*, Vol. 3, No. 2, 1968.

24. M. T. Jakub and R. A. Moen, "Translating Elevated Temperature Material Properties into Rules for Structural Design," *Proceedings of the First International Conference on Structural Mechanics in Reactor Technology* (held in Berlin, Germany, September 1971) T. A. Jaeger, Luxembourg, 1971.

25. C. H. A. Townley and J. F. Poynor, "Creep and the Combined Effects of Creep and Fatigue," Chapter 3 of *Pressure Vessel Engineering Technology*, Edited by R. W. Nichol, Elsevier Publishing Company, Ltd., Amsterdam, 1971.

26. R. K. Penny and D. L. Marriotts, *Design for Creep*, McGraw-Hill, New York 1971.

27. B. F. Langer, "Design of Vessels Involving Fatigue," Chapter 2 of *Pressure Vessel Engineering Technology*, Edited by R. W. Nichols, Elsevier Publishing Company, Ltd., Amsterdam, 1971.

28. W. J. O'Donnell and J. Porowski, "Upper Bounds for Accumulated Strains Due to Creep Ratchetting," *Welding Research Council Bulletin No. 195*, June 1974. Also Presented at the ASME Pressure Vessel, Piping and Materials Conference in Miami, June 1974, to be published in the ASME Transactions.

30.* J. M. Corum, and W. K. Sartory, "Elastic-Plastic-Creep Analysis of Thermal Ratchetting in Straight Pipe and Comparisons with Test Results," ASME Paper No. 73-WA/PVP-4. Contributed by the Pressure Vessels and Piping Division of ASME for presentation at the Winter Annual Meeting, Detroit, November 1973.

31. T. W. Pickel, G. T. Yahr, W. K. Sartory, and J. M. Corum, Studies of Shakedown and Ratchetting of Structures, pp. 161-171 in "High-Temperature Structural Design Methods for LMFBR Components Quarterly Progress Report for Period Ending June 30, 1973," USAEC Report ORNL-TM-4356, Oak Ridge National Laboratory, December 1973.

32. C. D. Walker, "Strain Fatigue Properties of Some Steels at 950°F (510°C) – With a Hold in the Tension Part of the Cycle," Paper No. 24, *Joint International Conference on Creep*, Institution of Mechanical Engineers, London, 1963.

*Reference 29 omitted.

33. H. G. Edmunds, and D. J. White, "Observations of the Effect of Creep Relaxation on High Strain Fatigue," *Journal of Mechanical Engineering Science*, Vol. 8, No. 3, 1966, pp. 310-321.

34. R. A. T. Dawson, W. J. Elder, G. S. Hill, and A. T. Price. "High Strain Fatigue of Austenitic Steels," Thermal and High Strain Fatigue, *Proceedings of International Conference organized by Institute of Metals in association with the Iron and Steel Institute*, Church House, London, June, 1967, p. 239.

35. E. L. Robinson, "Effects of Temperature Variations on the Long-Term Rupture Strength of Steels," *Transactions of The American Society of Mechanical Engineers*, Vol. 74, 1952, pp. 777-780.

36. S. Taira, "Lifetime of Structures Subjected to Varying Load and Temperature," *Creep in Structures*, J. Nicholas Hoff, ed., Academic Press, New York, 1962, pp. 96-124.

37. D. A. Spera, "The Calculation of Elevated Temperature Cyclic Life Considering Low-Cycle Fatigue and Creep," NASA TND-5317, NASA Lewis Research Center, Cleveland, Ohio.

38. S. S. Manson, G. R. Halford, and D. A. Spera, "The Role of Creep in High Temperature Low Cycle Fatigue," pp. 229-249. Ch. 12 in *Advances in Creep Design*, A. I. Smith and A. M. Nicolson, eds., Applied Science Publications Ltd., London, 1971.

39. R. D. Campbell, "Creep/Fatigue Interaction Correlation for 304 Stainless Steel Subjected to Strain-Controlled Cycling with Hold Times at Peak Strain," ASME Paper No. 71-PVP-6.

40. B. M. Wundt, "Cumulative Damage Due to Combined Creep and Low Cycle Fatigue of 1% Cr-1% Mo-¼% V Steel at 1000 F," Consulting Memorandum No. 9, The Metals Property Council, New York, November 9, 1970.

41. R. Lagneberg, and R. Altermo, "The Effect of Combined Low Cycle Fatigue and Creep on the Life of Austenitic Stainless Steels," *Met. Transactions* Vol. 2, 1971, p. 1821.

42. E. P. Esztergar, and J. R. Ellis, "Considerations of Creep-Fatigue Interaction in Design Analysis," *Design for Elevated Temperature Environment*, American Society of Mechanical Engineers, 1972.

43. S. S. Manson, G. R. Halford, and M. H. Hirshberg, "Creep Fatigue Analysis by Strain Range Partitioning," *Design for Elevated Temperature Environment*, American Society of Mechanical Engineers, 1972, pp. 12-28 (NASA TMX-67838, 1971).

44. J. F. Polhemus, C. E. Spaeth, and W. H. Vogel, "A Ductility Exhaustion Model for Prediction of Thermal Fatigue and Creep Interaction," *Fatigue at Elevated Temperatures*, ASTM STP 520, American Society for Testing and Materials, 1973, pp. 625-636.

45. E. P. Esztergar and J. R. Ellis, "Cumulative Damage Concepts in Creep-Fatigue Life Prediction," *Central Electricity Generating Board, International Conference on Thermal Stresses and Thermal Fatigue*, Berkeley, Glos., England, September, 1969, Paper No. 28.

46. M. M. Abo El Ata and Jain Finnie, "A Study of Creep Damage Rules," ASME Paper 71-WA/Met-1.

47. M. Kitagawa and R. W. Weeks, "Analysis of Hold Time Fatigue Test Results of AISI 304 Stainless Steel by Five Existing Methods," Submitted to the *1974 Symposium on Mechanical Behavior of Materials*, Kyoto, Japan, August 1974.

48. J. B. Conway, "An Analysis of the Relaxation Behavior of AISI 304 and 316 Stainless Steel at Elevated Temperatures," GEMP-730, General Electric Nuclear Systems Programs, Cincinnati, Ohio, December 1969.

49. J. T. Berling and J. B. Conway, "Effect of Hold Time on the Low Cycle Fatigue Resistance of 304 Stainless Steel at 1200°F," Part II, Materials and Fabrication, *First International Conference on Pressure Vessel Technology* (Delft, Netherlands, September 1969), published by The American Society of Mechanical Engineers, 1970.

50. J. T. Berling, and T. Slot, "Effects of Temperature and Strain Rate on Low Cycle Fatigue Resistance of AISI 304, 316 and 348 Stainless Steels" ASTM STP 459, *Fatigue at High Temperatures*, pp. 3-30. (Also available as General Electric Report GEMP-642, General Electric Nuclear Systems Programs, Cincinnati, Ohio, June 1968).

51. J. B. Conway, "Evaluation of Plastic Fatigue Properties of Heat-Resistant Alloys," GEMP-740, General Electric Nuclear Systems Programs, Cincinnati, Ohio, December 1969.

52. G. R. Halford, M. H. Hirshberg, and S. S. Manson, "Temperature Effects on the Strain Range Partitioning Approach for Creep/Fatigue Analysis," ASTM STP 520, 1973, pp. 658-667, (NASA TMX-68023, 1972).

53. E. Krempl, and C. D. Walker, "Effect of Creep-Rupture Ductility and Hold Time on the 1000°F Strain-Range Behavior of a 1 Cr - 1 Mo - 0.25V Steel," ASTM STP 459, pp. 75-98.

54. J. M. Corum, "Examination of K-Factor Used In Code Case 1331 and Recommended Modifications," pp. 172-179, High Temperature Structural Design Methods for LMFBR Components Quarterly Progress Report For Period Ending June 30, 1973, Oak Ridge National Laboratory Report, ORNL-TM-4356.

55. R. W. Weeks, D. R. Diercks, and C. F. Cheng, "ANL Low-Cycle Fatigue Studies—Program, Results and Analysis," U. S. AEC Report ANL-8009, March 1973.

56. C. R. Brinkman, G. E. Korth, and R. R. Hobbins, "Estimates of Creep-Fatigue Interaction in Irradiated and Unirradiated Austenitic Stainless Steels," *Nuclear Technology*, Vol. 16, 1972.

57. C. E. Jaske, H. Mindlin, and J. S. Perrin, "Combined Low-Cycle Fatigue and Stress Relaxation of Alloy 800 and Type 304 Stainless Steel at Elevated Temperatures," *Fatigue at Elevated Temperatures*, ASTM STP 520, American Society for Testing and Materials, 1973, pp. 365-376.

58. J. G. Y. Chow, J. R. Hare, R. H. Jones, and Tremel, "Quarterly Progress Report on High Cycle Fatigue of LMFBR Materials," BNL 50363, October 1972.

59. C. E. Jaske, H. Mindlin, and J. S. Perrin, "Low-Cycle-Fatigue Evaluation of Reactor Materials," in BMI-1914, July 1971, pp. A2-A44, Battelle Memorial Institute report.

60. L. F. Coffin, Jr., "Predictive Parameters and Their Application to High Temperature Low Cycle Fatigue," *Second International Conference on Fracture* (Brighton, England, 1969) published by Chapman and Hall, London, and Barnes & Noble, New York, 1969.

61. S. Y. Zamrik, Study of the Effects of Biaxality in Creep-Fatigue at Elevated Temperatures, pp. 177-189 in "High Temperature Structural Design Methods for LMFBR Components Quarterly Progress Report for Period Ending September 30, 1972," USAEC Report ORNL-TM-4058, Oak Ridge National Laboratory, December 1973.

62. S. S. Manson, *Thermal Stresses and Low Cycle Fatigue*, pp. 193-273, McGraw-Hill, 1966.

63. C. R. Brinkman, G. E. Korth, and J. M. Beeston, "Comparison of the Fatigue and Creep-Fatigue Properties of Unirradiated Type 304 and 316 Stainless Steel at 593°C (1100°F)," ANCR-1078, August 1972.

64. C. E. Jaske, H. Mindlin, and J. S. Perrin, "Low Cycle Fatigue and Creep Fatigue of Incoloy 800," BMI-1921, February 1972.

65. C. E. Brinkman, G. E. Korth, and J. M. Beeston, "Influence of Irradiation on Creep-Fatigue Behavior of Several Austenitic Stainless Steels and Incoloy 800 at 700°C," *Effects of Radiation on Substructures and Mechanical Properties of Metals and Alloys*, ASTM STP 529, 1973.

66. E. Krempl, "The Effect of Stress Concentration on the Low-Cycle Fatigue of Three Low-Strength Structural Steels at Room Temperature and 550°F," GEAP-10170, March 1970.

67. E. Z. Stowell, "Stress and Strain Concentration at a Circular Hole in an Infinite Plate," NACA-TN-2073, April 1950.

68. H. Neuber, "Theory of Stress Concentration for Shear-Strained Prismatical Bodies with Arbitrary Nonlinear Stress-Strain Law," *Transactions of The American Society of Mechanical Engineers, Series E, Journal of Applied Mechanics*, pp. 544-550.

69. D. F. Mowbray and McConnelee, "Application of Finite Element Elastic-Plastic Stress Analysis to Notched Fatigue Specimen Behavior," *First International Conference on Structural Mechanics in Reactor Technology* (West Berlin, Germany, September 1971), published by T. A. Jaeger, Luxembourg.

70. T. H. Topper and C. V. Byre Gowda, "Local Stress-Strain Approach to Fatigue Analysis and Design," ASME Paper 70-DE-24. Presented at the *Design Engineering Conference and Show*, Chicago, Ill., May 11-14, 1970.

71. Ernest L. Robinson, "Steam-Piping Design to Minimize Creep Concentrations," ASME Transactions, 1955, pp. 1147-1162.

72. J. Spence, "An Analysis for Pipework Systems Under Creep Conditions," *Proceedings of the First International Conference on Pressure Vessel Technology*, Part 1 – Design and Analysis, ASME, 1969.

73. W. Gorczynski, "A Method of Assessing Structural Efficiency of Pipework Designed for High Temperature Service," *Proc. Instn. Mechanical Engineers*, 1963-1964, Vol. 178.

APPENDIX A

PROCEDURES EMPLOYED TO ESTABLISH THE BASIC TIME AND TEMPERATURE STRESS INTENSITIES AND ISOCHRONOUS STRESS-STRAIN CURVES[1]

A.1 MAXIMUM ALLOWABLE VALUE OF GENERAL PRIMARY MEMBRANE STRESS INTENSITY FOR DESIGN CONDITIONS

The symbol S_o is used for this value. The S_o values are identical to the values for S given in Section VIII, Division 1 of the Code.

A.2 TIME-INDEPENDENT DESIGN STRESS INTENSITY

The symbol S_m is used for this value. These values are based on tensile and yield strengths of the material. The criteria employed are defined as follows:

(a) The allowable stress intensity value, S_m, for ferritic steels and nonferrous metals and alloys, except those covered in paragraph (b) below, is the least of the following four values:

(1) one-third of the specified minimum tensile strength at room temperature

(2) one-third of the short-term tensile strength at temperature (as defined in A.2.1 in this Appendix).

The ratio of UTS_T/UTS_{RT}, for austenitic stainless steel, is found in ASTM DS5-S2.

(3) two-thirds of the specified minimum yield strength at room temperature

(4) two-thirds of the short-term 0.2% offset yield strength at temperature (defined as the ratio of yield strength at temperature divided by the yield strength at room temperature, multiplied by the minimum specified room temperature yield strength).

The ratio of YS_T/YS_{RT}, for austenitic stainless steel, is found in ASTM DS-S2. The strength is determined at a strain rate of 0.0005 min.$^{-1}$

(b) The allowable stress intensity value, S_m, for austenitic steels, nickel-chromium-iron and nickel-iron-chromium alloys is the lowest of the following four values:

(1) one-third of the specified minimum tensile strength at room temperature

(2) one-third of the tensile strength at the operating temperature

(3) two-thirds of the specified minimum yield strength at room temperature

(4) 90% of the yield strength at the operating temperature

A.2.1 YIELD AND TENSILE STRENGTH

The procedures for establishing yield and ultimate strengths are discussed below:

The yield and tensile strength data available for a particular material grade are normalized by ratioing the elevated temperature strength of individual lots to the room temperature strength of the same lots, and then all sets of such ratios representing a

[1] Not applicable to bolting materials.

particular grade are evaluated by the method of least squares to establish the curve of best fit for the data. The resulting *strength-ratio trend curve* is considered to represent the typical or characteristic variation of yield or tensile strength with temperature. Using such a ratio trend curve, it becomes possible to compute strength trend curves for any particular room temperature strength level of interest within the limits encompassed by the original data.

Since the design stress intensity criteria include fractions of the specified yield and tensile strengths, it is necessary to factor the ratio trend curves against the specified minimum yield and tensile strengths to define what may be termed minimum position yield and tensile strength curves. At temperatures above room temperature, the property *yield strength at temperature* is taken, for purposes of the criteria, to be this minimum position value. However, the property *tensile strength at temperature* is taken as the smaller of:

(a) specified minimum tensile strength at room temperature; or
(b) a value 10% greater than the minimum position value cited above.

A.3 TIME-DEPENDENT DESIGN STRESS INTENSITY[2]

The symbol S_t is used for the basic time and temperature dependent allowable stress intensity for load-controlled stresses. S_t values are the least of each of the three quantities:

(a) two-thirds of the minimum stress to cause rupture in time t;
(b) 80% of the minimum stress to cause the onset of tertiary creep in time t; and
(c) the minimum stress to produce one percent total strain in time t.

A.3.1 MINIMUM STRESS-TO-CAUSE-RUPTURE IN TIME t

The basic data and a description of the rupture strength evaluation procedures employed for several of the materials included in Case 1592 (i.e., Types 304 and 316 Stainless Steel) may be found in Metal Property Council data evaluations [Smith (17) and Simmons and Van Echo (18)].

Two principal procedures are employed in evaluating the dependence of the stress-to-rupture upon time and temperature. A choice between the results, based on engineering judgment, is then made.

In the first procedure, the isothermal relation between stress and time for rupture of individual lots is interpolated or extrapolated, as required, to identify the stress-to-cause-rupture in 100, 1000, 10,000, etc., hr. Plotting on log-log coordinates tends to linearize the variation, and thereby facilitate extrapolation, particularly at lower temperatures. At higher temperatures, the variation tends to curvilinearity at longer times, and extrapolation involves greater risk. The results of such interpolations or extrapolations for individual lots, as they vary with temperature, are then evaluated by the method of least squares to define an average rupture strength-temperature trend curve. A trend curve for minimum rupture strength is derived from the mean trend curve by subtracting 1.65 multiples of the standard deviation of the sample. If certain implicit assumptions hold (e.g., that the data are normally distributed, or that the average is without error), this minimum trend curve defines a lower boundary for 95% of the data. Inspection of the data plots has always shown that this is approximately true.

[2] Based on data determined from tests performed on air.

The second evaluation procedure that has been employed is an indirect one, involving one or another time-temperature parameter. One of the simplest of these, widely used, is Larson and Miller's

$$P = T(C + \log t) = F(S)$$

where T is the temperature in degrees Rankin, t is the time for rupture in hours, C is a material constant, and $F(S)$ denotes that the parameter depends upon stress. Ordinarily, the available data are not adequate to permit evaluation of individual lots by the parameter procedure, as would be desirable; instead, the total data population must be treated as a common population on a universalized basis, assuming the constant C to remain invariant from lot to lot within the data population. Accordingly, the scatter band for the stress-parameter variation is evaluated by the method of least squares to determine an average curve of best fit, from which average values of rupture strength as dependent upon temperature can be derived. A minimum curve is developed, as in the previously described procedure, by subtracting 1.65 multiples of the standard deviation of the sample from the average curve.

A.3.2 MINIMUM STRESS-TO-INITIATE-TERTIARY-CREEP IN TIME t

For the ferrous alloys included in Case 1592, Leyda and Rowe (19) had reported that the time to initiate tertiary creep is a fixed fraction of the time for rupture for a given material at a specific temperature. Thus, for 2¼ Cr-1 Mo and Types 304 and 316, the minimum stress-to-initiate-tertiary-creep was computed from the minimum-stress-to-rupture data. For the high-nickel alloys, tertiary creep information was developed by examination of available creep curves. In all instances, the initiation of tertiary creep was assessed visually. Extrapolations to lower temperatures were made by time-temperature parameter methods exactly analogous to those described for rupture strength, except that the time for tertiary creep to begin became the measured quantity.

A.3.3 MINIMUM STRESS TO CAUSE 1% TOTAL STRAIN IN TIME t

In common with the criterion for stress to initiate tertiary creep, the criterion on minimum stress for 1% total strain is new to the ASME Code. For purposes of Section I and Section VIII, Division 1, creep strength has for many years been evaluated in terms of the stress causing a secondary creep rate of 0.01% per 1000 hr. In the new criterion, stress to cause 1% total strain can be evaluated in an exactly analogous manner as the stress to cause rupture or to initiate tertiary creep—the dependence upon stress tends to parallel that of rupture time—or it can be derived directly from the isochronous stress-strain curves. Both approaches have been employed in developing the material for Case 1592.

A.4 ISOCHRONOUS STRESS-STRAIN CURVES

For relatively short times, isochronous stress-strain curves may be derived by taking constant time sections through a family of creep curves, such as those of Fig. 2. However, this approach to their derivation is not generally practicable (unless forming only a part of a multi-approach procedure) since the time scale of interest extends beyond the feasible limit of experimental testing. Extrapolative procedures are required for the longer test times and for strains below 1 %. For generating the isochronous stress-strain curves in Case 1592, two procedures have been employed. In one of these, the curves are developed by performing evaluations exactly analogous to those described for developing information on the stress to reduce 1% strain, except that other specific strains encompassing the range of interest are also evaluated and the various parts assembled in plots of stress versus strain for different fixed times.

In a second procedure, the strain has been expressed as an analytical function of time according to the general form:

$$\epsilon = \epsilon_{loading} + \epsilon_{transient} + \epsilon_{steady\ state}$$

where each of the parts is a function of stress and temperature. The individual parameters of the equation are then evaluated from the experimental results generated in conventional creep tests.

More complete descriptions of these procedures may be found in *The Generation of Isochronous Stress-Strain Curves*, ASME, 1972(4).

LIST OF FIGURES

Fig. 1(a) *Histories from a Loading at Low Temperature* 9

Fig. 1(b) *Histories from a Load-Controlled Loading at Elevated Temperature* 9

Fig. 1(c) *Histories from a Strain-Controlled Loading at Elevated Temperature* 10

Fig. 2 *Effect of Stress Level on Elevated Temperature Behavior* 11

Fig. 3 *Data from the Standard Creep Test* 12

Fig. 4 *Stress-Rupture Data from Constant Temperature Creep Tests* 12

Fig. 5 *Isochronous Stress-Strain Curves from Creep Tests at Constant Temperature* 13

Fig. 6 *Effect of Tension Hold Time on the Fatigue Life of AISI Type 304 Stainless Steel at 1000 F in Air* 14

Fig. 7 *Flow Diagram for Elevated Temperature Analysis* 16

Fig. 8 *S_{mt} Allowable Stress, Type 316 Stainless Steel* 17

Fig. 9 *Elastically Calculated Primary Bending Stress Distribution Compared to Actual Time-Dependent Inelastic Stress Distribution* 19

Fig. 10 *Steady-State Creep Stress Distributions Across a Rectangular Beam in Pure Bending and Having a Steady-State Creep Law of the Form, $\dot{\epsilon}_c = A\sigma^n$* 20

Fig. 11 *Steady-State Creep Stress Distribution Across a Thin, Circular Tube in Pure Bending and Having a Steady-State Creep Law of the Form $\dot{\epsilon}_c = A\sigma^n$* 21

Fig. 12 *Stress Regimes* 23

Fig. 13(a) *Effect of Prior Creep Deformation on Tensile Elongation of Type 304 Stainless Steel* 25

Fig. 13(b) *Variation of Creep Ductility with Rupture Life for Selected Austenitic Stainless Steel Submerged-Arc Weldments* 26

Fig. 14 *Typical Strain-Time Responses* 27

Fig. 15 *Strain-Time History Schematic* 28

Fig. 16 *Simple Example of Conditions Leading to Elevated Temperature Ratcheting* 29

Fig. 17 *Effective Creep Stress, σ_c, for Upper Bounds on Total Accumulated Inelastic Strain with Creep Ratcheting* 33

Fig. 18 *Load History for an Example with Ratcheting* 34

Fig. 19 *Stress History for an Example with Ratcheting* 35

Fig. 21 Effect of Hold-Time on Fatigue Life of Austenitic Stainless Steel 37

Fig. 22 Effect of Hold-Time on Fatigue Life of Various Steels 38

Fig. 23 Creep vs. Fatigue Damage at 5% Load Drop-off, Type 304 Stainless Steel at 1200 F. 42

Fig. 24 Average and Minimum Trend Curves for Creep-Fatigue Interaction for Types 304 and 316 Stainless Steels 43

Fig. 25 Comparison of Code Creep-Fatigue Allowables to Experimental Data 44

Fig. 26 Distribution of Actual-to-Calculated Life Ratios for Strain-Controlled Creep-Fatigue Test Specimens 45

Fig. 27 Creep-Fatigue Damage Interaction for Tension Hold-Time Tests of Solution Annealed Ni-Fe-Cr, Alloy 800H 46

Fig. 28 Strain Rate Effects on Fatigue Life Reduction 47

Fig. 29 Hold-Time Effects on Fatigue Life Reduction for Types 304 and 316 Stainless Steel 48

Fig. 30 Comparison of Analytical and Experimental Strain Ranges for a Notched Bar 50–53

Fig. 31 Sample Problem in Plane Stress 56

Fig. 32 Analysis Flow Diagram 57

Fig. 33 Typical Buckling Behavior 59

Fig. 34 Creep Buckling Deflection-Time Characteristics 59

Fig. 35 Behavior of a Bolt in an Unyielding Flange 65

Fig. 36 Balanced Loop Behavior 66

Fig. 37 Four Large Bending Loops in Series with Four Smaller Loops of Half-Size Pipe in Parallel 67

Fig. 38 Two-Bar Model with Strain Concentration but no Elastic Follow-up 68

Fig. 39 Two-Bar Model with no Strain Concentration or Elastic Follow-up 68

Fig. 40 Two-Bar Model with Elastic Follow-up and Strain Concentration 69

Fig. 41 Built-in Cylinder with Elastic Follow-up 70